

SOLID-STATE SCIENCES

E. N. Economou

Green's Functions in Quantum Physics

Third Edition

 Springer

Springer Series in
SOLID-STATE SCIENCES

Series Editors:

M. Cardona P. Fulde K. von Klitzing R. Merlin H.-J. Queisser H. Störmer

- 90 **Earlier and Recent Aspects of Superconductivity**
Editor: J.G. Bednorz and K.A. Müller
- 91 **Electronic Properties and Conjugated Polymers III**
Editors: H. Kuzmany, M. Mehring, and S. Roth
- 92 **Physics and Engineering Applications of Magnetism**
Editors: Y. Ishikawa and N. Miura
- 93 **Quasicrystals**
Editor: T. Fujiwara and T. Ogawa
- 94 **Electronic Conduction in Oxides**
2nd Edition By N. Tsuda, K. Nasu, A. Fujimori, and K. Siratori
- 95 **Electronic Materials**
A New Era in Materials Science
Editors: J.R. Chelikowski and A. Franciosi
- 96 **Electron Liquids**
2nd Edition By A. Isihara
- 97 **Localization and Confinement of Electrons in Semiconductors**
Editors: F. Kuchar, H. Heinrich, and G. Bauer
- 98 **Magnetism and the Electronic Structure of Crystals**
By V.A. Gubanov, A.I. Liechtenstein, and A.V. Postnikov
- 99 **Electronic Properties of High- T_c Superconductors and Related Compounds**
Editors: H. Kuzmany, M. Mehring, and J. Fink
- 100 **Electron Correlations in Molecules and Solids**
3rd Edition By P. Fulde
- 101 **High Magnetic Fields in Semiconductor Physics III**
Quantum Hall Effect, Transport and Optics By G. Landwehr
- 102 **Conjugated Conducting Polymers**
Editor: H. Kiess
- 103 **Molecular Dynamics Simulations**
Editor: F. Yonezawa
- 104 **Products of Random Matrices in Statistical Physics** By A. Crisanti, G. Paladin, and A. Vulpiani
- 105 **Self-Trapped Excitons**
2nd Edition
By K.S. Song and R.T. Williams
- 106 **Physics of High-Temperature Superconductors**
Editors: S. Maekawa and M. Sato
- 107 **Electronic Properties of Polymers**
Orientation and Dimensionality of Conjugated Systems
Editors: H. Kuzmany, M. Mehring, and S. Roth
- 108 **Site Symmetry in Crystals**
Theory and Applications
2nd Edition
By R.A. Evarestov and V.P. Smirnov
- 109 **Transport Phenomena in Mesoscopic Systems**
Editors: H. Fukuyama and T. Ando
- 110 **Superlattices and Other Heterostructures**
Symmetry and Optical Phenomena
2nd Edition
By E.L. Ivchenko and G.E. Pikus
- 111 **Low-Dimensional Electronic Systems**
New Concepts
Editors: G. Bauer, F. Kuchar, and H. Heinrich
- 112 **Phonon Scattering in Condensed Matter VII**
Editors: M. Meissner and R.O. Pohl
- 113 **Electronic Properties of High- T_c Superconductors**
Editors: H. Kuzmany, M. Mehring, and J. Fink
-

Springer Series in
SOLID-STATE SCIENCES

Series Editors:

M. Cardona P. Fulde K. von Klitzing R. Merlin H.-J. Queisser H. Störmer

- | | |
|---|--|
| <p>114 Interatomic Potential and Structural Stability
Editors: K. Terakura and H. Akai</p> <p>115 Ultrafast Spectroscopy of Semiconductors and Semiconductor Nanostructures
By J. Shah</p> <p>116 Electron Spectrum of Gapless Semiconductors
By J.M. Tsidilkovski</p> <p>117 Electronic Properties of Fullerenes
Editors: H. Kuzmany, J. Fink, M. Mehring, and S. Roth</p> <p>118 Correlation Effects in Low-Dimensional Electron Systems
Editors: A. Okiji and N. Kawakami</p> <p>119 Spectroscopy of Mott Insulators and Correlated Metals
Editors: A. Fujimori and Y. Tokura</p> <p>120 Optical Properties of III-V Semiconductors
The Influence of Multi-Valley Band Structures By H. Kalt</p> <p>121 Elementary Processes in Excitations and Reactions on Solid Surfaces
Editors: A. Okiji, H. Kasai, and K. Makoshi</p> <p>122 Theory of Magnetism
By K. Yosida</p> <p>123 Quantum Kinetics in Transport and Optics of Semiconductors
By H. Haug and A.-P. Jauho</p> <p>124 Relaxations of Excited States and Photo-Induced Structural Phase Transitions
Editor: K. Nasu</p> <p>125 Physics and Chemistry of Transition-Metal Oxides
Editors: H. Fukuyama and N. Nagaosa</p> | <p>126 Physical Properties of Quasicrystals
Editor: Z.M. Stadnik</p> <p>127 Positron Annihilation in Semiconductors
Defect Studies
By R. Krause-Rehberg and H.S. Leipner</p> <p>128 Magneto-Optics
Editors: S. Sugano and N. Kojima</p> <p>129 Computational Materials Science
From Ab Initio to Monte Carlo Methods. By K. Ohno, K. Esfarjani, and Y. Kawazoe</p> <p>130 Contact, Adhesion and Rupture of Elastic Solids
By D. Maugis</p> <p>131 Field Theories for Low-Dimensional Condensed Matter Systems
Spin Systems and Strongly Correlated Electrons
By G. Morandi, P. Sodano, A. Tagliacozzo, and V. Tognetti</p> <p>132 Vortices in Unconventional Superconductors and Superfluids
Editors: R.P. Huebener, N. Schopohl, and G.E. Volovik</p> <p>133 The Quantum Hall Effect
By D. Yoshioka</p> <p>134 Magnetism in the Solid State
By P. Mohn</p> <p>135 Electrodynamics of Magnetoactive Media
By I. Vagner, B.I. Lembrikov, and P. Wyder</p> |
|---|--|
-

Springer Series in SOLID-STATE SCIENCES

Series Editors:

M. Cardona P. Fulde K. von Klitzing R. Merlin H.-J. Queisser H. Störmer

The Springer Series in Solid-State Sciences consists of fundamental scientific books prepared by leading researchers in the field. They strive to communicate, in a systematic and comprehensive way, the basic principles as well as new developments in theoretical and experimental solid-state physics.

- | | | | |
|-----|--|-----|--|
| 136 | Nanoscale Phase Separation and Colossal Magnetoresistance
The Physics of Manganites and Related Compounds
By E. Dagotto | 144 | Physics of Transition Metal Oxides
By S. Maekawa, T. Tohyama, S.E. Barnes, S. Ishihara, W. Koshibae, and G. Khaliullin |
| 137 | Quantum Transport in Submicron Devices
A Theoretical Introduction
By W. Magnus and W. Schoenmaker | 145 | Point-Contact Spectroscopy
By Y.G. Naidyuk and I.K. Yanson |
| 138 | Phase Separation in Soft Matter Physics
Micellar Solutions, Microemulsions, Critical Phenomena
By P.K. Khabibullaev and A.A. Saidov | 146 | Optics of Semiconductors and Their Nanostructures
Editors: H. Kalt and M. Hetterich |
| 139 | Optical Response of Nanostructures
Microscopic Nonlocal Theory
By K. Cho | 147 | Electron Scattering in Solid Matter
A Theoretical and Computational Treatise
By J. Zabloudil, R. Hammerling, L. Szunyogh, and P. Weinberger |
| 140 | Fractal Concepts in Condensed Matter Physics
By T. Nakayama and K. Yakubo | 148 | Physical Acoustics in the Solid State
By B. Lüthi |
| 141 | Excitons in Low-Dimensional Semiconductors
Theory, Numerical Methods, Applications By S. Glutsch | 149 | Solitary Waves in Complex Dispersive Media
Theory · Simulation · Applications
By V.Yu. Belashov and S.V. Vladimirov |
| 142 | Two-Dimensional Coulomb Liquids and Solids
By Y. Monarkha and K. Kono | 150 | Topology in Condensed Matter
Editor: M.I. Monastyrsky |
| 143 | X-Ray Multiple-Wave Diffraction
Theory and Application
By S.-L. Chang | 151 | Particle Penetration and Radiation Effects
By P. Sigmund |
| | | 152 | Magnetism
From Fundamentals to Nanoscale Dynamics
By H.C. Siegmann and J. Stöhr |

Volumes 90–135 are listed at the end of the book.

Eleftherios N. Economou

Green's Functions in Quantum Physics

Third Edition

With 60 Figures

 Springer

Eleftherios N. Economou
University of Crete
Foundation for Research and Technology-Hellas (FORTH)
Department of Physics
P. O. Box 1527
711 10 Heraklion, Crete, Greece
E-mail: economou@admin.forth.gr

Series Editors:

Professor Dr., Dres. h. c. Manuel Cardona
Professor Dr., Dres. h. c. Peter Fulde*
Professor Dr., Dres. h. c. Klaus von Klitzing
Professor Dr., Dres. h. c. Hans-Joachim Queisser
Max-Planck-Institut für Festkörperforschung, Heisenbergstrasse 1, 70569 Stuttgart, Germany
* Max-Planck-Institut für Physik komplexer Systeme, Nöthnitzer Strasse 38
01187 Dresden, Germany

Professor Dr. Roberto Merlin
Department of Physics, 5000 East University, University of Michigan
Ann Arbor, MI 48109-1120, USA

Professor Dr. Horst Störmer
Dept. Phys. and Dept. Appl. Physics, Columbia University, New York, NY 10027 and
Bell Labs., Lucent Technologies, Murray Hill, NJ 07974, USA

Library of Congress Control Number: 2006926231

ISSN 0171-1873
ISBN-10 3-540-28838-4 3rd ed. Springer Berlin Heidelberg New York
ISBN-13 978-3-540-28838-1 3rd ed. Springer Berlin Heidelberg New York
ISBN 3-540-12266-4 2nd ed. Springer-Verlag Berlin Heidelberg New York

This work is subject to copyright. All rights are reserved, whether the whole or part of the material is concerned, specifically the rights of translation, reprinting, reuse of illustrations, recitation, broadcasting, reproduction on microfilm or in any other way, and storage in data banks. Duplication of this publication or parts thereof is permitted only under the provisions of the German Copyright Law of September 9, 1965, in its current version, and permission for use must always be obtained from Springer. Violations are liable to prosecution under the German Copyright Law.

Springer is a part of Springer Science+Business Media
springer.com

© Springer-Verlag Berlin Heidelberg 1979, 1983, 2006
Printed in Germany

The use of general descriptive names, registered names, trademarks, etc. in this publication does not imply, even in the absence of a specific statement, that such names are exempt from the relevant protective laws and regulations and therefore free for general use.

Typesetting by the author and LE- \TeX GbR
Cover concept: eStudio Calamar Steinen
Cover production: *design & production* GmbH, Heidelberg
Production: LE- \TeX Jelonek, Schmidt & Vöckler GbR, Leipzig

Printed on acid-free paper 57/3100/YL - 5 4 3 2 1 0

To Sophia

Preface to the Third Edition

In this third edition the book has been expanded in three directions:

1. Problems have been added at the end of each chapter (40% of which are solved in the last section of the book) together with suggestions for further reading. Furthermore, the number of appendices (marked with a grey stripe) has been substantially enlarged in order to make the book more self-sufficient. These additions, together with many clarifications in the text, render the book more suitable as a companion in a course on Green's functions and their applications.
2. The impressive developments of the 1980s and 1990s in mesoscopic physics, and in particular in transport properties, found their way – to a certain extent – in the new Chaps. 8 and 9 (which also contain some of the material of the old Chap. 7). This is a natural expansion, since Green's functions have played an important role as a theoretical tool in this new field of physics, a role that continues in nanoregime research (see, e.g., recent publications dealing with carbon nanotubes). Thus, the powerful and unifying formalism of Green's functions finds applications not only in standard physics subjects such as perturbation and scattering theory, bound-state formation, etc., but also at the forefront of current and, most likely, future developments.
3. Over the last 15 years or so Green's functions have found applications not only in condensed matter electronic motion but in classical wave propagation in both periodic and random media; photonic and phononic crystals are the outcomes of this line of research whose underlying basic theoretical principles are summarized in Sect. 7.2.4.

I would like to thank Ms. Mina Papadakis and Dr. Stamatis Stamatiadis whose help was invaluable during the writing and typesetting of this drastically revised third edition of my book.

Heraklion, Crete, March 2005

E. N. Economou

Preface to the Second Edition

In this edition, the second and main part of the book has been considerably expanded so as to cover important applications of the formalism of Green's functions.

In Chap. 5 a section was added outlining the extensive role of the tight-binding (or, equivalently, the linear combination of atomiclike orbitals) approach to many branches of solid-state physics. Some additional information (including a table of numerical values) regarding square and cubic lattice Green's functions were incorporated.

In Chap. 6 the difficult subjects of superconductivity and the Kondo effect are examined employing an appealingly simple connection to the question of the existence of a bound state in a very shallow potential well. The existence of such a bound state depends entirely on the form of the unperturbed density of states near the end of the spectrum: if the density of states blows up, there is always at least one bound state. If the density of states approaches zero continuously, a critical depth (and/or width) of the well must be reached in order to have a bound state. The borderline case of a finite discontinuity (which is very important to superconductivity and the Kondo effect) always produces a bound state with an exponentially small binding energy.

Chapter 7 has been expanded to cover details of the new and fast-developing field of wave propagation in disordered media. The coherent potential approximation (a simple but powerful method) is presented with an extensive list of references to the current literature. Then the electrical conductivity is examined both because it is an interesting quantity in its own right and because it plays a central role in demonstrating how disorder can create a qualitatively different behavior. Since the publication of the first edition of this book, significant advances in the field of random media have taken place. An effort has been made to present in a simple way the essential points of these advances (for the reader with a casual interest in this subject) and to review the current literature (for the benefit of the reader whose research activities are or will be related to the field of disordered systems).

In this edition, each chapter is preceded by a short outline of the material to be covered and concluded by a summary containing the most important equations numbered as in the main text.

I would like to thank A. Andriotis and A. Fertis for pointing out to me several misprints in the first edition. I would also like to express my gratitude to Exxon Research and Engineering Company for its hospitality during the final stages of this work.

Heraklion, Crete, January 1983

E. N. Economou

Preface to the First Edition

This text grew out of a series of lectures addressed to solid-state experimentalists and students beginning their research career in solid-state physics.

The first part, consisting of Chaps. 1 and 2, is a rather extensive mathematical introduction that covers material related to Green's functions usually included in a graduate course on mathematical physics. Emphasis is given to those topics that are important in quantum physics. On the other hand, little attention is given to the important question of determining the Green's functions associated with boundary conditions on surfaces at finite distances from the source. The second and main part of the book is, in my opinion, the first attempt at integrating, in a systematic but concise way, various topics of quantum physics, where Green's functions (as defined in Part I) can be successfully applied. Chapter 3 is a direct application of the formalism developed in Part I. In Chap. 4 the perturbation theory for Green's functions is presented and applied to scattering and to the question of bound-state formation. Next, the Green's functions for the so-called tight-binding Hamiltonian (TBH) are calculated. The TBH is of central importance for solid-state physics because it is the simplest example of wave propagation in periodic structures. It is also important for quantum physics in general because it is rich in physical phenomena (e.g., negative effective mass, creation of a bound state by a repulsive perturbation) and, at the same time, simple in its mathematical treatment. Thus one can derive simple, exact expressions for scattering cross sections and for bound and resonance levels. The multiple scattering formalism is presented within the framework of the TBH and applied to questions related to the behavior of disordered systems (such as amorphous semiconductors). The material of Part II is of interest not only to solid-state physicists but to students in a graduate-level course in quantum mechanics (or scattering theory) as well.

In Part III, with the help of the second quantization formalism, many-body Green's functions are introduced and utilized in extracting physical information about interacting many-particle systems. Many excellent books have been devoted to the material of Part III (e.g., Fetter and Walecka: Quantum Theory

of Many-Particle Systems [20]). Thus the present treatment must be viewed as a brief introduction to the subject; this introduction may help the solid-state theorist approach the existing thorough treatments of the subject and the solid-state experimentalist become acquainted with the formalism.

I would like to thank the “Demokritos” Nuclear Research Center and the Greek Atomic Energy Commission for their hospitality during the writing of the second half of this book.

Athens, Greece, November 1978

E. N. Economou

Contents

Part I Green's Functions in Mathematical Physics

1	Time-Independent Green's Functions	3
1.1	Formalism	3
1.2	Examples	9
1.2.1	Three-Dimensional Case ($d = 3$)	10
1.2.2	Two-Dimensional Case ($d = 2$)	11
1.2.3	One-Dimensional Case ($d = 1$)	13
1.2.4	Finite Domain Ω	13
1.3	Summary	14
1.3.1	Definition	14
1.3.2	Basic Properties	15
1.3.3	Methods of Calculation	15
1.3.4	Use	16
	Further Reading	17
	Problems	17
2	Time-Dependent Green's Functions	21
2.1	First-Order Case	21
2.1.1	Examples	24
2.2	Second-Order Case	26
2.2.1	Examples	30
2.3	Summary	33
2.3.1	Definition	33
2.3.2	Basic Properties	33
2.3.3	Definition	34
2.3.4	Basic Properties	34
2.3.5	Use	35
	Further Reading	36
	Problems	36

Part II Green's Functions in One-Body Quantum Problems

3	Physical Significance of G.	
	Application to the Free-Particle Case	41
3.1	General Relations	41
3.2	The Free-Particle ($\mathcal{H}_0 = p^2/2m$) Case	43
	3.2.1 3-d Case	44
	3.2.2 2-d Case	45
	3.2.3 1-d Case	45
3.3	The Free-Particle Klein–Gordon Case	47
3.4	Summary	50
	Further Reading	51
	Problems	51
4	Green's Functions and Perturbation Theory	55
4.1	Formalism	55
	4.1.1 Time-Independent Case	55
	4.1.2 Time-Dependent Case	60
4.2	Applications	64
	4.2.1 Scattering Theory ($E > 0$)	64
	4.2.2 Bound State in Shallow Potential Wells ($E < 0$)	67
	4.2.3 The KKR Method for Electronic Calculations in Solids	70
4.3	Summary	71
	Further Reading	74
	Problems	74
5	Green's Functions for Tight-Binding Hamiltonians	77
5.1	Introductory Remarks	77
5.2	The Tight-Binding Hamiltonian (TBH)	80
5.3	Green's Functions	87
	5.3.1 One-Dimensional Lattice	88
	5.3.2 Square Lattice	89
	5.3.3 Simple Cubic Lattice	94
	5.3.4 Green's Functions for Bethe Lattices (Cayley Trees)	98
5.4	Summary	101
	Further Reading	102
	Problems	102
6	Single Impurity Scattering	111
6.1	Formalism	111
6.2	Explicit Results for a Single Band	118
	6.2.1 Three-Dimensional Case	118
	6.2.2 Two-Dimensional Case	123
	6.2.3 One-Dimensional Case	124

6.3	Applications	125
6.3.1	Levels in the Gap	125
6.3.2	The Cooper Pair and Superconductivity	127
6.3.3	The Kondo Problem	133
6.3.4	Lattice Vibrations in Crystals Containing “Isotope” Impurities	135
6.4	Summary	137
	Further Reading	139
	Problems	140
7	Two or More Impurities; Disordered Systems	141
7.1	Two Impurities	141
7.2	Infinite Number of Impurities	150
7.2.1	Virtual Crystal Approximation (VCA)	151
7.2.2	Average t -Matrix Approximation (ATA)	152
7.2.3	Coherent Potential Approximation (CPA)	153
7.2.4	The CPA for Classical Waves	158
7.2.5	Direct Extensions of the CPA	163
7.2.6	Cluster Generalizations of the CPA	165
7.3	Summary	168
	Further Reading	169
	Problems	169
8	Electrical Conductivity and Green’s Functions	173
8.1	Electrical Conductivity and Related Quantities	173
8.2	Various Methods of Calculation	176
8.2.1	Phenomenological Approach	176
8.2.2	Boltzmann’s Equation	177
8.2.3	A General, Independent-Particle Formula for Conductivity	178
8.2.4	General Linear Response Theory	180
8.3	Conductivity in Terms of Green’s Functions	183
8.3.1	Conductivity Without Vertex Corrections	184
8.3.2	CPA for Vertex Corrections	186
8.3.3	Vertex Corrections Beyond the CPA	190
8.3.4	Post-CPA Corrections to Conductivity	192
8.4	Summary	195
	Further Reading	197
	Problems	197
9	Localization, Transport, and Green’s Functions	199
9.1	An Overview	199
9.2	Disorder, Diffusion, and Interference	203
9.3	Localization	208
9.3.1	Three-Dimensional Systems	210

9.3.2	Two-Dimensional Systems	212
9.3.3	One-Dimensional and Quasi-One-Dimensional Systems	214
9.4	Conductance and Transmission	216
9.5	Scaling Approach	219
9.6	Other Computational Techniques	224
9.6.1	Quasi-One-Dimensional Systems and Scaling	225
9.6.2	Level Spacing Statistics	225
9.7	Localization and Green's Functions	226
9.7.1	Green's Function and Localization in One Dimension	227
9.7.2	Renormalized Perturbation Expansion (RPE) and Localization	230
9.7.3	Green's Functions and Transmissions in Quasi-One-Dimensional Systems	235
9.8	Applications	238
9.9	Summary	240
	Further Reading	243
	Problems	243

Part III Green's Functions in Many-Body Systems

10	Definitions	249
10.1	Single-Particle Green's Functions in Terms of Field Operators	249
10.2	Green's Functions for Interacting Particles	253
10.3	Green's Functions for Noninteracting Particles	257
10.4	Summary	260
	Further Reading	261
	Problems	261
11	Properties and Use of the Green's Functions	263
11.1	Analytical Properties of g_s and \tilde{g}_s	263
11.2	Physical Significance and Use of g_s and \tilde{g}_s	268
11.3	Quasiparticles	275
11.4	Summary	281
11.4.1	Properties	281
11.4.2	Use	282
	Further Reading	283
	Problems	283
12	Computational Methods for g	285
12.1	Equation of Motion Method	285
12.2	Diagrammatic Method for Fermions at $T = 0$	289
12.3	Diagrammatic Method for $T \neq 0$	298
12.4	Partial Summations. Dyson's Equation	300
12.5	Other Methods of Calculation	306

12.6 Summary	306
Further Reading	307
Problems	307
13 Applications	309
13.1 Normal Fermi Systems. Landau Theory	309
13.2 High-Density Electron Gas	312
13.3 Dilute Fermi Gas	319
13.4 Superconductivity	322
13.4.1 Diagrammatic Approach	322
13.4.2 Equation of Motion Approach	324
13.5 The Hubbard Model	327
13.6 Summary	332
Further Reading	333
Problems	334
A Dirac's delta Function	337
B Dirac's bra and ket Notation	341
C Solutions of Laplace and Helmholtz Equations in Various Coordinate Systems	345
C.1 Helmholtz Equation $(\nabla^2 + k^2) \psi(\mathbf{r}) = 0$	345
C.1.1 Cartesian Coordinates x, y, z	345
C.1.2 Cylindrical Coordinates z, ϕ, ϱ	345
C.1.3 Spherical coordinates r, θ, ϕ	346
C.2 Vector Derivatives	347
C.2.1 Spherical Coordinates r, θ, ϕ	347
C.2.2 Cylindrical Coordinates z, ϱ, ϕ	348
C.3 Schrödinger Equation in Centrally Symmetric 3- and 2-Dimensional Potential V	348
D Analytic Behavior of $G(z)$ Near a Band Edge	351
E Wannier Functions	355
F Renormalized Perturbation Expansion (RPE)	357
G Boltzmann's Equation	363
H Transfer Matrix, S-Matrix, etc.	369
I Second Quantization	379
Solutions of Selected Problems	391
References	447
Index	461

Green's Functions in Mathematical Physics

Time-Independent Green's Functions

Summary. In this chapter, the time-independent Green's functions are defined, their main properties are presented, methods for their calculation are briefly discussed, and their use in problems of physical interest is summarized.

1.1 Formalism

Green's functions can be defined as solutions of inhomogeneous differential equations of the type¹

$$[z - L(\mathbf{r})] G(\mathbf{r}, \mathbf{r}'; z) = \delta(\mathbf{r} - \mathbf{r}') , \quad (1.1)$$

subject to certain boundary conditions (BCs) for \mathbf{r} or \mathbf{r}' lying on the surface S of the domain Ω of \mathbf{r} and \mathbf{r}' . Here we assume that z is a complex variable with $\lambda \equiv \text{Re}\{z\}$ and $s \equiv \text{Im}\{z\}$ and that $L(\mathbf{r})$ is a time-independent, linear, hermitian² differential operator that possesses a complete set of eigenfunctions $\{\phi_n(\mathbf{r})\}$, i.e.,

$$L(\mathbf{r})\phi_n(\mathbf{r}) = \lambda_n\phi_n(\mathbf{r}) , \quad (1.2)$$

where $\{\phi_n(\mathbf{r})\}$ satisfy the same BCs as $G(\mathbf{r}, \mathbf{r}'; z)$. The subscript n may stand for more than one index specifying uniquely each eigenfunction and the corresponding eigenvalue. The set $\{\phi_n\}$ can be considered as orthonormal without loss of generality (see Problem 1.1s at the end of Chap. 1), i.e.,

$$\int_{\Omega} \phi_n^*(\mathbf{r})\phi_m(\mathbf{r}) d\mathbf{r} = \delta_{nm} . \quad (1.3)$$

¹ Several authors write the right-hand side (rhs) of (1.1) as $4\pi\delta(\mathbf{r} - \mathbf{r}')$ or $-4\pi\delta(\mathbf{r} - \mathbf{r}')$.

² A linear operator, L , acting on arbitrary complex functions, $\phi(\mathbf{r})$ and $\psi(\mathbf{r})$, defined on Ω and satisfying given BCs is called hermitian if $\int_{\Omega} \phi^*(\mathbf{r})[L\psi(\mathbf{r})]d\mathbf{r} = \{\int_{\Omega} \psi^*(\mathbf{r})[L\phi(\mathbf{r})]d\mathbf{r}\}^* = \int_{\Omega} [L\phi(\mathbf{r})]^*\psi(\mathbf{r})d\mathbf{r}$.

The completeness of the set $\{\phi_n(\mathbf{r})\}$ means that (Problem 1.2s)

$$\sum_n \phi_n(\mathbf{r})\phi_n^*(\mathbf{r}') = \delta(\mathbf{r} - \mathbf{r}') . \quad (1.4)$$

(For the definition and properties of Dirac's delta function, δ , see Appendix A.)

Note that n may stand for a set of indices that can take either discrete values (for the discrete part of the spectrum of L , if any) and/or continuous values (for the continuous part of the spectrum of L , if any). Similarly, the symbol \sum_n should be interpreted as $\sum_n' + \int dc$, where \sum_n' indicates a genuine summation over the eigenfunctions belonging to the discrete spectrum (if any) and $\int dc$ denotes (multiple) integration over the continuous spectrum (if any).³

Working with Green's functions is greatly facilitated by introducing an abstract vector space, a particular representation of which is the various functions we are dealing with. The most convenient way of achieving this is by using Dirac's bra and ket notation, according to which one can write (Appendix B):

$$\phi_n(\mathbf{r}) = \langle \mathbf{r} | \phi_n \rangle , \quad \phi_n^*(\mathbf{r}) = \langle \phi_n | \mathbf{r} \rangle , \quad \text{etc.} , \quad (1.5)$$

$$\delta(\mathbf{r} - \mathbf{r}') L(\mathbf{r}) \equiv \langle \mathbf{r} | L | \mathbf{r}' \rangle , \quad (1.6)$$

$$G(\mathbf{r}, \mathbf{r}'; z) \equiv \langle \mathbf{r} | G(z) | \mathbf{r}' \rangle , \quad (1.7)$$

$$\langle \mathbf{r} | \mathbf{r}' \rangle = \delta(\mathbf{r} - \mathbf{r}') , \quad (1.8)$$

$$\int d\mathbf{r} |\mathbf{r}\rangle \langle \mathbf{r}| = 1 , \quad (1.9)$$

where $|\mathbf{r}\rangle$ is the eigenvector of the position operator; in the new notation we can write (1.1) to (1.4) as follows:

$$(z - L)G(z) = 1 , \quad (1.1')$$

$$L|\phi_n\rangle = \lambda_n |\phi_n\rangle , \quad (1.2')$$

$$\langle \phi_n | \phi_m \rangle = \delta_{nm} , \quad (1.3')$$

$$\sum_n |\phi_n\rangle \langle \phi_n| = 1 . \quad (1.4')$$

The ordinary \mathbf{r} -representation is recaptured by using (1.5)–(1.9); e.g., taking the $\langle \mathbf{r} |, |\mathbf{r}' \rangle$ matrix element of (1.1') we have

$$\langle \mathbf{r} | (z - L)G(z) | \mathbf{r}' \rangle = \langle \mathbf{r} | 1 | \mathbf{r}' \rangle = \langle \mathbf{r} | \mathbf{r}' \rangle = \delta(\mathbf{r} - \mathbf{r}') .$$

³ The continuous spectrum and the integration $\int dc$ can be obtained by considering a finite domain Ω and taking the limit as Ω becomes infinite. For example, for plane waves, $\phi_{\mathbf{k}} = \frac{1}{\sqrt{\Omega}} \exp(i\mathbf{k} \cdot \mathbf{r})$, and in d -dimensional space,

$$\sum_{\mathbf{k}} \xrightarrow{\Omega \rightarrow \infty} \left[\frac{\Omega}{(2\pi)^d} \right] \int d\mathbf{k} . \quad (\text{For a proof see Problem 1.5s.})$$

The left-hand side (lhs) of the last relation can be written as follows:

$$zG(\mathbf{r}, \mathbf{r}'; z) - \langle \mathbf{r} | LG(z) | \mathbf{r}' \rangle .$$

By introducing the unit operator, $\int d\mathbf{r}'' |\mathbf{r}''\rangle \langle \mathbf{r}''|$, between L and G in the last expression we rewrite it in the form

$$zG(\mathbf{r}, \mathbf{r}'; z) - \int d\mathbf{r}'' \langle \mathbf{r} | L | \mathbf{r}'' \rangle \langle \mathbf{r}'' | G(z) | \mathbf{r}' \rangle .$$

Finally, taking into account (1.6) we obtain

$$zG(\mathbf{r}, \mathbf{r}'; z) - L(\mathbf{r})G(\mathbf{r}, \mathbf{r}'; z) = \delta(\mathbf{r} - \mathbf{r}') ,$$

which is identical to (1.1). The usefulness of the bra and ket notation is that

- (i) The intermediate algebraic manipulations are facilitated and
- (ii) One is not restricted to the \mathbf{r} -representation (e.g., one can express all equations in the \mathbf{k} -representation, which is equivalent to taking the Fourier transform with respect to \mathbf{r} and \mathbf{r}' of the original equations).

If all eigenvalues of $z - L$ are nonzero, i.e., if $z \neq \{\lambda_n\}$, then one can solve (1.1') formally as

$$G(z) = \frac{1}{z - L} . \quad (1.10)$$

Multiplying (1.10) by (1.4') we obtain

$$G(z) = \frac{1}{z - L} \sum_n |\phi_n\rangle \langle \phi_n| = \sum_n \frac{1}{z - L} |\phi_n\rangle \langle \phi_n| = \sum_n \frac{|\phi_n\rangle \langle \phi_n|}{z - \lambda_n} . \quad (1.11)$$

The last step follows from (1.2'), and the general relation $F(L) |\phi_n\rangle = F(\lambda_n) |\phi_n\rangle$ valid by definition for any well-behaved function F . Equation (1.11) can be written more explicitly as

$$G(z) = \sum_n' \frac{|\phi_n\rangle \langle \phi_n|}{z - \lambda_n} + \int dc \frac{|\phi_c\rangle \langle \phi_c|}{z - \lambda_c} , \quad (1.12)$$

or, in the \mathbf{r} -representation,

$$G(\mathbf{r}, \mathbf{r}'; z) = \sum_n' \frac{\phi_n(\mathbf{r})\phi_n^*(\mathbf{r}')}{z - \lambda_n} + \int dc \frac{\phi_c(\mathbf{r})\phi_c^*(\mathbf{r}')}{z - \lambda_c} . \quad (1.13)$$

Since L is a hermitian operator, all of its eigenvalues $\{\lambda_n\}$ are real. Hence, if $\text{Im}\{z\} \neq 0$, then $z \neq \{\lambda_n\}$, which means that $G(z)$ is an analytic function in the complex z -plane except at those points or portions of the real z -axis that correspond to the eigenvalues of L . As can be seen from (1.12) or (1.13), $G(z)$ exhibits simple poles at the position of the discrete eigenvalues of L ; the inverse is also true: *the poles of $G(z)$ give the discrete eigenvalues of L .*

$z = \lambda$, where λ belongs to the continuous spectrum of L , $G(\mathbf{r}, \mathbf{r}'; \lambda)$ is not well defined since the integrand in (1.13) has a pole. Then one can attempt to define $G(\mathbf{r}, \mathbf{r}'; \lambda)$ by a limiting procedure. In the usual case, where the eigenstates associated with the continuous spectrum are propagating or extended (i.e., not decaying as $r \rightarrow \infty$), the side limits of $G(\mathbf{r}, \mathbf{r}'; \lambda \pm is)$ as $s \rightarrow 0^+$ exist but are different from each other. Thus, this type of continuous spectrum produces a branch cut in $G(z)$ along part(s) of the real z -axis. We mention here in passing, and we shall return to the point in a later chapter, that in disordered systems there is the possibility of a continuous spectrum associated with localized eigenstates [i.e., states decaying fast enough as $r \rightarrow \infty$ so that the normalized $\{\phi_n(\mathbf{r})\}$ approach a nonzero limit as $\Omega \rightarrow \infty$]. For such an unusual spectrum even the side limits $\lim_{s \rightarrow 0^+} G(\mathbf{r}, \mathbf{r}'; \lambda \pm is)$ do not exist; the line of singularity corresponding to such a spectrum is not a branch cut but what is called a natural boundary. In what follows we restrict ourselves to the normal case of a continuous spectrum consisting of extended eigenstates. For λ belonging to such a spectrum we define two Green's functions as follows:

$$G^+(\mathbf{r}, \mathbf{r}'; \lambda) \equiv \lim_{s \rightarrow 0^+} G(\mathbf{r}, \mathbf{r}'; \lambda + is) , \quad (1.14)$$

$$G^-(\mathbf{r}, \mathbf{r}'; \lambda) \equiv \lim_{s \rightarrow 0^+} G(\mathbf{r}, \mathbf{r}'; \lambda - is) , \quad (1.15)$$

with similar definitions for the corresponding operators $G^+(\lambda)$, $G^-(\lambda)$. From (1.13) one can easily see that

$$G^*(\mathbf{r}, \mathbf{r}'; z) = G(\mathbf{r}', \mathbf{r}; z^*) . \quad (1.16)$$

If z is real, $z = \lambda$, and $\lambda \neq \{\lambda_n\}$, it follows from (1.16) that $G(\mathbf{r}, \mathbf{r}'; \lambda)$ is hermitian; in particular, $G(\mathbf{r}, \mathbf{r}; \lambda)$ is real. On the other hand, for λ belonging to the continuous spectrum, we have from (1.16) and definitions (1.14) and (1.15) that

$$G^-(\mathbf{r}, \mathbf{r}'; \lambda) = [G^+(\mathbf{r}', \mathbf{r}; \lambda)]^* , \quad (1.17)$$

which shows that

$$\text{Re} \{G^-(\mathbf{r}, \mathbf{r}; \lambda)\} = \text{Re} \{G^+(\mathbf{r}, \mathbf{r}; \lambda)\} \quad (1.18)$$

and

$$\text{Im} \{G^-(\mathbf{r}, \mathbf{r}; \lambda)\} = -\text{Im} \{G^+(\mathbf{r}, \mathbf{r}; \lambda)\} . \quad (1.19)$$

Using the identity (see the solution of Problem 1.3s)

$$\lim_{y \rightarrow 0^+} \frac{1}{x \pm iy} = \text{P} \frac{1}{x} \mp i\pi\delta(x) \quad (1.20)$$

and (1.13) we can express the discontinuity, $\tilde{G}(\lambda)$, in terms of delta function

$$\tilde{G}(\lambda) \equiv G^+(\lambda) - G^-(\lambda) = -2\pi i\delta(\lambda - L) , \quad (1.21)$$

or, in the \mathbf{r}, \mathbf{r}' representation,

$$\begin{aligned}\tilde{G}(\mathbf{r}, \mathbf{r}'; \lambda) &= -2\pi i \sum_n \delta(\lambda - \lambda_n) \phi_n(\mathbf{r}) \phi_n^*(\mathbf{r}') \\ &= -2\pi i \sum_n' \delta(\lambda - \lambda_n) \phi_n(\mathbf{r}) \phi_n^*(\mathbf{r}') \\ &\quad - 2\pi i \int \delta(\lambda - \lambda_c) \phi_c(\mathbf{r}) \phi_c^*(\mathbf{r}') dc .\end{aligned}\tag{1.22}$$

For the diagonal matrix element we obtain from (1.13) and (1.20)

$$G^\pm(\mathbf{r}, \mathbf{r}; \lambda) = P \sum_n \frac{\phi_n(\mathbf{r}) \phi_n^*(\mathbf{r})}{\lambda - \lambda_n} \mp i\pi \sum_n \delta(\lambda - \lambda_n) \phi_n(\mathbf{r}) \phi_n^*(\mathbf{r}) .\tag{1.23}$$

Integrating (1.23) over \mathbf{r} we have

$$\begin{aligned}\int d\mathbf{r} G^\pm(\mathbf{r}, \mathbf{r}; \lambda) &= \int d\mathbf{r} \langle \mathbf{r} | G^\pm(\lambda) | \mathbf{r} \rangle \equiv \text{Tr} \{G^\pm(\lambda)\} \\ &= P \sum_n \frac{1}{\lambda - \lambda_n} \mp i\pi \sum_n \delta(\lambda - \lambda_n) .\end{aligned}\tag{1.24}$$

The quantity $\sum_n \delta(\lambda - \lambda_n)$ is the density of states (DOS) at λ , $\mathcal{N}(\lambda)$; $\mathcal{N}(\lambda)d\lambda$ gives the number of states in the interval $[\lambda, \lambda + d\lambda]$. The quantity

$$\begin{aligned}\varrho(\mathbf{r}; \lambda) &\equiv \sum_n \delta(\lambda - \lambda_n) \phi_n(\mathbf{r}) \phi_n^*(\mathbf{r}) \\ &= \sum_n' \delta(\lambda - \lambda_n) \phi_n(\mathbf{r}) \phi_n^*(\mathbf{r}) + \int \delta(\lambda - \lambda_c) \phi_c(\mathbf{r}) \phi_c^*(\mathbf{r}) dc\end{aligned}\tag{1.25}$$

is the DOS per unit volume at point \mathbf{r} . Obviously,

$$\mathcal{N}(\lambda) = \int \varrho(\mathbf{r}; \lambda) d\mathbf{r} .\tag{1.26}$$

Using (1.22)–(1.25) we obtain

$$\varrho(\mathbf{r}; \lambda) = \mp \frac{1}{\pi} \text{Im} \{G^\pm(\mathbf{r}, \mathbf{r}; \lambda)\} = -\frac{1}{2\pi i} \tilde{G}(\mathbf{r}, \mathbf{r}; \lambda) ,\tag{1.27}$$

and

$$\mathcal{N}(\lambda) = \mp \frac{1}{\pi} \text{Im} \{\text{Tr} G^\pm(\lambda)\} .\tag{1.28}$$

$G(z)$ can be expressed in terms of the discontinuity $\tilde{G}(\lambda) \equiv G^+(\lambda) - G^-(\lambda)$:

$$\begin{aligned}G(\mathbf{r}, \mathbf{r}'; z) &= \sum_n \frac{\phi_n(\mathbf{r}) \phi_n^*(\mathbf{r}')}{z - \lambda_n} = \int_{-\infty}^{\infty} d\lambda \sum_n \delta(\lambda - \lambda_n) \frac{\phi_n(\mathbf{r}) \phi_n^*(\mathbf{r}')}{z - \lambda} \\ &= \frac{i}{2\pi} \int_{-\infty}^{\infty} d\lambda \frac{\tilde{G}(\mathbf{r}, \mathbf{r}'; \lambda)}{z - \lambda} ,\end{aligned}\tag{1.29}$$

where (1.22) was taken into account. In particular, for the diagonal matrix elements of G we have

$$G(\mathbf{r}, \mathbf{r}; z) = \int_{-\infty}^{\infty} d\lambda' \frac{\varrho(\mathbf{r}; \lambda')}{z - \lambda'} . \quad (1.30)$$

Note that $\varrho(\mathbf{r}; \lambda')$ versus λ' may consist of a sum of δ functions (corresponding to the discrete spectrum of L) and a continuous function (corresponding to the continuous spectrum of L) as shown in (1.25). Equation (1.30) shows that the DOS per unit volume [i.e., the imaginary part of $\mp G^{\pm}(\mathbf{r}, \mathbf{r}; \lambda')/\pi$] enables us to calculate $G(\mathbf{r}, \mathbf{r}; z)$ (both $\text{Re}\{G\}$ and $\text{Im}\{G\}$) for all values of $z = \lambda + is$.

Consider the expression

$$\mathbf{E}(z) \equiv E_x(x, y) - iE_y(x, y) = \int_C dz' \frac{2\varrho(z')}{z - z'} , \quad (1.30')$$

giving the x and y component of the electric field $\mathbf{E}(x, y)$ in two-dimensional (2-d) space in terms of the charge density $\varrho(z') \equiv \varrho(x', y')$ along line C . Comparing with (1.30) we see that $G(\mathbf{r}, \mathbf{r}; z)$ can be thought of as the electric field generated by a positive charge distribution on the x -axis given by one half the DOS per unit volume, $\varrho/2$. More explicitly, the correspondence is

$$\begin{aligned} \text{Re}\{G(\mathbf{r}, \mathbf{r}; z)\} &\leftrightarrow E_x(z) , \\ \text{Im}\{G(\mathbf{r}, \mathbf{r}; z)\} &\leftrightarrow -E_y(z) ; \\ \varrho(\mathbf{r}; \lambda) &\leftrightarrow 2\varrho(z') , \\ z \equiv \lambda + is &\leftrightarrow z = x + iy , \\ \lambda' &\leftrightarrow z' = x' + iy' . \end{aligned}$$

This analogy is often helpful in visualizing the z dependence of $G(\mathbf{r}, \mathbf{r}; z)$ for complex values of z . For example, we see immediately that

$$\text{Re}\{G^+(\mathbf{r}, \mathbf{r}; \lambda)\} = \text{Re}\{G^-(\mathbf{r}, \mathbf{r}; \lambda)\}$$

while

$$\text{Im}\{G^+(\mathbf{r}, \mathbf{r}; \lambda)\} = -\text{Im}\{G^-(\mathbf{r}, \mathbf{r}; \lambda)\} ,$$

with $\text{Im}\{G^+(\mathbf{r}, \mathbf{r}; \lambda)\}$ being always negative or zero. Of course, when λ is not an eigenvalue of L , $G^+(\mathbf{r}, \mathbf{r}; \lambda)$ is real; it satisfies the relation

$$\frac{dG(\mathbf{r}, \mathbf{r}; \lambda)}{d\lambda} = -\langle \mathbf{r} | (\lambda - L)^{-2} | \mathbf{r} \rangle < 0 . \quad (1.31)$$

To prove (1.31) we write

$$\frac{dG(\mathbf{r}, \mathbf{r}; \lambda)}{d\lambda} = \frac{d[\langle \mathbf{r} | (\lambda - L)^{-1} | \mathbf{r} \rangle]}{d\lambda} = -\langle \mathbf{r} | (\lambda - L)^{-2} | \mathbf{r} \rangle ,$$

which is negative since, for λ real and not coinciding with any eigenvalue of L , $(\lambda - L)^{-2}$ is a positive definite operator.

To summarize our findings: $G(\mathbf{r}, \mathbf{r}'; z)$ is analytic on the complex z -plane except on portions or points of the real axis. The positions of the poles of $G(\mathbf{r}, \mathbf{r}'; \lambda)$ on the real axis give the discrete eigenvalues of L . The residue at each pole gives the product $\phi_n(\mathbf{r})\phi_n^*(\mathbf{r}')$ if the corresponding nondegenerate eigenfunction is $\phi_n(\mathbf{r})$. Otherwise it gives the sum $\sum_m \phi_m(\mathbf{r})\phi_m^*(\mathbf{r}')$, where m runs over all eigenstates corresponding to the eigenvalue λ_n . The branch cuts of $G(\mathbf{r}, \mathbf{r}'; \lambda)$ along the real λ -axis correspond to the continuous spectrum of L , and the discontinuity of the diagonal matrix element $G(\mathbf{r}, \mathbf{r}; \lambda)$ across the branch cut gives the DOS per unit volume times -2π . Note that the analytic continuation of $G(\mathbf{r}, \mathbf{r}'; z)$ across the branch cut does not coincide with $G(\mathbf{r}, \mathbf{r}'; z)$, and it may develop singularities in the complex z -plane.

Knowledge of the Green's function $G(\mathbf{r}, \mathbf{r}'; z)$ permits us to obtain immediately the solution of the general inhomogeneous equation

$$[z - L(\mathbf{r})] u(\mathbf{r}) = f(\mathbf{r}), \quad (1.32)$$

where the unknown function $u(\mathbf{r})$ satisfies on S the same BCs as $G(\mathbf{r}, \mathbf{r}'; z)$; $f(\mathbf{r})$ is a given function. By taking into account (1.1), it is easy to show that the solution of (1.32) is

$$u(\mathbf{r}) = \begin{cases} \int G(\mathbf{r}, \mathbf{r}'; z) f(\mathbf{r}') d\mathbf{r}', & z \neq \{\lambda_n\}, \quad (1.33a) \\ \int G^\pm(\mathbf{r}, \mathbf{r}'; \lambda) f(\mathbf{r}') d\mathbf{r}' + \phi(\mathbf{r}), & z = \lambda, \quad (1.33b) \end{cases}$$

where in (1.33b) λ belongs to the branch cut of $G(z)$ (i.e., λ belongs to the continuous spectrum of L) and $\phi(\mathbf{r})$ is the general solution of the corresponding homogeneous equation. If z coincides with a discrete eigenvalue of L , say, λ_n , there is no solution of (1.32) unless $f(\mathbf{r})$ is orthogonal to all eigenfunctions associated with λ_n (Problem 1.4). If $u(\mathbf{r})$ describes physically the response of a system to a source $f(\mathbf{r})$, then $G(\mathbf{r}, \mathbf{r}')$ describes the response of the same system to a unit point source located at \mathbf{r}' . Note that the symmetry relation (1.16) is a generalized reciprocity relation: the response at \mathbf{r} from a source at \mathbf{r}' is essentially the same as the response at \mathbf{r}' from a source at \mathbf{r} . Equation (1.33a) means that the response to the general source $f(\mathbf{r})$ can be expressed as the sum of the responses to point sources distributed according to $f(\mathbf{r})$.

1.2 Examples

In this section we consider the case where $L(\mathbf{r}) = -\nabla^2$ and the domain Ω extends eventually over the whole real space. The BC is that the eigenfunctions of L must be finite at infinity. Then the eigenfunctions are

$$\langle \mathbf{r} | \mathbf{k} \rangle = \frac{1}{\sqrt{\Omega}} e^{i\mathbf{k} \cdot \mathbf{r}}, \quad (1.34)$$

and the eigenvalues are

$$\lambda_n = \mathbf{k}^2, \quad (1.35)$$

where the components of the vector \mathbf{k} are real to satisfy the BCs. Thus, the spectrum is continuous, extending from 0 to $+\infty$. The Green's function can be obtained by either solving the defining equation, which in the present case is

$$(z + \nabla_r^2) G(\mathbf{r}, \mathbf{r}'; z) = \delta(\mathbf{r} - \mathbf{r}'), \quad (1.36)$$

or from (1.13), which in the present case can be written as

$$G(\mathbf{r}, \mathbf{r}'; z) = \sum_{\mathbf{k}} \frac{\langle \mathbf{r} | \mathbf{k} \rangle \langle \mathbf{k} | \mathbf{r}' \rangle}{z - k^2} = \int \frac{d\mathbf{k}}{(2\pi)^d} \frac{e^{i\mathbf{k} \cdot (\mathbf{r} - \mathbf{r}')}}{z - k^2}, \quad (1.37)$$

where d is the dimensionality.⁴ For $d = 3$ we will use (1.37) to evaluate G , while for $d = 2$ or 1 we will compute G from (1.36).

1.2.1 Three-Dimensional Case ($d = 3$)

If ϱ is the difference $\mathbf{r} - \mathbf{r}'$ and θ the angle between \mathbf{k} and ϱ , we can write (1.37) as

$$\begin{aligned} G(\mathbf{r}, \mathbf{r}'; z) &= \frac{1}{4\pi^2} \int_0^\infty \frac{k^2 dk}{z - k^2} \int_0^\pi d\theta \sin \theta e^{ik\varrho \cos \theta} \\ &= \frac{1}{4\pi^2} \int_0^\infty \frac{k^2 dk}{z - k^2} \frac{e^{ik\varrho} - e^{-ik\varrho}}{ik\varrho} \\ &= \frac{1}{4i\pi^2\varrho} \int_{-\infty}^\infty \frac{ke^{ik\varrho}}{z - k^2} dk. \end{aligned} \quad (1.38)$$

The integration path can be closed by an infinite semicircle in the upper half plane. Unless z is real and nonnegative, one of the poles (denoted by \sqrt{z}) of the integrand in (1.38) has a positive imaginary part and hence lies within the integration contour, and the other (denoted by $-\sqrt{z}$) has a negative imaginary part and lies outside the integration contour. By employing the residue theorem we obtain from (1.38)

$$G(\mathbf{r}, \mathbf{r}'; z) = -\frac{\exp(i\sqrt{z}|\mathbf{r} - \mathbf{r}'|)}{4\pi|\mathbf{r} - \mathbf{r}'|}; \quad \text{Im}\{z\} > 0. \quad (1.39)$$

If $z = \lambda$, where $\lambda \geq 0$ (i.e., if z coincides with the eigenvalues of $-\nabla^2$), the two poles lie on the integration contour and G is not well defined. The side limits $G^\pm(\mathbf{r}, \mathbf{r}'; \lambda)$ are well defined and are given by

⁴ Use was made of the relation $\sum_{\mathbf{k}} \rightarrow [\Omega/(2\pi)^d] \int d\mathbf{k}$ as $\Omega \rightarrow \infty$. For a proof and comments see Problem 1.5s.

$$G^{\pm}(\mathbf{r}, \mathbf{r}'; \lambda) = -\frac{e^{\pm i\sqrt{\lambda}|\mathbf{r}-\mathbf{r}'|}}{4\pi|\mathbf{r}-\mathbf{r}'|}; \quad \sqrt{\lambda}, \lambda \geq 0. \quad (1.40)$$

For $z = \lambda$, where $\lambda < 0$, we obtain from (1.39)

$$G(\mathbf{r}, \mathbf{r}'; \lambda) = -\frac{e^{-\sqrt{|\lambda}|\mathbf{r}-\mathbf{r}'|}}{4\pi|\mathbf{r}-\mathbf{r}'|}; \quad \lambda < 0, \quad \sqrt{|\lambda|} > 0. \quad (1.41)$$

For the particular case $z = 0$ we have

$$G(\mathbf{r}, \mathbf{r}'; 0) = -\frac{1}{4\pi|\mathbf{r}-\mathbf{r}'|}. \quad (1.42)$$

As can be seen from (1.36), $G(\mathbf{r}, \mathbf{r}'; 0)$ is the Green's function corresponding to a Laplace equation with a point source, i.e.,

$$\nabla_r^2 G(\mathbf{r}, \mathbf{r}'; 0) = \delta(\mathbf{r} - \mathbf{r}') . \quad (1.43)$$

By employing (1.33b) we can write the general solution of Poisson's equation

$$\nabla^2 V(\mathbf{r}) = -4\pi\varrho(\mathbf{r})$$

as

$$\begin{aligned} V(\mathbf{r}) &= \int G(\mathbf{r}, \mathbf{r}'; 0)(-4\pi)\varrho(\mathbf{r}') d\mathbf{r}' + \text{const.} \\ &= \int \frac{\varrho(\mathbf{r}') d\mathbf{r}'}{|\mathbf{r}-\mathbf{r}'|} + \text{const.} \end{aligned} \quad (1.44)$$

The constant has been added since the most general eigenfunction of $-\nabla^2$ corresponding to eigenvalue 0 is a constant, as can be seen from (1.34) and (1.35). Equation (1.44) is the basic result in electrostatics.

1.2.2 Two-Dimensional Case ($d = 2$)

Because of symmetry considerations, $G(\mathbf{r}, \mathbf{r}'; z)$ is a function of the magnitude of the 2-d vector $\boldsymbol{\varrho} = \mathbf{r} - \mathbf{r}'$ and z . Furthermore, it satisfies the homogeneous equation

$$(z + \nabla^2)G(\varrho; z) = 0 \quad \text{for } \varrho \neq 0. \quad (1.45)$$

The δ function source can be transformed into an equivalent BC as $\varrho \rightarrow 0$; indeed, by applying Gauss' theorem, $\int \nabla \cdot (\nabla G) d\Omega = \int \nabla G \cdot d\mathbf{S}$, which in the present 2-d case takes the form

$$\int_0^{\varrho} \nabla^2 G 2\pi\varrho' d\varrho' = 2\pi\varrho \frac{\partial G}{\partial \varrho},$$

we obtain from (1.36)

$$2\pi\varrho \frac{\partial G}{\partial \varrho} + 2\pi z \int_0^\varrho G \varrho' d\varrho' = 1 ,$$

which, as $\varrho \rightarrow 0$, leads to

$$G(\varrho) \xrightarrow{\varrho \rightarrow 0} \frac{1}{2\pi} \ln \varrho + \text{const.} \quad (1.46)$$

Furthermore, $G(\varrho)$ must satisfy the condition

$$G(\varrho) \xrightarrow{\varrho \rightarrow \infty} 0 . \quad (1.47)$$

The only solution of (1.45) that is symmetric and satisfies BCs (1.46) and (1.47) is

$$G(\mathbf{r}, \mathbf{r}'; z) = -\frac{i}{4} H_0^{(1)}(\sqrt{z} |\mathbf{r} - \mathbf{r}'|) ; \quad \text{Im} \{\sqrt{z}\} > 0 , \quad (1.48)$$

where $H_0^{(1)}$ is the Hankel function of zero order of the first kind.⁵ This can be seen from the fact that the general solution of (1.45) is a superposition of terms like $[A_n H_n^{(1)}(\sqrt{z}\varrho) + B_n H_n^{(2)}(\sqrt{z}\varrho)] e^{\pm in\theta}$ (Appendix C). Since we are looking for a θ -independent solution, $n = 0$; furthermore, the Hankel function $H_0^{(2)}(\sqrt{z}\varrho)$, for $\text{Im} \{\sqrt{z}\} > 0$, blows up as $\varrho \rightarrow \infty$ and must be excluded. Finally, (1.46) together with the relation $H_0^{(1)}(\sqrt{z}\varrho) \rightarrow (2i/\pi) \ln(\varrho)$ as $\varrho \rightarrow 0$ fixes the coefficient A_0 . For $z = \lambda$, where $\lambda \geq 0$, (i.e., for z coinciding with the spectrum of $-\nabla^2$) $\text{Im} \{\sqrt{z}\} = 0$, and only the side limits are well defined as

$$G^\pm(\mathbf{r}, \mathbf{r}'; \lambda) = -\frac{i}{4} H_0^{(1)}(\pm\sqrt{\lambda}\varrho) ; \quad \sqrt{\lambda} > 0 , \quad (1.49)$$

where⁵

$$H_0^{(1)}(-\sqrt{\lambda}\varrho) = -H_0^{(2)}(\sqrt{\lambda}\varrho) . \quad (1.50)$$

G^+ describes an outgoing wave, while G^- is an ingoing wave; this can be seen from the asymptotic form of $H_0^{(1)}$ and $H_0^{(2)}$.

Equation (1.48) for the particular case $z = -|\lambda|$ can be recast as

$$G^\pm(\mathbf{r}, \mathbf{r}'; -|\lambda|) = -\frac{1}{2\pi} K_0(\sqrt{|\lambda|} |\mathbf{r} - \mathbf{r}'|) ; \quad \sqrt{|\lambda|} > 0 , \quad (1.51)$$

where K_0 is the modified Bessel function of zero order.⁵

The Green's function corresponding to the 2-d Laplace equation can be obtained from (1.48) by letting $z \rightarrow 0$ and keeping the leading $|\mathbf{r} - \mathbf{r}'|$ -dependent term. We find that

⁵ For definitions and properties of Bessel and Hankel functions see the book by Abramowitz and Stegun [1].

$$G(\mathbf{r}, \mathbf{r}'; 0) = \frac{1}{2\pi} \ln |\mathbf{r} - \mathbf{r}'| + \text{const.} \quad (1.52)$$

The solution of Poisson's equation in 2-d is then

$$V(\mathbf{r}) = -2 \int \varrho(\mathbf{r}') \ln |\mathbf{r} - \mathbf{r}'| d\mathbf{r}' + \text{const.} \quad (1.53)$$

Taking the $-\nabla$ of (1.53) we obtain the expression for the 2-d electric field given before in (1.30').

1.2.3 One-Dimensional Case ($d = 1$)

The basic equation (1.36) becomes

$$\left(z + \frac{d^2}{dx^2} \right) G(x, x'; z) = \delta(x - x') . \quad (1.54)$$

For $x < x'$ we have $G = A \exp(-i\sqrt{z}x)$ with $\text{Im}\{\sqrt{z}\} > 0$, while for $x > x'$ we obtain $G = B \exp(i\sqrt{z}x)$; the choice of signs in the exponents ensures that $G \rightarrow 0$ as $|x| \rightarrow \infty$. By integrating (1.54) we find that $G(x'^-, x'; 0) = G(x'^+, x'; z)$ and $(dG/dx)_{x=x'^+} - (dG/dx)_{x=x'^-} = 1$. We thus determine the constants A and B . We obtain finally

$$G(x, x'; z) = \frac{\exp(i\sqrt{z}|x - x'|)}{2i\sqrt{z}} ; \quad \text{Im}\{\sqrt{z}\} > 0 . \quad (1.55)$$

For $z = \lambda \geq 0$ (i.e., within the continuous spectrum of $-d^2/dx^2$) we have for the side limits

$$G^\pm(x, x'; \lambda) = \mp \frac{i}{2\sqrt{\lambda}} \exp(\pm i\sqrt{\lambda}|x - x'|) ; \quad \lambda > 0, \sqrt{\lambda} > 0 . \quad (1.56)$$

For $z = -|\lambda|$ we obtain from (1.55)

$$G(x, x'; -|\lambda|) = -\frac{1}{2\sqrt{|\lambda|}} \exp(-\sqrt{|\lambda|}|x - x'|) ; \quad \sqrt{|\lambda|} > 0 . \quad (1.57)$$

The Green's function for the 1-d Laplace equation can be found either by solving (1.54) for $z = 0$ directly or by taking the limit of $(G^+ + G^-)/2$ as $\lambda \rightarrow 0$. We find

$$G(x, x'; 0) = \frac{1}{2} |x - x'| + \text{const.} \quad (1.58)$$

1.2.4 Finite Domain Ω

The problem of determination of G becomes more tedious when the surface S bounding our domain Ω consists in part (or in whole) of pieces at a finite distance from the point \mathbf{r}' of the source. One can then employ any of the following methods to determine G :

1. Use general equation (1.13) where the eigenvalues and eigenfunctions are the ones associated with the BCs on S .
2. Write G as $G = G^\infty + \phi$, where G^∞ is the Green's function associated with the infinite domain (which is assumed to be known) and ϕ is the general solution of the corresponding homogeneous equation. Then determine the arbitrary coefficients in ϕ by requiring that $G^\infty + \phi$ satisfy the given BCs on S . It is then clear that G satisfies both the differential equation and the BCs.
3. Divide the domain Ω into two subdomains by a surface S' passing through the source point \mathbf{r}' . Then G in the interior of each subdomain satisfies a homogeneous equation. Find in each subdomain the general solution of the homogeneous equation subject to the given BCs on S . Next, match the two solutions on S' in a way obtained by integrating the differential equation for G around \mathbf{r}' . An elementary example of this technique was used in Sect. 1.2.3.
4. Write, e.g., in 3-d,

$$\begin{aligned} \delta(\mathbf{r} - \mathbf{r}') &= \frac{1}{r^2} \delta(r - r') \delta(\phi - \phi') \delta(\cos\theta - \cos\theta') \\ &= \frac{1}{r^2} \delta(r - r') \sum_{\ell m} Y_{\ell m}(\theta, \phi) Y_{\ell m}^*(\theta', \phi') \end{aligned}$$

so as to reduce the problem to 1-d with respect to r and r' .

The interested reader may find a brief presentation of these techniques in the book by Mathews and Walker [2]. A more comprehensive and rigorous presentation is given in the second volume of the book by Byron and Fuller [3]; see also the books by Duffy [4], Barton [5], Roach [6], Stakgold [7] and Morse and Feshbach [8]. Several books on electromagnetism, such as those by Smythe [9] or Jackson [10], contain several interesting examples of Green's functions.

Finally, it should be mentioned that for more complicated operators L (such as those describing the quantum-mechanical motion of a particle in an external field), the determination of G is a very complicated problem. More often than not one has to employ approximate techniques such as perturbation expansions. We will return to this very interesting subject in Chap. 4. Examples of methods (1) to (4) mentioned above are presented in the solutions of the problems in Chap. 1 (see also Appendix C).

1.3 Summary

1.3.1 Definition

The Green's function, corresponding to the linear, hermitian, time-independent differential operator $L(\mathbf{r})$ and the complex variable $z = \lambda + is$, is defined

as the solution of the equation⁶

$$[z - L(\mathbf{r})]G(\mathbf{r}, \mathbf{r}'; z) = \delta(\mathbf{r} - \mathbf{r}') , \quad (1.1)$$

subject to certain homogeneous BCs on the surface S of the domain Ω of \mathbf{r} and \mathbf{r}' . Equation (1.1) can be considered as the \mathbf{r} -representation of the operator equation

$$(z - L)G = 1 . \quad (1.1')$$

1.3.2 Basic Properties

1. If $\{|\phi_n\rangle\}$ is the complete orthonormal set of eigenfunctions (subject to the same BCs on the surface S) of L , and $\{\lambda_n\}$ is the set of the corresponding eigenvalues, then one can write

$$G = (z - L)^{-1} \quad (1.10)$$

$$= \sum_n \frac{|\phi_n\rangle \langle \phi_n|}{z - \lambda_n}, \quad z \neq \{\lambda_n\} . \quad (1.11)$$

2. From (1.11) one can see that $G(z)$ is uniquely defined if and only if $z \neq \{\lambda_n\}$. If z coincides with any of the discrete eigenvalues of L , G does not exist, since, as can be seen from (1.11), $G(z)$ has simple (first-order) poles at the positions of the discrete eigenvalues. If z belongs to the continuous spectrum of L , then G usually exists, but it is not uniquely defined because one can add to any particular G the general solution of the homogeneous equation corresponding to (1.1). Two particular explicit expressions, G^+ and G^- , are usually employed in the case where the continuous spectrum of L corresponds to a branch cut. For infinite disordered systems, part of the continuous spectrum may give rise to the so-called natural boundary, i.e., a singular line to be examined in a later chapter. The analytic behavior of $G(z)$ is summarized in Fig. 1.1, p. 16. Because L is hermitian, all its eigenvalues are real; hence, the singularities of $G(z)$ are on the real z -axis. As was mentioned above, for the branch cuts of $G(z)$ (which correspond to the continuous spectrum associated with extended eigenstates) we define the side limits

$$G^\pm(\lambda) = \lim_{s \rightarrow 0^+} G(\lambda \pm is) . \quad (1.15')$$

1.3.3 Methods of Calculation

$G(z)$ is calculated either by solving the defining equation (1.1) or by using (1.11).

⁶ The numbering of the equations appearing in each summary is that of the main text of the corresponding chapter.

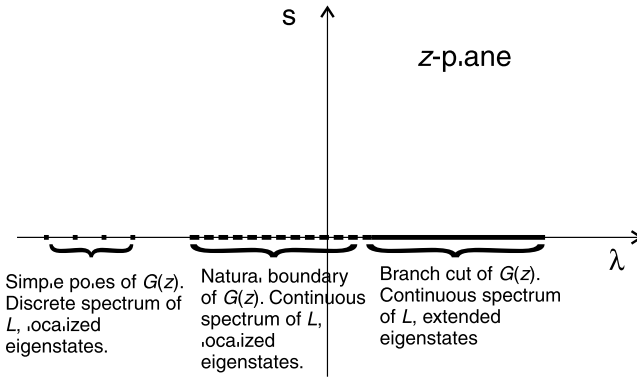


Fig. 1.1. Analytic behavior of $G(z) \equiv (z - L)^{-1}$. The singular *points* or *lines* are on the real z -axis (when L is Hermitian) and provide information about the eigenvalues and eigenfunctions of L

1.3.4 Use

Once $G(z)$ is known one can:

1. Obtain information about the homogeneous equation corresponding to (1.1), i.e., about the eigenvalues and eigenfunctions of L . Thus the position of the poles of $G(z)$ give the discrete eigenvalues of L , and the residues at these poles provide information about the corresponding eigenfunctions. The branch cuts (or the natural boundaries, if any) give the location of the continuous spectrum, and the discontinuity across the branch cut gives the density of states $\mathcal{N}(\lambda)$

$$\mathcal{N}(\lambda) = \mp \frac{1}{\pi} \text{Im} \{ \text{Tr} \{ G^\pm(\lambda) \} \} . \tag{1.28}$$

2. Solve the inhomogeneous equation

$$[z - L(\mathbf{r})] u(\mathbf{r}) = f(\mathbf{r}) , \tag{1.32}$$

where the unknown function $u(\mathbf{r})$ satisfies on S the same BCs as $G(\mathbf{r}, \mathbf{r}'; z)$, and $f(\mathbf{r})$ is given. We have

$$u(\mathbf{r}) = \begin{cases} \int G(\mathbf{r}, \mathbf{r}'; z) f(\mathbf{r}') d\mathbf{r}' ; & z \neq \{\lambda_n\} , \tag{1.33a} \\ \int G^\pm(\mathbf{r}, \mathbf{r}'; \lambda) f(\mathbf{r}') d\mathbf{r}' + \phi(\mathbf{r}) ; & z = \lambda , \tag{1.33b} \end{cases}$$

where λ in (1.33b) belongs to the branch cut of $G(z)$ and $\phi(\mathbf{r})$ is the general solution of the corresponding homogeneous equation for the given value of λ . For z coinciding with any of the discrete eigenvalues of L , say, λ_n , there is no solution of (1.32) unless $f(\mathbf{r})$ is orthogonal to all eigenfunctions associated with λ_n .

3. Use $G_0(z)$ and L_1 to obtain information about the eigenfunctions and eigenvalues of $L = L_0 + L_1$; $G_0(z) \equiv (z - L_0)^{-1}$. Discussion of this third use of the Green's function formalism will be given in Chap. 4.

Some very common applications of the formalism outlined above were discussed in Sect. 1.2.

Further Reading

- A short and clear introduction to Green's functions is given in the book by Mathews and Walker [2], pp. 267–277.
- A more extensive introduction with several examples is given in the book by Byron and Fuller [3], pp. 395–441.
- In the book by Duffy [4] there is a more systematic development of the subject with many examples on how to construct Green's functions for different operators and more complicated boundaries.
- A more mathematically oriented approach is presented in the book by Stakgold [7].
- Interesting examples referring to more complicated boundaries can be found in the book by Smythe [9], pp. 155–158, pp. 177–180, pp. 189–191.
- For an extensive list of integrals and other mathematical data, see the book by Gradshteyn and Ryzhik [11].

Problems⁷

1.1s. Prove that two eigenfunctions belonging to different eigenvalues of a hermitian operator are orthogonal. Then prove (1.3).

1.2s. Prove (1.4).

1.3s. Prove (1.20).

1.4. Show that inhomogeneous equation (1.32) has no solution if z coincides with a discrete eigenvalue of L unless $f(\mathbf{r})$ is orthogonal to all eigenfunctions associated with this eigenvalue.

Hint: Expand both $u(\mathbf{r})$ and $f(\mathbf{r})$ in terms of the orthonormal complete set of the eigenfunctions of L :

$$u = \sum_{i=1}^s b_{ni} \phi_{ni} + \sum_{m \neq ni} b_m \phi_m, \quad (1)$$

$$f = \sum_{i=1}^s c_{ni} \phi_{ni} + \sum_{m \neq ni} c_m \phi_m, \quad (2)$$

⁷ Problem numbering followed by a letter "s" indicates that this problem is solved in the last part of the book.

where ϕ_{ni} ($i = 1, \dots, s$) belong to the eigenvalue λ_n for which $z = \lambda_n$

$$L\phi_{ni} = \lambda_n\phi_{ni}, \quad i = 1, \dots, s, \quad (3)$$

$$L\phi_m = \lambda_m\phi_m, \quad \lambda_m \neq \lambda_n. \quad (4)$$

Replace (1) and (2) in (1.32), use the orthonormality of the set $\{\phi_{ni}, \phi_m\}$, and then take $z = \lambda_n$.

1.5s. Show that $d\mathbf{r}d\mathbf{p}/h^d$ gives the number of states associated with the volume element $d\mathbf{r}d\mathbf{p}$ of the phase space for a free particle moving in a d -dimensional real space; \mathbf{p} is the particle's momentum.

1.6s. Calculate the 1-d Green's function $G(x, x'; z)$ for the operator $L = -d^2/dx^2$ defined in the domain $(0, 1)$, with BCs $G(x, x'; z) = 0$ for either x or $x' = 0, 1$. Employ all methods of calculations mentioned on p. 14. What is the $z \rightarrow 0$ limit of G ? Use your results to calculate the sum $\sum_{n=0}^{\infty} [a^2 + n^2]^{-1}$.

1.7s. Calculate the Green's function $G(\varrho, \varrho'; z)$ for the 2-d operator $L \equiv -\nabla_{\varrho}^2$ and the BCs $G(\varrho, \varrho'; z) = 0$ for $\varrho, \varrho' = a$ ($0 \leq \varrho, \varrho' \leq a$). Employ all methods of calculation. Find the limit $z = 0$. What is the application in electrostatics?

1.8s. Calculate the Green's function $G(\mathbf{r}, \mathbf{r}'; z)$ for the 3-d operator $L = -\nabla_r^2$ and the BCs $G(\mathbf{r}, \mathbf{r}'; z) = 0$ for $|\mathbf{r}|, |\mathbf{r}'| = a$ ($0 \leq r, r' \leq a$). Employ two different methods of calculation. Find the limit $z = 0$. What is the application in electrostatics?

1.9s. Calculate the diagonal matrix element of the Green's function given the density of states (DOS)

$$\varrho(E) = \frac{1}{\pi\sqrt{4V^2 - E^2}}, \quad |E| \leq 2|V|.$$

1.10. The same as Problem 1.9s but for

$$\varrho(E) = \frac{2\sqrt{(6V)^2 - E^2}}{\pi(6V)^2}.$$

1.11s. Consider the operator

$$L \equiv \nabla_r (f(\mathbf{r})\nabla_r) + g(\mathbf{r}),$$

where $f(\mathbf{r})$ and $g(\mathbf{r})$ are known well-behaved functions of \mathbf{r} . Consider also the differential equation for the unknown function $\psi(\mathbf{r})$

$$L\psi(\mathbf{r}) = u(\mathbf{r}),$$

where $u(\mathbf{r})$ is a known well-behaved function; the unknown function $\psi(\mathbf{r})$ satisfies the BC $\psi(\mathbf{r}_s) = u_1(\mathbf{r}_s)$ or $\nabla\psi(\mathbf{r})_{\mathbf{r}=\mathbf{r}_s} = \mathbf{u}_2(\mathbf{r}_s)$ for \mathbf{r}_s on the closed surface S bounding the domain Ω ; $u_1(\mathbf{r}_s)$ and $\mathbf{u}_2(\mathbf{r}_s)$ are known functions. If the Green's function $G(\mathbf{r}, \boldsymbol{\rho}; z)$ is defined by the equation

$$LG(\mathbf{r}, \boldsymbol{\rho}; z) = \delta(\mathbf{r} - \boldsymbol{\rho})$$

and appropriate BC for $\mathbf{r} = \mathbf{r}_s$, show that $\psi(\boldsymbol{\rho})$ can be obtained by the relation

$$\begin{aligned} \psi(\boldsymbol{\rho}) &= \int_{\Omega} d\mathbf{r} G(\mathbf{r}, \boldsymbol{\rho}) u(\mathbf{r}) \\ &+ \int_S d\mathbf{r}_s [\psi(\mathbf{r}_s) \nabla_r G(\mathbf{r}_s, \boldsymbol{\rho}) - G(\mathbf{r}_s, \boldsymbol{\rho}) \nabla_r \psi(\mathbf{r}_s)] f(\mathbf{r}_s) . \end{aligned}$$

If the BC for $\psi(\mathbf{r})$ is $\psi(\mathbf{r}_s) = u_1(\mathbf{r}_s)$, then the appropriate BC for G is $G = 0$ for $\mathbf{r} = \mathbf{r}_s$; if the BC for $\psi(\mathbf{r})$ is $\nabla_r \psi(\mathbf{r}_s) = \mathbf{u}_2(\mathbf{r}_s)$, then we must choose $\nabla G = 0$ for $\mathbf{r} = \mathbf{r}_s$.

Examine the special case $f(\mathbf{r}) = 1$ and $g(\mathbf{r}) = z$.

1.12. If the operator L is not hermitian, we define its adjoint operator, L^\dagger , by the relation

$$[\langle u |, L |v \rangle]^* = \langle v |, L^\dagger |u \rangle$$

for arbitrary bra and ket.

Show that:

- (a) If $|\phi_n\rangle$ and λ_n are the eigenvectors and eigenvalues of L , then the eigenvalues of L^\dagger are λ_n^* :

$$L^\dagger |\psi_n\rangle = \lambda_n^* |\psi_n\rangle ,$$

where $|\psi_n\rangle$ are the eigenvectors of L^\dagger .

- (b) For nondegenerate eigenvalues of L and proper normalization

$$\langle \psi_n | \phi_n \rangle = \langle \phi_n | \psi_n \rangle = \delta_{nm} .$$

- (c) $\sum_n |\phi_n\rangle \langle \psi_n| = 1$ and $\sum_n |\psi_n\rangle \langle \phi_n| = 1$.

- (d) The Green's function G satisfying the relation $(z - L)G = 1$ is given by

$$G(z) = \sum_n \frac{|\phi_n\rangle \langle \psi_n|}{z - \lambda_n} ,$$

and the Green's function G^\dagger satisfying the relation $(z^* - L^\dagger)G^\dagger = 1$ is given by

$$G^\dagger(z^*) = \sum_n \frac{|\psi_n\rangle \langle \phi_n|}{z^* - \lambda_n^*} .$$

Time-Dependent Green's Functions

Summary. The Green's functions corresponding to linear partial differential equations of first and second order in time are defined; their main properties and uses are presented.

2.1 First-Order Case

The Green's function $g(\mathbf{r}, \mathbf{r}', t - t')$ associated with the first-order (in time) homogeneous and inhomogeneous partial differential equations

$$\left[\frac{i}{c} \frac{\partial}{\partial t} - L(\mathbf{r}) \right] \phi(\mathbf{r}, t) = 0, \quad (2.1)$$

$$\left[\frac{i}{c} \frac{\partial}{\partial t} - L(\mathbf{r}) \right] \psi(\mathbf{r}, t) = f(\mathbf{r}, t) \quad (2.2)$$

is defined as the solution of

$$\left[\frac{i}{c} \frac{\partial}{\partial t} - L(\mathbf{r}) \right] g(\mathbf{r}, \mathbf{r}', t, t') = \delta(\mathbf{r} - \mathbf{r}') \delta(t - t'), \quad (2.3)$$

subject to the same BCs on the bounding surface S as $\phi(\mathbf{r}, t)$ and $\psi(\mathbf{r}, t)$. For the time being we shall assume that c is a positive constant. The operator $L(\mathbf{r})$ is as in Chap. 1. Expressing $g(\mathbf{r}, \mathbf{r}', \tau)$, where $\tau = t - t'$, in terms of its Fourier transform

$$g(\tau) = \int_{-\infty}^{\infty} \frac{d\omega'}{2\pi} e^{-i\omega'\tau} g(\omega'), \quad (2.4)$$

and substituting in (2.3) we obtain

$$\left(\frac{\omega}{c} - L \right) g(\omega) = \delta(\mathbf{r} - \mathbf{r}') . \quad (2.5)$$

The \mathbf{r}, \mathbf{r}' dependence of $g(\tau)$ and $g(\omega)$ is not displayed explicitly. Comparing with (1.1) we see that

$$g(\omega) = G\left(\frac{\omega}{c}\right), \tag{2.6}$$

where $G(z)$ is the Green's function associated with L and examined in detail in Chap. 1.

Using the results of Chap. 1, one concludes that $g(\omega)$ is an analytic function of the complex variable ω with singularities (poles and/or branch cuts) on the real ω -axis. Because of this property, (2.4) is not well defined as it stands. One has to use a limiting procedure in order to unambiguously define $g(\tau)$:

$$g^C(\tau) = \lim_{C \rightarrow C_0} \int_C \frac{d\omega}{2\pi} G\left(\frac{\omega}{c}\right) e^{-i\omega\tau}. \tag{2.7}$$

One can obtain infinitely many Green's functions depending on how path C approaches the real ω -axis C_0 . However, there are only two choices of physical interest shown in Fig. 2.1 as g^+ and g^- ; they give

$$g^\pm(\tau) = \int_{-\infty}^\infty \frac{d\omega'}{2\pi} G^\pm\left(\frac{\omega'}{c}\right) e^{-i\omega'\tau}. \tag{2.8}$$

It is useful to consider quantities denoted by the symbol $\tilde{g}^{CC'}$ and defined as the difference of two Green's functions g^C and $g^{C'}$. Obviously the quantities $\tilde{g}^{CC'}$ can be expressed as integrals of $g(\omega)e^{-i\omega\tau}/2\pi$ over closed contours enclosing the real ω -axis, either in part or in its entirety. Because each $\tilde{g}^{CC'}$ is the difference of two Green's functions, it satisfies homogeneous equation (2.1) and not (2.3). Thus, strictly speaking, the various $\tilde{g}^{CC'}$ s are not Green's functions.

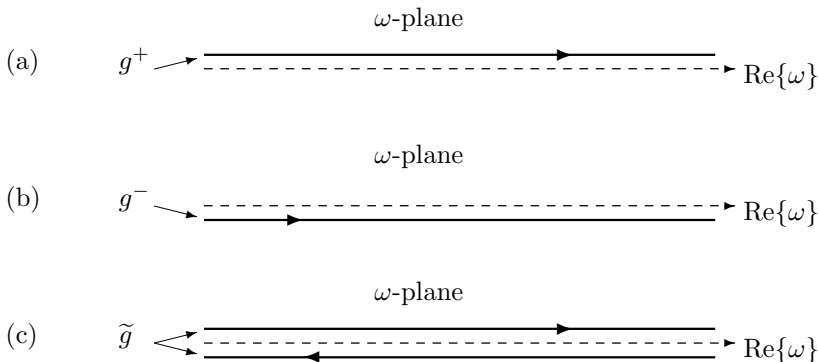


Fig. 2.1. Integration paths (solid lines) in the ω -plane for obtaining (a) $g^+(\tau)$, (b) $g^-(\tau)$, and (c) $\tilde{g}(\tau) = g^+(\tau) - g^-(\tau)$, where $g^+(\tau)$ and $g^-(\tau)$ satisfy a first-order (in time) differential equation. The singularities of the integrand lie on the real ω -axis

In the present case, because we introduce only two Green's functions of interest, there is only one $\tilde{g}^{CC'}$ of interest defined by

$$\tilde{g}(\tau) = g^+(\tau) - g^-(\tau). \quad (2.9)$$

By inspection of Fig. 2.1 and taking into account (2.9) we see that $\tilde{g}(\tau)$ is given by integrating $g(\omega)e^{-i\omega\tau}d\omega/2\pi$ along the contour shown in Fig. 2.1c.

For $\tau > 0$ (< 0) the paths for g^\pm can be closed by an infinite semicircle in the lower (upper) ω half-plane. Taking into account that all singularities of $g(\omega)$ or $G(\omega/c)$ are on the real axis, we have from Fig. 2.1 that

$$g^\pm(\tau) = \pm\theta(\pm\tau)\tilde{g}(\tau), \quad (2.10)$$

where the step function, $\theta(\tau)$, is defined as

$$\theta(\tau) = \begin{cases} 1, & \tau > 0, \\ 0, & \tau < 0. \end{cases} \quad (2.11)$$

Taking into account (1.16) and (2.8) we obtain

$$g^-(\mathbf{r}, \mathbf{r}', \tau) = [g^+(\mathbf{r}', \mathbf{r}, -\tau)]^*. \quad (2.12)$$

From Fig. 2.1 we can see that the function $\tilde{g}(\tau)$ can be written as

$$\begin{aligned} \tilde{g}(\tau) &= \int_{-\infty}^{\infty} \frac{d\omega'}{2\pi} e^{-i\omega'\tau} \tilde{G}\left(\frac{\omega'}{c}\right) \\ &= -2\pi i \int_{-\infty}^{\infty} \frac{d\omega'}{2\pi} e^{-i\omega'\tau} \sum_n \delta\left(\frac{\omega'}{c} - \lambda_n\right) \phi_n(\mathbf{r}) \phi_n^*(\mathbf{r}') \\ &= -ic \sum_n e^{-ic\lambda_n\tau} \phi_n(\mathbf{r}) \phi_n^*(\mathbf{r}'). \end{aligned} \quad (2.13)$$

We have used (1.21) and (1.22) to express the difference $G^+ - G^- \equiv \tilde{G}$ in terms of λ_n , $\phi_n(\mathbf{r}) \phi_n^*(\mathbf{r}')$, and the presence of the delta function to do the integral over ω' .

The corresponding operator $\tilde{g}(\tau)$ is then

$$\tilde{g}(\tau) = -ic \sum_n e^{-ic\lambda_n\tau} |\phi_n\rangle \langle \phi_n| = -ice^{-icL\tau}; \quad (2.14)$$

the operator

$$U(t-t') \equiv e^{-icL(t-t')} \quad (2.15)$$

is a time-evolution operator or a propagator because

$$|\phi(t)\rangle = U(t-t') |\phi(t')\rangle \quad (2.16)$$

satisfies (2.1). Thus the operator $U(t-t')$ propagates $|\phi\rangle$ from time t' to t .

We see that

$$U(t - t') = \frac{i}{c} \tilde{g}(t - t') . \quad (2.17)$$

Notice that in the \mathbf{r} -representation, (2.13), when $\tau = 0$, i.e., when $t = t'$, becomes

$$\tilde{g}(\mathbf{r}, \mathbf{r}', 0) = -ic\delta(\mathbf{r} - \mathbf{r}') . \quad (2.18)$$

Notice also

$$U(t_1 - t_2) = U(t_1 - t_3)U(t_3 - t_2) . \quad (2.19)$$

$g(t_1 - t_2)$ obeys a similar relation. Combining (2.16) and (2.17) and transforming to the \mathbf{r} -representation we obtain (Problem 2.1)

$$\phi(\mathbf{r}, t) = \frac{i}{c} \int \tilde{g}(\mathbf{r}, \mathbf{r}', t - t') \phi(\mathbf{r}', t') d\mathbf{r}' , \quad (2.20)$$

which, with the help of (2.10), can be expressed in terms of $g^+(\tau)$ and $g^-(\tau)$ for $\tau > 0$ and $\tau < 0$, respectively. The solution of inhomogeneous equation (2.2), $\psi(\mathbf{r}, t)$, can be expressed in terms of the general solution of homogeneous equation (2.1), $\phi(\mathbf{r}, t)$, and the Green's function $g^+(t - t')$ as follows:

$$\psi(\mathbf{r}, t) = \phi(\mathbf{r}, t) + \int d\mathbf{r}' dt' g^+(\mathbf{r}, \mathbf{r}', t - t') f(\mathbf{r}', t') . \quad (2.21)$$

To prove this, substitute (2.21) in (2.2) and take into account (2.1) and (2.3). Note that if we had used $g^-(\tau)$ instead of $g^+(\tau)$, the resulting $\psi(\mathbf{r}, t)$ would again have satisfied (2.2). We have excluded the solution corresponding to $g^-(\tau)$ on the basis of the physical argument that the response of a system at a time t depends only on what the source, $f(\mathbf{r}', t')$, was in the past ($t' < t$). Using (2.10) we can rewrite (2.21) as

$$\psi(\mathbf{r}, t) = \phi(\mathbf{r}, t) + \int d\mathbf{r}' \int_{-\infty}^t dt' \tilde{g}(\mathbf{r}, \mathbf{r}', t - t') f(\mathbf{r}', t') . \quad (2.22)$$

2.1.1 Examples

Here we calculate the various Green's functions for the case $L = -\nabla^2$. It is enough to calculate $\tilde{g}(t)$; $g^\pm(\tau)$ can be obtained from (2.10). For the present case the most convenient way of calculating $\tilde{g}(t)$ is (2.13); $\phi_n(\mathbf{r}) = e^{i\mathbf{k} \cdot \mathbf{r}} / \sqrt{\Omega}$, and $\lambda_n = k^2$. We have

$$\begin{aligned} \tilde{g}(\mathbf{r}, \mathbf{r}', \tau) &= -ic \sum_{\mathbf{k}} \frac{e^{i\mathbf{k} \cdot (\mathbf{r} - \mathbf{r}')}}{\Omega} e^{-ick^2\tau} \\ &= -ic \int \frac{d^d k}{(2\pi)^d} e^{i\mathbf{k} \cdot \boldsymbol{\rho} - ick^2\tau} , \end{aligned} \quad (2.23)$$

where $\boldsymbol{\rho} \equiv \mathbf{r} - \mathbf{r}'$ and d is the dimensionality. Taking into account that $\mathbf{k} \cdot \boldsymbol{\rho} = \sum_{i=1}^d k_i \rho_i$ and $k^2 = \sum_{i=1}^d k_i^2$, where k_i and ρ_i are the cartesian coordinates of \mathbf{k} and $\boldsymbol{\rho}$, respectively, we can rewrite (2.23) as (Problem 2.2s)

$$\begin{aligned} \tilde{g}(\mathbf{r}, \mathbf{r}', \tau) &= -ic \prod_{i=1}^d \int_{-\infty}^{\infty} \frac{dk_i}{2\pi} \exp(ik_i \rho_i - ic k_i^2 \tau) \\ &= -ic \prod_{i=1}^d \int_{-\infty}^{\infty} \frac{dk}{2\pi} \exp(i\rho_i^2/4c\tau) \exp(-ic\tau k^2) \\ &= -ic \prod_{i=1}^d \exp(i\rho_i^2/4c\tau) \frac{1}{2\pi} \sqrt{\frac{\pi}{ic\tau}} \\ &= -ic \left(\frac{1}{4\pi ic\tau} \right)^{d/2} \exp(i\rho^2/4c\tau), \end{aligned} \quad (2.24)$$

where $\sqrt{\pi/ic\tau}$ is the square root with a positive real part. Equation (2.24), together with (2.20), allows us to study how a free quantum-mechanical wave packet evolves in time. An example of particular interest is the evolution of the minimum uncertainty wave packet (see, e.g., Problem 3.2s in the next chapter or the book by Landau and Lifshitz [12], p. 48, or the book by Merzbacher [13]), pp. 18–24.

Note that if we choose $c = -iD$ and $L = -\nabla^2$, where D is a positive constant called the diffusion coefficient, we obtain the diffusion equation $-\partial n/D\partial t + \nabla^2 n = 0$ ¹. For such an equation we must consider the evolution toward the future, and as a result we should keep $g^+(\tau)$ only. Instead of the Fourier transform, it is more convenient to consider the Laplace transform. The final result for $g^+(\tau)$ is obtained by substituting $c = -iD$ in (2.24) and taking into account (2.10). Dividing this result by $-D$ we find

$$\begin{aligned} \frac{g^+(\mathbf{r}, \mathbf{r}', t - t')}{-D} &= \theta(t - t') \left(\frac{1}{4\pi D(t - t')} \right)^{d/2} \\ &\quad \times \exp \left[-\frac{(\mathbf{r} - \mathbf{r}')^2}{4D(t - t')} \right]. \end{aligned} \quad (2.25)$$

Note that $g^+(-D) \rightarrow \delta(\mathbf{r} - \mathbf{r}')$ as $t - t' \rightarrow 0^+$. As t increases, $g^+(-D)$ describes the diffusion of this local initial pulse. It must be stressed that the average diffusion range increases as the square root of $t - t'$: $\Delta \rho = \sqrt{2D\tau}$ where $\boldsymbol{\rho} = \mathbf{r} - \mathbf{r}'$, $\tau = t - t'$, and $\Delta \rho = \sqrt{\langle \rho^2 \rangle}$. For further details see Problem 2.3 and/or [8], p. 862.

¹ An equivalent equation governs the time and space dependence of the temperature, $T(\mathbf{r}, t)$, in a medium; in this case, D is replaced by K/c , where K is the thermal conductivity and c is the specific heat per unit volume.

2.2 Second-Order Case

The Green's functions associated with the second-order (in time) differential equations

$$\left[-\frac{1}{c^2} \frac{\partial^2}{\partial t^2} - L(\mathbf{r}) \right] \phi(\mathbf{r}, t) = 0, \quad (2.26)$$

$$\left[-\frac{1}{c^2} \frac{\partial^2}{\partial t^2} - L(\mathbf{r}) \right] \psi(\mathbf{r}, t) = f(\mathbf{r}, t), \quad (2.27)$$

are defined as the solutions of

$$\left[-\frac{1}{c^2} \frac{\partial^2}{\partial t^2} - L(\mathbf{r}) \right] g(\mathbf{r}, \mathbf{r}', t - t') = \delta(\mathbf{r} - \mathbf{r}') \delta(t - t'), \quad (2.28)$$

subject to the same BCs on S as $\phi(\mathbf{r})$ and $\psi(\mathbf{r})$; c is a positive constant. Expressing the general solution $g(\tau)$ of (2.28) as

$$g(\tau) = \int_{-\infty}^{\infty} \frac{d\omega'}{2\pi} e^{-i\omega'\tau} g(\omega'), \quad (2.29)$$

and substituting in (2.28), we obtain for $g(\omega)$

$$g(\omega) = G\left(\frac{\omega^2}{c^2}\right). \quad (2.30)$$

Since $G(z)$ is analytic in the complex plane except on the real z -axis, it follows that $g(\omega)$ is analytic in the complex ω -plane except in the real or imaginary ω -axis. The singularities of $g(\omega)$ on the real (imaginary) ω -axis come from the singularities of $G(z)$ in the positive (negative) real semiaxis. Here we will restrict ourselves on physical grounds to the case where there are no singularities off the real ω -axis (i.e., all eigenfrequencies ω_n are real), which means that the singularities of $G(z)$ are located on the positive real z -semiaxis.

Since $G(z)$ has singularities for z real and positive, $g(\omega)$ may not be well defined when ω is real. We again need to employ a limiting procedure:

$$g^C(\tau) = \lim_{C \rightarrow C_0} \int_C \frac{d\omega}{2\pi} g(\omega) e^{-i\omega\tau} = \lim_{C \rightarrow C_0} \int_C \frac{d\omega}{2\pi} G\left(\frac{\omega^2}{c^2}\right) e^{-i\omega\tau}. \quad (2.31)$$

Of all the infinite choices for C , only three are of physical interest. These three choices are shown in Fig. 2.2a–c. Note that the fourth case shown in Fig. 2.2d can be expressed in terms of the other three because

$$g^R + g^A = g + g^-, \quad (2.32)$$

as can be seen from Fig. 2.2.

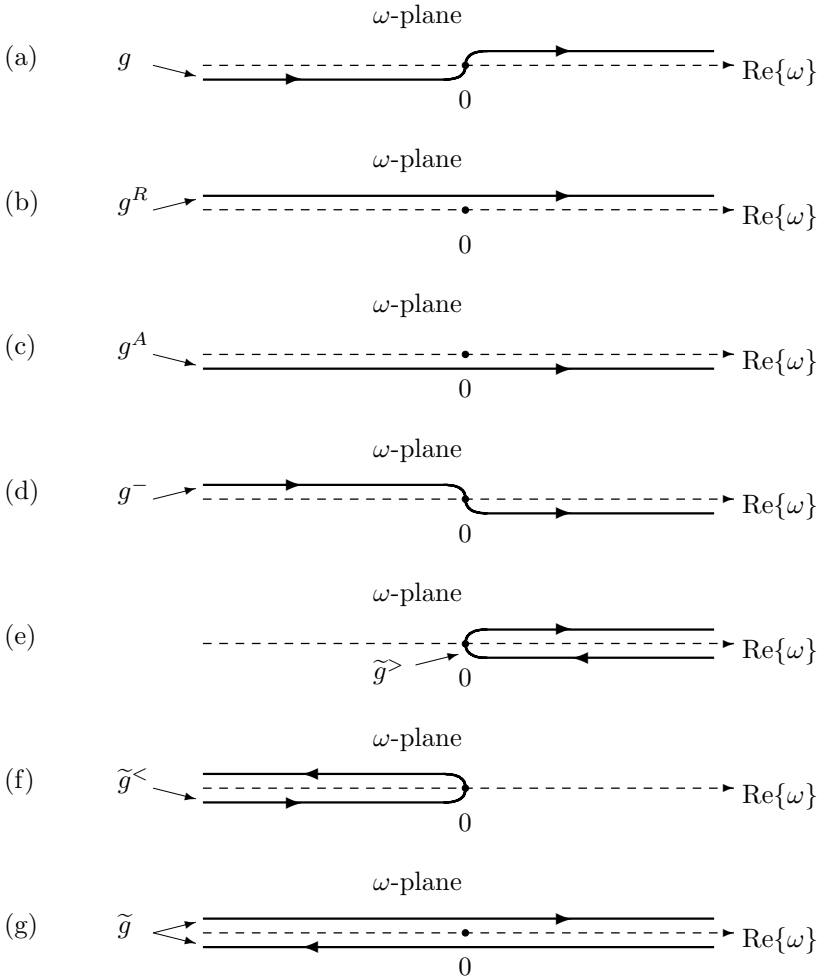


Fig. 2.2. Integration paths (*solid lines*) in the ω -plane for obtaining various Green's functions satisfying a second-order (in time) differential equation. The singularities of the integrand are located on the real ω -axis. The functions \tilde{g}^{\lessgtr} and \tilde{g} are differences of pairs of Green's function (see text)

Usually we take g , g^R , and g^A as the three basic Green's functions; $g(\tau)$ is called the causal Green's function, or simply the Green's function, in many-body and field theory; as we will see in Part III, it is widely used. $g^R(\tau)$ and $g^A(\tau)$ are the retarded and advanced Green's functions, respectively; they are used in solutions of inhomogeneous equations; the names retarded and advanced are connected with the properties that $g^R(\tau) = 0$ for $\tau < 0$ and $g^A(\tau) = 0$ for $\tau > 0$, as we shall see below. The Fourier transforms of $g(\tau)$, $g^R(\tau)$, $g^A(\tau)$, and $g^-(\tau)$ are given by

$$\begin{aligned}
g(\omega') &= \lim_{s \rightarrow 0^+} g(\omega' + is\omega') = \lim_{s \rightarrow 0^+} G \left(\frac{\omega'^2}{c^2} + \frac{2i\omega'^2}{c^2} s \right) \\
&= G^+ \left(\frac{\omega'^2}{c^2} \right), \tag{2.33}
\end{aligned}$$

$$g^R(\omega') = \lim_{s \rightarrow 0^+} g(\omega' + is) = \lim_{s \rightarrow 0^+} G \left(\frac{\omega'^2}{c^2} + \frac{2i\omega'}{c^2} s \right), \tag{2.34}$$

$$g^A(\omega') = \lim_{s \rightarrow 0^+} g(\omega' - is) = \lim_{s \rightarrow 0^+} G \left(\frac{\omega'^2}{c^2} - \frac{2i\omega'}{c^2} s \right), \tag{2.35}$$

$$\begin{aligned}
g^-(\omega') &= \lim_{s \rightarrow 0^+} g(\omega' - is\omega') = \lim_{s \rightarrow 0^+} G \left(\frac{\omega'^2}{c^2} - \frac{2i\omega'^2}{c^2} s \right) \\
&= G^- \left(\frac{\omega'^2}{c^2} \right), \tag{2.36}
\end{aligned}$$

where

$$\omega' s = \begin{cases} 0^+ & \text{for } \omega' > 0, \\ 0^- & \text{for } \omega' < 0, \end{cases} \tag{2.37a}$$

$$\tag{2.37b}$$

and ω' is real.

Since there are three independent g s of interest, we can define three \tilde{g} s, each as a difference of a pair of g s. More explicitly we have

$$\tilde{g}^> = g - g^A, \tag{2.38}$$

$$\tilde{g}^< = g - g^R, \tag{2.39}$$

$$\tilde{g} = g^R - g^A = \tilde{g}^> - \tilde{g}^<. \tag{2.40}$$

Obviously $\tilde{g}^{\leq}(\tau)$ and $\tilde{g}(\tau)$ can be obtained by integrating $g(\omega)e^{-i\omega\tau}/2\pi$ along the contours shown in Fig. 2.2e–g, respectively. We remind the reader that the \tilde{g} s satisfy homogeneous equation (2.26) and not (2.28).

Taking into account that the paths for the various g s can be closed in the lower (upper) ω -plane when τ is larger (smaller) than zero and that there are no singularities of $g(\omega)$ for ω off the real axis, we obtain by inspection of Fig. 2.2

$$g(\tau) = \theta(\tau)\tilde{g}^>(\tau) + \theta(-\tau)\tilde{g}^<(\tau), \tag{2.41}$$

$$g^R(\tau) = \theta(\tau)\tilde{g}(\tau), \tag{2.42}$$

$$g^A(\tau) = -\theta(-\tau)\tilde{g}(\tau), \tag{2.43}$$

$$g^-(\tau) = -\theta(\tau)\tilde{g}^<(\tau) - \theta(-\tau)\tilde{g}^>(\tau). \tag{2.44}$$

As we can see from (2.40)–(2.44), knowledge of $\tilde{g}^>$ and $\tilde{g}^<$ allows us to determine all g s and \tilde{g} .

From Fig. 2.2 we can see that

$$\begin{aligned}
 \tilde{g}^>(\mathbf{r}, \mathbf{r}', \tau) &= \lim_{s \rightarrow 0^+} \int_0^\infty \frac{d\omega}{2\pi} e^{-i\omega\tau} [g(\omega + is) - g(\omega - is)] \\
 &= \int_0^\infty \frac{d\omega}{2\pi} e^{-i\omega\tau} \tilde{G}\left(\frac{\omega^2}{c^2}\right) \\
 &= - \int_0^\infty \frac{d\omega}{2\pi} e^{-i\omega\tau} 2\pi i \sum_n \phi_n(\mathbf{r}) \phi_n^*(\mathbf{r}') \delta\left(\frac{\omega^2}{c^2} - \lambda_n\right) \\
 &= -\frac{ic}{2} \sum_n \frac{\phi_n(\mathbf{r}) \phi_n^*(\mathbf{r}')}{\sqrt{\lambda_n}} \exp\left(-ic\sqrt{\lambda_n}\tau\right), \tag{2.45}
 \end{aligned}$$

where $\sqrt{\lambda_n} \geq 0$. To obtain (2.45) we have used (1.21), (1.22), (2.34) and (2.35), as well as (A.3) of Appendix A. Similarly, we have

$$\tilde{g}^<(\mathbf{r}, \mathbf{r}', \tau) = -\frac{ic}{2} \sum_n \frac{\phi_n(\mathbf{r}) \phi_n^*(\mathbf{r}')}{\sqrt{\lambda_n}} e^{ic\sqrt{\lambda_n}\tau}. \tag{2.46}$$

From (2.45) and (2.46) it follows that

$$\tilde{g}^<(\mathbf{r}, \mathbf{r}', \tau) = -[\tilde{g}^>(\mathbf{r}', \mathbf{r}, \tau)]^*, \tag{2.47}$$

$$\tilde{g}(\mathbf{r}, \mathbf{r}', \tau) = -c \sum_n \frac{\phi_n(\mathbf{r}) \phi_n^*(\mathbf{r}')}{\sqrt{\lambda_n}} \sin\left(c\sqrt{\lambda_n}\tau\right). \tag{2.48}$$

It follows from (2.48) that $\tilde{g}(\mathbf{r}, \mathbf{r}', 0) = 0$ and $d\tilde{g}/d\tau = -c^2\delta(\mathbf{r} - \mathbf{r}')$ for $\tau = 0$. Equation (2.48) in operator form is

$$\tilde{g}(\tau) = -c \frac{\sin\left(c\sqrt{L}\tau\right)}{\sqrt{L}}, \quad \tau = t - t'. \tag{2.49}$$

Consider now the expression

$$|\phi(t)\rangle = -\frac{1}{c^2} \left[\tilde{g}(t - t') |\dot{\phi}(t')\rangle + \tilde{g}(t - t') |\phi(t')\rangle \right], \tag{2.50}$$

where the dot denotes differentiation with respect to t and $\dot{\phi}(t')$ is $d\phi/dt$ for $t = t'$. Since $\tilde{g}(t - t')$ satisfies homogeneous equation (2.26), so does the function $|\phi(t)\rangle$ given by (2.50). Furthermore, $\phi(t) \rightarrow \phi(t')$ and $\dot{\phi}(t) \rightarrow \dot{\phi}(t')$ as $t \rightarrow t'$, in view of the initial conditions satisfied by $\tilde{g}(\mathbf{r}, \mathbf{r}', \tau)$ for $\tau \rightarrow 0$. Thus (2.50) determines the solution of (2.26) for an arbitrary time t in terms of $\phi(t')$ and $\dot{\phi}(t')$ at a particular time t' . Rewriting (2.50) in the \mathbf{r} -representation we have

$$\begin{aligned}
 \phi(\mathbf{r}, t) &= -\frac{1}{c^2} \int d\mathbf{r}' \tilde{g}(\mathbf{r}, \mathbf{r}', t - t') \dot{\phi}(\mathbf{r}', t') \\
 &\quad -\frac{1}{c^2} \int d\mathbf{r}' \tilde{g}(\mathbf{r}, \mathbf{r}', t - t') \phi(\mathbf{r}', t'). \tag{2.51}
 \end{aligned}$$

It is easy to verify that

$$\begin{aligned}\psi(\mathbf{r}, t) &= \phi(\mathbf{r}, t) + \int d\mathbf{r}' dt' g^R(\mathbf{r}, \mathbf{r}', t - t') f(\mathbf{r}', t') \\ &= \phi(\mathbf{r}, t) + \int d\mathbf{r}' \int_{-\infty}^t dt' \tilde{g}(\mathbf{r}, \mathbf{r}', t - t') f(\mathbf{r}', t')\end{aligned}\quad (2.52)$$

satisfies inhomogeneous equation (2.27), where $\phi(\mathbf{r}, t)$ is the general solution of (2.26). We have used g^R in (2.52) because of the physical argument that the response $\psi(\mathbf{r}, t)$ at time t depends on the values of the source, $f(\mathbf{r}', t')$, at times t' prior to t .

2.2.1 Examples

Consider first the case $L = -\nabla^2$ in 3-d space for which $G^\pm(\lambda)$ are given by (1.40). Substituting in (2.45) we obtain

$$\tilde{g}^>(\varrho, \tau) = -\frac{1}{4\pi\varrho} \int_0^\infty \frac{d\omega}{2\pi} e^{-i\omega\tau} \left(e^{i\omega\varrho/c} - e^{-i\omega\varrho/c} \right), \quad (2.53)$$

where $\varrho = \mathbf{r} - \mathbf{r}'$. Using (2.47) we have

$$\tilde{g}^<(\varrho, \tau) = -\frac{1}{4\pi\varrho} \int_0^\infty \frac{d\omega}{2\pi} e^{i\omega\tau} \left(e^{i\omega\varrho/c} - e^{-i\omega\varrho/c} \right). \quad (2.54)$$

Subtracting (2.54) from (2.53) and changing the integration variable from ω to $-\omega$ in the integral involving $\exp[-i\omega(\varrho/c + \tau)] - \exp[-i\omega(\varrho/c - \tau)]$ we get

$$\begin{aligned}\tilde{g}(\varrho, \tau) &= \frac{1}{4\pi\varrho} \int_0^\infty \frac{d\omega}{2\pi} \left(e^{i\omega\varrho/c} - e^{-i\omega\varrho/c} \right) (e^{+i\omega\tau} - e^{-i\omega\tau}) \\ &= \frac{1}{4\pi\varrho} \int_{-\infty}^\infty \frac{d\omega}{2\pi} \left(e^{i\omega(\varrho/c + \tau)} - e^{i\omega(\varrho/c - \tau)} \right) \\ &= \frac{1}{4\pi\varrho} [\delta(\varrho/c + \tau) - \delta(\varrho/c - \tau)] \\ &= \frac{c}{4\pi\varrho} [\delta(\varrho + c\tau) - \delta(\varrho - c\tau)].\end{aligned}\quad (2.55)$$

Using (2.55), (2.42), and 2.43) we obtain

$$g^R(\mathbf{r}, \mathbf{r}', t - t') = -\frac{c}{4\pi |\mathbf{r} - \mathbf{r}'|} \delta(|\mathbf{r} - \mathbf{r}'| - c(t - t')), \quad (2.56)$$

$$g^A(\mathbf{r}, \mathbf{r}', t - t') = -\frac{c}{4\pi |\mathbf{r} - \mathbf{r}'|} \delta(|\mathbf{r} - \mathbf{r}'| + c(t - t')). \quad (2.57)$$

The solution of the inhomogeneous wave equation,

$$\left(\nabla^2 - \frac{\partial^2}{c^2 \partial t^2} \right) \psi(\mathbf{r}, t) = f(\mathbf{r}, t),$$

is then, according to (2.52),

$$\begin{aligned}\psi(\mathbf{r}, t) &= \phi(\mathbf{r}, t) - \frac{1}{4\pi} \int d\mathbf{r}' dt' \delta\left(\frac{\varrho}{c} - (t - t')\right) f(\mathbf{r}', t') / \varrho \\ &= \phi(\mathbf{r}, t) - \frac{1}{4\pi} \int d\mathbf{r}' \frac{f(\mathbf{r}', t - |\mathbf{r} - \mathbf{r}'|/c)}{|\mathbf{r} - \mathbf{r}'|} .\end{aligned}\quad (2.58)$$

Equation (2.58) is the basic result in electromagnetic theory.

In order to obtain the Green's functions associated with the 2-d wave equation, we will use the following argument, as presented in [8]. A point source at the point (x'_1, x'_2) of a 2-d space is equivalent to a uniformly distributed source along a line parallel to the x_3 -axis and passing through the point $(x'_1, x'_2, 0)$. Hence, the 2-d g can be obtained by integrating the 3-d g over the third component of \mathbf{r}' , x'_3 . Writing $\mathbf{r} = \mathbf{R} + x_3 \mathbf{i}_3$, $\mathbf{r}' = \mathbf{R}' + x'_3 \mathbf{i}_3$ and $\varrho^2 = (\mathbf{R} - \mathbf{R}')^2 + (x_3 - x'_3)^2$, we obtain for the 2-d \tilde{g}

$$\tilde{g}(\mathbf{R}, \mathbf{R}', \tau) = \int_{-\infty}^{\infty} dx'_3 \tilde{g}(\varrho, \tau) = \int_{-\infty}^{\infty} dy \tilde{g}\left(\sqrt{P^2 + y^2}, \tau\right), \quad (2.59)$$

where $P = |\mathbf{R} - \mathbf{R}'|$ and $y = x_3 - x'_3$. Substituting (2.55) into (2.59), taking into account (A.3), and performing the integration, we get the final result for the 2-d \tilde{g} ,

$$\tilde{g}(\mathbf{R}, \mathbf{R}', \tau) = -\frac{\bar{\varepsilon}(\tau)\theta(c|\tau| - P)c}{2\pi\sqrt{c^2\tau^2 - P^2}}, \quad (2.60)$$

where $\bar{\varepsilon}(\tau) = 1$ for $\tau > 0$ and $\bar{\varepsilon}(\tau) = -1$ for $\tau < 0$.

The 2-d g^R is then

$$g^R(\mathbf{R}, \mathbf{R}', \tau) = -\frac{\theta(c\tau - P)c}{2\pi\sqrt{c^2\tau^2 - P^2}}. \quad (2.61)$$

The 1-d g^R can be obtained by integrating the 2-d g^R once more over x'_2 . We find

$$g^R(x, x', \tau) = -\frac{c}{2}\theta(c\tau - |x - x'|). \quad (2.62)$$

A very interesting discussion of the physical significance of the results for g^R associated with the wave equation in 3-d, 2-d, and 1-d is given in [8], pp. 838–853.

We will conclude this chapter by obtaining the various Green's functions associated with the 3-d Klein-Gordon equation, which corresponds to $L(\mathbf{r})$ being equal to $-\nabla^2 + \mu^2$, where μ is a positive constant. The eigenvalues are $\lambda_n = k^2 + \mu^2$ and the eigenfunctions $\langle \mathbf{r} | \phi_n \rangle = e^{i\mathbf{k} \cdot \mathbf{r}} / \sqrt{\Omega}$. Substituting in (2.46) we obtain

$$\tilde{g}^<(\mathbf{r}, \mathbf{r}', \tau) = -\frac{ic}{2} \int \frac{d^3k}{(2\pi)^3} \frac{\exp[i(\mathbf{k} \cdot \varrho + ck_0\tau)]}{k_0}, \quad (2.63)$$

where $k_0 = \sqrt{\lambda_n} = \sqrt{k^2 + \mu^2}$ and $\boldsymbol{\varrho} = \mathbf{r} - \mathbf{r}'$. After performing the integration over the angle variables, we obtain

$$\tilde{g}^<(\mathbf{r}, \mathbf{r}', \tau) = -\frac{c}{4\pi\varrho} \int_{-\infty}^{\infty} \frac{dk}{2\pi} \frac{k}{k_0} \exp[i(k\varrho + ck_0\tau)] = \frac{c}{4\pi\varrho} \frac{\partial f}{\partial \varrho}, \quad (2.64)$$

where

$$f = i \int_{-\infty}^{\infty} \frac{dk}{2\pi} \frac{\exp[i(k\varrho + ck_0\tau)]}{k_0}; \quad (2.65)$$

changing the integration variable in (2.65) to ϕ , where

$$k = \mu \sinh(\phi); \quad k_0 = \mu \cosh(\phi),$$

we obtain

$$f = \frac{i}{2\pi} \int_{-\infty}^{\infty} d\phi \exp\{i\mu[\varrho \sinh(\phi) + c\tau \cosh(\phi)]\}. \quad (2.66)$$

In evaluating the integral (2.66) one has to distinguish four cases according to the signs of $c^2\tau^2 - \varrho^2$ and τ . For example, for $\tau > 0$ and $c^2\tau^2 - \varrho^2 > 0$ the quantity $\varrho \sinh(\phi) + c\tau \cosh(\phi)$ can be written as $\sqrt{c^2\tau^2 - \varrho^2} \cosh(\phi + \phi_0)$, where $\tanh(\phi_0) = \varrho/c\tau$. Substituting in (2.66) we obtain

$$\begin{aligned} f &= \frac{i}{2\pi} \int_{-\infty}^{\infty} d\phi \exp\left[i\mu\sqrt{c^2\tau^2 - \varrho^2} \cosh(\phi + \phi_0)\right] \\ &= -\frac{1}{2} \mathcal{H}_0^{(1)}\left(\mu\sqrt{c^2\tau^2 - \varrho^2}\right). \end{aligned} \quad (2.67)$$

Similar expressions are obtained for the other three cases. Performing the differentiation with respect to ϱ implied by (2.64) (and keeping in mind the discontinuities of f at $c^2\tau^2 = \varrho^2$, which produce δ functions), we obtain, finally, for $\tilde{g}^<$ the following expression:

$$\begin{aligned} \tilde{g}^<(\mathbf{r}, \mathbf{r}', t - t') &= \bar{\varepsilon}(\tau)\delta(\nu)\frac{c}{4\pi} - \theta(\nu)\bar{\varepsilon}(\tau)\frac{\mu c}{4\pi\sqrt{\nu}} J_1(\mu\sqrt{\nu}) \\ &\quad - \theta(\nu)\frac{i\mu c}{8\pi\sqrt{\nu}} Y_1(\mu\sqrt{\nu}) \\ &\quad + \theta(-\nu)\frac{i\mu c}{4\pi^2\sqrt{-\nu}} K_1(\mu\sqrt{-\nu}), \end{aligned} \quad (2.68)$$

where

$$\nu = c^2\tau^2 - \varrho^2, \quad \tau = t - t'; \quad \boldsymbol{\varrho} = \mathbf{r} - \mathbf{r}'. \quad (2.69)$$

From (2.47) we obtain for $\tilde{g}^>$ ($\mathbf{r}, \mathbf{r}', t - t'$)

$$\tilde{g}^>(\mathbf{r}, \mathbf{r}', t - t') = -\text{Re}\{\tilde{g}^<(\mathbf{r}, \mathbf{r}', t - t')\} + i \text{Im}\{\tilde{g}^<(\mathbf{r}, \mathbf{r}', t - t')\}. \quad (2.70)$$

The remaining g s and \tilde{g} s are then

$$\tilde{g}(\mathbf{r}, \mathbf{r}', t - t') = -\bar{\varepsilon}(\tau)\delta(\nu)\frac{c}{2\pi} + \theta(\nu)\bar{\varepsilon}(\tau)\frac{\mu c}{4\pi\sqrt{\nu}}J_1(\mu\sqrt{\nu}), \quad (2.71)$$

$$g(\mathbf{r}, \mathbf{r}', t - t') = -\delta(\nu)\frac{c}{4\pi} + \theta(\nu)\frac{\mu c}{8\pi\sqrt{\nu}}J_1(\mu\sqrt{\nu}) \\ + i\text{Im}\{\tilde{g}^<(\mathbf{r}, \mathbf{r}', t - t')\}, \quad (2.72)$$

$$g^R(\mathbf{r}, \mathbf{r}', t - t') = -\theta(\tau)\frac{c}{2\pi}\left[\delta(\nu) - \frac{\mu}{2\sqrt{\nu}}\theta(\nu)J_1(\mu\sqrt{\nu})\right], \quad (2.73)$$

$$g^A(\mathbf{r}, \mathbf{r}', t - t') = -\theta(-\tau)\frac{c}{2\pi}\left[\delta(\nu) - \frac{\mu}{2\sqrt{\nu}}\theta(\nu)J_1(\mu\sqrt{\nu})\right]. \quad (2.74)$$

As $\mu \rightarrow 0^+$, the above expressions reduce to those obtained for the wave equation. To obtain this reduction, take into account that $\delta(\nu) = \delta(c^2\tau^2 - \varrho^2) = [\delta(c\tau - \varrho) + \delta(c\tau + \varrho)]/2\varrho$. More information about the g s and \tilde{g} s associated with various relativistic equations can be found in the book by Bogoliubov and Shirkov [14]. Note the following correspondence of our notation with that of [14]: $g^R \rightarrow -D^{\text{ret}}$, $g^A \rightarrow -D^{\text{adv}}$, $g \rightarrow -D^c$, $\tilde{g} \rightarrow -D$, $\tilde{g}^> \rightarrow -D^-$, $\tilde{g}^< \rightarrow D^+$.

2.3 Summary

2.3.1 Definition

The Green's function g associated with a first-order (in time) partial differential equation of the form $i\partial\phi/c\partial t - L(\mathbf{r})\phi = 0$ is defined as the solution of the equation

$$\left[\frac{i}{c}\frac{\partial}{\partial t} - L(\mathbf{r})\right]g(\mathbf{r}, \mathbf{r}', t, t') = \delta(\mathbf{r} - \mathbf{r}')\delta(t - t'), \quad (2.3)$$

subject to certain homogeneous BCs on the surface S of the domain Ω of \mathbf{r}, \mathbf{r}' . Here $L(\mathbf{r})$ is a linear, hermitian, time-independent operator possessing a complete set of eigenfunctions as in Chap. 1. The constant c is either real (in which case it will be taken as positive without loss of generality) or imaginary. The former case corresponds to a Schrödinger-type equation, while the latter corresponds to a diffusion-type equation.

2.3.2 Basic Properties

The Green's function g is a function of the difference $\tau \equiv t - t'$. The Fourier transform of $g(\mathbf{r}, \mathbf{r}', \tau)$ with respect to τ , $g(\mathbf{r}, \mathbf{r}'; \omega)$ is directly related to the time-independent Green's function examined in Chap. 1. More explicitly, $g(\mathbf{r}, \mathbf{r}'; \omega) = G(\mathbf{r}, \mathbf{r}'; \omega/c) \equiv \langle \mathbf{r} | (\omega/c - L)^{-1} | \mathbf{r}' \rangle$. For real ω , $G(\omega/c)$ may

not be well defined; thus we must obtain $g(\tau)$ by a limiting procedure of the type

$$g^C(\tau) = \lim_{C \rightarrow C_0} \int_C \frac{d\omega}{2\pi} G\left(\frac{\omega}{c}\right) e^{-i\omega\tau}, \quad (2.7)$$

as the integration path C approaches the real ω -axis C_0 . One can obtain infinitely many $g(\tau)$ s depending on how C approaches the real axis. However, there are only two “natural” (i.e., corresponding to situations of physical interest) choices of C shown in Fig. 2.1; the Green's functions corresponding to these two paths, $g^\pm(\tau)$, are then given by

$$g^\pm(\tau) = \int_{-\infty}^{\infty} \frac{d\omega'}{2\pi} G^\pm\left(\frac{\omega'}{c}\right) e^{-i\omega'\tau}. \quad (2.8)$$

For $\tau > 0$ ($\tau < 0$) we can close the integration paths with an infinite semicircle in the lower (upper) ω half-plane. Consequently, $g^+(\tau) = 0$ for $\tau < 0$ and $g^-(\tau) = 0$ for $\tau > 0$.

Some particular examples of $g(\tau)$ associated with $L = -\nabla^2$ were presented in §2.1.1.

2.3.3 Definition

The Green's function $g(\tau)$ associated with a second-order (in time) differential equation is defined as the solution of

$$\left[-\frac{1}{c^2} \frac{\partial^2}{\partial t^2} - L(\mathbf{r}) \right] g(\mathbf{r}, \mathbf{r}', t - t') = \delta(\mathbf{r} - \mathbf{r}') \delta(t - t'), \quad (2.28)$$

where $\tau \equiv t - t'$.

2.3.4 Basic Properties

The Fourier transform of $g(\tau)$, $g(\omega)$, is related to $G(z)$ defined in Chap. 1 by

$$g(\omega) = G(\omega^2/c^2). \quad (2.30)$$

Because of the singularities of $G(z)$ on the real axis, one needs to employ a limiting procedure:

$$g^C(\tau) = \lim_{C \rightarrow C_0} \int_C \frac{d\omega}{2\pi} g(\omega) e^{-i\omega\tau} = \lim_{C \rightarrow C_0} \int_C \frac{d\omega}{2\pi} G\left(\frac{\omega^2}{c^2}\right) e^{-i\omega\tau}. \quad (2.31)$$

Again there are infinitely many $g^C(\tau)$ s one can obtain depending on the way path C approaches the real axis C_0 . In the present case there are only three independent “natural” (i.e., of physical interest) choices, shown in Fig. 2.2 as g , g^R , and g^A . In particular, $g(\tau)$ or its Fourier transform $g(\omega')$ is the

so-called causal Green's function or simply Green's function in many-body or field theory. It is given by the Fourier transform of (2.33)

$$g(\tau) = \int_{-\infty}^{\infty} \frac{d\omega'}{2\pi} G^+(\omega'^2/c^2) e^{-i\omega'\tau} . \quad (2.33')$$

$g^R(\tau)$ is the retarded Green's function, which has the property $g^R(\tau) = 0$ for $\tau < 0$; $g^A(\tau)$ is the advanced Green's function, which satisfies the relation $g^A(\tau) = 0$ for $\tau > 0$; $g^-(\tau) = g^R(\tau) + g^A(\tau) - g(\tau)$. All these Green's functions are interrelated.

Some particular examples associated with $L = -\nabla^2$ or $L = -\nabla^2 + \mu^2$ were presented in Sect. 2.2.1.

2.3.5 Use

Having $g^\pm(\tau)$, which satisfies (2.3), we can:

1. Solve the homogeneous equation $i\partial\phi(\mathbf{r}, t)/c\partial t = L(\mathbf{r})\phi(\mathbf{r}, t)$ as

$$\phi(\mathbf{r}, t) = \frac{i}{c} \int \tilde{g}(\mathbf{r}, \mathbf{r}', t - t') \phi(\mathbf{r}', t') d\mathbf{r}' , \quad (2.20)$$

where

$$\tilde{g}(\tau) = g^+(\tau) - g^-(\tau) , \quad (2.9)$$

in terms of the initial value of ϕ , $\phi(\mathbf{r}', t')$.

2. Solve the inhomogeneous equation

$$i \frac{\partial\psi(\mathbf{r}, t)}{c\partial t} - L(\mathbf{r})\psi(\mathbf{r}, t) = f(\mathbf{r}, t) . \quad (2.2)$$

The function $\psi(\mathbf{r}, t)$ is given by

$$\psi(\mathbf{r}, t) = \phi(\mathbf{r}, t) + \int d\mathbf{r}' dt' g^+(\mathbf{r}, \mathbf{r}', t - t') f(\mathbf{r}', t') , \quad (2.21)$$

where $\phi(\mathbf{r}, t)$ is the solution of the homogeneous equation.

3. Use $g_0(\tau)$ and $L_1(t)$ to obtain information about the solution of

$$i \frac{\partial\psi(\mathbf{r}, t)}{c\partial t} - L_0\psi - L_1\psi = 0 ,$$

where g_0 corresponds to L_0 . This aspect will be discussed in Chap. 4.

4. Relate $g^\pm(\tau)$ to the commutators or anticommutators of field operators in quantum field theory. These relations will be given in Part III.

Similarly, the various Green's functions satisfying (2.28) can also be used for solving the corresponding homogeneous and inhomogeneous equations

$$\begin{aligned}\phi(\mathbf{r}, t) &= -\frac{1}{c^2} \int d\mathbf{r}' \tilde{g}(\mathbf{r}, \mathbf{r}', t - t') \dot{\phi}(\mathbf{r}', t') \\ &\quad - \frac{1}{c^2} \int d\mathbf{r}' \ddot{g}(\mathbf{r}, \mathbf{r}', t - t') \phi(\mathbf{r}', t') ,\end{aligned}\quad (2.51)$$

$$\begin{aligned}\psi(\mathbf{r}, t) &= \phi(\mathbf{r}, t) + \int d\mathbf{r}' dt' g^R(\mathbf{r}, \mathbf{r}', t - t') f(\mathbf{r}', t') \\ &= \phi(\mathbf{r}, t) + \int d\mathbf{r}' \int_{-\infty}^t dt' \tilde{g}(\mathbf{r}, \mathbf{r}', t - t') f(\mathbf{r}', t') ,\end{aligned}\quad (2.52)$$

as well as for carrying out a perturbative approach; they are also related to the commutators and anticommutators of field operators. It is worthwhile pointing out that the general solution of the inhomogeneous wave equation $(\nabla^2 - \partial^2/c^2 \partial t^2) \psi(\mathbf{r}, t) = f(\mathbf{r}, t)$ is given by

$$\begin{aligned}\psi(\mathbf{r}, t) &= \phi(\mathbf{r}, t) - \frac{1}{4\pi} \int d\mathbf{r}' dt' \delta\left(\frac{\rho}{c} - (t - t')\right) \frac{f(\mathbf{r}', t')}{\rho} \\ &= \phi(\mathbf{r}, t) - \frac{1}{4\pi} \int d\mathbf{r}' \frac{f(\mathbf{r}', t - |\mathbf{r} - \mathbf{r}'|/c)}{|\mathbf{r} - \mathbf{r}'|} ,\end{aligned}\quad (2.58)$$

where $\phi(\mathbf{r}, t)$ is the general solution of the homogeneous wave equation.

Further Reading

- Several interesting applications of time-dependent Green's functions are given in the first volume of the classic two-volume text by Morse and Feshbach [8], pp. 837–867.
- In the book by Bogoliubov and Shirkov [14], time-dependent Green's functions are connected to unequal time commutators of field operators for noninteracting quantum fields. See pp. 136–153.
- The book by Byron and Fuller [3], pp. 442–459, gives an introduction to time-dependent Green's functions.
- A more systematic approach with many examples is presented in the book by Duffy [4].

Problems

2.1. Prove (2.20).

Hint: Replace (2.17) in (2.16), take the product $\langle \mathbf{r} | \phi(t) \rangle$, and on the rhs of (2.16) introduce the unit operator $\int d\mathbf{r}' |\mathbf{r}'\rangle \langle \mathbf{r}'|$ directly in front of $|\phi(t')\rangle$.

2.2s. Prove (2.24).

2.3. Consider the 1-d diffusion equation

$$\frac{\partial n}{\partial t} - D \frac{\partial^2 n}{\partial x^2} = 0,$$

where D is the diffusion constant and $n(x, t)$ is the concentration of particles. Show that:

(a) The $\tilde{g}(x, x'; t)$ for the diffusion equation is given by

$$g^+(x, x'; t) = \tilde{g}(x, x'; t) = \frac{1}{2} \sqrt{\frac{1}{\pi Dt}} \exp \left[-\frac{(x - x')^2}{4Dt} \right], \quad t \geq 0.$$

(b) If $n(x, 0)$ is given by

$$n(x, 0) = \frac{1}{\delta x \sqrt{2\pi}} \exp \left[-\frac{x^2}{2\delta x^2} \right],$$

then

$$n(x, t) = \frac{1}{\sqrt{2\pi(\delta x^2 + 2Dt)}} \exp \left[-\frac{x^2}{2(\delta x^2 + 2Dt)} \right], \quad t \geq 0.$$

Thus $[\delta x(t)]^2 = \delta x^2 + 2Dt$, $t \geq 0$.

2.4. Consider the time-dependent scalar wave equation in d -dimensions ($d = 1, 2, 3$) with BC $\psi(\mathbf{r}) = 0$ for $r = a$ ($r^2 = \sum_{i=1}^d x_i^2$). The initial condition is $\psi(\mathbf{r}, 0) = A\delta(\mathbf{r})$, $\dot{\psi}(\mathbf{r}, 0) = 0$.

(a) Will the initial pulse be refocused at the point $r = 0$?

(b) For the case $d = 2$ give a graph of $\psi(\mathbf{r}, t)$ for various values of t in the interval $(0 < t < 10a/c)$.

Hint: See [8], pp. 851–853.

2.5. Calculate the Green's functions satisfying the equation

$$\nabla^2 G - a^2 \frac{\partial G}{\partial t} - \frac{1}{c^2} \frac{\partial^2 G}{\partial t^2} = \delta(\mathbf{r} - \mathbf{r}') \delta(t - t')$$

for $d = 1, 2, 3$ spatial dimensions and proper BCs at infinity. Take the limits $c \rightarrow \infty$ or $a \rightarrow 0$ and verify that you obtain the diffusion (with $D = a^{-2}$) and the wave Green's function, respectively.

What is the physical interpretation of this G ?

Hint: See [8], p. 865.

**Green's Functions
in One-Body Quantum Problems**

Physical Significance of G . Application to the Free-Particle Case

Summary. The general theory developed in Chap. 1 can be applied directly to the time-independent one-particle Schrödinger equation by making the substitutions $L(\mathbf{r}) \rightarrow \mathcal{H}(\mathbf{r})$, $\lambda \rightarrow E$, where $\mathcal{H}(\mathbf{r})$ is the Hamiltonian. The formalism presented in Chap. 2, Sects. 2.1,2.2 is applicable to the time-dependent one-particle Schrödinger equation.

3.1 General Relations

The nonrelativistic, one-particle, time-independent Schrödinger equation has the form

$$[E - \mathcal{H}(\mathbf{r})]\psi(\mathbf{r}) = 0, \quad (3.1)$$

and the corresponding Green's function satisfies the equation

$$[E - \mathcal{H}(\mathbf{r})]G(\mathbf{r}, \mathbf{r}'; E) = \delta(\mathbf{r} - \mathbf{r}'). \quad (3.2)$$

Here $\mathcal{H}(\mathbf{r})$ is the Hamiltonian operator in the \mathbf{r} -representation, and $G(\mathbf{r}, \mathbf{r}'; E)$ as a function of \mathbf{r} or \mathbf{r}' satisfies the same boundary conditions as the wavefunction $\psi(\mathbf{r})$, i.e., continuity of $\psi(\mathbf{r})$ and $\nabla\psi$ (unless the potential has an infinite discontinuity) and finite (or zero) value at infinity. It is clear that the general formalism developed in Chap. 1 is directly applicable to the present case with the substitutions

$$L(\mathbf{r}) \rightarrow \mathcal{H}(\mathbf{r}), \quad (3.3a)$$

$$\lambda \rightarrow E, \quad (3.3b)$$

$$\lambda + is = z \rightarrow z = E + is, \quad (3.3c)$$

$$\lambda_n \rightarrow E_n, \quad (3.3d)$$

$$\phi_n(\mathbf{r}) \rightarrow \phi_n(\mathbf{r}). \quad (3.3e)$$

Thus, the basic relation expressing G in terms of the eigenvalues E_n and the complete set of orthonormal eigenfunctions ϕ_n of \mathcal{H} is

$$G(\mathbf{r}, \mathbf{r}'; z) = \sum_n \frac{\phi_n(\mathbf{r})\phi_n^*(\mathbf{r}')}{z - E_n}, \quad (3.4)$$

or, in the bra and ket notation,

$$G(z) = \sum_n \frac{|\phi_n\rangle\langle\phi_n|}{z - E_n} = \frac{1}{z - \mathcal{H}}. \quad (3.5)$$

The operator $G^+(E) \equiv \lim(E + is - \mathcal{H})^{-1}$ as $s \rightarrow 0^+$ is also known as the *resolvent operator* [13], p. 525.

The singularities of $G(z)$ vs. z are on the real z -axis. They can be used as follows:

1. The position of the poles of $G(z)$ coincide with the discrete eigenenergies corresponding to \mathcal{H} , and vice versa.
2. The residue at each pole E_n of $G(\mathbf{r}, \mathbf{r}'; z)$ equals $\sum_i \phi_i(\mathbf{r})\phi_i^*(\mathbf{r}')$, where the summation runs over the f_n degenerate eigenstates corresponding to the discrete eigenenergy E_n .
3. The degeneracy f_n can be found by integrating the residue (Res) of the diagonal matrix element $G(\mathbf{r}, \mathbf{r}; E_n)$ over \mathbf{r} , i.e.,

$$f_n = \int d\mathbf{r} \text{Res}\{G(\mathbf{r}, \mathbf{r}; E_n)\} = \text{Tr}\{\text{Res}\{G(E_n)\}\}. \quad (3.6)$$

For a nondegenerate eigenstate, $f_n = 1$, and consequently

$$\phi_n(\mathbf{r})\phi_n^*(\mathbf{r}') = \text{Res}\{G(\mathbf{r}, \mathbf{r}'; E_n)\}. \quad (3.7)$$

From (3.7) we see that

$$|\phi_n(\mathbf{r})| = \sqrt{|\text{Res}\{G(\mathbf{r}, \mathbf{r}; E_n)\}|}, \quad (3.8)$$

$$p_n(\mathbf{r}) = -i \ln \left\{ \frac{\text{Res}\{G(\mathbf{r}, 0; E_n)\}}{\sqrt{|\text{Res}\{G(\mathbf{r}, \mathbf{r}; E_n)\} \times \text{Res}\{G(0, 0; E_n)\}|}} \right\}, \quad (3.9)$$

where $p_n(\mathbf{r})$ is the phase of $\phi_n(\mathbf{r})$ [assuming that the phase of $\phi_n(\mathbf{r})$ for $\mathbf{r} = 0$ is zero].

4. The branch cuts of $G(z)$ along the real z -axis coincide with the continuous spectrum of \mathcal{H} , and vice versa. [We assume that the continuous spectrum of \mathcal{H} consists of extended (or propagating) eigenstates. For the case of localized eigenstates and continuous spectrum see Problem 3.1s].
5. The density of states per unit volume $\varrho(\mathbf{r}, E)$ is given by

$$\varrho(\mathbf{r}; E) = \mp \frac{1}{\pi} \text{Im}\{G^\pm(\mathbf{r}, \mathbf{r}; E)\}. \quad (3.10)$$

6. The density of states $\mathcal{N}(E)$ is given by integrating $\varrho(\mathbf{r}, E)$ over \mathbf{r} , i.e.,

$$\mathcal{N}(E) = \int d\mathbf{r} \varrho(\mathbf{r}; E) = \mp \frac{1}{\pi} \text{Tr}\{\text{Im}\{G^\pm(E)\}\}. \quad (3.11)$$

7. Using the results of Chap. 2 we can write the solution of the time-dependent Schrödinger equation,¹

$$\left(i\hbar \frac{\partial}{\partial t} - \mathcal{H} \right) |\psi(t)\rangle = 0, \quad (3.12)$$

as follows:

$$|\psi(t)\rangle = U(t - t_0) |\psi(t_0)\rangle, \quad (3.13)$$

where the time-evolution operator,

$$U(t - t_0) = \exp[-i(t - t_0)\mathcal{H}/\hbar], \quad (3.14)$$

can be expressed simply in terms of the Green's function

$$U(t - t_0) = i\hbar \tilde{g}(t - t_0) = i\hbar \int_{-\infty}^{\infty} \frac{d\omega}{2\pi} \exp[-i\omega(t - t_0)] \tilde{G}(\hbar\omega). \quad (3.15)$$

Equation (3.13) can be written in the \mathbf{r} -representation as

$$\psi(\mathbf{r}, t) = i\hbar \int \tilde{g}(\mathbf{r}, \mathbf{r}', t - t_0) \psi(\mathbf{r}', t_0) d\mathbf{r}'. \quad (3.13')$$

3.2 The Free-Particle ($\mathcal{H}_0 = p^2/2m$) Case

We denote by \mathcal{H}_0 the free-particle Hamiltonian

$$\mathcal{H}_0 = \frac{p^2}{2m} = -\frac{\hbar^2}{2m} \nabla^2 \quad (3.16)$$

and by $G_0(z)$ the corresponding Green's function

$$\left(z + \frac{\hbar^2}{2m} \nabla_r^2 \right) G_0(\mathbf{r}, \mathbf{r}'; z) = \delta(\mathbf{r} - \mathbf{r}'). \quad (3.17)$$

Equation (3.17) can be written as

$$\left(\frac{2mz}{\hbar^2} + \nabla_r^2 \right) \left[\frac{\hbar^2}{2m} G_0(\mathbf{r}, \mathbf{r}'; z) \right] = \delta(\mathbf{r} - \mathbf{r}'). \quad (3.18)$$

Comparing (3.18) with (1.36) we see that

$$G_0(\mathbf{r}, \mathbf{r}'; z) = \frac{2m}{\hbar^2} G\left(\mathbf{r}, \mathbf{r}'; \frac{2mz}{\hbar^2}\right), \quad (3.19)$$

where $G(\mathbf{r}, \mathbf{r}'; z)$ is the Green's function corresponding to the operator $L = -\nabla_r^2$; this Green's function was calculated in Sect. 1.2.

¹ $\hbar \equiv h/2\pi$, where h is Planck's constant.

The free time-dependent nonrelativistic Schrödinger equation has the form of (2.1) with $c = 1/\hbar$ and $L = -(\hbar^2/2m)\nabla^2$. Thus, the only difference from (2.23) is that the eigenvalue k^2 must be replaced by $\hbar^2 k^2/2m$. By changing variables from k^2 to $q^2 = \hbar^2 k^2/2m$, the integral is reduced to the one in (2.24) times $(2m/\hbar^2)^{d/2}$ with q^2 replaced by $q^2 (2m/\hbar^2)$. Putting $c = 1/\hbar$ at the end we find \tilde{g} for the free-particle time-dependent Schrödinger equation:

$$\tilde{g}(\mathbf{r}, \mathbf{r}'; t - t') = -\frac{i}{\hbar} \left(\frac{m}{2\pi i \hbar t} \right)^{d/2} \exp \left[i \frac{m(\mathbf{r} - \mathbf{r}')^2}{2\hbar(t - t')} \right]. \quad (3.20)$$

(For an application of (3.13') and (3.20) see Problem 3.2s).

For the Green's function of the free-particle time-independent Schrödinger equation we have the following explicit results.

3.2.1 3-d Case

$$G_0(\mathbf{r}, \mathbf{r}'; E) = -\frac{m}{2\pi\hbar^2} \frac{\exp(-k_0 |\mathbf{r} - \mathbf{r}'|)}{|\mathbf{r} - \mathbf{r}'|}, \quad E \leq 0, \quad (3.21)$$

$$G_0^\pm(\mathbf{r}, \mathbf{r}'; E) = -\frac{m}{2\pi\hbar^2} \frac{\exp(\pm i k_0 |\mathbf{r} - \mathbf{r}'|)}{|\mathbf{r} - \mathbf{r}'|}, \quad E \geq 0, \quad (3.22)$$

where

$$k_0 = \sqrt{\frac{2m|E|}{\hbar^2}} \geq 0. \quad (3.23)$$

Here $G_0(z)$ has a branch cut along the positive E -axis; this branch cut corresponds to the continuous spectrum of \mathcal{H}_0 . The discontinuity of G across the branch cut, \tilde{G} , where

$$\tilde{G}(\mathbf{r}, \mathbf{r}'; E) = G^+(\mathbf{r}, \mathbf{r}'; E) - G^-(\mathbf{r}, \mathbf{r}'; E), \quad (3.24)$$

is given in the present case by

$$\tilde{G}_0(\mathbf{r}, \mathbf{r}'; E) = -2\pi i \frac{m}{2\pi^2 \hbar^2} \frac{\sin(k_0 |\mathbf{r} - \mathbf{r}'|)}{|\mathbf{r} - \mathbf{r}'|} \theta(E). \quad (3.25)$$

In particular, the DOS per unit volume is

$$\varrho_0(\mathbf{r}; E) = \frac{\tilde{G}_0(\mathbf{r}, \mathbf{r}; E)}{-2\pi i} = \frac{m k_0}{2\pi^2 \hbar^2} \theta(E) = \theta(E) \frac{m^{3/2}}{\sqrt{2\pi^2 \hbar^3}} \sqrt{E}. \quad (3.26)$$

Note that $\varrho_0(\mathbf{r}; E)$ does not depend on \mathbf{r} due to the translational invariance of the Hamiltonian \mathcal{H}_0 .

3.2.2 2-d Case

$$G_0(\mathbf{r}, \mathbf{r}'; E) = -\frac{m}{\pi\hbar^2} K_0(k_0 |\mathbf{r} - \mathbf{r}'|) , \quad E < 0 , \quad (3.27)$$

$$G_0^\pm(\mathbf{r}, \mathbf{r}'; E) = -\frac{im}{2\hbar^2} H_0^{(1)}(\pm k_0 |\mathbf{r} - \mathbf{r}'|) , \quad E > 0 , \quad (3.28)$$

where k_0 is given by (3.23), K_0 is the zeroth-order modified Bessel function, and $H_0^{(1)}$ is the Hankel function of the first kind of zero order. The quantity $\tilde{G}_0(\mathbf{r}, \mathbf{r}'; E)$ is then

$$\tilde{G}_0(\mathbf{r}, \mathbf{r}'; E) = -2\pi i \theta(E) \frac{m}{2\pi\hbar^2} J_0(k_0 |\mathbf{r} - \mathbf{r}'|) , \quad (3.29)$$

where $J_0(x)$ is the Bessel function of the first kind of zero order and k_0 is given by (3.23). To obtain (3.29) from (3.28) we have used the relations [1]

$$H_0^{(1)}(-x) = -H_0^{(2)}(x)$$

and

$$H_0^{(1)} = J_0 + iY_0 ; \quad H_0^{(2)} = J_0 - iY_0 ,$$

where Y_0 is the Bessel function of the second kind of zero order, see [1]. The DOS per unit area is

$$\varrho_0(\mathbf{r}; E) = \frac{\tilde{G}_0(\mathbf{r}, \mathbf{r}; E)}{-2\pi i} = \theta(E) \frac{m}{2\pi\hbar^2} . \quad (3.30)$$

3.2.3 1-d Case

$$G_0(x, x'; E) = -\frac{m}{\hbar^2 k_0} \exp(-k_0 |x - x'|) , \quad E < 0 , \quad (3.31)$$

$$G_0^\pm(x, x'; E) = \mp \frac{im}{\hbar^2 k_0} \exp(\pm i k_0 |x - x'|) , \quad E > 0 , \quad (3.32)$$

where k_0 is given by (3.23). The quantity \tilde{G}_0 is then

$$\tilde{G}_0(x, x'; E) = -2\pi i \theta(E) \frac{m}{\pi\hbar^2 k_0} \cos(k_0 |x - x'|) . \quad (3.33)$$

The DOS per unit length is

$$\varrho(x; E) = \frac{\tilde{G}_0(x, x; E)}{-2\pi i} = \theta(E) \frac{m}{\pi\hbar^2 k_0} = \theta(E) \frac{\sqrt{m}}{\sqrt{2}\pi\hbar} \frac{1}{\sqrt{E}} . \quad (3.34)$$

It must be stressed that the DOS is a quantity of great importance for most branches of physics. The reason is that most quantities of physical interest depend on the DOS. For example, the thermodynamic properties of a system

of noninteracting particles can be expressed in terms of the DOS of each particle; transition probabilities, scattering amplitudes, etc., depend on the DOS of the final and initial states.

In Fig. 3.1 we plot the DOS vs. E for a free particle whose motion in 3-d, 2-d, and 1-d space is governed by the nonrelativistic Schrödinger equation. In all cases the spectrum has a lower bound (at $E = 0$) below which the DOS is zero. Energies at which the continuous spectrum terminates are called band edges in solid-state physics. We will adopt this name here.

As we shall see later, the behavior of $\varrho(E)$, $\tilde{G}(E)$, and $G(z)$ for E or z near a band edge E_B is of great physical interest. It should be noted that the analytic structures of $\varrho_0(E)$ and $\tilde{G}_0(E)$ near the band edge, $E_B = 0$, are

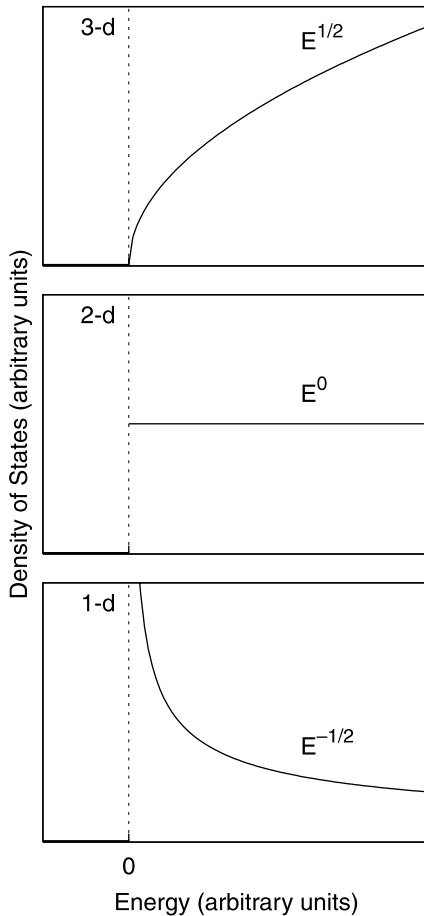


Fig. 3.1. Density of states $\mathcal{N}(E)$ ($\mathcal{N}(E)dE$ gives the number of eigenstates in the energy interval $[E, E+dE]$) vs. E for a free particle obeying the Schrödinger equation (energy-momentum relation $E = \hbar^2 k^2 / 2m$) in a d -dimensional ($d = 1, 2, 3$) space

identical [compare (3.25), (3.29), and (3.33) with (3.26), (3.30), and (3.34), respectively]. Furthermore, the analytic behavior of $\tilde{G}(E)$ or $\varrho(E)$ around an arbitrary energy E_0 determines the analytical properties of $G(z)$ for z around E_0 . (See Appendix D and the book by Muskhelishvili [15].) Thus, if $\tilde{G}(E)$ or $\varrho(E)$ is continuous around E_0 , then $G^\pm(E)$ are continuous functions of E for E in the vicinity of E_0 ; if $\tilde{G}(E)$ (or $\varrho(E)$) has a discontinuity at E_0 , then $G^\pm(E)$ exhibit a logarithmic singularity; finally, if $\tilde{G}(E)$ (or $\varrho(E)$) blows up at E_0 as $(E - E_0)^{-\gamma}$ where $0 < \gamma < 1$, then $G^\pm(E)$ also approach infinity as $(E - E_0)^{-\gamma}$.

The present results (see, e.g., Fig. 3.1) show that the behavior of $\varrho_0(E)$ (and hence $\tilde{G}_0(E)$ and $G_0^\pm(E)$) near the band edge $E_B = 0$ depends critically on the dimensionality of the system.

In the 3-d case the DOS and $\tilde{G}(E)$ are continuous functions of E approaching zero like $\sqrt{E - E_B}$ in the limit $E \rightarrow E_B^+$, [see (3.25) and (3.26)]. As a result of the general theorem stated in Appendix D, $G^\pm(E)$ are continuous functions of E as E crosses the band edge [compare (3.21) with (3.22)].

In the 2-d case the DOS and $\tilde{G}(E)$ are discontinuous at $E = 0$, see (3.29) and (3.30). As a result the Green's function $G(z)$ develops a logarithmic singularity as $z \rightarrow 0$ [see (3.27) and (3.28) and take into account that $K_0(x) \rightarrow -\ln(x)$ and $H_0^{(1)}(\pm x) \rightarrow (2i/\pi) \ln(x)$ as $x \rightarrow 0^+$].

Finally, in the 1-d case the DOS and $\tilde{G}(E)$ approach infinity as $1/\sqrt{E}$ in the limit $E \rightarrow 0^+$. As a result of the general theorems stated in Appendix D, $G(z)$ blows up like $1/\sqrt{z}$ as $z \rightarrow 0$, see (3.31) and (3.32).

The above statements connecting the dimensionality with the behavior of $G(z)$, $\tilde{G}(E)$, and the DOS near a band edge were based upon the results for the free-particle case. We shall see in Chap. 5 that the same connection exists for almost all cases where the Hamiltonian \mathcal{H} is periodic.

3.3 The Free-Particle Klein–Gordon Case

In this section we calculate the density of states (i.e., the number of eigenstates in the energy interval $[E, E + dE]$ divided by dE) for a free particle of rest mass m obeying the time-independent Klein–Gordon equation, which has the form

$$\left(\frac{E^2}{\hbar^2 c^2} - \mu^2 + \nabla_r^2 \right) \psi(\mathbf{r}) = 0, \quad (3.35)$$

with $\mu = cm/\hbar$. The formalism developed in Chap. 1 is directly applicable to the present case if one makes the substitutions

$$L(\mathbf{r}) \rightarrow -\nabla_r^2, \quad (3.36)$$

$$\lambda \rightarrow \frac{E^2}{\hbar^2 c^2} - \mu^2. \quad (3.37)$$

The DOS $\mathcal{N}(E)$ and $\varrho(E)$ with respect to the energy variable E can be obtained from the DOS $\mathcal{N}_\lambda(\lambda)$ and $\varrho_\lambda(\lambda)$ with respect to the variable λ by a simple change of variables according to (3.37), i.e.,

$$\mathcal{N}(E) = \mathcal{N}_\lambda(\lambda(E)) \frac{d\lambda}{dE} = \mathcal{N}_\lambda \left(\frac{E^2}{\hbar^2 c^2} - \mu^2 \right) \frac{2E}{\hbar^2 c^2}, \quad (3.38)$$

$$\varrho(E) = \varrho_\lambda(\lambda) \frac{d\lambda}{dE} = \varrho_\lambda \left(\frac{E^2}{\hbar^2 c^2} - \mu^2 \right) \frac{2E}{\hbar^2 c^2}, \quad (3.39)$$

where $\mathcal{N}_\lambda(\lambda)$, $\varrho_\lambda(\lambda)$ can be obtained immediately by use of (1.27), (1.28), (1.40), (1.49), and (1.56). After some simple algebra we obtain for the DOS of a free particle of rest mass m obeying the Klein–Gordon equation

$$\varrho(E) = \begin{cases} \theta(E - mc^2) \frac{E\sqrt{E^2 - m^2 c^4}}{2\pi^2 \hbar^3 c^3}, & \text{3-d,} & (3.40) \\ \theta(E - mc^2) \frac{E}{2\pi \hbar^2 c^2}, & \text{2-d,} & (3.41) \\ \theta(E - mc^2) \frac{E}{\pi \hbar c \sqrt{E^2 - m^2 c^4}}, & \text{1-d.} & (3.42) \end{cases}$$

In (3.40)–(3.42) we have kept only the positive energy solutions. If we want to keep the negative energy solutions as well, we must replace E by $|E|$ in the above equations.

Note first that (3.40)–(3.42) reduce to (3.26), (3.30), and (3.34), respectively, by introducing $E' = E - mc^2$ and assuming that $E' \ll mc^2$. Secondly, when $m = 0$, we obtain the case of a free particle obeying the wave equation. Examples of such particles are those resulting from quantizing classical wave equations such as the electromagnetic equations (the corresponding particles are, of course, the photons and c is the velocity of light) or the equation describing the propagation of sound waves in a fluid continuous medium (the corresponding particles are called phonons and c is the velocity of sound). Thus, for particles whose energy E is related to their momentum $\hbar |\mathbf{k}|$ by the relation

$$E = \hbar c |\mathbf{k}|, \quad (3.43)$$

the DOS is obtained from (3.40)–(3.42) by setting $m = 0$. We have explicitly

$$\varrho(E) = \begin{cases} \theta(E) \frac{E^2}{2\pi^2 \hbar^3 c^3}, & \text{3-d,} & (3.44) \\ \theta(E) \frac{E}{2\pi \hbar^2 c^2}, & \text{2-d,} & (3.45) \\ \theta(E) \frac{1}{\pi \hbar c}, & \text{1-d.} & (3.46) \end{cases}$$

It should be noted that the DOS given in (3.40)–(3.42) and (3.44)–(3.46) are not related to the corresponding Green's functions in the way described in

Sect. 3.2. The reason is that the relation between λ and E is not the same as in the Schrödinger case but is given by (3.37).

In Fig. 3.2 we plot the DOS vs. E for the case where the energy vs. \mathbf{k} is given by (3.43).

In most cases it is easier to obtain first the number of states per unit volume $R(E) \equiv \int_{-\infty}^E dE' \varrho(E')$ and then to calculate $\varrho(E)$ by $dR(E)/dE$. As is pointed out in Problem 1.5s, the states of a particle moving in a homogeneous or periodic medium are characterized by their wavevector \mathbf{k} ; the corresponding eigenenergy is a function of \mathbf{k} : $\varepsilon = f(\mathbf{k})$. For isotropic media $\varepsilon = f(|\mathbf{k}|)$ and the surfaces of constant energy are spheres.

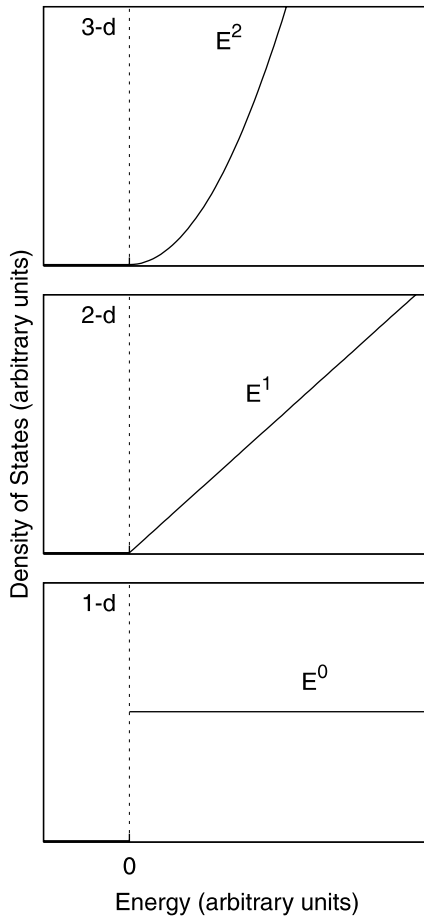


Fig. 3.2. Density of states $\mathcal{N}(E)$ ($\mathcal{N}(E)dE$ gives the number of eigenstates in the energy interval $[E, E + dE]$) vs. E for a free particle obeying the wave equation (energy–momentum relation $E = \hbar c|\mathbf{k}|$) in a d -dimensional ($d = 1, 2, 3$) space

The number of states per unit volume, $R(E)$, for a homogeneous (or periodic) medium is given by

$$R(E) = \frac{\Omega_{\mathbf{k}}(E)}{(2\pi)^d}, \quad (3.47)$$

where $\Omega_{\mathbf{k}}(E)$ is the volume of the region(s) in \mathbf{k} -space containing all points \mathbf{k} for which $f(\mathbf{k}) < E$. For the Klein–Gordon case, where $f(k) = \sqrt{m^2c^4 + c^2\hbar^2k^2}$, the inequality $f(k) < E$ defines a d -dimensional sphere of radius $k = \sqrt{(E^2 - m^2c^4)}/\hbar c$. Hence the number of states per unit volume, $R(E)$, is given by (when $E \geq mc^2$)

$$R(E) = \begin{cases} \frac{1}{(2\pi)^3} \frac{4\pi}{3} \frac{(E^2 - m^2c^4)^{3/2}}{\hbar^3 c^3}, & \text{3-d,} & (3.48a) \\ \frac{1}{(2\pi)^2} \frac{\pi (E^2 - m^2c^4)}{\hbar^2 c^2}, & \text{2-d,} & (3.48b) \\ \frac{1}{2\pi} \frac{2\sqrt{E^2 - m^2c^4}}{\hbar c}, & \text{1-d.} & (3.48c) \end{cases}$$

By differentiating (3.48a)–(3.48c) we obtain (3.40–3.42).

3.4 Summary

Knowledge of $G(z) \equiv (z - \mathcal{H})^{-1}$ permits us to obtain the discrete eigenenergies, the corresponding eigenfunctions, and the density of states in the continuous parts of the spectrum of \mathcal{H} . Knowledge of $\tilde{g}(\tau)$ allows us to calculate the time development of the wavefunction.

For the simple case where $\mathcal{H} = \mathcal{H}_0 \equiv p^2/2m$, we obtain the density of states per unit volume (area or length) as follows:

$$\varrho_0(E) = \begin{cases} \theta(E) \frac{m^{3/2}}{\sqrt{2\pi^2} \hbar^3} \sqrt{E}, & \text{3-d,} & (3.26) \end{cases}$$

$$\begin{cases} \theta(E) \frac{m}{2\pi \hbar^2}, & \text{2-d,} & (3.30) \end{cases}$$

$$\begin{cases} \theta(E) \frac{m^{1/2}}{\sqrt{2\pi} \hbar} \frac{1}{\sqrt{E}}, & \text{1-d.} & (3.34) \end{cases}$$

The behavior of $\varrho_0(E)$ near the boundary of the spectrum ($E = 0$) depends strongly on the dimensionality. The behavior of $\varrho(E)$ around an energy E_0 determines the analytical structure of $G^\pm(E)$ around E_0 . Thus, continuity of $\varrho(E)$ (as in the 3-d case) implies continuity of $G^\pm(E)$; discontinuity of $\varrho(E)$ (as in the 2-d case) implies a logarithmic singularity in $G^\pm(E)$; and divergence of $\varrho(E)$ (as in the 1-d case) implies divergence of $G^\pm(E)$ with the same critical exponent. The quantity $\varrho_0(E)$ is plotted in Fig. 3.1.

We calculated also the density of states for a free particle of mass m obeying the Klein–Gordon equation. In the particular case where $m = 0$, we have the wave equation, which implies an energy–momentum relation of the form $E = \hbar c |\mathbf{k}|$ and for which the density of states per unit volume (area or length) is

$$\varrho(E) = \begin{cases} \theta(E) \frac{E^2}{2\pi^2 \hbar^3 c^3}, & 3\text{-d}, & (3.44) \\ \theta(E) \frac{E}{2\pi \hbar^2 c^2}, & 2\text{-d}, & (3.45) \\ \theta(E) \frac{1}{\pi \hbar c}, & 1\text{-d}. & (3.46) \end{cases}$$

$\varrho(E)$ is plotted in Fig. 3.2.

The number of states per unit volume, $R(E) = \int_{-\infty}^E dE' \varrho(E')$, for a particle moving in a d -dimensional homogeneous or periodic space is given by

$$R(E) = \frac{\Omega_{\mathbf{k}}}{(2\pi)^d}, \quad (3.47)$$

where $\Omega_{\mathbf{k}}$ is the volume of the region(s) in \mathbf{k} -space whose points satisfy the inequality $f(\mathbf{k}) < E$.

Further Reading

There are many excellent textbooks on quantum mechanics. In addition to the book by Merzbacher [13] and the book by Landau and Lifshitz [12], we mention here Sakurai’s book [16], which uses a more modern approach and notation (see in particular pp. 51–60), the book by Bethe [17], which includes a very brief introduction to the Klein–Gordon equation (pp. 181–183), and the Flügge book [18], which in a problem-solution format provides an extensive list of applications (see in particular Problem 17). Finally, we mention the classical book by Schiff [19].

Problems

3.1s. Consider a quantum nonrelativistic particle moving within a d -dimensional cube of “volume” L^d . Assume that the spectrum becomes continuous in the limit $L \rightarrow \infty$ and that all eigenstates are of the form $\psi(\mathbf{r} - \mathbf{r}_i)$, where $|\psi(\mathbf{r} - \mathbf{r}_i)| < \exp(-|\mathbf{r} - \mathbf{r}_i|/L_c)$ as $|\mathbf{r} - \mathbf{r}_i| \rightarrow \infty$, where the decay length, L_c , is finite for all eigenstates. Strongly disordered potentials could produce such a situation, as we shall see in Chap. 9.

Show that the limit $L \rightarrow \infty$ of the integral of the local DOS $R(\mathbf{r}, E) = \int_{-\infty}^E dE' \varrho(\mathbf{r}, E')$, develops finite discontinuities (most of them exponentially

small) for almost all energies E . Hence $R(E)$ cannot be defined in the limit $L \rightarrow \infty$ since it develops singularities almost everywhere of the form known as the devil's staircase. On the other hand, if the states are ordinary propagating states (extended over the whole "volume" L^d), the number of states $R(E)$ approaches a regular function as $L \rightarrow \infty$.

3.2s. Consider the time evolution of a free quantum-mechanical particle obeying the 1-d Schrödinger equation

$$[i\hbar\partial_t + (\hbar^2/2m)\partial_{xx}] \psi(x, t) = 0 ,$$

with initial ($t = 0$) wavefunction of the form

$$\psi(x, 0) = \frac{1}{\sqrt{\delta x}(2\pi)^{1/4}} \exp \left[\frac{i}{\hbar} p_0 x - \frac{x^2}{4(\delta x)^2} \right] .$$

Find:

- (a) $\psi(x, t)$
- (b) $\hat{\psi}(p, t) = \int_{-\infty}^{\infty} dx e^{-ipx/\hbar} \psi(x, t)$
- (c) $\delta x(t) = \sqrt{\langle x(t)^2 \rangle - \langle x(t) \rangle^2}$
- (d) $\delta p_x(t) = \sqrt{\langle p_x(t)^2 \rangle - \langle p_x(t) \rangle^2}$
- (e) $\delta x(t)\delta p_x(t)$

3.3. Show that for a particle moving in a d -dimensional space and whose energy-wavevector relation is $\varepsilon \sim |\mathbf{k}|^s$ the DOS per unit volume is of the form

$$\varrho(E) \begin{cases} \sim E^{(d/s)-1}, & E > 0, \\ = 0 & , \quad E < 0. \end{cases}$$

Hint: See the solution of Problem 1.5s.

3.4s. The energy of a quantum in liquid He-4 depends on the wavevector \mathbf{k} as in Fig. 3.3. Give a schematic plot of the number of states per unit volume, $R(E)$, and then the DOS in the three regions $0 < E < \Delta$, $\Delta < E < \Delta'$, and $\Delta' < E$.

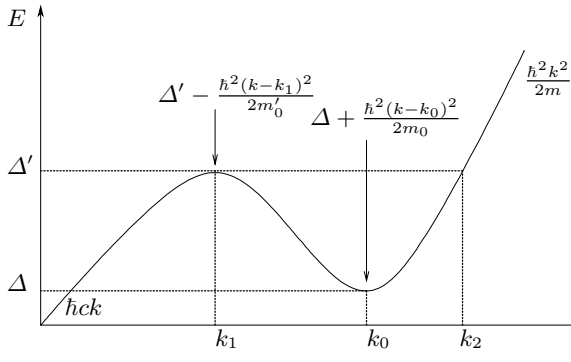


Fig. 3.3. Energy–wavevector relation of elementary excitations in liquid He-4

Green's Functions and Perturbation Theory

Summary. The problem of finding the eigenvalues and eigenfunctions of a Hamiltonian $\mathcal{H} = \mathcal{H}_0 + \mathcal{H}_1$ can be solved in three steps: 1) Calculate the Green's function $G_0(z)$ corresponding to \mathcal{H}_0 . 2) Express $G(z)$ as a perturbation series in terms of $G_0(z)$ and \mathcal{H}_1 , where $G(z)$ is the Green's function associated with \mathcal{H} . 3) Extract from $G(z)$ information about the eigenvalues and eigenfunctions of \mathcal{H} .

4.1 Formalism

4.1.1 Time-Independent Case

In this chapter we consider the very important and common case where the one-particle Hamiltonian \mathcal{H} can be separated into an unperturbed part \mathcal{H}_0 and a perturbation \mathcal{H}_1

$$\mathcal{H} = \mathcal{H}_0 + \mathcal{H}_1 . \quad (4.1)$$

It is implicitly assumed that \mathcal{H}_0 is such that its eigenvalues and eigenfunctions can be easily obtained. The question is to determine the eigenvalues and eigenfunctions of \mathcal{H} . Very often this goal is achieved by taking the following indirect path:

1. Determine first the Green's function G_0 associated with the unperturbed part \mathcal{H}_0 .
2. Express the Green's function G associated with the total Hamiltonian \mathcal{H} in terms of G_0 and \mathcal{H}_1 .
3. Obtain information about the eigenvalues and eigenfunctions of \mathcal{H} from G .

Step 3 above has been examined in detail in Chap. 1 and Sect. 3.1. The implementation of step 1 depends on \mathcal{H}_0 . For the very common and important case where $\mathcal{H}_0 = p^2/2m$, G_0 has been obtained in Sect. 3.2. In the next chapter a whole class of \mathcal{H}_0 s will be introduced, and the corresponding G_0 s will be calculated. In the present section we examine in some detail step 2, i.e., how G can be expressed in terms of G_0 and \mathcal{H}_1 .

The Green's functions $G_0(z)$ and $G(z)$ corresponding to \mathcal{H}_0 and \mathcal{H} , respectively, are

$$G_0(z) = (z - \mathcal{H}_0)^{-1} \quad \text{and} \quad (4.2)$$

$$G(z) = (z - \mathcal{H})^{-1} . \quad (4.3)$$

Using (4.1) and (4.2) we can rewrite (4.3) as follows:

$$\begin{aligned} G(z) &= (z - \mathcal{H}_0 - \mathcal{H}_1)^{-1} = \left\{ (z - \mathcal{H}_0) \left[1 - (z - \mathcal{H}_0)^{-1} \mathcal{H}_1 \right] \right\}^{-1} \\ &= \left[1 - (z - \mathcal{H}_0)^{-1} \mathcal{H}_1 \right]^{-1} (z - \mathcal{H}_0)^{-1} \\ &= [1 - G_0(z) \mathcal{H}_1]^{-1} G_0(z) . \end{aligned} \quad (4.4)$$

Expanding the operator $(1 - G_0 \mathcal{H}_1)^{-1}$ in power series we obtain

$$G = G_0 + G_0 \mathcal{H}_1 G_0 + G_0 \mathcal{H}_1 G_0 \mathcal{H}_1 G_0 + \dots . \quad (4.5)$$

Equation (4.5) can be written in a compact form

$$G = G_0 + G_0 \mathcal{H}_1 (G_0 + G_0 \mathcal{H}_1 G_0 + \dots) = G_0 + G_0 \mathcal{H}_1 G \quad (4.6)$$

or

$$G = G_0 + (G_0 + G_0 \mathcal{H}_1 G_0 + \dots) \mathcal{H}_1 G_0 = G_0 + G \mathcal{H}_1 G_0 . \quad (4.7)$$

In the \mathbf{r} -representation, (4.6) becomes

$$\begin{aligned} G(\mathbf{r}, \mathbf{r}'; z) &= G_0(\mathbf{r}, \mathbf{r}'; z) \\ &\quad + \int d\mathbf{r}_1 d\mathbf{r}_2 G_0(\mathbf{r}, \mathbf{r}_1; z) \mathcal{H}_1(\mathbf{r}_1, \mathbf{r}_2) G(\mathbf{r}_2, \mathbf{r}'; z) . \end{aligned} \quad (4.6')$$

Usually $\mathcal{H}_1(\mathbf{r}_1, \mathbf{r}_2)$ has the form $\delta(\mathbf{r}_1 - \mathbf{r}_2) V(\mathbf{r}_1)$; then (4.6') becomes

$$\begin{aligned} G(\mathbf{r}, \mathbf{r}'; z) &= G_0(\mathbf{r}, \mathbf{r}'; z) \\ &\quad + \int d\mathbf{r}_1 G_0(\mathbf{r}, \mathbf{r}_1; z) V(\mathbf{r}_1) G(\mathbf{r}_1, \mathbf{r}'; z) , \end{aligned} \quad (4.8)$$

i.e., $G(\mathbf{r}, \mathbf{r}'; z)$ satisfies a linear inhomogeneous integral equation with a kernel $G_0(\mathbf{r}, \mathbf{r}_1; z) V(\mathbf{r}_1)$. Equation (4.7) can be written also in a similar form. If we use the \mathbf{k} -representation, we can rewrite (4.6) as follows:

$$G(\mathbf{k}, \mathbf{k}'; z) = G_0(\mathbf{k}, \mathbf{k}'; z) + \sum_{\mathbf{k}_1 \mathbf{k}_2} G_0(\mathbf{k}, \mathbf{k}_1; z) \mathcal{H}_1(\mathbf{k}_1, \mathbf{k}_2) G(\mathbf{k}_2, \mathbf{k}'; z) . \quad (4.9)$$

Taking into account that $\langle \mathbf{r} | \mathbf{k} \rangle = e^{i\mathbf{k} \cdot \mathbf{r}} / \sqrt{\Omega}$ and that

$$\sum_{\mathbf{k}} = \Omega \int \frac{d\mathbf{k}}{(2\pi)^d} , \quad (4.10)$$

where d is the dimensionality, one can easily show that (4.9) is the Fourier transform of (4.6'), as it should be.

At this point we introduce the so-called t -matrix, which is of central importance in scattering theory and is directly related to G and G_0 . The t -matrix, $T(z)$, corresponding to the unperturbed Hamiltonian \mathcal{H}_0 , the perturbation part \mathcal{H}_1 , and the parameter z , is defined by the operator equation

$$T(z) \equiv \mathcal{H}_1 G(z) (z - \mathcal{H}_0) . \quad (4.11)$$

The above definition of $T(z)$ is valid for $z \neq \{E_n\}$, where $\{E_n\}$ are the eigenvalues of \mathcal{H} . If $z = E$, where E belongs to the continuous spectrum of \mathcal{H} , we define

$$T^\pm(E) = \mathcal{H}_1 G^\pm(E) (E - \mathcal{H}_0) . \quad (4.12)$$

Finally, if z coincides with one of the discrete eigenvalues of \mathcal{H} , say, E_n , then $T(E_n)$ is not defined because $G(z)$ [and hence $T(z)$] has a simple pole at E_n . This statement is correct except in the pathological case where the eigenvalue E_n and the corresponding eigenfunction $|\psi_n\rangle$ of \mathcal{H} satisfy the relation $\mathcal{H}_0 |\psi_n\rangle = E_n |\psi_n\rangle$. In this case, the pole of $G(z)$ at E_n is cancelled by the zero of $z - \mathcal{H}_0$ at $z = E_n$, and $T(z)$ is analytic around E_n .

The analytic structure of $T(z)$ is quite similar to $G(z)$: $T(z)$ is analytic in the complex z -plane; it has singularities on the real z -axis. The positions of the poles of $T(z)$ on the real axis give the discrete eigenvalues of \mathcal{H} and vice versa. The continuous spectrum of \mathcal{H} produces a branch cut in $T(z)$. Note that the analytic continuation of $T(z)$ across the branch cut does not coincide with $T(z)$, and it may develop singularities for complex values of z .

Using (4.5) and (4.11), we obtain the following expansion for $T(z)$:

$$T(z) = \mathcal{H}_1 + \mathcal{H}_1 G_0(z) \mathcal{H}_1 + \mathcal{H}_1 G_0(z) \mathcal{H}_1 G_0(z) \mathcal{H}_1 + \cdots . \quad (4.13)$$

The summation in (4.13) can be performed to give

$$T(z) = \mathcal{H}_1 + \mathcal{H}_1 (G_0 + G_0 \mathcal{H}_1 G_0 + \cdots) \mathcal{H}_1 = \mathcal{H}_1 + \mathcal{H}_1 G \mathcal{H}_1 \quad (4.14)$$

$$= \mathcal{H}_1 + \mathcal{H}_1 G_0 (\mathcal{H}_1 + \mathcal{H}_1 G_0 \mathcal{H}_1 + \cdots) = \mathcal{H}_1 + \mathcal{H}_1 G_0 T \quad (4.15)$$

$$= \mathcal{H}_1 + (\mathcal{H}_1 + \mathcal{H}_1 G_0 \mathcal{H}_1 + \cdots) G_0 \mathcal{H}_1 = \mathcal{H}_1 + T G_0 \mathcal{H}_1 . \quad (4.16)$$

With the help of T , the basic equation (4.5) can be rewritten as

$$G(z) = G_0(z) + G_0(z) T(z) G_0(z) , \quad (4.17)$$

which means that knowledge of T allows immediate determination of G .

Equations (4.15) and (4.16) in the \mathbf{r} - or \mathbf{k} -representation will become linear inhomogeneous integral equations for the unknown quantity $T(\mathbf{r}, \mathbf{r}'; z)$ or $T(\mathbf{k}, \mathbf{k}'; z)$; e.g., (4.15) in the \mathbf{k} -representation is

$$T(\mathbf{k}, \mathbf{k}'; z) = \mathcal{H}_1(\mathbf{k}, \mathbf{k}') + \sum_{\mathbf{k}_1 \mathbf{k}_2} \mathcal{H}_1(\mathbf{k}, \mathbf{k}_1) G_0(\mathbf{k}_1, \mathbf{k}_2; z) T(\mathbf{k}_2, \mathbf{k}'; z) , \quad (4.18)$$

where

$$\begin{aligned} \mathcal{H}_1(\mathbf{k}, \mathbf{k}') &\equiv \langle \mathbf{k} | \mathcal{H}_1 | \mathbf{k}' \rangle \\ &= \frac{1}{\Omega} \int d\mathbf{r} d\mathbf{r}' \exp(-i\mathbf{k} \cdot \mathbf{r} + i\mathbf{k}' \cdot \mathbf{r}') \mathcal{H}_1(\mathbf{r}, \mathbf{r}') , \end{aligned} \quad (4.19)$$

$$\begin{aligned} G_0(\mathbf{k}_1, \mathbf{k}_2; z) &\equiv \langle \mathbf{k}_1 | G_0(z) | \mathbf{k}_2 \rangle \\ &= \frac{1}{\Omega} \int d\mathbf{r}_1 d\mathbf{r}_2 \exp(-i\mathbf{k}_1 \cdot \mathbf{r}_1 + i\mathbf{k}_2 \cdot \mathbf{r}_2) G_0(\mathbf{r}_1, \mathbf{r}_2; z) , \end{aligned} \quad (4.20)$$

$$\begin{aligned} T(\mathbf{k}, \mathbf{k}'; z) &\equiv \langle \mathbf{k} | T(z) | \mathbf{k}' \rangle \\ &= \frac{1}{\Omega} \int d\mathbf{r} d\mathbf{r}' \exp(-i\mathbf{k} \cdot \mathbf{r} + i\mathbf{k}' \cdot \mathbf{r}') T(\mathbf{r}, \mathbf{r}'; z) . \end{aligned} \quad (4.21)$$

If $\mathcal{H}_1(\mathbf{r}, \mathbf{r}') = \delta(\mathbf{r} - \mathbf{r}') V(\mathbf{r})$, then $\mathcal{H}_1(\mathbf{k}, \mathbf{k}')$ reduces to

$$\mathcal{H}_1(\mathbf{k}, \mathbf{k}') = \frac{V(\mathbf{k} - \mathbf{k}')}{\Omega} , \quad (4.22)$$

where $V(\mathbf{q})$ is the Fourier transform of $V(\mathbf{r})$, i.e.,

$$V(\mathbf{q}) = \int d\mathbf{r} V(\mathbf{r}) e^{-i\mathbf{q} \cdot \mathbf{r}} . \quad (4.23)$$

In the usual case, where $G_0(\mathbf{r}_1, \mathbf{r}_2)$ is a function of the difference $(\mathbf{r}_1 - \mathbf{r}_2)$ only, we have from (4.20) that

$$G_0(\mathbf{k}_1, \mathbf{k}_2; z) = \delta_{\mathbf{k}_1, \mathbf{k}_2} G_0(\mathbf{k}_1; z) , \quad (4.24)$$

where $G_0(\mathbf{k}; z)$ is the Fourier transform of $G(\mathbf{r}_1, \mathbf{r}_2; z)$ with respect to the variable $\mathbf{q} = \mathbf{r}_1 - \mathbf{r}_2$. Under these conditions, (4.18) can be written as

$$\begin{aligned} T'(\mathbf{k}, \mathbf{k}'; z) &= V(\mathbf{k} - \mathbf{k}') \\ &+ \int \frac{d\mathbf{k}_1}{(2\pi)^d} V(\mathbf{k} - \mathbf{k}_1) G_0(\mathbf{k}_1; z) T'(\mathbf{k}_1, \mathbf{k}'; z) , \end{aligned} \quad (4.25)$$

where $T'(\mathbf{k}, \mathbf{k}'; z) = \Omega T(\mathbf{k}, \mathbf{k}'; z)$.

As was mentioned before, knowledge of $G(z)$ [or, equivalently, $T(z)$] allows us to determine the discrete eigenvalues and the corresponding eigenfunctions of \mathcal{H} ; it permits us also to obtain the DOS of the continuous part of the spectrum of \mathcal{H} . Now we would like to examine how the eigenstates associated with the continuous spectrum of \mathcal{H} can be obtained. The time-independent Schrödinger equation, $(E - \mathcal{H})|\psi\rangle = 0$, can be written as

$$(E - \mathcal{H}_0)|\psi\rangle = \mathcal{H}_1|\psi\rangle ; \quad (4.26)$$

E belongs to the continuous spectrum of \mathcal{H} . Equation (4.26) can be considered as an inhomogeneous equation whose general solution is [according to (1.33b)]

$$|\psi^\pm\rangle = |\phi\rangle + G_0^\pm(E)\mathcal{H}_1|\psi^\pm\rangle, \quad (4.27)$$

where $|\phi\rangle$ is the general solution of $(E - \mathcal{H}_0)|\phi\rangle = 0$ assuming that E belongs to the continuous spectrum of both \mathcal{H} and \mathcal{H}_0 ; superscripts \pm have been introduced in order to distinguish the solutions associated with G_0^+ from those associated with G_0^- . Equation (4.27) is an integral equation for the unknown functions $|\psi^\pm\rangle$; in the \mathbf{r} -representation we can rewrite (4.27) as

$$\psi^\pm(\mathbf{r}) = \phi(\mathbf{r}) + \int d\mathbf{r}_1 d\mathbf{r}_2 G_0^\pm(\mathbf{r}, \mathbf{r}_1; E) \mathcal{H}_1(\mathbf{r}_1, \mathbf{r}_2) \psi^\pm(\mathbf{r}_2), \quad (4.27')$$

or, in the usual case where $\mathcal{H}(\mathbf{r}_1, \mathbf{r}_2) = \delta(\mathbf{r}_1 - \mathbf{r}_2)V(\mathbf{r}_1)$,

$$\psi^\pm(\mathbf{r}) = \phi(\mathbf{r}) + \int d\mathbf{r}_1 G_0^\pm(\mathbf{r}, \mathbf{r}_1; E) V(\mathbf{r}_1) \psi^\pm(\mathbf{r}_1). \quad (4.28)$$

Equation (4.27') or (4.28) is the *Lippman-Schwinger equation*. If E does not belong to the spectrum of \mathcal{H}_0 , (4.28) becomes homogeneous because then $\phi(\mathbf{r}) = 0$,

$$\psi(\mathbf{r}) = \int d\mathbf{r}_1 G_0(\mathbf{r}, \mathbf{r}_1; E) V(\mathbf{r}_1) \psi(\mathbf{r}_1). \quad (4.29)$$

Usually, \mathcal{H}_0 and \mathcal{H}_1 are chosen in such a way that the continuous spectra of \mathcal{H}_0 and \mathcal{H} coincide. Then (4.27) and (4.28) are appropriate for finding the eigenfunctions of \mathcal{H} associated with the continuous spectrum (of either \mathcal{H}_0 or \mathcal{H}) while (4.29) gives the discrete eigenfunctions and eigenvalues of \mathcal{H} , assuming that the discrete eigenvalues of \mathcal{H}_0 and \mathcal{H} do not coincide. It should be recalled that once $G(z)$ [or $T(z)$] is known, one need not solve (4.29) to obtain the discrete spectrum since the latter can be determined directly from G or T .

By iterating (4.27) we obtain

$$|\psi^\pm\rangle = |\phi\rangle + G_0^\pm\mathcal{H}_1|\phi\rangle + G_0^\pm\mathcal{H}_1G_0^\pm\mathcal{H}_1|\phi\rangle + \dots \quad (4.30)$$

Using (4.13), we can express (4.30) in terms of T^\pm :

$$|\psi^\pm\rangle = |\phi\rangle + G_0^\pm T^\pm |\phi\rangle. \quad (4.31)$$

By multiplying (4.5) from the left or from the right by \mathcal{H}_1 and using (4.13), we have

$$\mathcal{H}_1 G = T G_0 \quad \text{or} \quad G \mathcal{H}_1 = G_0 T. \quad (4.32)$$

Substituting (4.32) into (4.31) we have

$$|\psi^\pm\rangle = |\phi\rangle + G^\pm \mathcal{H}_1 |\phi\rangle. \quad (4.33)$$

Equations (4.31) and (4.33) are important because they express the eigenfunctions $|\psi^\pm\rangle$ in terms of T^\pm or G^\pm in a closed form. Comparing (4.31) with (4.27) and assuming that G_0^\pm is not zero, we obtain

$$T^\pm |\phi\rangle = \mathcal{H}_1 |\psi^\pm\rangle. \quad (4.34)$$

4.1.2 Time-Dependent Case

Similar expressions can be obtained for the solution of the time-dependent Schrödinger equation, which is written as

$$\left(i\hbar \frac{\partial}{\partial t} - \mathcal{H}_0 \right) |\psi(t)\rangle = \mathcal{H}_1(t) |\psi(t)\rangle, \quad (4.35)$$

where \mathcal{H}_1 can be time dependent. From the general relation (2.21) we have

$$|\psi(t)^\pm\rangle = |\phi(t)\rangle + \int_{-\infty}^{\infty} dt' g_0^\pm(t-t') \mathcal{H}_1(t') |\psi^\pm(t')\rangle. \quad (4.36)$$

On physical grounds one keeps the $|\psi^+(t)\rangle$ solution because it is causal, i.e., the effects of \mathcal{H}_1 on the eigenfunction appear after \mathcal{H}_1 has been applied. Equation (4.36) can be iterated to give

$$\begin{aligned} |\psi^+(t)\rangle &= |\phi(t)\rangle \\ &+ \int dt_1 g_0^+(t-t_1) \mathcal{H}_1(t_1) |\phi(t_1)\rangle \\ &+ \int dt_1 dt_2 g_0^+(t-t_1) \mathcal{H}_1(t_1) g_0^+(t_1-t_2) \mathcal{H}_1(t_2) |\phi(t_2)\rangle \\ &+ \dots \end{aligned} \quad (4.37)$$

Let us assume that $\mathcal{H}_1(t) = 0$ for $t < t_0$ and that $|\phi(t_0)\rangle$ is an eigenfunction of \mathcal{H}_0 , say, $|\phi_n\rangle$. From (2.16) and (2.17) we have that

$$\begin{aligned} |\phi(t)\rangle &= \exp[-iE_n(t-t_0)/\hbar] |\phi_n\rangle = \exp[-i\mathcal{H}_0(t-t_0)/\hbar] |\phi_n\rangle \\ &= i\hbar \tilde{g}_0(t-t_0) |\phi_n\rangle. \end{aligned} \quad (4.38)$$

Under these initial conditions, (4.37) can be written as

$$|\psi^+(t)\rangle = A(t, t_0) |\phi_n\rangle, \quad (4.39)$$

where

$$\begin{aligned} A(t, t_0) &= i\hbar \tilde{g}(t-t_0) + i\hbar \int_{t_0}^t dt_1 \tilde{g}_0(t-t_1) \mathcal{H}_1(t_1) \tilde{g}_0(t_1-t_0) \\ &+ i\hbar \int_{t_0}^t dt_1 \int_{t_0}^{t_1} dt_2 \tilde{g}_0(t-t_1) \mathcal{H}_1(t_1) g_0^+(t_1-t_2) \mathcal{H}_1(t_2) \tilde{g}_0(t_2-t_0) \\ &+ \dots \end{aligned} \quad (4.40)$$

In obtaining (4.39) and (4.40) we have taken into account (4.38) and the relation $g^+(\tau) = \theta(\tau) \tilde{g}(\tau)$.

The probability amplitude for a transition from state $|\phi_n\rangle$ to state $|\phi_m\rangle$ as a result of $\mathcal{H}_1(t)$ acting during the time interval $[t_0, t]$ can be calculated from (4.38)–(4.40) as

$$\begin{aligned}
\langle \phi_m | A(t, t_0) | \phi_n \rangle &= \exp\left(\frac{-iE_m t + iE_n t_0}{\hbar}\right) \\
&\times \left[\langle \phi_m | \phi_n \rangle + \frac{-i}{\hbar} \int_{t_0}^t dt_1 \left\langle \phi_m \left| \exp\left(\frac{i\mathcal{H}_0 t_1}{\hbar}\right) \mathcal{H}_1(t_1) \exp\left(\frac{-i\mathcal{H}_0 t_1}{\hbar}\right) \right| \phi_n \right\rangle \right. \\
&\quad + \frac{-i}{\hbar} \int_{t_0}^t dt_1 dt_2 \\
&\quad \times \left\langle \phi_m \left| \exp\left(\frac{i\mathcal{H}_0 t_1}{\hbar}\right) \mathcal{H}_1(t_1) g_0^+(t_1 - t_2) \mathcal{H}_1(t_2) \exp\left(\frac{-i\mathcal{H}_0 t_2}{\hbar}\right) \right| \phi_n \right\rangle \\
&\quad \left. + \dots \right]. \tag{4.41}
\end{aligned}$$

In order to get rid of the unimportant phase factor in (4.41) we define an operator $S(t, t_0)$ as follows:

$$S(t, t_0) \equiv \exp\left(\frac{i\mathcal{H}_0 t}{\hbar}\right) A(t, t_0) \exp\left(\frac{-i\mathcal{H}_0 t_0}{\hbar}\right). \tag{4.42}$$

The matrix element $\langle \phi_m | S(t, t_0) | \phi_n \rangle$ is the quantity in parentheses in (4.41), which can be rewritten as

$$\begin{aligned}
\langle \phi_m | S(t, t_0) | \phi_n \rangle &= \delta_{mn} + \frac{-i}{\hbar} \int_{t_0}^t dt_1 \exp(i\omega_{mn} t_1) \langle \phi_m | \mathcal{H}_1(t_1) | \phi_n \rangle \\
&\quad + \frac{-i}{\hbar} \int_{t_0}^t dt_1 dt_2 \int \frac{d\omega}{2\pi} \exp[it_1(\omega_m - \omega)] \exp[it_2(\omega - \omega_n)] \\
&\quad \quad \times \langle \phi_m | \mathcal{H}_1(t_1) G_0^+(\hbar\omega) \mathcal{H}_1(t_2) | \phi_n \rangle \\
&\quad + \dots, \tag{4.43}
\end{aligned}$$

where $\omega_n = E_n/\hbar$, $\omega_m = E_m/\hbar$, and $\omega_{mn} = \omega_m - \omega_n$.

Equation (4.43) implies that the probability amplitude (apart from unimportant phase factors) for a transition between two different states $|\phi_n\rangle$ and $|\phi_m\rangle$ as a result of $\mathcal{H}_1(t)$ acting during the infinite period from $-\infty$ to $+\infty$ is

$$\langle \phi_m | S | \phi_n \rangle = \frac{-i}{\hbar} \int_{-\infty}^{\infty} dt_1 \exp(i\omega_{mn} t_1) \langle \phi_m | \mathcal{H}_1(t_1) | \phi_n \rangle + \dots, \tag{4.44}$$

where

$$S \equiv \lim_{\substack{t \rightarrow +\infty \\ t_0 \rightarrow -\infty}} S(t, t_0) \tag{4.45}$$

is the so-called S -matrix. Equation (4.44) is the basic result in time-dependent perturbation theory.

To obtain S for the particular case where \mathcal{H}_1 is a time-independent operator, we have to take the limits $t \rightarrow \infty$ and $t_0 \rightarrow -\infty$ symmetrically, i.e., $t = -t_0 \rightarrow \infty$. We have then

$$\begin{aligned}
\langle \phi_m | S | \phi_n \rangle &= \delta_{mn} \\
&+ \langle \phi_m | \mathcal{H}_1 | \phi_n \rangle \frac{-i}{\hbar} \int_{-\infty}^{\infty} dt_1 \exp(i\omega_{mn}t_1) \\
&+ \frac{-i}{\hbar} \int \frac{d\omega}{2\pi} \langle \phi_m | \mathcal{H}_1 G_0^+(\hbar\omega) \mathcal{H}_1 | \phi_n \rangle \\
&\quad \times \int_{-\infty}^{\infty} dt_1 \int_{-\infty}^{\infty} dt_2 \exp[it_1(\omega_m - \omega)] \exp[it_2(\omega - \omega_n)] + \dots \\
&= \delta_{mn} - 2\pi i \delta(E_n - E_m) [\langle \phi_m | \mathcal{H}_1 | \phi_n \rangle \\
&\quad + \langle \phi_m | \mathcal{H}_1 G_0^+(E_n) \mathcal{H}_1 | \phi_n \rangle + \dots] \\
&= \delta_{mn} - 2\pi i \delta(E_n - E_m) \langle \phi_m | T^+(E_n) | \phi_n \rangle ; \tag{4.46}
\end{aligned}$$

to arrive at the last result we employ the relation

$$\int_{-\infty}^{\infty} dt e^{iEt/\hbar} = 2\pi\hbar\delta(E) . \tag{4.47}$$

Notice that the result (4.46) is equivalent to the following expression for $\langle \phi_m | S(t, t_0) | \phi_n \rangle$ in the limits $t = -t_0 \rightarrow \infty$:

$$\begin{aligned}
&\langle \phi_m | S(t, t_0) | \phi_n \rangle \\
&= \delta_{mn} - \frac{i}{\hbar} \langle \phi_m | T^+(E_n) | \phi_n \rangle \int_{t_0}^t \exp(i\omega_{mn}t') dt' . \tag{4.46'}
\end{aligned}$$

Equation (4.46') allow us to obtain the *rate* of the transition probability (for \mathcal{H}_1 being independent of t); indeed, for $m \neq n$ we have

$$\begin{aligned}
&|\langle \phi_m | S(t, t_0) | \phi_n \rangle|^2 \\
&= \frac{1}{\hbar^2} |\langle \phi_m | T^+(E_n) | \phi_n \rangle|^2 \int_{t_0}^t dt_1 \int_{t_0}^t dt_2 \exp[i\omega_{mn}(t_1 - t_2)] .
\end{aligned}$$

Changing variables from t_1, t_2 to $T = (t_1 + t_2)/2$, $\tau = t_1 - t_2$ and taking the limit $t_0 \rightarrow -\infty$, we have

$$\begin{aligned}
&|\langle \phi_m | S(t, t_0) | \phi_n \rangle|^2 \\
&= \frac{1}{\hbar^2} |\langle \phi_m | T^+(E_n) | \phi_n \rangle|^2 \int_{-\infty}^t dT \int_{-\infty}^{\infty} d\tau \exp(i\omega_{mn}\tau) .
\end{aligned}$$

Hence, taking into account (4.47), we obtain

$$\begin{aligned}
W_{mn} &\equiv \lim_{t_0 \rightarrow -\infty} \frac{d}{dt} |\langle \phi_m | S(t, t_0) | \phi_n \rangle|^2 \\
&= \frac{2\pi}{\hbar} |\langle \phi_m | T^+(E_n) | \phi_n \rangle|^2 \delta(E_m - E_n) . \tag{4.48}
\end{aligned}$$

The exact equation (4.48) to the first order of perturbation theory, where $\langle \phi_m | T^+(E_n) | \phi_n \rangle$ is replaced by $\langle \phi_m | \mathcal{H}_1 | \phi_n \rangle$, reduces to the well-known and extensively used *Fermi's "golden rule."*

Since $|\phi_n\rangle$ is assumed normalized, we have that $|\psi^+(t)\rangle$ is normalized, i.e.,

$$1 = \langle \psi^+(t) | \psi^+(t) \rangle = \langle \phi_n | A^+(t, t_0) A(t, t_0) | \phi_n \rangle ,$$

which implies that $A(t, t_0)$ is unitary. Using definition (4.42) it is easy to show then that $S(t, t_0)$ is unitary, too. Thus for the S -matrix we have

$$S^\dagger S = S S^\dagger = 1 . \quad (4.49)$$

Equation (4.49) can be expressed in terms of the t -matrix using (4.46):

$$\begin{aligned} & \langle \phi_n | T^+(E_n) | \phi_\ell \rangle - \langle \phi_n | T^-(E_n) | \phi_\ell \rangle = \\ & -2\pi i \sum_m \langle \phi_n | T^-(E_n) | \phi_m \rangle \langle \phi_m | T^+(E_n) | \phi_\ell \rangle \delta(E_m - E_n) . \end{aligned} \quad (4.50)$$

Equation (4.50) can also be derived from $T = \mathcal{H}_1 + \mathcal{H}_1 G \mathcal{H}_1$, which implies that $T^+ - T^- = \mathcal{H}_1(G^+ - G^-)\mathcal{H}_1 = -2\pi i \mathcal{H}_1 \delta(E - H) \mathcal{H}_1$. The rest of the proof is left to the reader. As we shall see in the next section, (4.50) is equivalent to the so-called optical theorem in scattering theory; in other words, the optical theorem stems from the unitarity of S .

Before we conclude the present discussion we will recast the expression for the S -matrix in a form that is convenient for future manipulations:

$$\begin{aligned} S = 1 + & \frac{-i}{\hbar} \int_{-\infty}^{\infty} dt_1 \mathcal{H}_1^I(t_1) \\ & + \left(\frac{-i}{\hbar} \right)^2 \int_{-\infty}^{\infty} dt_1 \mathcal{H}_1^I(t_1) \int_{-\infty}^{t_1} dt_2 \mathcal{H}_1^I(t_2) + \dots , \end{aligned} \quad (4.51)$$

where

$$\mathcal{H}_1^I(t) \equiv \exp(i\mathcal{H}_0 t/\hbar) \mathcal{H}_1(t) \exp(-i\mathcal{H}_0 t/\hbar) . \quad (4.52)$$

To obtain (4.51) we have used the relation

$$\begin{aligned} g_0^+(t_1 - t_2) &= \theta(t_1 - t_2) \tilde{g}_0(t_1 - t_2) \\ &= \theta(t_1 - t_2) \frac{-i}{\hbar} \exp[-i\mathcal{H}_0(t_1 - t_2)/\hbar] . \end{aligned} \quad (4.53)$$

The restrictions in the intermediate integrations in (4.51) can be relaxed if at the same time we divide the n th term ($n = 1, 2, 3, \dots$) by $n!$ [20]. However, in writing products of \mathcal{H}_1^I s, one must make certain that the original ordering of the operators is preserved, i.e., the product is ordered in such a way that earlier times appear to the right. To make this chronological ordering explicit, we define the time-ordered product of operators \mathcal{H}_1^I as

$$T [\mathcal{H}_1^I(t_i) \cdots \mathcal{H}_1^I(t_j) \cdots] = \mathcal{H}_1^I(t_1) \mathcal{H}_1^I(t_2) \cdots \mathcal{H}_1^I(t_n) , \quad (4.54)$$

where t_1, t_2, \dots, t_n satisfy the relations $t_1 > t_2 > \dots > t_n$ and $t_i \cdots t_j \cdots$ is any permutation of t_1, t_2, \dots, t_n . With this definition (4.51) becomes

$$\begin{aligned}
S &= \sum_{n=0}^{\infty} \left(\frac{-i}{\hbar} \right)^n \frac{1}{n!} \int dt_1 dt_2 \cdots dt_n T [\mathcal{H}_1^I(t_1) \cdots \mathcal{H}_1^I(t_n)] \\
&= T \exp \left[-\frac{i}{\hbar} \int dt \mathcal{H}_1^I(t) \right]. \tag{4.55}
\end{aligned}$$

The last expression in (4.55) is simply a compact way of writing the sum.

4.2 Applications

4.2.1 Scattering Theory ($E > 0$)

In this and the next section we take $\mathcal{H}_0 = p^2/2m = -\hbar^2 \nabla^2/2m$; the perturbation $\mathcal{H}_1(\mathbf{r}, \mathbf{r}')$ is of the form $\delta(\mathbf{r} - \mathbf{r}')V(\mathbf{r})$, where $V(\mathbf{r})$ is of finite extent [i.e., $V(\mathbf{r})$ decays fast enough as $r \rightarrow \infty$]. Here \mathcal{H}_0 has a continuous spectrum that extends from zero to $+\infty$. The continuous spectrum of \mathcal{H} coincides with that of \mathcal{H}_0 ; \mathcal{H} , however, may develop discrete levels of negative eigenenergies if $V(\mathbf{r})$ is negative in some region(s). In this section we will examine questions related to the continuous spectrum ($E > 0$), while in the next section we examine the question of a discrete level for very shallow $V(\mathbf{r})$.

The problem of physical interest for $E > 0$ is scattering: an incident particle of energy $E = \hbar^2 k^2/2m$, described by the unperturbed wave function $e^{i\mathbf{k} \cdot \mathbf{r}}/\sqrt{\Omega}$, comes under the influence of the perturbation $V(\mathbf{r})$, and as a result its wave function is modified. The question is to find the asymptotic behavior (as $r \rightarrow \infty$) of this modification.

The solution of the scattering problem can be obtained immediately from (4.31), which in the \mathbf{r} -representation becomes

$$\psi^{\pm}(\mathbf{r}) = \frac{1}{\sqrt{\Omega}} e^{i\mathbf{k} \cdot \mathbf{r}} + \frac{1}{\sqrt{\Omega}} \int d\mathbf{r}_1 d\mathbf{r}_2 G_0^{\pm}(\mathbf{r}, \mathbf{r}_1) T^{\pm}(\mathbf{r}_1, \mathbf{r}_2) e^{i\mathbf{k} \cdot \mathbf{r}_2}. \tag{4.56}$$

Using the expression for the 3-d $G_0^{\pm}(\mathbf{r}, \mathbf{r}_1)$, which we obtained in Sect. 3.2, we can rewrite (4.56) as

$$\begin{aligned}
\sqrt{\Omega} \psi^{\pm}(\mathbf{r}) &= e^{i\mathbf{k} \cdot \mathbf{r}} \\
&\quad - \frac{2m}{4\pi\hbar^2} \int d^3 r_1 d^3 r_2 \frac{\exp(\pm i k |\mathbf{r} - \mathbf{r}_1|)}{|\mathbf{r} - \mathbf{r}_1|} T^{\pm}(\mathbf{r}_1, \mathbf{r}_2) \exp(i\mathbf{k} \cdot \mathbf{r}_2), \tag{4.57}
\end{aligned}$$

where $k = \sqrt{2mE/\hbar^2}$. As was mentioned before, we are interested in the asymptotic behavior of $\psi^{\pm}(\mathbf{r})$ as $r \rightarrow \infty$. In this limit we can omit \mathbf{r}_1 in the denominator of the rhs of (4.57); in the exponent we can write $|\mathbf{r} - \mathbf{r}_1| \approx r - r_1 \cos \theta + O(r_1^2/r)$.¹ Thus $k|\mathbf{r} - \mathbf{r}_1| \approx kr - kr_1 \cos \theta = kr - \mathbf{k}_f \cdot \mathbf{r}_1$, where \mathbf{k}_f is a vector of magnitude k in the direction of \mathbf{r} . For large r we can then write (4.57) as

¹ The symbol O means “of the order of.”

$$\begin{aligned}
 \sqrt{\Omega}\psi^\pm(\mathbf{r}) &\xrightarrow{r\rightarrow\infty} e^{i\mathbf{k}\cdot\mathbf{r}} \\
 -\frac{m}{2\pi\hbar^2}\frac{e^{\pm ikr}}{r} \int d^3r_1 d^3r_2 \exp(\mp i\mathbf{k}_f\cdot\mathbf{r}_1) \langle \mathbf{r}_1 | T^\pm(E) | \mathbf{r}_2 \rangle \exp(i\mathbf{k}\cdot\mathbf{r}_2) \\
 &= e^{i\mathbf{k}\cdot\mathbf{r}} - \frac{m}{2\pi\hbar^2}\frac{e^{\pm ikr}}{r} \langle \pm\mathbf{k}_f | T'^\pm(E) | \mathbf{k} \rangle . \tag{4.58}
 \end{aligned}$$

To obtain (4.58) we have used the relations $\langle \mathbf{r} | \mathbf{k} \rangle = e^{i\mathbf{k}\cdot\mathbf{r}}/\sqrt{\Omega}$, $T' = \Omega T$, and $\int d^3r |\mathbf{r}\rangle \langle \mathbf{r}| = 1$. Equation (4.58) shows that the solution ψ^- must be excluded because it produces a physically unacceptable ingoing spherical wave asymptotically.

The quantity of physical importance is the scattering amplitude $f(\mathbf{k}_f, \mathbf{k})$, which is defined by the relation

$$\psi(\mathbf{r}) \xrightarrow{r\rightarrow\infty} \text{const.} \times \left[e^{i\mathbf{k}\cdot\mathbf{r}} + f(\mathbf{k}_f, \mathbf{k}) \frac{e^{ikr}}{r} \right] . \tag{4.59}$$

Comparing (4.58) with (4.59) we obtain for the scattering amplitude

$$f(\mathbf{k}_f, \mathbf{k}) = -\frac{m}{2\pi\hbar^2} \langle \mathbf{k}_f | T'^+(E) | \mathbf{k} \rangle , \tag{4.60}$$

where $E = \hbar^2 k_f^2/2m = \hbar^2 k^2/2m$, i.e., the energy argument of $T'^+(E)$ coincides with the eigenenergy of $|\mathbf{k}\rangle$ and $|\mathbf{k}_f\rangle$; this is described in the literature as T'^+ being calculated “on the shell.” Thus, the t -matrix in the \mathbf{k} -representation is essentially the scattering amplitude, which is directly related to the differential cross section, $d\sigma/d\mathcal{O}^2$

$$\frac{d\sigma}{d\mathcal{O}} = |f|^2 = \frac{m^2}{4\pi^2\hbar^4} |\langle \mathbf{k}_f | T'^+(E) | \mathbf{k} \rangle|^2 . \tag{4.61}$$

Substituting (4.60) into (4.25) we obtain the following integral equation for the scattering amplitude f :

$$f(\mathbf{k}_f, \mathbf{k}) = -\frac{m}{2\pi\hbar^2} V(\mathbf{k}_f - \mathbf{k}) + \int \frac{d^3k_1}{(2\pi)^3} \frac{V(\mathbf{k}_f - \mathbf{k}_1)}{E - \hbar^2 k_1^2/2m + is} f(\mathbf{k}_1, \mathbf{k}) ; \tag{4.62}$$

we have taken into account that

$$G_0^+(k_1; E) = \lim_{s\rightarrow 0^+} \left(E - \frac{\hbar^2 k_1^2}{2m} + is \right)^{-1} .$$

Thus, to the first order in the scattering potential

$$f(\mathbf{k}_f, \mathbf{k}) \approx -\frac{m}{2\pi\hbar^2} V(\mathbf{k}_f - \mathbf{k}) , \tag{4.63}$$

where $V(\mathbf{q})$ is the Fourier transform of $V(\mathbf{r})$ [see (4.23)]. Equation (4.63) is the *Born approximation* for the scattering amplitude.

² \mathcal{O} is the symbol for the solid angle.

Equation (4.61) can be derived in an alternative way. The differential cross section is defined as the probability per unit time for the transition $\mathbf{k} \rightarrow \mathbf{k}_f$, $W_{\mathbf{k}_f \mathbf{k}}$, times the number of final states divided by the solid angle, 4π , and by the flux, $j = v/\Omega$, of the incoming particle:

$$\frac{d\sigma}{d\mathcal{O}} = \frac{\Omega}{4\pi v} \int dE_f \mathcal{N}(E_f) W_{\mathbf{k}_f \mathbf{k}} . \quad (4.64)$$

Substituting $W_{\mathbf{k}_f \mathbf{k}}$ from (4.48) and $\mathcal{N}(E_f)$ from (3.26) we obtain (4.61). The total cross section

$$\sigma = \int d\mathcal{O} \frac{d\sigma}{d\mathcal{O}} \quad (4.65)$$

can be written in view of (4.64), (4.48), and (4.50) as

$$\begin{aligned} \sigma &= \frac{\Omega}{v} \sum_{\mathbf{k}_f} W_{\mathbf{k}_f \mathbf{k}} = \frac{\Omega}{v} \frac{2\pi}{\hbar} \sum_{\mathbf{k}_f} |\langle \mathbf{k}_f | T^+(E) | \mathbf{k} \rangle|^2 \delta(E_f - E) \\ &= \frac{2\pi\Omega}{\hbar v} \sum_{\mathbf{k}_f} \langle \mathbf{k} | T^-(E) | \mathbf{k}_f \rangle \langle \mathbf{k}_f | T^+(E) | \mathbf{k} \rangle \delta(E_f - E) \\ &= \frac{2\pi}{\hbar v} \frac{\Omega i}{2\pi} [\langle \mathbf{k} | T^+(E) | \mathbf{k} \rangle - \langle \mathbf{k} | T^-(E) | \mathbf{k} \rangle] \\ &= -\frac{2\Omega}{\hbar v} \text{Im} \{ \langle \mathbf{k} | T^+(E) | \mathbf{k} \rangle \} . \end{aligned} \quad (4.66)$$

Taking (4.60) into account we can rewrite (4.66) as

$$\sigma = \frac{4\pi}{k} \text{Im} \{ f(\mathbf{k}, \mathbf{k}) \} . \quad (4.67)$$

Equation (4.67) is the so-called *optical theorem*, which connects the total cross section with the forward scattering amplitude.

As was already mentioned, the scattering amplitude f for positive energies is directly related to an observable quantity of great physical importance, namely, the differential cross section. The behavior of f , extended for negative energies, is also of physical significance because the poles of $f(E)$ [which coincide with the poles of $T(E)$, as can be seen from (4.60)] give the discrete eigenenergies of the system. In other words, if the scattering problem has been solved and f vs. E has been obtained, one only need find the position of the poles of f in order to find the discrete levels of the system. Of course, these poles are on the negative E -semiaxis. We should mention also that, frequently, f vs. E (or T^+ vs. E) exhibits sharp peaks at certain positive energies. The states associated with such peaks in f are called *resonances*; their physical significance will be discussed in Chap. 6.

An elementary example of the above comments is provided by the case where $V(\mathbf{r})$ is an *attractive* Coulomb potential $V(\mathbf{r}) = -e^2/r$. Then the scattering amplitude is [12, 19]

$$f = \frac{-t\Gamma(1-it)}{\Gamma(1+it)} \times \frac{\exp\{2it \ln[\sin(\theta/2)]\}}{2k \sin^2(\theta/2)}, \quad (4.68)$$

where

$$k = \sqrt{2mE/\hbar^2}, \quad \text{Im}\{k\} \geq 0, \quad (4.69)$$

$$t = \frac{me^2}{\hbar^2 k}, \quad (4.70)$$

and θ is the angle between \mathbf{k} and \mathbf{k}_f . The poles of f occur when the argument of $\Gamma(1-it)$ is a nonpositive integer, i.e., when $1-it = -p$, where $p = 0, 1, 2, \dots$, i.e., when

$$it = 1 + p = n; \quad n = 1, 2, 3, \dots \quad (4.71)$$

Substituting (4.69) and (4.70) into (4.71) we obtain for the discrete eigenenergies of the attractive Coulomb potential

$$E = -\frac{e^4 m}{2\hbar^2} \frac{1}{n^2}; \quad n = 1, 2, \dots \quad (4.72)$$

which is the standard result. If the potential were repulsive, the scattering amplitude would be given by (4.68) with i replaced by $-i$. In this case the argument in the gamma function in the numerator in (4.68) cannot become a nonpositive integer given (4.69) and (4.70); thus, f has no poles, which means that there are no discrete levels. This result was expected since the scattering potential is repulsive.

4.2.2 Bound State in Shallow Potential Wells ($E < 0$)

Here we assume that

$$V(\mathbf{r}) = \begin{cases} -V_0 & \text{for } \mathbf{r} \text{ inside } \Omega_0, \\ 0 & \text{for } \mathbf{r} \text{ outside } \Omega_0, \end{cases} \quad (4.73)$$

where Ω_0 is a finite region in real space and V_0 is positive and very small: $V_0 \rightarrow 0^+$. We are interested in finding whether or not a discrete level E_0 appears and how it varies with V_0 . To answer this question, it is enough to find the position of the pole of $G(E)$, if any, for E in the range $[-V_0, 0]$.

The basic equation (4.5) has the following form in the present case:

$$\begin{aligned} G(\mathbf{r}, \mathbf{r}'; z) &= G_0(\mathbf{r}, \mathbf{r}'; z) \\ &\quad - V_0 \int_{\Omega_0} d\mathbf{r}_1 G_0(\mathbf{r}, \mathbf{r}_1; z) G_0(\mathbf{r}_1, \mathbf{r}'; z) \\ &\quad + V_0^2 \int_{\Omega_0} d\mathbf{r}_1 \int_{\Omega_0} d\mathbf{r}_2 G_0(\mathbf{r}, \mathbf{r}_1; z) G_0(\mathbf{r}_1, \mathbf{r}_2; z) G_0(\mathbf{r}_2, \mathbf{r}'; z) \\ &\quad + \dots \end{aligned} \quad (4.74)$$

3-d Case

$$G_0(\mathbf{r}, \mathbf{r}_1; E) = -\frac{m}{2\pi\hbar^2} \frac{\exp(-k_0 |\mathbf{r} - \mathbf{r}_1|)}{|\mathbf{r} - \mathbf{r}_1|}, \quad k_0 = \sqrt{\frac{2m|E|}{\hbar^2}},$$

[see (3.21)]. In this case $G(E)$ remains finite for E around 0. As a result the various integrals in (4.74) are finite. Thus for sufficiently small V_0 the power series expansion in (4.74) converges, which means that the difference $G - G_0$ approaches zero as $V_0 \rightarrow 0^+$. This in turn means that G remains finite for small V_0 and E in the range $[-V_0, 0]$ and consequently has no poles in this range. The conclusion is that in 3-d sufficiently shallow potential wells do not produce discrete levels; the product $mV_0\Omega_0^{2/3}/\hbar^2$ has to exceed a critical value before the first discrete level is formed (Problem 4.7s).

2-d Case

$$G_0(\mathbf{r}, \mathbf{r}_1; E) = -\frac{m}{\pi\hbar^2} K_0(k_0 |\mathbf{r} - \mathbf{r}_1|), \quad k_0 = \sqrt{\frac{2m|E|}{\hbar^2}},$$

[see (3.27)]. Since $V_0 \rightarrow 0^+$, it follows that $|E| \rightarrow 0^+$ and $k_0 \rightarrow 0^+$. Using the small argument expansion for K_0 we obtain

$$G_0(\mathbf{r}, \mathbf{r}_1; E) = \frac{m}{\pi\hbar^2} \ln(k_0 |\mathbf{r} - \mathbf{r}_1|) + c_1 + O(k_0 |\mathbf{r} - \mathbf{r}_1|), \quad (4.75)$$

where c_1 is a known constant. Substituting (4.75) into (4.74) and keeping the leading terms only, we obtain

$$\begin{aligned} G(\mathbf{r}, \mathbf{r}'; E) &\approx G_0(\mathbf{r}, \mathbf{r}'; E) \sum_{n=0}^{\infty} \left[-\frac{V_0\Omega_0 m}{\pi\hbar^2} \ln(k_0 \sqrt{S_n}) \right]^n \\ &= \frac{G(\mathbf{r}, \mathbf{r}'; E)}{1 + V_0\Omega_0 m \ln(k_0 \sqrt{S}) / \pi\hbar^2}, \end{aligned} \quad (4.76)$$

where $\{S_n\}$ and S are constants of the order of the extension of the potential well Ω_0 ; the exact value of S requires explicit evaluation of integrals of the type

$$\int_{\Omega_0} d^2r_1 \cdots \int_{\Omega_0} d^2r_n \ln |\mathbf{r} - \mathbf{r}_1| \times \ln |\mathbf{r}_1 - \mathbf{r}_2| \cdots \times \ln |\mathbf{r}_n - \mathbf{r}'|.$$

From (4.76) one finds for the pole of $G(\mathbf{r}, \mathbf{r}'; E)$, E_0 the following result:

$$E_0 \xrightarrow{V_0 \rightarrow 0^+} -\frac{\hbar^2}{2mS} \exp\left(-\frac{2\pi\hbar^2}{mV_0\Omega_0}\right) = -\frac{\hbar^2}{2mS} \exp\left(-\frac{1}{\varrho_0 V_0 \Omega_0}\right), \quad (4.77)$$

where $\varrho_0 = m/2\pi\hbar^2$ is the unperturbed DOS per unit area [see (3.30)]. The conclusion is that in the 2-d case a discrete level is always formed no matter

how shallow the potential well is. This property stems from the fact that $G_0(E)$ blows up as E approaches the band edges $E = 0$. As was discussed in Chap. 3, the logarithmic divergence of $G_0(E)$ is linked to the discontinuity of the unperturbed DOS at the band edge. The logarithmic singularity of $G_0(E)$ at $E = 0$ produces a discrete level that depends on V_0 as $\exp(-1/\varrho_0 V_0 \Omega_0)$, where ϱ_0 is the discontinuity in the unperturbed DOS per unit area, V_0 is the depth of the potential well, and Ω_0 is its 2-d extent. As we will see in Chap. 6, this result is valid in all cases where the unperturbed DOS exhibits a discontinuity at the band edge. The connection of this result with the theory of superconductivity will be discussed in Chap. 6.

For the particular case of a circular potential well, the problem can be solved directly from the Schrödinger equation, and the result for the discrete level is

$$E_0 \xrightarrow{V_0 \rightarrow 0^+} -\frac{2\pi}{e^{2\gamma}} \frac{\hbar^2}{m\Omega_0} \exp\left(-\frac{2\pi\hbar^2}{mV_0\Omega_0}\right), \quad (4.78)$$

where $\Omega_0 = \pi a^2$ is the area of the circular potential well and $\gamma = 0.577\dots$ is Euler's constant. For other shapes of the potential well (even simple ones like the square potential well) it becomes extremely complicated to solve the problem directly from the Schrödinger equation. Thus one can appreciate the power of the Green's function approach, which allowed us to obtain (4.77) for every shape of the 2-d potential well. Note that the shape of the potential well influences the preexponential factor S in (4.77) but not the dominant exponential factor.

1-d Case

$$G_0(x, x'; E) = -\frac{m}{\hbar^2 k_0} \exp(-k_0 |x - x'|), \quad k_0 = \sqrt{\frac{-2mE}{\hbar^2}},$$

[see (3.31)]. In the limit $V_0 \rightarrow 0^+$, $E_0 \rightarrow 0^-$ and $k_0 \rightarrow 0^+$. Thus G_0 can be approximated by

$$G_0(x, x'; E) \xrightarrow{E \rightarrow 0^-} -\sqrt{\frac{m}{-2\hbar^2 E}}. \quad (4.79)$$

Substituting in (4.74) we obtain

$$G \approx G_0 \sum_{n=0}^{\infty} (-G_0 V_0 \Omega_0)^n = \frac{G_0}{1 + G_0 V_0 \Omega_0} = \frac{G_0}{1 - \Omega_0 V_0 \sqrt{-m/2\hbar^2 E}}. \quad (4.80)$$

Thus the discrete level, E_0 , as given by the pole of $G(E)$, is

$$E_0 = -\frac{m\Omega_0^2 V_0^2}{2\hbar^2}; \quad (4.81)$$

Ω_0 is the linear extent of the 1-d potential well. In the 1-d case, as in the 2-d case, a potential well, no matter how shallow, always creates a discrete

level. In contrast to the 2-d case, the level E_0 is an analytic function of $V_0\Omega_0$ [$E_0 \sim -(V_0\Omega_0)^2$] as $V_0\Omega_0 \rightarrow 0^+$. This behavior is a consequence of the square root singularity of $G_0(E)$ or $\varrho_0(E)$ at the band edge.

The material of this section will be discussed again in detail in Chap. 6.

4.2.3 The KKR Method for Electronic Calculations in Solids

A widely used method for obtaining the electronic eigenfunctions and eigenenergies in periodic solids was introduced by Korringa, Kohn, and Rostoker (KKR) and employs Green's function techniques, namely, (4.28). The unperturbed Hamiltonian is $\mathcal{H}_0 = -(\hbar^2/2m)\nabla^2$; the periodic potential, $V(\mathbf{r})$, produced by the ions and all the other electrons is treated as the perturbation. It is assumed that $V(\mathbf{r})$ is of the following form:

$$V(\mathbf{r}) = \sum_{\mathbf{n}} v(|\mathbf{r} - \mathbf{R}_{\mathbf{n}}|) , \quad (4.82)$$

where the local potential, $v(|\mathbf{r} - \mathbf{R}_{\mathbf{n}}|)$, around the atom located at the site $\mathbf{R}_{\mathbf{n}}$ is assumed to be spherically symmetric and nonzero only inside a sphere centered at $\mathbf{R}_{\mathbf{n}}$ and of radius r_0 ; these spheres do not overlap.

Since there is no external incoming electronic beam, $\phi(\mathbf{r}) = 0$ in (4.28). Furthermore, because of the periodicity, the eigenfunction $\psi(\mathbf{r})$ obeys *Bloch's theorem* (see next chapter):

$$\psi_{\mathbf{k}}(\mathbf{r}) = \frac{1}{\sqrt{\Omega}} e^{i\mathbf{k} \cdot \mathbf{r}} w_{\mathbf{k}}(\mathbf{r}) , \quad (4.83)$$

where $w_{\mathbf{k}}(\mathbf{r})$ is periodic with the same periodicity as $V(\mathbf{r})$, i.e., $w_{\mathbf{k}}(\mathbf{r}) = w_{\mathbf{k}}(\mathbf{r} - \mathbf{R}_{\mathbf{n}})$. We have then by substituting (4.82) and (4.83) into (4.28):

$$\psi_{\mathbf{k}}(\mathbf{r}) = \frac{1}{\sqrt{\Omega}} \sum_{\mathbf{n}} \int d\mathbf{r}' G_0(\mathbf{r} - \mathbf{r}') v(|\mathbf{r}' - \mathbf{R}_{\mathbf{n}}|) e^{i\mathbf{k} \cdot (\mathbf{r}' - \mathbf{R}_{\mathbf{n}})} e^{i\mathbf{k} \cdot \mathbf{R}_{\mathbf{n}}} w_{\mathbf{k}}(\mathbf{r}' - \mathbf{R}_{\mathbf{n}}) ,$$

or, by replacing \mathbf{r}' by $\boldsymbol{\varrho} + \mathbf{R}_{\mathbf{n}}$,

$$\begin{aligned} \psi_{\mathbf{k}}(\mathbf{r}) &= \frac{1}{\sqrt{\Omega}} \sum_{\mathbf{n}} \int d\boldsymbol{\varrho} G_0(\mathbf{r} - \boldsymbol{\varrho} - \mathbf{R}_{\mathbf{n}}) \exp(i\mathbf{k} \cdot \mathbf{R}_{\mathbf{n}}) v(\boldsymbol{\varrho}) e^{i\mathbf{k} \cdot \boldsymbol{\varrho}} w_{\mathbf{k}}(\boldsymbol{\varrho}) \\ &= \int d\boldsymbol{\varrho} G_{\mathbf{k}}(\mathbf{r} - \boldsymbol{\varrho}) v(\boldsymbol{\varrho}) \psi_{\mathbf{k}}(\boldsymbol{\varrho}) . \end{aligned} \quad (4.84)$$

In the last relation we have defined the lattice unperturbed Green's function $G_{\mathbf{k}}(\mathbf{r} - \boldsymbol{\varrho})$ as follows:

$$G_{\mathbf{k}}(\mathbf{r} - \boldsymbol{\varrho}) = \sum_{\mathbf{n}} G_0(\mathbf{r} - \boldsymbol{\varrho} - \mathbf{R}_{\mathbf{n}}) \exp(i\mathbf{k} \cdot \mathbf{R}_{\mathbf{n}}) . \quad (4.85)$$

The advantage of (4.84) and (4.85) is the separation of lattice information [which is incorporated for each lattice and each \mathbf{k} in $G_{\mathbf{k}}(\mathbf{r} - \boldsymbol{\rho})$] from the local potential, $v(\boldsymbol{\rho})$, which varies from material to material.

The solution of (4.84) proceeds as follows: in the interior of each sphere, $r < r_0$, the solution $\psi_{\mathbf{k}}(\mathbf{r})$ has the following form (because of the spherical symmetry):

$$\psi_{\mathbf{k}}(\mathbf{r}) = \sum_{\ell m} c_{\ell m} Y_{\ell m}(\theta, \phi) R_{\ell}(r); \quad r \leq r_0, \quad (4.86)$$

with

$$R_{\ell}'' + \frac{2}{r} R_{\ell}' + \frac{2m}{\hbar^2} \left(E - v(r) - \frac{\hbar^2 \ell(\ell + 1)}{2mr^2} \right) R_{\ell} = 0, \quad (4.87)$$

where each ' denotes differentiation with respect to r , and R_{ℓ} is regular at $r = 0$. Equation (4.87) is solved numerically, and the solution is substituted into (4.86), which in turn is substituted into (4.84) to obtain $\psi_{\mathbf{k}}(\mathbf{r})$ outside the sphere ($r \geq r_0$).

However, because of the continuity of $\psi_{\mathbf{k}}(\mathbf{r})$ we must have

$$\lim_{r \rightarrow r_0^-} \psi_{\mathbf{k}}(\mathbf{r}) = \lim_{r \rightarrow r_0^+} \psi_{\mathbf{k}}(\mathbf{r}), \quad (4.88)$$

where the left side of (4.88) is obtained from (4.86, 4.87), while the right side of (4.88) by employing (4.84). To implement (4.88) we employ the identity

$$\begin{aligned} & \int d\phi d\theta \sin \theta G_{\mathbf{k}}(r_0, \theta', \phi', r_0, \theta, \phi) \left. \frac{\partial}{\partial \varrho} \psi(\varrho, \theta, \phi) \right|_{\varrho=r_0} \\ &= \int d\phi d\theta \sin \theta \psi(r_0, \theta, \phi) \left. \frac{\partial}{\partial \varrho} G_{\mathbf{k}}(r_0, \theta', \phi', \varrho, \theta, \phi) \right|_{\varrho=r_0}, \quad (4.89) \end{aligned}$$

where the integration is over the angles θ and ϕ of $\boldsymbol{\rho}$, while both r and ϱ are equal to r_0 . The final step is to substitute into (4.89) $\psi(\boldsymbol{\rho})$ from (4.86), to multiply both sides of (4.89) by $Y_{\ell' m'}^*(\theta', \phi')$, and to integrate over the solid angle $d\phi' d\theta' \sin \theta'$.

We end up with a linear homogeneous system for the unknown coefficient $c_{\ell m}$, which is solved numerically by truncating it to a finite number of unknowns and equations.

4.3 Summary

In this chapter we were interested in finding the eigenvalues and eigenfunctions of a Hamiltonian \mathcal{H} , which can be decomposed as

$$\mathcal{H} = \mathcal{H}_0 + \mathcal{H}_1, \quad (4.1)$$

where \mathcal{H}_0 is such that its eigenvalues and eigenfunctions can be easily determined. This problem was solved by

1. Calculating $G_0(z)$ corresponding to \mathcal{H}_0 ;
2. Expressing $G(z)$ in terms of $G_0(z)$ and \mathcal{H}_1 , where $G(z)$ is the Green's function associated with \mathcal{H} ; and
3. Extracting from $G(z)$ information about the eigenvalues and eigenfunctions of \mathcal{H} .

Here $G(z)$ is related to $G_0(z)$ and \mathcal{H}_1 as follows:

$$G = G_0(z) + G_0(z)\mathcal{H}_1G_0(z) + G_0(z)\mathcal{H}_1G_0(z)\mathcal{H}_1G_0(z) + \cdots \quad (4.5)$$

$$= G_0(z) + G_0(z)\mathcal{H}_1G(z) \quad (4.6)$$

$$= G_0(z) + G(z)\mathcal{H}_1G_0(z) . \quad (4.7)$$

Equations (4.6) and (4.7) are inhomogeneous integral equations for $G(z)$. It is very helpful to introduce an auxiliary quantity, which is called t -matrix and is given by

$$T(z) = \mathcal{H}_1 + \mathcal{H}_1G_0(z)\mathcal{H}_1 + \mathcal{H}_1G_0(z)\mathcal{H}_1G_0(z)\mathcal{H}_1 + \cdots \quad (4.13)$$

$$= \mathcal{H}_1 + \mathcal{H}_1G(z)\mathcal{H}_1 \quad (4.14)$$

$$= \mathcal{H}_1 + \mathcal{H}_1G_0(z)T(z) \quad (4.15)$$

$$= \mathcal{H}_1 + T(z)G_0(z)\mathcal{H}_1 . \quad (4.16)$$

$G(z)$ can be easily expressed in terms of $T(z)$:

$$G(z) = G_0(z) + G_0(z)T(z)G_0(z) . \quad (4.17)$$

Here $T(z)$ has the same analytic structures as $G(z)$, i.e., it may have poles and/or branch cuts on the real z -axis. For E belonging to a branch cut we define the side limits $T^\pm(E) = \lim T(E \pm is)$ as $s \rightarrow 0^+$.

Information about the eigenvalues and eigenfunctions of \mathcal{H} are extracted as follows:

1. The poles of $T(z)$ and $G(z)$ give the discrete eigenenergies of \mathcal{H} .
2. The residue of $G(z)$ [or $T(z)$] at each pole determines the corresponding eigenfunction (if it is nondegenerate).
3. The eigenfunction(s) of \mathcal{H} associated with E belonging to the continuous spectrum of \mathcal{H} is (are) given by

$$|\psi^\pm(E)\rangle = |\phi(E)\rangle + G_0^\pm(E)T^\pm(E)|\phi(E)\rangle \quad (4.31)$$

$$= |\phi(E)\rangle + G^\pm(E)\mathcal{H}_1|\phi(E)\rangle , \quad (4.33)$$

where $\phi(E)$ is any eigenfunction of \mathcal{H}_0 corresponding to the same eigenvalue E . In most physical applications the solution $|\psi^-(E)\rangle$ is excluded on physical grounds.

4. The discontinuity of $G(z)$ across the branch cut gives the density of states (times 2π), as was discussed before.

In the time-dependent case the time evolution of the system can be described in terms of an infinite series involving $g_0(\tau)$ and \mathcal{H}_1 . The main quantity of physical interest in this case is the probability amplitude for a transition from the eigenstate (of \mathcal{H}_0) $|\phi_n\rangle$ to the eigenstate $|\phi_m\rangle$ as a result of \mathcal{H}_1 acting during the infinite time interval $[-\infty, +\infty]$. This probability amplitude is expressed as the $\langle\phi_m|, |\phi_n\rangle$ matrix element of the so-called S -matrix, which can be expressed as an infinite series involving $g_0(\tau)$ and \mathcal{H}_1 . This series for the S -matrix can be written as

$$\begin{aligned} S &= 1 + \frac{-i}{\hbar} \int_{-\infty}^{\infty} dt_1 \mathcal{H}_1^I(t_1) \\ &+ \left(\frac{-i}{\hbar}\right)^2 \int_{-\infty}^{\infty} dt_1 \mathcal{H}_1^I(t_1) \int_{-\infty}^{t_1} dt_2 \mathcal{H}_1^I(t_2) \\ &+ \cdots, \end{aligned} \quad (4.51)$$

where

$$\mathcal{H}_1^I(t) \equiv \exp(i\mathcal{H}_0 t/\hbar) \mathcal{H}_1(t) \exp(-i\mathcal{H}_0 t/\hbar) .$$

The S -matrix is unitary;

$$S^\dagger S = S S^\dagger = 1 . \quad (4.49)$$

If \mathcal{H}_1 is time independent and E_n and E_m belong to the continuous spectrum of \mathcal{H}_0 , one finds that S is related to T^+ as follows:

$$\langle\phi_m | S | \phi_n\rangle = \delta_{mn} - 2\pi i \delta(E_n - E_m) \langle\phi_m | T^+(E_n) | \phi_n\rangle , \quad (4.46)$$

where $\mathcal{H}_0 |\phi_n\rangle = E_n |\phi_n\rangle$ and $\mathcal{H}_0 |\phi_m\rangle = E_m |\phi_m\rangle$. The probability per unit time for the transition $|\phi_n\rangle \rightarrow |\phi_m\rangle$ ($n \neq m$) is

$$W_{mn} = \frac{2\pi}{\hbar} |\langle\phi_m | T^+(E_n) | \phi_n\rangle|^2 \delta(E_m - E_n) . \quad (4.48)$$

Knowledge of $T(z)$ permits us to obtain immediately the scattering amplitude, $f(\mathbf{k}_f, \mathbf{k})$, associated with a time-independent \mathcal{H}_1 ; indeed we have

$$f(\mathbf{k}_f, \mathbf{k}) = -\frac{m}{2\pi\hbar^2} \langle\mathbf{k}_f | T^+(E) | \mathbf{k}\rangle , \quad (4.60)$$

where $E = \hbar^2 k^2/2m = \hbar^2 k_f^2/2m$ and $T'(z) = \Omega T(z)$. From the unitarity of S and (4.46) and (4.60), the optical theorem follows:

$$\sigma = \frac{4\pi}{k} \text{Im} \{f(\mathbf{k}, \mathbf{k})\} , \quad (4.67)$$

where σ is the total cross section. Since f is proportional to T^+ , it follows that the poles of scattering amplitude (if any) considered as a function of energy E give the discrete levels of the system (E should not be restricted to positive values, but it must be allowed to take negative values as well; this implies imaginary values for $k = k_f$).

The formalism just outlined is applied to the question of the existence of a discrete level in very shallow potential wells. It was found that:

1. In the 3-d case, the product of the square of the linear extent times the depth of the well³ must exceed a critical value for a discrete level to appear.
2. For the 2-d case, a discrete level at E_0 always exists no matter how shallow the potential well is; E_0 is given by

$$E_0 \sim -\exp\left(-\frac{1}{\varrho_0 V_0 \Omega_0}\right), \quad \text{as } V_0 \Omega_0 \rightarrow 0^+, \quad (4.77)$$

where ϱ_0 is the unperturbed DOS per unit area, V_0 is the depth, and Ω_0 is the 2-d extent of the potential well.

3. For the 1-d case, a discrete level is always present; it is given by

$$E_0 \xrightarrow{V_0 \Omega_0 \rightarrow 0^+} -\frac{m\Omega_0^2 V_0^2}{2\hbar^2}, \quad (4.81)$$

where Ω_0 is the linear extent of the well. The characteristic behavior summarized in steps 1, 2, and 3 above is directly related to the analytic structure of the unperturbed DOS at the band edge.

Further Reading

- The S -matrix is discussed in some books on quantum mechanics (see, e.g., [12] pp. 503–512) and in books of field theory (e.g., [14] and [20]).
- Scattering theory is presented in all books on quantum mechanics (see in particular [16], pp. 379–441 and [12, 19], pp. 502–590 and pp. 96–121).
- The problem of a bound state in a shallow potential well is treated in all books on quantum mechanics for $d = 1$ and $d = 3$; the interesting case of $d = 2$ is usually ignored.
- The Green's function perturbation approach for the wave equation can be found in the book by Sheng [21], pp. 15–26, pp. 51–55, and pp. 58–66.

Problems

- 4.1. Express (4.16) in the \mathbf{r} -representation.
- 4.2. Express (4.27) in the \mathbf{k} -representation.
- 4.3s. Prove (4.50) starting either from (4.46) or from $T = \mathcal{H}_1 + \mathcal{H}_1 G \mathcal{H}_1$.
- 4.4. Prove (4.51).

³ This product can be expressed in more physical terms as the dimensionless ratio of the depth, V_0 , of the potential well over the kinetic energy, $\hbar^2/2m\Omega_0^{2/3}$, that the particle would have if it were confined entirely within Ω_0 .

4.5. Using the exact result (4.68), calculate the differential cross section for the Coulomb potential $-e^2/r$. Obtain the same quantity by employing the Born approximation; how does the latter compare with the exact result?

4.6s. By minimizing the total energy of a particle in a very shallow potential well, show that $d = 2$ is the critical dimensionality for the existence of a bound state.

4.7s. Consider a potential well of depth V_0 and radius a in 1-, 2-, and 3-d space. Plot the eigenenergy $-E_d$ ($d = 1, 2, 3$) of the ground state as a function of the square of the dimensionless variable $V_0/(\hbar^2/2ma^2)$. Plot also the decay length L_d ($d = 1, 2, 3$) of the ground state as a function of the square of $V_0/(\hbar^2/2ma^2)$. What are the analytic expressions for E_d and L_d ($d = 1, 2, 3$) as $V_0/(\hbar^2/2ma^2)$ tends to infinity or to its critical value for the appearance of the first bound state?

4.8. Consider the unperturbed wave equation $(\omega^2/c^2 - \mathcal{H}_0)|\phi\rangle = 0$, where $\mathcal{H}_0 = -\nabla^2$, and a time-independent perturbation \mathcal{H}_1 . Taking into account that the role of λ (Chap. 1) or E (Chap. 3) is played by $k^2 = \omega^2/c^2$, show that the transition probability per unit time is given by (Fermi's golden rule for the scalar wave equation)

$$W_{\mathbf{k}_f \mathbf{k}} = \frac{\pi c^2}{\omega_k} |\langle \mathbf{k}_f | T^+(k^2) | \mathbf{k} \rangle|^2 \delta(k_f^2 - k^2) . \quad (1)$$

Then, following the derivation of (4.66), prove that the total cross section σ is related to the $\text{Im}\{T^+\}$ as follows:

$$\sigma = -\frac{\Omega}{k} \text{Im} \{ \langle \mathbf{k} | T^+(k^2) | \mathbf{k} \rangle \} . \quad (2)$$

Furthermore, show that, for a wave equation in 3-d, the differential cross section is related to the t -matrix by

$$f(\mathbf{k}_f, \mathbf{k}) = -\frac{\Omega}{4\pi} \langle \mathbf{k}_f | T^+(k^2) | \mathbf{k} \rangle . \quad (3)$$

Combining (2) and (3) we obtain (4.67) for the 3-d wave equation as well.

4.9. Prove (4.89) by showing first that

$$\left(E + \frac{\hbar^2}{2m} \nabla_{\boldsymbol{\rho}}^2 \right) G_{\mathbf{k}}(\mathbf{r} - \boldsymbol{\rho}) = \delta(\mathbf{r} - \boldsymbol{\rho})$$

and by employing the Schrödinger equation

$$\left(-\frac{\hbar^2}{2m} \nabla_{\boldsymbol{\rho}}^2 + v(\boldsymbol{\rho}) - E \right) \psi_{\mathbf{k}}(\boldsymbol{\rho}) = 0 .$$

Green's Functions for Tight-Binding Hamiltonians

Summary. We introduce the so-called tight-binding Hamiltonians (TBH), which have the form

$$\mathcal{H} = \sum_{\ell} |\ell\rangle \varepsilon_{\ell} \langle \ell| + \sum_{\ell m} |\ell\rangle V_{\ell m} \langle m| ,$$

where each state $|\ell\rangle$ is an atomiclike orbital centered at the site ℓ ; the sites $\{\ell\}$ form a lattice. Such Hamiltonians are very important in solid-state physics. Here we calculate the Green's functions associated with the TBH for various simple lattices. We also review briefly some applications in solid-state physics.

5.1 Introductory Remarks

In this chapter we examine the Green's functions associated with a class of *periodic* Hamiltonians, i.e., Hamiltonians remaining invariant under a translation by any vector ℓ , where $\{\ell\}$ form a regular lattice in d -dimensional space

$$\ell = \sum_{a=1}^d \ell_a \mathbf{r}_a , \quad \ell_a = 0, \pm 1, \pm 2, \dots \quad (5.1)$$

and \mathbf{r}_a ($a = 1, \dots, d$) are d linear independent vectors forming the basis of the lattice.

The reasons for considering here periodic Hamiltonians are the following.

1. They produce continuous spectra that possess not only a lower bound, as in the free-particle case, but an *upper* bound (or bounds) as well. Thus, the physics is not only richer but more symmetric and in some sense more satisfying.
2. They are of central importance for understanding the electronic behavior of perfect crystalline solids.
3. They provide the basis for understanding the electronic properties of real, imperfect crystalline solids, since the imperfections can be treated as a perturbation \mathcal{H}_1 using techniques developed in Chap. 4.

4. They are mathematically equivalent to a system of coupled 1-d harmonic oscillators and, as a result, they describe (by direct generalization to 3-d) the ionic motions in a crystalline solid. Furthermore, imperfections can be treated by techniques presented in Chap. 4.
5. The class of simplified periodic Hamiltonians we consider here allows us to obtain simple closed-form results for certain perturbation problems. Thus the physics presented in Sect. 4.1 can be better appreciated without the burden of a complicated algebra. This point will be examined in detail in the next chapter.

Before we introduce the class of Hamiltonians under consideration, we remind the reader of some of the basic properties of the eigenfunctions and eigenvalues of a periodic Hamiltonian [22–30].

The eigenfunctions, which are called *Bloch functions*, are plane wavelike, i.e.,

$$\psi_{n\mathbf{k}}(\mathbf{r}) = \frac{1}{\sqrt{\Omega}} e^{i\mathbf{k}\cdot\mathbf{r}} u_{n\mathbf{k}}(\mathbf{r}) , \quad (5.2)$$

where the preexponential $u_{n\mathbf{k}}(\mathbf{r})$ is not a constant, as in the genuine plane waves, but a periodic function of \mathbf{r} of the same periodicity as the potential; the quantum number \mathbf{k} determines how much the phase changes when we propagate by a lattice vector $\boldsymbol{\ell}$:

$$\psi_{n\mathbf{k}}(\mathbf{r} + \boldsymbol{\ell}) = e^{i\mathbf{k}\cdot\boldsymbol{\ell}} \psi_{n\mathbf{k}}(\mathbf{r}) . \quad (5.3)$$

Note that the quantity \mathbf{k} is restricted to a finite region in \mathbf{k} -space, called the *first Brillouin zone*. The other quantum number n , which is called the *band index*, takes integer values; the presence of n compensates somehow the restriction of \mathbf{k} in the first Brillouin zone. It is worthwhile to stress that eigenstates of the type (5.2) imply propagation without any resistance similar (but not identical) to the free-particle case.

Periodicity has more profound and characteristic effects on the energy spectrum, which consists of continua, called *bands*, that may or may not overlap; there are also energy regions, called *gaps*, which do not belong to any band and, as a result, correspond to zero density of states. The boundary points between bands and gaps are called *band edges*. The eigenenergies $E_n(\mathbf{k})$ are continuous functions of \mathbf{k} within each band n . The band edges correspond to absolute minima or maxima of E vs. \mathbf{k} for a given n or a set $\{n\}$ of overlapping bands.

There are two simple diametrically opposite starting points for obtaining the electronic eigenenergies, $E_n(\mathbf{k})$, and the eigenfunctions, $\psi_{n\mathbf{k}}(\mathbf{r})$, in crystalline solids.

One, the nearly-free electron (NFE) model, takes the point of view that in a solid the total *effective* potential felt by each electron is weak enough to be treated by perturbation methods (the unperturbed solutions being plane waves). Developments based on this approach led to the pseudopotential

method, which was proven to be very fruitful indeed, especially for simple metals and semiconductors [31–38].

The other approach views the solids as being made up of atoms brought together from an infinite relative distance. It is then natural (following the usual practice for molecules) to try to express the unknown electronic wave functions as linear combinations of atomic orbitals (LCAO). In this chapter we shall deal with the simpler possible version of this approach by considering only one atom per primitive crystal cell, only one atomic orbital per atom, nearest-neighbor coupling only, and orthonormality of the atomic orbitals. We shall refer to this oversimplified version of the LCAO as the tight-binding model (TBM); the atomic orbital associated with the atom located at site ℓ will be symbolized by

$$w(\mathbf{r} - \boldsymbol{\ell}) = \langle \mathbf{r} | \boldsymbol{\ell} \rangle . \quad (5.4)$$

For more realistic calculations one needs to take into account several complicating factors:

1. Usually one needs several orbitals per atom, e.g., tetrahedral solids (C, Si, Ge, etc.) require at least four orbitals per site (one *s*-like and three *p*-like), while transition metals require in addition five *d*-like orbitals. Furthermore, one may need to employ hybrid atomic orbitals, or modified, atomiclike orbitals such as Wannier functions (see Appendix E).
2. One may have more than one atom per primitive crystalline cell.
3. The matrix elements between orbitals at different sites may not decay fast enough so that more than nearest-neighbor matrix elements may be needed.
4. The atomiclike orbitals at different sites may not be orthogonal to each other. Indeed, true atomic orbitals are not orthogonal.

Note that there is freedom in choosing the atomiclike orbitals. The Wannier functions, mentioned before (Appendix E), are one possible choice; it has the advantage of orthonormality and completeness and the disadvantage of weak decay (and hence many appreciable matrix elements). One may employ this freedom in choosing the basis so as to simplify the problem, i.e., to reduce the number of appreciable matrix elements and facilitate their computation.

The direct calculation of the matrix elements in this atomiclike orbital basis is in general a very difficult task. To obtain them indirectly one fits the LCAO results to either alternative calculations (see, e.g., [39]) or to experimental data (see, e.g., [40–42]). Harrison [25, 26, 43, 44] obtained very simple, general, and more or less acceptable (but not accurate) expressions for the matrix elements by requiring that the NFE and the LCAO methods produce consistent results. Slater and Koster [45] were the first to study in detail the dependence of the off-diagonal matrix elements on the orientation of the orbitals relative to the vector joining two neighboring atoms. As shown in Harrison's book [25], the LCAO method is a very useful tool for analyzing many classes of materials such as covalent solids [39, 46–52], ionic solids [53], simple

metals [54], transition metals [55–57], transition-metal compounds [58–61], the A15 (such as Nb_3Sn) compounds [62, 63], high T_c oxide superconductors (such as $\text{YBa}_2\text{Cu}_3\text{O}_7$) [64], etc.

5.2 The Tight-Binding Hamiltonian (TBH)

As was mentioned in Sect. 5.1, the basic set of functions within the TBM consists of orthonormal, identical, atomiclike orbitals, each one centered at the lattice sites $\ell = \ell_1 \mathbf{r}_1 + \ell_2 \mathbf{r}_2 + \ell_3 \mathbf{r}_3$ (for $d = 3$), where each ℓ_i takes all integer values; thus $\langle \mathbf{r} | \ell \rangle = w(\mathbf{r} - \ell)$. The matrix elements of the Hamiltonian within this subspace are

$$\langle \ell | \mathcal{H} | \mathbf{m} \rangle = \varepsilon_\ell \delta_{\ell \mathbf{m}} + V_{\ell \mathbf{m}} . \quad (5.5)$$

Following the usual notation we have denoted the diagonal matrix elements by ε_ℓ and the off-diagonal matrix elements by $V_{\ell \mathbf{m}}$ ($V_{\ell \ell} \equiv 0$).

The periodicity of the Hamiltonian, i.e., its invariance under translations by a lattice vector ℓ , implies that

$$\varepsilon_\ell = \varepsilon_0 \quad \text{for all } \ell , \quad (5.6a)$$

$$V_{\ell \mathbf{m}} = V_{\ell - \mathbf{m}} . \quad (5.6b)$$

It should be stressed that the Hamiltonian, which describes a real periodic solid, has matrix elements outside the subspace spanned by the $|\ell\rangle$ vectors and that this subspace is coupled with the rest of the Hilbert space. Nevertheless, we restrict ourselves to this subspace for the sake of simplicity. The price for this approximation can be considered reasonable, since many important *qualitative* features are retained in spite of this drastic simplification. Furthermore, bands arising from atomic orbitals weakly overlapping with their neighbors (i.e., tightly bound to their atoms) can be described rather accurately by working within the above-defined subspace or its straightforward generalization [22, 25, 28]. For this reason, the Hamiltonian (5.5), which is confined within the subspace spanned by $\{|\ell\rangle\}$, where ℓ runs over all lattice sites, is called the tight-binding Hamiltonian (TBH) or the tight-binding model (TBM).

The TBH, (5.5), can be written equivalently as

$$\mathcal{H} = \sum_{\ell} |\ell\rangle \varepsilon_\ell \langle \ell| + \sum_{\ell \mathbf{m}} |\ell\rangle V_{\ell \mathbf{m}} \langle \mathbf{m}| , \quad V_{\ell \ell} = 0 , \quad (5.7)$$

where ε_ℓ and $V_{\ell \mathbf{m}}$ satisfy (5.6a) and (5.6b). We shall also consider the more general case where the lattice can be divided into two interpenetrating sublattices such that each point of sublattice 1 is surrounded by points belonging to sublattice 2; the Hamiltonian remains invariant under translation by vectors of sublattice 1 or sublattice 2. In this case

$$\varepsilon_\ell = \begin{cases} \varepsilon_1 & \text{if } \ell \text{ belongs to sublattice 1 ,} \\ \varepsilon_2 & \text{if } \ell \text{ belongs to sublattice 2 .} \end{cases} \quad (5.8a)$$

$$(5.8b)$$

For the sake of simplicity we assume in our explicit results that

$$V_{\ell\mathbf{m}} = \begin{cases} V, & \ell, \mathbf{m} \text{ nearest neighbors,} \\ 0, & \text{otherwise.} \end{cases} \quad (5.9a)$$

$$(5.9b)$$

This last assumption, although not necessary, simplifies the calculational effort. The set $\{|\ell\rangle\}$ is assumed orthonormal:

$$\langle \ell | \mathbf{m} \rangle = \delta_{\ell\mathbf{m}} . \quad (5.10)$$

Thus a TBH is characterized by:

1. The lattice structure associated with the points $\{\ell\}$.
2. The values of the diagonal matrix element $\{\varepsilon_\ell\}$; in the simple periodic case, where (5.6a) is satisfied, there is only one common value that can be taken as zero by a proper redefinition of the origin of energy; in the two-sublattice periodic case, where (5.8) is satisfied, the quantity of physical significance is the difference $\varepsilon_1 - \varepsilon_2 > 0$.
3. The off-diagonal matrix elements $V_{\ell\mathbf{m}}$, which in the periodic case depend only on the difference $\ell - \mathbf{m}$.

If the simplifying assumption (5.9) is made, there is only one quantity, V , which, following the usual practice in the literature, can be taken as negative (for s -like orbitals V is indeed negative; for p - or d -orbitals the sign and the magnitude of V depends on the relative orientation of the orbitals with respect to the direction of the line joining the two neighboring atoms). It must be pointed out that a negative V , in contrast to a positive V , preserves the well-known property that as the energy of real eigenfunctions increases so does the number of their sign alternation. In any case one can obtain the positive V Green's functions from those calculated here by employing the relation

$$G(\ell, \mathbf{m}; E + is, \{\varepsilon_\ell\}, V) = -G(\ell, \mathbf{m}; -E - is, \{-\varepsilon_\ell\}, -V) . \quad (5.11)$$

The first term on the rhs of (5.7) describes a particle that can be trapped around any particular lattice site ℓ with an eigenenergy ε_ℓ . The second term allows the particle to hop from site ℓ to site \mathbf{m} with a transfer matrix element $V_{\ell\mathbf{m}}$. The quantum motion associated with the Hamiltonian (5.7) is equivalent to the wave motion of the coupled pendula shown in Fig. 5.1. This can easily be seen by writing the time-independent Schrödinger equation $\mathcal{H}|\psi\rangle = E|\psi\rangle$ as

$$(\varepsilon_i - E) c_i + \sum_j V_{ij} c_j = 0 , \quad (5.12)$$

where $|\psi\rangle = \sum_i c_i |\mathbf{i}\rangle$ and (5.7) and (5.10) are used. The equations of motion of the coupled pendula are

$$\left(m_i \omega_i^2 + \sum_j \kappa_{ij} - m_i \omega^2 \right) u_i - \sum_j \kappa_{ij} u_j = 0 , \quad (5.13)$$

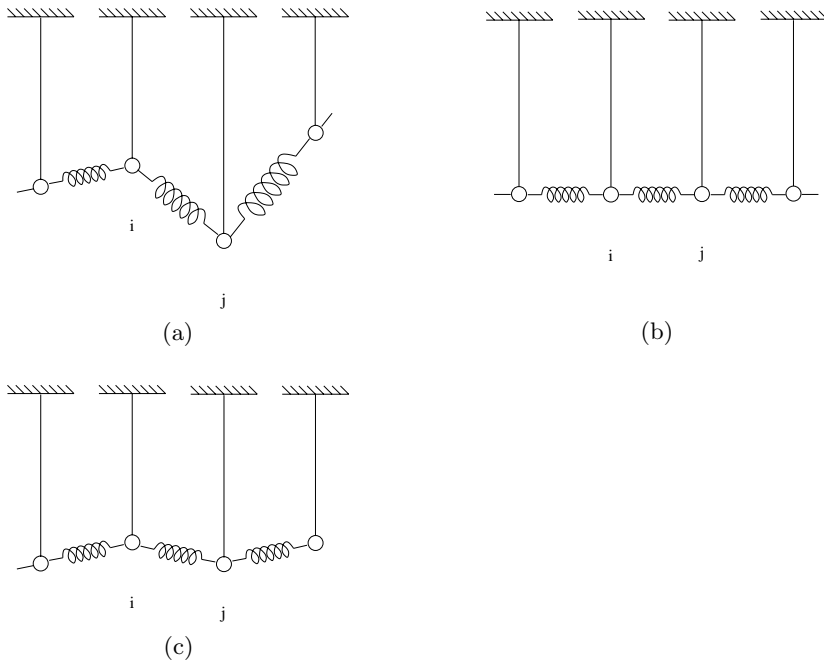


Fig. 5.1. One-dimensional coupled pendulum analog of the tight-binding Hamiltonian. Only nearest-neighbor couplings are shown (a). In the periodic case examined in this chapter, all pendula and all nearest-neighbor couplings are identical (b). The double spaced periodic case is also shown (c)

or

$$\left(\omega_i^2 + \frac{1}{m_i} \sum_{ij} \kappa_{ij} - \omega^2 \right) u_i - \frac{1}{m_i} \sum_{ij} \kappa_{ij} u_j = 0, \quad (5.13')$$

where u_i is the 1-d displacement of the pendulum located at site i , ω_i is its eigenfrequency in the absence of coupling, and $-\sum_j k_{ij}(u_i - u_j)$ is the force exercised on the pendulum at the i site as a result of the couplings with all the other pendula; m_i is the mass at i . The correspondence between the electronic and the pendulum case is illustrated in Table 5.1.

The simple mechanical system of coupled pendula is very important for solid-state physics: through the analogies in Table 5.1, it allows us to introduce the basic features of electronic behavior in crystalline solids and to obtain a clear physical picture of electronic propagation in periodic media. (Actually F. Bloch arrived at his famous explanation of almost unimpeded electronic propagation in crystalline metals by recalling the free propagation of motion in a periodic 1-d array of coupled pendula.) Furthermore, if we generalize to 3-d displacements, the problem of coupled pendula is reduced to that of the ionic (or atomic) motion in solids (by setting $\omega_i = 0$) since each ion (or atom)

Table 5.1. Analogy between the TBH and a system of coupled pendula

Electronic case	Pendulum case
c_i : component of eigenfunction at site i	u_i : displacement of pendulum located at site i
$-V_{ij}$: minus transfer matrix element between $ i\rangle$ and $ j\rangle$	κ_{ij}/m_i : spring constant coupling pendula at sites i and j over mass m_i
E : eigenenergy	ω^2 : square of eigenfrequency
ε_i : site energy	$\omega_i^2 + 1/m_i \sum_j \kappa_{ij}$: square of uncoupled eigenfrequency plus sum of spring constants connected to i over mass m_i

is indeed performing small oscillations around its equilibrium position with the restoring force being equal to $-\sum_j \mathbf{k}_{ij} (\mathbf{u}_i - \mathbf{u}_j)$. Thus for the periodic ($m_i = m_0$, $\omega_i = \omega_0$, and $\kappa_{ij} = \kappa_{i-j}$) case, the solution of system (5.13') is, according to (5.3):

$$u_j = u_i e^{i\mathbf{k} \cdot (\mathbf{j} - \mathbf{i})}, \quad \text{for each pair } \mathbf{i}, \mathbf{j}, \quad (5.14a)$$

and then

$$\omega^2(\mathbf{k}) = \omega_0^2 + \frac{1}{m_0} \sum_j \kappa_{0j} - \frac{1}{m_0} \sum_j \kappa_{0j} e^{i\mathbf{k} \cdot \mathbf{j}}. \quad (5.14b)$$

The reader may verify by direct substitution that (5.14a) and (5.14b) satisfy the system of equations (5.13').

Setting $\mathbf{i} = 0$ in (5.14a), replacing the dummy index \mathbf{j} by $\boldsymbol{\ell}$, and using the analogies in Table 5.1, we find for the electronic eigenfunctions and eigenenergies of the TBM:

$$|\mathbf{k}\rangle = \sum_{\boldsymbol{\ell}} c_{\boldsymbol{\ell}} |\boldsymbol{\ell}\rangle = c_0 \sum_{\boldsymbol{\ell}} e^{i\mathbf{k} \cdot \boldsymbol{\ell}} |\boldsymbol{\ell}\rangle, \quad (5.15a)$$

$$E(\mathbf{k}) = \varepsilon_0 + \sum_{\boldsymbol{\ell}} V_{0\boldsymbol{\ell}} e^{i\mathbf{k} \cdot \boldsymbol{\ell}}, \quad (5.15b)$$

where the orthonormality of the eigenstates $\{|\mathbf{k}\rangle\}$ imply that $c_0 = 1/\sqrt{N}$.

Equation (5.15a) means that the eigenmodes are propagating waves such that the amplitude at each site is the same and the phase changes in a regular

way: $\phi_{\ell} = \mathbf{k} \cdot \ell$. To obtain explicit results, we employ the simplifying equation (5.9) so that (5.15b) becomes

$$E(\mathbf{k}) = \varepsilon_0 + V \sum'_{\ell} e^{i\mathbf{k} \cdot \ell}, \quad (5.16)$$

where the summation extends over the sites neighboring the origin. For the 1-d case we have

$$E(k) = \varepsilon_0 + 2V \cos(ka), \quad 1\text{-d}, \quad (5.17)$$

where a is the lattice constant. For a 2-d square lattice

$$E(\mathbf{k}) = \varepsilon_0 + 2V [\cos(k_1 a) + \cos(k_2 a)], \quad 2\text{-d square.} \quad (5.18)$$

For the 3-d simple cubic we have

$$E(\mathbf{k}) = \varepsilon_0 + 2V [\cos(k_1 a) + \cos(k_2 a) + \cos(k_3 a)], \quad 3\text{-d simple cubic.} \quad (5.19)$$

In Fig. 5.2 we plot E vs. k for the 1-d case; k is restricted within the first Brillouin zone, which for the 1-d case extends from $-\pi/a$ to π/a . The function $E(k)$ has an absolute maximum (which corresponds to the upper band edge) for $k = \pi/a$ or $-\pi/a$ with a value $E_{\max} = \varepsilon_0 + 2|V|$; it has an absolute minimum (which corresponds to a lower band edge) for $k = 0$ with a value $E_{\min} = \varepsilon_0 - 2|V|$. Thus the spectrum is a continuum (a band) extending from $\varepsilon_0 - 2|V|$ to $\varepsilon_0 + 2|V|$. The bandwidth is $4|V|$. One can easily show that cases (5.17) to (5.19) produce a single band extending from $\varepsilon_0 - Z|V|$ to

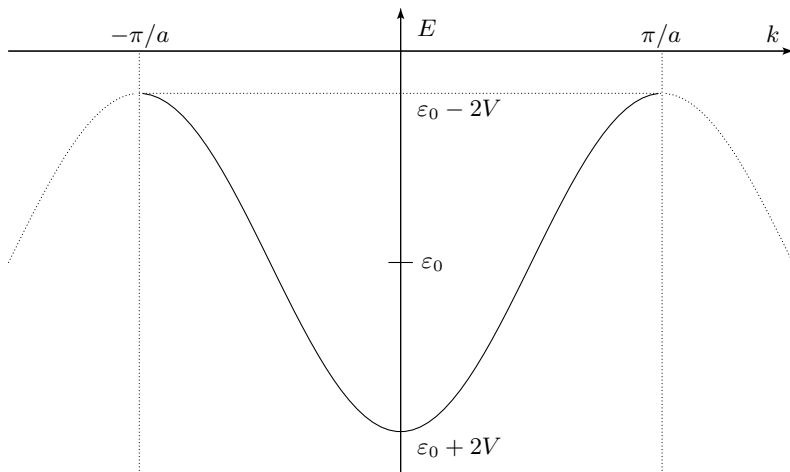


Fig. 5.2. E vs. k for the 1-d tight-binding case with nearest-neighbor coupling $V (< 0)$. $B = 2|V|$ is half the bandwidth

$\varepsilon_0 + Z|V|$, where Z is the number of nearest neighbors. The quantity $Z|V|$, which is equal to half the bandwidth, is usually symbolized by B . For 2-d and 3-d cases the functions $E(\mathbf{k})$ are presented either by plotting E vs. \mathbf{k} as \mathbf{k} varies along chosen directions or by plotting the lines (2-d case) or surfaces (3-d case) of constant energy (Figs. 5.3–5.5). In all cases \mathbf{k} is restricted within the first Brillouin zone.

For a 1-d periodic model of ionic vibration we obtain from (5.14b) (by setting $\omega_0 = 0$ and assuming only nearest-neighbor couplings) the following result:

$$m_0\omega^2(k) = 2\kappa[1 - \cos(ka)] = 4\kappa \sin^2\left(\frac{ka}{2}\right), \quad (5.20a)$$

or

$$\omega(k) = 2\sqrt{\frac{\kappa}{m_0}} \left| \sin\left(\frac{ka}{2}\right) \right| \xrightarrow{k \rightarrow 0} \sqrt{\frac{\kappa a}{\varrho}} k, \quad (5.20b)$$

where $\varrho = m_0/a$ is the average linear density and $\kappa a = B_m$ is the bulk modulus for the 1-d case. The quantity $\sqrt{B_m/\varrho}$ is the phase or group sound velocity for $ka \ll 1$. As ka approaches π , the phase velocity, ω/k , and the group velocity, $v_g \equiv d\omega/dk$, are different with $v_g \rightarrow 0$ as $ka \rightarrow \pi$.

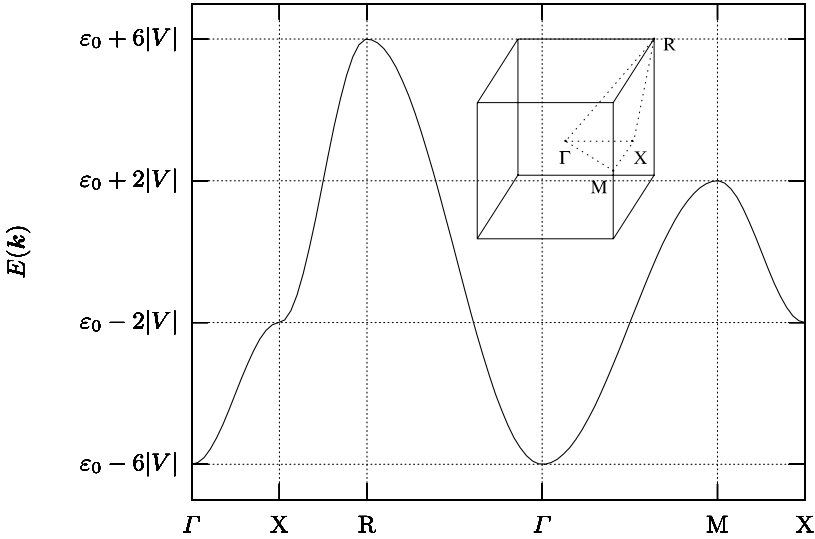


Fig. 5.3. E vs. \mathbf{k} for 3-d simple cubic tight-binding case with nearest-neighbor coupling $V(< 0)$, as \mathbf{k} varies along the straight-line segments of the first Brillouin zone (1BZ) shown in the insert

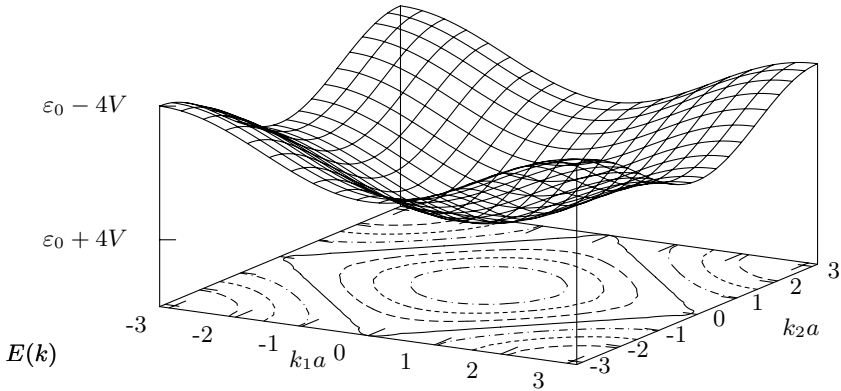


Fig. 5.4. Two-dimensional plot of E vs. \mathbf{k} according to (5.18) ($V < 0$). The first Brillouin zone (1BZ) is the square $-\pi < k_1a, k_2a \leq \pi$. The contours of equal energy are also shown within the 1BZ

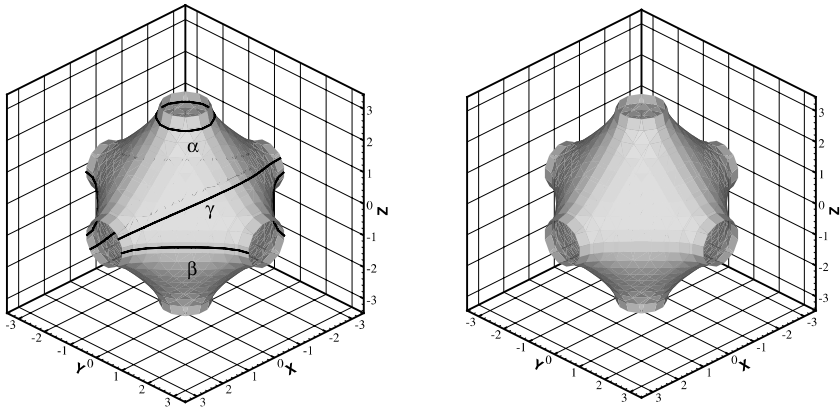


Fig. 5.5. Surface of constant energy [$E(\mathbf{k}) = \varepsilon_0 + 1.5V$] in \mathbf{k} -space for the case of (5.19). The 1BZ (shown) is the cube $-\pi < k_1a, k_2a, k_3a \leq \pi$; the lines α, β, γ are intersections of this surface by various planes, and they give the semiclassical electronic trajectories in the presence of a static magnetic field perpendicular to each plane

5.3 Green's Functions

The Green's function for the TBH examined in the previous section is

$$G(z) = \sum_{\mathbf{k}} \frac{|\mathbf{k}\rangle \langle \mathbf{k}|}{z - E(\mathbf{k})}, \quad (5.21)$$

where $|\mathbf{k}\rangle$ is given by (5.15a) and $E(\mathbf{k})$ by (5.16). The matrix elements of $G(z)$ are

$$\begin{aligned} G(\ell, \mathbf{m}; z) &\equiv \langle \ell | G(z) | \mathbf{m} \rangle = \sum_{\mathbf{k}} \frac{\langle \ell | \mathbf{k} \rangle \langle \mathbf{k} | \mathbf{m} \rangle}{z - E(\mathbf{k})} \\ &= \frac{\Omega}{N(2\pi)^d} \int_{\text{1BZ}} d\mathbf{k} \frac{e^{i\mathbf{k} \cdot (\ell - \mathbf{m})}}{z - E(\mathbf{k})}, \end{aligned} \quad (5.22)$$

where the symbol 1BZ denotes that the integration must be restricted within the first Brillouin zone. In particular, all diagonal matrix elements are equal to each other and are given by

$$G(\ell, \ell; z) = \frac{\Omega}{N(2\pi)^d} \int_{\text{1BZ}} \frac{d\mathbf{k}}{z - E(\mathbf{k})}. \quad (5.23)$$

For large z one can omit $E(\mathbf{k})$ in the denominator of the integrand in (5.23) so that

$$G(\ell, \ell; z) \xrightarrow{z \rightarrow \infty} \frac{1}{z} \frac{\Omega}{N(2\pi)^d} \int_{\text{1BZ}} d\mathbf{k}.$$

The volume of the first Brillouin zone equals $(2\pi)^d/\Omega_0$, where $\Omega_0 = \Omega/N$ is the volume of the primitive cell of the lattice. Hence,

$$G(\ell, \ell; z) \xrightarrow{z \rightarrow \infty} \frac{1}{z}. \quad (5.24)$$

This behavior can be understood if one expresses $G(\ell, \ell; z)$ in terms of the density of states per site $\varrho(E)$

$$G(\ell, \ell; z) = \int \frac{\varrho(E)}{z - E} dE \xrightarrow{z \rightarrow \infty} \frac{1}{z} \int \varrho(E) dE; \quad (5.25)$$

but $\int \varrho(E) dE = 1$ since there is one state per site. Below we give some explicit results for the various matrix elements of G for several lattices.

5.3.1 One-Dimensional Lattice

Substituting (5.17) into (5.22) we obtain (taking into account that $L/N = a$)

$$\begin{aligned} G(\ell, m; z) &= \frac{L}{2\pi N} \int_{-\pi/a}^{\pi/a} dk \frac{e^{ika(\ell-m)}}{z - \varepsilon_0 - 2V \cos(ka)} \\ &= \frac{1}{2\pi} \int_{-\pi}^{\pi} d\phi \frac{e^{i\phi(\ell-m)}}{z - \varepsilon_0 - 2V \cos \phi}, \quad \phi = ka. \end{aligned} \quad (5.26)$$

To evaluate the integral, we observe first that it depends on the absolute value $|\ell - m|$. Next we transform it into an integral over the complex variable $w = e^{i\phi}$ along the unit circle. Thus we have

$$G(\ell, m; z) = \frac{1}{2\pi i |V|} \oint dw \frac{w^{|\ell-m|}}{w^2 + 2xw + 1}, \quad (5.27)$$

where

$$x = \frac{z - \varepsilon_0}{B}, \quad B = 2|V|. \quad (5.28)$$

The two roots of $w^2 + 2xw + 1 = 0$ are given by

$$\varrho_1 = -x + \sqrt{x^2 - 1}, \quad (5.29a)$$

$$\varrho_2 = -x - \sqrt{x^2 - 1}, \quad (5.29b)$$

where by $\sqrt{x^2 - 1}$ we denote the square root whose imaginary part has the same sign as $\text{Im}\{x\}$. (For real x one has to follow a limiting procedure.) It follows that $\varrho_1 \varrho_2 = 1$. One can show that $|\varrho_1| < 1$ and $|\varrho_2| > 1$ unless x is real and satisfies the relation $-1 \leq x \leq 1$. In the latter case both roots lie on the unit circle, and the integral (5.27) is not well defined. Hence, this condition gives the continuous spectrum of \mathcal{H} which lies in the real E -axis between $\varepsilon_0 - 2|V|$ and $\varepsilon_0 + 2|V|$. For z not coinciding with this singular line, we obtain for $G(\ell, m; z)$ by the method of residues

$$G(\ell, m; z) = \frac{1}{|V|} \frac{\varrho_1^{|\ell-m|}}{\varrho_1 - \varrho_2} = \frac{1}{\sqrt{(z - \varepsilon_0)^2 - B^2}} \varrho_1^{|\ell-m|}, \quad (5.30)$$

where ϱ_1 is given by (5.29a). For z coinciding with the spectrum we have

$$G^\pm(\ell, m; E) = \frac{\mp i}{\sqrt{B^2 - (E - \varepsilon_0)^2}} \left(-x \pm i\sqrt{1 - x^2}\right)^{|\ell-m|}, \quad (5.31)$$

where $\varepsilon_0 - B \leq E \leq \varepsilon_0 + B$, $x = (E - \varepsilon_0)/B$ and the symbol $\sqrt{1 - x^2}$ denotes the positive square root.

The density of states per site is given by

$$\varrho(E) = \mp \frac{1}{\pi} \text{Im} \{G^\pm(\ell, \ell; E)\} = \frac{\theta(B - |E - \varepsilon_0|)}{\pi \sqrt{B^2 - (E - \varepsilon_0)^2}}. \quad (5.32)$$

In Fig. 5.6 we plot the real and the imaginary part of the diagonal matrix element $G(\ell, \ell; E)$ vs. E . Notice the square root singularities at both band edges. As was mentioned in Chap. 3, this behavior is characteristic of one-dimensionality. Note that the off-diagonal matrix elements $G(\ell, m; z)$ decay exponentially with the distance $|\ell - m|$ when z does not coincide with the spectrum. On the other hand, when z belongs to the spectrum, $|\varrho_1| = 1$, and the matrix elements $G(\ell, m; z)$ do not decay with the distance $|\ell - m|$.

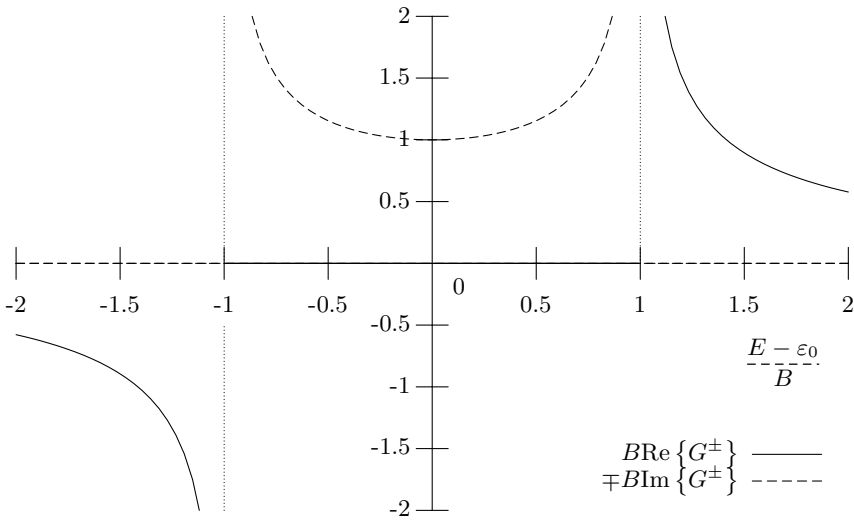


Fig. 5.6. The diagonal matrix element $G^\pm(\ell, \ell; E)$ vs. E for the 1-d lattice. $B = 2|V|$ is half the bandwidth

5.3.2 Square Lattice

For the square lattice we have, by substituting (5.18) into (5.23),

$$G(\ell, \mathbf{m}; z) = \frac{a^2}{(2\pi)^2} \int_{\text{1BZ}} d^2k \frac{e^{i\mathbf{k} \cdot (\ell - \mathbf{m})}}{z - \varepsilon_0 - 2V[\cos(k_1 a) + \cos(k_2 a)]}, \quad (5.33)$$

where

$$\mathbf{k} \cdot (\ell - \mathbf{m}) = a [k_1 (\ell_1 - m_1) + k_2 (\ell_2 - m_2)]. \quad (5.34)$$

Here ℓ_1 , ℓ_2 , m_1 , and m_2 are integers, a is the lattice constant; in the present case, the first Brillouin zone is the square

$$-\pi/a \leq k_1 < \pi/a, \quad -\pi/a \leq k_2 < \pi/a.$$

Thus (5.33) can be rewritten as

$$\begin{aligned} G(\boldsymbol{\ell}, \mathbf{m}; z) &= \frac{1}{(2\pi)^2} \int_{-\pi}^{\pi} d\phi_1 \int_{-\pi}^{\pi} d\phi_2 \frac{\exp[i\phi_1(\ell_1 - m_1) + i\phi_2(\ell_2 - m_2)]}{z - \varepsilon_0 - 2V(\cos\phi_1 + \cos\phi_2)} \\ &= \frac{1}{\pi^2} \int_0^{\pi} d\phi_1 \int_0^{\pi} d\phi_2 \frac{\cos[\phi_1(\ell_1 - m_1)] \cos[\phi_2(\ell_2 - m_2)]}{z - \varepsilon_0 - 2V(\cos\phi_1 + \cos\phi_2)} \quad (5.35a) \\ &= \frac{1}{\pi^2} \int_0^{\pi} d\phi_1 \int_0^{\pi} d\phi_2 \left\{ \frac{\cos[(\ell_1 - m_1 + \ell_2 - m_2)\phi_1]}{z - \varepsilon_0 - 4V \cos\phi_1 \cos\phi_2} \right. \\ &\quad \left. \times \cos[(\ell_1 - m_1 - \ell_2 + m_2)\phi_2] \right\}. \quad (5.35b) \end{aligned}$$

For a derivation of the last expression see [65]. By taking matrix elements of the operator equation, $(z - \mathcal{H})G = 1$, one obtains recurrence relations that allow one to express the arbitrary matrix element $G(\boldsymbol{\ell}, \mathbf{m}; z)$ in terms of the matrix elements $G(\boldsymbol{\ell}, \mathbf{m}; z)$ with $\ell_1 - m_1 = \ell_2 - m_2$ [65] [see also (5.47) below]. Furthermore, the matrix elements $G(\boldsymbol{\ell}, \mathbf{m}; z)$ with $\ell_1 - m_1 = \ell_2 - m_2$ can be expressed by recurrence relations in terms of the diagonal matrix element $G(\boldsymbol{\ell}, \boldsymbol{\ell}; z)$ and the matrix element $G(\boldsymbol{\ell}, \mathbf{m}; z)$ with $\ell_1 - m_1 = \ell_2 - m_2 = 1$, which will be denoted by $G(1; z)$ [65] (see also Problem 5.3). For the diagonal matrix element $G(\boldsymbol{\ell}, \boldsymbol{\ell}; z)$ we have

$$\begin{aligned} G(\boldsymbol{\ell}, \boldsymbol{\ell}; z) &= \frac{1}{2\pi} \int_{-\pi}^{\pi} d\phi_1 \frac{1}{2\pi} \int_{-\pi}^{\pi} d\phi_2 \frac{1}{z - \varepsilon_0 + B \cos\phi_1 \cos\phi_2} \\ &= \frac{1}{2\pi} \int_{-\pi}^{\pi} d\phi_1 \frac{1}{\sqrt{(z - \varepsilon_0)^2 - B^2 \cos^2\phi_1}} \\ &= \frac{1}{\pi(z - \varepsilon_0)} \int_0^{\pi} \frac{d\phi}{\sqrt{1 - \lambda^2 \cos^2\phi}}, \quad (5.36) \end{aligned}$$

where

$$\lambda = \frac{B}{z - \varepsilon_0}; \quad B = 4|V|, \quad (5.37)$$

hence

$$G(\boldsymbol{\ell}, \boldsymbol{\ell}; z) = \frac{2}{\pi(z - \varepsilon_0)} \mathcal{K}(\lambda), \quad (5.38)$$

where \mathcal{K} is the complete elliptic integral of the first kind. In a similar way, by performing the integration over ϕ_2 we obtain from (5.35b)

$$G(1; z) = \frac{1}{\pi} \int_0^\pi d\phi_1 \frac{\cos(2\phi_1)}{\sqrt{(z - \varepsilon_0)^2 - B^2 \cos^2 \phi_1}} \quad (5.39a)$$

$$= \frac{2}{\pi(z - \varepsilon_0)} \left[\left(\frac{2}{\lambda^2} - 1 \right) \mathcal{K}(\lambda) - \frac{2}{\lambda^2} \mathcal{E}(\lambda) \right], \quad (5.39b)$$

where $\mathcal{E}(\lambda)$ is the complete elliptic integral of the second kind.

For $z = E + is$, $s \rightarrow 0^\pm$ and E within the band, one may use the analytic continuation of $\mathcal{K}(\lambda)$ and $\mathcal{E}(\lambda)$ [1] to obtain explicit expressions for $G^\pm(\ell, \ell; E)$ and $G^\pm(1; z)$; e.g., for $G^\pm(\ell, \ell; E)$ we have

$$\begin{aligned} G(\ell, \ell; E) &= \frac{2}{\pi(E - \varepsilon_0)} \mathcal{K}\left(\frac{B}{E - \varepsilon_0}\right), \quad |E - \varepsilon_0| > 4|V| = B, \\ \text{Re}\{G^\pm(\ell, \ell; E)\} &= -\frac{2}{\pi B} \mathcal{K}\left(\frac{E - \varepsilon_0}{B}\right), \quad -B < E - \varepsilon_0 < 0, \\ \text{Re}\{G^\pm(\ell, \ell; E)\} &= \frac{2}{\pi B} \mathcal{K}\left(\frac{E - \varepsilon_0}{B}\right), \quad 0 < E - \varepsilon_0 < B, \\ \text{Im}\{G^\pm(\ell, \ell; E)\} &= \mp \frac{2}{\pi B} \mathcal{K}\left(\sqrt{1 - \frac{(E - \varepsilon_0)^2}{B^2}}\right), \quad |E - \varepsilon_0| < B. \end{aligned} \quad (5.40)$$

The density of states per site is given by

$$\begin{aligned} \varrho(E) &= \mp \frac{1}{\pi} \text{Im}\{G^\pm(\ell, \ell; E)\} \\ &= \frac{2}{\pi^2 B} \theta(B - |E - \varepsilon_0|) \mathcal{K}\left(\sqrt{1 - \frac{(E - \varepsilon_0)^2}{B^2}}\right). \end{aligned} \quad (5.41)$$

These functions are plotted in Fig. 5.7. Note that the DOS exhibits at both band edges a discontinuity that produces the logarithmic singularities of the $\text{Re}\{G\}$ at the band edges. As was discussed before, this behavior is characteristic of the two-dimensionality of the system. Note also the singularity at the interior of the band (at $E = \varepsilon_0$); the $\text{Re}\{G^\pm\}$ is discontinuous there and $\text{Im}\{G^\pm\}$ has a logarithmic singularity. The singularities of G^\pm within the band are associated with saddle points in the function $E(\mathbf{k})$. A minimum number of such saddle points exists and depends on the number of independent variables k_1, \dots, k_d [66, 67] (see Problem 5.8 at the end of this chapter).

As was mentioned before, recurrence relations allow one to express all $G(\ell, \mathbf{m}; z)$ in terms of $G(0; z) \equiv G(\ell, \ell; z)$, (5.38), and $G(1; z)$, (5.39). These recurrence relations develop numerical instabilities for $|E - \varepsilon_0| \geq B$, especially along the direction of the x - and y -axes. The reason is that the recurrence relations are satisfied not only by the Green's functions, which decay to zero as $|\ell - \mathbf{m}| \rightarrow \infty$, but by an independent set as well, which blows up as $|\ell - \mathbf{m}| \rightarrow \infty$. Because of numerical errors, a very small component of this divergent set is present in $G(0; z)$ and $G(1; z)$ and magnified as $|\ell - \mathbf{m}|$ increases,

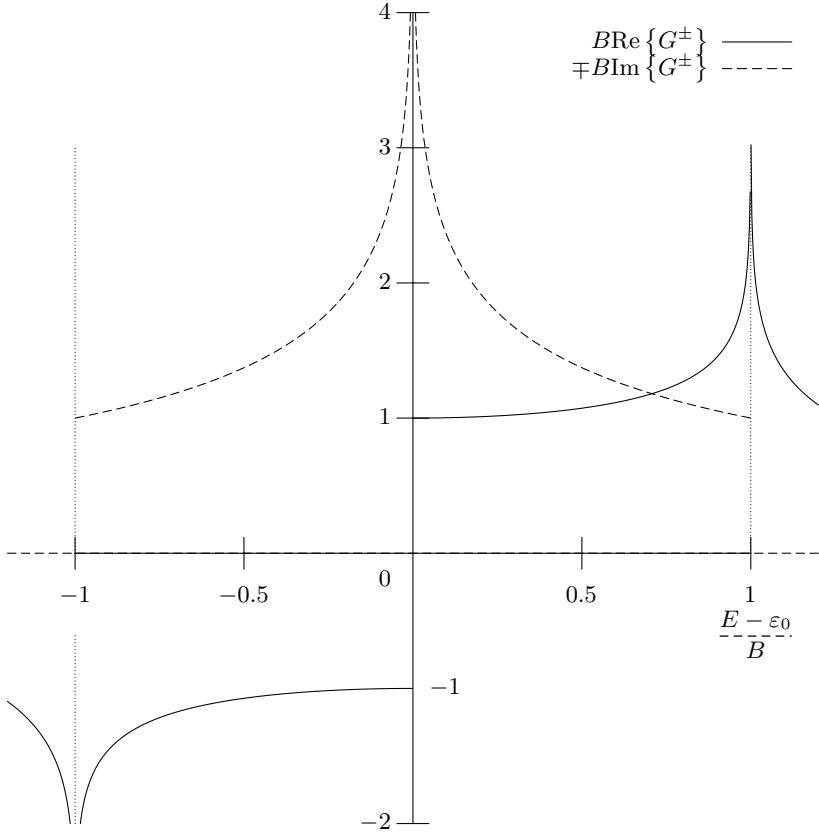


Fig. 5.7. Diagonal matrix elements $G^\pm(\ell, \ell; E)$ vs. E for the 2-d square lattice. $B = 4|V|$ is half the bandwidth

until it eventually dominates the solution. To avoid this difficulty, one has to use asymptotic expansions of $G(\mathbf{m}, 0; z)$, which are valid for $|\mathbf{m}| \gg R_0$ [see (5.42) below] and which can be obtained using the method of stationary phase in evaluating the integral for $G(\mathbf{m}, 0; z)$ [68]. See also the solution of Problem 5.2s, equation (15). Setting $\mathbf{k}_0 \cdot \mathbf{R} = k_{01}am_1 + k_{02}am_2 = \phi_{01}m_1 + \phi_{02}m_2$, $R = |\mathbf{m}|a$, $|\mathbf{m}| = \sqrt{m_1^2 + m_2^2}$, and

$$R_0 \equiv \frac{\sqrt{\sin^2 \phi_{01} + \sin^2 \phi_{02}}}{\left| \frac{\varepsilon_0 - E}{2|V|} (1 - \cos \phi_{01} \cos \phi_{02}) \right|}, \tag{5.42}$$

we find for $|E - \varepsilon_0| < B$ and for $|\mathbf{m}| \gg R_0$

$$2|V|G^+(\mathbf{m}, 0; E) = \frac{\pm 1 - i}{2\sqrt{\pi}} \frac{\exp[i(m_1\phi_{01} + m_2\phi_{02})]}{\sqrt{|\mathbf{m}|/R_0}}, \tag{5.43}$$

where the upper (lower) sign corresponds to $E > \varepsilon_0$ ($E < \varepsilon_0$), m_1 and m_2 are the cartesian components of \mathbf{m} , and ϕ_{01} and ϕ_{02} are solutions of the following relations:

$$(\varepsilon_0 - E) / 2|V| = \cos \phi_{01} + \cos \phi_{02} , \quad (5.44)$$

$$m_2 \sin \phi_{01} = m_1 \sin \phi_{02} , \quad (5.45)$$

$$m_1 \sin \phi_{01} \geq 0 . \quad (5.46)$$

It follows from (5.42)–(5.46) that the length R_0 (in units of the lattice spacing a) depends on the direction m_1/m_2 as well as the energy E . In particular, as we approach the singular points $E = \varepsilon_0$ and $E = \varepsilon_0 \pm B$, the quantity $R_0 \rightarrow \infty$.

In the limit $E \rightarrow \varepsilon_0$, $\cos \phi_{01} \rightarrow -\cos \phi_{02}$, $\sin^2 \phi_{01} \rightarrow \sin^2 \phi_{02}$, and thus

$$R_0 \rightarrow \left| \frac{2V}{E - \varepsilon_0} \right| \frac{\sqrt{2} |\sin \phi_{01}|}{1 + \cos^2 \phi_{01}} \rightarrow \infty \quad \text{as } E \rightarrow \varepsilon_0 . \quad (5.42')$$

R_0 being infinite implies that $G(\mathbf{m}, 0; E)$ does not decay as $|\mathbf{m}| \rightarrow \infty$ when $E = \varepsilon_0$. Indeed, by using the defining equation $(E - \mathcal{H})G = 1$, or more explicitly

$$(E - \varepsilon_0) G(\mathbf{m}, 0; E) - \sum_{\ell \neq \mathbf{m}} \langle \mathbf{m} | \mathcal{H} | \ell \rangle \langle \ell | G | 0 \rangle = \delta_{\mathbf{m}, 0} , \quad (5.47)$$

we find in the limit $E = \varepsilon_0$ that

$$G^\pm(\mathbf{m}, 0; E) = \frac{(-1)^{m_1}}{4V} = \frac{(-1)^{m_1+1}}{4|V|} , \quad m_1 - m_2 = \text{odd} ,$$

when the difference $m_1 - m_2$ is an odd integer. In the case where $m_1 - m_2$ is an even integer, all $G(\mathbf{m}, 0; E)$ blow up as $E \rightarrow \varepsilon_0$. We can show that, to the leading order in $E - \varepsilon_0 \rightarrow 0$, we have

$$G(\mathbf{m}, 0; E) \simeq (-1)^{m_1} G(0, 0; E) , \quad m_1 - m_2 = \text{even} .$$

To prove this last relation, show first that the difference $\delta G(\mathbf{m}, 0; E) \equiv G(\mathbf{m}, 0; E) - (-1)^{m_1} G(0, 0; E)$ is finite in the limit $E \rightarrow \varepsilon_0$; then use the recursion relation (5.47).

In the limit $E \rightarrow \varepsilon_0 - B$, the quantity $R_0 \rightarrow \sqrt{|V| / |E - \varepsilon_0 + B|} \rightarrow \infty$. Hence $G(\mathbf{m}, 0; E)$ does not decay as $E \rightarrow \varepsilon_0 - B$ since $R \rightarrow \infty$; furthermore, all $G(\mathbf{m}, 0; E)$ blow up in the limit $E \rightarrow \varepsilon_0 - B$. In the same limit, the differences $\delta G(\mathbf{m}, 0; E) \equiv G(\mathbf{m}, 0; E) - G(0; E)$ are finite numbers [69] that obey the same recurrence relations as the G s; the starting values for $\delta G(\mathbf{m}, 0; E)$ with $m_1 = m_2$ are $\delta G(0; E) = 0$ and $\delta G(1; E) = -1/(\pi|V|)$. Using these values and the recurrence relations obtained by Morita [65] or by solving Problem 5.3, we obtain first $\delta G(\mathbf{m}, 0; E)$ for $m_1 = m_2$ and then, by employing (5.47), we can calculate the Green's function elements for $m_1 \neq m_2$. However, these recurrence relations may eventually develop numerical instabilities.

For E outside the band, the quantities ϕ_1 and ϕ_2 in (5.43) become imaginary, and consequently $G(\mathbf{m}, 0; E)$ decays exponentially with the distance $|\mathbf{m}|$. In particular, for $E = \varepsilon_0 - B - \delta E$, $\delta E > 0$, and $\delta E/B \ll 1$, one obtains for large $|\mathbf{m}|$

$$2|V|G(\mathbf{m}, 0; \varepsilon_0 - B - \delta E) = -\frac{\exp\left(-|\mathbf{m}|\sqrt{\delta E/|V|}\right)}{\sqrt{2\pi}\left(|\mathbf{m}|^2\delta E/|V|\right)^{1/4}}. \quad (5.48)$$

Similar relations appear at the upper band edge $E = \varepsilon_0 + B$. Several other 2-d lattices have been studied. Thus, Horiguchi [70] has expressed Green's functions for the triangular and honeycomb lattices in terms of the complete elliptic integrals of the first and second kind. Horiguchi and Chen [71] obtained the Green's function for the diced lattice. For all these lattices, the DOS exhibits the characteristic discontinuity at the band edges and $\text{Re}\{G\}$ has a logarithmic singularity. There are singular points within the band where the $\text{Re}\{G\}$ exhibits a discontinuity and the DOS has a logarithmic singularity.

If we are not interested in quantitative details, we can approximate the Green's functions for 2-d lattices by a simple function that retains the correct analytic behavior near the band edges and that gives one state per site. This simple approximation is

$$G(\ell, \ell; z) = \frac{1}{2B} \ln\left(\frac{z - \varepsilon_0 + B}{z - \varepsilon_0 - B}\right), \quad (5.49)$$

which gives the following DOS:

$$\varrho(E) = \frac{1}{2B} \theta(B - |E - \varepsilon_0|). \quad (5.50)$$

We must stress that the simple expression (5.49) does not correspond to a real 2-d lattice and that it does not possess any Van Hove singularity in the interior of the band. In Fig. 5.8 we plot $G(\ell, \ell; E)$ as given by (5.49) vs. E .

5.3.3 Simple Cubic Lattice

The first Brillouin zone for the simple cubic lattice is the cube

$$-\pi/a \leq k_1 < \pi/a, \quad -\pi/a \leq k_2 < \pi/a, \quad -\pi/a \leq k_3 < \pi/a,$$

where a is the lattice constant. Substituting (5.19) into (5.22) and introducing the variables $\phi_i = k_i a$ ($i = 1, 2, 3$) we obtain

$$G(\ell, \mathbf{m}; z) = \frac{1}{(2\pi)^3} \int_{-\pi}^{\pi} d\phi_1 \int_{-\pi}^{\pi} d\phi_2 \int_{-\pi}^{\pi} d\phi_3 \times \frac{\cos[(\ell_1 - m_1)\phi_1 + (\ell_2 - m_2)\phi_2 + (\ell_3 - m_3)\phi_3]}{z - \varepsilon_0 - 2V(\cos\phi_1 + \cos\phi_2 + \cos\phi_3)}. \quad (5.51)$$

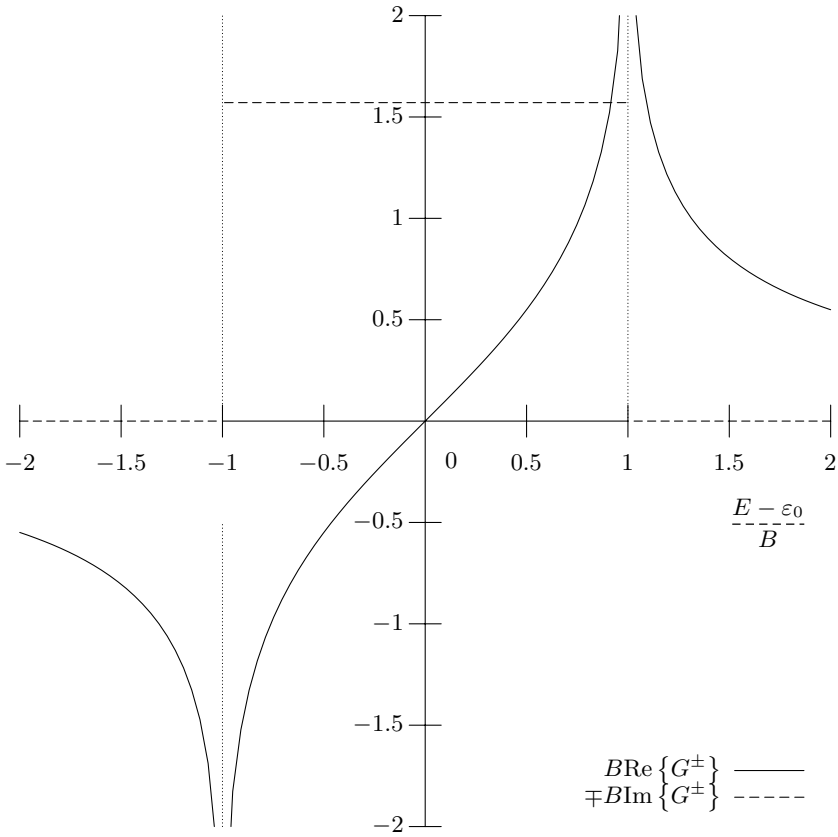


Fig. 5.8. Plot of $\text{Re}\{G^\pm\}$ and $\mp\text{Im}\{G^\pm\}$ vs. E for approximate expression $G(\ell, \ell; z) = \ln[(z - \varepsilon_0 + B)/(z - \varepsilon_0 - B)]/2B$, where $B = 4|V|$ is half the bandwidth. Compare with the exact expression for the square lattice (Fig. 5.7)

In particular, the diagonal matrix element $G(\ell, \ell; z)$ is

$$G(\ell, \ell; z) = \frac{1}{(2\pi)^3} \int_{-\pi}^{\pi} d\phi_1 \int_{-\pi}^{\pi} d\phi_2 \int_{-\pi}^{\pi} d\phi_3 \times \frac{1}{z - \varepsilon_0 - 2V(\cos \phi_1 + \cos \phi_2 + \cos \phi_3)}; \quad (5.52)$$

the integration over ϕ_2 and ϕ_3 in (5.52) can be done as in the square lattice case yielding $t\mathcal{K}(t)/2\pi V$, where

$$t = \frac{4V}{z - \varepsilon_0 - 2V \cos \phi_1}; \quad (5.53)$$

thus

$$G(\ell, \ell; z) = \frac{1}{2\pi^2 V} \int_0^\pi d\phi_1 t \mathcal{K}(t). \tag{5.54}$$

The last integral can be calculated numerically [72]. $\text{Re}\{G^\pm(\ell, \ell; E)\}$ and $\mp \text{Im}\{G^\pm(\ell, \ell; E)\}$ for real E are plotted in Fig. 5.9. The behavior is typical for a 3-d system: near both band edges, the DOS, $-\text{Im}\{G^+\}/\pi$, approaches zero continuously as $\sqrt{|\Delta E|}$, where $|\Delta E|$ is the difference of E and the corresponding band edge. $\text{Re}\{G\}$ remains finite around the band edges, although its derivative with respect to E blows up as we approach the band edges from outside the band. Within the band are two Van Hove singularities, where both $\text{Im}\{G\}$ and $\text{Re}\{G\}$ are continuous while their derivatives are discontinuous and blow up sideways (however, see point 4 in Problem 5.8).

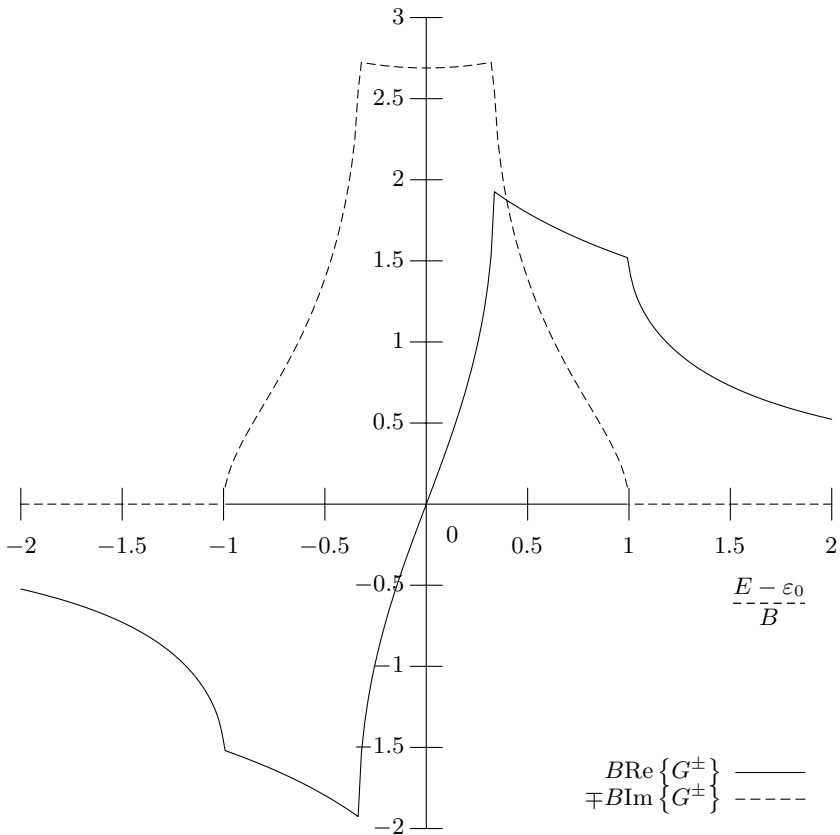


Fig. 5.9. Diagonal matrix elements $G(\ell, \ell; E)$ vs. E for simple cubic lattice. $B = 6|V|$ is half the bandwidth

When $|\boldsymbol{\ell} - \mathbf{m}|$ is along an axis (e.g., the x -axis), one can perform the integration over ϕ_2 and ϕ_3 in (5.51) as in the square lattice, yielding again $t\mathcal{K}(t)/2\pi V$; thus

$$G(\ell_1 - m_1, 0, 0; z) = \frac{1}{2\pi^2 V} \int_0^\pi d\phi_1 \cos[(\ell_1 - m_1)\phi_1] t\mathcal{K}(t). \quad (5.55)$$

Details concerning the evaluation of integral (5.55) are given in [73]; in the same reference some recurrence relations¹ are obtained that allow the computation of $G(\boldsymbol{\ell}, \mathbf{m}; z)$ for small $|\boldsymbol{\ell} - \mathbf{m}|$ in terms of $G(\ell_1 - m_1, 0, 0; z)$. Using these techniques, Table 5.2 at the end of this chapter was constructed. Joyce [74] was able to prove that $G(\boldsymbol{\ell}, \boldsymbol{\ell}; z)$ can be expressed as a product of two complete elliptic integrals of the first kind. Morita [75] obtained recurrence relations for the simple cubic lattice that allow the evaluation of all $G(\boldsymbol{\ell}, \mathbf{m})$ in terms of $G(0, 0, 0) \equiv G(\boldsymbol{\ell}, \boldsymbol{\ell})$, $G(2, 0, 0)$, and $G(3, 0, 0)$. The last two Green's functions were expressed by Horiguchi and Morita [76] in closed forms in terms of complete elliptic integrals. The reader is also referred to the papers by Austen and Loly [77], by Hioe [78], by Rashid [79], by Inawashiro et al. [80], by Katsura et al. [81], and by Joyce [82]. Asymptotic expansions valid for large values of $|\boldsymbol{\ell} - \mathbf{m}|$ were obtained [68]; within the band $G(\boldsymbol{\ell}, \mathbf{m})$ decays slowly as $|\boldsymbol{\ell} - \mathbf{m}|^{-1}$; outside the band it decays exponentially (Problem 5.4.)

The Green's functions for other 3-d lattices, such as face- and body-centered cubic, have been calculated [72, 75, 77–79, 83–88]. Note that the Green's functions for the fcc and bcc lattices blow up at the upper band edge and in the interior of the band, respectively [72] (Problem 5.5s). This behavior is atypical for a 3-d system. A small perturbation such as the inclusion of second-nearest-neighbor transfer matrix elements will eliminate these pathological infinities.

In many cases where quantitative details are not important, it is very useful to have a simple approximate expression (for G) that can be considered as typical for a 3-d lattice. Such an expression must exhibit the correct analytic behavior near the band edges and must give one state per site. Such a simple expression, widely used and known as the Hubbard Green's function, is the following:

$$G(\boldsymbol{\ell}, \boldsymbol{\ell}; z) = \frac{2}{z - \varepsilon_0 + \sqrt{(z - \varepsilon_0)^2 - B^2}}, \quad (5.56)$$

where the sign of $\text{Im} \left\{ \sqrt{(z - \varepsilon_0)^2 - B^2} \right\}$ is the same as the sign of $\text{Im} \{z\}$. The DOS corresponding to (5.56) is of a semicircular form: the real and imaginary parts of G as given by (5.56) are shown in Fig. 5.10. Note that the simple approximation (5.56) does not reproduce any Van Hove singularity within the band.

¹ There is a typographical error in (3.8) and (3.9) of [73]: $G_{sc}(t; 1, 0, 0)$ must be multiplied by t^3 instead of t^2 .

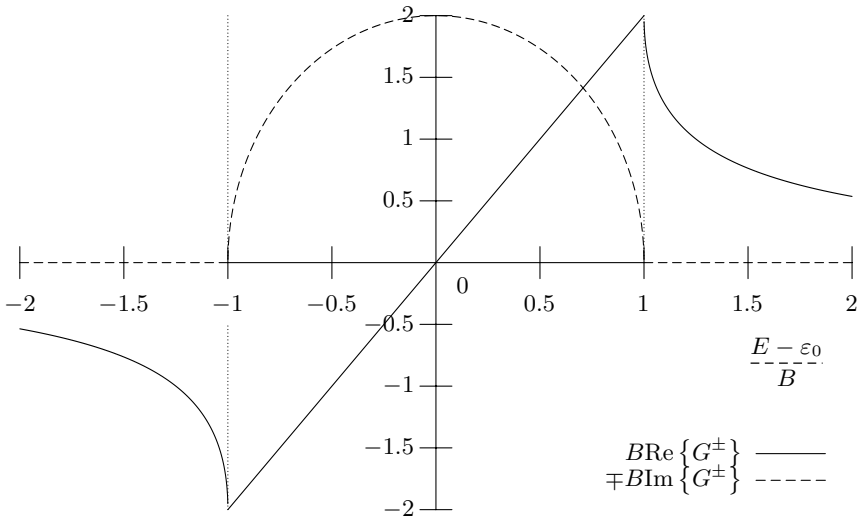


Fig. 5.10. $\text{Re}\{G^\pm\}$ and $\mp\text{Im}\{G^\pm\}$ vs. E for approximate 3-d $G(\ell, \ell; z) = 2 / \left[(z - \varepsilon_0) + \sqrt{(z - \varepsilon_0)^2 - B^2} \right]$, where B is half the bandwidth. Compare with the exact $G(\ell, \ell; z)$ for the simple cubic lattice (Fig. 5.9)

5.3.4 Green's Functions for Bethe Lattices (Cayley Trees)

Bethe lattices or Cayley trees are lattices which have no closed loops and are completely characterized by the number of nearest neighbors Z or the connectivity $K = Z - 1$. In Fig. 5.11 we show a portion of a Bethe lattice for $K = 2$ ($Z = 3$). The 1-d lattice is a Cayley tree with $K = 1$ ($Z = 2$).

Calculation of Green's functions in Bethe lattices can be performed by using the renormalized perturbation expansion (RPE) as explained in Appendix F.

For the double spacing periodic case shown in Fig. 5.11 (with $\varepsilon_1 > \varepsilon_2$), the result for $G(\ell, \ell; z)$ is (Appendix F)

$$\begin{aligned}
 G(\ell, \ell; z) = G_1(z) &\equiv \frac{2K(z - \varepsilon_2)}{D}; & \varepsilon_\ell = \varepsilon_1, \\
 G_2(z) &\equiv \frac{2K(z - \varepsilon_1)}{D}; & \varepsilon_\ell = \varepsilon_2.
 \end{aligned}
 \tag{5.57}$$

Here D is given by

$$\begin{aligned}
 D = & (K - 1)(z - \varepsilon_1)(z - \varepsilon_2) \\
 & + (K + 1)\sqrt{(z - \varepsilon_1)(z - \varepsilon_2)[(z - \varepsilon_1)(z - \varepsilon_2) - 4KV^2]},
 \end{aligned}
 \tag{5.58}$$

where the sign of the imaginary part of the square root in (5.58) is the same as the sign of $\text{Im}\{(z - \varepsilon_1)(z - \varepsilon_2)\}$. For the off-diagonal matrix element

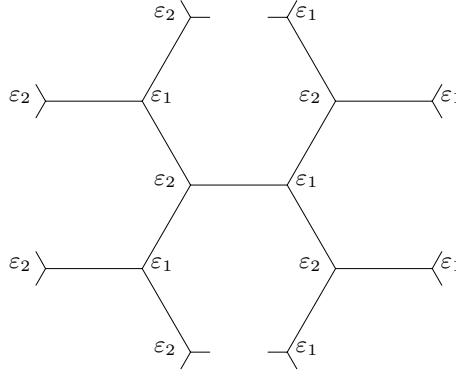


Fig. 5.11. Part of a Bethe lattice (Cayley tree) with $Z = 3$ nearest neighbors. The site energies $\{\varepsilon_\ell\}$ are arranged in an alternating periodic manner

$G(\ell, m; z)$ we have (Appendix F)

$$G(\ell, m) = G(\ell, \ell) V^{|m-\ell|} [G(\ell+1, \ell+1[\ell])]^{|m-\ell|/2} \times [G(\ell, \ell[\ell+1])]^{|m-\ell|/2}, \quad (5.59a)$$

when $|m - \ell|$ even,

$$G(\ell, m) = G(\ell, \ell) V^{|m-\ell|} [G(\ell+1, \ell+1[\ell])]^{(|m-\ell|+1)/2} \times [G(\ell, \ell[\ell+1])]^{(|m-\ell|-1)/2}; \quad (5.59b)$$

when $|m - \ell|$ odd, and

$$G(\ell+1, \ell+1[\ell]; z) = \frac{K+1}{z - \varepsilon_{\ell+1} + K [G(\ell+1, \ell+1; z)]^{-1}}, \quad (5.60)$$

$$G(\ell, \ell[\ell+1]; z) = \frac{K+1}{z - \varepsilon_\ell + K [G(\ell, \ell; z)]^{-1}}. \quad (5.61)$$

As can be seen from (5.58), the spectrum consists of two subbands, the lower one extending from $(\varepsilon_1 + \varepsilon_2)/2 - \sqrt{(\varepsilon_1 - \varepsilon_2)^2/4 + 4KV^2}$ to ε_2 and the upper one from ε_1 to $(\varepsilon_1 + \varepsilon_2)/2 + \sqrt{(\varepsilon_1 - \varepsilon_2)^2/4 + 4KV^2}$. There is a gap from ε_2 to ε_1 . The DOS at sites with $\varepsilon_1(\varepsilon_2)$ is $\varrho_1(\varrho_2)$, where

$$\varrho_i(E) = -\frac{1}{\pi} \text{Im} \{G_i^+(E)\}; \quad i = 1, 2. \quad (5.62)$$

A plot of $G_1(z)$ is shown in Fig. 5.12. Note the analytic behavior at the band edges, which is typical 3-d except at one of the interior band edges, where a square root divergence appears.

The double spacing periodic case in a Cayley tree describes the basic qualitative features of ionic crystals such as NaCl and CsCl. Indeed, in these materials, the lower subband is fully occupied by electrons while the upper subband

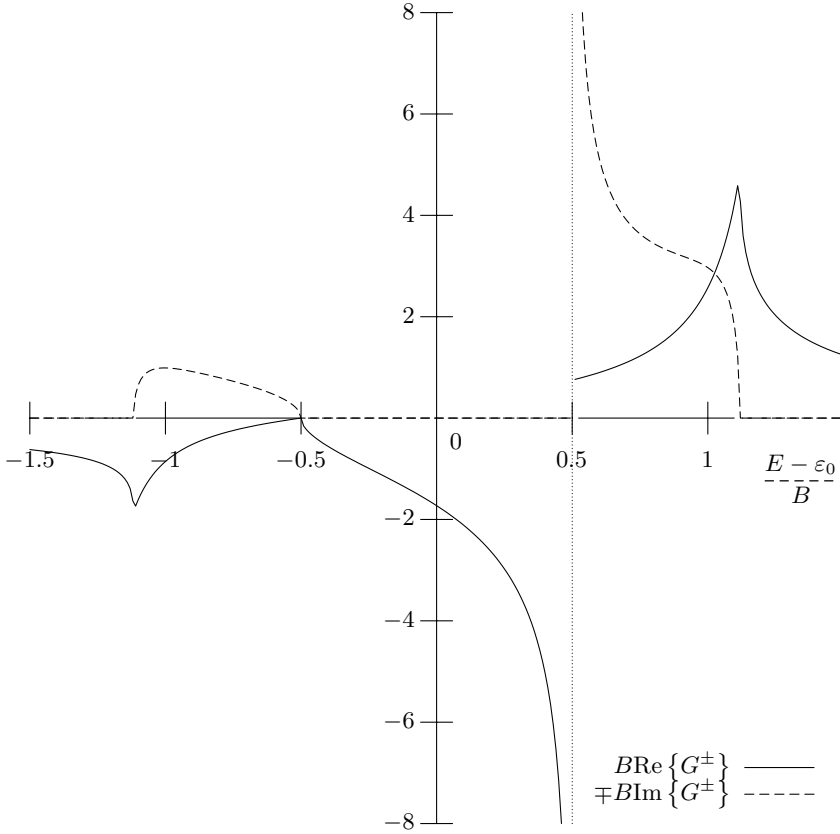


Fig. 5.12. $\text{Re}\{G^\pm(\ell, \ell)\}$ and $\mp\text{Im}\{G^\pm(\ell, \ell)\}$ vs. E for a Bethe lattice with four nearest neighbors ($K = 3$); $\varepsilon_{\ell+2n} = \varepsilon_1$, $\varepsilon_{\ell+2n+1} = \varepsilon_2$, where n integer and $\varepsilon_1 \geq \varepsilon_2$; $\varepsilon_0 = (\varepsilon_1 + \varepsilon_2)/2$, $B = 2\sqrt{K\bar{V}^2}$ and the difference $\varepsilon_1 - \varepsilon_2$ has been taken equal to B . $\text{Re}\{G^\pm(\ell + 1, \ell + 1; E)\} = -\text{Re}\{G^\pm(\ell, \ell; -E + 2\varepsilon_0)\}$; $\text{Im}\{G^\pm(\ell + 1, \ell + 1; E)\} = \text{Im}\{G^\pm(\ell, \ell; -E + 2\varepsilon_0)\}$

is completely empty. Any electronic excitation has to overcome the gap width, E_g , in order to take place. Thus E_g plays an important role in optical absorption, photoconductivity, electronic polarizability, lattice vibrations, etc. Our simple model gives E_g as being equal to $\varepsilon_1 - \varepsilon_2$. If we make the approximation that ε_1 and ε_2 are equal to the corresponding atomic levels, we find $E_g = 14.52$ eV for LiF (the experimental value is 13.6 eV), $E_g = 8.83$ eV for NaCl (the experimental value is 8.5 eV), and $E_g = 7.6$ eV for CsI (the experimental value is 6.2 eV). The subband widths, W , in the large-gap case, where $E_g \gg 4\sqrt{K}|V|$, are given by $W \simeq 4KV^2/E_g = B^2/E_g$, where $B \equiv 2\sqrt{K\bar{V}^2}$ is half the bandwidth in the case where $\varepsilon_1 = \varepsilon_2$. (In Fig. 5.12 we have taken $\varepsilon_1 = -\varepsilon_2 = B/2$ so that $E_g = B$ and the width of the subbands is $0.618B$.)

The simple periodic case is obtained by setting $\varepsilon_1 = \varepsilon_2 = \varepsilon_0$. We then have

$$G(\ell, \ell; z) = \frac{2K}{(K-1)(z - \varepsilon_0) + (K+1)\sqrt{(z - \varepsilon_0)^2 - 4KV^2}}, \quad (5.63)$$

where the sign of the imaginary part of the square root is the same as the sign of $\text{Im}\{z\}$. We obtain thus a single band centered around ε_0 with a half bandwidth $B = 2|V|\sqrt{K}$. Note that (5.63) reduces to the Hubbard Green's function in the limit $K \rightarrow \infty$ with $B = 2|V|\sqrt{K}$ remaining constant. For the quantity $G(\ell, \ell[\ell+1])$ we have when $\varepsilon_1 = \varepsilon_2 = \varepsilon_0$:

$$G(\ell, \ell[\ell+1]) = \frac{2}{(z - \varepsilon_0) + \sqrt{(z - \varepsilon_0)^2 - 4KV^2}}. \quad (5.64)$$

Hence the off-diagonal matrix elements are

$$G(\ell, m) = \frac{2K}{(K-1)(z - \varepsilon_0) + (K+1)\sqrt{(z - \varepsilon_0)^2 - 4KV^2}} \times \left[\frac{2V}{(z - \varepsilon_0) + \sqrt{(z - \varepsilon_0)^2 - 4KV^2}} \right]^{|\ell-m|}. \quad (5.65)$$

For $K = 1$ the Bethe lattice is identical to the 1-d lattice, and consequently (5.65) reduces to (5.30) when $K = 1$. Similarly, (5.57), (5.59a), and (5.59b) give the double spacing periodic 1-d results when $K = 1$.

Note that the Green's functions for Bethe lattices have several applications in solid-state physics, especially for analyzing amorphous solids [89–92] by the method of “cluster–Bethe–lattice.” For a review the reader is referred to a paper by Thorpe [93].

5.4 Summary

In this chapter we introduced the tight-binding Hamiltonian (TBH)

$$\mathcal{H} = \sum_{\ell} |\ell\rangle \varepsilon_{\ell} \langle \ell| + \sum_{\ell m} |\ell\rangle V_{\ell m} \langle m|, \quad V_{\ell\ell} = 0, \quad (5.7)$$

where each state $|\ell\rangle$ is an atomiclike orbital centered at site ℓ and $\langle \ell | \mathbf{n} \rangle = \delta_{\ell\mathbf{n}}$. The $\{\ell\}$ sites form a regular lattice. The quantity ε_{ℓ} is the energy of an electron located at site ℓ in the absence of $V_{\ell m}$. The quantity $V_{\ell m}$ is the matrix element for transferring an electron from site ℓ to site m . The electronic motion governed by the TBH (5.7) is mathematically equivalent to the motion of a coupled set of 1-d pendula (Table 5.1).

We examined the case of a periodic TBH with the same period as the lattice. This periodicity implies that

$$\varepsilon_{\ell} = \varepsilon_0 \quad \text{for all } \ell, \quad (5.6a)$$

$$V_{\ell m} = V_{\ell - m}. \quad (5.6b)$$

The eigenfunctions and eigenvalues of the periodic TBH are of the following form:

$$|\mathbf{k}\rangle = \frac{1}{\sqrt{N}} \sum_{\mathbf{i}} e^{i\mathbf{k} \cdot \mathbf{i}} |\mathbf{i}\rangle, \quad (5.15a)$$

$$E(\mathbf{k}) = \varepsilon_0 + \sum_{\ell} V_{0\ell} e^{i\mathbf{k} \cdot \ell}, \quad (5.15b)$$

where \mathbf{k} is restricted to a finite region called the first Brillouin zone. Using the general formula $G(z) = \sum_{\mathbf{k}} (|\mathbf{k}\rangle \langle \mathbf{k}|) / [z - E(\mathbf{k})]$ together with (5.15a) and (5.15b), we can calculate $G(z)$. In the case where

$$V_{\ell m} = \begin{cases} V, & \ell, m \text{ nearest neighbors,} \\ 0, & \text{otherwise,} \end{cases} \quad (5.9a)$$

$$(5.9b)$$

we obtain explicit expressions for $G(z)$ for various lattices such as the 1-d lattice, the 2-d square, the 3-d simple cubic, and the Bethe lattice (Figs. 5.6, 5.7, 5.9, and 5.12). The analytic behavior of these Green's functions near the band edges depends in general on the dimensionality as in the free-particle case (although exceptions do exist; see Problem 5.5s).

Finally, we discussed briefly the applications of the TBH [or the linear combination of atomic orbitals (LCAO) method] to the problem of the electronic structure of solids.

Further Reading

Several textbooks present the subject of solid-state physics at the introductory level, such as those by Kittel [22] and Ibach and Lüth [23], and to a more advanced level such as the books by Ashcroft and Mermin [28], Marder [30], and Harrison [25].

Problems

5.1s. Prove that $|\varrho_2| > |\varrho_1|$ unless $-1 \leq x \leq 1$, where ϱ_1 and ϱ_2 are given by (5.29).

5.2s. Using (5.43)–(5.46) prove (5.42).

5.3. Define the functions

$$F_n(k^2) \equiv \int_0^\pi dx \frac{\cos(nx)}{\sqrt{1 - k^2 \cos^2 x}}, \quad (1)$$

$$G_n(k^2) \equiv \int_0^\pi dx \cos(nx) \sqrt{1 - k^2 \cos^2 x}. \quad (2)$$

Show that

$$G_n(k^2) = -\frac{k^2}{4} F_{n+2}(k^2) + \left(1 - \frac{k^2}{2}\right) F_n(k^2) - \frac{k^2}{4} F_{n-2}(k^2). \quad (3)$$

Show also by partial integration of (2) that

$$G_n(k^2) = -\frac{k^2}{4n} [F_{n-2}(k^2) - F_{n+2}(k^2)]. \quad (4)$$

Comparing (3) and (4) obtain a recurrence relation of F_{n+2} in terms of F_n and F_{n-2} . Use this recurrence relation to obtain a recurrence relation for $G(\mathbf{m}, 0; E)$ when $m_1 = m_2$.

5.4. Following the procedures of Problem 5.2s, prove that the asymptotic expansion of (5.51) for large values of $|\ell - \mathbf{m}|$ are given by

$$G(\mathbf{R}) = \frac{-1}{4\pi |V|} \frac{\exp(i\mathbf{k}_0 \cdot \mathbf{R})}{(R/a)} \times \sqrt{\frac{\sin^2 \phi_1 + \sin^2 \phi_2 + \sin^2 \phi_3}{\sin^2 \phi_1 \cos \phi_2 \cos \phi_3 + \sin^2 \phi_2 \cos \phi_3 \cos \phi_1 + \sin^2 \phi_3 \cos \phi_1 \cos \phi_2}}.$$

5.5s. Find the E vs. \mathbf{k} for the body-centered cubic (bcc) and the face-centered cubic (fcc) lattices within the framework of the Hamiltonian (5.7). Then determine the energies where the DOS blows up.

5.6. To describe qualitatively elemental semiconductors we can consider the simplest possible model, i.e., a 1-d TBM with two atomiclike orbitals per site (one s and one p along the direction of the chain). For the diagonal matrix elements of the Hamiltonian we shall choose the values appropriate for Si ($\varepsilon_s = -14.79$ eV and $\varepsilon_p = -7.58$ eV). For the off-diagonal matrix elements we shall make the following choices (see [25]):

$$\begin{aligned} \langle n, s | \mathcal{H} | n+1, s \rangle &= V_2 = -1.32 \frac{\hbar^2}{md^2} = -1.32 \frac{7.61}{d^2} \text{ eV} \stackrel{\text{Si}}{\equiv} -1.82 \text{ eV}, \\ \langle n, p | \mathcal{H} | n+1, p \rangle &= V'_2 = 2.22 \frac{\hbar^2}{md^2} = 2.22 \frac{7.61}{d^2} \text{ eV} \stackrel{\text{Si}}{\equiv} 3.06 \text{ eV}, \\ \langle n, s | \mathcal{H} | n+1, p \rangle &= -\langle n, p | \mathcal{H} | n+1, s \rangle \\ &= V''_2 = 1.42 \frac{\hbar^2}{md^2} = 1.42 \frac{7.61}{d^2} \text{ eV} \stackrel{\text{Si}}{\equiv} 1.96 \text{ eV}, \end{aligned} \quad (1)$$

where d is the bond length (in the last expressions d is in \AA). For Si $d = 2.35 \text{\AA}$.

Show that:

1. For each k there are now two solutions, $E(k)$, given by setting the determinant D equal to zero:

$$D \equiv \begin{vmatrix} E - \varepsilon_s - 2V_2 \cos(kd) & -2iV_2'' \sin(kd) \\ 2iV_2'' \sin(kd) & E - \varepsilon_p - 2V_2' \cos(kd) \end{vmatrix} = 0. \quad (2)$$

2. For d very large, two bands are formed around ε_s and ε_p of widths $4|V_2|$ and $4V_2'$, respectively. The gap is $E_g = \varepsilon_p - \varepsilon_s - 2(V_2' + |V_2|)$.
3. For $d = d_{\text{SI}}$, two bands are formed around $\varepsilon_h - |V_{2h}|$ and $\varepsilon_h + |V_{2h}|$ of width $\varepsilon_p - \varepsilon_s \pm 1.8\hbar^2/md^2$ for the upper and lower band, respectively, where $\varepsilon_h = (\varepsilon_s + \varepsilon_p)/2$, $V_{2h} = -\frac{1}{2}(|V_2| + V_2' + 2V_2'')$. So the gap is approximately equal to $2|V_{2h}| - (\varepsilon_p - \varepsilon_s)$. Substituting the values for Si we find $E_g \simeq 1.59$ eV, to be compared with the experimental value of $E_g = 1.16$ eV.
4. Interpret the results in item 3 above by changing the basis from $|s\rangle$ and $|p\rangle$ to the atomic hybrids $|\chi_1\rangle = \frac{1}{\sqrt{2}}(|s\rangle + |p\rangle)$ and $|\chi_2\rangle = \frac{1}{\sqrt{2}}(|s\rangle - |p\rangle)$ and then to the bonding, $|\psi_{bn}\rangle \equiv \frac{1}{\sqrt{2}}(|\chi_{1,n}\rangle + |\chi_{2,n+1}\rangle)$, and the antibonding, $|\psi_{an}\rangle \equiv \frac{1}{\sqrt{2}}(|\chi_{1,n}\rangle - |\chi_{2,n+1}\rangle)$, orbitals. By appropriate approximation, the two sets $\{|\psi_{bn}\rangle\}$ and $\{|\psi_{an}\rangle\}$ are decoupled.
5. Plot the four band edges of the two bands as a function of d ($2\text{\AA} < d < \infty$) by employing the solutions of (2). Are there values of d where the gap disappears?

5.7s. Starting from (F.10)–(F.13) prove (5.60) and (5.61).

5.8. The states of a quantum particle moving in a periodic potential are characterized by the crystal wavevector \mathbf{k} and the band index n . In what follows we shall not display explicitly the band index. (In the TBM we considered in this chapter there is only one band).

Prove that the density of states (DOS) exhibits a singularity, as shown in Fig. 5.13, near an energy E_0 such that $\nabla_{\mathbf{k}}E(\mathbf{k}) = 0$ for an *isolated* point, $\mathbf{k} = \mathbf{k}_0$, satisfying the relation $E_0 = E(\mathbf{k}_0)$.

The quantities A_i are defined by the relations $A_i \equiv \partial^2 E(\mathbf{k}) / \partial k_i^2$ for $\mathbf{k} = \mathbf{k}_0$; the components i are along the principal axes, which by definition satisfy the relations $\partial^2 E(\mathbf{k}) / \partial k_i \partial k_j = 0$ for $i \neq j$.

Hints:

1. It is better and easier to work first with the quantity $R(E, E_0)$ representing the number of states whose eigenenergies fall between E and E_0 . Then the DOS is obtained by taking the derivative

$$\varrho(E) = \frac{dR(E, E_0)}{dE} \quad \text{as } E \rightarrow E_0. \quad (1)$$

The number of states, $R(E, E_0)$, per primitive cell (and per band) is given by the general formula

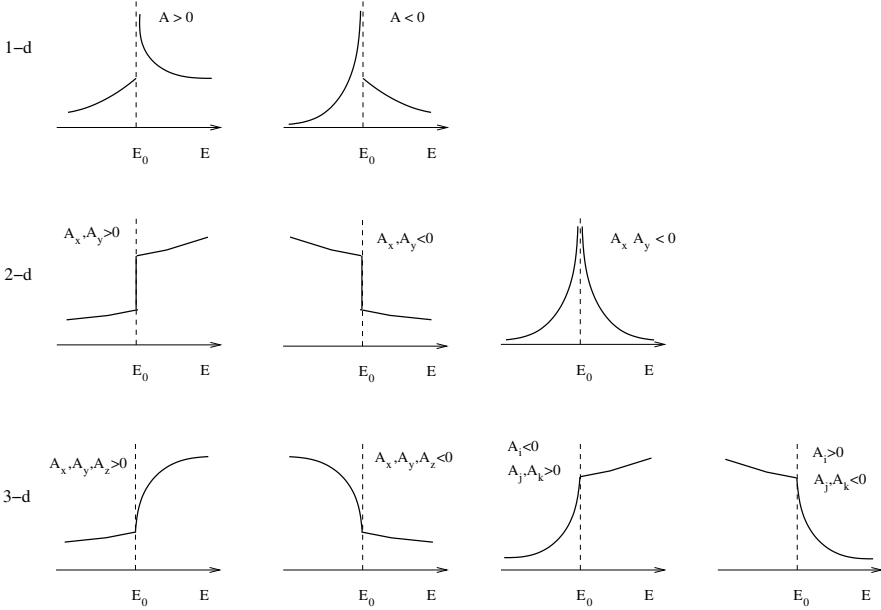


Fig. 5.13. Behavior of DOS near an isolated energy E_0 corresponding to an extremum or a saddle point of $E(\mathbf{k})$ for 1-d, 2-d, and 3-d systems

$$R(E, E_0) = \frac{\Omega_0}{(2\pi)^d} \Omega_{\mathbf{k}}, \quad (2)$$

where d is the dimensionality of space ($d=1,2,3$), Ω_0 the “volume” of the primitive cell (a, a^2, a^3 for $d = 1, 2, 3$ and for the examples we have considered), and $\Omega_{\mathbf{k}}$ the extent (volume, area, length for $d = 3, 2, 1$, respectively) of the region in \mathbf{k} -space whose points satisfy the inequalities $E_0 < E(\mathbf{k}) < E$. Notice that the total number of states in the whole first Brillouin zone is exactly one (per band).

- Consider the $E(k)$ vs. k in the 1-d case as shown schematically in the figure below. When E is below the local minimum E_m , there is only one k point such that $E = E(k)$, and consequently $R(E + \delta E, E) \equiv \varrho(E)\delta E$ is, according to (2), $(a/2\pi)\delta k$. Thus

$$\varrho(E) = \frac{a}{2\pi} \frac{1}{|dE/dk|}, \quad E < E_m, \quad (3)$$

where the derivative is computed at point k such that $E(k) = E$. If E is between E_m and E_M , then there are three k points such that $E(k_i) = E$ and the DOS is equal to $(a/2\pi) \sum_{i=1}^3 |dE/dk|_i^{-1}$. For E higher but close to E_m , $R(E, E_m) = (a/2\pi) [k_1 + k_3 - k_2]$. But around k_m we can write

$$E = E_m + \frac{1}{2} A (k_i - k_m)^2, \quad i = 2, 3, \quad E \rightarrow E_m^+. \quad (4)$$

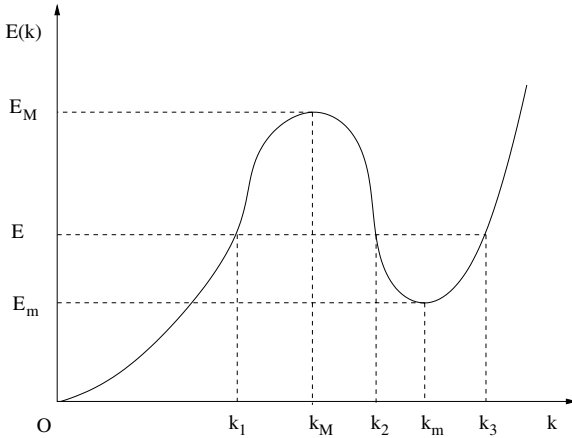


Fig. 5.14. Example of E vs. k for 1-d system

Thus $k_3 - k_m = k_m - k_2 = \sqrt{2(E - E_m)/A}$. Substituting in $R(E, E_m)$ and differentiating with respect to E we find

$$\rho(E) = \begin{cases} \frac{a}{2\pi} \left(\frac{1}{|dE/dk|_1} + \sqrt{\frac{2}{A} \frac{1}{\sqrt{E - E_m}}} \right), & E \rightarrow E_m^+, \\ \frac{a}{2\pi} \frac{1}{|dE/dk|_1}, & E \rightarrow E_m^-. \end{cases} \quad (5)$$

In a similar way show that

$$\rho(E) = \begin{cases} \frac{a}{2\pi} \frac{1}{|dE/dk|_3}, & E \rightarrow E_M^+, \\ \frac{a}{2\pi} \left(\frac{1}{|dE/dk|_3} + \sqrt{\frac{2}{A} \frac{1}{(E - E_M)}} \right), & E \rightarrow E_M^-. \end{cases} \quad (6)$$

3. In two dimensions we have for E close to E_0 , such that $E(\mathbf{k}_0) = E_0$, and $\nabla_{\mathbf{k}} E(\mathbf{k}) = 0$ for $\mathbf{k} = \mathbf{k}_0$, where \mathbf{k}_0 is an isolated point:

$$E = E(\mathbf{k}) = E_0 + \frac{1}{2} A_x (k_x - k_{x0})^2 + \frac{1}{2} A_y (k_y - k_{y0})^2, \quad (7)$$

where x and y are the principal axes.

If both $A_x > 0$ and $A_y > 0$, then \mathbf{k}_0 corresponds to a local minimum; if both $A_x < 0$ and $A_y < 0$, then \mathbf{k}_0 corresponds to a local maximum; finally, if $A_x A_y < 0$, then \mathbf{k}_0 is a saddle point.

Show that:

- (a) If $A_x, A_y > 0$, then for E just above E_0 an extra $\delta R(E, E_0)$ is added corresponding to an ellipse in \mathbf{k} -space of area proportional to $\delta E = E - E_0$. Thus a discontinuity in the DOS would result in the form

$$\varrho(E_0^+) - \varrho(E_0^-) = \frac{a^2}{2\pi} \frac{1}{\sqrt{A_x A_y}}. \quad (8)$$

(b) If $A_x, A_y < 0$, then we find a similar expression

$$\varrho(E_0^+) - \varrho(E_0^-) = -\frac{a^2}{2\pi} \frac{1}{\sqrt{A_x A_y}}. \quad (9)$$

(c) If $A_x A_y < 0$, then the area in \mathbf{k} space corresponding to $R(\pm E \mp E_0)$ is between the two straight lines $k_y - k_{0y} = \pm \sqrt{-A_x/A_y} (k_x - k_{x0})$ and the hyperbola $2(E - E_0) = A_x (k_x - k_{x0})^2 + A_y (k_y - k_{y0})^2$, where $E - E_0$ is either positive or negative. The corresponding area in \mathbf{k} -space is

$$\Omega_{\mathbf{k}} = \frac{2}{\sqrt{-A_x A_y}} |E - E_0| |\ln |E - E_0|| + O(|E - E_0|).$$

Hence

$$\varrho(E) = \frac{a^2}{(2\pi)^2} \frac{2}{\sqrt{-A_x A_y}} |\ln |E - E_0|| \quad \text{as } E \rightarrow E_0. \quad (10)$$

4. Following a similar approach in three dimensions show that

$$\varrho(E) \rightarrow \begin{cases} +\frac{a^3}{\sqrt{2}\pi^2} \sqrt{\frac{E - E_0}{A_x A_y A_z}} + \text{const.} & \text{as } E \rightarrow E_0^\pm, \quad (11a) \\ -\frac{a^3}{\sqrt{2}\pi^2} \sqrt{\frac{E - E_0}{A_x A_y A_z}} + \text{const.} & \text{as } E \rightarrow E_0^\pm, \quad (11b) \end{cases}$$

where (11a) is for E_0 being an extremum (either minimum or maximum) while (11b) is for E_0 being a saddle point of $E(\mathbf{k})$.

Note that if $\nabla_{\mathbf{k}} E(\mathbf{k})$ is zero along a line, then the 2-d singularity is as in 1-d. Similarly, if $\nabla_{\mathbf{k}} E(\mathbf{k})$ is zero along a line in 3-d, then the singularities are as in the 2-d case, and if $\nabla_{\mathbf{k}} E(\mathbf{k}) = 0$ in a surface in 3-d, then the singularities are as in the 1-d case.

Apply (11a) and (11b) to sketch the shape of the DOS for the case of $E(k) = \varepsilon_0 + 2V [\cos(k_x a) + \cos(k_y a) + \cos(k_z a)]$.

5.9. Using (5.47) prove that $G(1; z) = B^{-1} - G(l, l; z)/\lambda$. Then show (5.39b).

Table 5.2. Numerical values for the simple cubic Green's functions $G(\ell_1 - m_1, \ell_2 - m_2, \ell_3 - m_3)$ [in units of $(2|V|)^{-1}$]

$E/2 V $	$\text{Re}\{G(0, 0, 0)\}$	$\text{Im}\{G(0, 0, 0)\}$	$\text{Re}\{G(1, 0, 0)\}$	$\text{Im}\{G(1, 0, 0)\}$	$\text{Re}\{G(1, 0, 0)\}$	$\text{Im}\{G(1, 0, 0)\}$	$\text{Re}\{G(1, 1, 0)\}$	$\text{Im}\{G(1, 1, 0)\}$	$\text{Re}\{G(1, 1, 1)\}$	$\text{Im}\{G(1, 1, 1)\}$
0.0	0.0	0.896441	-0.333333	0.0	0.0	0.0	-0.185788	0.275664	0.0	0.0
0.2	0.074176	0.896927	-0.328388	0.059795	-0.036758	-0.183040	0.265774	-0.082250	-0.163723	-0.163723
0.4	0.152660	0.898396	-0.312979	0.119786	-0.073595	-0.174773	0.234932	0.234932	-0.204031	-0.204031
0.5	0.195323	0.899508	-0.300780	0.149918	-0.092168	-0.168550	0.210461	0.210461	-0.178622	-0.178622
0.6	0.241798	0.900881	-0.284974	0.180176	-0.111043	-0.160914	0.178622	0.178622	-0.083045	-0.083045
0.8	0.356091	0.904444	-0.238376	0.241185	-0.151676	-0.141336	0.083045	0.083045	-0.201461	-0.201461
1.0	0.642882	0.909173	-0.119039	0.303058	-0.239523	-0.115850	0.006621	0.006621	-0.195407	-0.195407
1.2	0.623924	0.617641	-0.083764	0.247056	-0.210658	0.006621	0.049291	0.049291	-0.183703	-0.183703
1.4	0.606577	0.506449	-0.050264	0.236343	-0.180223	0.049291	0.067430	0.067430	-0.175882	-0.175882
1.5	0.598434	0.463545	-0.034116	0.231772	-0.164446	0.067430	0.082687	0.082687	-0.166779	-0.166779
1.6	0.590611	0.425657	-0.018341	0.227017	-0.148310	0.082687	0.106135	0.106135	-0.144801	-0.144801
1.8	0.575841	0.360233	0.012171	0.216140	-0.115001	0.106135	0.121426	0.121426	-0.117903	-0.117903
2.0	0.562116	0.303994	0.041411	0.202662	-0.080371	0.121426	0.129014	0.129014	-0.086194	-0.086194
2.2	0.549312	0.253400	0.069496	0.185826	-0.044490	0.129014	0.128408	0.128408	-0.049765	-0.049765
2.4	0.537326	0.205800	0.096528	0.164640	-0.007418	0.128408	0.124557	0.124557	-0.029803	-0.029803
2.5	0.531612	0.182285	0.109677	0.151904	0.011546	0.124557	0.117828	0.117828	-0.008689	-0.008689
2.6	0.526070	0.158374	0.122594	0.137257	0.030785	0.117828	0.092137	0.092137	0.036969	0.036969
2.8	0.515470	0.105986	0.147772	0.098920	0.070069	0.092137	0.0	0.0	0.087157	0.087157
3.0	0.505462	0.0	0.172129	0.0	0.110383	0.0	0.0	0.0	0.025989	0.025989
3.2	0.400104	0.0	0.093444	0.0	0.042757	0.0	0.0	0.0	0.015398	0.015398
3.4	0.357493	0.0	0.071825	0.0	0.028498	0.0	0.0	0.0	0.012450	0.012450
3.5	0.341048	0.0	0.064556	0.0	0.024187	0.0	0.0	0.0	0.010270	0.010270
3.6	0.326621	0.0	0.058612	0.0	0.020855	0.0	0.0	0.0	0.007296	0.007296
3.8	0.302143	0.0	0.049381	0.0	0.016041	0.0	0.0	0.0	0.002870	0.002870
4.5	0.242855	0.0	0.030949	0.0	0.007868	0.0	0.0	0.0		

Table 5.2. (continued)

$E/2 V $	$\text{Re}\{G(2, 0, 0)\}$	$\text{Im}\{G(2, 1, 0)\}$	$\text{Re}\{G(2, 1, 0)\}$	$\text{Im}\{G(2, 1, 1)\}$	$\text{Re}\{G(2, 1, 1)\}$	$\text{Im}\{G(2, 1, 1)\}$	$\text{Re}\{G(2, 2, 0)\}$	$\text{Im}\{G(2, 2, 0)\}$
0.0	0.0	-0.153291	0.057669	0.0	0.0	0.185788	0.0	-0.051116
0.2	-0.058501	-0.140847	0.055263	-0.014153	0.072194	0.172074	-0.035756	-0.041527
0.4	-0.108662	-0.103475	0.048608	-0.025972	0.136244	0.131113	-0.065024	-0.012416
0.5	-0.127430	-0.075392	0.044234	-0.030162	0.162322	0.100539	-0.074501	0.010095
0.6	-0.139596	-0.041012	0.039726	-0.032830	0.182491	0.063357	-0.078274	0.038275
0.8	-0.130786	0.046798	0.033989	-0.032481	0.195967	-0.030276	-0.054995	0.112685
1.0	0.077131	0.160342	0.081196	-0.022246	0.105070	-0.148591	0.169476	0.214911
1.2	0.017674	-0.027190	0.026381	-0.094125	0.054332	-0.122370	0.131214	-0.003198
1.4	-0.026422	-0.041854	-0.018346	-0.094170	0.008767	-0.117578	0.088374	-0.056319
1.5	-0.042997	-0.037947	-0.036071	-0.087016	-0.011436	-0.111042	0.066251	-0.070590
1.6	-0.056060	-0.029951	-0.052177	-0.076716	-0.029587	-0.101889	0.044256	-0.079012
1.8	-0.072019	-0.006670	-0.074373	-0.049538	-0.058760	-0.076806	0.002587	-0.081221
2.0	-0.074987	0.020951	-0.084251	-0.017244	-0.076833	-0.044847	-0.032527	-0.067062
2.2	-0.065573	0.048180	-0.081178	0.016267	-0.081929	-0.009132	-0.056640	-0.040003
2.4	-0.044321	0.070841	-0.064567	0.046857	-0.072205	0.026283	-0.064998	-0.004542
2.5	-0.029411	0.079009	-0.051010	0.059461	-0.061218	0.042154	-0.061705	0.014298
2.6	-0.011721	0.084050	-0.033863	0.069106	-0.045846	0.055489	-0.052563	0.032255
2.8	0.031780	0.079419	0.011450	0.073435	-0.001059	0.067703	-0.014039	0.056992
3.0	0.085779	0.0	0.071863	0.0	0.063931	0.0	0.056110	0.0
3.2	0.026911	0.0	0.017389	0.0	0.012685	0.0	0.009106	0.0
3.4	0.016927	0.0	0.009670	0.0	0.006405	0.0	0.004293	0.0
3.5	0.014093	0.0	0.007649	0.0	0.004862	0.0	0.003180	0.0
3.6	0.011965	0.0	0.006197	0.0	0.003792	0.0	0.002428	0.0
3.8	0.008988	0.0	0.004279	0.0	0.002443	0.0	0.001513	0.0
4.5	0.004213	0.0	0.001588	0.0	0.000743	0.0	0.000428	0.0

Table 5.2. (continued)

$E/2 V $	$\text{Re}\{G(3, 0, 0)\}$	$\text{Im}\{G(3, 0, 0)\}$	$\text{Re}\{G(3, 0, 0)\}$	$\text{Im}\{G(3, 1, 0)\}$	$\text{Re}\{G(3, 1, 0)\}$	$\text{Im}\{G(3, 1, 0)\}$	$\text{Re}\{G(4, 0, 0)\}$	$\text{Im}\{G(4, 0, 0)\}$
0.0	0.102658	0.0	0.0	0.0	0.018619	0.0	0.0	0.078814
0.2	0.083937	-0.059520	0.008731	0.015606	0.007660	0.057151	0.079233	0.054616
0.4	0.031616	-0.098678	0.013680	0.007660	0.002605	0.069084	0.069084	-0.006106
0.5	-0.003588	-0.104662	0.013690	0.011602	-0.002458	0.043454	0.043454	-0.039691
0.6	-0.041447	-0.098070	0.011602	-0.000094	-0.009563	-0.039781	-0.039781	-0.066840
0.8	-0.106839	-0.036386	-0.000094	-0.054831	-0.006713	0.039227	0.039227	-0.066765
1.0	-0.051484	0.106611	-0.054831	0.016421	0.048606	-0.033782	-0.033782	0.079732
1.2	0.020657	0.064189	0.016421	0.049369	0.020362	-0.031992	-0.031992	-0.013180
1.4	0.049665	0.023146	0.049369	0.054050	0.002144	-0.017774	-0.017774	0.025213
1.5	0.051810	0.002450	0.054050	0.052321	-0.015436	-0.000717	-0.000717	0.036722
1.6	0.047658	-0.015996	0.052321	0.034211	-0.042968	0.028959	0.028959	0.040510
1.8	0.026051	-0.042000	0.034211	0.004549	-0.054598	0.039365	0.039365	0.027341
2.0	-0.004357	-0.049882	0.004549	-0.026625	-0.047353	0.025540	0.025540	-0.002085
2.2	-0.033303	-0.038901	-0.038901	-0.048773	-0.022359	-0.005390	-0.005390	-0.029932
2.4	-0.051000	-0.012029	-0.012029	-0.053043	-0.004865	-0.021874	-0.021874	-0.039145
2.5	-0.052691	0.005294	0.005294	-0.050898	0.014238	-0.034762	-0.034762	-0.033078
2.6	-0.048091	0.023380	0.023380	-0.021571	0.047283	-0.032872	-0.032872	-0.019427
2.8	-0.015603	0.052086	0.052086	0.051046	0.0	0.040578	0.040578	0.023128
3.0	0.055090	0.0	0.051046	0.007147	0.0	0.003578	0.003578	0.0
3.2	0.009231	0.0	0.007147	0.003231	0.0	0.001389	0.001389	0.0
3.4	0.004594	0.0	0.003231	0.002360	0.0	0.000962	0.000962	0.0
3.5	0.003499	0.0	0.002360	0.001782	0.0	0.000695	0.000695	0.0
3.6	0.002749	0.0	0.001782	0.001091	0.0	0.000396	0.000396	0.0
3.8	0.001809	0.0	0.001091	0.000299	0.0	0.000094	0.000094	0.0
4.5	0.000611	0.0	0.000299	0.0	0.0	0.0	0.0	0.0

Single Impurity Scattering

Summary. In this chapter we examine (using techniques developed in Chap. 4) a model tight-binding Hamiltonian describing the problem of a substitutional impurity in a perfect periodic lattice. We obtain explicit results for bound and scattering states. Certain important applications, such as gap levels in solids, Cooper pairs in superconductivity, resonance and bound states producing the Kondo effect, and impurity lattice vibrations, are presented.

6.1 Formalism

We consider here the case of a tight-binding Hamiltonian (TBH) whose perfect periodicity has been broken at just one site (the ℓ site); there, the diagonal matrix element ε_ℓ equals $\varepsilon_0 + \varepsilon$; at every other site it has the unperturbed value ε_0 . This situation can be thought of physically as arising by substituting the host atom at the ℓ site by a foreign atom having a level lying by ε higher than the common level of the host atoms. Thus our TBH can be written as

$$\mathcal{H} = \mathcal{H}_0 + \mathcal{H}_1, \quad (6.1)$$

where the unperturbed part \mathcal{H}_0 is chosen as the periodic TBH examined in Chap. 5, i.e.,

$$\mathcal{H}_0 = \sum_{\mathbf{m}} |\mathbf{m}\rangle \varepsilon_0 \langle \mathbf{m}| + V \sum'_{n\mathbf{m}} |\mathbf{n}\rangle \langle \mathbf{m}|, \quad (6.2)$$

and \mathcal{H}_1 is the perturbation arising from the substitutional impurity, which for simplicity is assumed to not affect the off-diagonal matrix elements:

$$\mathcal{H}_1 = |\ell\rangle \varepsilon \langle \ell|. \quad (6.3)$$

The Green's function G_0 corresponding to \mathcal{H}_0 was examined in detail for various lattices in Chap. 5. In this chapter we would like to find the Green's function G corresponding to $\mathcal{H} \equiv \mathcal{H}_0 + \mathcal{H}_1$; having G (or, equivalently, the

t -matrix T), one can extract all information about the eigenvalues and eigenfunctions of \mathcal{H} . Our starting point is (4.5), which expresses G in terms of G_0 and \mathcal{H}_1 , i.e.,

$$G = G_0 + G_0 \mathcal{H}_1 G_0 + G_0 \mathcal{H}_1 G_0 \mathcal{H}_1 G_0 + \cdots . \quad (6.4)$$

One could use the equivalent equation for T ,

$$T = \mathcal{H}_1 + \mathcal{H}_1 G_0 \mathcal{H}_1 + \mathcal{H}_1 G_0 \mathcal{H}_1 G_0 \mathcal{H}_1 + \cdots . \quad (6.5)$$

Substituting (6.3) into (6.5), we obtain

$$\begin{aligned} T &= |\ell\rangle \varepsilon \langle \ell| + |\ell\rangle \varepsilon \langle \ell| G_0 |\ell\rangle \varepsilon \langle \ell| + |\ell\rangle \varepsilon \langle \ell| G_0 |\ell\rangle \varepsilon \langle \ell| G_0 |\ell\rangle \varepsilon \langle \ell| + \cdots \\ &= |\ell\rangle \varepsilon \left\{ 1 + \varepsilon G_0(\ell, \ell) + [\varepsilon G_0(\ell, \ell)]^2 + \cdots \right\} \langle \ell| \\ &= |\ell\rangle \frac{\varepsilon}{1 - \varepsilon G_0(\ell, \ell)} \langle \ell| , \end{aligned} \quad (6.6)$$

where

$$G_0(\ell, \ell) \equiv \langle \ell| G_0 |\ell\rangle . \quad (6.7)$$

Having obtained a closed expression for T we have immediately G :

$$G = G_0 + G_0 T G_0 = G_0 + G_0 |\ell\rangle \frac{\varepsilon}{1 - \varepsilon G_0(\ell, \ell)} \langle \ell| G_0 . \quad (6.8)$$

As discussed in previous chapters, the poles of $G(E)$ [or $T(E)$] correspond to the discrete eigenvalues of \mathcal{H} . In the present case the poles of G (or T) are given by

$$G_0(\ell, \ell; E_p) = 1/\varepsilon , \quad (6.9)$$

as can be seen by inspection of (6.8) or (6.6). Note that the poles E_p must lie outside the band of \mathcal{H}_0 , because inside the band $G_0(\ell, \ell; E)$ has a nonzero imaginary part and consequently (6.9) cannot be satisfied. Using (6.8) we obtain for the residue of $G(\mathbf{n}, \mathbf{m})$ at the pole E_p

$$\text{Res}\{G(\mathbf{n}, \mathbf{m}; E_p)\} = -\frac{G_0(\mathbf{n}, \ell; E_p) G_0(\ell, \mathbf{m}; E_p)}{G'_0(\ell, \ell; E_p)} , \quad (6.10)$$

where the prime denotes differentiation with respect to E . The degeneracy f_p of the level E_p can be found by using (3.6) and (6.10):

$$\begin{aligned} f_p &= \text{Tr}\{\text{Res}\{G(E_p)\}\} = \sum_{\mathbf{n}} \text{Res}\{(\mathbf{n}, \mathbf{n}; E_p)\} \\ &= -\frac{1}{G'_0(\ell, \ell)} \sum_{\mathbf{n}} G_0(\mathbf{n}, \ell) G_0(\ell, \mathbf{n}) = -\frac{\langle \ell| (E_p - \mathcal{H}_0)^{-2} |\ell\rangle}{G'(\ell, \ell)} \\ &= 1 , \end{aligned} \quad (6.11)$$

where the last step follows because of (1.31). Since the level E_p is nondegenerate, the discrete eigenfunction $|b\rangle$ satisfies (3.7), which in the present case can be written as

$$\langle \mathbf{n}|b\rangle \langle b|\mathbf{m}\rangle = \text{Res} \{G(\mathbf{n}, \mathbf{m}; E_p)\} . \quad (6.12)$$

Substituting (6.10) into (6.12) we obtain for $|b\rangle$

$$|b\rangle = \frac{G_0(E_p)}{\sqrt{-G'_0(\boldsymbol{\ell}, \boldsymbol{\ell}; E_p)}} |\boldsymbol{\ell}\rangle , \quad (6.13)$$

or more explicitly

$$|b\rangle = \sum_{\mathbf{n}} b_{\mathbf{n}} |\mathbf{n}\rangle , \quad (6.14)$$

where $b_{\mathbf{n}}$ is given by

$$b_{\mathbf{n}} = \frac{G_0(\mathbf{n}, \boldsymbol{\ell}; E_p)}{\sqrt{-G'_0(\boldsymbol{\ell}, \boldsymbol{\ell}; E_p)}} . \quad (6.15)$$

We remind the reader that $G'_0(\boldsymbol{\ell}, \boldsymbol{\ell}; E_p)$ is always negative for E not belonging to the spectrum [see (1.31)].

We have seen in Chap. 5 that for E outside the band, $G_0(\mathbf{n}, \boldsymbol{\ell}; E)$ decays exponentially with the distance $R_{\mathbf{n}\boldsymbol{\ell}} \equiv |\mathbf{n} - \boldsymbol{\ell}|$, i.e.,

$$G_0(\mathbf{n}, \boldsymbol{\ell}; E) \xrightarrow{R_{\mathbf{n}\boldsymbol{\ell}} \rightarrow \infty} \text{const.} \times \exp[-\alpha(E)R_{\mathbf{n}\boldsymbol{\ell}}] , \quad (6.16)$$

with $\alpha(E) > 0$. Hence, (6.14) and (6.15) imply that the eigenfunction $|b\rangle$ is localized in the vicinity of the impurity site $\boldsymbol{\ell}$ and decays far away from it as $\exp[-\alpha(E_p)R_{\boldsymbol{\ell}\mathbf{n}}]$. The quantity $\alpha^{-1}(E_p)$ is a measure of the linear extent of the eigenfunction. In the 1-d case $\alpha(E)$ is given by

$$a(E) = -\frac{1}{a} \ln \left[\frac{|E - \varepsilon_0|}{B} - \sqrt{\frac{(E - \varepsilon_0)^2}{B^2} - 1} \right] , \quad |E - \varepsilon_0| > B . \quad (6.17)$$

Let us now examine the effects of the perturbation on the continuous spectrum of \mathcal{H}_0 (i.e., for E inside the band).

The partial DOS at site \mathbf{n} is given by $\varrho(\mathbf{n}; E) = -\text{Im} \{ \langle \mathbf{n} | G^+(E) | \mathbf{n} \rangle \} / \pi$ which, by using (6.8), becomes

$$\varrho(\mathbf{n}; E) = \varrho_0(\mathbf{n}; E) - \frac{1}{\pi} \text{Im} \left\{ \frac{\varepsilon \langle \mathbf{n} | G_0^+(E) | \boldsymbol{\ell} \rangle \langle \boldsymbol{\ell} | G_0^+(E) | \mathbf{n} \rangle}{1 - \varepsilon G_0^+(\boldsymbol{\ell}, \boldsymbol{\ell}; E)} \right\} . \quad (6.18)$$

In particular, the DOS at the impurity site $\boldsymbol{\ell}$ can be written after some simple algebraic manipulations as

$$\varrho(\boldsymbol{\ell}; E) = \frac{\varrho_0(\boldsymbol{\ell}; E)}{|1 - \varepsilon G_0^\pm(\boldsymbol{\ell}, \boldsymbol{\ell}; E)|^2} . \quad (6.19)$$

Taking into account that $G_0(E) \xrightarrow{E \rightarrow \infty} 1/E$, we can easily see from (6.8) that $G(E) \xrightarrow{E \rightarrow \infty} 1/E$; hence

$$G(\mathbf{n}, \mathbf{n}; E) \equiv \langle \mathbf{n} | G(E) | \mathbf{n} \rangle \xrightarrow{E \rightarrow \infty} \frac{1}{E} .$$

This relation implies (by Cauchy's theorem; see Problem 6.1) that

$$\int_{-\infty}^{\infty} \varrho(\mathbf{n}; E) dE = -\frac{1}{\pi} \text{Im} \left\{ \int_{-\infty}^{\infty} G^+(\mathbf{n}, \mathbf{n}; E) dE \right\} = 1 . \quad (6.20)$$

Equation (6.18) implies that the DOS $\varrho(\mathbf{n}; E)$ is a nonzero continuous function of E within the unperturbed band (except possibly at isolated points) and that the continuous band of \mathcal{H} coincides with the band of \mathcal{H}_0 . Unlike $\varrho_0(\mathbf{n}; E)$, the quantity $\varrho(\mathbf{n}; E)$ exhibits a δ -function singularity outside the band at the energy E_p of the bound state, where (6.18) can be recast as

$$\begin{aligned} \varrho(\mathbf{n}; E) &= \frac{G_0(\mathbf{n}, \boldsymbol{\ell}; E_p) G_0(\boldsymbol{\ell}, \mathbf{n}; E_p)}{-G'_0(\boldsymbol{\ell}, \boldsymbol{\ell}; E_p)} \delta(E - E_p) \\ &= |b_{\mathbf{n}}|^2 \delta(E - E_p) , \quad E \approx E_p . \end{aligned} \quad (6.21)$$

To obtain the last result we have used (6.15). Equation (6.20) can be written then as

$$\int_{E_\ell}^{E_u} \varrho(\mathbf{n}; E) dE + \sum_p |b_{\mathbf{n}}|^2 = 1 , \quad (6.22)$$

where the summation is over all the poles of G (if any), and E_ℓ and E_u are the lower and upper band edges, respectively. If we sum over all sites \mathbf{n} and take into account that the bound eigenfunctions are normalized, we obtain

$$\int_{E_\ell}^{E_u} \mathcal{N}(E) dE + P = N , \quad (6.23)$$

where $P = \sum_p$ is the total number of poles (i.e., of discrete levels; $P = 0$ or 1 in the present model) and $\mathcal{N}(E)$ is the total DOS within the continuous band. Here N is the number of lattice sites, which coincides with the total number of independent states in our Hilbert space. Equation (6.23) means that any discrete levels were formed at the expense of the continuous spectrum. Equation (6.22) means that this "sum rule" is valid for each site \mathbf{n} and that the transfer of weight from the continuum at \mathbf{n} to each discrete level equals the overlap $|b_{\mathbf{n}}|^2$ of this discrete level with site \mathbf{n} .

The eigenstates in the band are of the scattering type and are given by (4.31), which, in the present case, can be written as

$$|\psi_E\rangle = |\mathbf{k}\rangle + G_0^+(E) T^+(E) |\mathbf{k}\rangle , \quad (6.24)$$

where $|\mathbf{k}\rangle$ is the Bloch wave given by (5.15a) and (5.15b); as was discussed in Chap. 4, G^+T^+ selects the physically admissible outgoing solutions.

Substituting (6.6) into (6.24), we obtain (after some simple algebraic manipulations) the \mathbf{n} -site amplitude of $|\psi_E\rangle$, $\langle \mathbf{n}|\psi_E\rangle$

$$\langle \mathbf{n}|\psi_E\rangle = \langle \mathbf{n}|\mathbf{k}\rangle + \frac{\langle \mathbf{n}|G_0^+(E)|\ell\rangle \varepsilon \langle \ell|\mathbf{k}\rangle}{1 - \varepsilon G_0^+(\ell, \ell; E)}. \quad (6.25)$$

In particular, the amplitude of $|\psi_E\rangle$ at the site of the impurity is

$$\langle \ell|\psi_E\rangle = \frac{\langle \ell|\mathbf{k}\rangle}{1 - \varepsilon G_0^+(\ell, \ell; E)}. \quad (6.26)$$

We saw in Chap. 4 that the cross section $|f|^2$ for an incident wave $|\mathbf{k}_i\rangle$ to be scattered to the final state $|\mathbf{k}_f\rangle$ is proportional to $|\langle \mathbf{k}_f|T^+(E)|\mathbf{k}_i\rangle|^2$, where T is the t -matrix. Using (6.6), (5.15a), and (5.15b), we obtain for the scattering cross section

$$|f|^2 \sim \frac{\varepsilon^2}{|1 - \varepsilon G_0^+(\ell, \ell; E)|^2}. \quad (6.27)$$

We have pointed out that $1 - \varepsilon G_0^\pm(\ell, \ell; E)$ cannot become zero for E within the band. However, it is possible, under certain conditions, that the magnitude $|1 - \varepsilon G_0^\pm(\ell, \ell; E)|^2$ becomes quite small for $E \approx E_r$. Then, for $E \approx E_r$, the quantity $|\langle \ell|\psi_E\rangle|^2$ will become very large, as can be seen from (6.26). On the other hand, for \mathbf{n} far away from ℓ , i.e., $R_{n\ell} \rightarrow \infty$, $|\langle \mathbf{n}|\psi_E\rangle|^2 \rightarrow |\langle \mathbf{n}|\mathbf{k}\rangle|^2$, because $\langle \mathbf{n}|G_0(E)|\ell\rangle$ goes to zero as $R_{n\ell} \rightarrow \infty$. Thus the eigenfunction $|\psi_{E_r}\rangle$ reduces to the unperturbed propagating Bloch wave $|\mathbf{k}\rangle$ for $R_{n\ell} \rightarrow \infty$, while around the impurity site ℓ it is considerably enhanced, as shown in Fig. 6.1b. For comparison we have also plotted schematically a bound eigenstate (Fig. 6.1a) and a regular (i.e., one for which $|1 - \varepsilon G_0(\ell, \ell; E)|^2$ is not small) band state (Fig. 6.1c). Eigenstates of the type shown in Fig. 6.1b are called *resonance* eigenstates. They resemble, somehow, local (or bound) eigenstates in the sense that it is much more probable to find the particle around site ℓ than around any other site. On the other hand, they share with the other band states the property of being propagating and nonnormalizable. Note that the resonance eigenenergies E_r will appear as peaks, both in the scattering cross section [see (6.27)] and in the perturbed DOS $\varrho(\ell; E)$ [see (6.19)]. For the DOS $\varrho(\ell; E)$, the peak may be shifted somehow if the unperturbed DOS $\varrho_0(\ell; E)$ has a strong E dependence around E_r .

The quantity $|1 - \varepsilon G_0^\pm(\ell, \ell; E)|^2$ can be written as

$$(1 - \varepsilon \operatorname{Re}\{G_0^\pm\})^2 + \varepsilon^2 (\operatorname{Im}\{G_0^\pm\})^2.$$

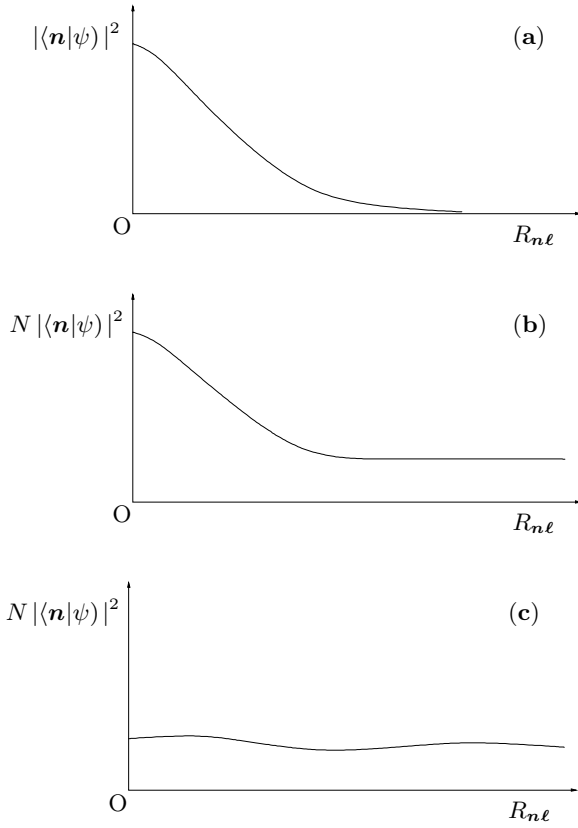


Fig. 6.1. Schematic plot of $|\langle \mathbf{n} | \psi \rangle|^2$ or $N |\langle \mathbf{n} | \psi \rangle|^2$ vs. distance $R_{n\ell}$ of site \mathbf{n} from site ℓ ; for an eigenstate $|\psi\rangle$ localized around site ℓ (a); for a resonance eigenstate (b); and for an ordinary propagating (or extended) eigenstate (c)

If $\text{Im} \{G_0^\pm(\ell, \ell; E)\}$ is a slowly varying function of E (for E around E_r), then the resonance energy will be given approximately as a solution of

$$1 - \varepsilon \text{Re} \{G_0(\ell, \ell; E)\} \approx 0. \quad (6.28)$$

Obviously a sharp resonance requires that $\varepsilon^2 (\text{Im} \{G_0(\ell, \ell; E_r)\})^2$ must be much smaller than 1. If, furthermore, the derivative of $\text{Re} \{G_0(\ell, \ell; E)\}$ is a slowly varying function of E (for E around E_r), then we can write

$$|1 - \varepsilon G_0(\ell, \ell; E)|^2 \approx A^{-2} [(E - E_r)^2 + \Gamma^2]; \quad E \simeq E_r, \quad (6.29)$$

where

$$\Gamma = \frac{|\text{Im} \{G_0(\ell, \ell; E_r)\}|}{|\text{Re} \{G_0'(\ell, \ell; E)\}|},$$

and $A^{-1} = |\varepsilon \text{Re} \{G_0'(\ell, \ell; E)\}|$ for $E = E_r$.

Substituting the approximate expression (6.29) into (6.19), (6.26), and (6.27), we obtain

$$\varrho(\ell; E) \approx \frac{A^2 \varrho_0(\ell; E)}{(E - E_r)^2 + \Gamma^2} = \frac{A^2 \varrho_0(\ell; E)}{|E - z_r|^2}, \quad (6.30)$$

$$|\langle \ell | \psi_E \rangle|^2 \approx \frac{1}{N} \frac{A^2}{(E - E_r)^2 + \Gamma^2} = \frac{A^2/N}{|E - z_r|^2}, \quad (6.31)$$

$$|f|^2 \propto \frac{A^2 \varepsilon^2}{(E - E_r)^2 + \Gamma^2} = \frac{A^2 \varepsilon^2}{|E - z_r|^2}, \quad (6.32)$$

where

$$z_r \equiv E_r - i\Gamma. \quad (6.33)$$

Thus, assuming the validity of (6.29), the resonance eigenstates appear as poles in the *lower* [upper] *half plane* of the *analytic continuation* of $G^+(\ell, \ell; E)$ [$G^-(\ell, \ell; E)$], across the branch cut; remember that $G^\pm(\ell, \ell; E)$ equals $G_0^\pm(\ell, \ell; E) / [1 - \varepsilon G_0^\pm(\ell, \ell; E)]$. The inverse is also true: if the analytic continuation of $G^+(\ell, \ell; E)$ across the branch cut exhibits a pole near the real axis (with $\Gamma/B \ll 1$, B being the half bandwidth), then a resonance appears. Note, though, that the analytic continuation of $G^\pm(\ell, \ell; E)$ may possess a more complicated structure, in which case the quantities $\varrho(\ell; E)$, $|\langle \ell | \psi_E \rangle|^2$, and $|f|^2$ do not have the simple form shown in (6.30)–(6.32). An example of this case is resonances appearing close to the band edges. We will see later that these resonances appear when the real pole E_p lies very close to the band edge.

Consider a particle whose motion is described by \mathcal{H} , placed initially ($t = 0$) at site ℓ , i.e., $c_{\mathbf{n}}(0) = \delta_{\mathbf{n}\ell}$. Using (2.20), (2.10), and (2.8) we obtain for the probability amplitude, $c_{\ell}(t)$, of still finding the particle at the same site later ($t > 0$) the following expression:

$$c_{\ell}(t) = \frac{i}{2\pi} \int_{-\infty}^{\infty} e^{-iEt/\hbar} G^+(\ell, \ell; E) dE. \quad (6.34)$$

The contribution to $c_{\ell}(t)$ from a bound state [i.e., a pole of $G^+(\ell, \ell; E)$], $c_{\ell b}(t)$, is

$$\begin{aligned} c_{\ell b}(t) &= -2\pi i \frac{i}{2\pi} \text{Res} \{ G^+(\ell, \ell; E_p) \} \exp(-iE_p t/\hbar) \\ &= |b_{\ell}|^2 \exp(-iE_p t/\hbar), \end{aligned} \quad (6.35)$$

where (6.8) and (6.15) were taken into account. Equation (6.35) means physically that in the presence of the local eigenstate $|b\rangle$ the particle will not diffuse away; even as $t \rightarrow \infty$ there will be a finite probability $|b_{\ell}|^4$ of finding the particle at site ℓ . The contribution, $c_{\ell B}(t)$, to $c_{\ell}(t)$ from all the states (of the type as in Fig. 6.1c) belonging to the band decays with time in a power law.

In particular,

$$c_{\ell B}(t) = \begin{cases} J_0(Bt/\hbar), & (6.36a) \\ 2J_0(Bt/\hbar) + 2J_0''(Bt/\hbar), & (6.36b) \end{cases}$$

where (6.36a) is the result of the 1-d DOS, (5.30), and (6.36b) is for the Hubbard DOS, (5.55), and $J_0(x)$ is the Bessel function of the first kind and zero order (Problem 6.2). Thus, the ordinary band eigenstates help the particle to diffuse away at a characteristic time of the order \hbar/B , where B is the half bandwidth. Finally, the contribution to $c_{\ell}(t)$ from resonance eigenstates, $c_{\ell r}(t)$, is, assuming a single pole representation of the resonance as in (6.30)–(6.32),

$$c_{\ell r}(t) \sim \exp(-\Gamma t/\hbar) \exp(-iE_r t/\hbar). \quad (6.37)$$

Thus for $t \ll \hbar/\Gamma$ the resonance behaves similarly to the bound state as far as the quantity $c_{\ell}(t)$ is concerned. The width Γ must be much smaller than B ; otherwise the concept of a resonance eigenstate has no meaning at all.

To summarize this section: Any discrete eigenvalues of \mathcal{H} are found as solutions of (6.9). The corresponding eigenfunctions are local (or bound) and are given by (6.14) and (6.15). The DOS in the continuum is given by (6.18) and (6.19) and the scattering eigenfunctions by (6.25) and (6.26). Resonance eigenstates may appear in the continuum; these are propagating states that are considerably enhanced in the vicinity of the impurity site. The corresponding eigenenergies E_r appear as a sharp maximum in the DOS or in the scattering cross section. This maximum may come from a single pole z_r in the analytic continuation of $G^+(\ell, \ell; E)$ across the branch cut; then the real part of this pole gives the resonance eigenenergy and the inverse of the imaginary part determines a “lifetime” for the diffusion of a particle initially placed at the impurity site.

6.2 Explicit Results for a Single Band

6.2.1 Three-Dimensional Case

As was discussed in Chap. 5, the typical 3-d DOS behaves as $C_{\ell}\sqrt{E - E_{\ell}}$ (or $C_u\sqrt{E_u - E}$) near the lower (or upper) band edge E_{ℓ} (or E_u). As a result of this, $\text{Re}\{G_0(\ell, \ell; E_{\ell})\} \equiv I_{\ell}$ and $\text{Re}\{G_0(\ell, \ell; E_u)\} \equiv I_u$ are finite;¹ furthermore, because dG/dE is negative outside the band and $G(E) \rightarrow 0$ as $E \rightarrow \infty$, we have

$$I_{\ell} \leq G_0(\ell, \ell; E) < 0 \quad \text{for } E \leq E_{\ell}, \quad (6.38)$$

and

$$0 < G_0(\ell, \ell; E) \leq I_u \quad \text{for } E_u \leq E. \quad (6.39)$$

¹ Exceptions appear in some cases; see Chap. 5.

Hence, the solution of (6.9) requires us to distinguish several cases:

1. $\varepsilon \leq I_\ell^{-1}$; then (6.9) has one and only one solution E_p lying below E_ℓ . This is shown in Fig. 6.2 for the case of a simple cubic lattice.
2. $I_\ell^{-1} < \varepsilon \leq 0$; then there is no solution of (6.9) because $1/\varepsilon$ lies below I_ℓ and consequently there is no intersection of G_0 with $1/\varepsilon$ for $E - \varepsilon_0 < -B$ (Fig. 6.2). The physical interpretation of this result is that an attractive ($\varepsilon < 0$) impurity potential can create a bound eigenstate only when its strength $|\varepsilon|$ exceeds a critical value, $1/|I_\ell|$.
3. For positive ε , the behavior is similar: $|\varepsilon|$ needs to exceed a critical value, $1/|I_u|$ before one (and only one) bound level appears; this level lies above the upper band edge E_u .

Thus a *repulsive* ($\varepsilon > 0$) potential can trap a quantum particle in a level above the upper bound of the unperturbed continuum the same way that

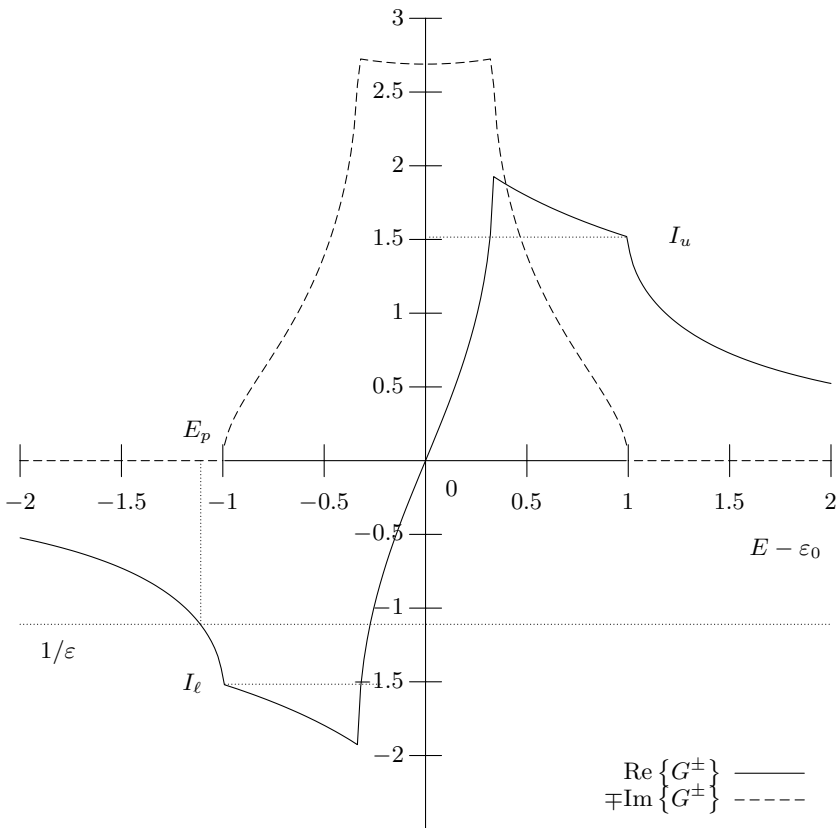


Fig. 6.2. Graphical solution of the equation $\varepsilon G_0^\pm(\ell, \ell; E) = 1$ for the simple cubic lattice and for $\varepsilon < I_\ell^{-1} < 0$ ($B = 1$)

an attractive potential can trap a particle in a level below the lower bound of the continuum. This is a purely wave mechanical property of the same nature as the appearance of an *upper bound* to the continuous spectrum, or the appearance of gaps. One can “understand” the connection better if one keeps in mind that in the vicinity of an upper bound of the spectrum the so-called *effective mass*² is negative; hence the acceleration in a repulsive perturbing potential is attractive and a bound state is formed. Note that for $\mathcal{H}_0 = p^2/2m$ (free particle) the continuous spectrum has a lower bound at $E = 0$ but no upper bound; in this case repulsive perturbing potentials cannot trap a particle.

We can conclude by pointing out that for $\varepsilon < -1/|I_\ell|$ there is one bound level below the continuum; for $-1/|I_\ell| < \varepsilon < 1/I_u$ there is no bound level; finally, for $1/I_u < \varepsilon$ there is one discrete (bound) level above the band.

It is interesting to see how the spectrum of \mathcal{H} changes as $|\varepsilon|$ gradually increases from zero. To simplify the calculations, we use the Hubbard $G_0(\ell, \ell; E)$ (with $\varepsilon_0 = 0$), i.e., $G_0(\ell, \ell; E) = 2/(E \pm \sqrt{E^2 - B^2})$. For this simple case $|I_\ell|^{-1} = I_u^{-1} = B/2$, and $E_p = (B^2 + 4\varepsilon^2)/4\varepsilon$ for $|\varepsilon| > B/2$. The DOS $\varrho(\ell; E)$ is given by

$$\begin{aligned} \varrho(\ell; E) &= \varrho_0(E) \left| \left(1 - \frac{2E\varepsilon}{B^2} + i \frac{2\varepsilon\sqrt{B^2 - E^2}}{B^2} \right) \right|^{-2} \\ &= \frac{2}{\pi} \frac{\sqrt{B^2 - E^2}}{B^2 + 4\varepsilon^2 - 4E\varepsilon}, \quad |E| < B. \end{aligned} \quad (6.40)$$

$\varrho(\ell; E)$ exhibits a maximum at $E = E_r$, where

$$E_r = \frac{4\varepsilon B^2}{B^2 + 4\varepsilon^2}, \quad (6.41)$$

which can be considered as a resonance eigenenergy³ if the maximum is sharp enough. In Fig. 6.3 we plot $\varrho(\ell; E)$ for various negative values of ε . As

² In the 1-d case the effective mass, m^* , is defined as $m^* = \hbar^2 (\partial^2 E / \partial k^2)^{-1} = \hbar^2 / A$ (Problem 5.8). In higher dimensions m^* is a tensor given by the relation $(\hbar^2 / m^*)_{ij} = \partial^2 E / \partial k_i \partial k_j$; its eigenvalues m_i^* satisfy the relation $m_i^* = \hbar^2 / A_i$, where A_i is defined in Problem 5.8.

³ Notice that for the Hubbard G_0 and for $|\varepsilon|$ less than the critical value, $B/2$, $\text{Re}\{1 - \varepsilon G_0\} = 1 - (2E\varepsilon/B^2)$ cannot become zero for $|E| < B$, i.e., for $|E|$ within the band. This is obvious if in Fig. 6.2 we replace the simple cubic G_0 by the Hubbard whose plot is given in Fig. 5.10. Thus for the Hubbard G_0 and for $|\varepsilon| < B/2$ the resonance energy is not given by (6.29). In contrast, for the simple cubic G_0 and for $|\varepsilon|$ less than the critical value $|\varepsilon_c|$ the quantity $1 - \varepsilon \text{Re}\{G_0\}$ can become zero for E within the band; this is clear from Fig. 6.2, which shows that for $1/|\varepsilon|$ between $|I_\ell| = 1.516/B$ and $1.929/B$ there is a value of $|E|$ between B and $B/3$ that makes $1 - \varepsilon \text{Re}\{G_0(E)\}$ equal to zero. However, this difference between the simple Hubbard G_0 and the more complicated G_0 shown in Fig. 6.2

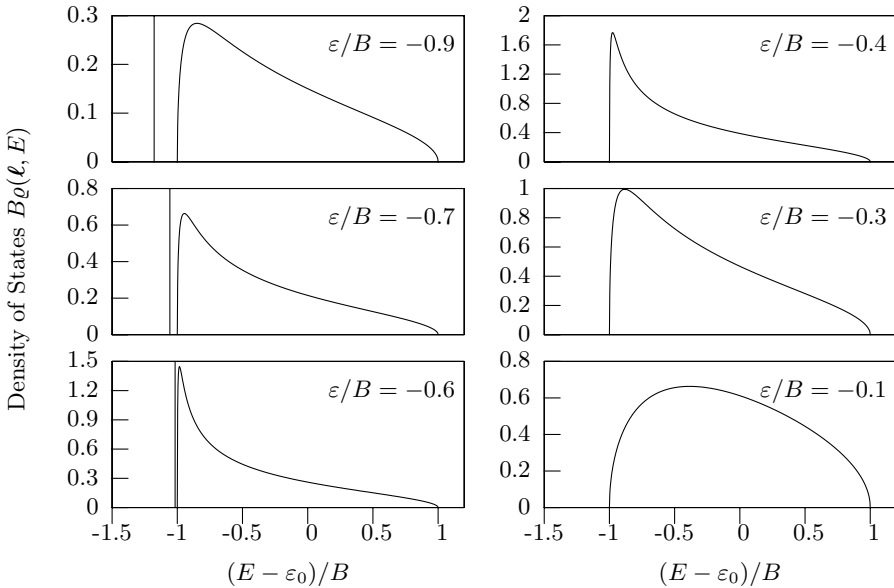


Fig. 6.3. Perturbed DOS $\varrho(\ell; E)$ vs. E for different values of attractive local potential. As $|\varepsilon|$ increases from zero, states are pushed toward the lower band edge, and at a critical value ($|\varepsilon|/B = 0.5$) a discrete level is split off the continuum. The unperturbed DOS $\varrho_0(\ell; E)$ has been taken as in (5.56)

$|\varepsilon|$ increases from zero, states are pushed toward the lower band edge; the maximum of $\varrho(\ell; E)$ moves toward lower values and becomes sharper until a well-defined resonance near the lower band edge appears. This resonance coincides with the band edge for the critical value of $|\varepsilon| = B/2$. As $|\varepsilon|$ exceeds $B/2$, part of the resonance is split off the continuum to form a δ -function (which corresponds to the bound level) at $E = E_p$ of weight

$$|b_\ell|^2 = \frac{\sqrt{E_p^2 - B^2}}{|\varepsilon|} = \frac{4\varepsilon^2 - B^2}{4\varepsilon^2}.$$

Further increase of $|\varepsilon|$ lowers the energy of the bound level and increases its weight $|b_\ell|^2$ at the expense of the continuum; at the same time the resonance recedes toward the center of the band and becomes ill defined. This resonance

does not show up in a substantial way in the plot of the DOS. The reader may verify this by approximating the simple cubic $G_0(E)$ as $E \rightarrow -B^+$ as follows:

$$\begin{aligned} B \operatorname{Re} \{G_0\} &\simeq -1.5164 - 0.6184(B + E)/B, \\ B \operatorname{Im} \{G_0^+\} &\simeq 1.1695\sqrt{(B + E)/B}, \end{aligned}$$

or by looking at the plot of the DOS vs. E/B for the simple cubic lattice and for various values of ε in the solution of Problem 6.3s.

is associated with the appearance of the pole of $G(E)$ on the real axis and at the vicinity of the band edge and not with a complex pole in the analytic continuation of G^\pm . Similar behavior is exhibited around the upper band edge E_u for repulsive ($\varepsilon > 0$) potentials.

In Fig. 6.4 we summarize the above discussion by plotting: (a) The trajectories of the band edges E_ℓ and E_u , (b) the bound level E_p , and (c) the resonance [as defined from the peak of $\varrho(\ell; E)$] as a function of parameter ε , for the simple case of the Hubbard Green's function.

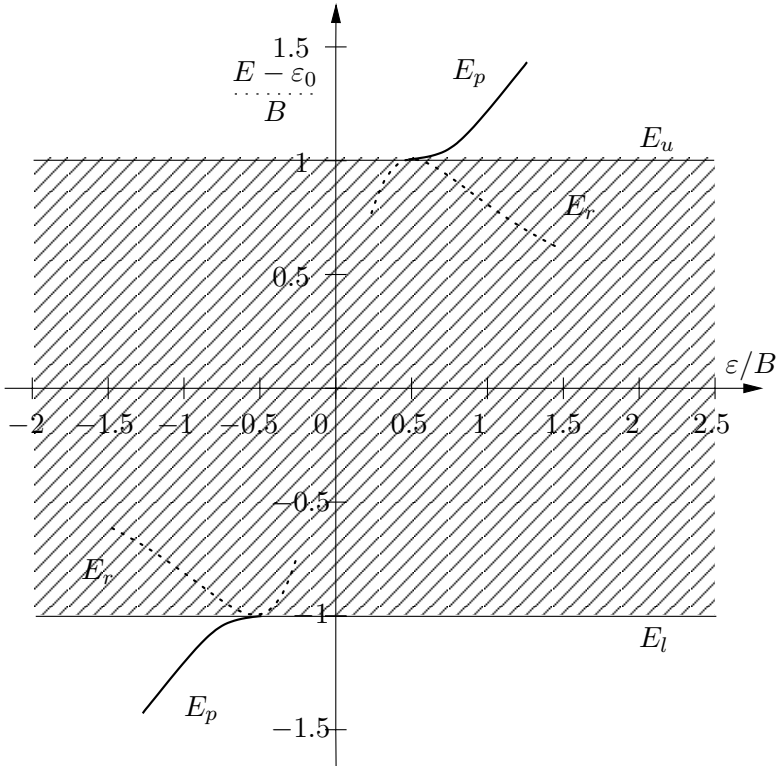


Fig. 6.4. Discrete level (E_p), resonance level (E_r), and band edges (E_ℓ , E_u) vs. local attractive ($\varepsilon < 0$) or repulsive ($\varepsilon > 0$) potential. The shaded area corresponds to the continuous spectrum. The unperturbed DOS $\varrho_0(\ell; E)$ has been taken as in (5.56)

Note that in more complicated systems consisting of overlapping simple bands more than one bound level and resonance may appear, as in the case of a potential well examined in Chap. 4. A typical case is shown schematically in Fig. 6.5.

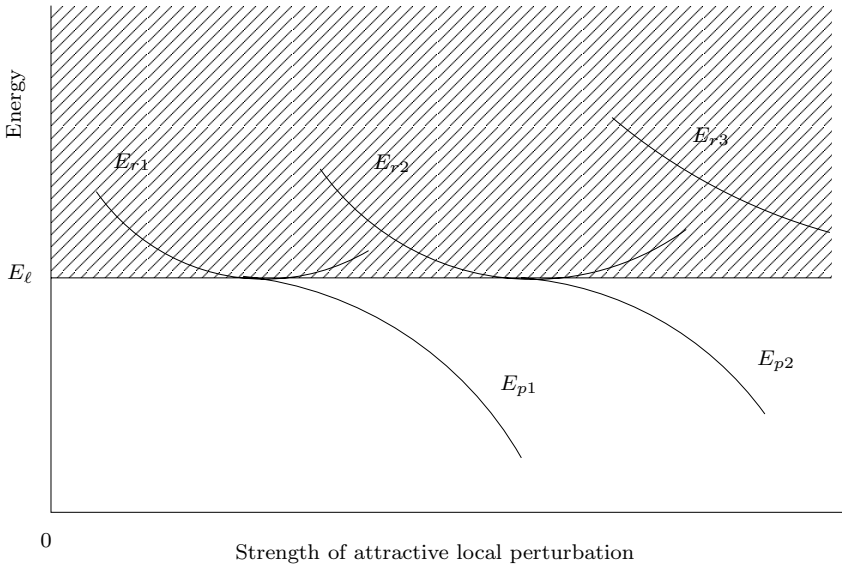


Fig. 6.5. Schematic plot of various discrete (E_{pi}) and resonance (E_{ri}) levels vs. magnitude of attractive local perturbation. E_{ℓ} is the lower edge of a composite band consisting of overlapping simple bands and corresponding to more than one state per site

6.2.2 Two-Dimensional Case

As discussed in Chap. 5, the unperturbed DOS, $\varrho_0(\ell; E)$, exhibits a discontinuity as E approaches the band edge, i.e.,

$$\varrho_0(\ell; E) \xrightarrow{E \rightarrow E_{\ell}^+} \varrho_d. \quad (6.42)$$

As a result

$$G_0(\ell, \ell; E) \xrightarrow{E \rightarrow E_{\ell}^-} \varrho_d \ln \left| \frac{(E - E_{\ell})}{C} \right| \xrightarrow{E \rightarrow E_{\ell}^-} -\infty, \quad (6.43)$$

where C is a positive constant. A similar behavior appears in the upper band edge. Thus, both I_{ℓ} and I_u are infinite, and consequently there is always one solution to (6.9) no matter how small $|\varepsilon|$ is. For very small $|\varepsilon|$, E_p lies very close to the band edge, and one can use (6.43) for $G_0(\ell, \ell; E)$. Substituting in (6.9) we obtain

$$E_p - E_{\ell} \approx -C \exp \left(-\frac{1}{|\varepsilon| \varrho_d} \right); \quad \varepsilon \leq 0. \quad (6.44)$$

Thus the binding energy $|E_p - E_\ell|$ for weak perturbation depends exponentially on the inverse of the strength of the perturbation. This dependence stems directly from the discontinuity of the unperturbed DOS at the band edge, which in turn is a characteristic feature of 2-d systems. For the case of the square lattice one obtains, by taking the limit⁴ $E \rightarrow (\varepsilon_0 - B)^-$ in (5.38),

$$G_0(\ell, \ell; E) \xrightarrow{E \rightarrow (\varepsilon_0 - B)^-} \frac{1}{\pi B} \ln \left(\frac{|E - \varepsilon_0 + B|}{8B} \right),$$

which means that $\varrho_d = 1/\pi B$ and $C = 8B$. Thus for a square lattice

$$E_p - E_\ell \xrightarrow{\varepsilon \rightarrow 0^-} -8B e^{-\pi B/|\varepsilon|}. \quad (6.45)$$

It should be noted that (6.44) is applicable to the case of a particle of mass m moving in a 2-d potential well of depth V_0 and 2-d extent Ω_0 ; in this case $\varrho_d = \varrho_0 \Omega_0$, where ϱ_0 is the free-particle DOS per unit area and $|\varepsilon| = V_0$. Substituting in (6.44) we obtain (4.77). The relevance of (6.44) to the theory of superconductivity will be discussed in the next section.

The interested reader may calculate explicitly various quantities of physical interest and construct a diagram of the type shown in Fig. 6.4 by employing for the 2-d $G_0(\ell, \ell; E)$ the simple model (5.49).

6.2.3 One-Dimensional Case

In the 1-d case the unperturbed DOS near a lower band edge behaves as

$$\varrho_0(\ell; E) \xrightarrow{E \rightarrow E_\ell^+} \frac{C}{\sqrt{E - E_\ell}}, \quad (6.46)$$

which implies that

$$G_0(\ell, \ell; E) \xrightarrow{E \rightarrow E_\ell^-} -\frac{\pi C}{\sqrt{E_\ell - E}} \rightarrow -\infty. \quad (6.47)$$

Thus I_ℓ (and I_u) is infinite, and consequently there is always a bound state no matter how small $|\varepsilon|$ is. For small negative ε the bound level is very close to the lower band edge, and thus one can use expression (6.47) in (6.9). We then obtain for the binding energy E_b the following expression:

$$E_b = |E_p - E_\ell| \xrightarrow{\varepsilon \rightarrow 0^-} \varepsilon^2 \pi^2 C^2. \quad (6.48)$$

For a particle of mass m moving in an ordinary potential well of depth V_0 and linear extent Ω_0 , we have that $|\varepsilon| = V_0$ and $C = \Omega_0 \hbar^{-1} \pi^{-1} \sqrt{m/2}$ [see (4.79)], then E_b is

⁴ $\mathcal{K}(k) \rightarrow \ln(4/\sqrt{1-k^2})$ as $k \rightarrow 1^-$.

$$E_b \xrightarrow{V_0, \Omega_0 \rightarrow 0} \frac{mV_0^2 \Omega_0^2}{2\hbar^2}, \quad (6.49)$$

which agrees with (4.81).

The question of resonances in 1-d systems requires special attention. Firstly, instead of the scattering cross section, one defines the transmission and reflection coefficients, $|t|^2$ and $|r|^2$, which in the present case are given by (Problem 6.4s)

$$|t|^2 = \frac{1}{|1 - \varepsilon G_0(\ell, \ell; E)|^2}, \quad (6.50)$$

$$|r|^2 = \frac{|\varepsilon G_0(\ell, \ell; E)|^2}{|1 - \varepsilon G_0(\ell, \ell; E)|^2}. \quad (6.51)$$

Secondly, the quantity $G_0(\ell, \ell; E)$ is purely imaginary for E within the band so that $|r|^2 + |t|^2 = 1$. The perturbed DOS $\varrho(\ell; E)$ is given by combining (6.19) and (6.50); so

$$\varrho(\ell; E) = \varrho_0(\ell; E) |t|^2. \quad (6.52)$$

Similarly, the quantity $|\langle \ell | \psi \rangle|^2$ is

$$|\langle \ell | \psi \rangle|^2 = \frac{|t|^2}{N}. \quad (6.53)$$

Since $|t|^2 \leq 1$, a resonance would appear as a sharp peak in $|t|^2$ vs. E , where $|t|^2$ rises from values much smaller than one to values approaching one. As an example of such behavior, see [13], p. 109.

For a 1-d lattice, $G_0(\ell, \ell; E)$ is (for $\varepsilon_0 = 0$)

$$G_0(\ell, \ell; E) = \frac{1}{\sqrt{E^2 - B^2}}, \quad |E| > B. \quad (6.54)$$

Thus, the bound level is

$$E_p = \pm \sqrt{B^2 + \varepsilon^2}, \quad (6.55)$$

for $\varepsilon \gtrless 0$, respectively. The transmission coefficient is given by

$$|t|^2 = \frac{B^2 - E^2}{B^2 + \varepsilon^2 - E^2}, \quad (6.56)$$

which does not exhibit any resonance structure. Our model is too simple (no possibility for interference effects) for a resonance to appear.

6.3 Applications

6.3.1 Levels in the Gap

The Hamiltonian we considered in this chapter is an oversimplified model for describing what happens to the electronic properties of a crystalline solid in

the presence of a substitutional impurity. The present model, in spite of its simplicity, retains the essential *qualitative* features of a real solid.

However, if quantitative features are of interest, one has to incorporate several complicating factors, the most important of which is the presence of more than one state for each atom located at site \mathbf{n} (see Problem 5.6 on the presence of two states in each primitive cell). As we have seen in the case of double spacing periodic Cayley tree and in Problem 5.6, the presence of more than one atomiclike orbital per primitive cell may lead to the appearance of a gap separating a fully occupied lower band (called valence band) from a completely empty upper band (called conduction band). This happens to important classes of materials such as semiconductors and insulators, and it is crucial in determining electric, optical, and other properties of these materials. The presence of substitutional or other local defects usually introduces bound levels in the gap. These levels dramatically affect the conductivity and other properties, especially in semiconductors. Some impurities (such as P or Ga atoms in the Si lattice) produce extremely beneficial behavior from a technological point of view. Others (such as vacancies, which can be described mathematically by setting the impurity level $\varepsilon_0 + \varepsilon$ equal to infinity) are detrimental to the function of devices based on doped semiconductors (i.e., semiconductors including desirable substitutional impurities). In the next chapter, Problem 7.2s, we shall examine the appearance of a bound level within the gap of a simple model such as the one in Problem 5.6. A detailed discussion can be found in the original papers by Koster and Slater [94, 95], in subsequent work by Callaway and coworkers [68, 96–98], in a paper by Papaconstantopoulos and Economou [52], in a paper by Bernholc et al. [99, 100], and in a book by Lannoo and Bourgoin [101], where a more extensive list of references is given.

To perform realistic electronic calculations in the presence of isolated defects, one must determine the impurity potential. Even if this potential is known for a perfect periodic solid consisting only of impurity atoms, still in the environment of the host material the electronic charge will be redistributed around the defect, thus modifying the local potential. To face this problem one has to carry out a self-consistent calculation [101, 102]: start with a given impurity potential; calculate the Green's function as explained earlier; then determine the change in the electronic charge density [101]; using Poisson's equation obtain the local (impurity) potential; repeat the procedure until self-consistency is reached.

A further complication of the defect problem stems from the lattice relaxation (i.e., the displacement of the ions around the impurity to new equilibrium positions), which modifies directly as well as indirectly the electronic potential. The first-principle determination of this relaxation is a very difficult problem that requires an accurate calculation of the total (electronic as well as ionic) energy for various plausible relaxations; the actual relaxation is the one that minimizes the total energy. Such a sophisticated calculation

was carried out by Baraff et al. [103] and by Lipari et al. [104] for an isolated vacancy in Si.

6.3.2 The Cooper Pair and Superconductivity

Consider a system of identical fermions, each of mass m , interacting through an attractive pairwise potential: $V(r) = -V_0$ for $r \equiv |\mathbf{r}_i - \mathbf{r}_j| < a$ and zero otherwise. We will examine the motion of a pair of particles omitting the interactions of the pair with the rest of the particles. We shall take into account, however, that the Pauli principle forbids any member of the pair to be in an already occupied state.

In the absence of the interaction V , the eigenstate of the pair is $|\mathbf{k}_1, s_1, \mathbf{k}_2, s_2\rangle$, where the momenta $\mathbf{k}_1, \mathbf{k}_2$ lie outside the Fermi sea defined by the rest of the particles. The spins s_1 and s_2 are arbitrary.

It is more convenient to transform to the center of mass and relative coordinates. Then the Hamiltonian of the pair, \mathcal{H}_{12} , can be written as

$$\mathcal{H}_{12} = \mathcal{H}_{CM} + \mathcal{H}_r = \frac{\hbar^2 K^2}{2M} - \frac{\hbar^2 \nabla_r^2}{2\mu} + V(|\mathbf{r}|) , \quad (6.57)$$

where $M = 2m$, $\mu = m_1 m_2 / (m_1 + m_2) = m/2$, and $\mathbf{r} \equiv \mathbf{r}_1 - \mathbf{r}_2$. The total momentum $\mathbf{K} = \mathbf{k}_1 + \mathbf{k}_2$ is a good quantum number of \mathcal{H}_{12} . Thus, the problem has been reduced to the examination of \mathcal{H}_r , which is the Hamiltonian of a spherical potential well, i.e., the problem examined in this chapter. All we need then is the unperturbed Green's function, which in turn depends on the unperturbed DOS, $\varrho_0(E; \mathbf{K})$, per unit volume for the noninteracting pair of total momentum \mathbf{K} . The quantity $\varrho_0(E; \mathbf{K})$ is given by the volume in \mathbf{k} -space subject to the restriction $E = \varepsilon(\mathbf{k}_1) + \varepsilon(\mathbf{k}_2)$, i.e.,

$$\varrho_0(E; \mathbf{K}) = \frac{1}{(2\pi)^3} \int d\mathbf{k} \delta(E - \varepsilon(\mathbf{k}_1) - \varepsilon(\mathbf{k}_2)) \times \theta(\varepsilon(\mathbf{k}_1) - E_F) \theta(\varepsilon(\mathbf{k}_2) - E_F) , \quad (6.58)$$

where $\mathbf{k} = (\mathbf{k}_1 - \mathbf{k}_2)/2$ is the momentum for the relative motion; \mathbf{k}_1 and \mathbf{k}_2 in (6.58) must be replaced by $\mathbf{K}/2 + \mathbf{k}$ and $\mathbf{K}/2 - \mathbf{k}$, respectively. The two step functions assure that neither electron of the pair can occupy levels below the Fermi energy E_F as required by Pauli's principle; for finite temperatures the product $\theta\theta$ has to be replaced by $[1 - f(\varepsilon(\mathbf{k}_1))][1 - f(\varepsilon(\mathbf{k}_2))]$, where f is the Fermi distribution. Note that (6.58) remains valid even when the pair moves in an external periodic potential (such as in crystalline solids), in which case $\mathbf{k}_1, \mathbf{k}_2, \mathbf{K}$, and \mathbf{k} are crystal momenta and $\varepsilon(\mathbf{k})$ is in general more complicated than $\varepsilon(\mathbf{k}) = \hbar^2 \mathbf{k}^2 / 2m$. It is clear from (6.58) that the presence of the Fermi sea drastically modifies the unperturbed DOS reducing it to zero for $E < 2E_F$, i.e.,

$$\varrho_0(E; \mathbf{K}) = 0 \quad \text{for } E < 2E_F . \quad (6.59)$$

Furthermore for $\mathbf{K} = 0$, ϱ_0 becomes

$$\varrho_0(E; 0) = \frac{1}{2}\varrho(E/2)\theta(E/2 - E_F), \quad (6.60)$$

where $\varrho(E)$ is the DOS per unit volume for a noninteracting particle of energy E and given spin orientation. Then it follows that

$$\varrho_0(E; 0) \xrightarrow{E \rightarrow 2E_F^+} \frac{1}{2}\varrho_F, \quad K = 0, \quad (6.61)$$

where $\varrho_F = \varrho(E_F)$. On the other hand

$$\varrho_0(E; K) \xrightarrow{E \rightarrow 2E_F^+} \text{const.} \times \frac{E - 2E_F}{K}, \quad K \neq 0. \quad (6.62)$$

Thus only for $K = 0$ does the unperturbed DOS drop discontinuously at $E = 2E_F$ from $\varrho_F/2$ to 0. Under these conditions, as we have shown, a bound state will be formed no matter how weak the attractive potential is. The binding energy of the $K = 0$ pair is given for weak attraction by (6.44), i.e.,

$$E_b(0) = C \exp\left(-\frac{2}{V_0\varrho_F a^3}\right). \quad (6.63)$$

The basic result (6.63) was first obtained by Cooper [105]. For pairs with $K \neq 0$, the bound state, in order to appear at all, will require an attractive potential of strength proportional to K and, in any case, will have weaker binding energy than $E_b(0)$. For spherically symmetric potentials $V(|\mathbf{r}_1 - \mathbf{r}_2|)$ (as the one we consider here) the bound pair, which is the ground state, is spherically symmetric and consequently remains invariant under the transformation $\mathbf{r} \rightarrow -\mathbf{r}$, i.e., under exchanging the two particles of the pair. Since the total wave function is odd under the exchange $1 \leftrightarrow 2$, the spin part must be odd, i.e., the pair must be in a singlet state. For spherically asymmetric potentials it is possible that the orbital ground state is odd under the exchange $1 \leftrightarrow 2$, and then the pair must be in a triplet spin state.

It should be stressed that the binding energy shown in (6.63) stemmed from the discontinuity in the unperturbed DOS for the relative motion of the pair. This discontinuity arose because of the presence of the other fermions, which made the states below $2E_F$ unavailable to the pair. Thus a system of fermions in the presence of an attractive interaction achieves its lowest energy by complete pair formation with each pair having a momentum $\mathbf{K} = 0$. This means that in the ground state ($T = 0$) all pairs undergo a quantum condensation. The existence of a condensate implies that independent pair excitations are suppressed. Thus the low-lying excitations are either pair-breaking individual fermions [each of which has a minimum energy $E_b(0)$ as in (6.63)] or collective density fluctuations (i.e., quantized sound waves for neutral fermions or plasmons for charged fermions). Under these conditions, conservation of energy and momentum (see, e.g., Landau and Lifshitz [106] and [107]) implies

that no elementary excitations can appear in a slow-moving “condensed” system. Hence, such a system will be either superfluid (for neutral fermions as in He^3) or superconducting (for charged fermions as in various metallic superconductors).

The picture that emerged from our simple considerations is in qualitative agreement with the results of a sophisticated many-body theory of superconductivity [108–114]. However, there are quantitative discrepancies: the correct result for the binding energy of the pair is proportional to $\exp(-1/V_0 \varrho_F a^3)$ rather than $\exp(-2/V_0 \varrho_F a^3)$ as in (6.63). The resolution of this discrepancy is directly related to the answer to the following apparent paradox: Consider a system of noninteracting fermions moving in an external, 3-d, static weak potential unable to bind any particle. Clearly, it is enough to find the levels (none of which is bound) of a single fermion in this potential and then occupy these levels according to the Fermi distribution $f(E)$. However, if we consider a given fermion in the presence of all the others, then the available unperturbed DOS is $\varrho(E)[1 - f(E)]$, which at $T = 0$ exhibits a discontinuity ϱ_F ; consequently, and in contrast to what was concluded before, it seems that there should be a bound level with binding energy proportional to $\exp(-1/|V| \varrho_F a^3)$.

The origin of these difficulties is our omission of some processes, to be termed indirect, that take place as a result of the indistinguishability of the fermions. The DOS for the single-fermion problem was found to be $\varrho(E)[1 - f(E)]$, because it was assumed that all the other fermions of the Fermi sea played no role other than the passive one dictated by the Pauli principle. However, the fermions of the Fermi sea make possible additional processes (the indirect ones): a Fermi sea fermion can jump to the final state, and the fermion under consideration fills up the created hole. Obviously the DOS for these indirect processes involving the occupied levels equals $\varrho(E)f(E)$. Adding this DOS to the direct-process DOS $\varrho(E)[1 - f(E)]$ we obtain that the total DOS is $\varrho(E)$, i.e., the same as in the absence of the Fermi sea, which is the correct result.

There is an extensively studied case where the cancellation of the $f(E)$ -dependent term between the direct and the indirect processes is not complete: this case leads to the so-called Kondo effect, which will be summarized in the next subsection.

Returning now to the problem of the $\mathbf{K} = 0$ electronic pair we see that the omitted indirect processes involve two Fermi sea electrons jumping to the final states while the original electrons fill up the resulting holes. The corresponding DOS equals $\varrho(E/2)f(E/2)f(E/2)/2$. This DOS must be subtracted from the direct DOS $\varrho(E/2)[1 - f(E/2)][1 - f(E/2)]/2$. The subtraction rather than addition of the two DOS has to do with the antisymmetry of the pair function under particle exchange (Chap. 13). The total effective DOS is then

$$\varrho_0(E; 0) = \varrho(E/2) \frac{1 - 2f(E/2)}{2}. \quad (6.64)$$

Equation (6.64) shows that the discontinuity at $T = 0$ and $E = 2E_F$ is now ϱ_F instead of $\varrho_F/2$ as predicted by (6.60). This eliminates the spurious factor of 2 in the exponent of the rhs of (6.63).

Using the general expression

$$G_0(E; 0) = \int dE' \frac{\varrho_0(E'; 0)}{E - E'} \quad (6.65)$$

and (6.64) we obtain $G_0(E; 0)$. The integration limits in (6.65) are $2E_F - 2\hbar\omega_D$ and $2E_F + 2\hbar\omega_D$. The cutoff energy, $2\hbar\omega_D$, is introduced because the attractive potential is nonzero only when the pair energy is in the range $[2E_F - 2\hbar\omega_D, 2E_F + 2\hbar\omega_D]$. For low temperatures T , where $1 - 2f(E/2)$ varies rapidly at E_F , $|G_0(E; 0)|$ exhibits a maximum at $E = 2E_F$ proportional to $\varrho_F/k_B T$. As one lowers the temperature, this maximum becomes more pronounced until a critical temperature T_c is reached such that

$$a^3 |G_0(2E_F; 0)| V_0 = 1. \quad (6.66)$$

For $T < T_c$ the equation $1 - a^3 V_0 G_0(E; 0) = 0$ will be satisfied and consequently a bound pair will be formed. Thus T_c is the critical temperature below which superconductivity appears. Substituting (6.64) in (6.65) and assuming that $\varrho(E/2) \approx \varrho_F$ and that $\hbar\omega_D/k_B T_c \gg 1$, we obtain (Problem 6.7s)

$$G_0(2E_F; 0) = -\varrho_F \ln \left(\frac{2e^\gamma \hbar\omega_D}{\pi k_B T} \right). \quad (6.67)$$

Substituting (6.67) into (6.66) we obtain for T_c

$$T_c = \frac{2e^\gamma \hbar\omega_D}{\pi k_B} e^{-1/\lambda}, \quad (6.68)$$

where $\lambda = \varrho_F V_0 a^3$ and $\gamma = 0.577\dots$ is Euler's constant. Equation (6.68) is exactly the BCS [108, 109] result for T_c .

We conclude our brief summary of the theory of superconductivity by commenting on the origin of the attractive potential and on the so-called strong coupling modifications of (6.68).

The attraction required to overcome the Coulomb repulsion and bind the partners of each pair together can only be provided by the polarizable medium in which the electrons are embedded. The analogy of two persons on a mattress (which plays the role of the polarizable medium) suggests that the attractive interaction V between two electrons is proportional to the interaction of each electron with the polarizable medium V_{e-m} , and proportional to how easily the medium is polarized, which can be characterized by the inverse of a typical eigenfrequency ω_m of the medium. Thus V is given by

$$V \sim \frac{V_{e-m}^2}{\hbar\omega_m}. \quad (6.69)$$

In all well-understood cases, the polarizable medium is the ionic lattice; then $V_{e-m} = V_{e-p}$, where V_{e-p} is the electron-phonon interaction and ω_m is a typical phonon frequency, which can be taken to be equal to the Debye frequency ω_D . Much effort has been devoted to finding a V mediated by degrees of freedom other than the ionic ones, but no definite results have been established. The discovery of high T_c superconductivity in ceramic Copper oxides, such as $\text{YBa}_2\text{Cu}_3\text{O}_{7-x}$, and in other materials, such as alkali doped fullerenes or MgB_2 , has given new impetus to the search for alternative or complementary mechanisms to mediate electron-electron attraction. Despite intense efforts over the last 18 years, there is no consensus on any of the various other mechanisms proposed. Taking into account that V_{e-p} depends on the momenta of each electron we see that actually V_{e-m}^2 in (6.69) is an appropriate Fermi surface average, $\langle V_{e-p}^2 \rangle$, of the electron-phonon interaction. Furthermore, there is not simply one eigenfrequency, as was assumed in (6.69), but a continuum of eigenfrequencies characterized by a distribution $F(\omega)$. Thus (6.69) must be replaced by

$$V = \int d\omega F(\omega) \frac{\langle V_{e-p}^2 \rangle}{\hbar\omega}. \quad (6.70)$$

The quantity of interest is

$$\lambda = \varrho_F V_0 a^3 = \varrho_F \int V d^3r,$$

on which T_c depends exponentially. It is customary to express λ in terms of

$$\alpha^2(\omega) \equiv \frac{\varrho_F}{2\hbar} \int d^3r \langle V_{e-p}^2 \rangle;$$

taking into account (6.70) one obtains

$$\lambda = 2 \int d\omega F(\omega) \frac{\alpha^2(\omega)}{\omega}. \quad (6.71)$$

The phonon-mediated electron-electron attraction V depends on the square of the electron-phonon interaction V_{e-p}^2 . But the same quantity, V_{e-p}^2 , determines (in the Born approximation) the scattering probability of an electron by the lattice vibrations and, consequently, the phonon contribution to the electrical resistivity ϱ_e . Thus one expects that the materials with high lattice resistivity to have a high λ and hence to be high T_c superconductors. Such a correlation does indeed exist. As a matter of fact, one can show that at high temperatures the derivative of the metallic resistivity ϱ_e is given by

$$\frac{d\varrho_e}{dT} = \frac{8\pi^2 k}{\hbar} \frac{1}{\omega_p^2} \lambda_{tr}, \quad (6.72)$$

where ω_p is the plasma frequency and λ_{tr} results from λ by substituting $\langle V_{e-p}^2 \rangle$ by $\langle V_{e-p}^2 (1 - \cos\theta) \rangle$, where θ is the angle between the incoming wavevector,

\mathbf{k}_1 , and the wavevector, \mathbf{k}_2 , of the scattered wave. In [115], λ_{tr} , as obtained by (6.72), is compared with λ , as obtained from T_c measurements, and/or tunneling experiments, and/or first-principle calculations [116], for various metals. The overall agreement is impressive, suggesting that knowledge of ω_p , ω_D , and $d\rho_e/dT$ for a given metal provides a reasonable estimate of T_c through (6.72) and (6.68) (assuming of course that phonon-mediated attraction is the dominant mechanism).

From (6.70) one can see that a large V can be obtained if there are many low-frequency phonons. This means that a soft, not-so-stable lattice may imply a high T_c . Indeed, most high- T_c materials are not so stable structurally.

Let us examine finally how (6.68) can be improved. An obvious modification is the subtraction from V of a quantity V^* proportional to the screened Coulomb repulsion between the two electrons of the pair. This means that λ must be replaced by $\lambda - \mu^*$, where $\mu^* \equiv \rho_F \int d^3r V^*$. Usually μ^* is about 0.1.

The origin of other modifications is more subtle and requires for its comprehension concepts that will be presented in Part III of this book. Nevertheless, a simplified exposition of these so-called strong coupling modifications will be attempted now.

In arriving at (6.68) we have implicitly assumed that the electron-phonon interaction V and the Coulomb repulsion V_c are so weak that they have no effect on the propagation of the individual electrons that comprise the pairs. Actually, both V_{e-p} and V_c modify the properties of each electron; it is these modified electrons (which are called dressed or quasi electrons) that combine to make up the pairs. One important modification is that the discontinuity at the Fermi level is reduced by a factor $w_F \equiv (1 - \partial\Sigma^*/\hbar\partial\omega)^{-1}$ for each electron of the pair (see Part III, Sects. 12.4 and 13.1), where $\Sigma^*(\omega, \mathbf{k})$ is the so-called *proper self-energy*. One way to understand this reduction is by taking into account that only a fraction w_F of each electron propagates as a quasi electron, while the rest, $1 - w_F$, has no well-defined energy-momentum relation and thus does not produce any discontinuity at E_F . The net result is to multiply the DOS given by (6.64) by a factor w_F^2 .

Another important effect of V_{e-p} and V_c is that they change the electron velocity at the Fermi level from its unperturbed value \mathbf{v}_F to

$$\mathbf{v}'_F = \left(\mathbf{v}_F + \frac{\partial\Sigma^*}{\hbar\partial\mathbf{k}} \right) w_F .$$

Since the single-particle DOS is inversely proportional to the magnitude of the velocity, it follows that the DOS ρ_F must be replaced by $(v_F/v'_F)\rho_F$.

The result of the above two effects together is to multiply the quantity $\lambda - \mu^*$ by a factor equal to $w_F^2 (v_F/v'_F)$ and the outcome to replace λ in (6.68). To calculate this factor explicitly one needs to obtain the proper self-energy, $\Sigma^*(\omega, \mathbf{k})$, which depends on both V_{e-p} and V_c . It is usually assumed that the Coulomb interaction V_c has no significant effects on $\partial\Sigma^*/\partial\omega$; furthermore, calculations employing the Hubbard dielectric function give that the effect of V_c on $\partial\Sigma^*/\partial\mathbf{k}$ is negligible for the usual electronic densities [$r_s \approx 2.5$;

see (13.14)] [112]. Thus in calculating Σ^* we usually keep only V_{e-p} and we employ second-order perturbation theory to obtain [110, 112, 117]

$$\Sigma^*(\omega, \mathbf{p}) = -\lambda \hbar \omega, \quad (6.73)$$

from which we get $w_F = (1 + \lambda)^{-1}$, $v_F/v'_F = (1 + \lambda)$, and $w_F^2 (v_F/v'_F) = (1 + \lambda)^{-1}$. Hence the expression for T_c becomes

$$T_c = p \exp\left(-\frac{1 + \lambda}{\lambda - \mu^*}\right), \quad (6.74)$$

where the prefactor p is not equal to that of (6.68) because of contributions due to the non-quasi-particle smooth background of each electron propagator.

A more rigorous analysis based on the Eliashberg gap equations [117] gives the following expression for T_c [117, 118]:

$$T_c = p \exp\left(-\frac{1.04(1 + \lambda)}{\lambda - \mu^*(1 + 0.62\lambda)}\right), \quad (6.75)$$

which is remarkably close to our simplified result. According to McMillan [117], the prefactor in (6.75) is

$$p = \frac{\hbar \omega_D}{1.45 k_B}. \quad (6.76)$$

A more accurate value of p is given in [118].

6.3.3 The Kondo Problem

In most metals, when the temperature is lowered, the electrical resistivity decreases as a result of the decreasing amplitude of the thermal ionic vibrations. In some metals containing magnetic impurities the resistivity *rises* as the temperature is lowered below a certain characteristic temperature. In 1964, Kondo [119] examined a system of noninteracting electrons undergoing spin flip scatterings by external local moments. He was able to show that second-order contributions to the resistivity increased logarithmically with T as T was lowered. By keeping the most divergent contributions to all orders, Abrikosov [120] concluded that the resistivity blows up at a characteristic temperature T_K . Many attempts were made (see, e.g., [121–123]) to remove the nonphysical singularity and to understand the low-temperature ($T \ll T_K$) state of the system. Kondo [124] reviewed in detail the early literature. Anderson and Yuval [125, 126] introduced the idea of scaling and noticed the analogy of the Kondo problem with other problems in statistical physics; they managed thus to predict correctly the nature of the low-temperature state: one electron is bound to each local moment in a singlet state and each such combination is inaccessible to the other electrons. The difficult task is

how to follow continuously the solution from the high-temperature ($T \gg T_K$) weak-scattering region to the low-temperature ($T \ll T_K$) bound-state regime through the intermediate crossover ($T \approx T_K$) region. Some contributions [127] are reviewed in [128]. Finally, Wilson [129], by employing nonperturbative numerical treatment of the crossover regime, succeeded in connecting the high- T region to the low- T regime and thus obtained explicit numerical results for the $T = 0$ behavior. A clear presentation of the basic physical ideas is given in a review by Nozieres [130]. Subsequently, Andrei [131] and, independently, Wiegmann [132] managed to diagonalize exactly the Kondo Hamiltonian and to obtain quantities like the zero-temperature magnetic susceptibility in closed form. More recent treatments of the Kondo problem are given in [114] and in [133–135].

Here we give a brief simplified explanation of why the bound state appears for $T \ll T_K$ and why the resistivity exhibits the logarithmic increase for $T \gg T_K$ by considering a tight-binding version of the Kondo Hamiltonian. Assume that one local moment is located at site ℓ . The scattering potential \mathcal{H}_{1K} [instead of (6.3)] is given now by

$$\begin{aligned} \mathcal{H}_{1K} = & -J (|\ell \downarrow\rangle S_+ \langle \ell \uparrow| + |\ell \uparrow\rangle S_- \langle \ell \downarrow| \\ & + |\ell \uparrow\rangle S_z \langle \ell \uparrow| - |\ell \downarrow\rangle S_z \langle \ell \downarrow|) , \end{aligned} \quad (6.77)$$

where the arrows indicate the direction of the electronic spin and $S_+ \equiv S_x + iS_y$, $S_- \equiv S_x - iS_y$, and S_z are the spin components of the local moment. By considering the expansions (6.4) and (6.5) one sees immediately that the direct-process DOS (for a given electronic spin), $\varrho(1-f)$, is between a product of S s, say, $S_- S_+$. The corresponding indirect-process DOS, ϱf , is sandwiched between S_+ and S_- ; the reversal of the ordering of the S s reflects the reversal of the time sequence of the two consecutive spin flip events. Thus the total DOS (omitting terms that do not depend on f) is $(S_- S_+ - S_+ S_-)\varrho(1-f) = -S_z 2\varrho(1-f)$. Hence the problem is reduced to that of a local interaction J and an unperturbed DOS equal to $2\varrho(1-f)$. At $T = 0$, the latter has a discontinuity equal to $2\varrho_F$, which for negative J (antiferromagnetic coupling) will be responsible for a bound state of energy E_b given by

$$E_b = C \exp\left(-\frac{1}{2|J|\varrho'_F}\right) , \quad (6.78)$$

where $\varrho'_F = \varrho_F a^3$. Furthermore, by the same method as for the Cooper pair, one obtains that the bound state appears only for $T < T_K$, where T_K is

$$T_K = \frac{2e^\gamma}{\pi} \frac{D}{k_B} \exp\left(-\frac{1}{2|J|\varrho'_F}\right) , \quad (6.79)$$

with D being an energy cutoff analogous to the $\hbar\omega_D$ in superconductivity. Finally, for $T \gg T_K$ the t -matrix is proportional to $J/(1 - JG_0)$, where G_0 is the Green's function associated with the unperturbed DOS $2\varrho'(1-f)$.

Calculating G_0 at $E = E_F$ [see (6.67)] and taking into account that the resistivity ϱ_e is proportional to the square of the t -matrix, we obtain that

$$\varrho_e \sim \frac{|J|^2}{[1 - 2|J|\varrho'_F \ln(T_0/T)]^2}, \quad (6.80)$$

where T_0 is the prefactor on the rhs of (6.79). Equation (6.80) exhibits the observed logarithmic increase with decreasing T (for $T_K \ll T \ll T_0$).

We conclude this subsection by summarizing the physical origin of the Kondo effect: because of the S operators in (6.77), the f -dependent terms in the direct and indirect DOS do not cancel out as in the simple static case. As a result, the effective total DOS is proportional to $(1 - f)$. This factor creates a discontinuity at $T = 0$ and hence a bound state. The same factor accounts for a decrease in the binding energy with increasing T until a critical temperature T_K is reached beyond which no bound state exists. For $T > T_K$ there is, however, a resonance state that becomes less and less pronounced as T is further increased. This behavior of the resonance state accounts for the anomalous temperature dependence of the resistivity.

6.3.4 Lattice Vibrations in Crystals Containing “Isotope” Impurities

In this subsection we will examine the problem of small oscillations of a system of atoms of mass m placed at the $\{i\}$ sites of a periodic lattice and experiencing a harmonic interaction of the form

$$U = \frac{1}{2} \sum_{ij} \kappa_{ij} (u_i - u_j)^2, \quad (6.81)$$

where u_i is the displacement from equilibrium of the atom placed at the i site. We assume that $\kappa_{ij} = \kappa$ for i, j nearest neighbors, and $\kappa_{ij} = 0$ otherwise. For simplicity we consider here a 1-d lattice, where the number, Z , of nearest neighbors is $Z = 2$. Assuming a time dependence of the form $e^{-i\omega t}$, we obtain the following equation of motion:

$$-\omega^2 m_i u_i = F_i = -\frac{\partial V}{\partial u_i} = \sum_n \kappa_{in} (u_n - u_i) \quad (6.82)$$

or

$$(Z\kappa - \omega^2 m_i) u_i = \kappa \sum'_n u_n, \quad (6.83)$$

where the sum extends only over nearest neighbors of site i . Taking into account (5.9), we can rewrite (5.12) as follows:

$$(\varepsilon_i - E) c_i = -V \sum'_n c_n, \quad (6.84)$$

where the sum extends over nearest neighbors. A simple inspection of (6.83) and (6.84) shows that the problem of lattice vibrations is mathematically equivalent to the TBM (Sect. 5.2).

We consider now the so-called single-isotope impurity case, where

$$m_i = \begin{cases} m_0, & i \neq \ell, \\ m_0 + \Delta m, & i = \ell, \end{cases}$$

corresponding to a single impurity in the TBM. Below we put in columns the corresponding quantities in the two equivalent problems

Electrons	ε_0	V	E	ε	(6.85)
Lattice vibrations	$Z\kappa$	$-\kappa$	$\omega^2 m_0$	$-\Delta m \omega^2$	

The solution of the lattice problem at $\omega = 0$ is equivalent to the solution of the electronic problem at $E - \varepsilon_0 = 0 - Z\kappa = -Z|V|$ and $\varepsilon = 0$, i.e., at the lower band edge without any perturbation. As ω^2 increases from zero the equivalent parameters $E - \varepsilon_0$ and ε in the TBM change: $\varepsilon = -\omega^2 \Delta m$ and $E - \varepsilon_0 = m_0 \omega^2 - Z|V|$; by eliminating ω^2 and substituting $Z|V|$ by $Z\kappa$ we obtain

$$E = -\frac{m_0}{\Delta m} \varepsilon. \quad (6.86)$$

As ω^2 varies, the parameters E and ε of the equivalent TBM move along the straight line defined by (6.86). In Fig. 6.6 we plot the E vs. ε diagram for the TBM; we also draw two straight lines according to (6.86) (OAB corresponding to $\Delta m > 0$ and $0CD$ corresponding to $\Delta m < 0$). We see immediately from Fig. 6.6 that for $\Delta m > 0$ (i.e., the impurity mass heavier than the host mass) there is no discrete eigenfrequency; the spectrum is continuous and extends from 0 ($\omega^2 = 0$) to B ($\omega^2 = 2Z\kappa/m_0$). The frequency corresponding to any point A is

$$\omega_A^2 = \frac{2Z\kappa}{m_0} \frac{(OA)}{(OB)}. \quad (6.87)$$

Note that resonance eigenstates may appear at low frequencies if Δm becomes very large, so that the line OB would rotate counterclockwise until it crossed any dashed resonance line around the 0 point.

For $\Delta m < 0$ (i.e., impurity mass lighter than the host mass) there is a discrete eigenfrequency ω_D^2 because the ω^2 line crosses the E_p line (for typical 3-d cases $|\Delta m|$ must exceed a critical value for a discrete eigenfrequency to appear). The discrete eigenfrequency lies above the upper bound of the continuous spectrum and corresponds to a local oscillation, i.e., one confined around the impurity atom and decaying exponentially as one moves away from it. Using the analogies (6.85) and known results for the TBM, one can obtain all information about the lattice vibration problems.

We conclude this subsection by pointing out that a lighter impurity mass tends to push the eigenfrequencies up and to split off a discrete eigenfrequency

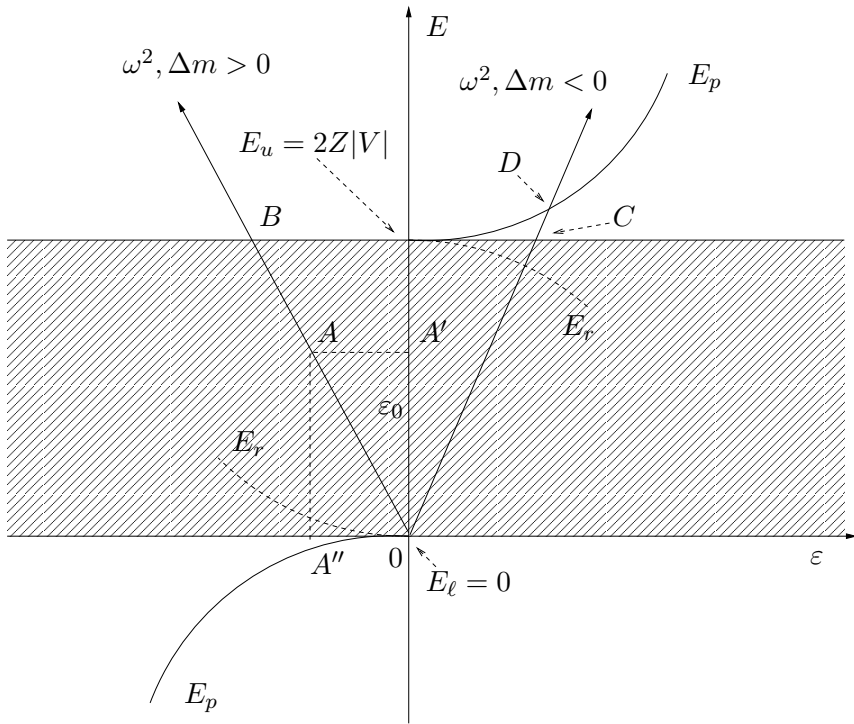


Fig. 6.6. The electronic spectrum vs. ϵ diagram (1-d case is shown) can be used to obtain the spectrum of the lattice vibration (see text)

above the upper bound(s) of the continuum(a). On the other hand, a heavier impurity mass tends to push the eigenfrequencies down; it cannot, of course, split a discrete eigenfrequency below $\omega^2 = 0$. However, if a lower band edge exists at a nonzero frequency (as in the case of an optic branch), then a heavier impurity mass can create a discrete level below the corresponding band.

6.4 Summary

In this chapter we examined (using the techniques developed in Chap. 4) a model Hamiltonian describing the problem of a substitutional impurity in a perfect periodic lattice. The Hamiltonian is given by $\mathcal{H} = \mathcal{H}_0 + \mathcal{H}_1$, where \mathcal{H}_0 is a periodic TBH of the type studied in Chap. 5 and \mathcal{H}_1 describes the change of the potential as a result of the impurity and is given by

$$\mathcal{H}_1 = |\ell\rangle \epsilon \langle \ell| . \quad (6.3)$$

As before, each state $|\mathbf{n}\rangle$ is centered around the corresponding lattice site \mathbf{n} .

The Green's function corresponding to \mathcal{H} can be evaluated exactly in terms of G_0 and ε . The result is

$$G(\mathbf{m}, \mathbf{n}; z) = G_0(\mathbf{m}, \mathbf{n}; z) + \varepsilon \frac{G_0(\mathbf{m}, \boldsymbol{\ell}; z) G_0(\boldsymbol{\ell}, \mathbf{n}; z)}{1 - \varepsilon G_0(\boldsymbol{\ell}, \boldsymbol{\ell}; z)}. \quad (6.8)$$

Any discrete levels E_p are given by the poles of $G(z)$, i.e., by

$$G_0(\boldsymbol{\ell}, \boldsymbol{\ell}; E_p) = 1/\varepsilon. \quad (6.9)$$

In typical 3-d cases the strength $|\varepsilon|$ of the perturbing potential must exceed a critical value for a discrete level to appear. On the other hand, in 2-d systems a discrete level appears no matter how small $|\varepsilon|$ is. For small $|\varepsilon|$, the binding energy E_b is given by

$$E_b = \text{const.} \times \exp\left[-\frac{1}{|\varepsilon| \varrho_d}\right], \quad d = 2, \quad (6.44)$$

where ϱ_d is the discontinuity of the unperturbed DOS per site at the band edge. Equation (6.44) follows from (6.9) and the logarithmic behavior of $G_0(\boldsymbol{\ell}, \boldsymbol{\ell}; E)$ near the band edge. As was pointed out earlier, this logarithmic behavior is a direct consequence of the discontinuity of $\varrho_0(\boldsymbol{\ell}; E)$. In 1-d systems $G_0(\boldsymbol{\ell}, \boldsymbol{\ell}; E)$ has a square root infinity at the band edge. As a result, (6.9) always has a solution E_p that for small values of $|\varepsilon|$ behaves as

$$E_b = |E_p - E_B| = \text{const.} \times \varepsilon^2, \quad (6.48)$$

where E_B is the band edge.

The eigenstate $|b\rangle$ associated with the nondegenerate discrete level E_p can be obtained as follows:

$$|b\rangle = \sum_{\mathbf{n}} b_{\mathbf{n}} |\mathbf{n}\rangle, \quad (6.14)$$

with

$$b_{\mathbf{n}} = \frac{G_0(\mathbf{n}, \boldsymbol{\ell}; E_p)}{\sqrt{-G_0'(\boldsymbol{\ell}, \boldsymbol{\ell}; E_p)}}, \quad (6.15)$$

where the prime denotes differentiation with respect to E .

The $|\psi_E\rangle$ eigenstates associated with the continuous part of the spectrum (scattering eigenstates) are given by

$$|\psi_E\rangle = |\mathbf{k}\rangle + \frac{G_0^+(E) |\boldsymbol{\ell}\rangle \varepsilon \langle \boldsymbol{\ell} | \mathbf{k}\rangle}{1 - \varepsilon G_0^+(\boldsymbol{\ell}, \boldsymbol{\ell}; E)}, \quad (6.25)$$

where $|\mathbf{k}\rangle$ is the unperturbed Bloch functions.

The DOS at each site \mathbf{n} can be obtained by taking the imaginary part of (6.8) with $\mathbf{m} = \mathbf{n}$. The DOS has a continuous part for E within the band and a δ -function contribution at the discrete level E_p , if the latter exists. As was mentioned above, infinities of G outside the band correspond to discrete

levels associated with eigenstates localized around the impurity. Sharp peaks of G (or equivalently of the t -matrix) within the band correspond to resonance levels associated with extended (or propagating) eigenstates, which are considerably enhanced around the impurity site. The question of the appearance of resonance eigenstates with increasing $|\varepsilon|$ is examined.

Among the various applications examined, two (superconductivity and Kondo effect) deserve special mention because the present formalism provides a very simple derivation of their basic features.

Indeed, if one considers a system of identical fermions, it is a simple matter to show that the DOS for the relative motion of a pair of total momentum $\mathbf{K} = 0$ is given by $\varrho(1 - 2f)/2$, where f is the Fermi distribution. This DOS at $T = 0$ exhibits a discontinuity equal to ϱ_F and hence, in the presence of an attraction between the partners of the pair, will be responsible for the creation of a bound state with binding energy of the form (6.44). Furthermore, for $T > 0$ this DOS exhibits no discontinuity at E_F but a maximum finite slope proportional to $1/T$; as a result the Green's function $|G_0|$ does not blow up at E_F but exhibits a maximum of the form

$$\max |G_0| = \varrho_F \ln(T_0/T) , \quad (6.67)$$

where $T_0 \equiv 2e^\gamma \hbar \omega_D / \pi k_B$ is proportional to the cutoff $\hbar \omega_D$. Combining (6.67) with (6.9) one sees immediately that the bound state (and hence superconductivity) exists only for $T < T_c$, where T_c is obtained by equating $\max |G_0|$ with $1/|\varepsilon|$, i.e.,

$$T_c = T_0 \exp\left(-\frac{1}{|\varepsilon| \varrho'_F}\right) , \quad (6.68)$$

where $\varrho'_F = a^3 \varrho_F$. Equation (6.68) is exactly the BCS result for T_c .

Similarly, for the Kondo problem (where a system of noninteracting fermions is scattered with strength J by a local moment undergoing spin flips), the DOS, instead of being independent of f (as in the case of a static scatterer), includes a term of the form $2\varrho(1 - f)$. Then, by the same simple reasoning as for the pair case above, one concludes that a bound electron-local moment state will be formed for $T < T_K$ [where T_K is given by (6.79)] and that the binding energy at $T = 0$ is as in (6.78). Furthermore, for $T_K < T$, the resistivity, which is proportional to the square of the t -matrix, will contain a factor

$$\left|1 - |J| \max |G_0|\right|^{-2} = \left|1 - 2|J| \varrho'_F \ln\left(\frac{T_0}{T}\right)\right|^{-2}$$

that accounts for the logarithmic increase of the resistivity with decreasing temperature for $T_K \ll T \ll T_0$.

Further Reading

An introduction to superconductivity and the Kondo effect can be found in solid-state physics books such as that by Ashcroft and Mermin [28]. A more

extensive treatment employing second quantization formalism is given in the recent book by Taylor and Heinonen [133]. Books on many-body theory, such as those by Mahan [114] and Abrikosov et al. [113], present the theory of superconductivity and the Kondo effect. Finally, there are many specialized books and articles devoted to those subjects. The book by Rickayzen [111] gives an extensive and clear presentation of superconductivity.

Problems

6.1. Define a closed contour in the upper half plane consisting of a straight line from $-\infty$ to $+\infty$ just above the real axis and a semicircle, c , at infinity. Show that

$$\oint G(\mathbf{n}, \mathbf{n}; z) dz = 0 = \int_{-\infty}^{\infty} G^+(\mathbf{n}, \mathbf{n}; z) dE + \int_c dz G(\mathbf{n}, \mathbf{n}; z) ,$$

$$\int_c dz G(\mathbf{n}, \mathbf{n}; z) = i\pi .$$

6.2. Using the relation $J_0(z) = (1/\pi) \int_0^\pi d\theta \cos(z \sin \theta)$ prove (6.36a) and (6.36b).

6.3s. Plot the DOS vs. E/B for the simple cubic lattice and for $\varepsilon/B = -0.6$, -0.8 , and -0.9 .

6.4s. Prove (6.50) and (6.51).

6.5s. Consider the Green's function for the double spacing periodic Cayley tree given by (5.57). Let us introduce a local perturbation $\mathcal{H}_1 = |\ell\rangle \varepsilon \langle \ell|$, where $\langle \ell | \mathcal{H}_0 | \ell \rangle = \varepsilon_\ell$ ($\ell = 1, 2$). Plot the bound, E_p , and the resonance, E_r , eigenenergies vs. ε for both $\ell = 1$ and $\ell = 2$ (following the examples of Figs.6.4 and 6.5). Choose $K = 3$, $\varepsilon_1 = B/2$, $\varepsilon_2 = -B/2$, ($B = 2\sqrt{KV^2}$). What qualitative changes would occur if $K = 1$?

Hint: In the solutions we plot schematically the E_p 's vs. ε for the case $K = 3, i = 1$.

6.6s. Prove (6.60) and (6.62).

6.7s. Prove (6.67) taking into account (6.64) and (6.65).

Two or More Impurities; Disordered Systems

Summary. In this chapter we examine first a system consisting of two “impurities” embedded in a periodic tight-binding model (TBM). This prepares the way for the approximate treatment of a disordered system containing a nonzero concentration of impurities. We examine in particular the average DOS, which depends on the average Green’s function, $\langle G \rangle$. For the calculation of the latter, various approximation methods are employed; prominent among them is the so-called coherent potential approximation (CPA).

7.1 Two Impurities

We consider here the case where two substitutional impurities have been introduced at two different sites of the lattice, ℓ and m . The Hamiltonian for such a system is assumed to be

$$\mathcal{H} = \mathcal{H}_0 + \mathcal{H}_\ell + \mathcal{H}_m , \quad (7.1)$$

where \mathcal{H}_0 is the periodic TBH studied in Chap. 5, and

$$\mathcal{H}_\ell = |\ell\rangle \varepsilon \langle \ell| , \quad (7.2)$$

$$\mathcal{H}_m = |m\rangle \varepsilon' \langle m| . \quad (7.3)$$

We define further

$$\mathcal{H}_{0\ell} = \mathcal{H}_0 + \mathcal{H}_\ell , \quad (7.4)$$

$$\mathcal{H}_{0m} = \mathcal{H}_0 + \mathcal{H}_m . \quad (7.5)$$

Hence,

$$\mathcal{H} = \mathcal{H}_{0\ell} + \mathcal{H}_m = \mathcal{H}_{0m} + \mathcal{H}_\ell . \quad (7.6)$$

We denote by G_0 , $G_{0\ell}$, G_{0m} , and G the Green’s functions corresponding to \mathcal{H}_0 , $\mathcal{H}_{0\ell}$, \mathcal{H}_{0m} , and \mathcal{H} , respectively. For simplicity we do not display the \pm superscripts in G , T , t_ℓ , etc.

We saw in Chap. 6 that

$$G_{0\ell} = G_0 + G_0 T_\ell G_0, \quad (7.7)$$

where the t -matrix, T_ℓ , associated with \mathcal{H}_0 and \mathcal{H}_ℓ is given by

$$T_\ell = |\ell\rangle t_\ell \langle \ell|; \quad t_\ell = \frac{\varepsilon}{1 - \varepsilon G_0(\ell, \ell)}. \quad (7.8)$$

By considering $\mathcal{H}_{0\ell}$ as the unperturbed part and \mathcal{H}_m as the perturbation, we obtain by applying the general formula (4.5)

$$G = G_{0\ell} + G_{0\ell} \mathcal{H}_m G_{0\ell} + G_{0\ell} \mathcal{H}_m G_{0\ell} \mathcal{H}_m G_{0\ell} + \cdots. \quad (7.9)$$

As before, the summation in (7.9) can be performed exactly, because of the simple form of \mathcal{H}_m . We obtain

$$G = G_{0\ell} + G_{0\ell} |m\rangle \frac{\varepsilon'}{1 - \varepsilon' G_{0\ell}(m, m)} \langle m| G_{0\ell}. \quad (7.10)$$

Substituting (7.7) and (7.8) into (7.10) we have, after some lengthy but straightforward algebra,

$$G = G_0 + G_0 T G_0, \quad (7.11)$$

where the t -matrix, T , associated with the unperturbed part \mathcal{H}_0 and the perturbation $\mathcal{H}_\ell + \mathcal{H}_m$ is given by

$$\begin{aligned} T &= f_{m\ell} (T_\ell + T_m + T_\ell G_0 T_m + T_m G_0 T_\ell) \\ &= f_{m\ell} [|\ell\rangle t_\ell \langle \ell| + |m\rangle t_m \langle m| + |\ell\rangle t_\ell G_0(\ell, m) t_m \langle m| \\ &\quad + |m\rangle t_m G_0(m, \ell) t_\ell \langle \ell|]. \end{aligned} \quad (7.12)$$

The quantity $f_{m\ell}$ is

$$f_{m\ell} = \frac{1}{1 - t_m t_\ell G_0(m, \ell) G_0(\ell, m)}, \quad (7.13)$$

and t_m equals $\varepsilon'/[1 - \varepsilon' G_0(m, m)]$.

The Green's function $G(j, i)$ is obtained by combining (7.11) and (7.12). The resulting expression can be represented in a diagrammatic way as shown in Fig. 7.1, where we have drawn all continuous paths starting from site i and ending at site j ; the intermediate sites (if any) are the scattering centers ℓ and m . With each path (diagram) we associate a product according to the rules given in the caption of Fig. 7.1. Thus the total contribution of the diagrams of subgroup (a) is

$$\begin{aligned} &G_0(j, \ell) t_\ell G_0(\ell, i) + G_0(j, \ell) t_\ell G_0(\ell, m) t_m G_0(m, \ell) t_\ell G_0(\ell, i) + \cdots \\ &= G_0(j, \ell) t_\ell G_0(\ell, i) \\ &\quad \times \left\{ 1 + t_\ell G_0(\ell, m) t_m G_0(m, \ell) + [t_\ell G_0(\ell, m) t_m G_0(m, \ell)]^2 + \cdots \right\} \\ &= G_0(j, \ell) t_\ell G_0(\ell, i) f_{m\ell}, \end{aligned} \quad (7.14)$$

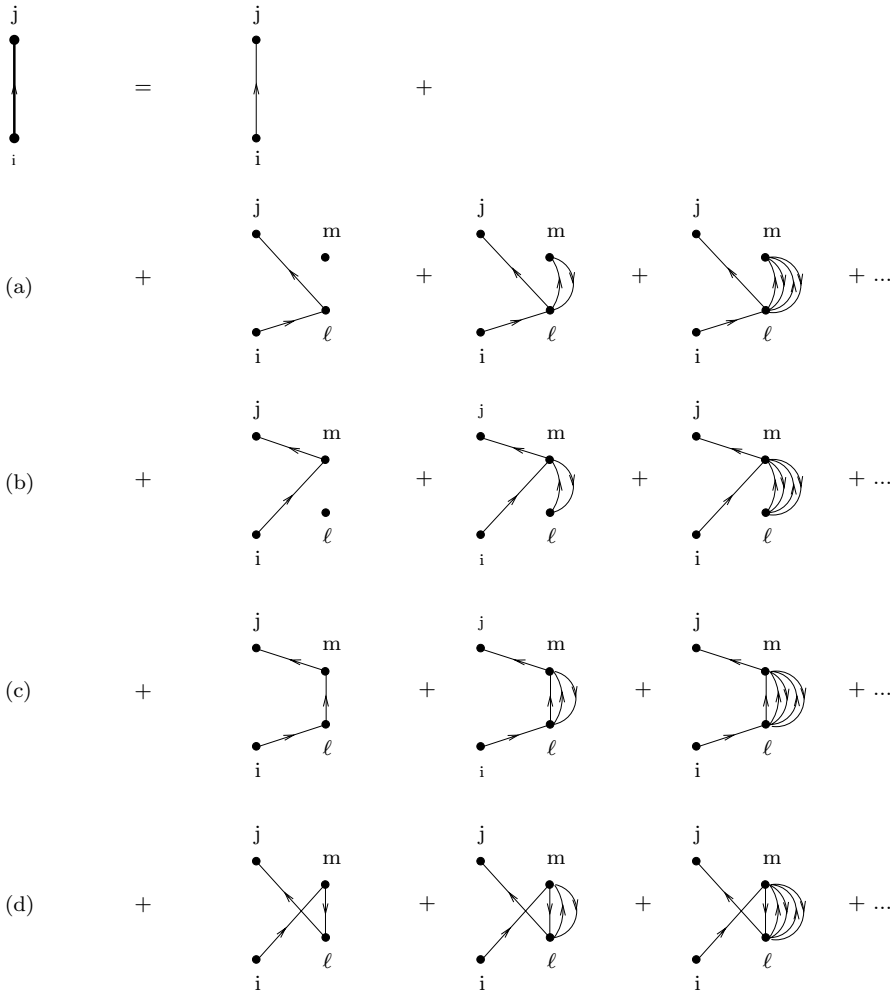


Fig. 7.1. Diagrammatic representation of the various terms contributing to the Green's function $G(j, i)$ (*thick line*) associated with two scatterers at sites l and m . Each diagram corresponds to a product of factors according to the following rules: a *thin line* starting from the arbitrary lattice site i and ending at the arbitrary lattice site j without visiting any other site corresponds to the factor $G_0(j, i)$; each time the scattering site l (m) is visited by the diagram a factor t_l (t_m) is introduced. The diagrams have been classified into four subgroups

where $f_{m\ell}$ is given by (7.13). Similarly, the total contribution of subgroups (b)–(d) in Fig. 7.1 are

$$\begin{aligned}
 &G_0(j, m) t_m G_0(m, i) f_{m\ell} , \\
 &G_0(j, m) t_m G_0(m, l) t_\ell G_0(l, i) f_{m\ell} ,
 \end{aligned}$$

and

$$G_0(\mathbf{j}, \boldsymbol{\ell}) t_{\boldsymbol{\ell}} G_0(\boldsymbol{\ell}, \mathbf{m}) t_{\mathbf{m}} G_0(\mathbf{m}, \mathbf{i}) f_{\mathbf{m}\boldsymbol{\ell}},$$

respectively. Hence the summation of all diagrams of the type shown in Fig. 7.1 is

$$G(\mathbf{j}, \mathbf{i}) = G_0(\mathbf{j}, \mathbf{i}) + \langle \mathbf{j} | G_0(T_{\boldsymbol{\ell}} + T_{\mathbf{m}} + T_{\boldsymbol{\ell}} G_0 T_{\mathbf{m}} + T_{\mathbf{m}} G_0 T_{\boldsymbol{\ell}}) G_0 | \mathbf{i} \rangle f_{\mathbf{m}\boldsymbol{\ell}}, \quad (7.15)$$

which agrees with (7.11) and (7.12).

The diagrams shown in Fig. 7.1 allow a physical interpretation of the various terms contributing to $G(\mathbf{j}, \mathbf{i})$. Thus, if the thick line from \mathbf{i} to \mathbf{j} [i.e., $G(\mathbf{j}, \mathbf{i})$] represents the propagation of the particle from site \mathbf{i} to site \mathbf{j} , the various terms can be interpreted as follows. The first diagram represents propagation without any scattering event [$G_0(\mathbf{j}, \mathbf{i})$, zero-order contribution]; the first diagram in subgroup (a) represents propagation from site \mathbf{i} to site $\boldsymbol{\ell}$, i.e., $G_0(\boldsymbol{\ell}, \mathbf{i})$, scattering at the impurity site $\boldsymbol{\ell}$ (of amplitude $t_{\boldsymbol{\ell}}$) and then propagation from $\boldsymbol{\ell}$ to \mathbf{j} , i.e., $G_0(\mathbf{j}, \boldsymbol{\ell})$; a similar interpretation can be given to any other diagram of the type shown in Fig. 7.1. Because $G_0(\mathbf{j}, \mathbf{i})$ can be interpreted as representing the propagation from site \mathbf{i} to site \mathbf{j} , it is customary to call the Green's function $G(\mathbf{j}, \mathbf{i})$ a *propagator*. Some authors use the name locator for the diagonal matrix elements $G(\mathbf{i}, \mathbf{i})$ for obvious reasons. Others use the name propagator for all matrix elements of G or for G itself so that the term propagator becomes synonymous with the term Green's function.

The diagrammatic representation has the advantage of allowing us to give a physical meaning to each term. This feature facilitates the development of various approximations, which in most cases are necessary. The vivid physical picture that emerges from the diagrams helps also in the memorization of the corresponding formula. It should be stressed that many types of diagrams appear in various branches of physics depending on the unperturbed part \mathcal{H}_0 , the perturbation \mathcal{H}_1 , the complete set of basic functions $|\mathbf{m}\rangle$, and the quantity calculated. The reader may see an example of this statement by comparing the diagrams of Fig. 7.1 with those introduced in Appendix F.

We would like to point out that the t -matrix, T , associated with two scattering centers at $\boldsymbol{\ell}$ and \mathbf{m} is not simply the sum of the t -matrices associated with the impurity at $\boldsymbol{\ell}$ and the impurity at \mathbf{m} . The difference is due to all the multiple scattering terms shown in Fig. 7.1. However, to the first order in $t_{\boldsymbol{\ell}}$ or $t_{\mathbf{m}}$ one keeps the zero-order diagram and the first diagrams in subgroups (a) and (b), and thus

$$T = T_{\boldsymbol{\ell}} + T_{\mathbf{m}} + O(T_{\boldsymbol{\ell}} T_{\mathbf{m}}). \quad (7.16)$$

Because $G_0(\boldsymbol{\ell}, \mathbf{m})$ decays to zero as $|\boldsymbol{\ell} - \mathbf{m}|$ approaches infinity (except in the 1-d case and for E within the band), it follows that the multiple scattering terms, which involve at least a factor $G_0(\boldsymbol{\ell}, \mathbf{m})$, approach zero as $|\boldsymbol{\ell} - \mathbf{m}| \rightarrow \infty$; thus, in the limit $|\boldsymbol{\ell} - \mathbf{m}| \rightarrow \infty$, $T = T_{\boldsymbol{\ell}} + T_{\mathbf{m}}$. The only exception is the 1-d case for E within the band, because in this case the

reflected or transmitted wave from one scattering center propagates with constant amplitude throughout the linear chain, and thus it can be scattered again by the other impurity no matter how far apart the two impurities are.

It is interesting to examine the question of discrete level(s) in the present case of two impurity atoms. The most convenient way to find these levels is by finding the poles of G as given by (7.10). These poles are solutions of

$$1 - \varepsilon' G_{0\ell}(\mathbf{m}, \mathbf{m}) = 0. \quad (7.17)$$

The quantity $G_{0\ell}(\mathbf{m}, \mathbf{m})$ has been examined in detail in Chap. 6. In Fig. 7.2 we plot schematically the quantity $\text{Re}\{G_{0\ell}(\mathbf{m}, \mathbf{m}; E)\}$ vs. E for the 1-d chain and for the special case where ℓ and \mathbf{m} are nearest neighbors; then we use this plot to obtain the qualitative features of the roots of (7.17). We examine first the case where both ε and ε' are negative. When $|\varepsilon|$ is small (Fig. 7.2a), there is only one intersection and, hence, only one discrete level no matter how large $|\varepsilon'|$ is. This discrete level lies below the discrete level of the Hamiltonian $\mathcal{H}_{0\ell}$. Thus, the additional attractive potential ε' simply pushes the discrete level further down. When $|\varepsilon| > B/2$, then $G_{0\ell}(E_\ell) < 0$, and, consequently, there is the possibility of two intersections (Fig. 7.2b). Thus, when $|\varepsilon| > B/2$, the additional attractive potential not only pushes the first discrete level further down but also creates a second level when $\varepsilon' < \varepsilon'_c$. The quantity ε'_c can be found as a solution of the equation $G_{0\ell}(E_\ell) = 1/\varepsilon'$, which gives

$$\frac{B}{\varepsilon'_c} + \frac{B}{\varepsilon} = -2. \quad (7.18)$$

Let us now examine the case $\varepsilon < 0$ but $\varepsilon' > 0$ (Fig. 7.2c). When ε' is very small, there is only one intersection below the band but above the discrete level of $\mathcal{H}_{0\ell}$. Thus an additional weak repulsion pushes the discrete level up, and if $|\varepsilon|$ is small ($< B/2$) and ε' is large ($\varepsilon' > \varepsilon'_c$), then this level is pushed all the way inside the continuum. On the other hand, a discrete level above the band (Fig. 7.2c) has already appeared (for $\varepsilon' > \varepsilon''_c$, where $\varepsilon''_c < \varepsilon'_c$). The quantity ε''_c is given as the solution of the equation $G_{0\ell}(E_u) = 1/\varepsilon'$, which, with the help of (5.30) and (6.8), becomes

$$\frac{B}{\varepsilon''_c} + \frac{B}{\varepsilon} = 2. \quad (7.19)$$

Similar behavior is exhibited in the case $\varepsilon > 0$. The hyperbolae (7.18) and (7.19) separate the $\varepsilon - \varepsilon'$ plane into regions such that one or two discrete levels appear below and/or above the band (Fig. 7.3a). It should be noted that the results depend on the separation of sites ℓ and m . As the distance $|\ell - m|$ increases the hyperbolae shown in Fig. 7.3a approach the $\varepsilon - \varepsilon'$ axes. In Fig. 7.3b we plot the results of a similar study in a Bethe lattice with $K = 4$ and for the sites ℓ and m being nearest neighbors. The boundaries are the hyperbolae

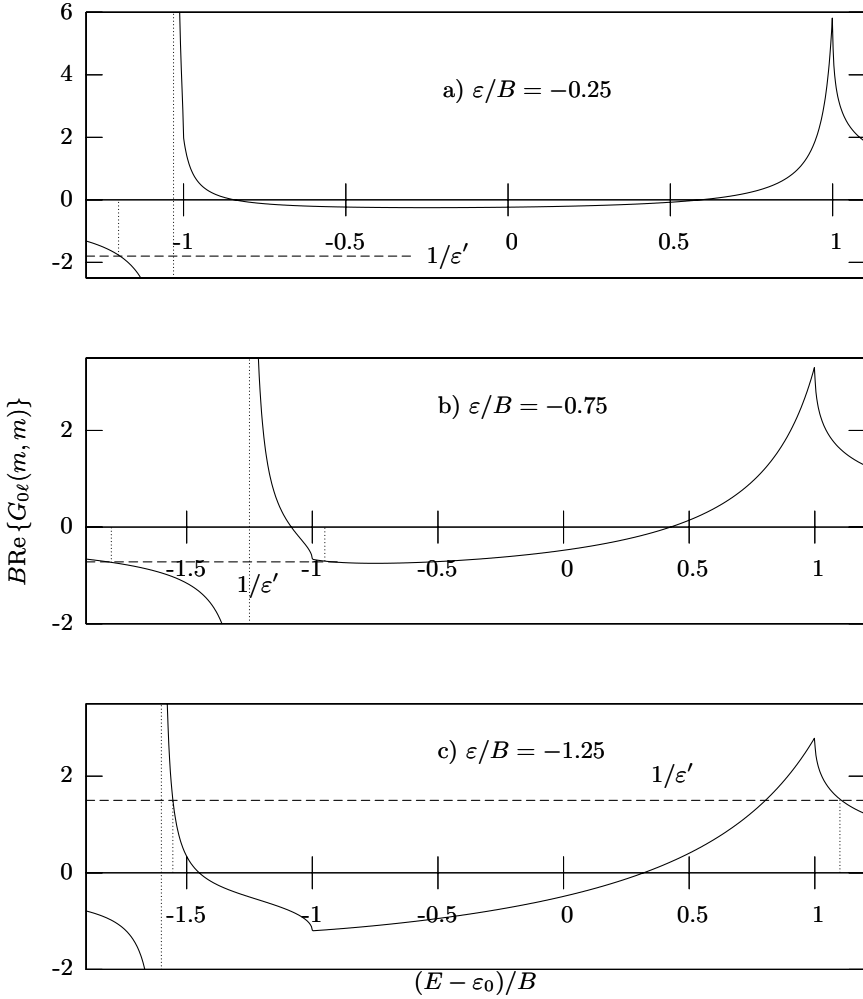


Fig. 7.2. $\text{Re}\{G_{0\ell}(m, m)\}$ vs. E for three different values of ϵ in the 1-d case. The intersections of $\text{Re}\{G_{0\ell}(m, m; E)\}$ with $1/\epsilon'$ are also shown. The sites ℓ and m are nearest neighbors

$$\left(\frac{2\epsilon}{B} \pm 1\right) \left(\frac{2\epsilon'}{B} \pm 1\right) = \frac{1}{4}. \tag{7.20}$$

The main qualitative difference from the 1-d case is the existence around the origin of the $\epsilon - \epsilon'$ plane of a region where no discrete levels appear at all; in the 1-d case this region has collapsed to a single point, namely, the origin.

Recall that intersections of $\text{Re}\{G_{0\ell}(\mathbf{m}, \mathbf{m}; E)\}$ with $1/\epsilon'$ within the band are not solutions of (7.17), since for E within the band $\text{Im}\{G_{0\ell}(\mathbf{m}, \mathbf{m}; E)\}$ is not zero. However, such intersections may produce resonances if they occur

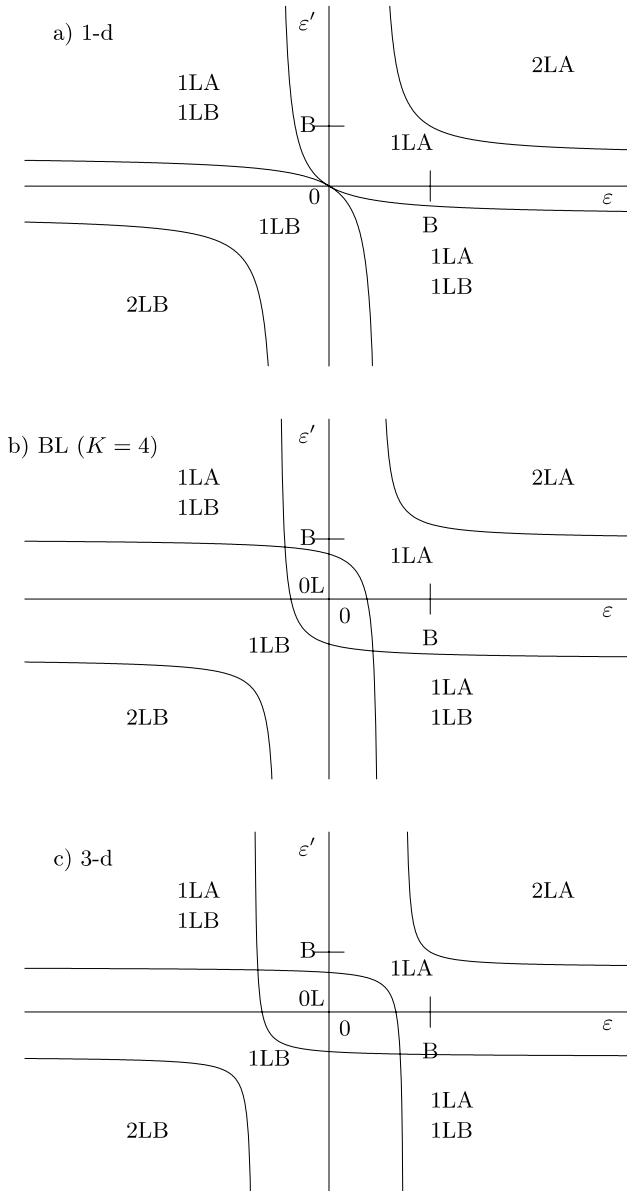


Fig. 7.3. The $\varepsilon - \varepsilon'$ plane is divided into regions where the following appear: no discrete levels (0L); one discrete level above the band (1LA); one discrete level below the band (1LB); two discrete levels, one above and the other below (1LA, 1LB); two discrete levels above the band (2LA); and two discrete levels below the band (2LB). In the 1-d case (a) the region 0L has collapsed to a single point (the origin). For a typical 3-d case such as a Bethe lattice with $K = 4$ (b), or the simple cubic lattice (c), the region 0L centered around the origin is of finite extent. The sites ℓ and m are nearest neighbors

at energies such that $\text{Im} \{G_{0\ell}(\mathbf{m}, \mathbf{m}; E)\}$ is small. In the 1-d case this occurs only for E near the band edges. We leave it to the reader to find the positions of any resonances as a function of the quantities ε and ε' .

We have derived the basic result (7.12) by repeating twice the method developed in Chap. 6. Equation (7.12) could be obtained in one step by considering $\mathcal{H}_1 \equiv \mathcal{H}_\ell + \mathcal{H}_m$ as the perturbation and applying (4.13). We have then, by introducing the unit operator $\sum_n |\mathbf{n}\rangle \langle \mathbf{n}| = \sum_i |\mathbf{i}\rangle \langle \mathbf{i}|$,

$$T = \mathcal{H}_1 + \mathcal{H}_1 \sum_n |\mathbf{n}\rangle \langle \mathbf{n}| G_0 \sum_i |\mathbf{i}\rangle \langle \mathbf{i}| \mathcal{H}_1 + \cdots ; \quad (7.21)$$

from the summation over all states we need to keep only two terms, namely, $|\mathbf{m}\rangle \langle \mathbf{m}| + |\ell\rangle \langle \ell|$, because all other terms give zero as a result of the form of $\mathcal{H}_1 = |\ell\rangle \varepsilon \langle \ell| + |\mathbf{m}\rangle \varepsilon' \langle \mathbf{m}|$. Now we can write

$$|\ell\rangle \langle \ell| + |\mathbf{m}\rangle \langle \mathbf{m}| = [|\ell\rangle, |\mathbf{m}\rangle] \begin{bmatrix} \langle \ell| \\ \langle \mathbf{m}| \end{bmatrix} ; \quad (7.22)$$

we denote by $|\alpha\rangle$ the matrix $[|\ell\rangle, |\mathbf{m}\rangle]$ and by $\langle \alpha|$ the adjoint matrix

$$\begin{bmatrix} \langle \ell| \\ \langle \mathbf{m}| \end{bmatrix} .$$

With this notation (7.21) can be rewritten as

$$T = \mathcal{H}_1 + \mathcal{H}_1 |\alpha\rangle \langle \alpha| G_0 |\alpha\rangle \langle \alpha| \mathcal{H}_1 + \mathcal{H}_1 |\alpha\rangle \langle \alpha| G_0 |\alpha\rangle \langle \alpha| \mathcal{H}_1 |\alpha\rangle \langle \alpha| G_0 |\alpha\rangle \langle \alpha| \mathcal{H}_1 + \cdots . \quad (7.23)$$

The quantity $\langle \alpha| G_0 |\alpha\rangle$ is a 2×2 matrix

$$\langle \alpha| G_0 |\alpha\rangle = \begin{bmatrix} G_0(\ell, \ell) & G_0(\ell, \mathbf{m}) \\ G_0(\mathbf{m}, \ell) & G_0(\mathbf{m}, \mathbf{m}) \end{bmatrix} ; \quad (7.24)$$

similarly,

$$\langle \alpha| \mathcal{H}_1 |\alpha\rangle = \begin{bmatrix} \varepsilon & 0 \\ 0 & \varepsilon' \end{bmatrix} , \quad (7.25)$$

and

$$\langle \alpha| T |\alpha\rangle = \begin{bmatrix} \langle \ell| T |\ell\rangle & \langle \ell| T |\mathbf{m}\rangle \\ \langle \mathbf{m}| T |\ell\rangle & \langle \mathbf{m}| T |\mathbf{m}\rangle \end{bmatrix} . \quad (7.26)$$

We obtain then from (7.23)

$$\begin{aligned} \langle \alpha| T |\alpha\rangle &= \langle \alpha| \mathcal{H}_1 |\alpha\rangle (1 + \langle \alpha| G_0 |\alpha\rangle \langle \alpha| \mathcal{H}_1 |\alpha\rangle + \cdots) \\ &= \langle \alpha| \mathcal{H}_1 |\alpha\rangle (1 - \langle \alpha| G_0 |\alpha\rangle \langle \alpha| \mathcal{H}_1 |\alpha\rangle)^{-1} . \end{aligned} \quad (7.27)$$

By calculating the inverse of the 2×2 matrix $1 - \langle \alpha| G_0 |\alpha\rangle \langle \alpha| \mathcal{H}_1 |\alpha\rangle$, one can easily show that (7.27) is equivalent to (7.12). This matrix approach is very

convenient for generalization to three, four, etc., impurities. If the number of impurities becomes very large, then the calculation becomes tedious because of the need to invert a large matrix. In this case it is sometimes useful to consider a third method of calculating the total t -matrix; this method is the following. Let

$$\mathcal{H}_1 = \sum_{\mathbf{m}} \mathcal{H}_{\mathbf{m}} \quad (7.28)$$

be the perturbative part of the Hamiltonian; the quantity $\mathcal{H}_{\mathbf{m}}$ has the form

$$\mathcal{H}_{\mathbf{m}} = |\mathbf{m}\rangle \varepsilon'_{\mathbf{m}} \langle \mathbf{m}|, \quad (7.29)$$

and the summation runs over all sites \mathbf{m} ; the sites occupied by the host atoms have $\varepsilon'_{\mathbf{m}} = 0$. We denote again by $T_{\mathbf{m}} = |\mathbf{m}\rangle t_{\mathbf{m}} \langle \mathbf{m}|$ the t -matrix associated with the unperturbed part \mathcal{H}_0 and the perturbation $\mathcal{H}_{\mathbf{m}}$; obviously, $t_{\mathbf{m}} = \varepsilon'_{\mathbf{m}}/[1 - \varepsilon'_{\mathbf{m}}G_0(\mathbf{m}, \mathbf{m})]$.

If T is the total t -matrix associated with the unperturbed part \mathcal{H}_0 and the perturbation \mathcal{H}_1 , we have

$$T = \mathcal{H}_1 + \mathcal{H}_1 G_0 T = \mathcal{H}_1 (1 + G_0 T) = \sum_{\mathbf{m}} \mathcal{H}_{\mathbf{m}} (1 + G_0 T) = \sum_{\mathbf{m}} Q_{\mathbf{m}}, \quad (7.30)$$

where $Q_{\mathbf{m}}$ is given by

$$Q_{\mathbf{m}} = \mathcal{H}_{\mathbf{m}} (1 + G_0 T). \quad (7.31)$$

From (7.30) $T = \sum_{\mathbf{n}} Q_{\mathbf{n}}$; substituting in (7.31) we have

$$Q_{\mathbf{m}} = \mathcal{H}_{\mathbf{m}} \left(1 + G_0 \sum_{\mathbf{n}} Q_{\mathbf{n}} \right)$$

or

$$(1 - \mathcal{H}_{\mathbf{m}} G_0) Q_{\mathbf{m}} = \mathcal{H}_{\mathbf{m}} \left(1 + G_0 \sum_{\mathbf{n} \neq \mathbf{m}} Q_{\mathbf{n}} \right) \quad (7.32)$$

or

$$Q_{\mathbf{m}} = (1 - \mathcal{H}_{\mathbf{m}} G_0)^{-1} \mathcal{H}_{\mathbf{m}} \left(1 + G_0 \sum_{\mathbf{n} \neq \mathbf{m}} Q_{\mathbf{n}} \right). \quad (7.33)$$

However, the quantity $(1 - \mathcal{H}_{\mathbf{m}} G_0)^{-1} \mathcal{H}_{\mathbf{m}}$ equals $T_{\mathbf{m}}$; thus, (7.33) becomes

$$Q_{\mathbf{m}} = T_{\mathbf{m}} \left(1 + G_0 \sum_{\mathbf{n} \neq \mathbf{m}} Q_{\mathbf{n}} \right). \quad (7.34)$$

If one solves (7.34) for all $Q_{\mathbf{m}}$, then one has managed to express $T = \sum Q_{\mathbf{m}}$ in terms of $T_{\mathbf{m}}$ s and G_0 . The reader is urged to solve (7.34) for the case of two impurities and recapture (7.12) in this way.

7.2 Infinite Number of Impurities

In this section we consider the case where a nonzero percentage of the lattice sites are occupied by impurity atoms in a random way. An example of such a system is the binary alloy A_xB_{1-x} where a fraction x of the lattice sites are occupied by A atoms with site energy $\varepsilon_0 + \varepsilon_A$ and the rest are occupied by B atoms with site energy $\varepsilon_0 + \varepsilon_B$. It should be mentioned that in reality we do not know the specific sites occupied by A and the specific sites occupied by B. What we may know is the probability for each particular configuration of As and Bs. Thus, we are led to the concept of a *random* or *disordered* system, the Hamiltonian of which is not known; what we know is the probability distribution of the matrix elements of the Hamiltonian. In the specific example of the binary alloy, if no correlations among the random variables $\{\varepsilon'_n\}$ are present, then their probability distribution is given by

$$P(\{\varepsilon'_n\}) = \prod_n p(\varepsilon'_n) , \quad (7.35)$$

with

$$p(\varepsilon'_n) = x\delta(\varepsilon'_n - \varepsilon_A) + (1-x)\delta(\varepsilon'_n - \varepsilon_B) . \quad (7.36)$$

In a random system we are interested in the average (over all configurations) of the physical quantities. More specifically, we would like to calculate the average of the Green's function $\langle G \rangle$ defined as

$$\langle G \rangle = \int d\{\varepsilon'_n\} P(\{\varepsilon'_n\}) G(\{\varepsilon_n\}) . \quad (7.37)$$

We assume that the average value is representative of the ensemble, i.e., that the probability distribution of $G(\{\varepsilon'_n\})$ is sharply peaked around the average value, $\langle G \rangle$. If this assumption is realistic, then the DOS observed experimentally will coincide with $-\text{Im}\{\langle G^+ \rangle\}/\pi$; this justifies our interest for calculating $\langle G \rangle$. However, there are quantities and/or conditions such that the average value is not representative of the ensemble. In this case, some other averages (e.g., geometric averages) may be representative of the ensemble, or it may be necessary to calculate the full probability distribution of the quantity under consideration.

In general, $\langle G \rangle$ cannot be calculated exactly; a notable exception, examined by Lloyd [136], is the case where $p(\varepsilon'_n)$ is a Lorentzian

$$p(\varepsilon'_n) = \frac{1}{\pi} \frac{\Gamma}{\varepsilon'^2_n + \Gamma^2} .$$

Then, because $p(\varepsilon'_n)$ has two poles $\varepsilon'_n = \pm i\Gamma$ in the complex ε'_n plane, each integration over ε'_n in (7.37) replaces ε'_n by $\mp i\Gamma$, with the upper sign corresponding to G^+ and the lower to G^- ; thus, finally, $\langle G^\pm(E) \rangle = G_0(E \pm i\Gamma)$. We mention that, besides the binary alloy and the Lorentzian, the rectangular

distribution

$$p(\varepsilon'_n) = \begin{cases} \frac{1}{W} & \text{for } |\varepsilon'_n| < W/2, \\ 0 & \text{otherwise,} \end{cases}$$

has been widely used in the literature.

Note that our Hamiltonian is the simplest one to model a random system. Even within the framework of a TBM there are physically important aspects that we ignored: the off-diagonal matrix elements V_{ij} may actually be random variables as well (off-diagonal disorder); the quantity ε'_n , and hence its probability distribution, may depend on the other sites in the vicinity of n , as, e.g., in the case of coupled pendula examined in Chap. 5 (environmental disorder); the random variables $\{\varepsilon'_n\}$ may be statistically correlated (short-range order), etc. Furthermore, in real systems, such as amorphous semiconductors, there is disorder resulting not from small displacements from the crystal sites but in association with new bonding configurations (topological disorder). Such disorder is much more difficult to treat. For more details concerning the various types of disorder the reader is referred to Ziman's book [137].

In spite of the drastic simplifications in our model Hamiltonian, one is still forced to develop approximate schemes for obtaining $\langle G \rangle$. Here we review briefly three of the most widely used methods.

7.2.1 Virtual Crystal Approximation (VCA)

Our Hamiltonian is $\mathcal{H} = \mathcal{H}_0 + \mathcal{H}_1$, where \mathcal{H}_0 is periodic tight-binding and \mathcal{H}_1 is given by (7.28) and (7.29). By averaging the basic equation (4.6) we obtain

$$\langle G \rangle = G_0 + G_0 \langle \mathcal{H}_1 G \rangle ; \quad (7.38)$$

G_0 does not depend on the random variables $\{\varepsilon'_n\}$, and hence $\langle G_0 \rangle = G_0$. Now, we make the approximation

$$\langle \mathcal{H}_1 G \rangle \simeq \langle \mathcal{H}_1 \rangle \langle G \rangle \quad (7.39)$$

and take into account that

$$\langle \mathcal{H}_1 \rangle = \sum_m \langle \mathcal{H}_m \rangle = \sum_m |\mathbf{m}\rangle \langle \varepsilon'_m \rangle \langle \mathbf{m}| = \langle \varepsilon'_m \rangle . \quad (7.40)$$

Since we are dealing with systems that are macroscopically homogeneous, the average $\langle \varepsilon'_m \rangle$ is independent of site \mathbf{m} and will be denoted by ε :

$$\varepsilon \equiv \langle \varepsilon'_m \rangle . \quad (7.41)$$

Substituting in (7.38) from (7.39)–(7.41) we obtain

$$\langle G \rangle = G_0 + G_0 \varepsilon \langle G \rangle ,$$

which can be rewritten as

$$\langle G(E) \rangle = \frac{1}{E - \mathcal{H}_0 - \varepsilon} = \frac{1}{E - \langle \mathcal{H} \rangle} . \quad (7.42)$$

Equation (7.42) is known as the VCA for $\langle G \rangle$; this approximation consists in calculating $\langle G(\mathcal{H}) \rangle$ as $G(\langle \mathcal{H} \rangle)$ and simply shifts the energy levels by $\varepsilon = \langle \varepsilon'_m \rangle$. This shift can be made equal to zero (which means that the VCA $\langle G \rangle$ equals G_0) by choosing $\mathcal{H}_0 \equiv \langle \mathcal{H} \rangle$, which means $\langle \varepsilon'_m \rangle = 0$ and $\mathcal{H}_1 \equiv \mathcal{H} - \langle \mathcal{H} \rangle$. Henceforth we adopt this notation.

The VCA fails completely for large values of $\langle \varepsilon'^2_m \rangle$. For more comments about this very simple method see the review article by Elliott et al. [138] and references therein.

7.2.2 Average t -Matrix Approximation (ATA)

If T is the t -matrix associated with \mathcal{H}_0 and \mathcal{H}_1 , we have

$$\langle G \rangle = G_0 + G_0 \langle T \rangle G_0 . \quad (7.43)$$

Here T is a complicated function of the individual t_m s

$$T = f(\{t_m\}) , \quad (7.44)$$

where

$$t_m = \frac{\varepsilon'_m}{1 - \varepsilon'_m G_0(\mathbf{m}, \mathbf{m})} . \quad (7.45)$$

The basic approximation in ATA is to set

$$\langle T \rangle = f(\{\langle t_m \rangle\}) . \quad (7.46)$$

Because the rhs of (7.46) has the same form as (7.44) with an \mathbf{m} -independent $\langle t_m \rangle$, it follows that $\langle T \rangle$ is the same as the t -matrix, T_e , associated with \mathcal{H}_0 and a periodic \mathcal{H}_{1e} of the form

$$\mathcal{H}_{1e} = \sum_{\mathbf{m}} |\mathbf{m}\rangle \Sigma \langle \mathbf{m}| = \Sigma , \quad (7.47)$$

provided [as can be seen from (7.45)] that Σ is chosen to satisfy the relation

$$\langle t_m \rangle = \Sigma [1 - \Sigma G_0(\mathbf{m}, \mathbf{m})]^{-1} . \quad (7.48)$$

Substituting T_e for $\langle T \rangle$ in (7.43) we obtain immediately

$$\langle G(E) \rangle = (E - \mathcal{H}_0 - \mathcal{H}_{1e})^{-1} = G_0(E - \Sigma) . \quad (7.49)$$

Thus the ATA calculates $\langle G \rangle$ from the periodic effective Hamiltonian $\mathcal{H}_e \equiv \mathcal{H}_0 + \mathcal{H}_{1e}$, which shifts the energy by the complex, energy-dependent quantity

Σ ; within the ATA, the so-called *self-energy* Σ is obtained from (7.48), which can be recast as

$$\Sigma = \frac{\langle t_{\mathbf{m}} \rangle}{1 + \langle t_{\mathbf{m}} \rangle G_0(\mathbf{m}, \mathbf{m})} . \quad (7.50)$$

The above derivation can be translated into a diagrammatic language [138].

In the limit of weak scattering, $\varepsilon'_{\mathbf{m}} \rightarrow 0$, we obtain from (7.50) and (7.45), in lowest order and taking into account our choice of $\langle \varepsilon'_{\mathbf{m}} \rangle = 0$, that

$$\Sigma \rightarrow \langle \varepsilon'^2_{\mathbf{m}} \rangle G_0(\mathbf{m}, \mathbf{m}) . \quad (7.51)$$

This is the correct limit. The ATA is also successful in the very dilute limit, where the concentration of impurities is $\ll 1$. The ATA has been used by Ehrenreich and Schwartz [139], Schwartz [140], Bansil [141–147], and coworkers to calculate the electronic structure of real random alloys, such as $\text{Cu}_x\text{Ni}_{1-x}$.

The concept of self-energy is more general and can be introduced outside the framework of any approximation. Indeed, we define the operator $\Sigma^\pm(E)$ from the relation

$$\langle G^\pm(E) \rangle^{-1} \equiv [G_0^\pm(E)]^{-1} - \Sigma^\pm(E) . \quad (7.52)$$

Taking into account (7.43) we can express $\Sigma^\pm(E)$ in terms of $\langle T(E) \rangle$ as follows (again for simplicity we omit the superscripts \pm):

$$\Sigma = \langle T \rangle [1 + \langle T \rangle G_0]^{-1} = \langle T \rangle [1 + G_0 \langle T \rangle]^{-1} , \quad (7.53)$$

which resembles (7.50). In the \mathbf{k} -representation both G_0 and $\langle T \rangle$ are diagonal because the unperturbed Hamiltonian as well as the *average* t -matrix possess the periodicity of the lattice. Hence Σ is also diagonal in the \mathbf{k} -representation. We have then from (7.52) and (7.53), respectively,

$$\langle G(E, \mathbf{k}) \rangle = [E - E_0(\mathbf{k}) - \Sigma(E, \mathbf{k})]^{-1} \quad (7.52')$$

$$\Sigma(E, \mathbf{k}) = \langle T(E, \mathbf{k}) \rangle \left[1 + \frac{\langle T(E, \mathbf{k}) \rangle}{E - E_0(\mathbf{k}) \pm i\delta} \right]^{-1} . \quad (7.53')$$

We see that in the general case the self-energy is a function of both E and \mathbf{k} . The ATA missed the \mathbf{k} dependence of the self-energy.

7.2.3 Coherent Potential Approximation (CPA)

As in the ATA case, the CPA calculates $\langle G \rangle$ through an effective Hamiltonian

$$\mathcal{H}_e = \sum_{\mathbf{n}} |\mathbf{n}\rangle \Sigma(E) \langle \mathbf{n}| + V \sum'_{\mathbf{m}\mathbf{n}} |\mathbf{n}\rangle \langle \mathbf{m}| ,$$

which in the simplest case is characterized by a single, complex, energy-dependent self-energy Σ . In other words, we assume that

$$\langle G(E) \rangle = G_e(E) = (E - \mathcal{H}_e)^{-1} = G_0(E - \Sigma) ,$$

with a \mathbf{k} -independent self-energy, $\Sigma(E)$, as in the ATA. In contrast to the ATA, the CPA determines the effective medium characterized by the as yet *unknown* self-energy Σ by expanding G in terms of $G_e \equiv (E - \mathcal{H}_e)^{-1}$ and $\mathcal{H}'_1 \equiv \mathcal{H} - \mathcal{H}_e$, i.e.,¹

$$G = G_e + G_e T' G_e , \quad (7.54)$$

and by demanding self-consistency, i.e., $\langle G \rangle = G_e$, which in view of (7.54) implies that

$$\langle T' \rangle = 0 . \quad (7.55)$$

The t -matrix, T' , is a complicated function of all the individual t -matrices, t'_m ,

$$T' = f(\{t'_m\}) , \quad (7.56)$$

$$t'_m = \frac{\varepsilon'_m - \Sigma}{1 - (\varepsilon'_m - \Sigma) G_e(\mathbf{m}, \mathbf{m})} . \quad (7.57)$$

The central approximation is again similar to that of the ATA

$$\langle T' \rangle \approx f(\{ \langle t'_m \rangle \}) . \quad (7.58)$$

Equation (7.55), in view of the approximation (7.58), leads to

$$\langle t'_m \rangle = 0 . \quad (7.59)$$

Equation (7.59) is an implicit equation for the self-energy Σ , which can be recast as

$$\Sigma = \left\langle \frac{\varepsilon'_m}{1 - (\varepsilon'_m - \Sigma) G_e(\mathbf{m}, \mathbf{m})} \right\rangle \quad (7.59a)$$

or as

$$\left\langle \frac{1}{1 - (\varepsilon'_m - \Sigma) G_e(\mathbf{m}, \mathbf{m})} \right\rangle = 1 . \quad (7.59b)$$

In (7.57), (7.59), (7.59a), and (7.59b) the quantity $G_e(\mathbf{m}, \mathbf{m})$ depends on Σ through (7.49)

$$G_e(\mathbf{m}, \mathbf{m}; E) = G_0(\mathbf{m}, \mathbf{m}; E - \Sigma) . \quad (7.60)$$

Having determined $\Sigma(E)$ [usually by solving iteratively (7.59a)] we can obtain approximately several quantities of physical interest:

(i) *The average DOS per site, $\varrho(E)$*

$$\varrho(E) = -\frac{1}{\pi} \text{Im} \{ G_e(\mathbf{m}, \mathbf{m}; E) \} = -\frac{1}{\pi} \text{Im} \{ G_0(\mathbf{m}, \mathbf{m}; E - \Sigma(E)) \} . \quad (7.61)$$

¹ The prime in (7.54)–(7.58) does not imply multiplication of T' or t'_m by Ω .

(ii) *The complex propagation constant, \mathbf{k} , given by the equations*

$$E_0(\mathbf{k}) = E - \Sigma(E), \quad (7.62a)$$

$$\left(\frac{\partial E_0(\mathbf{q})}{\hbar \partial \mathbf{q}} \right)_{\mathbf{q}=\mathbf{k}} \times t_0 = \mathbf{R}; \quad (7.62b)$$

[see (6a) and (6b) of the solution of Problem 5.2s].

In the simple case where the unperturbed $E_0(\mathbf{k})$ equals $\hbar^2 k^2 / 2m^*$, we have from (7.62a)

$$k = k_1 + ik_2 = \sqrt{\frac{2m^*}{\hbar^2}(E - \Sigma)} \quad (7.63)$$

or

$$k_1^2 = \frac{m^*}{\hbar^2} \left[E - \Sigma_1(E) + \sqrt{(E - \Sigma_1(E))^2 + \Sigma_2(E)^2} \right] \\ \rightarrow \frac{2m^*}{\hbar^2} |E - \Sigma_1|, \quad (7.63a)$$

$$k_2 = \frac{m^* |\Sigma_2|}{\hbar^2 k_1} = \frac{|\Sigma_2|}{\hbar v} \rightarrow \sqrt{\frac{m^*}{2\hbar^2} \frac{|\Sigma_2|}{\sqrt{|E - \Sigma_1|}}}, \quad (7.63b)$$

where $\Sigma_1(E)$ and $\Sigma_2(E)$ are the real and the imaginary parts of $\Sigma(E)$, $v = \hbar k_1 / m^*$ is the group velocity at energy E , and the limiting expressions are valid for $|\Sigma_2| \ll |E - \Sigma_1(E)|$.

From (7.63a) we see that the real part, k_1 , of the propagation constant is renormalized because of the presence of the self-energy $\Sigma(E)$ [compare with (3.23)]. The imaginary part k_2 would lead to a decay of the average of the off-diagonal matrix element $\langle G(\mathbf{n}, \mathbf{m}; E) \rangle$ as $|\mathbf{n} - \mathbf{m}| \rightarrow \infty$, so that in the simple case $E_0(\mathbf{k}) = \hbar^2 k^2 / 2m^*$ we shall have

$$\langle G(\mathbf{n}, \mathbf{m}; E) \rangle \simeq G_e(\mathbf{n}, \mathbf{m}; E) \\ = -\frac{m^* a^2 \exp(ik_1 a |\mathbf{n} - \mathbf{m}| - k_2 a |\mathbf{n} - \mathbf{m}|)}{2\pi \hbar^2 |\mathbf{n} - \mathbf{m}|}, \quad (7.64)$$

where a is the lattice constant of the simple cubic lattice.

(iii) *The renormalized wavelength, λ , and the mean free path ℓ .*

The renormalized wavelength, λ , corresponding to the energy E is given by

$$\lambda = \frac{2\pi}{k_1} \simeq \frac{2\pi \hbar}{\sqrt{2m^* |E - \Sigma_1|}}. \quad (7.65)$$

The mean free path ℓ is defined through the decay of the average Green's function $G(\mathbf{r}, \mathbf{r}'; E) \sim \exp(-|\mathbf{r} - \mathbf{r}'|/2\ell)$ for large values of $|\mathbf{r} - \mathbf{r}'|$. Comparing this definition with (7.64) we find that

$$\ell = \frac{1}{2k_2} = \frac{\hbar v}{2|\Sigma_2|}. \quad (7.66)$$

From the mean free path ℓ one defines the relaxation time $\tau = \ell/v$. We have then

$$\tau = \frac{\hbar}{2|\Sigma_2|}. \quad (7.67)$$

Thus the imaginary part of $\Sigma(E)$ is directly related to the inverse of the energy-dependent relaxation time.

It must be stressed that the decay of the *average* of $G(\mathbf{r}, \mathbf{r}'; E)$ does not necessarily imply that the eigenfunctions of the Hamiltonian \mathcal{H} are decaying as $r \rightarrow \infty$. Remember that

$$\begin{aligned} G(\mathbf{r}, \mathbf{r}'; E) &= \sum_i \frac{\psi_i(\mathbf{r}) \psi_i^*(\mathbf{r}')}{E - E_i} \\ &= \sum_i \frac{|\psi_i(\mathbf{r}) \psi_i^*(\mathbf{r}')| \exp\{i[\phi_i(\mathbf{r}) - \phi_i(\mathbf{r}')]\}}{E - E_i}. \end{aligned} \quad (7.68)$$

When we average over all configurations of the random variables involved in the Hamiltonian, the phase differences $\phi_i(\mathbf{r}) - \phi_i(\mathbf{r}')$ oscillate strongly (for large $|\mathbf{r} - \mathbf{r}'|$) and, as a result, contribute to the decay of $\langle G(\mathbf{r}, \mathbf{r}'; E) \rangle$ for $|\mathbf{r} - \mathbf{r}'| \gg \ell$. For weak disorder and for dimensionality larger than 2, this phase oscillation is the only source of decay; for strong disorder or for $d \leq 2$ the decay of the amplitude of the eigenfunctions contributes also to the decay of $\langle G(\mathbf{r}, \mathbf{r}'; E) \rangle$.

We conclude these remarks by pointing out that a reliable determination of the self-energy $\Sigma(E)$ is of central importance since it allows us to obtain quantities such as the DOS, ρ , the wavelength, λ , the phase velocity, v , the mean free path, ℓ , and the relaxation time, τ , as functions of energy. Almost all quantities of physical interest involve one or more of ρ , λ , v , ℓ , and τ .

The CPA has been proven impressively successful for obtaining $\Sigma(E)$. It gives the correct result in the weak scattering limit [where it reduces to (7.51) as can be seen from (7.59a)], in the strong scattering (or atomic) limit (i.e., when $\langle \varepsilon'_m{}^2 \rangle \gg V^2$), and in the dilute limit; and it interpolates properly between these limits.

Having mentioned the successes of the CPA, let us discuss now its limitations and failures. The only approximation we have employed is that $\langle t'_m \rangle = 0$ implies $\langle T' \rangle = 0$. The physical meaning of this approximation is revealed if we express T' in terms of the T'_m s by iterating (7.34) and substituting in (7.30):

$$T' = \sum_m T'_m + \sum_{n \neq m} T'_n G_e T'_m + \sum_{n \neq m \neq r} T'_n G_e T'_m G_e T'_r + \dots \quad (7.69)$$

In the present case where $\{\varepsilon'_m\}$ are independent random variables, the quantities $\{t'_m\}$ are independent random variables. By averaging (7.69) we can easily see that the average of the first three terms on the rhs of (7.69) are proportional to $\langle t'_m \rangle$; the fourth term is not in general proportional to $\langle t'_m \rangle$ because of contributions of the type

$$\begin{aligned} & \sum_{n \neq m} \langle T'_n G_e T'_m G_e T'_n G_e T'_m \rangle \\ &= \sum_{n \neq m} |n\rangle \langle t'_{n^2} \rangle \langle t'_{m^2} \rangle G_e(n, m) G_e(m, n) G_e(n, m) \langle m|, \end{aligned}$$

which are proportional to $\langle t'_{m^2} \rangle$. Similarly, higher-order terms in the expansion (7.69) corresponding to multiple scattering events from clusters of a fixed number of sites will introduce terms that are proportional to $\langle t'_{m^n} \rangle$, where n is any integer. Since, in general, $\langle t'_{m^2} \rangle = 0$ does not necessarily imply $\langle t'_{m^n} \rangle = 0$, we can conclude that the CPA incorrectly treats multiple scattering terms associated with clusters of a fixed number of neighboring sites. These multiple scattering events by the sites of a particular cluster are of great importance if they lead to a resonance behavior associated with a peak in the DOS and an enhancement of the corresponding eigenstates in the vicinity of the cluster that traps the particle for a long time. Hence, at energies where the DOS is dominated by contributions from resonance or localized (around a cluster of sites) eigenstates, the CPA is expected to fail. As we will discuss below, the near tails of the band are due, largely or entirely, to such cluster-localized eigenstates, and consequently the CPA is a poor approximation there; actually, the CPA predicts no tails at all when the probability distribution, $p(\varepsilon'_n)$, is terminating as in the binary, (7.36), or the rectangular case. On the contrary, for nonterminating distributions, such as the Gaussian, the near tail in the DOS is due mostly to states trapped around a cluster of sites, but the deeper tails are due to states trapped around a single site; the CPA treats these states correctly and produces reliable results for the deeper tails (Problem 7.6s). Cluster-localized eigenstates may, under certain circumstances, be responsible for the appearance of considerable structure in the DOS by creating peaks at certain energies or depleting states from other energies. Again the CPA tends to eliminate this structure. It should be noted that when the probability of occurrence of a cluster capable of trapping a particle in it is small, the role of cluster-localized eigenstates is small. If short-range order is absent, the probability of occurrence of such special clusters is small and decreases with increasing dimensionality. Thus the CPA works better in 3-d systems than in 1-d ones. A sketch in the preface of a book edited by Thorpe [93] summarizes the CPA situation best.

The CPA combines two basic ideas: one is to calculate the average of a given quantity associated with a random medium by introducing a periodic (or a position-independent) effective medium; the second is to determine this effective medium by a self-consistency requirement, i.e., by demanding that the fluctuations of the given quantity due to *local* fluctuations around the effective medium average out to zero. As was pointed out by Sen [148], these ideas can be traced back to Maxwell [149]. Hubbard [150] was probably the first to use the CPA in an electronic structure calculation. The CPA was brought to its present form by Taylor [151] and Soven [152], who are usually credited for the invention of the method. The basic equation (7.59a), which determines

the effective medium, has been rederived by various techniques. Among them must be mentioned diagrammatic methods based upon the expansion of G in powers of \mathcal{H}_1 [153–156]; these methods were first developed by Edwards [157], Langer [158], Klauder [159], and Matsubara and Toyozawa [160], with important contributions by Leath and Goodman [161, 162] and Yonezawa and Matsubara [163–165]. Other diagrammatic methods used to derive the CPA equations are based upon the expansion of G in powers of the off-diagonal matrix elements of the Hamiltonian. This so-called locator expansion, which is similar in spirit to the RPE discussed in Appendix F, was used by Leath [166] and by Matsubara and Kaneyoshi [167]. Contributions to our understanding of the CPA were made, among others, by Velicky et al. [168, 169], Onodera and Toyozawa [170], Yonezawa [171, 172], Butler [173], and Brouers et al. [174]. In addition to [138, 139], we mention also the review article by Yonezawa and Morigaki [175] and the book edited by Thorpe [93].

7.2.4 The CPA for Classical Waves

Starting in the late 1980s, the question of classical wave propagation in strongly scattering media, both disordered and periodic, has received increased attention. In the disordered case various versions of the CPA were employed to interpret novel experimental results. Usually the experiments were performed in composite materials, quite often consisting of two components (one of which could be air). There were two extreme types of topology. In the so-called *cermet topology*, there was a high concentration of inclusions in a host matrix; each inclusion, usually spherical and of the same material as all the others, was completely surrounded by the host material. In the other case the two components were topologically equivalent; e.g., each of the two components formed a continuous connected network (*network topology*).

The propagation of electromagnetic (em), acoustic (a), elastic (e), and other types of classical waves in such composite media was examined. For em waves each material component is characterized by its permittivity, $\varepsilon(\omega) = \varepsilon_R(\omega) + i\varepsilon_I(\omega)$, and possibly by its permeability, $\mu(\omega) = \mu_R(\omega) + i\mu_I(\omega)$. Usually, but not always, $\mu(\omega) \simeq 1$, especially at high frequency, and as a result only $\varepsilon(\omega)$ is of importance. To have strong scattering we need a large ratio of $\varepsilon_2(\omega)/\varepsilon_1(\omega)$ of the permittivities of the two components and a wavelength comparable to the size of the scatterers and to the average distance between neighboring scatterers. For acoustic waves in a two-component fluid medium there are two quantities characterizing each component: the density ϱ_i ($i = 1, 2$) and the velocity $c_i = \sqrt{B_i/\varrho_i}$ ($i = 1, 2$), where B_i is the bulk modulus. For elastic waves in a two-component solid system there are at least three quantities characterizing each component: the density ϱ_i ($i = 1, 2$), the longitudinal velocity $c_{li} = \sqrt{(B_i + 4\mu_i/3)/\varrho_i}$, and the transverse velocity $c_{ti} = \sqrt{\mu_i/\varrho_i}$ ($i = 1, 2$), where μ_i is the so-called transverse Lamé coefficient.

The simplest system that is mathematically equivalent to the Schrödinger equation is a composite fluid with a constant density, ϱ , and a position-

dependent sound velocity, $c(\mathbf{r})$ [or, equivalently, a position-dependent bulk modulus $B(\mathbf{r}) = \rho c^2(\mathbf{r})$]. [For a two-component system, $c(\mathbf{r}) = c_1$ if \mathbf{r} is within component 1 and $c(\mathbf{r}) = c_2$ if \mathbf{r} is within component 2]. The wave equation for the pressure, $p(\mathbf{r})$, is

$$\left(\frac{\omega^2}{c(\mathbf{r})^2} + \nabla^2 \right) p(\mathbf{r}) = 0 \quad (7.70)$$

or

$$\left(\frac{\omega^2}{c_0^2} + \nabla^2 \right) p(\mathbf{r}) = -\omega^2 \left(\frac{1}{c^2(\mathbf{r})} - \frac{1}{c_0^2} \right) p(\mathbf{r}), \quad (7.70')$$

where $1/c_0^2$ is the average value of $1/c^2(\mathbf{r})$. Equations (7.70) and (7.70') are to be compared with the Schrödinger equation

$$\left[\frac{2m}{\hbar^2} (E - V(\mathbf{r})) + \nabla^2 \right] \psi(\mathbf{r}) = 0 \quad (7.71)$$

or

$$\left[\frac{2m}{\hbar^2} (E - V_0) + \nabla^2 \right] \psi(\mathbf{r}) = \frac{2m}{\hbar^2} [V(\mathbf{r}) - V_0], \quad (7.71')$$

where V_0 is the average value of the potential $V(\mathbf{r})$. We see, by comparing (7.70) and (7.71), that the classical wave case corresponds to the Schrödinger case but for energy E above the maximum value of the potential $V(\mathbf{r})$ [since $E - V(\mathbf{r})$ must be positive to be identified with $\omega^2/c^2(\mathbf{r})$]. Furthermore, the fluctuating part $(2m/\hbar^2)(V(\mathbf{r}) - V_0)$ corresponds to $-\omega^2(c^{-2}(\mathbf{r}) - c_0^{-2})$, which means that potential wells (with respect to V_0) correspond to regions of velocity, $c(\mathbf{r})$, lower than c_0 ; more important in the classical wave case is that the fluctuation includes a factor ω^2 . Thus, for low frequencies we are in the weak scattering limit, and the scattering cross section, the mean free path, the relaxation time, and the t -matrix are all proportional to ω^4 or to $1/\lambda^4$. This is the so-called Rayleigh scattering for *scalar* classical waves. Notice also that at very high frequencies the ray approximation (which corresponds to the classical trajectories in the Schrödinger case and the geometric optics in the em case) is adequate. Thus the stronger effects of scattering for classical waves are expected at intermediate frequencies.

The Green's function for the unperturbed classical wave case [i.e., the left side of (7.70')] is given by (1.40) (1.49), and (1.56) for the 3-, 2-, and 1-d case, respectively, with $\sqrt{\lambda} = \omega/c_0 = k_0$, the unperturbed propagation constant. Employing these expressions for the unperturbed Green's functions (and their asymptotic expansions), the definition of the scattering amplitude, $f(\mathbf{k}_f, \mathbf{k}_0)$

$$p(\mathbf{r}) \xrightarrow{r \rightarrow \infty} \exp(i\mathbf{k}_0 \cdot \mathbf{r}) + f(\mathbf{k}_f, \mathbf{k}_0) \frac{\exp(ik_0 r)}{r^{(d-1)/2}}, \quad (7.72)$$

and (4.27), we find the following relations between the scattering amplitude f and the t -matrix (see [21], Sect. 3.4):

$$f(\mathbf{k}_f, \mathbf{k}_0) = \begin{cases} -\frac{\Omega}{4\pi} \langle \mathbf{k}_f | T^+(k_0^2) | \mathbf{k}_0 \rangle, & \text{3-d, (7.73a)} \\ -e^{i\pi/4} \sqrt{\frac{1}{8\pi k_0}} \Omega \langle \mathbf{k}_f | T^+(k_0^2) | \mathbf{k}_0 \rangle, & \text{2-d, (7.73b)} \\ -\frac{i\Omega}{2k_0} \langle \mathbf{k}_f | T^+(k_0^2) | \mathbf{k}_0 \rangle, & \text{1-d, (7.73c)} \end{cases}$$

where $\mathbf{k}_f^2 = \mathbf{k}_0^2$ and \mathbf{k}_f is along the direction of the observation vector \mathbf{r} . Ω is the volume, the area, or the length of the 3-, 2-, 1-d systems, respectively. From the general equation $T = \mathcal{H}_1 + \mathcal{H}_1 G_0 T$ it follows that $\Omega \langle \mathbf{k}_f | T^+(k_0) | \mathbf{k}_0 \rangle$ satisfies the following integral equation:

$$\begin{aligned} \Omega \langle \mathbf{k}_f | T^+(k_0^2) | \mathbf{k}_0 \rangle &= \Omega \langle \mathbf{k}_f | \mathcal{H}_1 | \mathbf{k}_0 \rangle \\ &+ \int \frac{d\mathbf{k}}{(2\pi)^d} \Omega \langle \mathbf{k}_f | \mathcal{H}_1 | \mathbf{k} \rangle \frac{1}{k_0^2 - k^2 + i\varepsilon} \Omega \langle \mathbf{k} | T^+(k_0^2) | \mathbf{k}_0 \rangle, \end{aligned} \quad (7.74)$$

where

$$\Omega \langle \mathbf{k}_f | \mathcal{H}_1 | \mathbf{k}_0 \rangle = -\omega^2 \int d\mathbf{r} \left[\frac{1}{c^2(\mathbf{r})} - \frac{1}{c_0^2} \right] \exp[-i(\mathbf{k}_f - \mathbf{k}_0) \cdot \mathbf{r}]. \quad (7.75)$$

In deriving (7.74) we have taken into account that

$$\langle \mathbf{k} | G_0^+(k_0^2) | \mathbf{k}' \rangle = \frac{\delta_{\mathbf{k}\mathbf{k}'}}{k_0^2 - k^2 + i\varepsilon}. \quad (7.76)$$

To first order we have that

$$\Omega \langle \mathbf{k}_f | T^+(k_0^2) | \mathbf{k}_0 \rangle \simeq \Omega \langle \mathbf{k}_f | \mathcal{H}_1 | \mathbf{k}_0 \rangle.$$

This last equation is always valid for sufficiently low frequencies. For a single scatterer of simple shape (e.g., spherical, cylindrical, etc.) and for intermediate frequencies and large fluctuations of $c^2(\mathbf{r})$, it is much easier to find first the scattering amplitude $f(\mathbf{k}_f, \mathbf{k}_0)$ by taking advantage of the boundary conditions at the surface of the scatterer rather than to solve the integral equation (7.74). For an infinite number of scatterers, intermediate frequencies, and large fluctuations of $c^2(\mathbf{r})$, exact analytical solutions are not possible and one is forced to use an approximation, e.g., the CPA. The CPA in its simplest version introduces a complex, k_0 -dependent effective propagation constant, $k_e(k_0) \equiv \omega/c_e$, which is related to the diagonal, in \mathbf{k} -space, matrix of the average Green's function $\langle G(k; k_0^2) \rangle$ and the self-energy $\Sigma(k_0^2)$ [as defined by (7.52)] as follows:

$$\langle G(k; k_0^2) \rangle \simeq G_e(k; k_0^2) = \frac{1}{k_e^2 - k^2} = \frac{1}{k_0^2 - \Sigma(k_0^2) - k^2}. \quad (7.77)$$

The next step is to replace locally (within a sphere or a cylinder or any other simple appropriate shape) the effective propagation constant, k_e , by the actual value, $k = \omega/c(\mathbf{r})$, of the propagation constant and calculate the corresponding t -matrix, which in principle is given by (7.74) and (7.75) with c_0 replaced by c_e and the integration in (7.75) restricted within the local region (be it spherical, cylindrical, etc.). The resulting t -matrix, or, equivalently, the scattering amplitude, f , must be averaged over various realizations of $c(\mathbf{r})$ within the chosen local shape. This average is set equal to zero

$$\langle f(\mathbf{k}_f, \mathbf{k}_e) \rangle = 0. \quad (7.78)$$

The quantity $\langle f \rangle$ depends not only on k_e (and $k_f = k_e$) but on the angle θ between \mathbf{k}_e and \mathbf{k}_f as well. Thus it is not in general possible to satisfy (7.78) for all angles θ . The reasonable choice is to satisfy (7.78) for $\theta = 0$, since, according to the optical theorem, the $\text{Im}\{f(\mathbf{k}, \mathbf{k})\}$ is connected to the total cross section σ . Actually we have (Problem 4.8)

$$\sigma = -\frac{\Omega}{k} \text{Im} \{ \langle \mathbf{k} | T^+ | \mathbf{k} \rangle \}. \quad (7.79)$$

Combining (7.79) (which is valid for systems of any dimensionality) with (7.73a) (which is valid for 3-d systems) we end up with (4.67).

To be more specific, let us consider a binary system consisting of two components, one with propagation constant $k_1 = \omega/c_1$ and the other with propagation constant $k_2 = \omega/c_2$. We shall assume that the two components are topologically symmetric with volume fractions x_1 and x_2 respectively ($x_1 + x_2 = 1$), and we shall choose a spherical region (of radius a) within which the effective medium (characterized by k_e) will be replaced either by medium 1 (with probability x_1) or by medium 2 (with probability x_2). In this case, (7.78) will take the form

$$x_1 f_1 + x_2 f_2 = 0, \quad (7.80a)$$

where

$$f_i = -\frac{i}{k_e} \sum_{n=0}^{\infty} (2n+1) r_{ni} \mathcal{P}_n(\cos \theta_i), \quad i = 1, 2, \quad (7.80b)$$

$$r_{ni} = -\frac{k_e j_n(k_i a) j'_n(k_e a) - k_i j_n(k_e a) j'_n(k_i a)}{k_e j_n(k_i a) h'_n(k_e a) - k_i h_n(k_e a) j'_n(k_i a)}, \quad i = 1, 2, \quad (7.80c)$$

and the angle θ_i between \mathbf{k}_e and \mathbf{k}_i is set to zero so that $\mathcal{P}_n(1) = 1$; the prime denotes differentiation with respect to the argument, e.g.,

$$j'_n(k_e a) = \left. \frac{dj_n(z)}{dz} \right|_{z=k_e a}.$$

In the case of acoustic waves in a two-component fluid where the densities ϱ_1 and ϱ_2 are different from each other as well as the velocities c_1 and c_2 ,

formulae (7.80) remain valid if k_e is replaced by k_e/ϱ_e and k_i by k_i/ϱ_i , while the arguments $k_e a$ and $k_i a$ do not change.

The quantity r_{ni} is directly related to the so-called phase shift, δ_{ni} , or to the quantity $S_{ni} \equiv \exp(2i\delta_{ni})$ through the relation

$$r_{ni} = \frac{1}{2}(S_{ni} - 1) = \frac{1}{2}[\exp(2i\delta_{ni}) - 1]. \quad (7.81)$$

Notice that the total cross section, σ , by a sphere of radius a and real propagation constant, k_i , embedded in a uniform medium of real propagation constant, k_e , is given by

$$\sigma = \frac{4\pi}{k_e} \text{Im}\{f_i\} = -\frac{4\pi}{k_e^2} \sum_{n=0}^{\infty} (2n+1) \text{Re}\{r_{ni}\} = \frac{4\pi}{k_e^2} \sum_{n=0}^{\infty} (2n+1) \sin^2 \delta_{ni}. \quad (7.82)$$

If there is absorption inside the sphere (i.e., if k_i is complex while k_e is real), the result for the total cross section is

$$\sigma_s = \frac{4\pi}{k_e^2} \sum_{n=0}^{\infty} (2n+1) |r_{ni}|^2 = \frac{\pi}{k_e^2} \sum_{n=0}^{\infty} (2n+1) |1 - S_{ni}|^2, \quad (7.83a)$$

$$\begin{aligned} \sigma_a &= -\frac{4\pi}{k_e^2} \sum_{n=0}^{\infty} (2n+1) \left[\text{Re}\{r_{ni}\} + |r_{ni}|^2 \right] \\ &= \frac{\pi}{k_e^2} \sum_{n=0}^{\infty} (2n+1) \left(1 - |S_{ni}|^2 \right), \end{aligned} \quad (7.83b)$$

$$\begin{aligned} \sigma_t &= -\frac{4\pi}{k_e^2} \sum_{n=0}^{\infty} (2n+1) \text{Re}\{r_{ni}\} \\ &= \frac{2\pi}{k_e^2} \sum_{n=0}^{\infty} (2n+1) (1 - \text{Re}\{S_{ni}\}), \end{aligned} \quad (7.83c)$$

where σ_s is the scattering-only cross section, σ_a is the absorption-only cross section, and σ_t is the extinction cross section, which is due to both scattering and absorption: $\sigma_t = \sigma_s + \sigma_a$. If the external medium possesses a complex k_e (as in the CPA case), more care is required in obtaining the scattering amplitude (Problem 7.9s). More effort is also required if we are dealing with vector classical fields such as the electromagnetic field (EM) and the elastic wave field in solid media. In the case of an EM field, the total cross sections involve two quantities of the type r_{ni} reflecting the fact that the EM field is transverse with two independent polarizations for each \mathbf{k} . These are given by the following expressions (see the books by Stratton [176], pp. 392–395, 414–420, 563–569, and by Bohren and Huffman [177] pp. 83–104, 181–183; the expressions for W_t and Q_t in Stratton's book should have a minus sign in front of them):

$$r_{ni}^{(\text{EM})} = \frac{\mu_i j_n(k_i a) [k_e a j_n(k_e a)]' - \mu_e j_n(k_e a) [k_i a j_n(k_i a)]'}{\mu_i j_n(k_i a) [k_e a h_n(k_e a)]' - \mu_e h_n(k_e a) [k_i a j_n(k_i a)]'}, \quad (7.84a)$$

$$\bar{r}_{ni}^{(\text{EM})} = \frac{\mu_i j_n(k_e a) [k_i a j_n(k_i a)]' - \mu_e (k_i/k_e)^2 j_n(k_i a) [k_e a j_n(k_e a)]'}{\mu_i h_n(k_e a) [k_i a j_n(k_i a)]' - \mu_e (k_i/k_e)^2 j_n(k_i a) [k_e a h_n(k_e a)]'}, \quad (7.84b)$$

$$\sigma_s = \frac{2\pi}{k_e^2} \sum_{n=1}^{\infty} (2n+1) \left(\left| r_{ni}^{(\text{EM})} \right|^2 + \left| \bar{r}_{ni}^{(\text{EM})} \right|^2 \right), \quad (7.85a)$$

$$\sigma_a = -\frac{2\pi}{k_e^2} \sum_{n=1}^{\infty} (2n+1) \left\{ \left| r_{ni}^{(\text{EM})} \right|^2 + \left| \bar{r}_{ni}^{(\text{EM})} \right|^2 + \text{Re} \left\{ r_{ni}^{(\text{EM})} \right\} + \text{Re} \left\{ \bar{r}_{ni}^{(\text{EM})} \right\} \right\}, \quad (7.85b)$$

$$\sigma_t = -\frac{2\pi}{k_e^2} \text{Re} \left\{ \sum_{n=1}^{\infty} (2n+1) \left[r_{ni}^{(\text{EM})} + \bar{r}_{ni}^{(\text{EM})} \right] \right\}. \quad (7.85c)$$

In the above expressions, μ_i and μ_e are the permeabilities, $k_e = \omega/c_e$, $k_i = \omega/c_i$, $c_e = c/\sqrt{\varepsilon_e \mu_e}$, $c_i = c/\sqrt{\varepsilon_i \mu_i}$, $h(z)$ is the spherical Hankel function of the first kind, and the prime denotes differentiation with respect to the argument $z = k_i a$ or $k_e a$.

For elastic waves in solids there are three components for each \mathbf{k} (two transverse and one longitudinal). The expressions for the scattered waves and the cross sections are more complicated (see the papers by Kafesaki et al. [178, 179] and by Penciu et al. [180]).

For the application of the CPA in the case for EM fields in random media see the papers by Economou and Soukoulis [181], Soukoulis et al. [182], Busch et al. [183, 184], and Jing et al. [185–187], and the book by Ping Sheng [21], Sect. 3.9, pp. 85–87. For the CPA applied to acoustic/elastic waves see the paper by Kafesaki and Economou [188].

7.2.5 Direct Extensions of the CPA

It must be stressed that in our derivation of the ATA and the CPA it was necessary to have the random part of the Hamiltonian \mathcal{H}_1 as a sum of local terms. The simple ATA and CPA we presented can be easily generalized in the case where each of the additive parts in \mathcal{H}_1 involves not just one local orbital but a finite number of them, e.g., if with each site \mathbf{m} a finite number of orbitals $|\mathbf{m}, \nu\rangle$, $\nu = 1, 2, \dots, j$ is associated, the random part of the Hamiltonian may have the form

$$\mathcal{H}_1 = \sum_{\mathbf{m}} \sum_{\nu \nu'} |\mathbf{m}, \nu\rangle \varepsilon'_{\mathbf{m}, \nu \nu'} \langle \nu', \mathbf{m} |. \quad (7.86)$$

In this case the effective part of the Hamiltonian will have the form

$$\mathcal{H}_{1e} = \sum_{\mathbf{m}} \sum_{\nu\nu'} |\mathbf{m}, \nu\rangle \Sigma_{\nu\nu'} \langle \nu', \mathbf{m} | ; \quad (7.87)$$

the $j \times j$ matrix Σ is determined by a matrix equation of the form (7.50) for the ATA or of the form (7.59a) for the CPA. Care must be exercised regarding the ordering of the matrices involved in $t_{\mathbf{m}}$. Another example is the special case of off-diagonal disorder where

$$V_{n\mathbf{m}} = V_{\mathbf{n}} + V_{\mathbf{m}} ; \quad (7.88)$$

then \mathcal{H}_1 is the sum of local terms each of which has the form

$$|\mathbf{m}\rangle \sum_{\mathbf{n}} (\varepsilon'_{\mathbf{m}} \delta_{\mathbf{m}\mathbf{n}} + V_{\mathbf{m}}) \langle \mathbf{n} | ,$$

where the summation is over the nearest neighbors of \mathbf{m} . In the special binary alloy case, (7.88) implies that $V_{AB} = (V_{AA} + V_{BB})/2$. A third, less obvious example is the case where

$$\varepsilon'_{\mathbf{m}} = - \sum_{\mathbf{n}} V_{m\mathbf{n}} , \quad \mathbf{n} \text{ nearest neighbor of } \mathbf{m} ; \quad (7.89)$$

this is realized in the case of pendula with random spring constants but fixed uncoupled eigenfrequencies and in the case of lattice vibrations, etc. When (7.89) is satisfied, \mathcal{H}_1 can be decomposed in *bond* contributions of the form

$$|\mathbf{n}\rangle V_{n\mathbf{m}} \langle \mathbf{m} | + |\mathbf{m}\rangle V_{m\mathbf{n}} \langle \mathbf{n} | - |\mathbf{m}\rangle V_{m\mathbf{n}} \langle \mathbf{m} | - |\mathbf{n}\rangle V_{n\mathbf{m}} \langle \mathbf{n} | .$$

In this connection it is worthwhile to mention the so-called homomorphic CPA developed by Yonezawa and Odagaki [189, 190], where *bond* additivity is forced by writing \mathcal{H}_1 as a sum of terms of the form

$$|\mathbf{n}\rangle V_{n\mathbf{m}} \langle \mathbf{m} | + |\mathbf{m}\rangle V_{m\mathbf{n}} \langle \mathbf{n} | + |\mathbf{m}\rangle \frac{\varepsilon'_{\mathbf{m}}}{Z} \langle \mathbf{m} | + |\mathbf{n}\rangle \frac{\varepsilon'_{\mathbf{n}}}{Z} \langle \mathbf{n} | .$$

Here Z is the number of nearest neighbors; if $\{\varepsilon'_{\mathbf{m}}\}$ are not random, then this decomposition is reasonable. However, if diagonal disorder is present, then these terms are not in general statistically independent, and hence the above decomposition may lead to erroneous results.

These extensions of the simple CPA have been employed to study the electronic structure, lattice vibrations, and magnetic excitations in real disordered systems. Thus the case (7.86) was examined by Faulkner [191], Faulkner and Stocks [192, 193], Papaconstantopoulos et al. [194], and Papaconstantopoulos and Economou [195] to treat electronic excitations. A variation of this case, developed in the framework of real space representation (instead of the TBM), is reviewed in [140, 141, 196, 197]; this so-called muffin-tin CPA avoids the difficulties associated with the off-diagonal randomness in TB CPA. In addition,

we mention contributions by Stocks et al. [198], Koringa and Mills [199], Roth [200], and Balanovski [201]. The case (7.88) was examined by Schwartz et al. [202] for the electronic problem, by Kaplan and Mostoller [203] for lattice vibrations, and by Harris et al. [204] for magnetic excitations. The case (7.89) has been studied by Tahir-Kheli and coworkers [205–207]; a generalization of this method incorporating environmental disorder was treated in [138] and [208].

According to the aforementioned, the CPA can treat off-diagonal disorder in the special case (7.88). Shiba [209] noted that the special case $V_{AB} = \sqrt{V_{AA}V_{BB}}$ can also be reduced to the simple CPA; this becomes apparent if one uses the locator expansion to derive the CPA. Among the efforts to treat off-diagonal disorder we mention work by Foo et al. [210] and by Brouers et al. [174]. Blackman et al. [211] obtained a solution to the problem for the case of binary distribution by introducing a 2×2 matrix version of the simple CPA, where the diagonal matrix elements refer to the AA, or BB configurations and the off-diagonal to the AB configuration; their method can be generalized to the n -component alloy distribution by working with $n \times n$ matrices. Whitelaw [212] succeeded in incorporating environmental disorder along with off-diagonal disorder; his method is briefly reviewed by Leath [213].

Up to now we have dealt with direct extensions of the CPA that map the problem back into the simple CPA. As a result, these extensions share with the simple CPA its desirable features: correct reproduction of the limiting cases, successful interpolation in between, and proper analytic behavior [214–216], which assures the nonnegativeness of the DOS. Some of these extensions incorporate cluster scattering as well. However, it must be realized that this was achieved only because of the special form of the random Hamiltonian. The question that arises is whether a systematic way to include cluster scattering in the simple CPA can be devised regardless of the form of the LCAO Hamiltonian. In the next subsection we review briefly the attempts to answer this question.

7.2.6 Cluster Generalizations of the CPA

It was already pointed out that the limitations of the simple CPA stem from its omission of multiple scattering from clusters of neighboring sites. Hence, it is obviously worthwhile to devise a general scheme for the incorporation of cluster scattering features in the simple CPA. A conceptual straightforward way to achieve this purpose is the following: replace the random part of the Hamiltonian \mathcal{H}_1 by an effective Hamiltonian \mathcal{H}_{1e} characterized by a number of as yet undetermined parameters $\Sigma_1, \Sigma_2, \dots, \Sigma_j$. Obviously \mathcal{H}_{1e} must possess the same periodicity as $\langle \mathcal{H}_1 \rangle + \mathcal{H}_0$. Then determine the self-energies $\Sigma_1, \dots, \Sigma_j$ by demanding that $\langle t_c \rangle = 0$, where t_c is the t -matrix associated with the fluctuations around the effective Hamiltonian within a chosen cluster c . Butler and Nickel [217] implemented such a scheme for a cluster of two neighboring sites. They found that serious nonanalyticities appear in the solutions when

the degree of disorder is large [218]. Furthermore, Ducastelle [215,216] demonstrated that this cluster generalization fails to reproduce the strong scattering limit. The nonanalyticities and the incorrect limiting behavior appeared routinely in the early schemes for cluster generalizations. Leath [219] attributed these failures to the fact that a particular site, as a result of the average periodicity, does not belong to a single fixed cluster but can be assigned to a number of overlapping, on average equivalent, clusters. According to this argument, one must break the average periodicity in order to obtain properly analytic solutions. An artificial way to do this is by introducing an effective Hamiltonian \mathcal{H}_{1e} that possesses a superlattice periodicity; the primitive cell of this superlattice equals the chosen cluster. This superperiodic \mathcal{H}_{1e} is characterized by self-energies Σ_i s connecting sites belonging to the same primitive cell; no self-energy refers to sites belonging to different primitive cells. Under these assumptions the problem becomes equivalent to that defined by (7.86) and (7.87), with the orbitals within the m^{th} supercell corresponding to the orbitals of the m th site in (7.86). Thus the problem has been mapped to that of the simple CPA, and consequently the solution is properly analytic. This has been achieved at the cost of introducing the incorrect superperiodicity on \mathcal{H}_{1e} , which produces small errors to quantities like $\langle G(\mathbf{m}, \mathbf{n}) \rangle$ when both \mathbf{m} and \mathbf{n} are well inside the supercell; on the other hand, when \mathbf{m} and \mathbf{n} belong to different supercells, the error is expected to be substantial.

A better way to break the average periodicity is by embedding an actual cluster in an effective medium. This means that the cluster is allowed to take all its possible configurations while the rest of the system is kept at its effective medium values. Again this method is appropriate for calculating $\langle G(\mathbf{m}, \mathbf{n}) \rangle$ only when both \mathbf{m} and \mathbf{n} belong to the cluster. The scheme can be subdivided into three categories depending on how the effective medium is determined. The simplest method is to determine it, say, from the simple CPA without attempting to make it consistent with the final result [220–222]. The method is easy to implement and has been very useful in treating real systems. In this connection one must mention the recursion method reviewed by Haydock [223] and the continued fraction method reviewed by Cyrot–Lackmann and Khanna [224]. In the second category there are many effective media, one for each particular configuration of the cluster [225, 226]; their determination is achieved by a slightly modified version of the simple CPA. Finally, in the third category one classifies all cases where an attempt is made to determine the effective medium so as to be consistent with the final result [174, 200, 217, 227–234]. There is no guarantee that the self-consistency requirement will not produce nonanalyticities; there is also no established self-consistency.

In Fig. 7.4 we plot the average density of states per site vs. E for a 1-d disordered system where the site energies $\{\varepsilon'_m\}$ have the binary distribution shown in (7.35) and (7.36) with $x = 0.5$, $|\varepsilon_A - \varepsilon_B|/B = 2$ ($B = 2|V|$), and $\varepsilon_A + \varepsilon_B = \varepsilon_0 = 0$. It should be stressed that the 1-d case with a binary alloy distribution is the most severe test of any approximation. The reason is that the 1-dimensionality and the binary distribution strongly en-

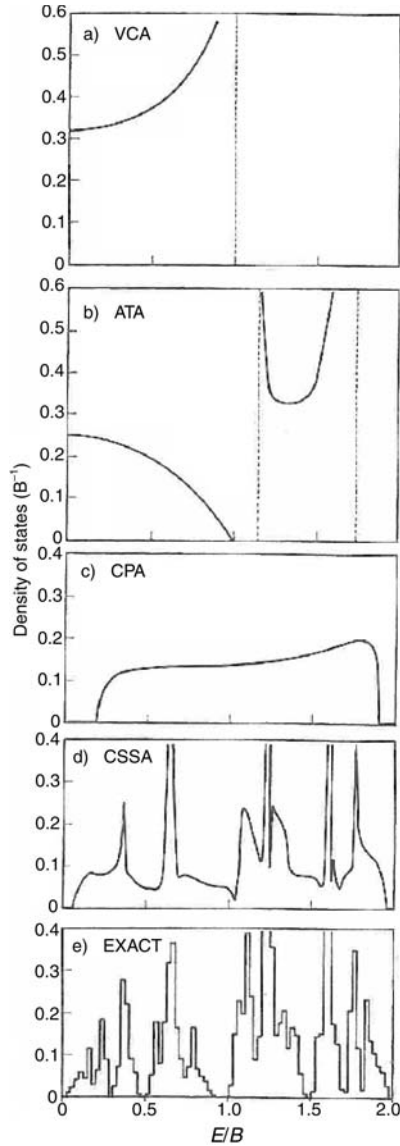


Fig. 7.4. Average density of states vs. E for a 1-d disordered system where the site energies have a binary distribution of the type shown in (7.35) and (7.36) with $x = 0.5$ and $|\varepsilon_A - \varepsilon_B|/B = 2$. Panel *d* (CSSA) is based on a generalization of the CPA [226]. In the present case $\rho(E) = \rho(-E)$

hance the probability of occurrence of certain special clusters capable of trapping electrons within them. Such clusters are responsible for the sharp peaks shown in Fig. 7.4e, which is based upon the numerical solution of

the exact equation (obtained by Schmidt [235]) for $\int^E \langle G(E') \rangle dE'$. Figure 7.4 shows that the ATA is a definite improvement over the VCA and that the CPA is a better approximation than the ATA. However, all these approximations fail to produce the fine structure of the exact results because, as was discussed before, even the CPA does not treat correctly the multiple scattering events responsible for the fine structure. On the other hand, the approximation termed CSSA [226] treats exactly clusters of up to three nearest-neighbor sites and as a result produces most of the fine structure.

We would like to point out once again that in higher dimensionality and/or for a smoother probability distribution there is no fine structure, and the CPA is a good approximation indeed; as a matter of fact, in the case where the probability distribution has a Lorentzian form, both the ATA and the CPA reproduce the exact result, because they replace each ε'_m by $\mp i\Gamma$ (for $E \pm i\Gamma$) (Sect. 7.2).

Despite the impressive success that embedded cluster CPA has in reproducing fine structure in the DOS (compare Figs. 7.4d and 7.4e), it cannot be considered as a complete solution to the problem of incorporating cluster effects because of its inherent inapplicability to the calculation of $\langle G(\mathbf{n}, \mathbf{m}) \rangle$ for large $|\mathbf{n} - \mathbf{m}|$.

Progress toward a general solution of this problem has been made. One important advance is the work by Mills and Ratanavararaksa [236], who developed a systematic diagrammatic way of assuring that a partial summation of a perturbation expansion is going to produce properly analytic results. Then they proceeded to sum up all diagrams associated with pair scattering, and they thus managed to produce the first properly analytic, properly periodic, fully self-consistent theory incorporating pair scattering.

Another powerful idea is to augment the Hilbert space through a new parameter that determines the component of the binary alloy occupying any site (this can be immediately generalized to multicomponent distributions). Then the process of configurational averaging corresponds to taking the “ground state quantum” average in this augmented space. This augmented space was first introduced by Mookerjee [237, 238]. Kaplan et al. [239] combined the augmented space idea and the pair-scattering method of [236] to produce a theory that is applicable not only to diagonal disorder but to off-diagonal and environmental disorder as well. Even short-range order can be treated within the framework of this theory [240]. These important developments are reviewed by Leath [213] and by Kaplan and Gray [241].

7.3 Summary

In this chapter we examined first a system consisting of two “impurities” embedded in a periodic tight-binding Hamiltonian (TBH). The total t -matrix associated with the two impurities is not simply the sum of t -matrices of each

impurity but includes infinitely many terms that correspond physically to multiple scattering events. A diagrammatic representation of this fact is shown in Fig. 7.1, where the propagation from site \mathbf{i} to site \mathbf{j} [described by $G(\mathbf{j}, \mathbf{i})$] is decomposed to unperturbed propagations [described by $G_0(\mathbf{n}, \mathbf{n}')$] and scattering events (described by the t -matrices t_ℓ and t_m) from the impurity sites ℓ and m .

In the case of two impurities the spectrum consists of a continuum (corresponding to extended scattering eigenstates) and no more than two discrete levels. The appearance and positions of the discrete levels depend on the magnitude and the sign of the impurity potentials. A typical behavior is shown in Fig. 7.3 for a 1-d system (a) and 3-d systems (b and c).

If the concentration of impurities is nonzero, we have what is called a random or disordered system. For such a system we are interested first in determining $\langle G \rangle$, where the symbol $\langle \rangle$ denotes averaging over the various configurations of impurities corresponding to the given concentration. In general, $\langle G \rangle$ cannot be determined exactly, and consequently schemes for approximations are needed. Three such schemes are reviewed briefly in Sect. 7.2. The most satisfactory one is the so-called coherent potential approximation (CPA) and its various extensions. The CPA, in its simplest form, determines $\langle G(E) \rangle$ as follows:

$$\langle G(E) \rangle = G_0(E - \Sigma(E)) , \quad (7.49)$$

where G_0 is the unperturbed periodic Green's function and the so-called self-energy Σ obeys the equation

$$\Sigma(E) = \left\langle \frac{\varepsilon'_m}{1 - (\varepsilon'_m - \Sigma(E)) G_0(\mathbf{m}, \mathbf{m}; E - \Sigma(E))} \right\rangle . \quad (7.59a)$$

The perturbation $\mathcal{H}_1 = \sum_m |\mathbf{m}\rangle \varepsilon'_m \langle \mathbf{m}|$ with $\langle \varepsilon'_m \rangle = 0$.

Further Reading

An extensive presentation of the CPA is given in the book by Gonis [242]. The classical wave case is treated in the books by P. Sheng [21, 243]. Scattering of electromagnetic waves is examined in the books by Stratton [176] and Bohren and Huffman [177].

Useful material can be found in older books and review articles such as those by Ziman [137], Lifshitz et al. [244], and Elliott et al. [138].

Problems

7.1s. Consider the two consecutive impurities problem,

$$\mathcal{H}_1 = |\ell\rangle \varepsilon \langle \ell| + |m\rangle \varepsilon' \langle m| , \quad (m = \ell + 1) ,$$

in an otherwise periodic 1-d Hamiltonian

$$\mathcal{H}_0 = \sum_n |n\rangle \varepsilon_0 \langle n| + V \sum' |n\rangle \langle m| .$$

Find the transmission and reflection coefficients for this model. Is there any resonance?

7.2s. Consider the simple 1-d model described in Problem 5.6. Derive the Green's function for this periodic model by employing a matrix notation where $|\ell\rangle = [|\ell_s\rangle, |\ell_p\rangle]$. Then introduce an impurity at site n that adds to the Hamiltonian a term \mathcal{H}_1 such that

$$\langle n | \mathcal{H}_1 | \ell \rangle = \begin{vmatrix} \varepsilon'_s & 0 \\ 0 & \varepsilon'_p \end{vmatrix} \delta_{n\ell} .$$

Find the bound states, if any, in the presence of \mathcal{H}_1 (especially those in the gap). Notice that a missing atom at n (a vacancy) corresponds in our model to $\varepsilon'_s \rightarrow \infty$ and $\varepsilon'_p \rightarrow \infty$, since by making ε'_s and ε'_p infinite site n becomes inaccessible to the electron.

7.3. Prove (checking carefully each step) that

$$\langle G^\pm(E) \rangle = G_0(E \pm i\Gamma)$$

if the probability distribution of each ε'_n is given by a Lorentzian: $p(\varepsilon'_n) = \Gamma/\pi (\varepsilon_n'^2 + \Gamma^2)$.

7.4. Starting from (7.52) prove (7.53). Also, starting from (7.59) prove (7.59a) and (7.59b).

7.5s. Calculate numerically the average DOS for a binary alloy case with $x = 0.5$: $p(\varepsilon'_n) = x\delta(\varepsilon'_n + \varepsilon) + (1-x)\delta(\varepsilon'_n - \varepsilon)$. For the unperturbed Green's function use the Hubbard one (5.56). Employ the CPA for your calculations and consider various values of ε/B . Plot your results for the DOS vs. E and the band edge trajectories vs. ε .

7.6s. Use the CPA to obtain the positions of the band "edges" as well as the tails in the DOS beyond the band "edges" for the case of a Gaussian distribution of each ε'_n and for a simple cubic lattice. Employ appropriate approximations to obtain analytical results in various limiting cases.

7.7. Prove (7.73a)–(7.73c).

7.8. Employing the boundary conditions that both $p(\mathbf{r})$ and the normal derivative, $\partial p/\partial r$, are continuous on the surface separating two media, prove (7.80b) and (7.80c). If the density of the two media is not the same, the boundary conditions are: p continuous and $\rho^{-1}\partial p/\partial r$ continuous; in this case find out how (7.80c) is modified.

7.9s. Consider sound propagation in an infinite, uniform host medium (characterized by density ϱ_0 and bulk modulus $B_0 = B_{0R} - iB_{0I}$) in which a sphere of radius a , bulk modulus $B = B_R - iB_I$, and density ϱ has been embedded. In this case of absorption in both media the various cross sections have to be calculated by the ratio of energy fluxes not at infinity but through a sphere of radius r ($r \rightarrow a^+$). To perform the calculation, introduce a scalar potential, ϕ , such that $\dot{\mathbf{u}} = \nabla\phi$, where \mathbf{u} is the displacement at point \mathbf{r} , connected to the pressure by the relation $p(\mathbf{r}) = -B\nabla \cdot \mathbf{u}$. The potential satisfies wave equation (7.70) and the boundary conditions $\varrho_i\phi_i$ and $\partial\phi_i/\partial r$ continuous at the interface. The energy flux is given by the expression

$$\mathbf{j} = -\frac{\varrho}{B + B^*} \left(B\dot{\phi}^* \nabla\phi + B^* \dot{\phi} \nabla\phi^* \right) .$$

Calculate the total cross section (both scattering and absorption) by taking into account that in the host medium $\phi = \phi_{\text{inc.}} + \phi_{\text{scat.}}$.

7.10. Express the tensor t -matrix, $\mathbf{t}(\mathbf{k}, \mathbf{k}'; \omega)$, for the EM field in a medium consisting of a dielectric sphere (radius a , ε_s , μ_s) in a uniform isotropic medium of ε_0 and μ_0 . Employ the eigenvectors $\mathbf{m}_{e^0nm}^{(i)}$ and $\mathbf{n}_{e^0nm}^{(i)}$ (see Stratton's book) and the coefficients $r_n^{(\text{EM})}$ and $\bar{r}_n^{(\text{EM})}$, as well as the connection between the t -matrix and the scattering amplitude.

Hint: See the article by Arya et al. in the book by Ping Sheng [243], especially the appendix on pp. 398–401.

Electrical Conductivity and Green's Functions

Summary. Disorder has a much more pronounced effect on transport properties than on the DOS. In fact, the DC metallic electrical conductivity is finite and not infinite (at $T = 0$), because of the presence of disorder, no matter how weak. As the disorder increases further, it may produce a metal–insulator transition, i.e., it may prevent the propagation of the carriers altogether, making the conductivity equal to zero (at $T = 0$ K). In the last 30 years there have been impressive developments in our understanding of these phenomena and in elucidating the role of elastic and inelastic scattering; Green's functions have played a central role as a theoretical tool. In this chapter, we shall introduce several transport quantities, such as electrical conductivity, and present several schemes for their calculation.

8.1 Electrical Conductivity and Related Quantities

The presence of an electric field, \mathcal{E} , in a system induces a current density, \mathbf{j} . The conductivity is defined as the coefficient of the linear (in \mathcal{E}) part of \mathbf{j} :

$$j_a(\mathbf{r}, t) = \int_0^\infty d\tau \int d\mathbf{r}' \sigma_{\alpha\beta}(\mathbf{r}, \mathbf{r}'; \tau) \mathcal{E}_\beta(\mathbf{r}', t - \tau), \quad (8.1)$$

where the subscripts α and β denote cartesian coordinates and a summation is implied over the repeated index β . In what follows we assume that both \mathcal{E} and \mathbf{j} are along the x -axis, so that we need to consider only σ_{xx} ; for simplicity we drop the subscripts. At the end it is easy to deduce from σ_{xx} the form of the other components of σ . Usually \mathcal{E} and \mathbf{j} vary slowly over distances of the order of ℓ_0 , where ℓ_0 is determined by the condition $\sigma \approx 0$ for $|\mathbf{r} - \mathbf{r}'| \gg \ell_0$. In this case one can perform the integration over \mathbf{r}' and the average over \mathbf{r} to obtain

$$j(t) = \int_0^\infty d\tau \sigma(\tau) \mathcal{E}(t - \tau), \quad (8.2)$$

where obviously

$$\sigma(\tau) = \frac{1}{\Omega} \int d\mathbf{r} d\mathbf{r}' \sigma(\mathbf{r}, \mathbf{r}'; \tau). \quad (8.3)$$

Henceforth we shall consider $\sigma(\tau)$ or its Fourier transform

$$\sigma(\omega) = \int_0^\infty d\tau \sigma(\tau) e^{i\omega\tau}. \quad (8.4)$$

At the end of the discussion we shall indicate how one can obtain $\sigma(\mathbf{r}, \mathbf{r}'; \tau)$ from $\sigma(\omega)$. If $\mathcal{E}(t)$ is given by

$$\mathcal{E}(t) = F e^{-i\omega t} + F^* e^{i\omega t}, \quad (8.5)$$

we have from (8.2) and (8.3) that

$$j(t) = \sigma(\omega) F e^{-i\omega t} + \sigma(-\omega) F^* e^{i\omega t}. \quad (8.6)$$

The reality of j requires that $\sigma(-\omega) = \sigma^*(\omega)$, from which it follows that the real (imaginary) part, $\sigma_1(\sigma_2)$, of σ is an even (odd) function of ω .

Note that as a result of causality, $\sigma(\tau)$ is nonzero only for $\tau \geq 0$; consequently, as can be seen from (8.4), $\sigma(\omega)$ is analytic for $\text{Im}\{\omega\} \geq 0$ with the possible exception of $\omega = 0$ (since the integral converges absolutely and the differentiation can be performed under the integration sign). Taking into account this analyticity and that $\sigma(\omega) \rightarrow 0$ for $\omega \rightarrow \infty$ (as we show later), we can see that the integral

$$\int_{-\infty}^{\infty} d\omega' \frac{\sigma(\omega')}{\omega' + i s - \omega}$$

is zero. By taking the limit $s \rightarrow 0^+$, and using (1.20), we obtain for the real (σ_1) and the imaginary (σ_2) parts of σ

$$\sigma_1(\omega) = \frac{1}{\pi} \text{P} \int_{-\infty}^{\infty} \frac{d\omega' \sigma_2(\omega')}{\omega' - \omega}, \quad (8.7)$$

$$\sigma_2(\omega) = -\frac{1}{\pi} \text{P} \int_{-\infty}^{\infty} \frac{d\omega' \sigma_1(\omega')}{\omega' - \omega} + \frac{A}{\omega}, \quad (8.8)$$

where iA is the residue (if any) of $\sigma(\omega)$ at $\omega = 0$. Thus knowing $\sigma_1(\omega)$ for $\omega \neq 0$ one can calculate $\sigma_2(\omega)$ and, consequently, $\sigma(\omega)$; the constant A can be obtained from the behavior of $\sigma(\omega)$ at infinity. Equations (8.7) and (8.8) are known as the *Kramers-Krönig relations*.

The conductivity tensor is related to several other quantities: by definition it is the inverse of the resistivity tensor, $\varrho_{\alpha\beta}(\mathbf{r}'', \mathbf{r}; t'' - t)$, i.e.,

$$\begin{aligned} \sum_{\gamma} \int \varrho_{\alpha\gamma}(\mathbf{r}'', \mathbf{r}; t'' - t) \sigma_{\gamma\beta}(\mathbf{r}, \mathbf{r}'; t - t') d\mathbf{r} dt \\ = \delta_{\alpha\beta} \delta(\mathbf{r}'' - \mathbf{r}') \delta(t'' - t'). \end{aligned} \quad (8.9)$$

It is connected to the diffusion function, $D_{\alpha\beta}(\mathbf{r}, \mathbf{r}''; t)$, by a generalized Einstein's relation

$$\sigma_{\alpha\beta}(\mathbf{r}, \mathbf{r}'; t) = q^2 \int d\mathbf{r}'' D_{\alpha\beta}(\mathbf{r}, \mathbf{r}''; t) [\delta n(\mathbf{r}'') / \delta \mu_0(\mathbf{r}')] , \quad (8.10)$$

where q is the charge of each of the diffusing particles ($-e$ for electrons), $n(\mathbf{r})$ is the local concentration of these particles at \mathbf{r} , and $\mu_0(\mathbf{r}')$ is the chemical potential at \mathbf{r}' in the absence of an electric field. For a proof see Problem 8.1s. In (8.10) it has been assumed that the relation between μ and n is nonlocal. If it is local,

$$\frac{\delta n(\mathbf{r})}{\delta \mu_0(\mathbf{r}')} = \delta(\mathbf{r} - \mathbf{r}') \frac{\partial n}{\partial \mu_0} ;$$

then, since as $T \rightarrow 0$ K, $n = 2 \int^{\mu_0} d\varepsilon \varrho(\varepsilon)$ (assuming spin $1/2$ particles), we have that $\partial n / \partial \mu_0 = 2\varrho_F$, where ϱ_F is the DOS per volume per spin at the Fermi level E_F ($E_F = \lim \mu$ as $T \rightarrow 0$ K). For free particles, $2\varrho_F = 3n/2E_F$ as $T \rightarrow 0$ K and $\partial n / \partial \mu_0 = 3n/2E_F$, while $\partial n / \partial \mu_0 = n/k_B T$ for $T \gg E_F/k_B$ (because $n = 2 \int d\varepsilon \varrho(\varepsilon) f(\varepsilon)$ with $f(\varepsilon) \approx \exp[(\mu - \varepsilon)/k_B T]$). Thus, we end up with the familiar Einstein's relations:

$$\sigma = \begin{cases} \frac{3}{2} q^2 (n/E_F) D , & T \ll E_F/k_B , \\ q^2 (n/k_B T) D , & T \gg E_F/k_B . \end{cases} \quad (8.11a)$$

$$(8.11b)$$

The DC conductivity, which, as we shall show below, can be written as

$$\sigma_{\text{DC}} = \int dE \sigma(E) \left(-\frac{\partial f}{\partial E} \right) , \quad (8.12)$$

is related to the averaged and the microscopic mobility, $\bar{\mu}_{\text{DC}}$ and $\mu_{\text{DC}}(E)$, respectively, as follows [245]:

$$\sigma_{\text{DC}} = |q| n \bar{\mu}_{\text{DC}} , \quad (8.13)$$

$$-\frac{d\sigma(E)}{dE} = |q| \varrho(E) \mu_{\text{DC}}(E) , \quad (8.14)$$

where q is the charge of each carrier ($-e$ for electrons), n is the concentration of carriers, $\varrho(E)$ is the DOS (including spin) per unit volume, and $f(E)$ is the occupation number of the single-particle state of energy E .

A very important relation is the one connecting the AC conductivity, $\sigma_{\alpha\beta}(\mathbf{r}, \mathbf{r}'; \omega)$, to the permittivity, $\varepsilon_{\alpha\beta}(\mathbf{r}, \mathbf{r}'; \omega)$:

$$\varepsilon_{\alpha\beta}(\mathbf{r}, \mathbf{r}'; \omega) = \delta_{\alpha\beta} + \frac{4\pi i}{\omega} \sigma_{\alpha\beta}(\mathbf{r}, \mathbf{r}'; \omega) . \quad (8.15)$$

(In the SI system $\delta_{\alpha\beta}$ is multiplied by ε_0 and the factor 4π is replaced by 1). The permittivity is connected to the electric susceptibility, $\chi_{\alpha\beta}^{(e)}$, as follows:

$$\chi_{\alpha\beta}^{(e)} = \frac{1}{4\pi} (\varepsilon_{\alpha\beta} - \delta_{\alpha\beta}) = \frac{i}{\omega} \sigma_{\alpha\beta} . \quad (8.16)$$

(In the SI, $\chi_{\alpha\beta}^{(e)} = i\sigma_{\alpha\beta}/\varepsilon_0\omega$). Notice that the susceptibility can be obtained in terms of the atomic (or ionic) polarizabilities.

The permittivity is a very important quantity because it determines the optical properties of materials, as mentioned in Chap. 7. But besides this, it gives the differential inelastic cross section, $d^2\sigma/d\mathcal{O}d\varepsilon_f$, of a charged particle by the solid:

$$\frac{d^2\sigma}{d\mathcal{O}d\varepsilon_f} \sim -\text{Im} \{ \varepsilon^{-1}(\mathbf{k}, \omega) \} ,$$

where $\hbar\omega = \varepsilon_i - \varepsilon_f$ and $\mathbf{k} = \mathbf{k}_i - \mathbf{k}_f$. Furthermore, it determines the Fourier transform of the screened Coulomb interaction of two charged particles (of charge q), $4\pi q^2/\varepsilon(\mathbf{k}, \omega)k^2$, and it allows us to express the total electronic potential energy in terms of $\text{Im} \{ \varepsilon^{-1}(\mathbf{k}, \omega) \}$. Finally, the zeros of $\varepsilon(\mathbf{k}, \omega)$ give the eigenfrequencies (vs. \mathbf{k}) of the collective *longitudinal* charge oscillations in a solid, while the infinities of $\varepsilon(\mathbf{k}, \omega)$ give the eigenfrequencies of the collective transverse oscillations in a solid [within the electrostatic approximation, $c \rightarrow \infty$; if this approximation is not valid, the transverse collective eigenfrequencies are given by $\varepsilon(\mathbf{k}, \omega) = c^2\mathbf{k}^2/\omega^2$].

8.2 Various Methods of Calculation

8.2.1 Phenomenological Approach

The simplest and crudest way to obtain approximately $\sigma(\omega)$ is by employing Newton's equation for the electronic drift velocity, v , in the presence of the field, $F e^{-i\omega t}$, and of a friction force, $-mv/\tau_{\text{tr}}$, (τ_{tr} is the transport relaxation time):

$$-i\omega mv = -\frac{mv}{\tau_{\text{tr}}} + qF , \quad (8.17)$$

where $q = -e$ is the electronic charge.

Since the current is given by $j = nqv$, where n is the electronic density, we obtain for $\sigma(\omega)$

$$\sigma(\omega) \approx \frac{ne^2\tau_{\text{tr}}}{m(1 - i\omega\tau_{\text{tr}})} . \quad (8.18)$$

For $\omega \rightarrow \infty$ the electronic motion is classical, all scattering is negligible, and only the electronic inertia (as measured by its mass m) matters. Hence, (8.18) (without the friction term) becomes exact:

$$\sigma(\omega) \xrightarrow{\omega \rightarrow \infty} i \frac{ne^2}{m\omega} . \quad (8.19)$$

A slight generalization of this approach (capable of treating nonspherical Fermi surfaces) consists in considering the whole equilibrium distribution transposed rigidly in \mathbf{k} -space by an amount $\delta\mathbf{k} = m\mathbf{v}/\hbar$, where v is again given by (8.17) [27].

The only forces we have used in (8.17) are the external one and the friction force. However, in reality, displacing a bound electron or an ion from its equilibrium position by x may set up a restoring harmonic force of the form $-m_i\omega_j^2x$, where ω_j is a natural frequency of the system. If such a force is present, instead of (8.18) we shall have

$$\sigma_j(\omega) = i \frac{q_j^2 n_j \omega}{m_j} \frac{1}{\omega^2 - \omega_j^2 + i\omega/\tau_j}, \quad (8.20)$$

where n_j is the concentration of those particles of mass m_j , charge q_j , and eigenfrequency ω_j . Now we can view phenomenologically the electrons in a solid as separated into several groups each one of which has its own eigenfrequency and its concentration n_j . Then the total conductivity from all groups shall be

$$\begin{aligned} \sigma(\omega) = & \frac{n_{\text{eff}} e^2 \tau_{\text{tr}}}{m_e (1 - i\omega\tau_{\text{tr}})} + \frac{ie^2\omega}{m_e} \sum_j \frac{n_{ej}}{\omega^2 - \omega_j^2 + i\omega/\tau_j} \\ & + \frac{iq^2 n_i \omega}{m_i (\omega^2 - \omega_{\text{TA}}^2 + i\omega/\tau_i)}, \end{aligned} \quad (8.21)$$

where the first two terms of the rhs are due to electrons and the last one to ions (assuming one ion per primitive cell), n_{eff} is the concentration of the free electrons, n_{ej} is the concentration of bound electrons of the group j , q is the charge per ion, n_i is the concentration of ions, and $\omega_{\text{TA}} = c_t k$ is the transverse sound velocity.

8.2.2 Boltzmann's Equation

A more sophisticated approach (but still semiclassical) is the one based on Boltzmann's equation, which determines the electron distribution in \mathbf{k} -space in the presence of an applied electric field and scattering mechanism, which tends to restore equilibrium [246, 247]. The advantage of this approach is that the phenomenological parameter τ_{tr} is related to the scattering potential $V(\mathbf{r})$ by

$$\frac{1}{\tau_{\text{tr}}} = \frac{2\pi}{\hbar} \varrho_F n_{\text{imp}} \frac{1}{4\pi} \int d\mathcal{O} |\langle \mathbf{k}_f | T'^+(E_F) | \mathbf{k} \rangle|^2 (1 - \cos\theta), \quad (8.22)$$

where ϱ_F is the DOS per volume per spin direction, n_{imp} is the number of scatterers per unit volume, the integration is over all directions of \mathbf{k}_f ($E(\mathbf{k}_f) = E(\mathbf{k}) = E_F$), and $T'^+(E)$ is the t -matrix associated with a single scatterer times the volume Ω . Equation (8.22) is equivalent to

$$\frac{1}{\ell_{\text{tr}}} = n_{\text{imp}} \sigma_{\text{tr}}, \quad (8.23)$$

where $\ell_{\text{tr}} = \tau_{\text{tr}} v_F$ and σ_{tr} is the cross section due to a single scatterer with the factor $(1 - \cos\theta)$ included. Equations (8.22) and (8.23) will be proven in Appendix G.

This extra factor, $(1 - \cos \theta)$, in (8.22) and (8.23) accounts for the fact that what matters for transport is the momentum change along the direction of initial propagation. If $|f(\mathbf{k}_j, \mathbf{k})|^2$ is isotropic (or, more generally, if it does not contain a p -spherical harmonic), then the $\cos \theta$ term averages out to zero, and $\tau_{\text{tr}} = \tau$, where τ is given by (8.22) without the $(1 - \cos \theta)$ factor. From τ we define the scattering mean free path $\ell = v_F \tau$; $\ell^{-1} = n_{\text{imp}} \sigma$, where σ is the total cross section due to a single scatterer [without the factor $(1 - \cos \theta)$].

8.2.3 A General, Independent-Particle Formula for Conductivity

We proceed now to obtain a general quantum-mechanical expression for $\sigma_1(\omega)$ within the independent-particle approximation and for $\omega \neq 0$ [248]. Then $\sigma(\omega)$ will be calculated by using (8.8) and (8.19). A more general, many-body way to obtain $\sigma(\omega)$ based on linear response theory will be given in §8.2.4 and Sect. 11.2 [110, 249, 250]. Using (8.5) and (8.6) we obtain, for the time average power $P = \Omega \bar{\mathcal{E}} \bar{j}$ consumed by the system, the expression

$$P = 2\Omega |F|^2 \sigma_1(\omega), \quad \omega \neq 0. \quad (8.24)$$

The average power P can also be calculated by multiplying the energy

$$\varepsilon_{\beta\alpha} \equiv \hbar\omega_{\beta\alpha} = E_\beta - E_\alpha$$

(absorbed by the system during the field-induced transition $|\alpha\rangle \rightarrow |\beta\rangle$) by the transition rate $p_{\alpha\beta}$ and by summing over all possibilities ($|\alpha\rangle \neq |\beta\rangle$)

$$P = \sum_{\alpha\beta} \varepsilon_{\beta\alpha} p_{\alpha\beta} = \frac{1}{2} \sum_{\alpha\beta} \varepsilon_{\beta\alpha} (p_{\alpha\beta} - p_{\beta\alpha}). \quad (8.25)$$

The summation includes a spin degeneracy factor equal to 2; the probability per unit time $p_{\alpha\beta}$ is given by

$$p_{\alpha\beta} = f_\alpha (1 - f_\beta) W_{\alpha\beta}, \quad (8.26)$$

where $f_\nu \equiv f(E_\nu)$, ($\nu = \alpha, \beta$), is the Fermi distribution and $W_{\alpha\beta}$ can be obtained (like Fermi's golden rule) by substituting into (4.48) the perturbation \mathcal{H}_1 instead of the t -matrix, since we are interested in the lowest-order response. In the present case the perturbation is

$$\mathcal{H}_1(t) = ex\mathcal{E}(t), \quad (8.27)$$

where the field is given by (8.5). The result is

$$W_{\alpha\beta} = \frac{2\pi}{\hbar} e^2 |F|^2 |\langle \alpha | x | \beta \rangle|^2 [\delta(\hbar\omega - \varepsilon_{\beta\alpha}) + \delta(\hbar\omega + \varepsilon_{\beta\alpha})]. \quad (8.28)$$

Combining (8.25), (8.26), and (8.28), and comparing with (8.24), we obtain

$$\sigma_1(\omega) = \frac{\pi e^2}{\Omega} \sum_{\alpha\beta} |\langle \alpha | x | \beta \rangle|^2 \omega_{\beta\alpha} (f_\alpha - f_\beta) \delta(\hbar\omega - \hbar\omega_{\beta\alpha}) . \quad (8.29)$$

We can recast this expression in terms of the momentum p_x matrix elements. Indeed, since

$$p_x = m \frac{dx}{dt} = im \frac{\mathcal{H}x - x\mathcal{H}}{\hbar} ,$$

we have

$$\langle \alpha | p_x | \beta \rangle = im\omega_{\alpha\beta} \langle \alpha | x | \beta \rangle . \quad (8.30)$$

Substituting (8.30) into (8.29) we obtain

$$\sigma_1(\omega) = \frac{\pi e^2}{\Omega m^2} \sum_{\alpha\beta} |\langle \alpha | p_x | \beta \rangle|^2 \frac{f_\alpha - f_\beta}{\omega_{\beta\alpha}} \delta(\hbar\omega - \hbar\omega_{\beta\alpha}) . \quad (8.31)$$

Because of the δ function in (8.31) it is trivial to perform the integration in (8.8); the constant A can be obtained by comparing with (8.19), and thus $\sigma_2(\omega)$ is calculated. Combining the expressions for $\sigma_1(\omega)$ and $\sigma_2(\omega)$ we have finally:

$$\begin{aligned} \sigma(\omega + is) &= \left(\frac{e^2 n}{m} - \frac{e^2}{\Omega m^2} \sum_{\alpha\beta} |\langle \alpha | p_x | \beta \rangle|^2 \frac{f_\alpha - f_\beta}{\hbar\omega_{\beta\alpha}} \right) \frac{i}{\omega + is} \\ &\quad - i \frac{e^2}{\Omega m^2} \sum_{\alpha\beta} |\langle \alpha | p_x | \beta \rangle|^2 \frac{f_\alpha - f_\beta}{\hbar\omega_{\beta\alpha}} \frac{1}{\omega_{\beta\alpha} - \omega - is} . \end{aligned} \quad (8.32)$$

The term $ie^2 n/m\omega \equiv \sigma_d(\omega)$ is the so-called *diamagnetic contribution* to $\sigma(\omega)$, and the rest, $\sigma_p(\omega)$, is the *paramagnetic* one, which can be recast as

$$\sigma_p(\omega) = -i \frac{e^2}{\Omega m^2 \hbar \omega} \sum_{\alpha\beta} |\langle \alpha | p_x | \beta \rangle|^2 \frac{f_\alpha - f_\beta}{\omega_{\beta\alpha} - \omega - is} . \quad (8.33)$$

The local conductivity $\sigma(\mathbf{r}, \mathbf{r}'; \omega)$ can be obtained from (8.32) by replacing the velocity, p_x/m , matrix elements by the current operator matrix elements, i.e.,

$$\frac{|\langle \alpha | p_x | \beta \rangle|^2}{\Omega} \rightarrow \lambda_{\alpha\beta}(\mathbf{r}) \lambda_{\alpha\beta}^*(\mathbf{r}') ,$$

where

$$\lambda_{\alpha\beta}(\mathbf{r}) = \frac{-i\hbar}{2} \left[\psi_\alpha^*(\mathbf{r}) \frac{\partial \psi_\beta(\mathbf{r})}{\partial x} - \psi_\beta(\mathbf{r}) \frac{\partial \psi_\alpha^*(\mathbf{r})}{\partial x} \right] , \quad (8.34)$$

$\psi_\alpha(\mathbf{r}) = \langle \mathbf{r} | \alpha \rangle$ and $\psi_\beta(\mathbf{r}) = \langle \mathbf{r} | \beta \rangle$. To obtain $\sigma_{\mu\nu}$, one replaces $|\langle \alpha | p_x | \beta \rangle|^2$ by $\langle \alpha | p_\mu | \beta \rangle \langle \beta | p_\nu | \alpha \rangle$ in (8.32).

For fixed boundary conditions (BCs) the term in parentheses in (8.32) vanishes identically. This can be proved by noticing that (8.30) implies the following equality:

$$\frac{|\langle \alpha | p_x | \beta \rangle|^2}{\omega_{\beta\alpha}} = -im \langle \alpha | x | \beta \rangle \langle \beta | p_x | \alpha \rangle .$$

Note that for a *perfect* conductor with *periodic boundary* conditions, the term in parentheses in (8.32) is not zero, because then (8.30) fails; in this case the only term that survives is the diamagnetic one.

Mott and Davis [248] gave an instructive way to obtain (8.18) (for $\omega = 0$) starting from (8.31). Their main assumption is that for weakly disordered systems the eigenfunctions have essentially constant amplitude (as in perfectly ordered systems) but phase coherence among different members of the ensemble is maintained only over a distance of the order of the transport mean free path, $\ell_{\text{tr}} \equiv v_F \tau_{\text{tr}}$ (for ordered systems $\ell_{\text{tr}} = \infty$). If the total volume Ω is divided into cells, each of volume $v_i \approx \ell_{\text{tr}}^d$, then

$$\langle \alpha | p_x | \beta \rangle = \sum_{v_i} \int_{v_i} d\mathbf{r} \psi_{\alpha}^* p_x \psi_{\beta} . \quad (8.35)$$

Multiplying (8.35) by its complex conjugate and cancelling the cross terms due to their random phases, one obtains

$$\langle |\langle \alpha | p_x | \beta \rangle|^2 \rangle = \sum_{v_i} \left| \int_{v_i} d\mathbf{r} \psi_{\alpha}^* p_x \psi_{\beta} \right|^2 = \frac{\Omega}{v} \left| \int_{v_i} \psi_{\alpha}^* p_x \psi_{\beta} d\mathbf{r} \right|^2 . \quad (8.36)$$

Within the volume v , ψ_{α} and ψ_{β} are assumed to be plane waves so that the integral can be performed explicitly. Substituting the result in (8.31) one obtains $\sigma_1 \approx e^2 n \ell_{\text{tr}} / 2m v_F$, which coincides with (8.18) apart from a factor of 2 (for $\omega = 0$), since $\ell_{\text{tr}} = v_F \tau_{\text{tr}}$.

Thouless [251] has also obtained (8.18) starting from (8.31) by assuming that ψ_{α} (and ψ_{β}) is a linear combination of plane waves with coefficients that are uncorrelated Gaussian random variables whose variance is $(\pi / \ell_{\text{tr}} k^2 \Omega) [(k - k_a)^2 + \ell_{\text{tr}}^2 / 4]$.

The general formulae we derived for σ or σ_1 are usually referred to in the literature as the *Kubo* [252, 253]–*Greenwood* [254] *formulae*.

8.2.4 General Linear Response Theory

Consider a system that initially (i.e., for $t < t_0$) is described by the thermodynamic equilibrium density matrix, ϱ_0 , where

$$\varrho_0 = \frac{\exp(-\beta \mathcal{H}_0)}{\text{Tr} \{ \exp(-\beta \mathcal{H}_0) \}} . \quad (8.37)$$

At time $t = t_0$ we apply a perturbation $\mathcal{H}_1(t)$. We would like to calculate how a physical quantity corresponding to operator X changes to first order in $\mathcal{H}_1(t)$. The answer to this is given by the following general formula (which we quote here without proof):

$$\langle X(t) \rangle = \langle X \rangle_0 - \frac{i}{\hbar} \int_{t_0}^t dt' \text{Tr} \{ \varrho_0 [X_I(t), \mathcal{H}_{1,I}(t')] \} , \quad (8.38)$$

where

$$\langle X \rangle_0 = \text{Tr} \{ \varrho_0 X \} , \quad (8.38a)$$

$$X_I(t) = \exp(i\mathcal{H}_0 t/\hbar) X \exp(-i\mathcal{H}_0 t/\hbar) , \quad (8.38b)$$

$$\mathcal{H}_{1,I}(t') = \exp(i\mathcal{H}_0 t'/\hbar) \mathcal{H}_1(t') \exp(-i\mathcal{H}_0 t'/\hbar) , \quad (8.38c)$$

and the brackets denote the commutator of the two operators.

If the time dependence of $\mathcal{H}_1(t)$ is of the form $e^{-i(\omega+is)t}$, and we take the limit $t_0 \rightarrow -\infty$ and $s \rightarrow 0^+$, we find

$$\begin{aligned} \langle X(t) \rangle - \langle X \rangle_0 &= \frac{e^{-i\omega t}}{\hbar} \sum_{n,m} \left(-\varrho_{0n} \frac{\mathcal{H}_{1,nm} X_{mn}}{\omega + \omega_{mn} + is} + \varrho_{0n} \frac{X_{nm} \mathcal{H}_{1,mn}}{\omega - \omega_{mn} + is} \right) , \end{aligned} \quad (8.39)$$

where $\varrho_{0n} = \exp(-\beta E_n)/Z$, $Z = \sum_n \exp(-\beta E_n)$, $\mathcal{H}_{1,nm} = \langle n | \mathcal{H}_1 | m \rangle$, $X_{mn} = \langle m | X | n \rangle$, $\mathcal{H}_0 |m\rangle = E_m |m\rangle$, $\mathcal{H}_0 |n\rangle = E_n |n\rangle$, and $\omega_{mn} = (E_m - E_n)/\hbar$. For a proof of (8.39), see Problem 8.6. The imaginary part of $\delta X(\omega) \equiv e^{i\omega t} [\langle X(t) \rangle - \langle X \rangle_0]$ is, according to (8.39),

$$\begin{aligned} \text{Im} \{ \delta X(\omega) \} &= \frac{\pi}{\hbar} \sum_{n,m} \varrho_{0n} [\mathcal{H}_{1,nm} X_{mn} \delta(\omega + \omega_{mn}) \\ &\quad - X_{nm} \mathcal{H}_{1,mn} \delta(\omega - \omega_{mn})] . \end{aligned} \quad (8.40)$$

Taking into account that

$$\delta(\omega + \omega_{mn}) = \frac{1}{2\pi} \int_{-\infty}^{\infty} \exp[-it(\omega + \omega_{mn})] dt , \quad (8.41)$$

and that

$$\begin{aligned} \mathcal{H}_{1,nm} \exp(-it\omega_{mn}) &= \mathcal{H}_{1,nm} \exp[it(E_n - E_m)/\hbar] \\ &= \langle n | \exp(i\mathcal{H}_0 t/\hbar) \mathcal{H}_1 \exp(-i\mathcal{H}_0 t/\hbar) | m \rangle \\ &= \langle n | \mathcal{H}_{1,I}(t) | m \rangle \end{aligned} \quad (8.42)$$

[and similarly for the second term in brackets in (8.40)], we find that

$$\begin{aligned} \text{Im} \{ \delta X(\omega) \} &= \frac{1}{2\hbar} \int_{-\infty}^{\infty} dt \text{Tr} \{ \varrho_0 [\mathcal{H}_{1,I}(t), X(0)] \} e^{-i\omega t} \\ &= -\frac{1}{2\hbar} \int_{-\infty}^{\infty} dt \langle [X(0), \mathcal{H}_{1,I}(t)] \rangle e^{-i\omega t} , \end{aligned} \quad (8.43)$$

where the symbol $\langle A \rangle$ indicates the average over the equilibrium canonical ensemble: $\langle A \rangle \equiv \text{Tr} \{ \varrho_0 A \}$. The last term on the rhs of (8.40) can be written as

$$\begin{aligned} & \frac{1}{Z} \exp(-\beta E_n) \mathcal{H}_{1,mn} X_{nm} \delta(\omega - \omega_{mn}) \\ &= \frac{1}{Z} \exp[-\beta(E_m - \hbar\omega)] \mathcal{H}_{1,mn} X_{nm} \delta(\omega - \omega_{mn}) . \end{aligned}$$

Now we interchange the dummy indices m and n so that the term above becomes

$$e^{\beta\hbar\omega} \frac{1}{Z} \exp(-\beta E_n) \mathcal{H}_{1,nm} X_{mn} \delta(\omega - \omega_{nm}) , \quad Z = \text{Tr} \{ \exp(-\beta \mathcal{H}_0) \} .$$

Since $\delta(\omega - \omega_{nm}) = \delta(\omega + \omega_{mn})$, the term above is the same as the first term on the rhs of (8.40) times the factor $e^{\beta\hbar\omega}$. Hence, we end up with the following expressions for $\text{Im} \{ \delta X(\omega) \}$:

$$\text{Im} \{ \delta X(\omega) \} = \frac{\pi}{\hbar} (1 - e^{\beta\hbar\omega}) \sum_{nm} \varrho_{0n} \mathcal{H}_{1,nm} X_{mn} \delta(\omega + \omega_{mn}) \quad (8.44)$$

$$= \frac{1}{2\hbar} (1 - e^{\beta\hbar\omega}) \int_{-\infty}^{\infty} dt \langle \mathcal{H}_{1,I}(t) X(0) \rangle e^{-i\omega t} , \quad (8.44')$$

where (8.44') was obtained from (8.44) by taking into account (8.41) and (8.42). Equation (8.44) is a general expression for the so-called *fluctuation-dissipation theorem*, which connects $\text{Im} \{ \delta X(\omega) \}$, i.e., the dissipation due to the departure from equilibrium as a result of the application of \mathcal{H}_1 , with the average of the quantity $\mathcal{H}_{1,I}(t) X(0)$ (which, for the cases of interest here, is related to the fluctuation in time of the quantity X) in the equilibrium state.

The imaginary part of the electric susceptibility, $\chi_{\alpha\beta}^{(e)}(\omega)$, can be obtained directly from (8.44) by setting $\mathcal{H}_1(t) = ex_a F e^{-i\omega t}$ [see (8.5) and (8.27)] and $X = -enx_\beta$, where $-e$ is the charge of the electron and n is the electronic concentration. We have then

$$\begin{aligned} \text{Im} \{ \chi_{\alpha\beta}^{(e)} \} &= \frac{P_{\alpha\beta}(\omega)}{F} \\ &= -\frac{e^2 n}{2\hbar} (1 - e^{\beta\hbar\omega}) \int_{-\infty}^{\infty} dt \langle x_{\alpha,I}(t) x_\beta(0) \rangle e^{-i\omega t} . \end{aligned} \quad (8.45)$$

From (8.16) and (8.45) we obtain $\text{Re} \{ \sigma_{\alpha\beta}(\omega) \}$

$$\text{Re} \{ \sigma_{\alpha\beta}(\omega) \} = -\frac{e^2 n \omega}{2\hbar} (1 - e^{\beta\hbar\omega}) \int_{-\infty}^{\infty} dt \langle x_{\alpha,I}(t) x_\beta(0) \rangle e^{-i\omega t} \quad (8.46a)$$

$$= -\frac{e^2 n \omega}{2\hbar} (1 - e^{\beta\hbar\omega}) \int_{-\infty}^{\infty} dt \langle x_\alpha(0) x_{\beta,I}(t) \rangle e^{i\omega t} \quad (8.46b)$$

$$= \frac{e^2 n \omega}{2\hbar} (1 - e^{-\beta\hbar\omega}) \int_{-\infty}^{\infty} dt \langle x_\beta(0) x_{\alpha,I}(t) \rangle e^{-i\omega t} . \quad (8.46c)$$

Equation (8.40) can be written by interchanging the dummy n and m indices in the second term of the rhs as follows:

$$\text{Im} \{ \delta X(\omega) \} = \frac{\pi}{\hbar} \sum_{nm} \mathcal{H}_{1,nm} X_{mn} \delta(\omega + \omega_{mn}) (\varrho_{0n} - \varrho_{0m}) ,$$

from which $\text{Re} \{ \sigma_{\alpha\beta}(\omega) \}$ can be recast as

$$\text{Re} \{ \sigma_{\alpha\beta}(\omega) \} = -\frac{\pi e^2 n \omega}{\hbar} \sum_{nm} x_{\alpha,nm} x_{\beta,mn} \delta(\omega + \omega_{mn}) (\varrho_{0n} - \varrho_{0m}) . \quad (8.47)$$

It must be stressed that in all formulae of this section up to now the Hamiltonians and their eigenfunctions refer to the whole system. Thus, these formulae are valid for the most general case where all correlations among particles are included. If we make the independent-particle approximation, the matrix elements in (8.39), (8.40), (8.44), and (8.47) are between single-particle states, and the many-body equilibrium density matrix elements must be replaced by the Fermi distribution, $f(\varepsilon_n)$ [divided by N in order to be normalized to 1, $\sum_n f(\varepsilon_n)/N = 1$, as the full density matrix $\sum_n \varrho_{0n} = 1$]. Thus, in the case of independent particles, (8.47) becomes (for $\alpha = \beta$)

$$\text{Re} \{ \sigma_{\alpha\alpha}(\omega) \} = \frac{\pi e^2}{\Omega} \sum_{nm} |\langle m | x_\alpha | n \rangle|^2 \delta(\hbar\omega - \hbar\omega_{nm}) \omega_{nm} (f_m - f_n) , \quad (8.48)$$

which coincides with (8.29). To arrive at (8.48) we have used the relations $n/N = 1/\Omega$, $\delta(\hbar\omega - \hbar\omega_{nm}) = \delta(\omega + \omega_{mn})/\hbar$, and $\omega = \omega_{nm}$ (because of the δ -function).

8.3 Conductivity in Terms of Green's Functions

Now we recast the general expression for $\sigma_1(\omega)$ or $\sigma(\omega)$ in an invariant form involving Green's functions. Among the various slightly different versions, we discuss here two. In the first used by Abrikosov et al. [113] and by Doniach and Sondheimer [135], $\sigma(\omega)$ is expressed in terms of the causal Green's function $g(E)$, which is of central importance in many-body theory (Part III). For the present purposes (where electrons are assumed to move independently of each other), $g(E)$ can be defined as $G^-(E)$ for $E < E_F$ and $G^+(E)$ for $E > E_F$, i.e.,

$$g(E) \equiv [E + is\bar{\varepsilon}(E - E_F) - \mathcal{H}]^{-1} , \quad (8.49)$$

from which it follows that

$$\langle \alpha | g(E) | \beta \rangle = \delta_{\alpha\beta} [E + is\bar{\varepsilon}(E - E_F) - E_\alpha]^{-1} .$$

At $T = 0$ one has

$$\frac{f_\alpha - f_\beta}{\varepsilon_{\beta\alpha} - \hbar\omega - is} = \frac{-1}{2\pi i} \int_{-\infty}^{\infty} dE \langle \alpha | g(E) | \alpha \rangle \langle \beta | g(E + \hbar\omega) | \beta \rangle . \quad (8.50)$$

To prove (8.50) close the integration path on its rhs by a semicircle either in the upper or in the lower half-plane and use residue theory.

Substituting (8.50) into (8.33), and performing the summation over intermediate states by employing (1.4'), one obtains

$$\sigma(\omega) = \frac{ie^2n}{m\omega} + \frac{e^2}{\Omega m^2\omega} \int \frac{dE}{2\pi} \text{Tr} \{p_x g(E) p_x g(E + \hbar\omega)\} , \quad (8.51)$$

where the Tr operation includes a factor of 2 due to spin summation. By using standard many-body techniques (see, e.g., Part III of this book), one can generalize (8.51) to nonzero temperatures. Abrikosov et al. [113], as well as Doniach and Sondheimer [135], starting from (8.51) expand the two g s in a perturbation series and after a lengthy calculation obtain the ensemble average of $\sigma(\omega)$ (over all configurations of the scatterers), which agrees with (8.18) and (8.22).

It is probably simpler and more convenient to express $\sigma_1(\omega)$ in terms of $\tilde{G} = G^+ - G^-$. For that purpose one notices first that

$$\begin{aligned} & \frac{f_\alpha - f_\beta}{\omega_{\beta\alpha}} \delta(\hbar\omega - \varepsilon_{\beta\alpha}) \\ &= \int dE \delta(E - E_\alpha) \delta(E - E_\beta + \hbar\omega) \frac{f(E) - f(E + \hbar\omega)}{\omega} . \end{aligned} \quad (8.52)$$

Substituting (8.52) into (8.31) we have

$$\begin{aligned} \sigma_1(\omega) &= \frac{\pi e^2 \hbar}{\Omega m^2} \int_{-\infty}^{\infty} dE \frac{f(E) - f(E + \hbar\omega)}{\hbar\omega} \text{Tr} \{p_x \delta(E + \hbar\omega - \mathcal{H}) p_x \delta(E - \mathcal{H})\} \\ &= \frac{e^2 \hbar}{\pi \Omega m^2} \int_{-\infty}^{\infty} dE \frac{f(E) - f(E + \hbar\omega)}{\hbar\omega} \\ &\quad \times \text{Tr} \{p_x \text{Im} \{G^+(E + \hbar\omega)\} p_x \text{Im} \{G^+(E)\}\} , \end{aligned} \quad (8.53)$$

where the Tr operation includes a factor of 2 due to spin summation. One can express $\sigma_1(\omega)$ in terms of G^\pm by noticing that $\text{Im} \{G^+\} = i(G^- - G^+)/2$ and substituting it into (8.53).

It is important to remember that in all expressions [(8.30), (8.31), (8.32), (8.33), (8.51), (8.53)] for $\sigma_1(\omega)$ or $\sigma(\omega)$ an appropriate ensemble average over all possible configurations of the scatterers has to be taken. One usually takes the arithmetic mean. However, explicit results in 1-d systems demonstrate [255–258] that it is the probability distribution of $\ln \sigma(0)$, and not that of $\sigma(0)$ itself, that is sharply peaked; thus the geometric, and not the arithmetic, mean of $\sigma(0)$ is representative of the ensemble. This anomalous behavior seems to be related to the exponential decrease of $\sigma(0)$ as one increases the linear dimension of 1-d systems.

8.3.1 Conductivity Without Vertex Corrections

To calculate the arithmetic mean of $\sigma_1(\omega)$, one has to average the product of two G s, which in general is different from the product of the averages. We

shall return to this important question later, but for the time being let us replace each G in (8.53) by its average value $\langle G \rangle$, which can be calculated with the use of the CPA. Working in the \mathbf{k} -representation, where both p and $\langle G \rangle$ are diagonal, we obtain from (8.53) in the limit $\omega \rightarrow 0$

$$\sigma^{(0)}(0) = \frac{2e^2\hbar}{\pi\Omega} \int dE \left(-\frac{\partial f}{\partial E} \right) \sum_{\mathbf{k}} |\langle \mathbf{k} | p_x/m | \mathbf{k} \rangle|^2 |\text{Im} \{ G^+(E, \mathbf{k}) \}|^2. \quad (8.54)$$

Taking into account that

$$\left\langle \mathbf{k} \left| \frac{p_x}{m} \right| \mathbf{k} \right\rangle = \frac{\partial E(\mathbf{k})}{\hbar \partial k_x} \equiv v_x(\mathbf{k}),$$

that $G^+(E, \mathbf{k}) = [E - \Sigma(E) - E(\mathbf{k})]^{-1}$, where $\Sigma = \Sigma_1 - i\Sigma_2$ is the self-energy, and that $(-\partial f/\partial E) \rightarrow \delta(E - E_F)$ as $T \rightarrow 0$, we obtain for the zero temperature conductivity

$$\sigma^{(0)}(0) = \frac{2e^2\hbar}{\pi\Omega} \sum_{\mathbf{k}} v_x^2(\mathbf{k}) \frac{\Sigma_2^2}{\left\{ [E_F - \Sigma_1 - E(\mathbf{k})]^2 + \Sigma_2^2 \right\}^2}. \quad (8.55)$$

The summation over \mathbf{k} is facilitated if one introduces an integration over $\delta(E' - E(\mathbf{k})) dE'$, so that

$$\begin{aligned} \sigma^{(0)}(0) &= \frac{2e^2\hbar}{\pi} \int dE' \left[\frac{1}{\Omega} \sum_{\mathbf{k}} v_x^2(\mathbf{k}) \delta(E' - E(\mathbf{k})) \right] \\ &\quad \times \frac{\Sigma_2^2}{\left\{ [E_F - \Sigma_1 - E']^2 + \Sigma_2^2 \right\}^2}. \end{aligned} \quad (8.56)$$

The quantity in the brackets depends only on the form of $E(\mathbf{k})$. For lattices of cubic symmetry v_x^2 can be replaced by $|\mathbf{v}|^2/d$, where d is the dimensionality. Furthermore, the \mathbf{k} summation can be replaced by an integration over the surface of constant energy E' , so that

$$\begin{aligned} \frac{1}{\Omega d} \sum_{\mathbf{k}} |\mathbf{v}(\mathbf{k})|^2 \delta(E' - E(\mathbf{k})) &= \frac{1}{(2\pi)^d d} \int dS_k \frac{1}{\hbar |\mathbf{v}(\mathbf{k})|} |\mathbf{v}(\mathbf{k})|^2 \\ &= \frac{1}{(2\pi)^d d \hbar} S(E') v(E'), \end{aligned}$$

where S is the area of the surface of energy E' and $v(E')$ is the average of the magnitude of the velocity over this surface. Equation (8.56) can be simplified considerably in the weak scattering limit, where Σ_2 is small, and Sv can be taken as a constant equal to its value at $E_F - \Sigma_1 \approx E_F$. Then the integration over E' can be performed explicitly, giving for σ

$$\sigma^{(0)}(0) = \frac{e^2 v_F}{|\Sigma_2|} \frac{S_F}{(2\pi)^d d}. \quad (8.57)$$

If we compare (8.57) with (2) of Problem 8.7, we see that we should identify $2|\Sigma_2|/\hbar$ with $1/\tau_{\text{tr}}$. However, (7.51) suggests that

$$|\Sigma_2| = \pi \varrho_m \langle \varepsilon'_m \rangle = \pi \varrho a^3 \langle \varepsilon'^2_m \rangle = \pi \varrho a^3 \frac{|V(0)|^2}{a^6} = \pi \varrho n_{\text{imp}} |V(q)|^2 ,$$

since, in this case, $V(q) = \varepsilon a^3 \delta_{q,0}$ and $n_{\text{imp}} = a^{-3}$. Hence $2|\Sigma_2|/\hbar$ equals $1/\tau$ and not $1/\tau_{\text{tr}}$. Thus our calculation reproduces the standard result apart from the $(1 - \cos \theta)$ factor, which is not present in $|\Sigma_2|$. The reason for this omission is our neglect of the difference $p_x \langle G p_x G \rangle - p_x \langle G \rangle p_x \langle G \rangle$, which is usually called a *vertex correction*. In the next subsection we present a CPA-like scheme for obtaining the vertex corrections. In the weak scattering limit, this scheme reduces to the standard theory for conductivity [113, 135] and reproduces the $\cos \theta$ correction.

One can rewrite (8.57) (with the $\cos \theta$ correction) in terms of τ_{tr} or $\ell_{\text{tr}} = v_F \tau_{\text{tr}}$ as follows (Problem 8.7):

$$\sigma^{(0)}(0) = \frac{2}{(2\pi)^d} \frac{e^2}{\hbar} v_F \tau_{\text{tr}} S_F = \frac{2}{(2\pi)^d} \frac{e^2}{\hbar} \ell_{\text{tr}} S_F . \quad (8.58)$$

(For $d=2$, S_F is the length of the Fermi line, and for $d=1$, $S_F = 2$.)

To summarize: Starting from the general equation (8.53) and utilizing the CPA to obtain both $\langle G \rangle$ and the vertex corrections produces a very satisfactory approximate result for $\sigma_1(\omega)$. In the weak scattering limit this result reduces to the standard expression for $\sigma_1(\omega)$ [113, 135, 157, 259]. Furthermore, the vertex corrections in the weak scattering limit are responsible for the appearance of the $\cos \theta$ term in $1/\tau_{\text{tr}}$.

Note that in the simple TBM the scattering is isotropic in \mathbf{k} -space (in fact, it is \mathbf{k} -independent), and as a result the $\cos \theta$ term gives zero contribution to $1/\tau_{\text{tr}}$. This means that the CPA vertex corrections for the *conductivity* and for the *simple TBM* are zero. In the next subsection we shall see that this is actually the case.

8.3.2 CPA for Vertex Corrections

As was mentioned before, transport properties depend on combinations of the form

$$\langle AG(z)BG(z') \rangle ,$$

where A and B are nonrandom operators. Following Velicky [260], we define the operator \tilde{T} by the relation

$$\langle G(z) \tilde{T} \langle G(z') \rangle \rangle = \langle G(z)BG(z') \rangle - \langle G(z) \rangle B \langle G(z') \rangle . \quad (8.59)$$

Within the CPA $\langle G(z) \rangle = G_e(z)$. Furthermore, according to (7.54), we can express G in terms of G_e and the t -matrix, T' , which is given by (7.30), i.e.,

$$T' = \sum_{\mathbf{m}} Q'_{\mathbf{m}} = \sum_{\mathbf{m}} \tilde{Q}'_{\mathbf{m}} . \quad (8.60)$$

The operators $Q'_{\mathbf{m}}$ and $\tilde{Q}'_{\mathbf{m}}$ satisfy the following equations:

$$Q'_{\mathbf{m}} = T'_{\mathbf{m}} \left(1 + G_e \sum_{\mathbf{n} \neq \mathbf{m}} Q'_{\mathbf{n}} \right) , \quad (8.61)$$

$$\tilde{Q}'_{\mathbf{m}} = \left(1 + \sum_{\mathbf{n} \neq \mathbf{m}} \tilde{Q}'_{\mathbf{n}} G_e \right) T'_{\mathbf{m}} , \quad (8.62)$$

where $T'_{\mathbf{m}} = |\mathbf{m}\rangle t'_{\mathbf{m}} \langle \mathbf{m}|$. Substituting the above relations into (8.59) we have

$$\tilde{\Gamma} = \sum_{\mathbf{m}\mathbf{n}} \tilde{\Gamma}_{\mathbf{m}\mathbf{n}} , \quad (8.63)$$

$$\tilde{\Gamma}_{\mathbf{m}\mathbf{n}} = \left\langle T'_{\mathbf{m}} \left(1 + G_e \sum_{\ell \neq \mathbf{m}} Q'_{\ell} \right) G_e B G_e \left(1 + \sum_{\mathbf{s} \neq \mathbf{n}} \tilde{Q}'_{\mathbf{s}} G_e \right) T'_{\mathbf{n}} \right\rangle . \quad (8.63')$$

The CPA for the vertex part $\tilde{\Gamma}_{\mathbf{m}\mathbf{n}}$ consists again in replacing the average of the product by a product of averages as follows:

$$\tilde{\Gamma}_{\mathbf{m}\mathbf{n}} \approx \left\langle T'_{\mathbf{m}} \left\langle \left(1 + G_e \sum_{\ell \neq \mathbf{m}} Q'_{\ell} \right) G_e B G_e \left(1 + \sum_{\mathbf{s} \neq \mathbf{n}} \tilde{Q}'_{\mathbf{s}} G_e \right) \right\rangle T'_{\mathbf{n}} \right\rangle . \quad (8.64)$$

Taking into account that the $t'_{\mathbf{m}}$ are independent random variables with zero mean (due to the CPA condition) we see that the rhs of (8.64) is nonzero only when $\mathbf{m} = \mathbf{n}$, i.e.,

$$\tilde{\Gamma}_{\mathbf{m}\mathbf{n}} = \delta_{\mathbf{m}\mathbf{n}} \tilde{\Gamma}_{\mathbf{n}} = \delta_{\mathbf{m}\mathbf{n}} |\mathbf{n}\rangle \tilde{\gamma}_{\mathbf{n}} \langle \mathbf{n}| . \quad (8.65)$$

Of the four terms inside the inner average sign in (8.64), two are proportional to $\langle Q'_{\ell} \rangle$ or $\langle \tilde{Q}'_{\mathbf{s}} \rangle$ and hence are zero within the CPA; the third is $G_e B G_e$, and the fourth is $\sum_{\ell, \mathbf{s} \neq \mathbf{n}} G_e \langle Q'_{\ell} G_e B G_e \tilde{Q}'_{\mathbf{s}} \rangle G_e$, which in view of (8.61), (8.62), (8.63'), (8.64), and (8.65) equals $G_e \sum_{\ell \neq \mathbf{n}} \tilde{\Gamma}_{\ell} G_e$. Hence we can rewrite (8.64) as

$$\tilde{\Gamma}_{\mathbf{n}} = \left\langle T'_{\mathbf{n}} G_e \left(B + \sum_{\ell \neq \mathbf{n}} \tilde{\Gamma}_{\ell} \right) G_e T'_{\mathbf{n}} \right\rangle . \quad (8.66)$$

System (8.66) for the unknown quantities $\tilde{\Gamma}_{\mathbf{n}}$ is a closed one, and consequently the problem has been solved formally. To be more explicit, we take matrix

elements in the local basis; we also write $\sum_{\ell \neq \mathbf{n}} \tilde{\Gamma}_\ell = \sum_\ell \tilde{\Gamma}_\ell - \tilde{\Gamma}_\mathbf{n}$. Then (8.66) becomes

$$\begin{aligned} \tilde{\gamma}_\mathbf{n} [1 + \langle t'_\mathbf{n} t'_\mathbf{n} \rangle G_e(\mathbf{n}\mathbf{n}) G_e(\mathbf{n}\mathbf{n})] \\ = \sum_{\ell \mathbf{m}} \langle t'_\mathbf{n} t'_\mathbf{n} \rangle G_e(\mathbf{n}, \ell) [B_{\ell \mathbf{m}} + \tilde{\gamma}_\ell \delta_{\ell \mathbf{m}}] G_e(\mathbf{m}, \mathbf{n}) . \end{aligned} \quad (8.67)$$

To display the energy dependencies explicitly and to make the expression more compact we introduce the quantity $u(z, z')$ defined by

$$\begin{aligned} u(z, z') \equiv \langle t'_\mathbf{n}(z) t'_\mathbf{n}(z') \rangle \\ \times [1 + \langle t'_\mathbf{n}(z) t'_\mathbf{n}(z') \rangle G_e(\mathbf{n}, \mathbf{n}; z) G(\mathbf{n}, \mathbf{n}; z')]^{-1} . \end{aligned} \quad (8.68)$$

Then $\tilde{\gamma}_\mathbf{n}(z, z')$ becomes

$$\tilde{\gamma}_\mathbf{n}(z, z') = \sum_{\ell \mathbf{m}} u(z, z') G_e(\mathbf{n}, \ell; z) [B_{\ell \mathbf{m}} + \tilde{\gamma}_\ell(z, z') \delta_{\ell \mathbf{m}}] G_e(\mathbf{m}, \mathbf{n}; z') . \quad (8.69)$$

Then $\tilde{\gamma}_\mathbf{n}$ can be factorized by defining the new quantity $\gamma_{\mathbf{n}\mathbf{m}}$ through the following relation:

$$\tilde{\gamma}_\mathbf{n} = \sum_{\mathbf{m} \ell \mathbf{s}} \gamma_{\mathbf{n}\mathbf{m}} G_e(\mathbf{m} \ell) B_{\ell \mathbf{s}} G_e(\mathbf{s} \mathbf{m}) . \quad (8.70)$$

Substituting (8.70) into (8.69) we find that $\gamma_{\mathbf{n}\mathbf{m}}$ obeys the B -independent equation

$$\gamma_{\mathbf{n}\mathbf{m}} = u \delta_{\mathbf{n}\mathbf{m}} + \sum_\ell u G_e(\mathbf{n}, \ell) G_e(\ell, \mathbf{n}) \gamma_{\ell \mathbf{m}} , \quad (8.71)$$

where the energy dependencies are not shown explicitly. The quantity $\gamma_{\mathbf{n}\mathbf{m}}$ corresponds more closely than $\tilde{\gamma}_\mathbf{n}$ to what is called the vertex part in many-body theory (Part III). Equation (8.71) can be solved immediately in \mathbf{k} -space

$$\gamma(\mathbf{q}; z, z') = u(z, z') [1 - u(z, z') A(\mathbf{q}; z, z')]^{-1} , \quad (8.72)$$

where

$$\begin{aligned} A(\mathbf{q}; z, z') &= \sum_{\mathbf{m}} e^{-i\mathbf{q} \cdot \mathbf{m}} G_e(\mathbf{0}, \mathbf{m}; z) G_e(\mathbf{m}, \mathbf{0}; z') \\ &= \frac{1}{N} \sum_{\mathbf{k}} G_e(\mathbf{k}; z) G_e(\mathbf{k} - \mathbf{q}; z') \end{aligned} \quad (8.73)$$

and

$$\gamma_{\mathbf{n}\mathbf{m}}(z, z') = \frac{1}{N} \sum_{\mathbf{q}} e^{i\mathbf{q} \cdot (\mathbf{n} - \mathbf{m})} \gamma(\mathbf{q}; z, z') . \quad (8.74)$$

The basic equation, (8.71), the series that results by iterating it, (8.70), and the vertex correction to $\text{Tr} \{A \langle G(z) B G(z') \rangle\}$ are shown graphically in Fig. 8.1

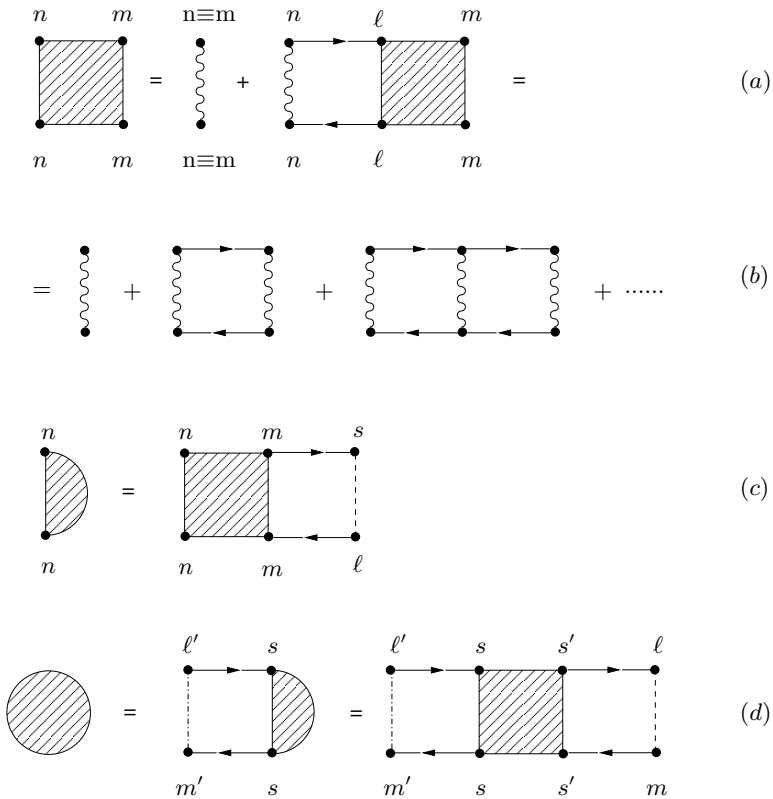


Fig. 8.1. Diagrammatic representation of the CPA for the vertex corrections in the local representation. Directed *solid lines* from \mathbf{n} to ℓ correspond to $G_e(\ell, \mathbf{n})$; the *upper* ones have an energy argument z' , and the *lower* ones have z . The *wavy lines*, which always connect identical sites, correspond to u [see (8.68)]. The *shaded square* is γ_{nm} , the *shaded semicircle* is $\tilde{\gamma}_n$, and the *shaded circle* is the vertex correction for the quantity $\text{Tr} \{A \langle G(z) B G(z') \rangle\}$; the *dashed lines* correspond to $B_{m\ell}$ and the *dashed-dot lines* to $A_{\ell'm'}$. Summation over all internal points is implied in **a** and **b**, while in **c** and **d** the summation is over m, ℓ , and s and $\ell', m', s, s', \ell, m$, respectively. Case **a** is equivalent to (8.71) and **b** to its iteration; **c** is equivalent to (8.70)

for the local basis representation. The same diagrams, with slightly different correspondence rules, can also be used for the \mathbf{k} -representation.

Let us comment on the CPA results. In the weak scattering limit, as follows from (8.68), $u \rightarrow \langle \varepsilon'_{\mathbf{n}} \rangle$. Then the terms summed in Fig. 8.1b are exactly the same as those used in the standard approach for the conductivity. Hence, in the weak scattering limit the CPA for the vertex corrections reduces to the standard result.

If we are interested in the vertex corrections to the conductivity tensor, we must take $A = B = \mathbf{p}$. Now the momentum operator \mathbf{p} in the \mathbf{k} representation is given by $m\partial E(\mathbf{k})/\hbar\partial\mathbf{k}$ and is an odd function of \mathbf{k} due to time reversal

symmetry. This implies that $p_{\ell s}$ is an odd function of $\ell - s$, which means that $\tilde{\gamma}_{\mathbf{n}}$ for this case is zero [see (8.70)]. As was mentioned before, the vanishing of the vertex corrections for σ is a consequence of the isotropy of the scattering potential in our model. The vertex corrections for other quantities do not vanish. We shall see in the next chapter that a quantity of importance is $\langle G(\mathbf{m}, \mathbf{0}; z') G(\mathbf{0}, \mathbf{m}; z) \rangle$, which corresponds to $A = |\mathbf{0}\rangle \langle \mathbf{0}|$ and $B = |\mathbf{m}\rangle \langle \mathbf{m}|$. Combining (8.72), (8.70), and (8.59) we obtain

$$\langle G(\mathbf{m}, \mathbf{0}; z') G(\mathbf{0}, \mathbf{m}; z) \rangle = \frac{1}{N} \sum_{\mathbf{k}} e^{i\mathbf{k} \cdot \mathbf{m}} \frac{A(\mathbf{k}; z; z')}{1 - u(z, z') A(\mathbf{k}; z, z')} . \quad (8.75)$$

The CPA does not, of course, keep all the terms that contribute to $\tilde{\Gamma}$, but the ones kept are very important, at least in the case where $z = E + is$ and $z' = E - is$: they are positive definite so that no possibility of self-cancellations exists, in contrast to other terms, which involve unpaired $G_e(\ell, \mathbf{m})$ s with $|\ell - \mathbf{m}|$ larger than the phase coherence length. As we shall see in the next section, the CPA terms can give a very large contribution, and, last but not least, they can be summed explicitly to produce a closed expression [see (8.72)]. Note also that the CPA preserves an exact relation between the self-energy and the vertex part $\tilde{\Gamma}$ for $B = 1$. By observing that

$$G(z)G(z') = \frac{G(z') - G(z)}{z - z'} ,$$

and by taking into account (8.59), one obtains (for $B = 1$)

$$\tilde{\Gamma}(z, z') = -\frac{\Sigma(z) - \Sigma(z')}{z - z'} , \quad (8.76)$$

where the exact self-energy, $\Sigma(z)$, satisfies by definition the relation

$$\langle G(z) \rangle = [z - \Sigma(z) - \mathcal{H}_0]^{-1} .$$

The CPA $\tilde{\Gamma}$ and Σ 's satisfy (8.76).

Equation (8.76) shows that, in the limit $z' \rightarrow z$ from opposite sides of the real axis (i.e., under the condition $\text{Im}\{z\} \text{Im}\{z'\} < 0$), the vertex part (for $B = 1$) blows up [since $\Sigma(z)$ is discontinuous across the real axis, i.e., $\Sigma^+(E) = -\Sigma^-(E)$]. This blowing up of the vertex part is indicative of its importance in the case where $\text{Im}\{z\} \text{Im}\{z'\} < 0$. We shall return to this point in §8.3.4.

8.3.3 Vertex Corrections Beyond the CPA

We now discuss a subgroup of terms contributing to the vertex corrections but omitted within the CPA. These terms have a structure quite similar to

the CPA terms and, as a result, may be equally important. They are shown diagrammatically in Fig. 8.2, from which one has

$$\begin{aligned} & \text{Tr} \{A \langle G(z)BG(z') \rangle\} - \text{Tr} \{A \langle G(z) \rangle B \langle G(z') \rangle\} \\ & \approx \sum A_{\ell s} G_e(\mathbf{s}, \mathbf{m}; z) \gamma'_{mn}(z, z') G_e(\mathbf{n}, \mathbf{i}; z) \\ & \quad \times B_{ij} G_e(\mathbf{j}, \mathbf{m}; z') G_e(\mathbf{n}, \mathbf{\ell}; z') . \end{aligned} \tag{8.77}$$

The quantity $\gamma'_{mn}(z, z')$ can be calculated explicitly by working in \mathbf{k} -space, and the result is similar to that of $\gamma_{nm}(z, z')$, except that A is now replaced by A' , where

$$A'(\mathbf{q}) = \sum_{\mathbf{m}} e^{-i\mathbf{q} \cdot \mathbf{m}} G_e(\mathbf{0}, \mathbf{m}) G_e(\mathbf{0}, \mathbf{m}) = \frac{1}{N} \sum_{\mathbf{k}} G_e(\mathbf{k}) G_e(\mathbf{q} - \mathbf{k}) , \tag{8.78}$$

and the first term of the series (in Fig. 8.2b) is $u^2 A'(\mathbf{q})$ and not u (since the term u is already counted in the CPA vertex corrections). Thus

$$\gamma'(\mathbf{q}) = u^2 A'(\mathbf{q}) [1 - uA'(\mathbf{q})]^{-1} , \tag{8.79}$$

$$\gamma'_{mn} = \frac{1}{N} \sum_{\mathbf{q}} e^{i\mathbf{q} \cdot (\mathbf{m}-\mathbf{n})} \gamma'(\mathbf{q}) . \tag{8.80}$$

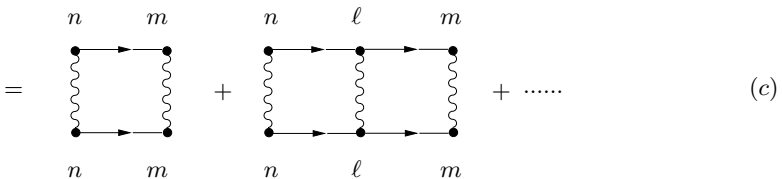
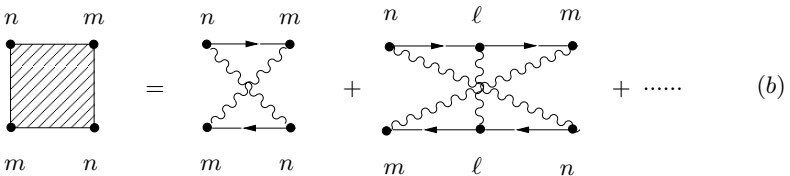
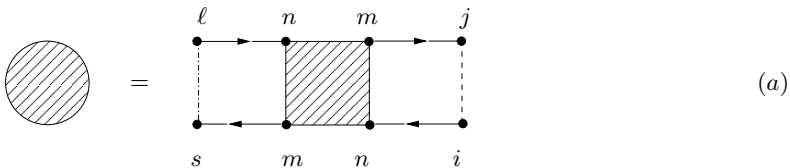


Fig. 8.2. **a** The shaded circle represents additional (beyond the CPA shown in Fig. 8.1) vertex corrections for the quantity $\text{Tr} \{A \langle G(z)BG(z') \rangle\}$. In the present case, the vertex part (shaded square) is given by the diagrams shown in **b** and called *maximally crossed diagrams*; they can be redrawn (without changing their values) as in **c**. The rules are as in Fig. 8.1

It must be pointed out that time reversal symmetry of the Hamiltonian implies that $G_e(\mathbf{0}, \mathbf{m})$ equals $G_e(\mathbf{m}, \mathbf{0})$, which in turn means that $A(\mathbf{q}) = A'(\mathbf{q})$. Recall that the presence of an external magnetic field destroys time reversal and, hence, the previous equality.

The post-CPA terms shown in Fig. 8.2b (or c) and known as maximally crossed diagrams, produce results for the vertex part γ'_{nm} , which are essentially equivalent to the CPA for γ_{nm} . The main difference between the two cases is the way the vertex part is connected to the G s [compare Fig. 8.1d with Fig. 8.2a: in Fig. 8.1d the two G s that connect to A (or B) start and end at the same site of the vertex part, while in Fig. 8.2 a the sites are different]. As a result of this difference, the vertex corrections to the conductivity, and *for our simple model Hamiltonian*, are identically zero for the CPA terms (because of the oddness of $p_{\ell m}$ with respect to the indices), while it is not zero for the post-CPA terms shown in Fig. 8.2. In fact, these terms make an extremely important contribution to the conductivity, which will be discussed in some detail below and in the next chapter in connection with the problem of localization.

8.3.4 Post-CPA Corrections to Conductivity

As was mentioned before, the vertex part (at least for the case $B = 1$) blows up in the limit z, z' approaching each other from opposite sides of the real axis. When $B = 1$, $\tilde{\gamma}_n(z, z')$ can be expressed as follows (Problem 8.12):

$$\tilde{\gamma}_n(z, z') = \frac{u(z, z') A(0; z, z')}{1 - u(z, z') A(0; z, z')} . \quad (8.81)$$

Comparing (8.81) with (8.76) we see immediately that $u(z, z') A(0; z, z')$ approaches 1 as $z \rightarrow z'$ from opposite sides of the real axis. Under these conditions, $\gamma(\mathbf{q}; z, z')$ has a singularity when $\mathbf{q} \rightarrow 0$. Since $\gamma(\mathbf{q}; z, z')$ is part of the integrand for the vertex corrections both within the CPA and beyond the CPA (if $A' = A$), it follows that the vertex corrections may become singular. This depends on the behavior of the integrand around the singularity, i.e., on the behavior of uA for small values of $z - z'$ and \mathbf{q}

$$u(z, z') A(\mathbf{q}; z, z') \approx 1 + a_1(z - z') - a_2 q^2 , \quad (8.82)$$

with $\text{Im}\{z\} \text{Im}\{z'\} < 0$. To be specific, we take $\text{Im}\{z\} > 0$. The constant a_1 can be found by comparing (8.81) with (8.76). The result is

$$a_1 = \frac{i}{2|\Sigma_2|} . \quad (8.83)$$

To find a_2 requires some algebra. We start with (8.73) and we expand $G_e(\mathbf{k} - \mathbf{q}; z')$ in powers of \mathbf{q} . The coefficient of the first power is

$$\frac{1}{N} \sum_{\mathbf{k}} G_e(\mathbf{k}) \nabla_{\mathbf{k}} G_e(\mathbf{k}) ,$$

which is zero, because $G_e(\mathbf{k})$ is an even function of \mathbf{k} . The next term is

$$\frac{q^2}{2d} \frac{1}{N} \sum_{\mathbf{k}} G_e(\mathbf{k}) \nabla_{\mathbf{k}}^2 G_e(\mathbf{k}) = -\frac{q^2}{2d} \frac{1}{N} \sum_{\mathbf{k}} \nabla_{\mathbf{k}} G_e(\mathbf{k}) \cdot \nabla_{\mathbf{k}} G_e(\mathbf{k}) , \quad (8.84)$$

where cubic symmetry is assumed and d is the dimensionality. Taking into account that

$$G_e(\mathbf{k}; z) = [z - \Sigma - E(\mathbf{k})]^{-1}$$

we see that

$$\nabla_{\mathbf{k}} G_e(\mathbf{k}; z) = G_e^2 \cdot \nabla_{\mathbf{k}} E(\mathbf{k}) ;$$

hence the coefficient of q^2 is proportional to $\sigma^{(0)}/\Sigma_2^2$, where $\sigma^{(0)}$ is the conductivity without vertex corrections (8.55). [Remember that the second G_e on the rhs of (8.84) depends on z' and in the limit $z' \rightarrow z$ with $\text{Im}\{z\} \text{Im}\{z'\} < 0$ $G_e(\mathbf{k}, z') = G_e^*(\mathbf{k}; z)$.] To find a_2 we also need

$$\begin{aligned} u(E^+, E^-) &= A^{-1}(0; E^+, E^-) = \left[\frac{1}{N} \sum_{\mathbf{k}} G_e^+(\mathbf{k}; E) G_e^-(\mathbf{k}; E) \right]^{-1} \\ &= \left[(\Sigma^- - \Sigma^+)^{-1} \frac{1}{N} \sum_{\mathbf{k}} (G_e^- - G_e^+) \right]^{-1} \\ &= 2i |\Sigma_2| [2i\pi \varrho'(E)]^{-1} = \frac{|\Sigma_2|}{\pi \varrho'} , \end{aligned}$$

where $\varrho'(E)$ is the DOS per unit cell per spin. The coefficient a_2 can be expressed in a more compact way in terms of the diffusion coefficient, $D^{(0)} = \sigma^{(0)}/2e^2 \varrho$ [see (8.10) and text thereafter]:

$$a_2 = \frac{\hbar D^{(0)}}{2 |\Sigma_2|} . \quad (8.85)$$

To find the vertex corrections to the conductivity, we start with expression (8.53) for the real part of the conductivity, which becomes at $T = 0$

$$\sigma_1(\omega) = \frac{e^2 \hbar}{\pi \Omega} \langle \text{Tr} \{ v_x \text{Im} \{ G^+(E_F + \hbar\omega) \} v_x \text{Im} \{ G^+(E_F) \} \} \rangle . \quad (8.86)$$

But

$$\text{Im} \{ G^+(E_F + \hbar\omega) \} = \frac{G^+(E_F + \hbar\omega) - G^-(E_F + \hbar\omega)}{2i}$$

with a similar expression for $\text{Im} \{ G^+(E_F) \}$. Of the four terms resulting from the multiplication of the two $\text{Im} \{ G \}$ s, two have their arguments on the same side of the real axis and, consequently, they are negligible in comparison with the other two, which give a divergent contribution to $\gamma(\mathbf{q}; z, z')$ as $\omega \rightarrow 0$. Thus the vertex correction to (8.86) becomes

$$\delta\sigma_1(\omega) = \phi_1(E_F, \omega) + \phi_1(E_F + \hbar\omega, -\omega) , \quad (8.87)$$

where

$$\phi_1(E_F, \omega) = \frac{e^2 \hbar}{4\pi\Omega} \delta \langle \text{Tr} \{ v_x G^+(E + \hbar\omega) v_x G^-(E) \} \rangle . \quad (8.88)$$

We consider here the post-CPA corrections shown in Fig. 8.2, since the CPA corrections vanish. From Fig. 8.2a, and transforming everything to the \mathbf{k} -representation, we have

$$\begin{aligned} \phi_1(E_F, \omega) &= \frac{2e^2 \hbar}{\pi\Omega} \frac{1}{4d} \frac{1}{N} \\ &\times \sum_{\mathbf{q}} \sum_{\mathbf{k}} [\mathbf{v}_{\mathbf{k}} \cdot \mathbf{v}_{\mathbf{q}-\mathbf{k}} G^+(\mathbf{k}; E + \hbar\omega) G^+(\mathbf{q} - \mathbf{k}; E + \hbar\omega) \\ &\quad \times G^-(\mathbf{k}; E) G^-(\mathbf{q} - \mathbf{k}; E) \gamma'(\mathbf{q}; E^+ + \hbar\omega^+, E^-)] . \end{aligned} \quad (8.89)$$

Because the integral (for $d = 2, 1$) is dominated by the region of the singularity at $\mathbf{q} = 0$, we can take $\mathbf{q} = 0$ in the $\mathbf{v}_{\mathbf{q}-\mathbf{k}}$ and G s and thus separate the \mathbf{k} -integration from the \mathbf{q} -integration. The former gives a result (as $\omega \rightarrow 0$) that is proportional to $-\sigma^{(0)}/\Sigma_2^2$ or $-D^{(0)}/\Sigma_2^2$. To perform the \mathbf{q} -integration, we need γ' , which we obtain from (8.79) and (8.82) ($A' = A$) as $\omega \rightarrow 0$:

$$\begin{aligned} \gamma'(\mathbf{q}, E^+ + \hbar\omega^+, E^-) &= \frac{u}{1 - uA} = \frac{|\Sigma_2|}{\pi \rho'} \frac{1}{-\frac{i\hbar\omega}{2|\Sigma_2|} + \frac{\hbar D^{(0)}}{2|\Sigma_2|} q^2} \\ &= \frac{2|\Sigma_2|^2}{\pi \rho' \hbar D^{(0)}} \frac{1}{q^2 - i \frac{\omega}{D^{(0)}}} . \end{aligned} \quad (8.90)$$

Substituting in (8.89) we obtain for $\phi_1(E_F, \omega)$

$$\phi_1(E_F, \omega) = -\frac{e^2}{\pi \hbar} \frac{1}{(2\pi)^d} \int d\mathbf{q} \frac{1}{q^2 - i(\omega/D^{(0)})} , \quad (8.91)$$

which, combined with

$$\phi_1(E_F + \hbar\omega, -\omega) \approx \phi_1(E_F, -\omega) ,$$

gives the final result for $\delta\sigma_1$:

$$\delta\sigma_1 = -\frac{e^2}{\pi \hbar} \frac{2}{(2\pi)^d} \int d\mathbf{q} \frac{q^2}{q^4 + (\omega^2/D^{(0)2})} . \quad (8.92)$$

For $d = 1$ no upper cutoff is needed; for $d = 2, 3$ we take as an upper cutoff L_m^{-1} , where L_m is of the order of the elastic mean free path. By introducing the length $L_\omega = \sqrt{D^{(0)}/\omega}$ we obtain from (8.92)

$$\delta\sigma_1 = \begin{cases} -\frac{e^2}{\sqrt{2}\pi\hbar} L_\omega , & 1\text{-d}, & (8.93a) \\ -\frac{e^2}{\pi^2\hbar} \ln\left(\frac{L_\omega}{L_m}\right) , & 2\text{-d}, & (8.93b) \\ \frac{e^2}{2\sqrt{2}\pi^2\hbar} \frac{1}{L_\omega} - \frac{e^2}{\pi^3\hbar} \frac{1}{L_m} , & 3\text{-d}. & (8.93c) \end{cases}$$

Notice that in the limit $\omega \rightarrow 0$, $L_\omega \rightarrow \infty$. Hence, the corrections due to the post-CPA vertex inclusion lead to a divergent and negative result for the DC conductivity in 1-d and 2-d. Clearly, this is physically unacceptable. However, this unphysical divergence may be indicative of a transition to a new state of the system that could not be properly described by the CPA and post-CPA vertex corrections. To this important open question we shall return in the next chapter. At this point, having in mind the physical analysis in Sect. 9.1 of the following chapter, we shall assume that (8.93a) and (8.93b) are satisfactory as long as L_ω is comparable to ℓ_{tr} , which implies that $|\delta\sigma_1| \ll \sigma_0$. The 3-d result in the limit $\omega \rightarrow 0$ may be considered reasonable as long as $e^2/\pi^3\hbar L_m$ is smaller than $\sigma_0 = (e^2/12\pi^3\hbar) S_F \ell_{\text{tr}}$. This inequality is satisfied when $S_F \ell_{\text{tr}} L_m > 12$ or assuming that $L_m \simeq \ell_{\text{tr}}$ when $S_F \ell_{\text{tr}}^2 \geq 12$.

8.4 Summary

In this chapter, the theory of electrical conductivity was developed. In Sect. 8.1 we defined the conductivity and connected it to other relevant quantities such as the permittivity, etc. Various methods for calculating σ were presented; among them the so-called Kubo–Greenwood formula was expressed in terms of Green’s functions as follows:

$$\sigma_{\mu\nu}(\omega) = \frac{ie^2 n}{m\omega} + \frac{e^2}{\Omega m^2 \omega} \int_{-\infty}^{\infty} \frac{dE}{2\pi} \text{Tr} \{ p_\mu g(E) p_\nu g(E + \hbar\omega) \} , \quad (8.51)$$

$$\begin{aligned} \sigma_{1\mu\nu}(\omega) &= \frac{e^2 \hbar}{\pi \Omega m^2} \int_{-\infty}^{\infty} dE \frac{f(E) - f(E + \hbar\omega)}{\hbar\omega} \\ &\times \text{Tr} \{ p_\mu \text{Im} \{ G^+(E + \hbar\omega) \} p_\nu \text{Im} \{ G^+(E) \} \} . \end{aligned} \quad (8.53)$$

In the above expressions $\sigma_1 = \text{Re} \{ \sigma \}$; the Tr operation includes a factor of 2 due to spin summation; p_ν is a cartesian component of the momentum operator. Equation (8.51) is valid at $T = 0$ and

$$g(E) \equiv \begin{cases} G^-(E) , & E < E_F , \\ G^+(E) , & E > E_F . \end{cases} \quad (8.49)$$

To obtain the ensemble average of $\sigma(\omega)$, we needed the average of the product of two G s, which is in general different from the product of the averages. A first approximation for $\sigma(\omega)$ was obtained by ignoring this difference and then utilizing the CPA for $\langle G \rangle$. The result in the weak scattering limit was (for $\omega = 0$)

$$\sigma^{(0)} = \frac{2}{(2\pi)^d d} \frac{e^2}{\hbar} \ell S_F , \quad (8.58)$$

where $\ell = v\tau$ is the mean free path, v is the average magnitude of the velocity over the Fermi surface S_F (which in the simplest case is $4\pi k_F^2$), d is the

dimensionality, and τ is the relaxation time given [in lowest order in $V(\mathbf{q})$] by

$$\frac{1}{\tau} = \frac{2\pi}{\hbar} \varrho_F n_{\text{imp}} \frac{1}{4\pi} \int d\mathcal{O} V^2(\mathbf{q}) . \quad (8.94)$$

In (8.94) ϱ_F is the DOS per volume per spin at E_F and n_{imp} is the concentration of the scatterers, each one of which is associated with a scattering potential whose Fourier transform is $V(\mathbf{q})$. The integration is over all directions of the vector \mathbf{q} [$E(\mathbf{q}) = E_F$].

Next we considered an extension of the CPA that allows the approximate evaluation of the difference between the average of the product of G s and the product of the average G s. The effect of this difference on σ (which is called vertex correction), according to the CPA, in the weak scattering limit, was to introduce a factor $(1 - \cos\theta)$ in (8.94) where θ is the angle of \mathbf{q} with respect to the direction of propagation. This factor by definition changes τ to τ_{tr} (transport relaxation time) and ℓ to ℓ_{tr} . Equation (8.58), with ℓ replaced by $\ell_{\text{tr}} = v\tau_{\text{tr}}$, is the semiclassical weak scattering result for σ , obtained usually by employing Boltzmann's equation. For strong scattering see (8.22).

In addition to the CPA contribution (Fig. 8.1) to the vertex corrections, another contribution (Fig. 8.2) was obtained. This post-CPA contribution to σ is of the form

$$\delta\sigma \sim - \int_{1/L_M}^{1/L_m} \frac{d\mathbf{q}}{q^2} , \quad (8.95)$$

where the upper cutoff length L_M is dominated by the shortest of several lengths and L_m is of the order of ℓ_{tr} . The contribution (8.95) is extremely important for 2-d systems, where $\delta\sigma$ diverges as $-\ln(L_M)$, and for 1-d systems, where $\delta\sigma$ diverges as $-L_M$, in the limit $L_M \rightarrow \infty$. It was found that the CPA contribution to σ , if combined with *electron-electron* interaction processes, yields a form similar to (8.95) with a different prefactor and somewhat different L_M (especially in the presence of external magnetic fields). These theoretical results have found impressive experimental confirmation in 2-d films or interfaces; in thin wires and in 3-d systems the agreement between theory and experiment is of qualitative or semiquantitative nature.

The physical interpretation of the divergence of $\delta\sigma$ as $L_M \rightarrow \infty$ in 1-d and 2-d, as we shall see in the next chapter, is that all eigenstates are localized (i.e., they decay to zero for large distances) no matter how weak the disorder. As $\delta\sigma$ increases (in absolute value) with increasing L_M , it eventually becomes comparable to $\sigma^{(0)}$, and finally the total $\sigma = \sigma^{(0)} + \delta\sigma$ must approach zero as $L_M \rightarrow \infty$. Equation (8.95) is appropriate for describing $\delta\sigma$ only when $|\delta\sigma|/\sigma^{(0)}$ is considerably smaller than 1. Thus, according to the above reasoning, 1-d and 2-d noninteracting systems are never truly metallic.

This nonmetallic nature is revealed when L_M becomes comparable to or larger than the localization length of the eigenfunctions. The fact that, for $d = 3$, (8.95) gives a $\delta\sigma \sim 1/L_M$ is interpreted as meaning that for weak disorder, the eigenstates in 3-d systems are extended with (more or less) uniform amplitude, at least for length scales exceeding a characteristic length ξ' .

When the disorder increases beyond a critical value, the eigenstates become localized.

Various approaches to this fundamental problem of disorder-induced localization are reviewed in the next chapter, and an extensive list of references to the literature is given.

Further Reading

The book by Doniach and Sondheimer [135] treats the question of electrical conductivity on pp. 96–122. The connection of electrical conductivity to the diffusion coefficient is presented in Janssen's book [261] (pp. 39–77).

Problems

8.1s. Prove (8.10), (8.11a), and (8.11b).

8.2. Solve Boltzmann's equation in the presence of both magnetic and electric fields (G.14) and calculate the magnetoconductivity. [See (G.17).]

Hint: Show first that the solution of

$$\frac{G_0}{\tau_{\text{tr}}} + \omega_c \frac{\partial G_0}{\partial \phi} = \delta(\phi - \phi')$$

is

$$G_0(\phi - \phi') = \theta(\phi - \phi') \frac{\exp[(\phi' - \phi)/\omega_c \tau]}{\omega_c}.$$

8.3. Prove (8.33) starting from (8.32).

8.4. Prove that the term in parentheses in (8.32) is identically equal to zero for fixed boundary conditions; for a perfect conductor with periodic boundary conditions show that the conductivity is equal to its diamagnetic contribution.

8.5. Starting from (8.31) and following the suggestions given by (8.35) and (8.36) show that

$$\sigma_1 \simeq \frac{e^2 n \ell_{\text{tr}}}{2m v_F}.$$

8.6. Prove (8.39) starting from (8.38), inserting a complete set of the eigenfunctions of \mathcal{H}_0 , where appropriate, and remembering that, by definition, $\text{Tr}\{A\} = \sum_n \langle n | A | n \rangle$, where the set $\{|n\rangle\}$ is complete.

8.7. Using the expression for the current density \mathbf{j} ,

$$\mathbf{j} = 2q \int \frac{d^3 k}{(2\pi)^3} \mathbf{v}_k f_1(\mathbf{k}), \quad (1)$$

where $f_1(\mathbf{k})$ is given by (G.9), prove that the 3-d DC conductivity at $T = 0$ K is given by

$$\sigma = \frac{1}{12\pi^3} \frac{e^2}{\hbar} S_F \ell_{\text{tr}}, \quad (2)$$

where S_F is the area of the Fermi surface in \mathbf{k} -space,

$$\begin{aligned} \ell_{\text{tr}} &= v_F \tau_{\text{tr}}, \\ S_F v_F &= \int d^2 k_{\parallel} v_{\mathbf{k}}, \end{aligned}$$

and τ_{tr} is given by (G.12). For finite temperatures we have for the DC conductivity

$$\sigma = \frac{1}{12\pi^3} \frac{e^2}{\hbar} \int d\varepsilon_{\mathbf{k}} \left(-\frac{\partial f_0}{\partial \varepsilon_{\mathbf{k}}} \right) S(\varepsilon_{\mathbf{k}}) \ell_{\text{tr}}(\varepsilon_{\mathbf{k}}), \quad (3)$$

where

$$S(\varepsilon_{\mathbf{k}}) \ell_{\text{tr}}(\varepsilon_{\mathbf{k}}) = \tau_{\text{tr}}(\varepsilon_{\mathbf{k}}) \int d^2 k_{\parallel} v(\mathbf{k}). \quad (4)$$

For $\varepsilon(k) = \hbar^2 k^2 / 2m$, (2) reduces to $\sigma = e^2 n \tau_{\text{tr}} / m$.

8.8. Starting from (8.69) and (8.70), prove (8.71).

8.9. Prove (8.72) and (8.73) using (8.71) and (8.74).

8.10. Prove (8.75).

Hint: Take into account that

$$\begin{aligned} A(\mathbf{q}; z, z') &= A(-\mathbf{q}; z, z'), \\ \frac{uA}{1-uA} &= -1 + \frac{1}{1-uA}, \end{aligned}$$

and

$$\begin{aligned} \frac{1}{N} \sum_{\mathbf{q}} e^{-i\mathbf{q} \cdot \mathbf{m}} \sum_{\boldsymbol{\ell}} e^{i\mathbf{q} \cdot \boldsymbol{\ell}} G(0, \boldsymbol{\ell}) G(\boldsymbol{\ell}, 0) &= G(0, \mathbf{m}) G(\mathbf{m}, 0) \\ &= \frac{1}{N} \sum_{\mathbf{q}} e^{\pm i\mathbf{q} \cdot \mathbf{m}} A(\mathbf{q}). \end{aligned}$$

8.11. Prove (8.81).

8.12. Prove that

$$A(0; z, z') \rightarrow \frac{\pi \varrho(\varepsilon)}{|\Sigma_2(\varepsilon)|}$$

in the limit $z \rightarrow \varepsilon + is$, $z' \rightarrow \varepsilon - is$, and $s \rightarrow 0^+$.

Hint: Take into account that in the above limits

$$G(\mathbf{k}; z) G(\mathbf{k}; z') = \frac{1}{\Sigma(z) - \Sigma(z')} [G(\mathbf{k}; z) - G(\mathbf{k}; z')].$$

8.13. Prove (8.46b), (8.46c), and (8.47).

Localization, Transport, and Green's Functions

9.1 An Overview

In Chap. 8 we obtained the basic formula for the metallic conductivity

$$\sigma_0 = \frac{2}{d(2\pi)^d} \frac{e^2}{\hbar} S_F \ell_{\text{tr}}, \quad d = 1, 2, 3, \quad (9.1)$$

where the transport mean path, ℓ_{tr} , is a length given by $\ell_{\text{tr}} = v\tau_{\text{tr}}$ [see (8.22) and (8.23)] and closely related to the scattering mean free path, $\ell = (n_{\text{imp}}\sigma)^{-1}$, where σ is the scattering cross section from one of the scatterers whose concentration is n_{imp} ; the mean free path, ℓ , as was shown by (7.64), (7.66), and (7.68), is related to the randomization of the phase among *different* members of the ensemble over which the average is taken. It is this randomization of the phase of the eigenfunctions that is responsible for the finite conductivity given by (9.1), as was shown in [248] and [251]. In deriving (9.1) it is implicitly assumed that the randomness and the resulting multiple scattering does not affect the average amplitude, $|\psi(\mathbf{r})|$, of the eigenfunctions. This assumption is actually a good approximation when the disorder is weak. As the disorder becomes stronger, multiple scattering events lead to constructive and destructive interference and hence to amplitude, $|\psi(\mathbf{r})|$, fluctuations. These amplitude fluctuations are responsible for the post-CPA corrections to σ_0 obtained in Chap. 8:

$$\delta\sigma = \begin{cases} -\frac{e^2}{\sqrt{2}\pi\hbar} L_M, & \text{1-d} & (9.2a) \\ -\frac{e^2}{\pi^2\hbar} \ln \frac{L_M}{L_m}, & \text{2-d} & (9.2b) \\ \frac{e^2}{2\sqrt{2}\pi^2\hbar} \frac{1}{L_M} - \frac{e^2}{\pi^3\hbar} \frac{1}{L_m}, & \text{3-d} & (9.2c) \end{cases}$$

where L_M is an upper cutoff length (identified as L_ω in Chap. 8) and L_m is assumed to be of the order of ℓ or ℓ_{tr} . Examples of upper cutoff lengths L_M ,

besides L_ω and the geometrical dimension L , are: the diffusion length during the inelastic phase incoherence time, τ_ϕ , to be discussed in Sect. 9.2

$$L_\phi = \sqrt{D\tau_\phi}, \quad (9.3)$$

and the cyclotron radius introduced by the presence of an external magnetic field \mathbf{B} ,

$$L_B = \sqrt{\frac{\hbar c}{eB}}; \quad (9.4)$$

(L_B must be multiplied by $e^{\gamma/2} \approx 1.33$ in order to reproduce more detailed calculations in 2-d systems). Kaveh [262] has pointed out that in the presence of more than one upper cutoff length a possible choice for L_M is

$$L_M^{-2} \approx c_1 L^{-2} + c_2 L_\phi^{-2} + L_\omega^{-2} + c_4 L_B^{-2} + \dots, \quad (9.5)$$

where the weights c_i are positive constants close to 1.

We have already shown that (9.2a) and (9.2b) lead to nonphysical results for L_M very large; even (9.2c) fails when L_M becomes very large and L_m sufficiently small so that $|\delta\sigma| \geq \sigma_0$. Thus the need arises for treating the disorder-induced amplitude variations in a more realistic way. In response to this need a new field has emerged establishing a firm connection with experimental data. In this chapter we present the basic ideas and results as well as some applications (far from complete) of this far-reaching field.

In principle, there are reasons to expect that disorder, if strong enough, may affect not only the phase but the amplitude as well. For this purpose consider the elementary example of two coupled pendula. The transfer of the motion from one to the other is facilitated by a strong mutual coupling and is opposed by a large *frequency mismatch*. If we have an array of pendula of random individual eigenfrequencies and then we couple them, it is not difficult to imagine that a wave propagating in such a medium may find regions of large frequency mismatch; such regions will be almost inaccessible to it. In fact, one may even think of the possibility of the wave surrounded by such regions so that it cannot escape to infinity; in other words, the wave may be confined to a finite region of space decaying to zero (usually in an exponential way) as one moves away from this region. These decaying eigenstates are termed *localized*. The ordinary propagating eigenstates are usually called *extended*.

In previous chapters we examined localized eigenstates associated with one or two isolated impurities; these states belonged to the discrete part of the spectrum. The continuous part of the spectrum was associated with extended eigenstates. Now imagine that a disordered system is created by allowing the number of impurities to become infinite. Then one expects the discrete spectrum associated with localized eigenstates to be smeared out to form a continuum that usually joins the main band as a tail. Obviously, the question arises as to whether or not the eigenstates (at least those in the tails where they started as localized) will become extended or remain localized.

The answer to this question can be sought within the framework of the random TBM introduced in Chap. 7 [see (7.35)]. This by now familiar model (also known as the Anderson model) is the simplest one that incorporates the essential competition between the transfer strength $|V|$ and the energy (or frequency) mismatch, which is characterized by the width $\delta\varepsilon$ ($\delta\varepsilon = |\varepsilon_A - \varepsilon_B|$), Γ , W for the binary, Lorentzian, and rectangular distributions, respectively) of the probability distribution of the random variable ε'_n . Thus the important parameter for localization is the dimensionless ratio

$$Q \equiv |V/\delta\varepsilon| . \quad (9.6)$$

As we shall see, another equally important parameter is the dimensionality d . Other aspects of the TBM, such as the shape of the probability distribution and the type of lattice, are of secondary importance and are believed not to influence the alleged universal features of the problem.

Before we proceed with our presentation, we shall state here the main results in the field. These results have not yet been rigorously proven but are accepted on the basis of considerable theoretical and experimental evidence in their support:

- (i) There is a critical dimensionality $d = 2$ for the localization problem. For $d \leq 2$ all eigenstates are localized (in the absence of magnetic interactions), no matter how weak the disorder. For $d > 2$, and for weak disorder, the tails of the band consist of localized eigenstates, while the interior corresponds to extended states. The localized regions are separated from the extended ones by critical energies termed *mobility edges*, E_c . As the disorder increases, the mobility edges move eventually toward the center of the band; they may merge together, eliminating the region of extended states. This behavior is shown in Fig. 9.1, where the mobility-edge trajectories (as the disorder W varies) separate the E - W plane into regions of localized and extended states.
- (ii) For weak disorder the vertex corrections to the conductivity are given by (9.2a), (9.2b), and (9.2c), which are known as weak localization equations. We repeat once more that the corrections (9.2a) and (9.2b) do not disappear as the upper cutoff length L_M becomes very large. On the contrary, they increase indefinitely with L_M , suggesting that eventually, for $L_M \rightarrow \infty$, $\sigma \rightarrow 0$. Thus a truly metallic behavior is not possible for $d \leq 2$ (in the absence of magnetic field and many-body interactions). This is, of course, consistent with the statement that all eigenstates are localized for $d \leq 2$. The nonmetallic nature of the conduction for $d \leq 2$ is usually masked by the fact that at high enough temperatures L_ϕ (and hence L_M) becomes quite short. We shall see in Sect. 9.2 that when $L_M \approx L_m$, $\delta\sigma \simeq 0$.
- (iii) The vertex corrections (9.2) come from the post-CPA terms shown in Fig. 8.2. The CPA terms, although quite similar to the post-CPA ones, produce no correction to the conductivity in the simple TBM because of the exact mutual cancellation of the terms shown in Fig. 8.1d. The presence of electron-electron interactions eliminates this cancellation. Indeed,

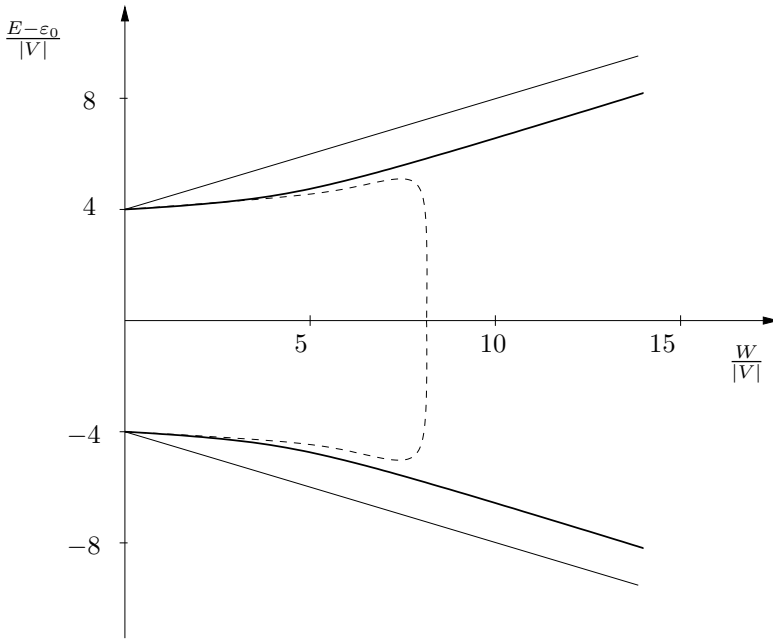


Fig. 9.1. Mobility-edge (*dashed line*) and band-edge trajectories (*heavy solid line* is based on the CPA; *light solid line* is exact) for a diamond lattice with a rectangular distribution of site energies centered at ε_0 and of total width W [263]

if the electron between points ℓ' and \mathbf{s} (Fig. 8.1d) interacts with the electron between \mathbf{s}' and ℓ , then the terms resulting from the exchange $\ell \leftrightarrow \mathbf{m}$ (or $\ell' \leftrightarrow \mathbf{m}'$) are no longer opposite to each other and hence the CPA vertex corrections, in the presence of electron–electron interaction, do not vanish. In fact, they produce a result like (9.2) with a similar, but not identical, proportionality factor. The cutoff L_M depends on the frequency ω or the temperature T , whichever is larger, more or less as in (9.5):

$$L_M^{-2} \approx \frac{k_B T}{\hbar D(0)} + \frac{\omega}{D(0)}. \quad (9.7)$$

The main difference is that L_M in the present case, and in contrast to the previous case, does not depend significantly on the external magnetic field \mathbf{B} . The reason is that the CPA terms involve $G_{nm}^+ G_{mn}^-$, which remains unaffected by \mathbf{B} , while the post-CPA terms of Fig. 8.2 involve $G_{nm}^+ G_{nm}^-$, which acquires an extra phase factor in the presence of \mathbf{B} .

- (iv) The theoretical results presented in (ii) and (iii) are in impressive agreement with experimental data, especially for the 2-d case.
- (v) Equation (9.2c) combined with (9.4) predicts a negative magnetoresistance proportional to \sqrt{B} . Such a behavior has been observed in impurity bands of heavily doped semiconductors at low temperatures (≈ 1 K) and remained a puzzle until the advance of the present explanation.

9.2 Disorder, Diffusion, and Interference

In order to see the physical origin of the corrections $\delta\sigma$ to the conductivity, formula (9.1), we consider a particle of charge q ($q = -e$ for electrons) located initially at the lattice site \mathbf{n} . The probability amplitude of finding it again at \mathbf{n} after time t is denoted by $c_{\mathbf{n}}(t)$. According to Feynman's path integral formulation, $c_{\mathbf{n}}(t)$ is given by

$$c_{\mathbf{n}}(t) = \sum_{\nu} A_{\nu}(t), \quad (9.8)$$

where the $A_{\nu}(t)$ s are the contributions from all *directed* paths starting at $t = 0$ from site \mathbf{n} and ending at time t again at \mathbf{n} . $A_{\nu}(t)$ is given by

$$A_{\nu}(t) = \exp \left[\frac{i}{\hbar} \int_0^t L[\mathbf{r}_{\nu}(t')] dt' \right], \quad (9.9)$$

where $\mathbf{r}_{\nu}(t')$ denotes the particular directed path ν and $L(\mathbf{r}_{\nu}(t'))$ is the Lagrangian of the particle. The probability of finding the particle at \mathbf{n} after time t is given by

$$|c_{\mathbf{n}}(t)|^2 = \sum_{\nu\nu'} A_{\nu}(t)A_{\nu'}^*(t) = \sum_{\nu} |A_{\nu}(t)|^2 + \sum_{\nu \neq \nu'} A_{\nu}(t)A_{\nu'}^*(t). \quad (9.10)$$

The omission of interference effects, which led to (9.1) with $\ell_{\text{tr}}^{-1} = n_{\text{imp}}\sigma_{\text{tr}}$, is the analog of omitting the last term (the interference term) on the rhs of (9.10). The usual justification for this omission is that the phases of the various path integrals, $A_{\nu}(t)$, are uncorrelated and widely varying so that the sum of $\nu \neq \nu'$ averages out to zero. However, there is a flaw in this argument. To see why, let us define for each closed path a forward and backward direction. Paths run in the forward direction will be denoted by greek letters α, β , etc., and those run in the backward direction by $\bar{\alpha}, \bar{\beta}$, etc. (α and $\bar{\alpha}$ refer to the same closed path run in opposite directions). With this notation, (9.10) can be written as follows:

$$\begin{aligned} \sum_{\nu\nu'} A_{\nu}(t)A_{\nu'}^*(t) &= \sum_{\alpha=\beta} [A_{\alpha}(t) + A_{\bar{\alpha}}(t)] [A_{\alpha}^*(t) + A_{\bar{\alpha}}^*(t)] + \\ &\quad + \sum_{\alpha \neq \beta} [A_{\alpha}(t) + A_{\bar{\alpha}}(t)] [A_{\beta}^*(t) + A_{\bar{\beta}}^*(t)] \\ &= \sum_{\alpha} A_{\alpha}(t)A_{\alpha}^*(t) + \sum_{\alpha} A_{\bar{\alpha}}(t)A_{\bar{\alpha}}^*(t) \\ &\quad + \sum_{\alpha} A_{\bar{\alpha}}(t)A_{\alpha}^*(t) + \sum_{\alpha} A_{\alpha}(t)A_{\bar{\alpha}}^*(t) \\ &\quad + \sum_{\alpha \neq \beta} [A_{\alpha}(t) + A_{\bar{\alpha}}(t)] [A_{\beta}^*(t) + A_{\bar{\beta}}^*(t)]. \quad (9.10') \end{aligned}$$

The first two sums on the last rhs of (9.10') are identical to the first sum on the rhs of (9.10). For the last sum on the rhs of (9.10'), one can argue that it is probably zero, since no phase correlations are expected to occur among the pairs of paths (α, β) , $(\alpha, \bar{\beta})$, $(\bar{\alpha}, \beta)$, $(\bar{\alpha}, \bar{\beta})$ with $\alpha \neq \beta$. However, the third and fourth sum on the last rhs of (9.10') [which, together with the last, correspond to $\sum_{\nu \neq \nu'} A_\nu(t) A_{\nu'}(t)$ in (9.10)] are not necessarily zero. On the contrary, if time reversal symmetry is obeyed by the Lagrangian of the system, $A_\alpha(t) = A_{\bar{\alpha}}(t)$ and

$$\sum_{\alpha} A_{\bar{\alpha}} A_{\alpha}^* + \sum_{\alpha} A_{\alpha} A_{\bar{\alpha}}^* = \sum_{\alpha} A_{\alpha} A_{\alpha}^* + A_{\bar{\alpha}} A_{\bar{\alpha}}^* .$$

Thus interference effects double the "classical" probability of finding the particle at the same site after time t and hence reduce the diffusion coefficient and the conductivity in agreement with (9.2a), (9.2b), and (9.2c).

Actually, this probability is less than double the "classical" one even if time reversal is obeyed. The reason is the presence of inelastic scattering events (due, e.g., to phonons) that introduce an uncertainty, δE_{in} , in the energy of the particle; this uncertainty introduces a phase randomness, $\delta\phi_{\alpha}$ and $\delta\phi_{\bar{\alpha}}$ with $\delta\phi_{\alpha} \neq \delta\phi_{\bar{\alpha}}$, and, as a result, destroys the perfect phase equality of A_{α} and $A_{\bar{\alpha}}$. The longer the path, the more severe the random phase difference, $\delta\phi_{\alpha} - \delta\phi_{\bar{\alpha}}$, between A_{α} and $A_{\bar{\alpha}}$, so that for very long paths ($L > L_{\phi}$)

$$\sum_{\alpha} A_{\bar{\alpha}} A_{\alpha}^* + \sum_{\alpha} A_{\alpha} A_{\bar{\alpha}}^* \simeq 0 .$$

The characteristic length, L_{ϕ} , over which coherence is lost is related to a characteristic time, τ_{ϕ} , through the diffusion relation $L_{\phi}^2 = D\tau_{\phi}$, where the inelastic phase incoherence time τ_{ϕ} is of the order $\hbar/\delta E_{\text{in}}$. It must be pointed out that this inelastic phase incoherence length, L_{ϕ} , is physically unrelated to the elastic scattering and transport mean free paths: the latter refer to phase randomness among different configurations/realizations of the ensemble that represent the random Hamiltonian. In other words, phase randomization appears only when we take the *average* of $e^{i\phi}$ over all members of the ensemble. Elastic scattering does not randomize the phase in each single member of the ensemble. In contrast, the phase incoherence length, L_{ϕ} , refers to the phase randomization in *each single* member of the ensemble as a result of repeated inelastic scattering.

To estimate the increase in $|c_n(t)|^2$, due to wave interference, we recall that the dominant contribution to $|c_n(t)|^2$ comes from closed paths adjacent to the classical one, i.e., from those inside a tube of cross section λ^2 (or λ^{d-1} for a d -dimensional system, where λ is the wavelength) around the classical trajectory. Take also into account that the probability of returning after time t to the original site is proportional to the probability of self-intersection of this orbital tube. Now, within time dt , the wave would move by vdt and would sweep a volume

$$d\Omega = \lambda^{d-1} v dt .$$

The total volume, $\Omega(t)$, swept by the wave during the entire time interval from zero to t is of the order of $L_D^d = (Dt)^{d/2}$. Hence the probability of self-intersection during the time dt after elapsed time t is of the order of the ratio

$$\frac{d\Omega}{\Omega(t)} = \frac{\lambda^{d-1}v}{(Dt)^{d/2}} dt.$$

It follows that the probability, p , of self-intersection during the time interval from $t = 0$ to $t = \tau_\phi$ is of the order

$$p \simeq \int_{\tau_{\text{tr}}}^{\tau_\phi} dt \frac{v\lambda^{d-1}}{(Dt)^{d/2}}. \quad (9.11)$$

The lower limit in the integral was set equal to τ_{tr} (the transport elastic relaxation time), since for $t \leq \tau_{\text{tr}}$ the motion of the wave is ballistic and the probability of returning is zero. The upper limit was taken as τ_ϕ (the inelastic phase incoherence time), because for $t \geq \tau_\phi$ phase coherence between a path α and its opposite, $\bar{\alpha}$, is lost and, as a result, there is no quantum increase in $|c_n(t)|^2$. Notice that at high temperatures, $\tau_\phi \simeq \tau_{\text{tr}}$, and consequently there are no quantum corrections to the classical result for the conductivity. On the other hand, for very low temperatures we have that $\tau_\phi \gg \tau_{\text{tr}}$, and, hence, the increase, p , in the probability of returning to the original site and the correction, $\delta\sigma$, to the classical conductivity σ_0 are appreciable.

Taking into account that

$$L_D = \sqrt{D\tau_{\text{tr}}} = \frac{\ell_{\text{tr}}}{\sqrt{d}},$$

where $\ell_{\text{tr}} = v\tau_{\text{tr}}$, we have by performing the integration in (9.11)

$$\delta\sigma \sim -p \simeq \begin{cases} 2 \left(1 - \sqrt{\frac{\tau_\phi}{\tau_{\text{tr}}}}\right) = 2 \left(1 - \frac{L_\phi}{L_D}\right), & d = 1, \quad (9.12a) \\ -\frac{\lambda\sqrt{2}}{L_D} \ln\left(\frac{\tau_\phi}{\tau_{\text{tr}}}\right) = -\frac{2\lambda\sqrt{2}}{L_D} \ln\left(\frac{L_\phi}{L_D}\right), & d = 2, \quad (9.12b) \\ -\frac{\sqrt{3}\lambda^2}{L_D^2} \left(1 - \sqrt{\frac{\tau_{\text{tr}}}{\tau_\phi}}\right) = -\frac{\lambda^2\sqrt{3}}{L_D^2} \left(1 - \frac{L_D}{L_\phi}\right), & d = 3. \quad (9.12c) \end{cases}$$

Notice that the dependence on L_ϕ in (9.12) is the same as the dependence on L_ω in (8.91) or the dependence on L_M in (9.2). This suggests that L_ϕ in (9.12) is the upper cutoff length L_M discussed in Sect. 9.1.

Note that the lengths L_ϕ , L_ω , L_B , etc. tend to infinity in some appropriate limits: $L_\omega \rightarrow \infty$ as $\omega \rightarrow 0$, $L_\phi \rightarrow \infty$ as $T \rightarrow 0\text{K}$ because τ_ϕ is proportional to $T^{-\alpha}$ (with $\alpha = 2/3$ for 1-d systems and $\alpha = 1$ for 2-d systems), $L_B \rightarrow \infty$ as $B \rightarrow 0$. Thus (9.2) are valid only in the case of relatively weak disorder (known in the field as weak localization) such that $\delta\sigma$ is considerably less than σ_0 .

We shall conclude this section by examining the role of the magnetic field in $\delta\sigma$. The presence of a magnetic field, \mathbf{B} , adds a term in the Lagrangian of the form $(q/c)\mathbf{A} \cdot \mathbf{v}$, where q is the electric charge of the particle, \mathbf{v} is its velocity, and \mathbf{A} is the vector potential: $\mathbf{B} = \nabla \times \mathbf{A}$. Obviously, the term $(q/c)\mathbf{A} \cdot \mathbf{v}$ breaks the time invariance of the Lagrangian [since $\mathbf{v}(t) = -\mathbf{v}(-t)$] and, as a result, the derivations of both (8.91) and (9.12) (which were based on time invariance) need to be reconsidered. The basic equation (9.9) in the presence of \mathbf{B} becomes

$$A_\alpha(t) = A_{\alpha 0}(t) \exp(i\phi_\alpha) , \quad (9.13)$$

where $A_{\alpha 0}(t)$ is the contribution of the path α in the absence of magnetic field and

$$\begin{aligned} i\phi_\alpha &= \frac{i}{\hbar} \frac{q}{c} \int_0^t \mathbf{A} \cdot \mathbf{v} dt' = \frac{iq}{\hbar c} \int \mathbf{A} \cdot d\mathbf{r}_\alpha \\ &= \frac{iq}{\hbar c} \int (\nabla \times \mathbf{A}) \cdot d\mathbf{S}_\alpha = \frac{iq}{\hbar c} \int \mathbf{B} \cdot d\mathbf{S}_\alpha = \frac{iq\Phi_\alpha}{\hbar c} . \end{aligned} \quad (9.14)$$

In deriving (9.14) we have changed the closed-path integral $\int \mathbf{A} \cdot d\mathbf{r}_\alpha$ to a surface integral over a surface terminated at the closed path and we have used the definition of the magnetic flux, $\Phi_\alpha = \int \mathbf{B} \cdot d\mathbf{S}_\alpha$. For an electron $q = -e$, and the extra phase ϕ_α becomes

$$\phi_\alpha = -\pi \frac{\Phi_\alpha}{\Phi_0} , \quad (9.15)$$

where Φ_0 is the quantum of magnetic flux defined as $\Phi_0 \equiv hc/2e$. For $\bar{\alpha}$, i.e., the same closed path run in the opposite direction, we have

$$A_{\bar{\alpha}}(t) = A_{\alpha 0}(t) \exp(-i\phi_\alpha) . \quad (9.16)$$

Substituting (9.13) and (9.16) into the third and fourth sum of the rhs of (9.10') and taking into account (9.15) we obtain

$$\sum_\alpha |A_{\alpha 0}|^2 [\exp(-2i\phi_\alpha) + \exp(2i\phi_\alpha)] = 2 \sum_\alpha |A_{\alpha 0}|^2 \cos(2\phi_\alpha) , \quad (9.17)$$

so that

$$|c_n(t)|^2 = 2 \sum_\alpha |A_{\alpha 0}|^2 [1 + \cos(2\phi_\alpha)] . \quad (9.18)$$

Thus, the presence of the magnetic field, by breaking the time reversal invariance, reduces the probability of returning to the original site and, hence, tends to restore the "classical" formula (9.1) for the conductivity. If we define the average flux $\bar{\Phi}(t)$ from the relation

$$2 \sum_\alpha |A_{\alpha 0}|^2 [1 + \cos(2\phi_\alpha)] \equiv 2 \left[1 + \cos \left(\frac{2\pi\bar{\Phi}(t)}{\Phi_0} \right) \right] \sum_\alpha |A_{\alpha 0}|^2 ,$$

then the change $\Delta\sigma(B) \equiv \delta\sigma(B) - \delta\sigma(0)$ is proportional to

$$\Delta\sigma(B) \sim \frac{v\lambda^{d-1}}{D_0^{d/2}} \int_{\tau}^{\tau_{\phi}} \frac{dt}{t^{d/2}} \left[1 - \cos\left(\frac{2\pi\Phi(t)}{\Phi_0}\right) \right]. \quad (9.19)$$

In the 2-d case, the quantity $\Delta\sigma(B)$ has been calculated explicitly [264–270], and the rigorous result in the limit $L_B \gg \ell$ was found to be

$$\Delta\sigma(B) = \frac{e^2}{2\pi^2\hbar} \left[\psi(x) - 2 \ln\left(\frac{L_B}{2L_{\phi}}\right) \right], \quad (9.20)$$

where $x = \frac{1}{2} + (L_B/2L_{\phi})^2$ and ψ is the digamma function [1], $\psi(x) \equiv \Gamma'(x)/\Gamma(x)$, where $\Gamma(x)$ is the gamma function.

For special geometries such that $\phi_{\alpha} \equiv -\pi\Phi_{\alpha}/\Phi_0$ is the same for all paths that count, the factor $[1 - \cos(2\pi\Phi/\Phi_0)]$ can be taken out of the integral in (9.19). In such a case, the conductivity will exhibit a sinusoidal periodic variation with the magnetic flux with the period $\Phi_0 = hc/2e$. This is the so-called *hc/2e Aharonov–Bohm effect* and has been observed in cylindrical tubes with very thin walls so that the flux Φ_{α} is an integer multiple of BS , where S is the cross section of the tube. If S is of the same order of magnitude as πL_{ϕ}^2 , then the only paths that count are those that go around the circumference of the tube only once; for all such paths $\Phi = BS$.

Another case where (9.18) produces impressive results is the one shown in Fig. 9.2. In this case, the probability amplitude, A , for a particle to go from point 1 to point 2 is

$$A = \sum_{\nu} A_{\nu} + \sum_{\nu'} A_{\nu'} = \sum_{\nu} A_{\nu 0} \exp(i\phi_{\nu}) + \sum_{\nu'} A_{\nu' 0} \exp(i\phi_{\nu'}), \quad (9.21)$$

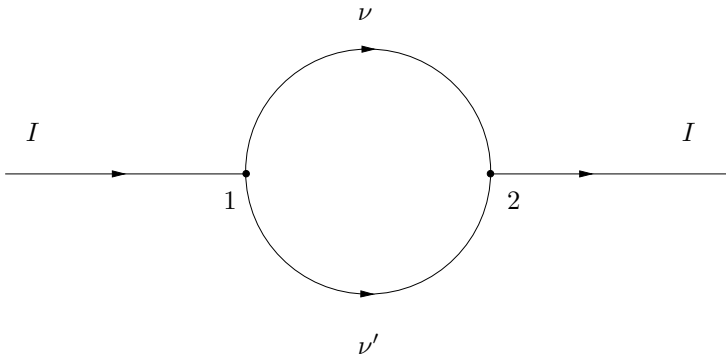


Fig. 9.2. The current I flowing from point 1 to point 2 follows the two paths (ν and ν') of a very thin ring-shaped wire

where

$$\phi_\nu = -\frac{e}{\hbar c} \int_1^2 \mathbf{A} d\mathbf{r}_\nu, \quad (9.22a)$$

$$\phi_{\nu'} = -\frac{e}{\hbar c} \int_1^2 \mathbf{A} d\mathbf{r}_{\nu'}. \quad (9.22b)$$

Denoting by A' each of the sums $\sum_\nu A_{\nu 0}$ and $\sum_{\nu'} A_{\nu' 0}$ (they are equal by symmetry) we have

$$A = A' [\exp(i\phi_\nu) + \exp(i\phi_{\nu'})]. \quad (9.23)$$

The probability $|A|^2$ is then

$$\begin{aligned} |A|^2 &= |A'|^2 [2 + 2 \cos(\phi_\nu - \phi_{\nu'})] = 2 |A'|^2 \left[1 + \cos\left(\frac{e}{\hbar c} \oint \mathbf{A} \cdot d\mathbf{r}\right) \right] \\ &= 2 |A'|^2 \left[1 + \cos\left(\frac{2\pi\Phi}{ch/e}\right) \right], \end{aligned} \quad (9.24)$$

where Φ is the magnetic flux through the ring. In this case, the conductivity would be a periodic sinusoidal function of Φ with period ch/e . This is the so-called *ch/e Aharonov-Bohm effect*.

9.3 Localization

There is a simple way to improve upon (9.2) by returning to (8.92). In obtaining (8.91) we started from (8.53) for the real part of σ . It would have been simpler to have chosen as our starting point (8.51); in this case, by a quite similar procedure, we would have obtained the vertex corrections for both the real and the imaginary part of σ , i.e.,

$$\delta\sigma = -\frac{e^2}{\pi\hbar} \frac{2}{(2\pi)^d} \int d\mathbf{q} \frac{1}{q^2 - i\omega/D^{(0)}}, \quad (9.25)$$

the real part of which coincides with (8.91), as it should. One can rewrite the lhs of (9.25) in terms of the diffusion coefficient,

$$\delta\sigma = \sigma - \sigma_0 = 2e^2 \varrho (D - D_0);$$

furthermore, (9.25) can be improved if one replaces the $D^{(0)}$ inside the integral by the corrected $D = D^{(0)} + \delta D$. We have then

$$D(\omega) = D^{(0)} - \frac{1}{(2\pi)^d \pi \hbar \varrho} \int d\mathbf{q} \frac{1}{q^2 - i\omega/D(\omega)}. \quad (9.26)$$

Equation (9.26) was obtained by Vollhardt and Wölfle [271]. Self-consistent equations for $D(\omega)$ were also obtained by Götze [272, 273] and by Kawabata [274, 275].

Equation (9.26) avoids the nonphysical behavior of (9.25) as ω approaches zero. Indeed, as ω becomes smaller and smaller, the last term of the rhs of (9.26) becomes larger and larger (at least for $d \leq 2$) and, hence, $D(\omega)$ becomes smaller and smaller until it finally approaches zero (in the limit of $L_\phi = L_B = \infty$). When $D(\omega) = 0$, the last term on the rhs of (9.26) must be finite and equal to $D^{(0)}$. For this to happen when $d \leq 2$ we must have $\omega/D(\omega) \rightarrow \text{const.}$ as $\omega \rightarrow 0$, or, equivalently, $D(\omega) \rightarrow -i\xi^2\omega$ as $\omega \rightarrow 0$, with the constant, $i\xi^2$, being imaginary to ensure that the integral is equal to the real quantity $(2\pi)^d \pi \hbar \rho D^{(0)}$. The same is true for $d = 3$ if $D^{(0)}$ is very small. Thus, the self-consistent equation (9.26) leads to the absence of static diffusion [$D(\omega) \rightarrow 0$ as $\omega \rightarrow 0$ and $L_M = \infty$] for $d \leq 2$ (no matter how weak the disorder) and for $d = 3$ (if the disorder is strong enough to produce sufficiently small values of $D^{(0)}$). The vanishing of the static diffusion coefficient or, equivalently, the vanishing of the DC conductivity implies localized states. Indeed, for localized states, the electric susceptibility, $\chi^{(e)}$, is finite as $\omega \rightarrow 0$. Hence the conductivity, $\sigma(\omega) = -i\omega\chi^{(e)}$ [see (8.16)], and the diffusion coefficient, $D(\omega)$, approach zero linearly in ω . As a result, $-i\omega/D(\omega) \rightarrow \xi^{-2}$ as $\omega \rightarrow 0$. The constant ξ , which has dimensions of length and is defined only in the localized regime, is given by

$$\pi \hbar \rho D^{(0)} = \frac{\pi \hbar}{2 e^2} \sigma_0 = \frac{\alpha_1}{(2\pi)^d} \int d\mathbf{q} \frac{1}{q^2 + \xi^{-2}}, \quad (9.27)$$

where the numerical constant α_1 is introduced to account for the fact that the q^2 dependence is valid only for small q .

It must be pointed out that $\delta\sigma(\omega)$ as given by (9.25) is, apart from a constant factor, the same as the unperturbed Green's function $G_0(\mathbf{r}, \mathbf{r}; z)$ with $z = i\omega/D^{(0)}$ [see (1.38)]. Thus the divergence of $\delta\sigma$ as $\omega \rightarrow 0$ for $d \leq 2$ (which leads to a finite ξ^2 no matter how weak the disorder is and hence can be interpreted as implying the localization of all eigenfunctions) is directly related to the divergence of the unperturbed Green's function at the band edge $z = 0$ for $d \leq 2$. Recall that it is precisely this divergence that always allows a local potential fluctuation to trap a particle (for $d \leq 2$). Hence, a mathematical connection was established between the problem of localization in a disordered system and that of a bound level in a single potential well [276, 277]. This connection can be further quantified in terms of the localization length. Indeed, for the shallow potential well problem, one can rewrite the basic equation (6.9) in terms of the effective mass m^* , defined by $E(\mathbf{k}) = \hbar^2 \mathbf{k}^2 / 2m^*$, and the localization length λ_p connected to the binding energy E_b by the relation $E_b = \hbar^2 / 2m^* \lambda_p^2$:

$$\frac{\hbar^2}{2m^* a^d |\varepsilon|} = \frac{\alpha_2}{(2\pi)^d} \int d\mathbf{q} \frac{1}{q^2 + \lambda_p^{-2}}, \quad (9.28)$$

where α_2 is introduced for the same reasons as in (9.27) and the integration is confined within the first Brillouin zone, i.e., for $q \leq \pi/a$, where a is the lattice constant. In (9.27) the integration is confined within a sphere of radius L_m^{-1} , where it was assumed that L_m is proportional to ℓ_{tr} or ℓ .

Thus, according to the self-consistent equation (9.27), the problem of determining the characteristic features of the eigenstates in a disordered system (for a given energy E and degree of disorder) is mathematically equivalent to finding the basic properties of the ground state in an equivalent potential well¹ whose linear extent, a_{eff} , is proportional to the mean free path at E and whose dimensionless depth, $\varepsilon_{\text{eff}}/|V_{\text{eff}}|$, is inversely proportional to $\sigma_0 \ell_{\text{tr}}^{d-2}$ or, equivalently, inversely proportional to $S_F \ell_{\text{tr}}^{d-1}$:

$$a_{\text{eff}} = c_1 \ell_{\text{tr}}, \quad (9.29)$$

$$\frac{\varepsilon_{\text{eff}}}{\hbar^2/2m^*a_{\text{eff}}^2} = \frac{c_2}{c_1^{d-2}} \frac{2e^2}{\pi \hbar} \frac{1}{\sigma_0 \ell_{\text{tr}}^{d-2}} = \frac{c_2 d (2\pi)^d}{c_1^{d-2} \pi} \frac{1}{S_F \ell_{\text{tr}}^{d-1}}, \quad (9.30)$$

where c_1 and c_2 are numerical factors dependent on the dimensionality; their values can be determined by fitting numerical data to the localization length, ξ , to the value of λ_p for a single site potential well of dimensionless depth $\varepsilon_{\text{eff}}/|V_{\text{eff}}|$ in a TBM of lattice spacing a_{eff} .

Employing the CPA we can calculate the average DOS, the mean free path ℓ or ℓ_{tr} , the conductivity σ_0 , and the renormalized Fermi surface, S_F ; using the post-CPA corrections to σ_0 we obtain the conductivity in the weak localization regime; finally, with the help of the potential well analogy, we can obtain the localization length ξ as well as the conductivity (in the presence of a finite L_M) in the so-called strong localization regime [278].

We conclude this section by summarizing results obtained through the procedure just outlined.

9.3.1 Three-Dimensional Systems

In Fig. 9.3 the effects of the disorder in a simple TBM are shown: (i) The Van Hove singularities associated with the perfect periodic system (Fig. 9.3a) are smoothed out as the disorder is introduced. (ii) The approximate band edges, $\pm E_B$, are moving away from the band center leading to a widening of the band by an amount proportional to $w^2/|V|$ (the proportionality factor is equal to 0.5 for the present case and for not so large values of w^2/V^2). (iii) The band edges $\pm E_B$ are not strictly defined because, beyond them, tails in the DOS appear that, over a considerable energy range and for not so large w , are of exponential form: $\varrho(E) \sim \exp(-|E|/E_0)$, where $E_0 \simeq c_2 w^2/|V|$ ($c_2 \simeq 0.12$ in the present case). These tails are important because they produce the so-called *Urbach tails* in the optical absorption in the semiconductors (as a result of electronic transitions from the valence to the conduction band involving the tails of either one). (iv) Two mobility edges, $\pm E_c$, appear such that the states corresponding to $|E| > E_c$ are localized, while those with $|E| < E_c$ are extended. For low disorder, the mobility edges, $\pm E_c$, are very close to the band

¹ If the potential well is defined within the framework of an effective TBM, then a_{eff} is the lattice spacing and $\varepsilon_{\text{eff}}/(\hbar^2/2m^*a_{\text{eff}}^2)$ must be interpreted as $\varepsilon_{\text{eff}}/|V_{\text{eff}}|$.

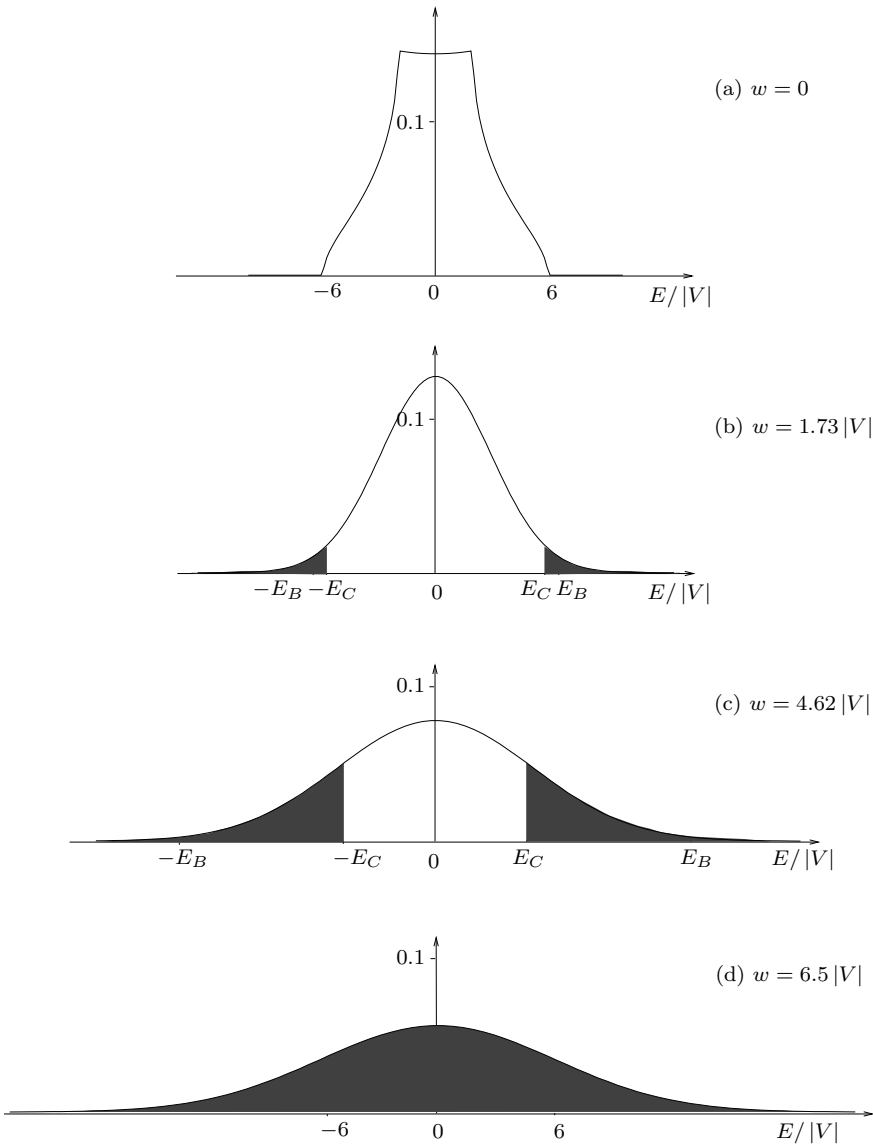


Fig. 9.3. The density of states vs. dimensionless energy for a simple cubic TBM whose diagonal matrix elements are independent random variables with a Gaussian probability distribution of standard deviation w ; V is the common value for the off-diagonal matrix elements. The regions of localized states (*black areas*), the mobility edges ($\pm E_c$), and the approximate band edges ($\pm E_B$) are also shown

edges, $\pm E_B$, respectively ($E_B - E_c \sim w^4/V^3$), moving initially outward with increasing disorder; for higher disorder they change direction and move inward toward the center of the band and eventually merge together, transforming all states to localized; this is known as the *Anderson transition* (in the present case it occurs when $w \simeq 6.2|V|$). Thus the trajectory of the mobility edges in the w - E plane is qualitatively similar to the one shown in Fig. 9.1. (v) As one approaches a mobility edge from the extended side, fluctuations in the amplitude, $|\psi(\mathbf{r})|$, of the eigenstates appear of multifractal nature [279,280] up to a maximum length ξ' . For $E \rightarrow E_c$ or $-E_c$, ξ' blows up: $\xi' \sim (|E_c| - |E|)^{-\gamma}$, where the exponent γ , according to the potential well analogy and the CPA, is equal to 1; however, detailed numerical analysis shows that $\gamma \simeq 1.54$ (in the absence of a magnetic field) and $\gamma \simeq 1.43$ (in the presence of a magnetic field). The quantity ξ' is important because it is connected to the conductivity $\sigma(E)$ for E belonging to the extended part of the spectrum

$$\sigma(E) \simeq \frac{e^2}{\hbar} \left(\frac{0.066}{\xi'} + \frac{A_1}{L_M} \right), \quad (9.31)$$

where the value of A_1 is of the order 0.05.

The quantity ξ' near the mobility edge can be obtained by extending the application of the effective potential well: if this potential well does not sustain a bound state, it means that the corresponding eigenstates of the disordered system are extended. However, as we saw in Chap. 6, as $a_{\text{eff}}^2 |\varepsilon_{\text{eff}}|$ approaches the critical value (for the appearance of a bound state) from below, a resonance state *shows up* at a resonance energy E_r ; the latter is connected to ξ' through the relation $E_r = \hbar^2/2m^* \xi'^2$.

In the localized regime the eigenstates exhibit multiple scale fluctuations and an exponential envelope of the form $e^{-r/\xi}$, where ξ is the localization length, which blows up in a power law, $\xi \sim (|E| - |E_c|)^{-\gamma}$, with the same exponent γ as the quantity ξ' . As $|E|$ moves away from a mobility edge, ξ soon becomes very small (comparable to the lattice spacing in the present case; this implies very strong localization in the vicinity of a single site).

9.3.2 Two-Dimensional Systems

Two-dimensional electronic systems can be realized approximately in very thin metallic films or rigorously at the interface of Si/SiO₂ or GaAs/Al_xGa_{1-x}As. The theory and arguments presented in this chapter as well as other approaches, together with extensive numerical work, converge at the conclusion that all eigenstates in a static disordered 2-d system (in the absence of magnetic forces and within the independent electron approximation) are localized (pathological exceptions do exist) no matter how weak the disorder.

In the presence of magnetic forces, and as the disorder is gradually turned on, a very narrow region of extended states at the center of the band remains until a critical value of the disorder where an Anderson-type transition takes

place (as in the 3-d case) and all eigenstates become localized. This picture is essential for the interpretation of the impressive Integral Quantum Hall Effect (IQHE) to be briefly discussed in Sect. 9.8.

The $d = 2$ is the critical dimensionality separating the $d < 2$ regime (where all states become localized even with a minute amount of disorder) from the $d > 2$ regime (where a critical value of disorder is needed to localize the eigenstates); as was mentioned earlier, the $d = 2$ case (in the absence of magnetic forces) belongs to the first regime but being in the borderline exhibits huge localization lengths (for not so strong disorder) given by the approximate formula

$$\xi \simeq 2.7\ell_{\text{tr}} \exp \left[\frac{S(E)\ell_{\text{tr}}(E)}{4} \right], \quad (9.32)$$

where $S(E)$ is the renormalized length of the line in the 2-d \mathbf{k} -space defined by the equation $E - \text{Re} \{ \Sigma(E) \} = E(\mathbf{k})$.

An approximate interpolation formula for the conductivity can be derived by employing the CPA and the potential well analogy (PWA) [278]:

$$\sigma = \sigma_0 \frac{\ln(L_M/L_m)}{K_0^2(L_m/\xi) \int_{L_m}^{L_M} dr \frac{1}{K_0^2(r/\xi)r}}, \quad (9.33)$$

where K_0 is the modified Bessel function of second kind and zero order [1].

In the weak localization case (weak disorder), $L_M \ll \xi$, this expression for σ reduces to (9.2b), while in the opposite limit $\xi \ll L_M$ we find

$$\sigma \simeq 2\sigma_0 \left(\frac{L_M}{\xi} \right) \exp \left(-\frac{2L_M}{\xi} \right).$$

Taking into account (9.5) in the case where $L_\phi \ll L, L_\omega$, i.e., when

$$\frac{1}{L_M^2} = \frac{1}{(1.33L_B)^2} + \frac{c_2}{L_\phi^2} \equiv \frac{eB}{1.78\hbar c} + \frac{c_2}{L_\phi^2},$$

we have, according to (9.2b) [see also (9.20)], that the magnetic-field-induced relative change of the resistance, $\Delta R/R \simeq -\Delta\sigma(B)/\sigma(0)$, is equal to

$$\frac{\Delta R}{R} \simeq -\frac{e^2}{2\pi^2\hbar\sigma(0)} \ln \left(1 + \frac{L_\phi^2}{c_2 L_B^2} \right) = -\frac{e^2}{2\pi^2\hbar\sigma(0)} \ln \left(1 + \frac{L_\phi^2 eB}{c_2 1.78\hbar c} \right), \quad (9.34)$$

i.e., the presence of a magnetic field reduces the resistance, or, in other words, a negative magnetoresistance is exhibited as a result of weak localization effects.

It must be pointed out that various interactions such as electron–electron, electron–phonon, etc. may produce effects similar to those of localization theory [see point (iii) in Sect. 9.1] or may significantly modify results of localization theory. For example, recent experiments in very clean interfaces of

GaAs/Al_xGa_{1-x}As or Si/SiO₂ have shown that $\sigma(T)$ ceases to decrease with decreasing temperature and instead starts increasing in clear violation of the formula $\delta\sigma \sim -\ln(L_\phi/L_m)$ with $L_\phi \rightarrow \infty$ as $T \rightarrow 0$ K [281].

9.3.3 One-Dimensional and Quasi-One-Dimensional Systems

Even during the early studies of 1-d disordered systems there were suggestions that the eigenstates may become localized [282]. Mott and Twose [283] were the first to propose that all eigenstates in a 1-d random system are localized. One may visualize this proposal by assuming that each backscattered wave at every elementary scattering event is lost, as far as the propagation is concerned, due to destructive interference; this picture suggests that the localization length ξ , defined by the relation

$$\frac{a}{\xi} = - \lim_{m \rightarrow \infty} \frac{\langle \ln |\psi_m| \rangle}{m}, \quad (9.35)$$

is of the same order of magnitude as the mean tree path ℓ ; ψ_m is the amplitude of the eigenfunction at site m and a is the lattice constant.

Borland [284–287] showed that for a random δ -function array the solutions of the differential equation (with fixed values of the function and its derivative at one end) grow exponentially on average with distance. This exponential growth was shown to be a direct result of the phase incoherence. The picture that emerged on the basis of Borland's proof is that at every energy there are two independent solutions of the Schrödinger equation, one increasing and the other decreasing exponentially (on the average) with increasing x . At a set of particular energies (the eigenenergies) the left decreasing solution matches at some point the right decreasing solution to form the eigenfunction that decays to zero as $|x| \rightarrow \infty$. According to this picture (which was not proven rigorously) the localization length is the same as the inverse of the average rate of growth of the solution of the differential equation. Wegner [288] demonstrated the localization of eigenfunctions through a different method. Borland's method is discussed very clearly in a review article by Halperin [289]. Relevant material can be found in books by Hori [290] and by Lieb and Mattis [291].

The exponential (on average) growth of the solutions of the differential equation can be shown rigorously [292] by employing the transfer matrix technique (Appendix H). The transfer matrix is a 2×2 matrix that connects, e.g., $\psi, d\psi/dx$ at x with $\psi, d\psi/dx$ at x' . The existence of such a 2×2 matrix is a direct consequence of the uniqueness of the path connecting x and x' in 1-d. The concept of the transfer matrix transforms the propagation of the wave in 1-d to a product of random 2×2 matrices. There are exact theorems [293] that state that under quite general conditions the product of n random matrices is a 2×2 matrix whose two eigenvalues, β_1 and $\bar{\beta}_1$, depend exponentially on n (as $n \rightarrow \infty$): $\beta_1 \sim e^{\varrho n}$ and $\bar{\beta}_1 \sim e^{-\varrho n}$, where ϱ is a positive number called the *Lyapunov exponent*. Thus, there is exponential growth of

the solution and exponential decay of the eigenfunction with a localization length $\xi = a/\varrho$, where a is the lattice spacing.

The transfer matrix technique can be used for the calculation of the transmission ($|t|^2$) or reflection ($|r|^2$) coefficient associated with a disordered segment of total length L . Using Furstenberg's theorem [292, 293], it is easy to prove that

$$\frac{1}{L} \left\langle \ln |t|^2 \right\rangle = -\frac{2}{\xi}, \quad (9.36)$$

where $1/\xi$ is the average rate of exponential growth of the solution.

Note that the probability distribution of $|t|^2$ possesses long tails that are responsible for a rather peculiar behavior of various averages [250, 251, 255–258, 294–297].

Abrikosov [258] found that, while $\langle \ln |t|^2 \rangle$ is given by (9.36), other averages give different results:

$$\left\langle |t|^{-2} \right\rangle = \frac{1}{2} \left(1 + e^{4L/\xi} \right), \quad (9.37)$$

$$\left\langle |t|^{-4} \right\rangle = \frac{1}{3} + \frac{1}{2} e^{4L/\xi} + \frac{1}{6} e^{12L/\xi}, \quad (9.38)$$

$$\left\langle |t|^{2n} \right\rangle \xrightarrow{L \rightarrow \infty} C_n \left(\frac{\xi}{2L} \right)^{3/2} e^{-L/2\xi}, \quad (9.39)$$

where the constant C_n depends only on n . The standard deviation of $\ln(|t|^2)$ is proportional to $\sqrt{L/\xi}$ for large values of L/ξ . Hence, in the strong disorder limit, $\ln(|t|^2)$ becomes sharply distributed, with a probability distribution that seems to be Gaussian. The interested reader may find additional material in [257, 298–300] and in review articles by Abrikosov and Ryzhkin [301] and Erdős and Herndon [302]. Note that a special case [295–297, 303, 304] exists such that $1/\xi = 0$. The vanishing of $1/\xi$ does not necessarily imply extended states. Indeed, in the case examined in [295–297], $\ln(|t|^2) \sim -\sqrt{L}$ as $L \rightarrow \infty$; on the other hand, the special case examined by Tong [305] shows the existence of a nondecaying wave at a particular energy.

The transfer matrix technique allows us to generalize the study to disordered quasi-one-dimensional systems consisting of M coupled 1-d channels. Then the transfer matrix is a $2M \times 2M$ matrix and the product of n such random matrices (as $n \rightarrow \infty$) is a $2M \times 2M$ matrix, whose $2M$ eigenvalues, $\beta_1, \beta_2, \dots, \beta_M, \bar{\beta}_1, \bar{\beta}_2, \dots, \bar{\beta}_M$, are given by

$$\beta_i = \exp(\varrho_i n) \quad \bar{\beta}_i = \exp(-\varrho_i n), \quad i = 1, \dots, M, \quad (9.40)$$

where the M positive Lyapunov exponents ϱ_i define M localization lengths $\xi_i = a/\varrho_i$. The decay of the eigenfunction is determined by the longest localization length ξ_i or the smallest positive Lyapunov exponent, ϱ_i .

Returning to the strictly 1-d systems, we find from the potential well analogy (PWA) that $\xi = c\ell_{\text{tr}}$, where $c = 4$ for the weak localization regime. In a subsequent section we shall present rigorous formulae for the evaluation of ξ in 1-d systems. Furthermore, the geometric average of the conductivity according to the PWA turns out to be equal to [278]

$$\sigma = \frac{e^2 L}{\pi \hbar} \frac{1}{e^{2L/\xi} - 1}. \quad (9.41)$$

In the weak localization regime, $L_M \ll \xi$, we find that

$$\sigma = \frac{e^2 \xi}{2\pi \hbar} - \frac{e^2 L}{2\pi \hbar} = \frac{2e^2 \ell_{\text{tr}}}{\pi \hbar} - \frac{e^2 L}{2\pi \hbar}. \quad (9.42)$$

In (9.42), the first term on the rhs coincides with σ_0 as given by (9.1) for $d = 1$, while the second term coincides with (9.2a) [by choosing $c_1 = 2$ in (9.5)].

9.4 Conductance and Transmission

By combining (9.41) and (9.36) we find the following important relation:

$$\mathcal{G}_s \equiv \frac{\sigma}{L} = \frac{e^2}{\pi \hbar} \left[\frac{1}{T} - 1 \right]^{-1} = \frac{e^2}{\pi \hbar} \frac{T}{R}, \quad (9.43)$$

where T is the geometric average of the transmission coefficient,

$$T \equiv \exp \left\langle \ln |t|^2 \right\rangle, \quad (9.44)$$

$R = 1 - T$, and $\mathcal{G}_s = \sigma/L$ is by definition the geometric average of the conductance of the disordered 1-d system. Equation (9.43), connecting the conductance to the transmission coefficient, was obtained and championed by Landauer [306]. The universal coefficient $e^2/\pi\hbar$ is written by many authors as $2e^2/h$ to stress the point that e^2/h is the conductance per channel and spin when $T/R = 1$. It is worthwhile to point out [307] that

$$\left(\frac{R}{T} \right)_{\text{total}} = \sum_{i=1}^N \frac{R_i}{T_i}$$

if we have N 1-d segments in series, each with a transmission coefficient T_i and reflection $R_i = 1 - T_i$. To obtain this additive feature of R_i/T_i , one must assume that the transmission and reflection *probabilities* (and not the *amplitudes* as in quantum mechanics) undergo multiple scatterings [307]. The additivity of R_i/T_i implies that the resistance grows linearly with L in agreement with the first term on the rhs of (9.42). This is valid as long as $L \ll \xi$.

For large L ($L \gg \xi$) one must take into account the wave nature of electronic propagation and do the multiple scatterings in terms of transmission and reflection amplitudes (not probabilities); this implies localization and, consequently, exponential growth of the resistance with L [as in (9.41)].

Economou and Soukoulis [255], employing the Kubo–Greenwood formalism, found that the conductance of a 1-d segment fed by a current source is given by

$$\mathcal{G} = \frac{2e^2}{h} T, \quad (9.45)$$

in apparent disagreement with (9.43). Equation (9.45), which has been generalized by Fisher and Lee [308] to the quasi-1-d case of M coupled parallel channels:

$$\mathcal{G} = \frac{2e^2}{h} \text{Tr} \{ \hat{t} \hat{t}^\dagger \} = \frac{2e^2}{h} M T, \quad (9.46)$$

where the matrix element, \hat{t}_{ij} , of the $M \times M$ matrix \hat{t} gives the transmission *current* amplitude from the left j th channel to the i th right channel (Appendix H); T is an average transmission coefficient per channel defined by $T \equiv \text{Tr} \{ \hat{t} \hat{t}^\dagger \} / M$.

Both the disagreement of (9.45) with (9.43) and the apparently paradoxical result of finite resistance $h/2e^2$ per channel for a perfect conductor led to some initial efforts to provide a physical explanation and possible reconciliation of the two results [309–315]. This controversial subject was clarified when a more careful analysis of the physical situation took place (Imry [316]).

Actually, the quasi-1-d system (with M channels) is connected (through leads or directly) to two macroscopic contacts, each one in internal thermal equilibrium with electrochemical potential $\mu_i = \mu_0 - |e| V_i$, $i = 1, 2$. The macroscopic nature of the contacts means that they consist of a huge number of channels, M_{ci} ($M_{ci} \rightarrow \infty$).

When a current enters a contact of M_{ci} channels from our quasi-1-d conductor with M channels ($M \ll M_{ci}$) it encounters a contact resistance. If there is no reflection as the current enters the contacts, one can show (see Datta [307], pp. 52–53) that this total contact resistance is given by

$$R_c = \mathcal{G}_c^{-1} = \left(\frac{2e^2}{h} M \right)^{-1}. \quad (9.47)$$

The total resistance of the system taking into account contacts is defined as the ratio $(\mu_1 - \mu_2) / |e| I$, where I is the current through our quasi-1-d system; hence, the total resistance is the sum of the contact resistance, R_c , and the resistance

$$R_s = \mathcal{G}_s^{-1} = \left[\frac{2e^2 T M}{h(1-T)} \right]^{-1}$$

of the quasi-1-d system per se:

$$\mathcal{G}^{-1} = \mathcal{G}_c^{-1} + \mathcal{G}_s^{-1} = \frac{h}{2e^2 M} \left(1 + \frac{1-T}{T} \right) = \frac{h}{2e^2 M T}. \quad (9.48)$$

Thus, the total conductance, $\mathcal{G} = (2e^2/h)MT$, is identical to that given by (9.46). One may conclude that \mathcal{G} , as given by (9.46), measures the ratio

$$-\frac{|e|I}{\mu_1 - \mu_2} \equiv \frac{I}{\Delta V},$$

while \mathcal{G}_s , as given by $(2e^2/h)MT/(1-T)$, measures the ratio $I/\Delta V'$ of Fig. 9.4. Actually, the latter is not always true because the presence of leads L'_1 and L'_2 in general modifies the corresponding voltages ΔV_0 and $\Delta V'_0$ existing under the same current ($I_0 = I$) but without leads L'_1 and L'_2 . To face this problem, Büttiker [317,318] treated all external contacts (be they either current sources or sinks of voltage probes) on equal footing and generalized the equation $I = \mathcal{G}(\mu_1 - \mu_2)/(-|e|)$, with $\mathcal{G} = (2e^2/h)\text{Tr}\{\hat{t}\hat{t}^\dagger\}$, to

$$I_p = \sum_q \mathcal{G}_{pq} [V_p - V_q], \quad (9.49)$$

where

$$\mathcal{G}_{pq} = \frac{2e^2}{h} \text{Tr}\{\hat{t}_{pq}\hat{t}_{pq}^\dagger\} \equiv \frac{2e^2}{h} \bar{T}_{pq}, \quad (9.50)$$

where \hat{t}_{pq} is a transmission *current* amplitude $M \times M'$ matrix whose matrix elements, \hat{t}_{pqij} , give the transmission *current* amplitude from the j th channel of the q lead to the i th channel of the p lead, and \bar{T}_{pq} is the average transmission probability per channel times the number MM' of channels. Furthermore,

$$V_p = \frac{\mu_p}{-|e|} \quad (9.51)$$

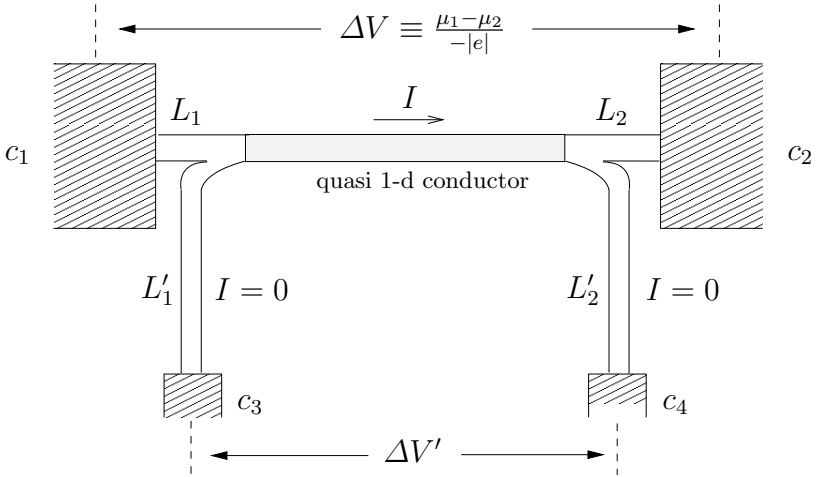


Fig. 9.4. Four-probe arrangement for measuring conductances of quasi-1-d conductor, which through leads L_1 and L_2 is connected to the contacts c_1 and c_2 of electrochemical potentials μ_1 and μ_2 , respectively. Two leads L'_1 and L'_2 (through which no current flows) connect the quasi-1-d conductor to voltage probes, c_3 and c_4

is the voltage at the contact p , and I_p is the total current entering from the contact p . Strictly speaking, (9.49) is valid at zero temperature where only channels at the Fermi level are involved; for finite temperatures the generalization is straightforward:

$$I_p = \int i_p(E) dE, \quad (9.52a)$$

where

$$i_p(E) = -\frac{2|e|}{h} \sum_q \bar{T}_{pq}(E) [f_p(E) - f_q(E)] \quad (9.52b)$$

and

$$f_p(E) = \left[\exp\left(\frac{E - \mu_p}{k_B T}\right) + 1 \right]^{-1}.$$

If the chemical potential difference $\mu_p - \mu_q$ is small compared with variations of $\bar{T}_{pq}(E)$ vs. E , then (9.52b) can be linearized by writing

$$f_p(E) - f_q(E) = -\frac{\partial f}{\partial E} (\mu_p - \mu_q) = |e| \frac{\partial f}{\partial E} (V_p - V_q),$$

and (9.52a) will be brought to the form of (9.49) with

$$\mathcal{G}_{pq} = \frac{2e^2}{h} \int \bar{T}_{pq}(E) \left(-\frac{\partial f}{\partial E} \right) dE. \quad (9.53)$$

The smoothness of $\bar{T}_{pq}(E)$ as a function of E is increased with increasing temperature and with increasing inelastic scatterings, which introduces an inelastic scattering energy scale δE_{in} . Thus the validity of linear equation (9.49) with \mathcal{G}_{pq} , given by (9.53), is guaranteed if

$$|\mu_p - \mu_q| \ll \delta E_{\text{in}} + \alpha k_B T, \quad (9.54)$$

where α is larger than 1.

9.5 Scaling Approach

In this section we present a work that played a decisive role in shaping our ideas in the field of localization. The basis of this work is the assumption that there is just one parameter Q (equal to the ratio of transfer strength $|V|$ over an average energy mismatch $\delta\varepsilon$) that completely characterizes the answer to the localization question for each dimensionality d . The existence of just *one* parameter Q is obvious in the simple TBM we have examined in Chaps. 5–8. What is not obvious is that a single parameter Q can still characterize more complicated models, where there are many energies per site and more than one transfer matrix element. Such complicated Hamiltonians may

arise even from the simple TBM if, e.g., one enlarges the unit cell of the lattice by a factor x so that the new “unit” cell has linear dimension $L_1 = ax$ and contains $n_1 = x^d$ original sites (a is the lattice spacing). If each new “unit” cell is considered as an effective “site,” there must be (according to our initial assumption) a quantity $Q(L_1)$ that characterizes the localization properties of the reformulated problem. By repeating the procedure of unit cell augmentation one produces a sequence, $Q(L_2), Q(L_3), \dots, Q(L_m), \dots$, where the “unit” cell after the m th step has linear dimension L_m equal to ax^m and contains $n_m = x^{md}$ sites. Abrahams et al. [319] realized that the derivative of $Q(L)$ with respect to L , or for that matter the logarithmic derivative β , where

$$\beta = \frac{d \ln[Q(L)]}{d \ln L}, \quad (9.55)$$

is an extremely important quantity for localization. Indeed, if β is larger than a positive number, no matter how small, the successive transformations will monotonically increase Q toward infinity as $L \rightarrow \infty$, which means that the initial problem is mapped into one, where the effective energy mismatch is zero and, hence, the eigenstates are extended. If β is less than a negative number, Q monotonically decreases toward zero; this means that the initial problem has been mapped into one where the effective transfer matrix element is zero, and consequently the eigenstates are localized. Hence the quantity β completely characterizes the localization problem. The assumption that there is just one parameter Q that determines localization forces the conclusion that β is a function of Q :

$$\beta = f(Q). \quad (9.56)$$

To proceed further with these ideas, one needs to identify what Q is in the general case. Thouless and coworkers [251,320] argued that in the general case, where the “unit” cell has linear dimension L , the role of $|V|$ in (9.6) is played by δE (where δE is a measure of how much the eigenenergies of an isolated “unit” cell change upon changing the boundary conditions from periodic to antiperiodic) and the role of $\delta \varepsilon$ is played by the level spacing, which is just the inverse of the total DOS. In other words

$$Q = \rho L^d \delta E. \quad (9.57)$$

It was further argued [320] that $\delta E = \hbar/\tau$, where τ is the time it takes a particle to diffuse from the center to the boundary of the “unit” cell: $\tau = (L/2)^2/D$, where D is the diffusion coefficient. Taking into account (9.27) we obtain that $\delta E = 4\hbar D/L^2$ equals $2\hbar\sigma/e^2\rho L^2$. Substituting in (9.57) we obtain that $Q = 2\hbar\sigma L^{d-2}/e^2$. But σL^{d-2} is the DC conductance \mathcal{G} of the unit cell,

$$\mathcal{G} = \sigma L^{d-2}. \quad (9.58)$$

Thus we reached the very important conclusion that the quantity Q is nothing else than the dimensionless DC conductance, i.e.,

$$Q = \frac{\hbar}{e^2} \mathcal{G}. \quad (9.59)$$

[In (9.59) we redefined Q as to eliminate a factor of 2].

In view of the fact that higher values of both Q and β favor extended states, it is not unreasonable to assume, as Abrahams et al. [319] did, that β is a monotonically increasing function of Q or of $\ln Q$. We are now in a position to find the qualitative features of β vs. $\ln Q$. In the weak scattering limit, when the conductance Q is very large, one is almost in the metallic regime, where σ is independent of L and $Q \sim L^{d-2}$. In this limit, $\beta = d \ln Q / d \ln L$ approaches $d-2$. In the other extreme of very strong disorder, the localization length is much less than L , and the conductance decays exponentially with L . Hence $\beta = \ln Q$ in this limit. This asymptotic behavior, together with the assumption of monotonicity, leads to a β vs. $\ln Q$ relation, as shown in Fig. 9.5. For $d = 1, 2$, β is always negative; hence by increasing the length L we decrease $\ln Q$, which in turn further decreases β . Thus, as we increase L , we slide down the curves, as shown in Fig. 9.5, and, at sufficiently large lengths L , we approach the regime of exponential localization, independently of what our starting point was. Hence all eigenstates are localized and a truly metallic behavior is not possible (at least for independent electrons). Only a quasimetal-

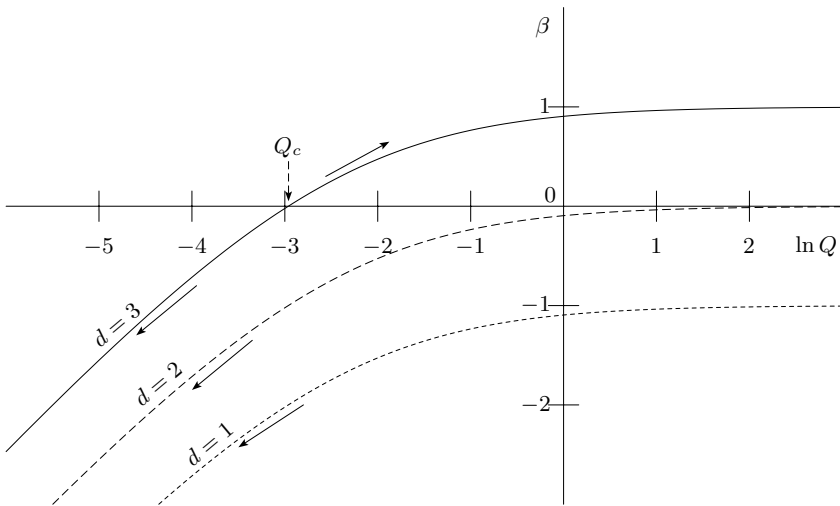


Fig. 9.5. Plot of β vs. $\ln Q$ for $d = 1$ -, 2 -, and 3 -d disordered systems assuming monotonicity. Q is the dimensionless conductance of a d -dimensional cube of length L and $\beta = d \ln Q / d \ln L$. As L increases, one moves along the curves in the direction indicated by the arrows

lic behavior can be observed when L is much larger than the total mean free path and much smaller than the localization length. In 1-d systems, in the presence of only elastic scattering, the mean free path ℓ is comparable to the localization length and, consequently, even a quasimetallic behavior is not possible. However, inelastic scattering changes this conclusion drastically, mainly because it allows electrons to jump from one localized state to another (of different energy), and hence it delocalizes them. This delocalization appears only after an electron has travelled a distance comparable to the inelastic diffusion length L_ϕ (9.3). As a result of this complication, localization effects become important only when L_ϕ becomes comparable to or larger than any characteristic localization length.

In the 3-d case there is a critical value, Q_c , of the conductance Q . For $Q < Q_c$, β is negative, and hence, by the same arguments as in $d = 1, 2$, the states are localized. On the other hand, for $Q > Q_c$, β is positive; as a result, by increasing the length, one increases Q and, hence, β itself. Thus one climbs up the β curve toward the flat metallic regime, associated with extended states of more or less uniform amplitude. It must be pointed out that the present analysis implies that the conductivity approaches zero continuously near the critical point. Indeed, for every length L , no matter how large, one can find a disorder such that Q is just above Q_c . Then the conductivity $\sigma \approx Q_c/L$ can become arbitrarily small by increasing the length L . There is considerable interest in finding how σ as a function of the energy or as a function of the disorder approaches zero. One assumes a power-law behavior, and then the question of finding the exponents arises [319, 321–336]. For a recent review see the article by Kawabata [337].

Let us now return to the weak scattering regime ($\ln Q \gg 1$), and let us assume that the classical limit $d - 2$ is approached as $1/Q$, i.e.,

$$\beta \approx d - 2 - \frac{A_d}{Q} + \dots ; \quad Q \rightarrow \infty . \quad (9.60)$$

One can then integrate (9.60) to find the first correction to the classical result for the conductance \mathcal{G} or for the DC conductivity σ . The final results are

$$\sigma \approx \begin{cases} \sigma_0 - \frac{e^2 A_1}{\hbar} L , & d=1 , & (9.61) \\ \sigma_0 - \frac{e^2 A_2}{\hbar} \ln L , & d=2 , & (9.62) \\ \sigma_0 - \sigma_1 + \frac{e^2 A_3}{\hbar} L^{-1} , & d=3 , & (9.63) \end{cases}$$

where σ_0 is the DC conductivity if vertex corrections were ignored. Equations (9.61)–(9.63) are of the same form as (9.2a)–(9.2c). Thus (9.60) can be justified by the post-CPA vertex corrections. The latter, of course, gives explicit value for the constant A_2 : $A_2 = 1/\pi^2$. The constants A_1 and A_3 depend on the relation between L and L_ω , i.e., on the constant $\sqrt{c_1}$ in (9.5). If we make the

choice $\sqrt{c_1} = 2\sqrt{2}$ for $d = 3$, then $A_3 = 1/\pi^2$, which is the usual value quoted in the literature. For the 1-d case (9.42) gives $A_1 = 1/2\pi$, which coincides with (9.2a) if we make the choice $\sqrt{c_1} = \sqrt{2}$.

As was pointed out earlier, the theoretical results (9.61)–(9.63) have been checked extensively experimentally in quasi-1- and 2-d systems and even in 3-d systems. For 2-d systems (thin films and interfaces) the experimental data [338–347] are in very good agreement with the theoretical results. For thin wires (quasi-1-d systems) the agreement is less impressive [348–353]. The situation is less clear for 3-d systems, where the theory is not well founded and the experimental data are limited to only impurity bands in semiconductors [328, 329, 333, 354]. Overall one can say that the scaling approach of Thouless [251] and of Abrahams et al. [319] has played a significant role in the field, and it has received strong experimental evidence in its support. Further support was given to it by various independent approximate theoretical and numerical treatments. Thus, although it is not a rigorous theory, it seems to be well accepted as a tool for studying the role of disorder in transport properties. However, there are already indications [265, 345–347, 355] suggesting that some of the basic assumptions of the method may not be generally true: e.g., spin-orbit scattering seems to *change the sign* of A_2 in (9.62) and to reduce its magnitude by two [265, 345–347, 355]. Thus the monotonicity of β vs. $\ln Q$ is not valid in the presence of an external magnetic field (which breaks the time reversal) or in the presence of spin-orbit interactions. As was mentioned before, in those cases, extended states at the center of a band of 2-d systems seem to survive up to a critical value of the disorder. The other basic assumption of the scaling approach, i.e., the one-parameter scaling, although accurate enough, does not seem to be exact. For a recent numerical study of this assumption see the article by Ohtsuki and Slevin [336].

Note that a full knowledge of β vs. $\ln Q$ would allow us to know both the critical value of Q in 3-d as well as the critical exponent, s , for the vanishing of the conductivity at a mobility edge:

$$\sigma(E) \sim (|E_c| - |E|)^s, \quad |E| \rightarrow |E_c|^- . \quad (9.64)$$

The critical exponent, s , which in the framework of the one-parameter scaling theory is equal to γ [where $-\gamma$ is the critical exponent of ξ' ; see also (9.31)] is given by

$$s = \frac{1}{Q_c (d\beta/dQ)_c}, \quad (9.65)$$

where Q_c is the critical value of Q such that $\beta(Q_c) = 0$. An approximate formula for β vs. Q for $d = 3$, which reproduces the correct behavior for the two limiting values, $Q \ll 1$ and $Q \gg 1$, and interpolates in between, is

$$\beta \simeq 2 - \left(1 + \frac{\pi^2 Q}{2}\right) \ln \left(1 + \frac{2}{\pi^2 Q}\right). \quad (9.66)$$

Based on (9.66) we get $\ln Q_c \simeq -2.96$ and $s \simeq 1.68$; accurate numerical estimates give $s \simeq 1.54 \pm 0.03$ [335, 336].

9.6 Other Computational Techniques

The question of localization has been studied extensively by various numerical techniques. In this subsection no attempt will be made to cover this diverse subject. The interested reader is referred to some of the original literature. Most of the authors supplemented their theoretical analysis with numerical computations that are consistent with the picture we already described. For higher-dimensional systems the initial numerical results can hardly be called conclusive because of the relatively small sizes of the samples; nevertheless, they were not inconsistent with the prevailing ideas in the field.

Yoshino and Okazaki [356] and Yonezawa [357] have found eigenenergies and corresponding eigenfunctions of finite 2-d (100×100) TBMs by direct diagonalization of the matrix equation; they took advantage of the fact that most of the matrix elements are zero. Licciardello and Thouless [320] examined numerically the sensitivity of the eigenenergies to changing boundary conditions. Stein and Krey [358, 359] implemented numerically the recursion method [223], according to which higher-dimensional disordered systems are mapped to 1-d systems with a much more complicated disorder; the 1-d systems are usually treated through the iteration (or continued fractions) to be presented in Sect. 9.7. Weaire and Srivastava [360] examined numerically the time evolution of a random trial function and used their results to draw conclusions about localization. Prelovšek [361, 362] employed a diffusion simulation technique. Lee [363, 364] and Sarker and Domany [321] implemented numerically the scaling ideas presented in §9.6.1; their results showed that $d = 2$ seems to be a borderline dimensionality but were nevertheless inconclusive regarding what is happening for $d = 2$.

There has also been considerable activity in trying to find the connection between the localization question and other extensively studied problems, where the borderline dimensionality is $d = 2$. As in the previous paragraph, we do not attempt to cover this diverse subject here; we only refer the interested reader to some of the original literature. Allen [365] connected the localization problem to the random-walk problem, in particular to $S(N)/N$, where $S(N)$ is the mean number of distinct sites visited during a random walk of N steps. Then $S(N)/N$ goes to zero as $N \rightarrow \infty$ for $d \leq 2$, while it remains finite for $d > 2$. Kaveh and Mott [262, 322, 366, 367] obtained the vertex corrections to the conductivity (9.61)–(9.63) by mapping the problem to the classical diffusion process. Wegner [323–325], Hikami [332], Efetov et al. [327], and Houghton et al. [326] have demonstrated that the localization problem is analogous to the nonlinear σ -model; then they employed sophisticated field-theoretical techniques to reach conclusions that are in agreement with the scaling approach. Schuster [368] pursued an analogy with the XY model; such an analogy, although in agreement with the conclusions of Pichard and Sarma [369, 370], is inconsistent with the numerical results of MacKinnon and Kramer [371] and of Soukoulis et al. [372], as well as with the conclusions of the scaling approach. The recursion method, which

maps the problem to a 1-d one, produces results [373–375] that are consistent with the prevailing ideas in the field. We mention also the work of Götze [272, 273].

9.6.1 Quasi-One-Dimensional Systems and Scaling

The most reliable numerical method for checking the scaling assumption and for producing results for various quantities of interest (such as critical disorder, mobility-edge trajectories, critical exponents, etc.) is the one proposed and applied by Pichard and Sarma [369, 370] and MacKinnon and Kramer [371] and reviewed by Kramer and Mackinnon [376]. Several other authors have used and extended this approach: Soukoulis et al. [372], Economou et al. [277, 377, 378], Zambetaki et al. [379], Q. Li et al. [380], Römer and Schreiber [335], Ohtsuki and Slevin [336], Kawabata [337], and many others (see references in a recent book edited by Brandes and Kettermann [381]).

The method determines numerically the longest localization length, λ_M , of a quasi-1-d system consisting of either M coupled channels arranged in a planar strip or $M \times M$ coupled channels forming a wire of a $Ma \times Ma$ square cross section (a is the lattice spacing). The probability distribution of the diagonal matrix elements is rectangular of total width W . For the wire case (which becomes 3-d as $M \rightarrow \infty$) the behavior depends on whether or not the disorder exceeds a critical value. For $W < W_c$, $\lambda_M(M)$ behaves as $M^2 a^2 / 4.82 \xi'$ (up to the largest M examined), and hence it seems to approach infinity parabolically as $M \rightarrow \infty$; the characteristic length ξ' (which depends on the disorder) can tentatively be given a physical interpretation as being the largest length beyond which the eigenfunctions look uniform in amplitude. Since a uniform amplitude implies a classical metallic behavior, the quantity ξ' can also be interpreted as the length (for a given disorder) at which β is almost 1. For $W > W_c$, $\lambda_M(M)$ increases with M slower than linearly, and it seems to saturate to a value $\lambda(\infty)$, which is the localization length ξ . For the strip case (which becomes 2-d as $M \rightarrow \infty$) $\lambda_M(M)$ increases with M slower than linearly and it seems to saturate to a finite value at least to disorders down to $W/|V| = 4$ [371]. Around $W/|V| \approx 6$ (which early work identified as a critical point), the localization length seems to change very fast (e.g., $\lambda \approx 40$ for $W/|V| = 6$, while $\lambda \approx 500$ for $W/|V| = 4$). Such large localization lengths make conclusive numerical work rather difficult. For a recent review, including various references, the reader is referred to [335, 376].

9.6.2 Level Spacing Statistics

This numerical method is based on the following basic difference between extended and localized eigenstates. Consider two localized eigenstates ψ_i and ψ_{i+1} belonging to *consecutive* eigenenergies; since the states are localized, we expect, with a probability that approaches 1 as the system becomes infinite,

that these two states will not overlap. On the contrary, if the states were extended, their overlap would be substantial. Thus

$$\langle \psi_i | \mathcal{H}_1 | \psi_{i+1} \rangle \simeq 0, \text{ if } \psi_i, \psi_{i+1} \text{ localized,}$$

while

$$\langle \psi_i | \mathcal{H}_1 | \psi_{i+1} \rangle \simeq \langle \psi_i | \mathcal{H}_1 | \psi_i \rangle \neq 0, \text{ if } \psi_i, \psi_{i+1} \text{ extended,}$$

where \mathcal{H}_1 is any perturbation. As a result of this basic difference, there is no level repulsion for localized states, in contrast to the case of extended states. This means that the probability distribution of consecutive level spacing is quite different for localized states (where very small values of level spacing are probable) and extended states (where very small values of level spacing are quite improbable), as shown in Fig. 9.6. This probability distribution can be obtained by diagonalizing an appropriately large number of realizations of the Hamiltonian of a finite segment of the random system under study. Note that, while the maximum possible size of this segment is adequate to show the difference in the probability distribution of level spacing, it is too small, in general, to determine directly by the calculation of the eigenstates whether the latter are localized or extended.

9.7 Localization and Green's Functions

Green's function techniques are heavily involved in the calculation of transport properties in general and in the localization problem in particular. Besides the examples we have already considered in Chaps. 8 and 9, Green's functions are used to obtain the longest localization length, ξ , in quasi-1-d systems

$$\frac{1}{\xi} = - \lim_{L \rightarrow \infty} \frac{1}{L} \langle \ln |G_{1L}^+(E)| \rangle, \quad (9.67)$$

where the calculation of the Green's function is obtained either from the equation of motion or by techniques analogous to those used in the transfer matrix approach.

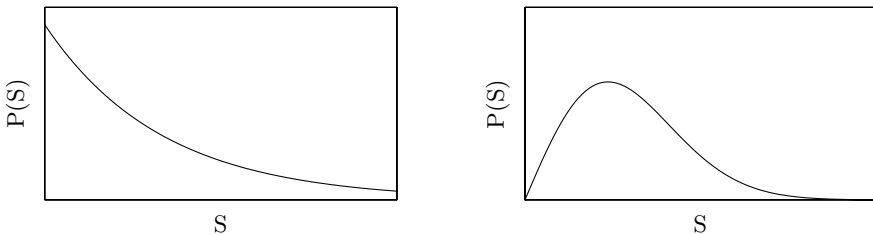


Fig. 9.6. The probability distribution of consecutive level spacing is quite different for localized (*left*) and extended (*right*) eigenstates

In this section we shall examine some examples where Green's functions are used to calculate transport and localization quantities of physical interest.

9.7.1 Green's Function and Localization in One Dimension

In this subsection we shall employ the renormalized perturbation expansion (RPE) (Appendix F) to obtain the 1-d Green's function. According to (F.6) we have

$$G(\ell, m) = G(\ell, \ell)VG(\ell + 1, \ell + 1[\ell])V \cdots G(m, m[m - 1]). \quad (9.68)$$

In writing (9.68) we have taken into account that there is only one self-avoiding path connecting ℓ to m in one dimension, and that $G(n, n[n - 1])$ does not depend on $\varepsilon_{n-2}, \varepsilon_{n-3}, \dots$. From (F.12) and (F.13) we have in the present case (where $K = 1$)

$$G(\ell + 1, \ell + 1[\ell]) = \frac{1}{E - \varepsilon'_{\ell+1} - V^2 G(\ell + 2, \ell + 2[\ell + 1])}. \quad (9.69)$$

Equation (9.69) allows us to express the probability distribution of $x \equiv G(\ell + 1, \ell + 1[\ell])$, $f_{\ell+1}(x; E)$, in terms of the probability distribution of $\varepsilon'_{\ell+1}$, $p(\varepsilon'_{\ell+1})$ and the probability distribution of $x' \equiv G(\ell + 2, \ell + 2[\ell + 1])$, $f_{\ell+2}(x'; E)$. The result is (in units where $|V| = 1$)

$$f_{\ell+1}(x; E) = \frac{1}{x^2} \int p \left(E - x' - \frac{1}{x} \right) f_{\ell+2}(x') dx'. \quad (9.70)$$

Because each site is equivalent on average, $f_{\ell+1} = f_{\ell+2} = f$. Thus (9.70) is an integral equation for f . From (9.67) and (9.68) we have (taking the lattice spacing $a = 1$)

$$\xi^{-1} = - \langle \ln |G(\ell + 1, \ell + 1[\ell])| \rangle = - \int_{-\infty}^{\infty} f(x; E) \ln |x| dx. \quad (9.71)$$

Substituting in (9.71) from (9.70) and changing variables, we can recast the expression for the inverse localization length, ξ^{-1} , in the following form:

$$\xi^{-1} = \frac{1}{2} \int_{-\infty}^{\infty} d\varepsilon \int_{-\infty}^{\infty} dx p(E + \varepsilon) f(x) \ln \left| 1 + \frac{\varepsilon}{x} \right|, \quad (9.72)$$

which is more convenient in the weak disorder regime. An alternative but equivalent expression for ξ^{-1} can be obtained by observing that the product in (9.68) can be expressed in terms of the eigenenergies of \mathcal{H} and those of \mathcal{H} with the sites $\ell, \ell + 1, \dots, m$ removed [see (F.18)]. When the states are localized and $|\ell - m| \rightarrow \infty$, the eigenenergies of \mathcal{H} can be separated into three groups: those associated with the semi-infinite segment to the left of ℓ , those associated

with the segment to the right of m , and those associated with the segment $\ell, \ell + 1, \dots, m$. Only the latter do not cancel in (F.18). Hence

$$\begin{aligned}\xi^{-1} &= \lim_{|\ell-m| \rightarrow \infty} \frac{1}{|\ell-m|} \left\langle \sum_j \ln |E - E_j| \right\rangle \\ &= \lim_{|\ell-m| \rightarrow \infty} \int_{-\infty}^{\infty} dE' \left\langle \frac{\sum_j \delta(|E' - E_j|)}{|\ell-m|} \right\rangle \ln |E - E'| \\ &= \int_{-\infty}^{\infty} \langle \varrho(E') \rangle \ln |E - E'| dE' .\end{aligned}\tag{9.73}$$

Equation (9.73) was first obtained by Thouless [382]. We point out that the average DOS per site,

$$\langle \varrho(E') \rangle = -\text{Im} \left\{ \frac{\langle G^+(\ell, \ell; E') \rangle}{\pi} \right\} ,$$

can be expressed in terms of $f(x)$ since $\Delta(\ell; E')$ in (F.10) is

$$\Delta(\ell; E') = V^2 G(\ell + 1, \ell + 1[\ell]) + V^2 G(\ell - 1, \ell - 1[\ell]) .\tag{9.74}$$

Hence (in units where $|V| = 1$)

$$\begin{aligned}\langle \varrho(E') \rangle &= \langle \delta(E' - \varepsilon_\ell - \Delta(\ell; E')) \rangle \\ &= \int d\varepsilon_\ell dx dx' p(\varepsilon_\ell) f(x; E') f(x'; E') \delta(E' - \varepsilon_\ell - x - x') \\ &= \int_{-\infty}^{\infty} dy f(y; E') f(1/y; E') .\end{aligned}\tag{9.75}$$

The last step follows by integrating over ε_ℓ , taking (9.70) into account, and changing the remaining integration variable from x to $y = 1/x$.

As an application of (9.72) we shall calculate ξ^{-1} to order σ^2 (where $\sigma^2 = \langle \varepsilon^2 \rangle$) at $E = 0$. To this order $f(x)$ in (9.72) can be replaced by $f_0(x)$, where $f_0(x)$ is the limit of $f(x)$ as $\sigma \rightarrow 0$. From (9.70) we find that

$$f_0(x) = \frac{1}{x^2} f_0(-1/x) ,\tag{9.76}$$

the solution of which is

$$f_0(x) = \frac{C}{\sqrt{1+x^4}} ;\tag{9.77}$$

the normalization constant $C = [2\mathcal{K}(\sqrt{1/2})]^{-1} \approx 0.27$. Substituting (9.77) in (9.72) and performing the integration we find (to order σ^2)

$$\xi^{-1} = \frac{2\mathcal{E}(\sqrt{1/2}) - \mathcal{K}(\sqrt{1/2})}{4\mathcal{K}(\sqrt{1/2})} \sigma^2 \approx 0.1142\sigma^2 .\tag{9.78}$$

For the rectangular distribution, where $\sigma^2 = W^2/12$, (9.78) becomes $\xi = 105.045/W^2$. This result was first obtained through different methods by Karpus and Wegner [383] and by Sarker [384].

Economou and coworkers [385–387] obtained with a similar technique an integral equation for the joint probability distribution of

$$x = \lim_{s \rightarrow 0^+} \operatorname{Re} \{G(\ell + 1, \ell + 1[\ell]; E + is)\}$$

and

$$y = - \lim_{s \rightarrow 0^+} \operatorname{Im} \left\{ \frac{G(\ell + 1, \ell + 1[\ell]; E + is)}{s} \right\}.$$

This allowed them to obtain averages of transport quantities like $sG^+(\ell, m; E + is) \times G^-(m, \ell; E - is)$ [see (9.92) below]; on the basis of their results they concluded that in the weak disorder limit the eigenfunctions are concentrated in a very small fraction of length ξ . To be more specific, let us introduce $L_e \equiv \left(\sum_m |\psi_m|^4\right)^{-1}$ as a measure of the number of sites participating in the eigenfunction $|\psi\rangle = \sum_m \psi_m |m\rangle$. Economou and coworkers [385–387] found that while $\xi \sim W^{-2}$ as $W \rightarrow 0$, the quantity L_e seems to behave like $W^{-\nu}$ with ν very close to 1.

Finally, we comment on the connection between the localization length ξ and the scattering mean free path ℓ . The latter is defined as

$$\ell = v\tau = \frac{\hbar v}{2|\Sigma_2|},$$

where v is the velocity at energy E . The so defined mean free path ℓ determines the exponential decay of the average of $G(m, n; E)$ or of $\psi_m \psi_n$, i.e.,

$$\langle G(m, n; E) \rangle \sim \langle \psi_m \psi_n \rangle \sim e^{-|m-n|a/2\ell}, \quad |m-n| \rightarrow \infty. \quad (9.79)$$

We remind the reader that the transport mean free path $\ell_{\text{tr}} = v\tau_{\text{tr}}$ is in general different from ℓ because of the $(1 - \cos\theta)$ term in (8.22). However, for the simple model we consider here $\ell_{\text{tr}} = \ell$. In 1-d, where θ takes only two values ($\theta = 0$, forward scattering, and $\theta = \pi$, backward scattering), ℓ^{-1} can be decomposed into two terms, ℓ_f^{-1} and ℓ_b^{-1} , corresponding to forward and backward scattering:

$$\ell^{-1} = \ell_f^{-1} + \ell_b^{-1}, \quad (9.80)$$

$$\ell_{\text{tr}}^{-1} = 2\ell_b^{-1}. \quad (9.81)$$

For our simple model, $\ell_f = \ell_b = 2\ell = 2\ell_{\text{tr}}$. In the weak scattering limit, using second-order perturbation expansion [see (7.51)], and taking into account that

$$\hbar v/a = |G_0(m, m)|^{-1} = \sqrt{(2V)^2 - E^2},$$

we find

$$\ell \approx \frac{a [(2V)^2 - E^2]}{2\sigma^2}, \quad (9.82)$$

where a is the lattice spacing and $\sigma^2 = \langle \varepsilon'_n{}^2 \rangle$. For a rectangular distribution of width W and at the center of the band ($E = 0$) we have (setting $a = 1$, $|V| = 1$)

$$\ell \approx 24/W^2. \quad (9.83)$$

Second-order perturbation theory gives

$$\langle \varrho(E') \rangle = -\text{Im} \left\{ \frac{G_0^+(m, m; E - \Sigma)}{\pi} \right\},$$

with $\Sigma = \sigma^2 G_0(m, m; E)$ [see (7.51)]. Substituting in (9.73) and integrating by parts one obtains

$$\xi \approx -\frac{2a}{\sigma^2 G_0^2(m, m; E)} = \frac{2a(4V^2 - E^2)}{\sigma^2}, \quad (9.84)$$

which is four times the mean free path ℓ . In the rectangular case and at the center of the band, one obtains $\xi = 96/W^2$ [251], to be compared with $\xi = 105.045/W^2$, which is the exact result to second order in W . An explanation of this discrepancy is given in [383].

It must be pointed out that the decay shown in (9.79) is partly due to the exponential decay of the amplitude (localization) and partly due to the phase incoherence among different members of the ensemble over which the average of $G(m, n)$ is taken [see (9.79)]. The latter is present even when there is no localization, and hence the exponential decay of $\langle G(m, n; E) \rangle$ as $|m - n| \rightarrow \infty$ cannot be used to deduce the existence of localization. To see the extent to which the decay shown in (9.79) is due to localization, one may consider the average

$$\langle |G(m, n; E)| \rangle \sim \langle |\psi_m \psi_n| \rangle \sim e^{-|m-n|/\lambda'}. \quad (9.85)$$

To calculate λ' one may approximately assume that $\ln |G(m, n; E)|$ has a Gaussian probability distribution with mean equal to $-|m - n|/\xi$ and standard deviation equal to $\sqrt{|m - n|/\xi}$. Then $\lambda' = 2\xi$, which to second order in W^2 and at the center of the band yields $\lambda' = 210.09/W^2$, to be compared with $\lambda' = 212.59/W^2$ obtained in [383].

9.7.2 Renormalized Perturbation Expansion (RPE) and Localization

Green's functions behave differently depending on whether the eigenstates are localized or extended. An example of such difference has already been encountered in 1-d, where for exponentially localized eigenstates $\langle \ln |G(\ell, m)| \rangle \sim -| \ell - m | / \lambda'$, while for extended states $\ln |G(\ell, m)|$ is independent of $|m - \ell|$, (5.31).

Before we proceed, let us further clarify the concepts of extended and localized eigenstates. We call extended those eigenstates that do not decay to zero at infinity; furthermore, we assume that these extended states look more or less uniform in amplitude at least beyond a characteristic length scale ξ' . On the other hand, we define localized states as those that decay to zero "sufficiently fast." There is no rigorous examination of what decay law qualifies for this characterization. It seems that exponential decay is "fast enough"; it is even possible that all normalizable eigenfunctions are localized in the above sense. These definitions leave in principle the possibility of having eigenstates that are neither extended nor localized in the above sense. A decaying but not normalizable eigenstate is an example of such an intermediate situation. It is usually assumed that the eigenstates will be either exponentially localized or extended. In 1-d this assumption is true in almost all cases. For higher dimensionalities there is no rigorous proof.

Let us consider here a finite system consisting of N unit cells. The diagonal matrix element of $G(E; N)$ in a Wannier representation can be written as

$$G(\mathbf{m}, \mathbf{m}; z; N) = \sum_{\nu} \frac{f_{\nu}}{z - E_{\nu}}, \quad (9.86)$$

where

$$f_{\nu} = \langle \mathbf{m} | \nu \rangle \langle \nu | \mathbf{m} \rangle, \quad (9.87)$$

and $|\nu\rangle$ is an eigenfunction of the Hamiltonian \mathcal{H} with eigenvalue E_{ν} ; we have dropped the index \mathbf{m} from f_{ν} for simplicity. Note that the symbol \sum_{ν} in (9.86) denotes a genuine summation since we are dealing with a finite system that possesses a discrete spectrum.

We consider now the limit $N \rightarrow \infty$, i.e., we allow the system to become infinite. A localized eigenstate $|\nu\rangle$ tends to a well-defined limit as $N \rightarrow \infty$; hence, if $|\nu\rangle$ is localized, $f_{\nu} \rightarrow f_{\nu}^{\infty}$ as $N \rightarrow \infty$, where f_{ν}^{∞} is in general a positive quantity. The magnitude of f_{ν}^{∞} (for localized eigenstates) depends strongly on how far away from site \mathbf{m} the localized state $|\nu\rangle$ is. If we assume exponential decay of the localized eigenfunctions, then $f_{\nu} \sim \exp(-2r_{\mathbf{m}\nu}/\xi_{\nu})$ as $r_{\mathbf{m}\nu} \rightarrow \infty$, where $r_{\mathbf{m}\nu}$ is the distance between site \mathbf{m} and the center of the localized state $|\nu\rangle$ and ξ_{ν} is its localization length; thus, the new f_{ν}^{∞} s that appear as $N \rightarrow \infty$ are extremely small since the distance $r_{\mathbf{m}\nu}$ of the new states $|\nu\rangle$ is proportional to $N^{1/d}a$, where a is the linear dimension of the unit cell. On the other hand, for extended or propagating eigenstates $|\nu\rangle$ (in the limit $N \rightarrow \infty$) the quantity f_{ν} behaves as $1/N$ in the limit $N \rightarrow \infty$; this behavior stems from the normalization factor $1/\sqrt{N}$ contained in every extended eigenstate $|\nu\rangle$. This basic difference in the behavior of f_{ν} as $N \rightarrow \infty$ produces the following characteristic properties.

Consider the quantity $c_{\mathbf{m}}(t)$, which is the probability amplitude for finding a particle in state $|\mathbf{m}\rangle$ at time t if initially ($t = 0$) the particle was in $|\mathbf{m}\rangle$.

This quantity was evaluated before and is given by (6.34). Substituting (9.86) into (6.34) we obtain

$$c_{\mathbf{m}}(t) = \sum_{\nu} f_{\nu} \exp(-iE_{\nu}t/\hbar). \quad (9.88)$$

The probability $|c_{\mathbf{m}}(t)|^2$ is

$$|c_{\mathbf{m}}(t)|^2 = \sum_{\nu\nu'} f_{\nu} f_{\nu'} \exp[-i(E_{\nu} - E_{\nu'})t/\hbar]. \quad (9.89)$$

Defining

$$|c_{\mathbf{m}}|^2 = \lim_{t \rightarrow \infty} \frac{1}{t} \int_0^t |c_{\mathbf{m}}(t')|^2 dt', \quad (9.90)$$

we obtain

$$|c_{\mathbf{m}}|^2 = \sum_{E_{\nu}} \sum_{i=1}^{g_{\nu}} \sum_{i'=1}^{g_{\nu}} f_{E_{\nu,i}} f_{E_{\nu,i'}}, \quad (9.91)$$

where g_{ν} is the degeneracy of the eigenenergy E_{ν} .

Using (9.86) it is easy to show that

$$|c_{\mathbf{m}}|^2 = \frac{s}{\pi} \int_{-\infty}^{\infty} dE G(\mathbf{m}, \mathbf{m}; E + is) G(\mathbf{m}, \mathbf{m}; E - is). \quad (9.92)$$

Equation (9.91) shows that the localized eigenstates make a nonzero contribution to the probability $|c_{\mathbf{m}}|^2$, while the extended eigenstates make no contribution to $|c_{\mathbf{m}}|^2$ as $N \rightarrow \infty$. Indeed, if all states were extended and nondegenerate, then all $f_{\nu} \sim 1/N$, and consequently

$$\sum_{\nu} f_{\nu}^2 \sim \sum_{\nu} \frac{1}{N^2} \sim \frac{1}{N}$$

(there are N terms in the summation). If the degeneracy, g_{ν} , is proportional to $N^{(d-1)/d}$ (which is probably its largest value), then the contribution of the extended states to $|c_{\mathbf{m}}|^2$ still goes to zero for $N \rightarrow \infty$ (as $N^{-1/d}$); d is the dimensionality. On the other hand, for localized eigenstates each f_{ν} tends to a definite limit and series (9.91) converges since f_{ν}^{∞} becomes quite small for eigenstates $|\nu\rangle$ appearing for large N . Equation (9.92), which is valid in the limit $s \rightarrow 0^+$ independently of whether or not the limit $N \rightarrow \infty$ has already been taken, shows that a branch cut in $G(E)$ makes no contribution to $|c_{\mathbf{m}}|^2$ and, hence, corresponds to states that are not localized. It is probably true, although no rigorous proof has been given, that a branch cut in $G(E)$ indicates a decay slower than $r^{-d/4}$. Under rather general conditions, it is true that extended states produce a branch cut in $G(E)$ (Problem 3.1s); this can be shown also by taking the limit $N \rightarrow \infty$ in (9.86); one must keep in mind that the average spacing of the levels goes as $1/N$ and f_{ν} (for extended states)

behaves as $1/N$ for $N \rightarrow \infty$. On the other hand, for localized eigenstates, the quantities f_ν approach a finite limit as $N \rightarrow \infty$, which means that in the limit of $N \rightarrow \infty$, we will have a dense distribution of poles whose residues remain finite; thus a line of singularity results that is not a branch cut and that is known as a natural boundary because the side limits $\lim G(E \pm is)$ do not exist as $s \rightarrow 0^+$.

Another way to distinguish between extended and localized eigenstates is to consider the convergence of $G(E)$ as $N \rightarrow \infty$. Note first that each term $f_\nu/(z - E_\nu)$ in (9.86) is important as $z \rightarrow E$ (where E belongs to the continuous spectrum), only if $|E - E_\nu| \leq Af_\nu$, i.e., if $E \in P_\nu$, where P_ν is the interval $[E_\nu - Af_\nu, E_\nu + Af_\nu]$ with $A \gg 1$. Then the contribution of all the terms with $\nu > \nu_0$ is important only if E belongs to the union \sum_0 of P_ν s with $\nu > \nu_0$. Assume now that the terms in (9.86) have been arranged in order of decreasing f_ν . For localized eigenstates the extent of the interval P_ν decreases at least as $r_{m\nu}^{-d-\varepsilon}$ (because the states are normalizable) with $\varepsilon > 0$ as $\nu \rightarrow \infty$. Hence the extent of the union \sum_0 approaches $N^{-\varepsilon/d}$, i.e., zero as $\nu_0 \rightarrow \infty$. Consequently, the probability of E belonging to \sum_0 approaches zero as $\nu_0 \rightarrow \infty$; hence series (9.86) converges as $N \rightarrow \infty$ with probability 1. It has been assumed that this last statement is equivalent to saying that for localized states the probability distribution of $G(E)$ converges as $N \rightarrow \infty$. For extended eigenstates the union \sum_0 approaches a nonzero value as $\nu_0 \rightarrow \infty$; this implies that for extended eigenstates $G(E)$ diverges with probability 1 as $N \rightarrow \infty$.

On the basis of the above discussion one can state certain criteria to decide about the nature of the eigenstates at E . These statements, although very plausible, cannot be considered as rigorously proven.

(i) Consider the quantity

$$\lim \langle sG(\mathbf{m}, \mathbf{m}; E + is) G(\mathbf{m}, \mathbf{m}; E - is) \rangle, \text{ as } s \rightarrow 0^+$$

or, more generally,

$$\lim \langle sG(\mathbf{m}, \mathbf{n}; E + is) G(\mathbf{n}, \mathbf{m}; E - is) \rangle, \text{ as } s \rightarrow 0^+.$$

If the above quantities are nonzero, the eigenstates at E are localized; if they approach zero linearly with s , the eigenstates are extended (or possibly very slowly decaying as $r^{-\nu}$ with $\nu \leq d/4$); if they approach zero more slowly than linearly with s , they probably decay as $r^{-\nu}$ with $d/4 \leq \nu \leq d/2$ (with logarithmic factors in s appearing when $\nu = d/2$ or $d/4$).

(ii) Consider the probability distribution of $G(E; N)$. If it converges as $N \rightarrow \infty$, the eigenstates at E are localized. If it diverges, the states are extended (or possibly slowly decaying but not normalizable).

(iii) Consider $G(\mathbf{m}, \mathbf{m}; E, N)$. If this quantity converges with probability 1 as $N \rightarrow \infty$, the states at E are localized. If it diverges, the states are extended (or possibly slowly decaying but not normalizable).

The first criterion has been employed in 1-d by Economou and coworkers [385–387]. We shall examine it in Problem 9.10s. The second criterion has been used in 1-d systems (§9.7.1). The third criterion was first used in conjunction with the renormalized perturbation expansion (RPE) by Anderson [388] in his paper that marked the birth of the field of localization. Anderson's work has been further developed by Ziman [389], Kikuchi [390], Herbert and Jones [391], Thouless [392], and Economou and coworkers [393, 394]. In all this work the RPE (presented in Appendix F) plays a key role; the reason is that the RPE is a closed expression for a finite system. Hence, its convergence or divergence as $N \rightarrow \infty$ is equivalent to the convergence or divergence of $G(\mathbf{m}, \mathbf{m}; E, N)$ as $N \rightarrow \infty$; the latter, according to (iii), is connected directly with the nature of the eigenstates.

According to (F.9), the RPE for the quantity $\Delta(\ell)$ has the structure

$$\Delta(\ell) = \sum_j t_j, \quad (9.93)$$

$$= \sum_{N=1}^{\infty} \sum_j' t_j^{(N)}, \quad (9.94)$$

where the summation in (9.93) is over all terms corresponding to self-avoiding paths starting from and ending at site ℓ . In (9.94) we have rearranged the series so as to perform first the summation over all paths of $N + 1$ steps and then sum from $N = 1$ to ∞ . We remind the reader that

$$t_j^{(N)} = V^{N+1} G(\mathbf{n}_1, \mathbf{n}_1[\ell]) G(\mathbf{n}_2, \mathbf{n}_2[\ell, \mathbf{n}_1]) \cdots, \quad (9.95)$$

where sites $\ell, \mathbf{n}_1, \mathbf{n}_2, \dots, \ell$ belong to the self-avoiding path j of $N + 1$ steps. The expansion (9.94) may diverge through two distinct mechanisms: one is the divergence of the series shown in (9.94); even if this series terminates (as in the 1-d case), the RPE may diverge as a result of the implicit iteration built in the RPE (Appendix F). Usually the assumption is made that the convergence of the series controls the convergence of the RPE; Abou-Chacra et al. [395] made the opposite assumption by terminating the series at $N = 1$ and explicitly taking into account the iteration procedure. To study the convergence of the series, one introduces the *localization function*, $L(E)$, defined by

$$L(E) = \lim_{N \rightarrow \infty} \left| \sum_j t_j^{(N)} \right|^{1/N}. \quad (9.96)$$

If $L(E)$ is less (more) than 1 with probability 1, then the series converges (diverges) in probability. Here it must be pointed out that there is the possibility of convergence (not absolute convergence) even when $L(E)$ is larger than 1. This possibility has been disregarded. To evaluate (9.96) one must make several approximations. First we set

$$L(E) \approx \tilde{L}(E), \quad (9.97)$$

where

$$\tilde{L}(E) = \lim_{N \rightarrow \infty} \left(\sum_j \left| t_j^{(N)} \right| \right)^{1/N}. \quad (9.98)$$

Equation (9.97) means that the sign fluctuations of the $t_j^{(N)}$ s are omitted. The second approximation is to replace each of the various G s in (9.95) by the first one

$$t_j^{(N)} \approx V^{N+1} G^N(\mathbf{n}_1, \mathbf{n}_1[\ell]). \quad (9.99)$$

The third approximation replaces the $G(\mathbf{n}_1, \mathbf{n}_1[\ell])$ by its CPA average. Thus $L(E)$ was calculated for various 3-d and 2-d lattices and various probability distributions of $\{\varepsilon'_n\}$. By setting $L(E) = 1$ one can obtain the trajectory of the mobility edge, i.e., the critical energy E_c separating extended from localized states as a function of the disorder or, equivalently, the critical disorder as a function of the energy (Fig. 9.1). The results were consistent with numerical data and with various limiting cases. The main drawback of the final result for $L(E)$ is that it failed to predict any qualitative difference between $d = 2$ and $d = 3$. To check the origin of this failure, Soukoulis and Economou [396] reexamined the three approximations mentioned above. In the process they prove (F.19), which allowed them to relax approximation (9.99); they worked in the limit of zero disorder so that no average was needed; and finally they calculated both $L(E)$ and $\tilde{L}(E)$. At the ends of the spectrum they found that $\tilde{L}(E) = L(E) \approx 1$ (with less than 1% error), which indicates that their calculations are quite accurate. For $d = 3$, they found that (9.97) is well satisfied and that $\tilde{L}(E)$ is well above 1 within the band, which shows that a finite amount of disorder is required to make $L(E) < 1$ and localize the eigenstates. In contrast, for a 2-d lattice, it was found that, while $\tilde{L}(E)$ is well above 1 within the band, $L(E)$ is (within numerical uncertainties) equal to 1. This is a strong indication that any amount of disorder, no matter how small, is enough to localize the states in 2-d. It was suggested [396] that the equation $\tilde{L}(E) \approx 1$ indicates a crossover region where the localization length varies very fast.

9.7.3 Green's Functions and Transmissions in Quasi-One-Dimensional Systems

In this subsection we expand further the topic presented in Sect. 9.4 and connect the quantity \hat{t}_{pqij} with the Green's function associated with a multilead, multichannel-per-lead system as shown schematically in Fig. 9.7.

The S -matrix as we defined it here [see (H.21)] connects the outgoing current amplitudes $\hat{D}_{pi} = \sqrt{v_{pi}} D_{pi}$ to the incoming current amplitudes $\hat{C}_{pj} = \sqrt{v_{qj}} C_{qj}$

$$\hat{D}_{pi} = \sum_q \sum_j \hat{s}_{pqij} \hat{C}_{qj}. \quad (9.100)$$

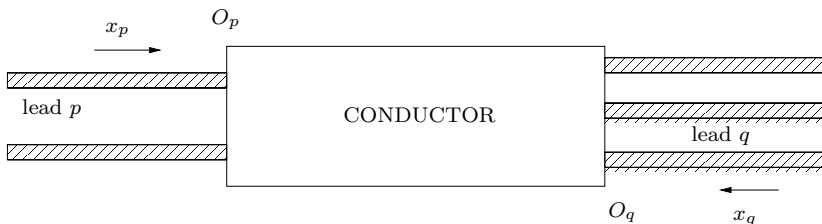


Fig. 9.7. The eigenfunctions associated with each lead p are either incoming of the form $C_{pi}\chi_{pi} \exp(ik_i x_p) / \sqrt{L_0}$ or outgoing of the form $D_{pi}\chi_{pi} \exp(-ik_i x_p) / \sqrt{L_0}$. The normalized wave functions χ_{pi} depend in general on the cartesian coordinates y_p and z_p , normal to the propagation direction. The eigenenergy $\varepsilon_{pi k_i}$ of the two states $|p, i, \pm k_i\rangle$ is of the form $\varepsilon_{pi k_i} = \varepsilon_{pi0} + \varepsilon_{pi}(k_i)$; usually $\varepsilon_{pi}(k_i) = \hbar^2 k_i^2 / 2m_i$

The quantities \hat{s}_{ppij} represent reflection current amplitudes, $\hat{s}_{ppij} = \hat{r}_{pij}$, while \hat{s}_{pqij} for $p \neq q$ represent transmission current amplitudes, $\hat{s}_{pqij} = \hat{t}_{pqij}$, from the j channel of the q lead to the i channel of the p lead.

We examine first the idealized case where each lead is strictly 1-d and as such sustains only one channel (or mode); thus index i drops out. Taking matrix elements of (4.17),² $G = G_0 + G_0 T G_0$, and remembering that³

$$\langle p, x_p | G_0 | q, x_q \rangle = \left(-\frac{i}{\hbar v_p} \right) \delta_{pq} \exp(ik |x_p + x_q|),$$

we obtain

$$\begin{aligned} \langle p, x_p | G | q, x_q \rangle &= \delta_{pq} \frac{-i}{\hbar v_p} \exp(ik_p |x_p + x_q|) \\ &+ \frac{-i}{\hbar v_p} \frac{-i}{\hbar v_q} \\ &\times \int dx'_p dx'_q \exp(ik_p |x_p - x'_p|) \exp(ik_q |x_q - x'_q|) \langle x_p | T | x_q \rangle. \end{aligned} \quad (9.101)$$

With the choice of coordinate systems shown in Fig. 9.7 we have $x_p < 0$, $x_q < 0$, $x_q < x'_q$, and $x_p < x'_p$. Thus

$$\begin{aligned} \langle p, x_p | G | q, x_q \rangle &= \frac{-i}{\hbar v_q} \exp[-i(k_p x_p + k_q x_q)] \\ &\times \left[\delta_{pq} + \frac{-i}{\hbar v_p} \int dx'_p dx'_q \exp(ik_p x'_p) \exp(ik_q x'_q) \langle x'_p | T | x'_q \rangle \right]. \end{aligned} \quad (9.102)$$

The integral over $dx'_p dx'_q$ can be written as follows:

$$L_0 \int dx'_p dx'_q \langle -k_p | x'_p \rangle \langle x'_p | T | x'_q \rangle \langle x'_q | k_q \rangle = \langle -k_p | T' | k_q \rangle, \quad (9.103)$$

² Everywhere G , G_0 , and T stand for G^+ , G_0^+ , T^+ .

³ When $p = q$, the origins O_p and O_q of the coordinate systems coincide and $x_q = -x'_p$.

where $T' = L_0 T$. Thus the quantity in brackets on the rhs of (9.102) equals, according to (H.26), the transmission amplitude⁴

$$t_{pq} = \delta_{pq} + \frac{-i}{\hbar v_p} \langle -k_p | T' | k_q \rangle . \quad (9.104)$$

For the reflection amplitude, r_{pp} , we have

$$r_{pp} = \frac{-i}{\hbar v_p} \langle -k_p | T' | k_p \rangle . \quad (9.105)$$

Combining (9.102)–(9.104) we end up with

$$\hat{t}_{pq} = \sqrt{\frac{v_p}{v_q}} t_{pq} = i\hbar \sqrt{v_p v_q} \exp [i(k_p x_p + k_q x_q)] G_{pq}(x_p, x_q) , \quad (9.106a)$$

$$\hat{r}_{pp} = r_{pp} = -\delta_{pq} + i\hbar v_p \exp (ik_p |x_p - x_p''|) G_{pq}(x_p - x_p''), \quad (9.106b)$$

$p = q, \quad \text{but } x_p \text{ is, in general, different from } x_q,$

where $G_{pq}(x_p, x_q) = \langle p, x_p | G | q, x_q \rangle$. Since t_{pq} is independent of x_p, x_q , and x_p'' , we can set $x_p = x_q = x_p'' = 0$ in (9.106a) and (9.106b).

For the multichannel case, (9.106a) and (9.106b) are generalized as follows:

$$\hat{t}_{pqij} = \sqrt{\frac{v_{pi}}{v_{qj}}} t_{pqij} = i\hbar \sqrt{v_{pi} v_{qj}} \exp [i(k_{pi} x_p + k_{qj} x_q)] \\ \times \int d\boldsymbol{\rho}_p d\boldsymbol{\rho}_q \chi_{pi}^*(\boldsymbol{\rho}_p) G_{pq}^+(\mathbf{r}_p, \mathbf{r}_q) \chi_{qj}(\boldsymbol{\rho}_q), \quad (9.107)$$

where $\mathbf{r}_\ell = x_\ell, \boldsymbol{\rho}_\ell, \ell = p, q$.

For \hat{r}_{ppi} we have to set $p = q$ and $x_q = -x_p''$ and add $-\delta_{ij}$ to the rhs of (9.107). Using (9.107) and setting $x_p = x_q = 0$, the quantity $\bar{T}_{pq} = \text{Tr} \{ \hat{t}_{pq} \hat{t}_{pq}^\dagger \}$ becomes

$$\bar{T}_{pq} = \sum_i \sum_j \hat{t}_{pqij} (\hat{t}_{pq}^\dagger)_{ji} \\ = \sum_{ij} \int d\boldsymbol{\rho}_p d\boldsymbol{\rho}_q d\boldsymbol{\rho}'_p d\boldsymbol{\rho}'_q \chi_{qj}(\boldsymbol{\rho}_q) \hbar v_{qj} \chi_{qj}^*(\boldsymbol{\rho}'_q) G_{qp}^-(\boldsymbol{\rho}'_q, \boldsymbol{\rho}_p) \\ \times \chi_{pi}(\boldsymbol{\rho}'_p) \hbar v_{pi} \chi_{pi}^*(\boldsymbol{\rho}_p) G_{pq}^+(\boldsymbol{\rho}_p, \boldsymbol{\rho}_q) . \quad (9.108)$$

We define

$$\Gamma_q(\boldsymbol{\rho}_q, \boldsymbol{\rho}'_q) = \sum_j \chi_{qj}(\boldsymbol{\rho}_q) \hbar v_{qj} \chi_{qj}^*(\boldsymbol{\rho}'_q) , \quad (9.109a)$$

$$\Gamma_p(\boldsymbol{\rho}'_p, \boldsymbol{\rho}_p) = \sum_i \chi_{pi}(\boldsymbol{\rho}'_p) \hbar v_{pi} \chi_{pi}^*(\boldsymbol{\rho}_p) , \quad (9.109b)$$

⁴ The bra $\langle -k_p |$ appears instead of the $\langle k_p |$ of (H.26) because of the opposite direction of the x_p -axis (Fig. 9.7).

and then we have

$$\bar{T}_{pq} = \text{Tr} \{ \Gamma_q G_{qp}^- \Gamma_p G_{pq}^+ \} = \text{Tr} \{ \Gamma_p G_{pq}^+ \Gamma_q G_{qp}^- \} , \quad (9.110)$$

where Tr means integrations over \mathbf{q}'_p , \mathbf{q}_p , \mathbf{q}_q , and \mathbf{q}'_q . In the case of a discrete system described by a TBM, (9.108)–(9.110) remain valid with the replacements

$$\begin{aligned} \mathbf{q}_\ell &\rightarrow \boldsymbol{\nu}_\ell a_\ell , \\ \mathbf{q}'_\ell &\rightarrow \boldsymbol{\nu}'_\ell a_\ell , \\ \hbar v_{\ell_i} &\rightarrow \hbar v_{\ell_i} / a_\ell , \\ \boldsymbol{\nu}_\ell &= (\nu_{\ell_2}, \nu_{\ell_3}) , \quad \boldsymbol{\nu}'_\ell = (\nu'_{\ell_2}, \nu'_{\ell_3}) , \quad \ell = p, q ; \end{aligned}$$

a_ℓ is the lattice spacing in the lead ℓ ; ν_{ℓ_2} , ν_{ℓ_3} , ν'_{ℓ_2} , and ν'_{ℓ_3} are integers determining the position of the atoms in the directions normal to x ; the eigenfunctions χ and the Green's functions G_{pq} are those corresponding to the TBH; finally, the trace operation in (9.110) means additions over the integers ν_{ℓ_2} , ν_{ℓ_3} , ν'_{ℓ_2} , and ν'_{ℓ_3} ($\ell = p, q$). For a 2-d TB system we have

$$\Gamma_\ell (\nu_{\ell_2}, \nu'_{\ell_2}) = \sum_i \chi_{\ell_i} (\nu_{\ell_2}) \frac{\hbar v_{\ell_i}}{a_\ell} \chi_{\ell_i}^* (\nu'_{\ell_2}) , \quad \ell = p, q , \quad (9.111)$$

$$\begin{aligned} \bar{T}_{pq} &= \sum_{\nu_{p_2}} \sum_{\nu'_{p_2}} \sum_{\nu_{q_2}} \sum_{\nu'_{q_2}} \Gamma_p (\nu'_{p_2}, \nu_{p_2}) G_{pq}^+ (\nu_{p_2}, \nu_{q_2}) \\ &\quad \times \Gamma_q (\nu_{q_2}, \nu'_{q_2}) G_{qp}^- (\nu'_{q_2}, \nu'_{p_2}) . \end{aligned} \quad (9.112)$$

9.8 Applications

We have already mentioned that the localization theory has found the most direct applications in the transport properties of thin wires, films, and interfaces. There are, however, classes of materials (such as quasi-1-d organic conductors [397], polymers [397,398], amorphous semiconductors [399,400], amorphous metals, etc. [400,401]) of high physical and/or technological importance that are, to some extent, disordered. The ideas and theoretical techniques presented in this chapter are indispensable tools in studying these materials. However, due to their complexity, our understanding has not yet reached a quantitative stage of development comparable to that of crystalline materials.

Band structure techniques and *localization theory* have also been applied to *electromagnetic waves* and other classical waves in strongly scattering periodic and disordered media [21, 243, 402–409]. The motivation for such studies is the fact that the classical waves are free from several complications that plague electronic waves in solids, such as inability to control their energy, finite temperature effects, electron–electron interactions, and other types of many-body effects. On the other hand, as was pointed out in the comments

following equations (7.70)–(7.71'), it is more difficult to localize classical waves than electronic waves. Furthermore, classical waves are subject to absorption, which contributes to the gradual extinction of an incoming beam; as a result, localization is not easily distinguished from the combined effect of diffusion and absorption.

Actually, the interpretation of the experiments of Wiersma et al. [404], where the transmission of electromagnetic waves through a highly disordered powder of GaAs was measured in three regimes identified by the authors as the extended, critical, and localized regimes (on the basis of different length dependence), was questioned by Scheffold et al. [409], who have argued that the results can be interpreted also on the basis of classical diffusion combined with absorption. One way to distinguish between localization on the one hand and diffusion/absorption on the other is to measure fluctuations as a function of the temperature T .

The basic equations (9.46) and (9.50) can be used to provide an easy interpretation of the impressive *integral quantum Hall effect* (IQHE). When a current, I , flows in a 2-d striplike conductor in the presence of a strong magnetic field, \mathbf{B} , normal to the strip, a so-called Hall voltage, V_H , develops between the two sides of the strip (i.e., perpendicular to the current flow). The Hall conductance, $\mathcal{G}_H \equiv I/V_H$, turns out to be quantized in units of e^2/h . This is what one should expect on the basis of (9.46), if the two directions of spin have been strongly separated in energy by the applied magnetic field, and *if* the 2-d conductor behaves as a perfect conductor with transmission $T = 1$. This last *if* seems unrealizable, since the conductor includes imperfections and the temperature is not zero. Actually, what makes this imperfect conductor behave perfectly is the presence of the strong magnetic field, which *separates spatially* the states with positive k (along the direction of the current) from those with negative k (opposite the direction of the current). The positive k states are highly localized along one edge of the strip and the negative k states along the other edge. Thus the scattering processes, $k \rightarrow -k$, or $-k \rightarrow k$, cannot take place (since there is no spatial overlap of the $|k\rangle$ and $|-k\rangle$ states), and the imperfect conductor behaves as a perfect one. For more details the reader is referred to the book by Datta [307].

Another system where (9.46) finds application is transport through double-barrier devices. The two barriers may trap the electron between them for a long time thereby creating approximate bound states at discrete energies, E_n , each with a width $\delta E_n \simeq \hbar/\tau_n$, where τ_n is their lifetime. When the energy of the electron transported through the double-barrier device coincides with one of the approximate levels, E_n , the transmission (and hence the conductance) exhibits a sharp peak of width δE_n . This resonance tunneling becomes even more interesting in very small devices, called *quantum dots* (QDs), where both electron–electron interactions and the discrete nature of electrons are important.

In these quantum dots, a critical voltage of the order $|e|/C$, where C is the capacitance of each barrier, is required in order to have conduction. This

phenomenon, called *Coulomb blockade*, is due to the fact that for very small voltages the charging energy of the quantum dot is positive and hence cannot take place until the critical voltage is reached and the charging energy becomes zero or negative. For more information the reader is referred to the books by Taylor and Heinonen [133], pp. 337–339, Datta [307], pp. 246–273, and, for more recent developments, the book edited by Brandes and Kettmann [381], pp. 157, 259, and 289.

Finally, we mention that the formalism presented in §9.7.3 finds application, among other situations, in transport through carbon and other nanotubes. These nanotubes are graphitelike strips that have been folded so as to create tubes of typical dimensions of the order of a nanometer. These tubes are connected to contacts and are studied as candidates for the next generation of nanoelectronics [410–413]. It is obvious that their conductance [and hence \bar{T}_{pq} as given by (9.110)] is of central importance for their device performance. To calculate \bar{T}_{pq} , one treats the coupling to each contact through a self-energy, Σ_p , which allows the calculation of both $\Gamma_p = i[\Sigma_p^+ - \Sigma_p^-]$ and $G = (E - \mathcal{H}_c - \Sigma)^{-1}$, where \mathcal{H}_c is the Hamiltonian of the isolated nanotube and $\Sigma = \sum_p \Sigma_p$. For details the reader is referred to the book by Datta [307] and the original literature (see, e.g., Andriotis and Menon [414–416]). A very idealized version of this approach is given in Problem 9.9.

We conclude this section by pointing out that the technology tendency toward miniaturization, which has already touched the nanoregime, requires conceptual and calculational tools such as the ones presented in Chaps. 8 and 9, where the quantum character of the transport and other phenomena becomes quite explicit.

9.9 Summary

In this chapter we have shown that quantum interference effects in disordered systems lead to eigenfunction amplitude fluctuations of increasing extent and size as the strength of the disorder increases; as a result, the static diffusion coefficient is reduced and eventually may become zero (for an infinite system and in the absence of inelastic scattering events and external magnetic fields). This is the phenomenon of Anderson localization whose physical manifestations depend on the relative size of various lengths such as the mean free path, ℓ , the minimum of several upper cutoff lengths, L_M , and the localization length, ξ ; L_M may be of the order of the geometrical length of the specimen, L , or the diffusion length, $L_\phi = \sqrt{D\tau_\phi}$, during the inelastic phase incoherence time τ_ϕ , or the cyclotron radius $L_D = \sqrt{\hbar c/eB}$, or the diffusion length, $L_c = \sqrt{D/\omega}$, in the presence of an AC electric field of angular frequency ω , whichever is smaller [see (9.5)]. If $\ell \ll L_M \ll \xi$, then we are in the so-called weak localization regime, where the quantum interference corrections to the conductivity are given by

$$\delta\sigma = \begin{cases} -\frac{e^2}{\sqrt{2\pi\hbar}}L_M, & \text{1-d,} & (9.2a) \\ -\frac{e^2}{\pi^2\hbar}\ln\frac{L_M}{L_m}, & \text{2-d,} & (9.2b) \\ \frac{e^2}{2\sqrt{2\pi^2\hbar}}\frac{1}{L_M} - \frac{e^2}{\pi^3\hbar}\frac{1}{L_m}, & \text{3-d,} & (9.2c) \end{cases}$$

and L_m is of the order of the mean free path ℓ . Notice that the presence of a magnetic field, B , reduces the value of L_M from $L_M = L_\phi/\sqrt{c_2}$ (when $B = 0$) to

$$L_M = L_\phi \left/ \sqrt{c_2 + \frac{L_\phi^2}{1.78L_B^2}} \right. .$$

Thus a negative magnetoresistance is exhibited that, in the 2-d case, is given by

$$\frac{\Delta R}{R} \simeq -\frac{\Delta\sigma}{\sigma(0)}, \quad (9.113)$$

where

$$\Delta\sigma = \sigma(B) - \sigma(0) \simeq \frac{e^2}{2\pi^2\hbar} \left[\psi(x) - 2\ln\left(\frac{L_B}{2L_\phi}\right) \right], \quad (9.20)$$

$x = 0.5 + (L_B/2L_\phi)^2$, and $\psi(x)$ is the digamma function, $\psi(x) \equiv \Gamma'(x)/\Gamma(x)$.

In special geometries such as cylindrical tubes with very thin walls and magnetic field parallel to the axis of the tube, the conductivity exhibits a sinusoidal periodic variation with the magnetic flux, $\Phi = BS$, with a period $\Phi_0 = hc/2e$, provided that the area S is of the same order of magnitude as πL_ϕ^2 . This is the so-called $\hbar c/2e$ Aharonov–Bohm effect. Similarly, in configurations such as those shown in Fig. 9.2, the conductivity would exhibit a periodic sinusoidal dependence on the magnetic flux, Φ , through the ring with the period of $2\Phi_0 = hc/e$; this is the $\hbar c/e$ Aharonov–Bohm effect.

If the localization length, ξ , is much smaller than L_M , an exponential dependence of the conductivity of the form

$$\sigma \sim \exp\left(-\frac{2L_M}{\xi}\right) \quad (9.114)$$

is expected. An approximate implicit expression for ξ is the following:

$$\frac{\pi}{2} \frac{\hbar}{e^2} \sigma_0 = \frac{\alpha_1}{(2\pi)^d} \int d\mathbf{q} \frac{1}{q^2 + \xi^{-2}}, \quad (9.27)$$

where σ_0 is the classical value of the conductivity.

The value of ξ as determined by (9.27) is the same as the value of the decay length of the lowest bound level in a potential well of linear extent

$$a_{\text{eff}} = c_1 \ell_{tr} \quad (9.29)$$

and depth ε_{eff} given by

$$\frac{\varepsilon_{\text{eff}}}{\hbar^2/2m^*a_{\text{eff}}^2} = \frac{c_2}{c_1^{d-2}} \frac{2e^2}{\pi\hbar} \frac{1}{\sigma_0 \ell_{\text{tr}}^{d-2}}. \quad (9.30)$$

It follows from (9.27)–(9.30) that $d = 2$ is the critical dimensionality; for $d < 2$ any amount of disorder, no matter how weak, is enough to localize the electron, while for $d > 2$ a critical amount of disorder is needed to produce localization.

For quasi-1-d systems consisting of a finite number of parallel running coupled 1-d channels the conductance, \mathcal{G} , is related to the transmission, T , per channel according to the formula

$$\mathcal{G} = \frac{2e^2}{h} MT, \quad (9.46)$$

where M is the number of channels and the factor 2 accounts for the two spin orientations. In the case where the quasi-1-d system is connected to several current or voltage leads, Büttiker generalized (9.46) to the following:

$$I_p = \sum_q \mathcal{G}_{pq} (V_p - V_q), \quad (9.49)$$

where

$$\mathcal{G}_{pq} = \frac{2e^2}{h} \bar{T}_{pq}, \quad (9.50)$$

$$\bar{T}_{pq} = \text{Tr} \{ \hat{t}_{pq} \hat{t}_{pq}^\dagger \}; \quad (9.50')$$

\hat{t}_{pq} is the transmission current amplitude $M_p \times M_q$ matrix whose matrix elements, \hat{t}_{pqij} , give the transmission current amplitude from the j th channel of the q lead to the i th channel of the p lead; I_p is the total current entering from contact p , $V_p = \mu_p/(-|e|)$, and μ_p is the chemical potential of contact p . The matrix elements \hat{t}_{pqij} are connected to the Green's function through (9.107), and the transmission coefficient, \bar{T}_{pq} , is given by

$$\bar{T}_{pq} = \text{Tr} [\Gamma_q G_{qp}^- \Gamma_p G_{pq}^+], \quad (9.110)$$

where

$$\Gamma_p (\nu_{p_2}, \nu'_{p_2}) = \sum_i \chi_{p_i} (\nu_{p_2}) \frac{\hbar v_{p_i}}{a_p} \chi_{p_i}^* (\nu'_{p_2}), \quad (9.111)$$

$$G = (E - \mathcal{H}_c - \Sigma)^{-1}, \quad (9.115)$$

$$\Sigma = \sum_p \Sigma_p, \quad (9.116)$$

and

$$\Gamma_p = i [\Sigma_p^+ - \Sigma_p^-]; \quad (9.117)$$

\mathcal{H}_c is the Hamiltonian of the isolated quasi-1-d conductor and Σ_p is the self-energy describing its coupling to contact p through lead p .

In Sect. 9.3 we presented the main results of the Anderson localization theory, in Sect. 9.5 we introduced the scaling approach to the localization problem, and in Sect. 9.6 we summarized several other theoretical techniques developed for this problem. Finally, in Sect. 9.7 the connection of the Green's function techniques to quantities related to the Anderson localization question and transport properties were presented.

Further Reading

Among the many books and review articles dealing with localization, quantum transport properties, and their calculation with the employment of Green's functions we mention the following:

- The book by Datta [307] provides an excellent introduction to the subject.
- Imry's book [250] gives a clear, physical insight to the subject and an extensive list of references to the original literature.
- The books by Sheng [21,243], as well as the book edited by Soukoulis [402], deal with classical waves in ordered and disordered media.
- A short account of the Coulomb blockade is given in the book by Taylor and Heinonen [133].
- The subject of quantum transport properties is treated in detail in the book by Ferry and Goodnick [417]. A shorter account is given in the book by Janssen [261]. Among the many excellent review articles we mention the one by Abrahams et al. [281] and the older one by Kramer and MacKinnon [376]. Some recent developments can be found in the book edited by Brandes and Kettermann [381].

Problems

9.1s. Prove (9.31), where

$$\xi' \simeq \frac{24.56\ell_{\text{tr}}}{S\ell_{\text{tr}}^2 - 12c_1'}.$$

Hint: Take into account (9.42) and (9.2c) and that the localization length, λ_A , of a quasi-1-d wire of cross section A in the extended regime is given by

$$\lambda_A = \frac{A}{4.82\xi'}$$

(see §9.6.1); $c_1' \simeq 0.75$ in order to reproduce the numerically determined critical value of $S\ell_{\text{tr}}^2 \simeq 9$, at which ξ' blows up, indicating the transition from extended to localized eigenstates. Notice that the present approximate approach

predicts a critical exponent $\gamma = 1$ in disagreement with accurate numerical data that give $\gamma \simeq 1.54$.

9.2. Using the potential well analogy with $c_2 = 1$ show that the 2-d localization length is proportional to $\ell_{\text{tr}} \exp[S\ell_{\text{tr}}/4]$.

9.3. Prove (9.34).

9.4. For a position-dependent conductivity, $\sigma(x)$, in a 1-d system, the local electric field is $E(x) = j/\sigma(x)$, where j is the current that is position independent since there is charge conservation. Hence the voltage drop, V , over a length L equals

$$V = j \int_0^L \frac{dx}{\sigma(x)}.$$

Then the conductance \mathcal{G} is

$$\frac{j}{V} = \left[\int_0^L dx \sigma^{-1}(x) \right]^{-1},$$

and the effective conductivity, σ_ε , is given by

$$\sigma_\varepsilon \equiv L\mathcal{G} = \frac{L}{\int_0^L dx \sigma^{-1}(x)}.$$

Assume that variations of $\sigma(x)$ with x are due to the fluctuations of the eigenfunctions

$$\sigma(x) = \sigma_0 \frac{|\psi(x)|^2}{|\psi_{\text{max}}|^2},$$

where $\psi(x) \sim e^{-x/\xi}$ for x outside an effective $1-d$ potential well. Following the above reasoning prove (9.41).

9.5s. Consider the T -shaped 1-d TBM shown in Fig. 9.8, where the off-diagonal matrix elements between all nearest neighbors are equal to V except the $\langle 0 | \mathcal{H} | 1_d \rangle$, which is equal to V' ; the diagonal matrix elements are taken as zero.

Calculate the 3×3 S -matrix for this model.

9.6s. Prove (9.65).

Hint: Q is a function of L/ξ' : $Q = f(L/\xi')$; ξ' blows up at the critical value Q_c with a power law: $\xi' \sim (Q - Q_c)^{-s}$.

9.7s. Prove (9.78).

9.8. For a binary diagonal disorder

$$p(\varepsilon_{\mathbf{m}}) = \frac{1}{2} \delta(\varepsilon_{\mathbf{m}} - \varepsilon) + \frac{1}{2} \delta(\varepsilon_p + \varepsilon)$$

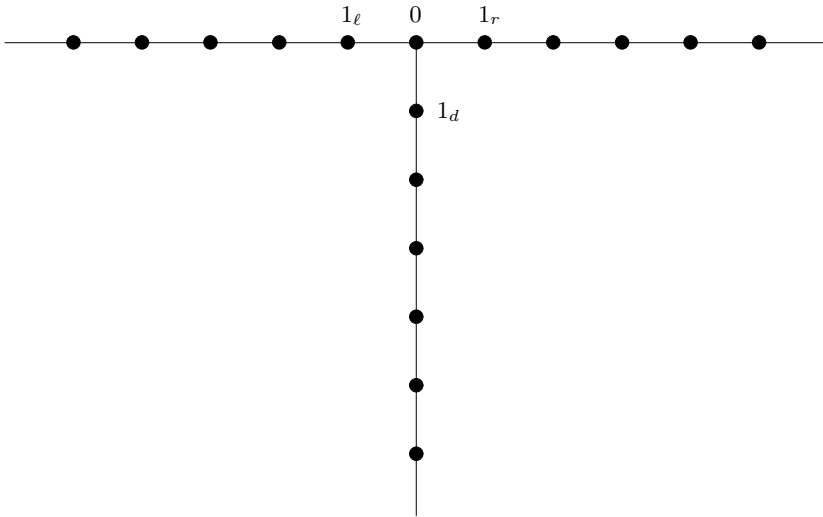


Fig. 9.8. A T-shaped TB system

of a TBM with off-diagonal matrix elements V , calculate the average DOS for $\varepsilon/B = 0, 4, \varepsilon/B = 0, 7, \varepsilon/B = 1$. Determine the positions of the mobility edges by setting $\tilde{L}(E) = K |V_2 \langle G(\mathbf{n}, \mathbf{n}[\ell]) \rangle| = 1$, where $K = Z - 1 = 5$. Employ the CPA for the calculation of the averages. Use the Bethe lattice periodic Green's functions. Plot the band-edge and the mobility-edge trajectories.

9.9. Consider the coupling, $\mathcal{H}_{c\ell}$, of a 2-d conductor to a lead as shown in Fig. 9.9. Let \mathcal{H}_c be the Hamiltonian of the isolated conductor and \mathcal{H}_ℓ that of the isolated semi-infinite ordered lead; the only nonzero matrix elements of the Hamiltonian $\mathcal{H}_{c\ell}$ are assumed to have the simple form

$$\langle \mu | \mathcal{H}_{c\ell} | \nu \rangle = \langle \nu | \mathcal{H}_{c\ell} | \mu \rangle = V_2 .$$

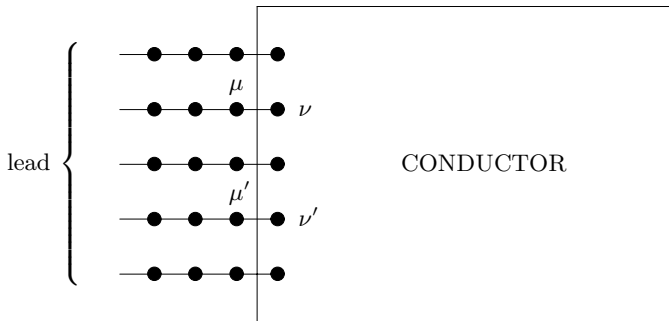


Fig. 9.9. A simple TB coupling of a conductor to a lead

Show that

$$\begin{aligned} [E - \mathcal{H}_\ell] G_{\ell c} - \mathcal{H}_{c\ell} G_c &= 0, \\ [E - \mathcal{H}_c] G_c - \mathcal{H}_{c\ell} G_{\ell c} &= 1, \end{aligned}$$

where

$$\begin{bmatrix} G_\ell & G_{\ell c} \\ G_{c\ell} & G_c \end{bmatrix} = \begin{bmatrix} E - \mathcal{H}_\ell & -\mathcal{H}_{\ell c} \\ -\mathcal{H}_{\ell c} & E - \mathcal{H}_c \end{bmatrix}^{-1}.$$

Then show that

$$G_c = [E - \mathcal{H}_c - \Sigma]^{-1},$$

where

$$\begin{aligned} \Sigma(\mu, \mu') &= V_2^2 g_\ell(\mu, \mu') = V_2^2 [E - \mathcal{H}_\ell]_{\mu\mu'}^{-1} \\ &= -|V_2| \Sigma \chi_i^*(\mu) \exp(ik_i a) \chi_i(\mu'); \end{aligned}$$

μ and μ' are points on the first column of the lead, $\chi_i(\mu)$ are the eigenfunctions for any column of the lead, and a is the lattice spacing of the lead.

9.10s. Using the CPA vertex corrections calculate the quantity

$$s \langle G(E + is) G(E - is) \rangle$$

as $s \rightarrow 0^+$, where $G(E \pm is)$ is the diagonal element of the Green's function corresponding to a random TBH.

Is the result nonzero? Comments?

Green's Functions in Many-Body Systems

Definitions

Summary. The Green's functions defined earlier are recast in a second quantized form. The resulting expressions can easily be generalized for the case where there are many *interacting* particles. The time evolution of the operators involves now the interaction terms in the Hamiltonian. As a result, the generalized Green's functions obey differential equations containing extra terms that depend on more complicated Green's functions.

10.1 Single-Particle Green's Functions in Terms of Field Operators

The Green's function formalism that has been developed up to now is appropriate for the problem of a single quantum particle moving in an external potential or for the propagation of a classical wave. Quite often we are dealing with systems involving many quantum particles interacting with each other or with quantized versions of classical waves. It is possible to generalize the definition of the Green's functions to obtain from them important physical information about the properties of these interacting many-particle systems. Such generalization is achieved in two steps. We first reexpress the single-body Green's functions (which we studied in the previous chapters) in the second quantization formalism, which is the most convenient language for the description of many-body systems [19, 20, 113, 114, 133, 418]. We can then generalize quite easily the definition of the Green's functions, as we shall see below.

In Appendix I we present very briefly the highlights of the second quantization formalism for two characteristic and very important cases: (1) the case of the field $\psi(\mathbf{r}, t)$ obeying the Schrödinger equation (first order in time); (2) the case of the field $u(\mathbf{r}, t)$ obeying the wave equation (second order in time). We express first the various Green's functions for the wave equation in

terms of the field operator $u(\mathbf{r}, t)$. The field $u(\mathbf{r}, t)$ can be expressed in terms of creation and annihilation operators $b_{\mathbf{k}}^\dagger$ and $b_{\mathbf{k}}$ as follows (Appendix I):

$$u(\mathbf{r}, t) = \sum_{\mathbf{k}} \sqrt{\frac{\hbar c^2}{2\omega_{\mathbf{k}}\Omega}} \left\{ b_{\mathbf{k}}^\dagger \exp[i(\omega_{\mathbf{k}}t - \mathbf{k} \cdot \mathbf{r})] + b_{\mathbf{k}} \exp[-i(\omega_{\mathbf{k}}t - \mathbf{k} \cdot \mathbf{r})] \right\}. \quad (10.1)$$

The above time dependence of the operator $u(\mathbf{r}, t)$ results from the general time evolution equation involving the commutator $[u, \mathcal{H}] \equiv u\mathcal{H} - \mathcal{H}u$

$$i\hbar \frac{\partial u(\mathbf{r}, t)}{\partial t} = [u(\mathbf{r}, t), \mathcal{H}], \quad (10.2)$$

which can be solved formally to give

$$u(\mathbf{r}, t) = e^{i\mathcal{H}t/\hbar} u(\mathbf{r}, 0) e^{-i\mathcal{H}t/\hbar}; \quad (10.3)$$

substituting in (10.3) the noninteracting Hamiltonian

$$\mathcal{H} = \sum_{\mathbf{k}} \hbar\omega_{\mathbf{k}} \left(b_{\mathbf{k}}^\dagger b_{\mathbf{k}} + \frac{1}{2} \right), \quad (10.4)$$

we obtain (10.1) by taking into account the commutation relations (I.23) obeyed by $b_{\mathbf{k}}^\dagger$ and $b_{\mathbf{k}}$. Since we ascribe the time dependence entirely to the operators and not at all to the state vectors, we are working within the so-called *Heisenberg picture*.

Now we express the various g s and \tilde{g} s associated with the wave equation and defined in Chap. 2 in terms of the operator $u(\mathbf{r}, t)$ given by (10.1). We have

$$\begin{aligned} \tilde{g}(\mathbf{r}, \mathbf{r}', t, t') &= -\frac{i}{\hbar} \langle 0 | [u(\mathbf{r}, t)u(\mathbf{r}', t') - u(\mathbf{r}', t')u(\mathbf{r}, t)] | 0 \rangle \\ &= -\frac{i}{\hbar} [u(\mathbf{r}, t), u(\mathbf{r}', t')], \end{aligned} \quad (10.5)$$

$$\tilde{g}^>(\mathbf{r}, \mathbf{r}', t, t') = -\frac{i}{\hbar} \langle 0 | u(\mathbf{r}, t)u(\mathbf{r}', t') | 0 \rangle, \quad (10.6)$$

$$\tilde{g}^<(\mathbf{r}, \mathbf{r}', t, t') = -\frac{i}{\hbar} \langle 0 | u(\mathbf{r}', t')u(\mathbf{r}, t) | 0 \rangle, \quad (10.7)$$

$$g^R(\mathbf{r}, \mathbf{r}', t, t') = -\frac{i}{\hbar} \theta(t - t') \langle 0 | [u(\mathbf{r}, t), u(\mathbf{r}', t')] | 0 \rangle, \quad (10.8)$$

$$g^A(\mathbf{r}, \mathbf{r}', t, t') = \frac{i}{\hbar} \theta(t' - t) \langle 0 | [u(\mathbf{r}, t), u(\mathbf{r}', t')] | 0 \rangle, \quad (10.9)$$

$$g(\mathbf{r}, \mathbf{r}', t, t') = -\frac{i}{\hbar} \langle 0 | T[u(\mathbf{r}, t)u(\mathbf{r}', t')] | 0 \rangle. \quad (10.10)$$

The Green's function g^- can be expressed in terms of g^R , g^A , and g as $g^- = g^R + g^A - g$. To prove the above relations we proceed as follows. For (10.5) we note that $\tilde{g}(\mathbf{r}, \mathbf{r}', t, t')$ is uniquely defined by the wave equation it obeys,

$$\left(\nabla^2 - \frac{1}{c^2} \frac{\partial^2}{\partial t^2}\right) \tilde{g}(\mathbf{r}, \mathbf{r}', t, t') = 0. \quad (10.11)$$

and the initial conditions $\tilde{g}(\mathbf{r}, \mathbf{r}', t, t) = 0$ and $\dot{\tilde{g}}(\mathbf{r}, \mathbf{r}', t, t) = -c^2 \delta(\mathbf{r} - \mathbf{r}')$. These initial conditions follow immediately from (2.48). All we need to show is that the rhs of (10.5) obeys the same equation and the same initial conditions. The wave equation (10.11) is obeyed by the rhs of (10.5) because the operator $u(\mathbf{r}, t)$ obeys it by definition. The initial conditions are obeyed as a consequence of the commutation relation (I.21). Thus (10.5) is proved. Note that the unequal time commutator $[u(\mathbf{r}, t), u(\mathbf{r}', t')]$, where $u(\mathbf{r}, t)$ is given by (10.1), is a c -number, and as such there was no need to take its mean value in the vacuum state. We prefer to use the mean value of $[u(\mathbf{r}, t), u(\mathbf{r}', t')]$ in defining \tilde{g} , first, because we can then generalize easily for interacting fields, and second, because we conform more to the definition of the other g s and \tilde{g} s. To prove (10.6) and (10.7), we use (10.1) on the rhs of (10.6, 10.7), and we take into account that $b_{\mathbf{k}}|0\rangle = 0$ and $[b_{\mathbf{k}}, b_{\mathbf{k}'}^\dagger] = \delta_{\mathbf{k}\mathbf{k}'}$; we find after some simple algebra that the rhs of (10.6) and (10.7) are, respectively,

$$-\frac{i c}{2} \sum_{\mathbf{k}} \frac{\left(e^{i\mathbf{k} \cdot \mathbf{r} / \sqrt{\Omega}}\right) \left(e^{-i\mathbf{k} \cdot \mathbf{r}' / \sqrt{\Omega}}\right)}{k} e^{-i\mathbf{k}c(t-t')}$$

and

$$\frac{-i c}{2} \sum_{\mathbf{k}} \frac{\left(e^{i\mathbf{k} \cdot \mathbf{r} / \sqrt{\Omega}}\right) \left(e^{-i\mathbf{k} \cdot \mathbf{r}' / \sqrt{\Omega}}\right)}{k} e^{i\mathbf{k}c(t-t')}.$$

These expressions coincide with the expressions (2.45) and (2.46), which were obtained previously for $\tilde{g}^>$ and $\tilde{g}^<$. To prove this last statement, take into account that for the present case $L = -\nabla^2$, $\lambda_n = k^2$, and $\phi_n(\mathbf{r}) = e^{i\mathbf{k} \cdot \mathbf{r} / \sqrt{\Omega}}$. The proof of (10.8) and (10.9) follows immediately from (10.5), (2.42), and (2.43). Finally, the proof of (10.10) follows by recalling the definition of the chronological operator T ,

$$T[u(\mathbf{r}, t)u(\mathbf{r}', t')] = \begin{cases} u(\mathbf{r}, t)u(\mathbf{r}', t'), & t > t', \\ u(\mathbf{r}', t')u(\mathbf{r}, t), & t < t', \end{cases} \quad (10.12)$$

and by taking into account (10.6), (10.7), and (2.41). We have thus succeeded in expressing the various g s and \tilde{g} s for the wave equation in terms of the vacuum expectation values of bilinear combinations of the field operator $u(\mathbf{r}, t)$, which obeys the wave equation. The relations (10.5)–(10.10) are valid for the general case where the g s and \tilde{g} s are associated with the general linear second-order equation $(-\partial^2/c^2 \partial t^2 - L)\phi = 0$ and $u(\mathbf{r}, t)$ obeys the same equation and the commutation relations (I.21).

Let us now try to express the g s and \tilde{g} s of a first-order equation (as the Schrödinger equation) in terms of the field operators ψ and ψ^\dagger . In writing expressions analogous to (10.5)–(10.10) we must take into account that the

operator ψ is not Hermitian and that it may satisfy an anticommutation (instead of commutation) relation; furthermore, its time dependence is

$$\psi(\mathbf{r}, t) = \sum_n a_n \psi_n(\mathbf{r}) \exp(-iE_n t/\hbar), \quad (10.13)$$

$$\psi^\dagger(\mathbf{r}, t) = \sum_n a_n^\dagger \psi_n^*(\mathbf{r}) \exp(iE_n t/\hbar). \quad (10.14)$$

Again this time dependence stems from the relation

$$\psi(\mathbf{r}, t) = e^{i\mathcal{H}t/\hbar} \psi(\mathbf{r}, 0) e^{-i\mathcal{H}t/\hbar}, \quad (10.15)$$

$$\psi^\dagger(\mathbf{r}, t) = e^{i\mathcal{H}t/\hbar} \psi^\dagger(\mathbf{r}, 0) e^{-i\mathcal{H}t/\hbar}, \quad (10.16)$$

where

$$\mathcal{H} = \sum_n E_n a_n^\dagger a_n, \quad (10.17)$$

and the creation and annihilation operators, a_n^\dagger and a_n , obey the relation (I.22).

In analogy to (10.5)–(10.10) we define for the fields $\psi(\mathbf{r}, t)$ and $\psi^\dagger(\mathbf{r}, t')$ the following \tilde{g} s and g s:

$$\begin{aligned} \tilde{g}(\mathbf{r}, \mathbf{r}', t, t') &= -\frac{i}{\hbar} \langle 0 | [\psi(\mathbf{r}, t) \psi^\dagger(\mathbf{r}', t') \mp \psi^\dagger(\mathbf{r}', t') \psi(\mathbf{r}, t)] | 0 \rangle \\ &= -\frac{i}{\hbar} [\psi(\mathbf{r}, t), \psi^\dagger(\mathbf{r}', t')]_{\mp}, \end{aligned} \quad (10.18)$$

$$\tilde{g}^>(\mathbf{r}, \mathbf{r}', t, t') = -\frac{i}{\hbar} \langle 0 | \psi(\mathbf{r}, t) \psi^\dagger(\mathbf{r}', t') | 0 \rangle, \quad (10.19)$$

$$\tilde{g}^<(\mathbf{r}, \mathbf{r}', t, t') = \mp \frac{i}{\hbar} \langle 0 | \psi^\dagger(\mathbf{r}', t') \psi(\mathbf{r}, t) | 0 \rangle, \quad (10.20)$$

$$g^R(\mathbf{r}, \mathbf{r}', t, t') = -\frac{i}{\hbar} \theta(t - t') \langle 0 | [\psi(\mathbf{r}, t), \psi^\dagger(\mathbf{r}', t')]_{\mp} | 0 \rangle, \quad (10.21)$$

$$g^A(\mathbf{r}, \mathbf{r}', t, t') = \frac{i}{\hbar} \theta(t' - t) \langle 0 | [\psi(\mathbf{r}, t), \psi^\dagger(\mathbf{r}', t')]_{\mp} | 0 \rangle, \quad (10.22)$$

$$g(\mathbf{r}, \mathbf{r}', t, t') = -\frac{i}{\hbar} \langle 0 | T [\psi(\mathbf{r}, t) \psi^\dagger(\mathbf{r}', t')] | 0 \rangle, \quad (10.23)$$

where

$$[A, B]_{\mp} = AB \mp BA \quad (10.24)$$

and

$$T [\psi(\mathbf{r}, t) \psi^\dagger(\mathbf{r}', t')] = \begin{cases} \psi(\mathbf{r}, t) \psi^\dagger(\mathbf{r}', t'), & t > t', \\ \pm \psi^\dagger(\mathbf{r}', t') \psi(\mathbf{r}, t), & t < t', \end{cases} \quad (10.25)$$

where the upper sign refers to bosons and the lower sign to fermions. It is easy to see that if the field operator ψ were Hermitian and were corresponding to bosons, then relations (10.18)–(10.23) would be identical to (10.5)–(10.10). We now show that the quantities defined by (10.18)–(10.23) are identical to the Green's functions g^+ , g^- , and \tilde{g} defined in Chap. 2 for a first-order equation.

We note first that $\tilde{g}^< = 0$ because $\psi|0\rangle = 0$. Next $\tilde{g}^> = \tilde{g}$ for the same reason. We now show that \tilde{g} as defined by (10.18) coincides with the \tilde{g} defined in Chap. 2 [see, e.g., (2.13)]. Both \tilde{g} s satisfy the same equation (Schrödinger equation) and obey the same initial condition, $g(\mathbf{r}, \mathbf{r}', t, t) = -i\delta(\mathbf{r} - \mathbf{r}')\hbar$ (for the Schrödinger case, $c = 1/\hbar$, $L = \mathcal{H}$, $\lambda_n = E_n$). We can easily see that

$$g(\mathbf{r}, \mathbf{r}', t, t') = g^R(\mathbf{r}, \mathbf{r}', t, t') = \theta(t - t')\tilde{g}(\mathbf{r}, \mathbf{r}', t, t') = g^+(\mathbf{r}, \mathbf{r}', t, t') ;$$

the last relation follows from (2.10). Similarly, $g^-(\mathbf{r}, \mathbf{r}', t, t') = g^A(\mathbf{r}, \mathbf{r}', t, t')$. Hence, in the case of a noninteracting field obeying a first-order (in time) equation, the \tilde{g} s and g s defined in terms of the vacuum expectation values of bilinear combinations of field operators ψ and ψ^\dagger are related to the g^+ , g^- , and \tilde{g} associated with the same equation as follows:

$$g^+(\mathbf{r}, \mathbf{r}', t, t') = g(\mathbf{r}, \mathbf{r}', t, t') = g^R(\mathbf{r}, \mathbf{r}', t, t') , \quad (10.26)$$

$$g^-(\mathbf{r}, \mathbf{r}', t, t') = g^A(\mathbf{r}, \mathbf{r}', t, t') , \quad (10.27)$$

$$\tilde{g}(\mathbf{r}, \mathbf{r}', t, t') \text{ [Eq. (2.9)]} = \tilde{g}(\mathbf{r}, \mathbf{r}', t, t') \text{ [Eq. (10.18)]} = \tilde{g}^>(\mathbf{r}, \mathbf{r}', t, t') , \quad (10.28)$$

$$\tilde{g}^<(\mathbf{r}, \mathbf{r}', t, t') = 0 . \quad (10.29)$$

The reader may wonder why we have introduced three g s and three \tilde{g} s since actually there are in the present case only two independent g s and one independent \tilde{g} . The reason is that when we generalize our definition to the many-particle systems, all three g s and three \tilde{g} s become independent.

10.2 Green's Functions for Interacting Particles

We now generalize the definition of Green's functions to systems of many interacting particles that are described by a Hamiltonian. We first define various g s and \tilde{g} s for the Schrödinger case characterized by the field operators $\psi^\dagger(\mathbf{r})$ and $\psi(\mathbf{r})$. The time dependence of these operators in the Heisenberg picture is given by the general equations (10.15) and (10.16). In what follows we assume for simplicity that there is no external potential felt by the particles, i.e., the quantity V_e introduced in Appendix I is zero. We also take $\hbar = 1$ so that we can use frequencies or energies indiscriminately. Furthermore, we write x for the four-vector \mathbf{r}, t , and we denote by $f(x, x')$ the function $f(\mathbf{r}, \mathbf{r}', t, t')$, where f is any of the g s or \tilde{g} s. For the sake of simplicity we omit the spin indices throughout the discussion. Because there is no external potential, the Hamiltonian is invariant under translation in space or time. This implies that all Green's functions depend on the difference $x - x'$. The definitions of the various g s and \tilde{g} s are the following:

$$\tilde{g}(x, x') = \tilde{g}(x - x') \equiv -i \left\langle [\psi(x), \psi^\dagger(x')]_{\mp} \right\rangle , \quad (10.30)$$

$$\tilde{g}^>(x, x') = \tilde{g}^>(x - x') \equiv -i \langle \psi(x)\psi^\dagger(x') \rangle , \quad (10.31)$$

$$\tilde{g}^<(x, x') = \tilde{g}^<(x - x') \equiv \mp i \langle \psi^\dagger(x') \psi(x) \rangle, \quad (10.32)$$

$$g^R(x, x') = g^R(x - x') \equiv -i\theta(t - t') \langle [\psi(x), \psi^\dagger(x')]_{\mp} \rangle, \quad (10.33)$$

$$g^A(x, x') = g^A(x - x') \equiv i\theta(t' - t) \langle [\psi(x), \psi^\dagger(x')]_{\mp} \rangle, \quad (10.34)$$

$$g(x, x') = g(x - x') \equiv -i \langle T [\psi(x) \psi^\dagger(x')] \rangle, \quad (10.35)$$

where the upper sign refers to bosons and the lower to fermions. The symbol $\langle A \rangle$ denotes thermal average of the arbitrary quantity A over the grand canonical ensemble:

$$\langle A \rangle = \frac{\sum_i \langle i | A | i \rangle \exp[-\beta(E_i - \mu N_i)]}{\sum_i \exp[-\beta(E_i - \mu N_i)]} = \frac{\text{Tr} \{ A e^{-\beta(\mathcal{H} - \mu N)} \}}{\text{Tr} \{ e^{-\beta(\mathcal{H} - \mu N)} \}}, \quad (10.36)$$

where \mathcal{H} is the total Hamiltonian of the system, N is the operator of the total number of particles, μ is the chemical potential, $\beta = 1/k_B T$ is the inverse temperature, and $\{|i\rangle\}$ are the common eigenfunctions (in the Heisenberg picture) of \mathcal{H} and N with eigenvalues E_i and N_i , respectively. In the limit $T \rightarrow 0$ we have

$$\langle A \rangle \rightarrow \langle \Psi_0 | A | \Psi_0 \rangle \text{ as } T \rightarrow 0^+, \quad (10.37)$$

where $|\Psi_0\rangle$ is the ground state (in the Heisenberg picture) of the whole system. Thus the generalization from (10.18)–(10.23) to (10.30)–(10.35) consists in taking the actual time development of the operators $\psi(x)$ and $\psi^\dagger(x')$ [instead of (10.13)] and in calculating the averages over the actual state of the system (instead of the vacuum). Obviously, if no particles are present in the system, the \tilde{g} s and g s defined by (10.30)–(10.35) reduce to those defined by (10.18)–(10.25), which, as we have seen, are identical to the g s and \tilde{g} s defined in Chap. 2. In other words, we can say by inspection of (10.18)–(10.25), that the g s and \tilde{g} s defined in Chap. 2 describe the propagation of a single particle from x' to x *in the absence of other particles*. On the other hand, the g s and \tilde{g} s defined by (10.30)–(10.35) describe the propagation of a *single* particle (or hole) from x' to x (or x to x') *in the presence of other particles*. For example, $\tilde{g}^>(x, x')$ from (10.31) can be interpreted as the probability amplitude of finding at x an extra particle that was added in our system at x' without any other modification in our system; thus, $\tilde{g}^>$ describes the propagation of an extra particle added to our system (such propagation has physical meaning for $t > t'$). Similarly, $\tilde{g}^<(x, x')$ describes the propagation of a hole from x to x' . It follows that $g(x, x')$ describes the propagation of an extra particle when $t > t'$ and the propagation of a hole when $t' > t$. If the system is the vacuum, as in (10.18)–(10.23), we cannot have holes, and as a result $\tilde{g}^< = 0$. On the other hand, for the general case (10.32) a hole can be created (i.e., a particle can be eliminated) and hence $\tilde{g}^<$ is not, in general, zero.

The various \tilde{g} s and g s defined by (10.30)–(10.35) are related to each other in exactly the same way as the \tilde{g} s and g s introduced in Chap. 2 for the second-order (in time) equation, i.e., by (2.38)–(2.44).

We introduce also the Fourier transform of $f(x - x')$ with respect to the variable $\boldsymbol{\rho} = \mathbf{r} - \mathbf{r}'$ and with respect to the four-vector $x - x'$, where f is any of the \tilde{g} s or g s, i.e.,

$$f(\mathbf{k}, \tau) = \int d\boldsymbol{\rho} e^{-i\mathbf{k} \cdot \boldsymbol{\rho}} f(x - x') \quad (10.38)$$

and

$$f(\mathbf{k}, \omega) = \int d\boldsymbol{\rho} d\tau e^{-i\mathbf{k} \cdot \boldsymbol{\rho} + i\omega\tau} f(x - x') , \quad (10.39)$$

where $\tau = t - t'$. The Fourier transform $f(\mathbf{k}, \omega)$ is the most widely used. The (\mathbf{k}, τ) Fourier transforms can be expressed in terms of the $a_{\mathbf{k}}^\dagger$ and $a_{\mathbf{k}}$ operators, creating and annihilating a particle with momentum \mathbf{k} as follows:

$$\tilde{g}^>(\mathbf{k}, \tau) = -i \langle a_{\mathbf{k}}(\tau + t') a_{\mathbf{k}}^\dagger(t') \rangle \quad (10.40)$$

with similar expressions for the other \tilde{g} s and g s. Equation (10.40) can be proved using (I.29), which relates $\psi(\mathbf{r})$ and $\psi^\dagger(\mathbf{r}')$ to $a_{\mathbf{k}'}$ and $a_{\mathbf{k}''}^\dagger$. Again, $a_{\mathbf{k}}(t) = \exp(i\mathcal{H}t) a_{\mathbf{k}} \exp(-i\mathcal{H}t)$ and $a_{\mathbf{k}}^\dagger(t) = \exp(i\mathcal{H}t) a_{\mathbf{k}}^\dagger \exp(-i\mathcal{H}t)$. One can use the relations (10.30)–(10.35) to define the Green's functions associated with any field. In particular, for the case of longitudinal acoustic (LA) phonons it is customary to use the scalar field $\phi(\mathbf{r}, t)$, which is real and depends on the LA phonon creation and annihilation operators $b_{\mathbf{k}}^\dagger$ and $b_{\mathbf{k}}$ as in (I.46). We have again that

$$\phi(\mathbf{r}, t) = e^{i\mathcal{H}t} \phi(\mathbf{r}, 0) e^{-i\mathcal{H}t} . \quad (10.41)$$

Denoting by D the Green's functions associated with the LA phonon field, we have, e.g.,

$$D(x, x') = D(x - x') = -i \langle T[\phi(x)\phi(x')] \rangle , \quad (10.42)$$

with similar expressions for D^R , D^A , \tilde{D} , $\tilde{D}^>$, and $\tilde{D}^<$. Again the \tilde{D} s and D s are related to each other by (2.38)–(2.43), i.e., in exactly the same way as the single-particle Green's functions.

In the case where the total Hamiltonian \mathcal{H} involves interactions, there is a basic difference between the Green's function defined in this section and those defined in Chap. 2. In the presence of interaction the field ψ (or ϕ) does not obey the same equation as in the noninteracting case. As a result, the differential equations obeyed by the \tilde{g} s or g s are more complicated than those examined in Chap. 2. To be more specific, consider the Schrödinger case with a total Hamiltonian $\mathcal{H} = T + V_i$, where T is the kinetic energy given by (I.32) and V_i is the interaction part given by (I.35). In this case we have shown in Appendix I that

$$\left(i \frac{\partial}{\partial t} + \frac{\nabla^2}{2m} \right) \psi(\mathbf{r}, t) = \int d\mathbf{r}' v(\mathbf{r} - \mathbf{r}') \psi^\dagger(\mathbf{r}', t) \psi(\mathbf{r}', t) \psi(\mathbf{r}, t) . \quad (10.43)$$

Thus, the application of the operator $i\partial/\partial t + \nabla_r^2/2m$ on $\psi(\mathbf{r}, t)$ does not produce zero as in the noninteracting case but an extra term involving the

interaction potential v and three ψ (or ψ^\dagger). As a result of this extra term, application of $i\partial/\partial t + \nabla_r^2/2m$ on $g(x, x')$ will give

$$\begin{aligned} & \left(i\frac{\partial}{\partial t} + \frac{\nabla^2}{2m} \right) g(x, x') \\ &= \delta(x - x') \pm i \int d^4x_1 v(\mathbf{r} - \mathbf{r}_1) g_2(x, x_1; x', x_1^+) \Big|_{t_1=t}, \end{aligned} \quad (10.44)$$

where x_1^+ means $\mathbf{r}_1, t_1 + s$ as $s \rightarrow 0^+$ and g_2 , the two-particle Green's function, is defined as

$$g_2(x_1, x_2; x'_1, x'_2) = (-i)^2 \langle T [\psi(x_1) \psi(x_2) \psi^\dagger(x'_2) \psi^\dagger(x'_1)] \rangle, \quad (10.45)$$

where the chronological operator T arranges the operators in chronological order so that the earliest time appears on the right and the latest on the left. In addition, for fermions only, we introduce a factor ± 1 depending on whether the time-ordered product is an even or odd permutation of the original ordering. Thus, for $t_1 > t_2 > t'_1 > t'_2$, we have that

$$g_2(x_1, x_2; x'_1, x'_2) = \langle \psi(x_1) \psi(x_2) \psi^\dagger(x'_1) \psi^\dagger(x'_2) \rangle;$$

in this case, g_2 describes the propagation of two extra particles added to our system. Equation (10.44) shows that in the presence of pairwise interactions the differential equation obeyed by $g(x, x')$ involves an extra term depending on the two-particle Green's function g_2 , which is unknown. In a similar way, one finds that the differential equation for g_2 involves the three-particle Green's function g_3 and so on, where the n -particle Green's function is defined by

$$\begin{aligned} & g_n(x_1, \dots, x_n; x'_1, \dots, x'_n) = \\ & (-i)^n \langle T [\psi(x_1) \cdots \psi(x_n) \psi^\dagger(x'_n) \cdots \psi^\dagger(x'_1)] \rangle. \end{aligned} \quad (10.46)$$

Thus, the existence of interaction complicates the calculation of g in an essential way: while in the noninteracting case g was determined by a single differential equation (and the appropriate initial conditions), in the presence of interactions we have an infinite hierarchy of equations, each connecting a Green's function of order n to one of order $n + 1$. We postpone the question of calculation of g until Chap. 12. In the next section we calculate g for the special case where there are no interactions among the particles.

Since the various g s and \tilde{g} s are so closely interrelated, there is no need to consider all of them. Most of the monographs on the subject develop the whole formalism by using the causal Green's function g defined by (10.35) or (10.42). Some other authors (see, e.g., [419, 424]) prefer to work with g^R .

In this section we have defined the various g s and \tilde{g} s for a system consisting of many particles. From these Green's functions one can obtain quantities of physical importance. We will discuss this question in the next chapter.

10.3 Green's Functions for Noninteracting Particles

Consider first the Schrödinger case $\psi(x)$. The Hamiltonian for noninteracting particles is [see (I.32)]

$$\mathcal{H} = \sum_{\mathbf{k}} \varepsilon_{\mathbf{k}} a_{\mathbf{k}}^{\dagger} a_{\mathbf{k}} , \quad (10.47)$$

where $\varepsilon_{\mathbf{k}} = k^2/2m$. From the general equation

$$i \frac{da_{\mathbf{k}}(t)}{dt} = [a_{\mathbf{k}}(t), \mathcal{H}]$$

we have in the present case

$$i \frac{da_{\mathbf{k}}(t)}{dt} = \varepsilon_{\mathbf{k}} a_{\mathbf{k}}(t) ,$$

which leads to

$$a_{\mathbf{k}}(t) = \exp(-i\varepsilon_{\mathbf{k}}t) a_{\mathbf{k}} . \quad (10.48)$$

Substituting this into (10.40) we obtain

$$\tilde{g}^>(\mathbf{k}, t) = -i \left\langle \exp(-i\varepsilon_{\mathbf{k}}t) a_{\mathbf{k}} a_{\mathbf{k}}^{\dagger} \right\rangle = -i \exp(-i\varepsilon_{\mathbf{k}}t) \left(1 \pm \left\langle a_{\mathbf{k}}^{\dagger} a_{\mathbf{k}} \right\rangle \right) . \quad (10.49)$$

Similarly,

$$\tilde{g}^<(\mathbf{k}, t) = \mp i \exp(-i\varepsilon_{\mathbf{k}}t) \left\langle a_{\mathbf{k}}^{\dagger} a_{\mathbf{k}} \right\rangle . \quad (10.50)$$

The average number operator, $\left\langle a_{\mathbf{k}}^{\dagger} a_{\mathbf{k}} \right\rangle$, is given by the Bose or Fermi function for noninteracting particles:

$$\left\langle a_{\mathbf{k}}^{\dagger} a_{\mathbf{k}} \right\rangle = f_{\mp}(\varepsilon_{\mathbf{k}}) = \frac{1}{\exp[\beta(\varepsilon_{\mathbf{k}} - \mu)] \mp 1} , \quad (10.51)$$

where μ is the chemical potential, $\beta = (k_B T)^{-1}$, and k_B is the Boltzmann constant. For the other g s and \tilde{g} s we have [using (2.40)–(2.43)]

$$g(\mathbf{k}, t) = \begin{cases} -i \exp(-i\varepsilon_{\mathbf{k}}t) [1 \pm f_{\mp}(\varepsilon_{\mathbf{k}})] , & t > 0 , \\ \mp i \exp(-i\varepsilon_{\mathbf{k}}t) f_{\mp}(\varepsilon_{\mathbf{k}}) , & t < 0 , \end{cases} \quad (10.52)$$

$$\tilde{g}(\mathbf{k}, t) = -i \exp(-i\varepsilon_{\mathbf{k}}t) , \quad (10.53)$$

$$g^R(\mathbf{k}, t) = -i\theta(t) \exp(-i\varepsilon_{\mathbf{k}}t) , \quad (10.54)$$

$$g^A(\mathbf{k}, t) = i\theta(-t) \exp(-i\varepsilon_{\mathbf{k}}t) . \quad (10.55)$$

We see that, for noninteracting systems, the quantities \tilde{g} , g^R , and g^A do not involve the temperature or μ and that they have exactly the same form as in the case of a single particle moving in the vacuum. On the other hand,

the quantities $\tilde{g}^>$, $\tilde{g}^<$, and g involve information pertaining not only to the motion of the added particle (or hole) but to the state of the system as well.

For fermions in the limit $T \rightarrow 0$ we have $\mu = \varepsilon_F = k_F^2/2m$; thus $g(\mathbf{k}, t)$ becomes

$$g(\mathbf{k}, t) = \begin{cases} -i \exp(-i\varepsilon_k t) \theta(k - k_F) , & t > 0 , \\ i \exp(-i\varepsilon_k t) \theta(k_F - k) , & t < 0 . \end{cases} \quad (10.56)$$

For bosons, the limit $T \rightarrow 0$ is more complicated because of the phenomenon of Bose condensation [20].

Let us now calculate the Fourier transforms with respect to t . It is easy to show that

$$\tilde{g}(\mathbf{k}, \omega) = -2\pi i \delta(\omega - \varepsilon_k) , \quad (10.57)$$

$$g^R(\mathbf{k}, \omega) = \lim_{s \rightarrow 0^+} \frac{1}{\omega + is - \varepsilon_k} , \quad (10.58)$$

$$g^A(\mathbf{k}, \omega) = \lim_{s \rightarrow 0^+} \frac{1}{\omega - is - \varepsilon_k} . \quad (10.59)$$

For $T = 0$ and for fermions we obtain from (10.56)

$$\begin{aligned} g(\mathbf{k}, \omega) &= \lim_{s \rightarrow 0^+} \left[\frac{\theta(k - k_F)}{\omega + is - \varepsilon_k} + \frac{\theta(k_F - k)}{\omega - is - \varepsilon_k} \right] \\ &= \lim_{s \rightarrow 0^+} \frac{1}{\omega - \varepsilon_k + is\bar{\varepsilon}(k - k_F)} , \end{aligned} \quad (10.60)$$

where $\bar{\varepsilon}(x) = 1$ for $x > 0$ and -1 for $x < 0$. By defining the function

$$G(\mathbf{k}, z) = \frac{1}{z - \varepsilon_k} , \quad (10.61)$$

we can rewrite (10.58)–(10.60) as

$$g^R(\mathbf{k}, \omega) = \lim_{s \rightarrow 0^+} G(\mathbf{k}, \omega + is) , \quad (10.62)$$

$$g^A(\mathbf{k}, \omega) = \lim_{s \rightarrow 0^+} G(\mathbf{k}, \omega - is) , \quad (10.63)$$

$$g(\mathbf{k}, \omega) = \lim_{s \rightarrow 0^+} G[\mathbf{k}, \omega + is\bar{\varepsilon}(\omega - \varepsilon_F)] . \quad (10.64)$$

Equations (10.58)–(10.60) can be proved by applying the residue theorem to show that the inverse Fourier transform of g^R , g^A , and g give (10.54)–(10.56).

We consider next the Green's functions for the LA phonon field $\phi(x)$. As was discussed in Appendix I, $\phi(x)$ can be expressed in terms of the phonon creation and annihilation operators $b_{\mathbf{k}}^\dagger$ and $b_{\mathbf{k}}$ as follows:

$$\phi(x) = \sum_{\mathbf{k}} \sqrt{\frac{\omega_{\mathbf{k}}}{2\Omega}} \left(b_{\mathbf{k}}^\dagger e^{i\mathbf{k}x} + b_{\mathbf{k}} e^{-i\mathbf{k}x} \right) , \quad (10.65)$$

where $kx = \omega_k t - \mathbf{k} \cdot \mathbf{r}$ and the summation over \mathbf{k} is restricted by $|\mathbf{k}| \leq k_D$. In obtaining (10.65) we have used the fact that the phonons do not interact, i.e., that their Hamiltonian is $\mathcal{H} = \sum_{\mathbf{k}} \omega_{\mathbf{k}} (b_{\mathbf{k}}^\dagger b_{\mathbf{k}} + 1/2)$. Substituting (10.65) into the definition of $\tilde{D}^>(x, x')$, we have

$$\begin{aligned} \tilde{D}^>(x, x') &= -i \langle \phi(x) \phi(x') \rangle \\ &= \frac{-i}{2\Omega} \sum_{\mathbf{k}\mathbf{k}'} \sqrt{\omega_{\mathbf{k}} \omega_{\mathbf{k}'}} \left[\exp(-ikx + ik'x') \langle b_{\mathbf{k}} b_{\mathbf{k}'}^\dagger \rangle \right. \\ &\quad \left. + \exp(ikx - ik'x') \langle b_{\mathbf{k}}^\dagger b_{\mathbf{k}'} \rangle \right]. \end{aligned} \quad (10.66)$$

Taking into account that

$$\langle b_{\mathbf{k}}^\dagger b_{\mathbf{k}'} \rangle = \langle b_{\mathbf{k}'} b_{\mathbf{k}}^\dagger \rangle - \delta_{\mathbf{k}\mathbf{k}'} = \delta_{\mathbf{k}\mathbf{k}'} n_{\mathbf{k}} = \delta_{\mathbf{k}\mathbf{k}'} (\exp(\beta\omega_{\mathbf{k}}) - 1)^{-1},$$

we obtain

$$\tilde{D}^>(x, x') = \frac{-i}{2\Omega} \sum_{\mathbf{k}} \omega(k) \left[e^{ik(x-x')} n_{\mathbf{k}} + e^{-ik(x-x')} (1 + n_{\mathbf{k}}) \right], \quad (10.67)$$

$[\omega(k) \equiv \omega_{\mathbf{k}}]$; in the $T = 0$ limit we have

$$\tilde{D}^>(x, x') = \frac{-i}{2\Omega} \sum_{\mathbf{k}} \omega(k) e^{-ik(x-x')}. \quad (10.68)$$

The quantity $\tilde{D}^<(x, x')$ can be obtained immediately from the relation

$$\tilde{D}^<(x, x') = \tilde{D}^>(x', x).$$

We have then for $\tilde{D}(x - x')$

$$\begin{aligned} \tilde{D}(x - x') &= \frac{-i}{2\Omega} \sum_{\mathbf{k}} \omega(k) \left[e^{-ik(x-x')} - e^{ik(x-x')} \right] \\ &= -\frac{1}{\Omega} \sum_{\mathbf{k}} \omega(k) \sin[k(x - x')]. \end{aligned} \quad (10.69)$$

The Green's functions D , D^R , and D^A can then be obtained by applying (2.41)–(2.43). Having obtained the various $D(x - x')$ s and $\tilde{D}(x - x')$ s, we can calculate their Fourier transforms easily. We find

$$\begin{aligned} \tilde{D}(\mathbf{k}, \omega) &= -i\pi\omega_{\mathbf{k}} [\delta(\omega - \omega_{\mathbf{k}}) - \delta(\omega + \omega_{\mathbf{k}})] \\ &\quad \times \theta(k_D - k), \quad k \equiv |\mathbf{k}|, \end{aligned} \quad (10.70)$$

$$D^R(\mathbf{k}, \omega) = \frac{\omega_{\mathbf{k}}^2}{(\omega + is)^2 - \omega_{\mathbf{k}}^2} \theta(k_D - k), \quad (10.71)$$

$$D^A(\mathbf{k}, \omega) = \frac{\omega_{\mathbf{k}}^2}{(\omega - is)^2 - \omega_{\mathbf{k}}^2} \theta(k_D - k). \quad (10.72)$$

In the $T \rightarrow 0$ limit we obtain for $D(\mathbf{k}, \omega)$

$$D(\mathbf{k}, \omega) = \frac{\omega_k^2}{\omega^2 - \omega_k^2 + i\epsilon} \theta(k_D - k) . \quad (10.73)$$

The factor $\theta(k_D - k) = \theta(\omega_D - \omega_k)$, where $\omega_D = ck_D$ comes from the restriction $k \leq k_D$ in the basic expression (10.65); physically, it is justified by the requirement that there are as many degrees of freedom in our continuous elastic model as there are degrees of freedom in an actual (discrete) solid.

10.4 Summary

Let $\psi(\mathbf{r})$ and $\psi^\dagger(\mathbf{r})$ be the field operators resulting from quantizing (second quantization) the wave function (and its complex conjugate) corresponding to the Schrödinger equation. We take $\hbar = 1$ and $(\mathbf{r}, t) = x$ and omit any external potential; we also omit for simplicity any spin indices. $\psi(\mathbf{r}, t) = \exp(i\mathcal{H}t)\psi(\mathbf{r})\exp(-i\mathcal{H}t)$ with an identical expression for $\psi^\dagger(\mathbf{r}, t)$, where \mathcal{H} is the total Hamiltonian describing our system. We define the one-particle Green's functions for our many-body system as follows:

$$\tilde{g}(x, x') = -i \left\langle [\psi(x), \psi^\dagger(x')]_{\mp} \right\rangle , \quad (10.30)$$

$$\tilde{g}^>(x, x') = -i \langle \psi(x)\psi^\dagger(x') \rangle , \quad (10.31)$$

$$\tilde{g}^<(x, x') = \mp i \langle \psi^\dagger(x')\psi(x) \rangle , \quad (10.32)$$

$$g^R(x, x') = \theta(t - t') \tilde{g}(x, x') , \quad (10.33)$$

$$g^A(x, x') = -\theta(t' - t) \tilde{g}(x, x') , \quad (10.34)$$

$$g(x, x') = -i \langle T [\psi(x)\psi^\dagger(x')] \rangle , \quad (10.35)$$

where $[A, B]_{\mp} = AB \mp BA$; the upper sign refers to bosons and the lower to fermions; the chronological operator T is defined as

$$T [\psi(x)\psi^\dagger(x')] = \begin{cases} \psi(x)\psi^\dagger(x') , & t > t' , \\ \pm \psi^\dagger(x')\psi(x) , & t < t' . \end{cases} \quad (10.25)$$

The symbol $\langle \rangle$ denotes the thermal average over the grand canonical ensemble, i.e.,

$$\langle A \rangle = \frac{\text{Tr} \{ A e^{-\beta(\mathcal{H} - \mu N)} \}}{\text{Tr} \{ e^{-\beta(\mathcal{H} - \mu N)} \}} . \quad (10.36)$$

For zero temperature $\langle A \rangle = \langle \Psi_0 | A | \Psi_0 \rangle$, where $|\Psi_0\rangle$ is the ground state (in the Heisenberg picture) of our system.

The Green's functions defined above describe the propagation of an extra particle (or hole) added to our system that is in thermal equilibrium. If our system contains no particles at all, the Green's functions defined by

(10.30)–(10.35) reduce to those introduced in Chap. 2, which describe the propagation of a particle in the vacuum. Using the commutation (anticommutation) relations of the field operators, one can prove that the \tilde{g} s and g s defined by (10.30)–(10.35) obey (2.38)–(2.44) as the Green's functions introduced in Chap. 2. Because the various g s and \tilde{g} s are interrelated, one can limit oneself to one of them; the most commonly used is the causal g defined by (10.35); a few authors use the retarded g^R .

The time evolution of the field operator $\psi(x)$ depends on the total Hamiltonian, which involves the other particles of the system if interactions are present. Thus, for interacting systems the differential equations obeyed by the g s or \tilde{g} s contain extra terms that involve more complicated Green's functions.

In practical calculations it is more convenient to work with the Fourier transforms of the various g s and \tilde{g} s with respect to the four-variable $x - x'$.

The definitions (10.30)–(10.35) can be applied to any quantized field. An example is given for the scalar field of the longitudinal acoustic phonons in a continuous elastic medium.

Finally, we calculated the Green's function for the simple case of noninteracting Schrödinger or phonon fields.

Further Reading

- Second quantization is presented in several books either by following a field-theoretical approach as in Appendix I (see, e.g., the book by Schiff [19] or the book by Mahan [114]) or by introducing creation and annihilation operators as a starting point (see, e.g., the books by Fetter and Walecka [20], Abrikosov et al. [113], and Taylor and Heinonen [133]).
- Green's functions for interacting particles are defined and extensively used in several books dealing with many-body theory: the book by Kadanoff and Baym [420] uses a notation similar to ours; the reader may find it profitable to consult the books by Mahan [114], Fetter and Walecka [20], and Abrikosov et al. [113].

Problems

10.1. Prove (I.22) and (I.23) starting from (I.20) and (I.21) and (I.12) and (I.13).

10.2. Show that the ordering of the operators in (I.35) is the correct one by calculating the matrix element $\langle \Psi_2 | V_i | \Psi_2 \rangle$ of V_i , where Ψ_2 is a state with two particles.

10.3. Prove (I.38) starting from (I.32) and (I.35).

10.4. Following the procedure outlined in Appendix I and starting from the Lagrangian density

$$\ell = \frac{1}{2} \rho \mathbf{d}^2 - \frac{1}{2} B (\nabla \cdot \mathbf{d})^2 ,$$

prove (I.39) and (I.46) by taking into account that $\nabla \times \mathbf{d} = 0$.

10.5. Prove (10.43) and (10.44).

10.6s. Using the invariance of the trace to cyclic permutations and the commutation relations (I.22) show that the Bose–Einstein and the Fermi–Dirac distributions are given by

$$\langle a_n^\dagger a_n \rangle = \frac{1}{\exp [\beta (\varepsilon_n - \mu)] \mp 1}$$

for noninteracting particles.

Properties and Use of the Green's Functions

Summary. The Green's functions defined in Chap. 10 have analytical properties that are similar but not identical to the Green's functions defined in Chap. 2 corresponding to second-order (in time) differential equations. They can all be expressed in terms of a generalized DOS and the Fermi or Bose thermal equilibrium distributions. From the Green's functions (or the generalized DOS) one can easily obtain all thermodynamic quantities and linear response functions like the conductivity. The poles of an appropriate analytic continuation of G in the complex E -plane can be interpreted as the energy (the real part of the pole) and the inverse lifetime (the imaginary part of the pole) of quasiparticles. The latter are entities that allow us to map an interacting system to a noninteracting one.

11.1 Analytical Properties of g_s and \tilde{g}_s

Let us consider first the quantity $\tilde{g}^>(\mathbf{k}, t)$. We have

$$\begin{aligned}
 \tilde{g}^>(\mathbf{k}, \tau) &= -i \left\langle a_{\mathbf{k}}(t) a_{\mathbf{k}}^\dagger(t') \right\rangle = -i \sum_m \varrho_m \left\langle m \left| a_{\mathbf{k}}(t) a_{\mathbf{k}}^\dagger(t') \right| m \right\rangle \\
 &= -i \sum_{m\ell} \varrho_m \left\langle m \left| e^{i\mathcal{H}t} a_{\mathbf{k}} e^{-i\mathcal{H}t} \right| \ell \right\rangle \left\langle \ell \left| e^{i\mathcal{H}t'} a_{\mathbf{k}}^\dagger e^{-i\mathcal{H}t'} \right| m \right\rangle \\
 &= -i \sum_{m\ell} \varrho_m \exp[-i\tau(E_\ell - E_m)] \left| \left\langle \ell \left| a_{\mathbf{k}}^\dagger \right| m \right\rangle \right|^2, \quad (11.1)
 \end{aligned}$$

where $|m\rangle$ and $|\ell\rangle$ are eigenfunctions of the total \mathcal{H} and N , i.e.,

$$\begin{aligned}
 \mathcal{H} |m\rangle &= E_m |m\rangle, & \mathcal{H} |\ell\rangle &= E_\ell |\ell\rangle, \\
 N |m\rangle &= N_m |m\rangle, & N |\ell\rangle &= N_\ell |\ell\rangle,
 \end{aligned}$$

$$\varrho_m = \frac{\exp[-\beta(E_m - \mu N_m)]}{\text{Tr} \{ \exp[-\beta(\mathcal{H} - \mu N)] \}},$$

$\tau = t - t'$, and the summation extends over all eigenstates.

By taking the Fourier transform with respect to τ we find

$$\tilde{g}^>(\mathbf{k}, \omega) = -2\pi i \sum_{m\ell} \varrho_m \left| \langle \ell | a_{\mathbf{k}}^\dagger | m \rangle \right|^2 \delta(\omega + E_m - E_\ell) . \quad (11.2)$$

In a similar way we can show that

$$\tilde{g}^<(\mathbf{k}, \omega) = \mp 2\pi i \sum_{mn} \varrho_m |\langle n | a_{\mathbf{k}} | m \rangle|^2 \delta(\omega + E_n - E_m) . \quad (11.3)$$

Equations (11.2) and (11.3) become in the $T = 0$ limit

$$\tilde{g}^>(\mathbf{k}, \omega) = -2\pi i \sum_{\ell} \left| \langle \ell | a_{\mathbf{k}}^\dagger | \Psi_0 \rangle \right|^2 \delta(\omega + E_g - E_\ell) , \quad (11.2')$$

$$\tilde{g}^<(\mathbf{k}, \omega) = \mp 2\pi i \sum_n |\langle n | a_{\mathbf{k}} | \Psi_0 \rangle|^2 \delta(\omega + E_n - E_g) , \quad (11.3')$$

where $|\Psi_0\rangle$ is the ground state and E_g the ground state energy.

One can easily show from (11.2) and (11.3) that

$$\tilde{g}^<(\mathbf{k}, \omega) = \pm e^{-\beta(\omega - \mu)} \tilde{g}^>(\mathbf{k}, \omega) . \quad (11.4)$$

In the $T = 0$ limit, (11.4) becomes

$$\begin{aligned} \tilde{g}^<(\mathbf{k}, \omega) &= 0 \text{ for } \omega > \mu , \\ \tilde{g}^>(\mathbf{k}, \omega) &= 0 \text{ for } \omega < \mu . \end{aligned} \quad (11.4')$$

Equation (11.4') can be proved directly from (11.2') and (11.3') by taking into account that $\mu = E_g(N + 1) - E_g(N) = E_g(N) - E_g(N - 1)$.

Let us now define a generalized DOS-like quantity $A(\mathbf{k}, \omega)$ as follows:

$$A(\mathbf{k}, \omega) \equiv i\tilde{g}(\mathbf{k}, \omega) = i[\tilde{g}^>(\mathbf{k}, \omega) - \tilde{g}^<(\mathbf{k}, \omega)] . \quad (11.5)$$

Taking into account (11.4,11.5) we can express both $\tilde{g}^>(\mathbf{k}, \omega)$ and $\tilde{g}^<(\mathbf{k}, \omega)$ in terms of $A(\mathbf{k}, \omega)$. We find

$$\tilde{g}^>(\mathbf{k}, \omega) = -iA(\mathbf{k}, \omega) [1 \pm f_{\mp}(\omega)] , \quad (11.6)$$

$$\tilde{g}^<(\mathbf{k}, \omega) = \mp iA(\mathbf{k}, \omega) f_{\mp}(\omega) , \quad (11.7)$$

where

$$f_{\mp}(\omega) = \frac{1}{e^{\beta(\omega - \mu)} \mp 1} \quad (11.8)$$

is the Bose (Fermi) distribution. Equations (11.6,11.7) become in the $T = 0$ limit and for fermions

$$\tilde{g}^>(\mathbf{k}, \omega) = -iA(\mathbf{k}, \omega)\theta(\omega - \mu) , \quad (11.6')$$

$$\tilde{g}^<(\mathbf{k}, \omega) = iA(\mathbf{k}, \omega)\theta(\mu - \omega) ; \quad (11.7')$$

for bosons the $T = 0$ limit is more complicated as a result of the phenomenon of Bose condensation.

From (11.2), (11.3), and (11.5) it is easy to see that the generalized DOS-like quantity $A(\mathbf{k}, \omega)$ is real. For fermions it is always nonnegative. For bosons it is nonnegative for $\omega > \mu$ and nonpositive for $\omega < \mu$. One can show further that $A(\mathbf{k}, \omega)$ obeys the following sum rule:

$$\int \frac{d\omega}{2\pi} A(\mathbf{k}, \omega) = 1. \quad (11.9)$$

Equation (11.9) can be proved with the aid of (11.2), (11.3), and (11.5) or as follows:

$$\begin{aligned} \int \frac{d\omega}{2\pi} A(\mathbf{k}, \omega) &= i \int \frac{d\omega}{2\pi} \int dt e^{i\omega t} [\tilde{g}^>(\mathbf{k}, t) - \tilde{g}^<(\mathbf{k}, t)] \\ &= i [\tilde{g}^>(\mathbf{k}, 0) - \tilde{g}^<(\mathbf{k}, 0)] = \langle a_{\mathbf{k}} a_{\mathbf{k}}^\dagger \mp a_{\mathbf{k}}^\dagger a_{\mathbf{k}} \rangle = 1. \end{aligned}$$

Consider now the Green's function $G(\mathbf{k}, \omega)$ defined by

$$G(\mathbf{k}, \omega) = \int_{-\infty}^{\infty} \frac{d\omega'}{2\pi} \frac{A(\mathbf{k}, \omega')}{\omega - \omega'}. \quad (11.10)$$

The function $G(\mathbf{k}, \omega)$ is analytic in the complex ω -plane and has singularities (branch cuts, in general) along those portions of the real axis where $A(\mathbf{k}, \omega) \neq 0$. From (11.10) and (11.5) it follows that

$$G(\mathbf{k}, \omega + is) - G(\mathbf{k}, \omega - is) = -iA(\mathbf{k}, \omega) = \tilde{g}(\mathbf{k}, \omega), \quad (11.11)$$

where ω is real and $s \rightarrow 0^+$. In view of (11.11) it follows immediately that $\tilde{g}(\mathbf{k}, t)$ is given by integrating $e^{-i\omega\tau} G/2\pi$ along the contour shown in Fig. 11.1f.

Now we can show that $g^R(\mathbf{k}, \tau)$ can be written as

$$g^R(\mathbf{k}, \tau) = \int_C \frac{d\omega}{2\pi} e^{-i\omega\tau} G(\mathbf{k}, \omega), \quad (11.12)$$

where the integration path C is shown in Fig. 11.1b. The proof is as follows. For negative τ we can close the integration path by a semicircle in the upper half-plane, and consequently $g^R(\mathbf{k}, t) = 0$ for $\tau < 0$, as it should be. For $\tau > 0$ we can close the path by a semicircle in the lower half-plane and the resulting contour can be deformed as in Fig. 11.1f. Hence for $\tau > 0$

$$\begin{aligned} \int_C \frac{d\omega}{2\pi} e^{-i\omega t} G(\mathbf{k}, \omega) &= \int_{-\infty}^{\infty} \frac{d\omega}{2\pi} e^{-i\omega\tau} [G(\mathbf{k}, \omega + is) - G(\mathbf{k}, \omega - is)] \\ &= \int_{-\infty}^{\infty} \frac{d\omega}{2\pi} e^{-i\omega\tau} \tilde{g}(\mathbf{k}, \omega) \\ &= \tilde{g}(\mathbf{k}, \tau) = \tilde{g}^R(\mathbf{k}, \tau). \end{aligned}$$

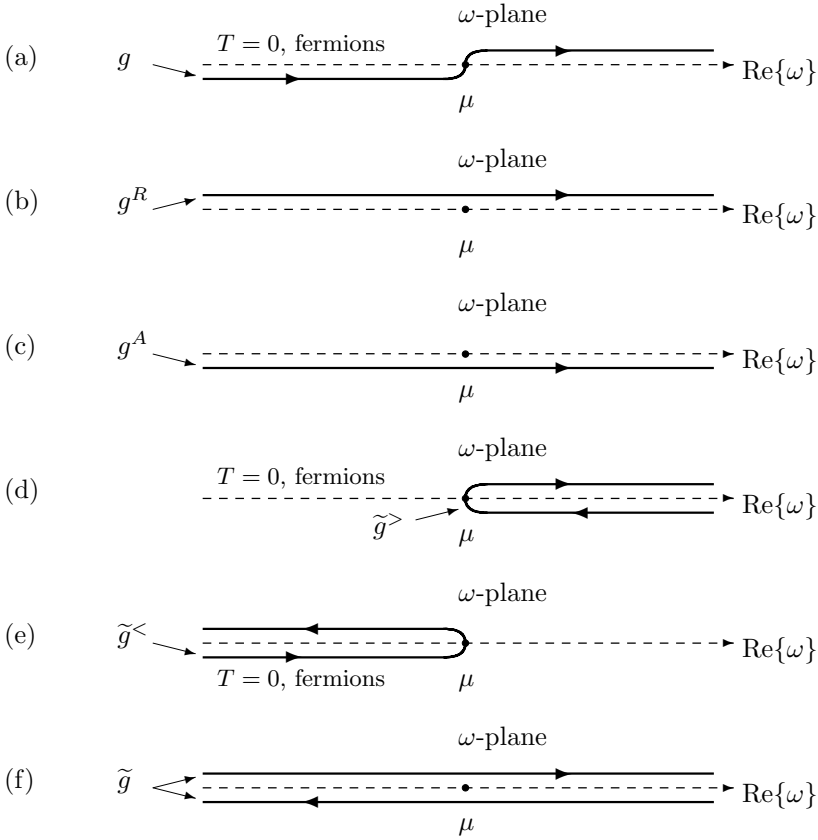


Fig. 11.1. Integration paths in the complex ω -plane for obtaining the various $g(\tau)$ s and $\tilde{g}(\tau)$ s. The quantities g , $\tilde{g}^>$, and $\tilde{g}^<$ are given by the corresponding integrals only for $T = 0$. The singularities of the integrand are located on the real ω -axis

In a similar way we can show that

$$g^A(\mathbf{k}, \tau) = \int_C \frac{d\omega}{2\pi} e^{-i\omega\tau} G(\mathbf{k}, \omega), \tag{11.13}$$

where path C is shown in Fig. 11.1c.

For the Fourier transforms we have

$$g^R(\mathbf{k}, \omega) = \lim_{s \rightarrow 0^+} G(\mathbf{k}, \omega + is), \tag{11.14}$$

$$g^A(\mathbf{k}, \omega) = \lim_{s \rightarrow 0^+} G(\mathbf{k}, \omega - is), \tag{11.15}$$

where ω is real. Equations (11.14) and (11.15) can be written by taking into account (11.10) as follows:

$$\operatorname{Re} \{g^R(\mathbf{k}, \omega)\} = \operatorname{Re} \{g^A(\mathbf{k}, \omega)\} = \mathcal{P} \int_{-\infty}^{\infty} \frac{d\omega'}{2\pi} \frac{A(\mathbf{k}, \omega')}{\omega - \omega'}, \quad (11.16)$$

$$\operatorname{Im} \{g^R(\mathbf{k}, \omega)\} = -\operatorname{Im} \{g^A(\mathbf{k}, \omega)\} = -\frac{1}{2}A(\mathbf{k}, \omega). \quad (11.17)$$

From the general relation $g = g^R + \tilde{g}^<$ [see (2.39)], with the aid of (11.7) and (11.17) we obtain for real ω

$$\operatorname{Re} \{g(\mathbf{k}, \omega)\} = \operatorname{Re} \{g^R(\mathbf{k}, \omega)\} = \operatorname{Re} \{g^A(\mathbf{k}, \omega)\} \quad (11.18)$$

$$\begin{aligned} \operatorname{Im} \{g(\mathbf{k}, \omega)\} &= -\frac{1}{2}A(\mathbf{k}, \omega) \mp A(\mathbf{k}, \omega)f_{\mp}(\omega) \\ &= -A(\mathbf{k}, \omega) \left[\frac{1}{2} \pm f_{\mp}(\omega) \right] \\ &= \operatorname{Im} \{g^R(\mathbf{k}, \omega)\} [1 \pm 2f_{\mp}(\omega)] \\ &= \operatorname{Im} \{g^R(\mathbf{k}, \omega)\} \times \left\{ \coth \left[\frac{\beta(\omega - \mu)}{2} \right] \right\}. \end{aligned} \quad (11.19)$$

Equation (11.19) in the limit $T = 0$ and for fermions becomes

$$\begin{aligned} \operatorname{Im} \{g(\mathbf{k}, \omega)\} &= \bar{\varepsilon}(\omega - \mu) \operatorname{Im} \{g^R(\mathbf{k}, \omega)\} = -\frac{1}{2}\bar{\varepsilon}(\omega - \mu)A(\mathbf{k}, \omega) \\ &= \lim_{s \rightarrow 0^+} \operatorname{Im} \{G(\mathbf{k}, \omega + is\bar{\varepsilon}(\omega - \mu))\}. \end{aligned} \quad (11.19')$$

From (11.19') and (11.18) it follows that, for $T = 0$ and for fermions, $g(\mathbf{k}, \tau)$ can be obtained by integrating $g(\mathbf{k}, \omega) \cdot e^{-i\omega\tau}/2\pi$ along the path shown in Fig. 11.1a. By taking into account (11.6'), (11.7'), and (11.11), we see that $\tilde{g}^>(\mathbf{k}, \tau)$ and $\tilde{g}^<(\mathbf{k}, \tau)$ (for $T = 0$ and for fermions) are given by integrating $G(\mathbf{k}, \tau) \cdot$

$e^{-i\omega\tau}/2\pi$ along the contours shown in Fig. 11.1d and e, respectively. With the aid of (11.18), (11.16), and 11.19) we can express the $\operatorname{Re} \{g(\mathbf{k}, \omega)\}$ in terms of $\operatorname{Im} \{g(\mathbf{k}, \omega)\}$ as follows:

$$\operatorname{Re} \{g(\mathbf{k}, \omega)\} = -2\mathcal{P} \int_{-\infty}^{\infty} \frac{d\omega'}{2\pi} \frac{\operatorname{Im} \{g(\mathbf{k}, \omega')\}}{\omega - \omega'} \times \left\{ \tanh \left[\frac{\beta(\omega - \mu)}{2} \right] \right\}. \quad (11.20)$$

We conclude this section with some remarks.

1. We see that all g s and \tilde{g} s can be expressed in terms of a single quantity, namely, $A(\mathbf{k}, \omega) = i\tilde{g}(\mathbf{k}, \omega)$, or in terms of the limiting values as $s \rightarrow 0^+$ of an analytic function $G(\mathbf{k}, \omega + is)$. Note that $\tilde{g}(\mathbf{k}, \omega)$, $g^R(\mathbf{k}, \omega)$, and $g^A(\mathbf{k}, \omega)$ depend only on $A(\mathbf{k}, \omega)$ [or $\lim G(\mathbf{k}, \omega + is)$]; on the other hand, $g(\mathbf{k}, \omega)$, $\tilde{g}^>(\mathbf{k}, \omega)$, and $\tilde{g}^<(\mathbf{k}, \omega)$ involve both $A(\mathbf{k}, \omega)$ and universal thermal factors; in other words, $\tilde{g}^>$, $\tilde{g}^<$, and g are not simply the limits of $G(\mathbf{k}, \omega \pm is)$ as $s \rightarrow 0^+$ (except when $T = 0$ and for fermions). This means that $\tilde{g}^>(\mathbf{k}, \omega)$, $\tilde{g}^<(\mathbf{k}, \omega)$, and $g(\mathbf{k}, \omega)$ cannot be continued off the real ω -axis to produce functions that are analytic everywhere off the real ω -axis. This could be

a serious drawback when one uses the residue theorem to evaluate integrals or when one attempts to uniquely determine $g(\mathbf{k}, \omega)$ by continuing off the real ω -axis the equation obeyed by $g(\mathbf{k}, \omega)$. We shall return to this last point in the next chapter.

2. Note the close analogy of the analytic properties of the various g s and \tilde{g} s for a many-body system and the g s and \tilde{g} s defined in Chap. 2. Thus the quantity $A(\mathbf{k}, \omega)$ is the analog of $2\pi\rho(\mathbf{k}, \omega)$, where $\rho(\mathbf{k}, E)$ is the density of states per unit volume in the \mathbf{k} -space. The function $G(\mathbf{k}, z) = \int d\omega'(z - \omega')^{-1}A(\mathbf{k}, \omega')/2\pi$ is the analog of the diagonal matrix element (in the \mathbf{k} -representation) of the Green's function $G(\mathbf{k}, z) = \langle \mathbf{k} | (z - \mathcal{H})^{-1} | \mathbf{k} \rangle$. Similarly, the quantities $\tilde{g}, \tilde{g}^>, \tilde{g}^<, g^R, g^A$, and g have their counterparts for the single-particle case. One must keep in mind that there are differences between the g s defined in Chap. 2 and those defined in Chap. 10. We mention some: the $\omega = 0$ point in the Chap. 2 case corresponds to the $\omega = \mu$ point in the Chap. 10 case (compare Fig. 2.2 and Fig. 11.1). This difference can be easily eliminated by slightly modifying the definition of Green's function, i.e., by replacing \mathcal{H} by $\mathcal{H} - \mu N$ in (10.15) and (10.16). This replacement implies that $\omega \rightarrow \omega' = \omega - \mu$. Many authors use this modified definition (see, e.g., [20, 113]). The quantities $\tilde{g}^>, \tilde{g}^<$, and g have the same analytic structure as the corresponding functions defined in Chap. 2 only for fermions at $T = 0$. The quantity $\rho(E)$ can become a δ -function in a proper representation, while $A(\omega)$ cannot, in general, become a δ -function no matter what representation we choose. Finally, we mention once more that the equations obeyed by the many-body Green's functions are not as simple as those obeyed by the g s (or \tilde{g} s) of Chap. 2 because an extra term is present involving higher-order Green's functions.
3. In Table 11.1 we present the connection of our notation with that used in various books [20, 113, 114, 130, 135, 420, 421] on the subjects. All these monographs deal mainly with the causal Green's function g .

11.2 Physical Significance and Use of g s and \tilde{g} s

In this section we examine the question of what physical information can be extracted from the various Green's functions. The thermodynamic average of any quantity that is the sum of one-body terms can be expressed immediately in terms of the Green's functions. As mentioned in Appendix I, such quantities can be written in the second quantized formalism as

$$F = \int d^3r \psi^\dagger(\mathbf{r}) F(\mathbf{r}) \psi(\mathbf{r}), \quad (11.21)$$

where $F(\mathbf{r})$ is the first quantized one-particle operator. Examples of operators F are the kinetic energy T with $T(\mathbf{r}) = -\nabla^2/2m$, the total number of particles N with $N(\mathbf{r}) = 1$, and the density operator $n(\mathbf{r}_0)$ with $n(\mathbf{r}) = \delta(\mathbf{r} - \mathbf{r}_0)$.

Table 11.1. Connection of the notation used in the present work with that used in other books on the subject. The symbol $(fT = 0)$ denotes the corresponding quantity for fermions at $T = 0$ K

Our notation	[20]	[113]	[420]	[130]	[135]	[421]	[114]
$g(\mathbf{k}, \omega)$	$\tilde{G}(\mathbf{k}, \omega - \mu)$	$G(\mathbf{k}, \omega - \mu)$	$G(\mathbf{k}, \omega)$	—	$G(\mathbf{k}, \omega)$	$G^T(\mathbf{k}, \omega)$	$G_t(\mathbf{k}, \omega)$
$g(\mathbf{k}, \omega) (fT = 0)$	$G(\mathbf{k}, \omega)$	$G(\mathbf{k}, \omega - \mu)$	—	—	$G(\mathbf{k}, \omega)$	$G(\mathbf{k}, \omega)$	—
$g^R(\mathbf{k}, \omega)$	$\tilde{G}^R(\mathbf{k}, \omega - \mu)$	$G^R(\mathbf{k}, \omega - \mu)$	—	—	$G^R(\mathbf{k}, \omega)$	—	G_{ret}
$g^R(\mathbf{k}, \omega) (fT = 0)$	$G^R(\mathbf{k}, \omega)$	$G_R(\mathbf{k}, \omega - \mu)$	—	—	$G^R(\mathbf{k}, \omega)$	—	—
$g^A(\mathbf{k}, \omega)$	$\tilde{G}^A(\mathbf{k}, \omega - \mu)$	$G^A(\mathbf{k}, \omega - \mu)$	—	—	—	—	—
$g^A(\mathbf{k}, \omega) (fT = 0)$	$G^A(\mathbf{k}, \omega)$	$G_A(\mathbf{k}, \omega - \mu)$	—	—	—	—	—
$\tilde{g}(\mathbf{k}, \omega)$	$-i\rho(\mathbf{k}, \omega - \mu)$	$2\pi i\rho(\mathbf{k}, \omega - \mu)$	$-iA(\mathbf{k}, \omega)$	—	—	—	—
$\tilde{g}(\mathbf{k}, \omega) (fT = 0)$	—	—	—	—	—	—	—
$A(\mathbf{k}, \omega)$	$\rho(\mathbf{k}, \omega - \mu)$	$-2\pi\rho(\mathbf{k}, \omega - \mu)$	$A(\mathbf{k}, \omega)$	—	—	—	$A(\mathbf{k}, \omega)$
$A(\mathbf{k}, \omega) (fT = 0)$	—	—	—	—	—	—	—
$\tilde{g}^>(\mathbf{k}, \omega)$	—	—	$G^>(\mathbf{k}, \omega)$	—	$-iJ_1(\mathbf{k}, \omega)$	—	$G^>(\mathbf{k}, \omega)$
$\tilde{g}^>(\mathbf{k}, \omega) (fT = 0)$	$-2\pi iA(\mathbf{k}, \omega - \mu)$	$-2\pi iA(\mathbf{k}, \omega - \mu)$	$G^<(\mathbf{k}, \omega)$	$-2\pi iA_+(\mathbf{k}, \omega - \mu)$	—	$-2\pi iA^+(\mathbf{k}, \omega - \mu)$	$G^<(\mathbf{k}, \omega)$
$\tilde{g}^<(\mathbf{k}, \omega)$	—	—	—	—	$\mp iJ_2(\mathbf{k}, \omega)$	—	—
$\tilde{g}^<(\mathbf{k}, \omega) (fT = 0)$	$2\pi iB(\mathbf{k}, \mu - \omega)$	$2\pi iB(\mathbf{k}, \mu - \omega)$	$G(\mathbf{k}, z)$	$2\pi iA_-(\mathbf{k}, \mu - \omega)$	—	$2\pi iA^-(\mathbf{k}, \mu - \omega)$	—
$G(\mathbf{k}, z)$	$\Gamma(\mathbf{k}, z - \mu)$	—	—	—	$G(\mathbf{k}, z)$	—	$\mathcal{G}(\mathbf{k}, z)$
$G(\mathbf{k}, z) (fT = 0)$	—	—	—	—	$G(\mathbf{k}, z)$	—	—

It follows from the definition of $\tilde{g}^<$ that

$$\begin{aligned}\langle F \rangle &= \pm i \int d^3r F(\mathbf{r}) \tilde{g}^<(\mathbf{r}, t, \mathbf{r}, t) \\ &= \pm i \int d^3r F(\mathbf{r}) \lim_{t' \rightarrow t^+} g(\mathbf{r}, t, \mathbf{r}, t').\end{aligned}\quad (11.22)$$

More specifically, we have the kinetic energy $\langle T \rangle$ and the density $\langle n(\mathbf{r}) \rangle$

$$\begin{aligned}\langle T \rangle &= \pm i \int d^3r \lim_{\substack{\mathbf{r}' \rightarrow \mathbf{r} \\ t' \rightarrow t^+}} \left[-\frac{\nabla^2}{2m} g(x, x') \right] \\ &= \pm i \sum_{\mathbf{k}} \int_{-\infty}^{\infty} \frac{d\omega}{2\pi} \tilde{g}^<(\mathbf{k}, \omega) \frac{k^2}{2m} \\ &= \sum_{\mathbf{k}} \int_{-\infty}^{\infty} \frac{d\omega}{2\pi} A(\mathbf{k}, \omega) f_{\mp}(\omega) \frac{k^2}{2m},\end{aligned}\quad (11.23)$$

$$\begin{aligned}\langle n(\mathbf{r}) \rangle &= \pm i \lim_{t' \rightarrow t^+} g(\mathbf{r}, t, \mathbf{r}, t') \\ &= \int \frac{d^3k}{(2\pi)^3} \int_{-\infty}^{\infty} \frac{d\omega}{2\pi} A(\mathbf{k}, \omega) f_{\mp}(\omega).\end{aligned}\quad (11.24)$$

The density in \mathbf{k} -space is

$$\langle n(\mathbf{k}) \rangle = \langle a_{\mathbf{k}}^{\dagger} a_{\mathbf{k}} \rangle = \int_{-\infty}^{\infty} \frac{d\omega}{2\pi} A(\mathbf{k}, \omega) f_{\mp}(\omega).\quad (11.25)$$

Operators that involve summation over pairs of particles such as the interaction energy V_i (Appendix I), contain four ψ s (two ψ s and two ψ^{\dagger} s). These operators can be expressed in terms of g_2 and not g . However, the interaction Hamiltonian V_i , which is connected through the Schrödinger equation with T , can be written in terms of g . To show this we use the basic equation (see Appendix I)

$$\left(i \frac{\partial}{\partial t} + \frac{\nabla^2}{2m} \right) \psi(\mathbf{r}, t) = \int d^3r_1 v(\mathbf{r} - \mathbf{r}_1) \psi^{\dagger}(\mathbf{r}_1, t) \psi(\mathbf{r}_1, t) \psi(\mathbf{r}, t)\quad (11.26)$$

and its adjoint

$$\begin{aligned}\left(-i \frac{\partial}{\partial t'} + \frac{\nabla'^2}{2m} \right) \psi^{\dagger}(\mathbf{r}', t') \\ = \psi^{\dagger}(\mathbf{r}', t') \int d^3r_2 v(\mathbf{r}' - \mathbf{r}_2) \psi^{\dagger}(\mathbf{r}_2, t') \psi(\mathbf{r}_2, t').\end{aligned}\quad (11.27)$$

Multiplying (11.26) from the left by $\psi^{\dagger}(\mathbf{r}', t')/4$ and (11.27) from the right by $\psi(\mathbf{r}, t)/4$, subtracting the resulting equations, setting $t' = t$ and $\mathbf{r}' = \mathbf{r}$ and integrating over \mathbf{r} we obtain

$$\frac{1}{4} \int d^3r \left[\left(i \frac{\partial}{\partial t} - i \frac{\partial}{\partial t'} \right) \langle \psi^{\dagger}(\mathbf{r}, t') \psi(\mathbf{r}, t) \rangle \right]_{t=t'} = \frac{1}{2} \langle T \rangle + \langle V_i \rangle.\quad (11.28)$$

Using (11.23) and the definition of g , we obtain from (11.28)

$$\begin{aligned} \langle V_i \rangle &= \pm \frac{i}{2} \int d^3r \lim_{\substack{t' \rightarrow t^+ \\ \mathbf{r}' \rightarrow \mathbf{r}}} \left[i \frac{\partial}{\partial t} + \frac{\nabla_r^2}{2m} \right] g(x, x') \\ &= \sum_{\mathbf{k}} \int \frac{d\omega}{2\pi} \frac{1}{2} \left(\omega - \frac{k^2}{2m} \right) A(\mathbf{k}, \omega) f_{\mp}(\omega) . \end{aligned} \quad (11.29)$$

Adding (11.23) and (11.29) we obtain for the total energy

$$\begin{aligned} \langle \mathcal{H} \rangle &= \pm \frac{i}{2} \int d^3r \lim_{\substack{t' \rightarrow t^+ \\ \mathbf{r}' \rightarrow \mathbf{r}}} \left[i \frac{\partial}{\partial t} - \frac{\nabla_r^2}{2m} \right] g(x, x') \\ &= \sum_{\mathbf{k}} \int \frac{d\omega}{2\pi} \frac{1}{2} \left(\omega + \frac{k^2}{2m} \right) A(\mathbf{k}, \omega) f_{\mp}(\omega) . \end{aligned} \quad (11.30)$$

To obtain all the other thermodynamic quantities it is enough to calculate the grand partition function $Z_G \equiv \text{Tr} \{ \exp[-\beta(\mathcal{H} - \mu N)] \}$ as a function of the volume Ω , the chemical potential μ , and the temperature $T \equiv 1/k_B\beta$. Z_G is directly related to the pressure by the general thermodynamic equation

$$Z_G = e^{\beta\Omega P} . \quad (11.31)$$

Furthermore, the pressure can be expressed in terms of the density as [420]

$$P(\beta, \mu) = \int_{-\infty}^{\mu} d\mu' n(\beta, \mu') . \quad (11.32)$$

Substituting in (11.32) from (11.24) we have

$$P(\beta, \mu) = \int_{-\infty}^{\mu} d\mu' \int \frac{d^3k}{(2\pi)^3} \int \frac{d\omega}{2\pi} A(\mathbf{k}, \omega) f_{\mp}(\omega) , \quad (11.33)$$

where both $A(\mathbf{k}, \omega)$ and $f_{\mp}(\omega)$ depend, in general, on the inverse temperature and the chemical potential μ' . Unfortunately, the integral over μ' can rarely be performed explicitly [420].

Another way to calculate Z_G (which avoids this difficulty) is based on the general thermodynamic relation [422]

$$\left\langle \frac{\partial \mathcal{H}}{\partial a} \right\rangle = -\Omega \left. \frac{\partial P}{\partial a} \right|_{T, \mu} , \quad (11.34)$$

where a is any parameter in the total Hamiltonian \mathcal{H} . We write for \mathcal{H}

$$\mathcal{H} = T + a V_i , \quad (11.35)$$

so that $a = 0$ corresponds to the noninteracting case and $a = 1$ corresponds to the actual case. Taking into account (11.31), (11.34), and (11.35) we obtain

$$-\beta \langle V_i \rangle = \frac{\partial}{\partial a} [\ln(Z_G)] . \tag{11.36}$$

Integrating (11.36) over a and using (11.29), we have, finally,

$$\begin{aligned} \ln(Z_G) &= \beta P \Omega \\ &= \beta P_0 \Omega - \beta \int_0^1 \frac{da}{a} \sum_{\mathbf{k}} \int \frac{d\omega}{2\pi} \frac{1}{2} \left(\omega - \frac{k^2}{2m} \right) A_a(\mathbf{k}, \omega) f_{\mp}(\omega) , \end{aligned} \tag{11.37}$$

where the subscript a in $A(\mathbf{k}, \omega)$ denotes that $A_a(\mathbf{k}, \omega)$ corresponds to the Hamiltonian (11.35), and P_0 is the pressure for the noninteracting system.

Another class of important physical quantities which are related to the Green's functions are the linear response functions introduced in §8.2.4. The system is perturbed from equilibrium at $t = t_0$ by an external Hamiltonian $\mathcal{H}_1(t)$ which has the form

$$\mathcal{H}_1(t) = \int d^3r B(\mathbf{r}, t) f(\mathbf{r}, t) , \tag{11.38}$$

where $B(\mathbf{r}, t)$ is an operator and $f(\mathbf{r}, t)$ is a c -number such that $f(\mathbf{r}, t) = 0$ for $t < t_0$. According to (8.38), the first order in \mathcal{H}_1 of the change, $\delta \langle X \rangle = \langle X \rangle - \langle X_0 \rangle$, of an operator $X(\mathbf{r}, t)$, as a result of the application of \mathcal{H}_1 , is given by (for $\hbar = 1$):

$$\delta X(\mathbf{r}, t) = -i \int dt' d^3r' \langle [X(\mathbf{r}, t), B(\mathbf{r}', t')] \rangle f(\mathbf{r}', t') , \tag{11.39}$$

where the time evolution of the operators $X(\mathbf{r}', t)$ and $B(\mathbf{r}', t')$ can be determined either by \mathcal{H}_0 or by $\mathcal{H}_0 + \mathcal{H}_1$, since we are interested in the linear response in \mathcal{H}_1 . For what follows we shall restrict ourselves to the usual case where $X = B$. We have then

$$\delta \langle B(\mathbf{r}, t) \rangle = \int_{-\infty}^{\infty} dt' \int d^3r' D^R(\mathbf{r}, t, \mathbf{r}', t') f(\mathbf{r}', t') . \tag{11.39'}$$

Equation (11.39') is the analog of (2.52) with $\psi - \phi$ replaced by $\delta \langle B(\mathbf{r}, t) \rangle$. The quantity $D^R(x, x')$ is

$$D^R(x, x') = -i\theta(t - t') \langle [B(x), B(x')] \rangle , \tag{11.40}$$

i.e., it has the form of a retarded Green's function with the field operator ψ replaced by the operator B . A specific example of the above, directly related to the one examined in §8.2.4, is the case of an external electrostatic potential $\phi_e(\mathbf{r}, t)$ applied to a system of electrons (each of charge $-e$) placed in a uniform positive background (to ensure overall electrical neutrality). In this

case, $B(\mathbf{r}, t) = \delta n(\mathbf{r}, t)$, where $\delta n(\mathbf{r}, t)$ is the deviation of the electronic density from its equilibrium value n_0 , $f(\mathbf{r}, t) = (-e)\phi_e(\mathbf{r}, t)$, and $\delta \langle B(\mathbf{r}, t) \rangle$ is $\langle \delta n(\mathbf{r}, t) \rangle$. Thus the Fourier transform of (11.39') takes the form

$$\langle \delta n(\mathbf{k}, \omega) \rangle = (-e)D^R(\mathbf{k}, \omega)\phi_e(\mathbf{k}, \omega), \quad (11.41)$$

where $D^R(\mathbf{k}, \omega)$ is the Fourier transform of $D^R(x, x')$ with respect to the variable $x - x'$ and

$$\begin{aligned} D^R(x, x') &= -i\theta(t - t') \langle [\delta n(x), \delta n(x')] \rangle \\ &= -i\theta(t - t') \langle [(\psi^\dagger(x)\psi(x) - n_0), (\psi^\dagger(x')\psi(x') - n_0)] \rangle \\ &= -i\theta(t - t') \langle [\psi^\dagger(x)\psi(x), \psi^\dagger(x')\psi(x')] \rangle. \end{aligned} \quad (11.42)$$

Equation (11.42) shows that $D^R(x, x')$ is related to the two-particle Green's function g_2 . Taking into account that the external potential ϕ_e is related to the external density n_e with Poisson's equation

$$\phi_e(\mathbf{k}, \omega) = -4\pi \frac{en_e(\mathbf{k}, \omega)}{k^2}, \quad (11.43)$$

and that the longitudinal dielectric function, $\varepsilon(\mathbf{k}, \omega)$, is defined by

$$\varepsilon(\mathbf{k}, \omega) \equiv \frac{en_e(\mathbf{k}, \omega)}{en_e(\mathbf{k}, \omega) + e \langle \delta n(\mathbf{k}, \omega) \rangle}, \quad (11.44)$$

we can express $\varepsilon(\mathbf{k}, \omega)$ in terms of D^R as follows:

$$\frac{1}{\varepsilon(\mathbf{k}, \omega)} - 1 = \frac{4\pi e^2}{k^2} D^R(\mathbf{k}, \omega). \quad (11.45)$$

Since the longitudinal conductivity $\sigma(\mathbf{k}, \omega)$ is related to $\varepsilon(\mathbf{k}, \omega)$ by (8.15)

$$\varepsilon(\mathbf{k}, \omega) = 1 - \frac{4\pi}{i\omega} \sigma(\mathbf{k}, \omega), \quad (11.46)$$

we conclude that the longitudinal conductivity can be expressed in terms D^R , i.e., in terms of g_2 . The quantity $\delta n(x)$ in (11.42) is related to the current operator by the continuity equation; as a result, D^R can be expressed in terms of the current-current commutator. This is a special case of the fluctuation-dissipation theorem [253], which connects the imaginary part of a response function (which determines the dissipation of energy) to the square of the fluctuation of the corresponding physical quantity. For more details on the evaluation of the transverse and longitudinal conductivity the reader is referred to [113, 135, 423].

As we can see from (11.23), (11.24), (11.29), (11.30), (11.33), and (11.37), the various thermodynamic quantities involve an integral of the type

$$I = \lim_{\sigma \rightarrow 0^-} I(\sigma) = \lim_{\sigma \rightarrow 0^-} \int \frac{d\omega}{2\pi} e^{-\omega\sigma} F(\omega) A(\mathbf{k}, \omega) f_{\mp}(\omega), \quad (11.47)$$

where $F(\omega)$ is a polynomial; the factor $e^{-\omega\sigma}$ was introduced in order to allow the transformations that follow. Taking into account (11.11) and subtracting the contribution of the pole of $f_-(\omega)$ at $\omega = \mu$ we can write for $I(\sigma)$

$$\begin{aligned}
 I(\sigma) + \frac{1}{\beta} e^{-z_0\sigma} F(z_0) G(\mathbf{k}, z_0) &= i \int_C \frac{d\omega}{2\pi} e^{-\omega\sigma} F(\omega) G(\mathbf{k}, \omega) f_{\mp}(\omega) \\
 &= i \int_{C_R} \frac{d\omega}{2\pi} e^{-\omega\sigma} F(\omega) G(\mathbf{k}, \omega) f_{\mp}(\omega) \\
 &\quad - i \int_{C_A} \frac{d\omega}{2\pi} e^{-\omega\sigma} F(\omega) G(\mathbf{k}, \omega) f_{\mp}(\omega), \tag{11.48}
 \end{aligned}$$

where $z_0 \equiv \mu$ and the contour $C = C_R - C_A$ and paths C_R and C_A are shown in Fig. 11.1f,b,c, respectively. For fermions the last term of the lhs of (11.48) must be taken as zero. The integral over the path C_R , I_R can be transformed as shown in Fig. 11.2. The new path $C_1 + C_2 + C_3 + C_4$ avoids the poles of the integrand in the upper ω -half-plane; these poles come from $f_{\mp}(\omega)$ and are given by

$$z_\nu = \mu + \frac{i\pi\nu}{\beta} \begin{cases} \nu = 2n & \text{for bosons,} \\ \nu = 2n - 1 & \text{for fermions,} \end{cases} \tag{11.49a}$$

$$\tag{11.49b}$$

where n is a positive integer. Assuming that

$$-\beta < \sigma < 0, \tag{11.50}$$

we can easily show that the contributions from C_1 and C_4 vanish. Thus

$$I_R(\sigma) = \mp \frac{1}{\beta} \sum_{\nu>0} \exp(-z_\nu\sigma) F(z_\nu) G(\mathbf{k}, z_\nu); \tag{11.51}$$

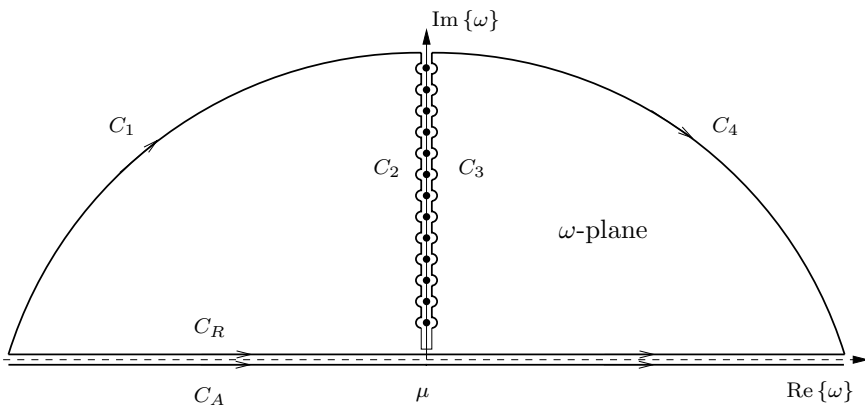


Fig. 11.2. The integration of $e^{-\omega\sigma} F(\omega) G(\mathbf{k}, \omega) f_{\mp}(\omega) / 2\pi$ (see text) along the path C_R can be equivalently performed along the composite path $C_1 + C_2 + C_3 + C_4$

in a similar way one shows that

$$I_A(\sigma) = \pm \frac{1}{\beta} \sum_{\nu < 0} e^{-z_\nu \sigma} F(z_\nu) G(\mathbf{k}, z_\nu) . \quad (11.52)$$

Combining (11.48), and (11.51), and (11.52) we have

$$\begin{aligned} I(\sigma) &= \mp \frac{1}{\beta} \sum_{\nu} e^{-z_\nu \sigma} F(z_\nu) G(\mathbf{k}, z_\nu) , \\ I &= \mp \frac{1}{\beta} \sum_{\nu} F(z_\nu) G(\mathbf{k}, z_\nu) . \end{aligned} \quad (11.53)$$

Equation (11.53) shows that the thermodynamic quantities can be obtained from the values of $G(\mathbf{k}, \omega)$ at the special points z_ν given by (11.49). The importance of this result stems from the fact that the quantities $G(\mathbf{k}, z_\nu)$ are easier to calculate than $A(\mathbf{k}, \omega)$. We shall return to this point in the next chapter.

The results of this section show that the quantity $A(\mathbf{k}, \omega)/2\pi$ not only reduces in the absence of interactions to the density of states $\varrho(\mathbf{k}, \omega)$ per unit volume in \mathbf{k} -space but also allows the calculation of various thermodynamic quantities in a way similar to the way that $\varrho(\mathbf{k}, \omega)$ gives the thermodynamics of noninteracting particles. Because of this property we can interpret the quantity $A(\mathbf{k}, \omega)/2\pi$ as a generalized density of states per unit frequency and unit volume in \mathbf{k} -space. Then, with the aid of (11.7), $\tilde{g}^<(\mathbf{k}, \omega)$ can be interpreted (apart from a factor $\pm i$) as the average number of particles per unit volume in \mathbf{k} - ω -space; similarly, with the aid of (11.6), $\tilde{g}^>(\mathbf{k}, \omega)$ can be interpreted as the average number of states (per unit volume in \mathbf{k} - ω -space) available for the addition of an extra particle to the system.

In the absence of interactions and for a translationally invariant system, we have

$$\frac{A(\mathbf{k}, \omega)}{2\pi} = \varrho(\mathbf{k}, \omega) = \delta(\omega - \varepsilon_k^0) , \quad (11.54)$$

where for Schrödinger particles $\varepsilon_k^0 = k^2/2m$. Equation (11.54) expresses simply the fact that in the absence of interactions a particle of momentum \mathbf{k} necessarily has energy ε_k^0 . A formal proof of (11.54) is obtained by combining (11.11) with (10.57). Substituting (11.54) in the basic formulae of Sects. 11.1 and 11.2, we rediscover the results of Sect. 10.3 and the well-known thermodynamic expressions for noninteracting particles.

11.3 Quasiparticles

Let us assume that $A(\mathbf{k}, \omega)$ has a sharp peak at $\omega = \varepsilon_{\mathbf{k}}$; for simplicity we assume further that the peak has a Lorentzian shape, i.e.,

$$A(\mathbf{k}, \omega) = A_b(\mathbf{k}, \omega) + \frac{2|\gamma_{\mathbf{k}}|w_{\mathbf{k}}}{(\omega - \varepsilon_{\mathbf{k}})^2 + \gamma_{\mathbf{k}}^2} . \quad (11.55)$$

Here $A_b(\mathbf{k}, \omega)$ is the smooth background, $\varepsilon_{\mathbf{k}}$ the position of the maximum, $|\gamma_{\mathbf{k}}|$ the width, and $w_{\mathbf{k}}$ ($0 < w_{\mathbf{k}} \leq 1$) the weight of the peak. It is natural to attempt to interpret the peak as representing a quasiparticle of momentum \mathbf{k} , energy $\varepsilon_{\mathbf{k}}$, and lifetime $\tau_{\mathbf{k}} = 1/|\gamma_{\mathbf{k}}|$; $w_{\mathbf{k}}$ can be interpreted as the percentage of a real particle participating in the creation of the corresponding quasiparticle. The quasiparticle can be thought of as a dressed particle consisting in part ($w_{\mathbf{k}}$) of a bare (real) particle and in part $(1 - w_{\mathbf{k}})$ of a cloud of other particles surrounding the bare one. As the interactions approach zero each quasiparticle tends to the corresponding bare particle, i.e.,

$$\varepsilon_{\mathbf{k}} \rightarrow \varepsilon_{\mathbf{k}}^0, \quad \tau_{\mathbf{k}} \rightarrow \infty, \quad |\gamma_{\mathbf{k}}| \rightarrow 0^+, \quad w_{\mathbf{k}} \rightarrow 1, \quad A_b \rightarrow 0.$$

The concept of quasiparticle is of fundamental importance in analyzing the behavior of many-body systems; it allows us to replace a system of strongly interacting particles by an equivalent system of weakly interacting quasiparticles. Then, in a first approximation, the interactions among the quasiparticles can be omitted, and the problem reduces to one that can be solved. A straightforward method to obtain the weakly interacting quasiparticles out of the strongly interacting particles is by a canonical transformation; this method, although conceptionally simple, is extremely difficult in practice since for every particular system one must find the appropriate canonical transformation. On the other hand, the Green's function method provides a general way to recognize the existence of weakly interacting quasiparticles as peaks in $A(\mathbf{k}, \omega)$. Furthermore, it gives basic information about the quasiparticles, i.e., it gives its energy as a function of its momentum; it gives its finite lifetime resulting from the weak interactions with the other quasiparticles; and, finally, it gives what percentage of the quasiparticle is made up of bare particle and what percentage is made up of cloud. For a more precise statement of the last sentence the reader is referred to Nozieres [423].

A peak in $A(\mathbf{k}, \omega)$ of the type shown in (11.55) will appear as a pole in the analytic continuation of $G(\mathbf{k}, \omega)$ across the discontinuity along the real ω -axis. The analytic continuation of $G(\mathbf{k}, \omega)$, *a.c.* $\{G(\mathbf{k}, \omega)\}$, to the lower ω -half-plane is, according to (11.11),

$$a.c.\{G(\mathbf{k}, \omega)\} = G(\mathbf{k}, \omega) - ia.c.\{A(\mathbf{k}, \omega)\}; \quad \text{Im}\{\omega\} < 0; \quad (11.56)$$

similarly,

$$a.c.\{G(\mathbf{k}, \omega)\} = G(\mathbf{k}, \omega) + ia.c.\{A(\mathbf{k}, \omega)\}; \quad \text{Im}\{\omega\} > 0. \quad (11.57)$$

Substituting (11.55) into (11.56) and (11.57) we obtain

$$\begin{aligned} a.c.\{G(\mathbf{k}, \omega)\} &= G(\mathbf{k}, \omega) \pm ia.c.\{A_b(\mathbf{k}, \omega)\} \pm \frac{2\gamma_{\mathbf{k}}w_{\mathbf{k}}i}{(\omega - \varepsilon_{\mathbf{k}})^2 + \gamma_{\mathbf{k}}^2} \\ &= G(\mathbf{k}, \omega) \pm ia.c.\{A_b(\mathbf{k}, \omega)\} \pm \frac{2\gamma_{\mathbf{k}}w_{\mathbf{k}}i}{(\omega - z_{\mathbf{k}})(\omega - z_{\mathbf{k}}^*)}, \\ \text{Im}\{\omega\} &\geq 0, \end{aligned} \quad (11.58)$$

where

$$z_{\mathbf{k}} = \varepsilon_{\mathbf{k}} + i\gamma_{\mathbf{k}}. \quad (11.59)$$

Thus, a sharp peak of Lorentzian shape in $A(\mathbf{k}, \omega)$ appears as a pole (near the real axis) of the analytic continuation $a.c.\{G(\mathbf{k}, \omega)\}$ of $G(\mathbf{k}, \omega)$ across the real axis. The real part of the pole gives the energy of the quasiparticle, the imaginary part gives the inverse lifetime, and the residue equals the weight $w_{\mathbf{k}}$. Taking into account (11.14), (11.15), and (11.58) we have

$$a.c.\{g^R(\mathbf{k}, \omega)\} = \begin{cases} G(\mathbf{k}, \omega), & \text{Im}\{\omega\} > 0, \quad (11.60a) \\ G(\mathbf{k}, \omega) - i.a.c.\{A_b\} \\ -\frac{2\gamma_{\mathbf{k}}w_{\mathbf{k}}i}{(\omega - z_{\mathbf{k}})(\omega - z_{\mathbf{k}}^*)}, & \text{Im}\{\omega\} < 0, \quad (11.60b) \end{cases}$$

$$a.c.\{g^A(\mathbf{k}, \omega)\} = \begin{cases} G(\mathbf{k}, \omega) + i.a.c.\{A_b\} \\ +\frac{2\gamma_{\mathbf{k}}w_{\mathbf{k}}i}{(\omega - z_{\mathbf{k}})(\omega - z_{\mathbf{k}}^*)}, & \text{Im}\{\omega\} > 0, \quad (11.61a) \\ G(\mathbf{k}, \omega), & \text{Im}\{\omega\} < 0. \quad (11.61b) \end{cases}$$

Equations (11.60) and (11.61) mean that a pole in the analytic continuation of $g^R(\mathbf{k}, \omega)[g^A(\mathbf{k}, \omega)]$ in the lower (upper) ω -half-plane describes a quasiparticle. The closer the pole to the real ω -axis, the better the quasiparticle is defined.

For fermions at $T = 0$ we obtain with the aid of (11.19') that the pole of the analytic continuation of $g(\mathbf{k}, \omega)$, $a.c.\{g(\mathbf{k}, \omega)\}$, appears, if at all, in the upper ω -half-plane when $\text{Re}\{\omega\} < \mu$ and in the lower ω -half-plane when $\text{Re}\{\omega\} > \mu$, i.e.,

$$a.c.\{g(\mathbf{k}, \omega)\} = \begin{cases} G(\mathbf{k}, \omega), & \text{Re}\{\omega\} > \mu, \text{Im}\{\omega\} > 0, \quad (11.62a) \\ a.c.\{G(\mathbf{k}, \omega)\}, & \text{Re}\{\omega\} < \mu, \text{Im}\{\omega\} > 0, \quad (11.62b) \\ G(\mathbf{k}, \omega), & \text{Re}\{\omega\} < \mu, \text{Im}\{\omega\} < 0, \quad (11.62c) \\ a.c.\{G(\mathbf{k}, \omega)\}, & \text{Re}\{\omega\} > \mu, \text{Im}\{\omega\} < 0, \quad (11.62d) \end{cases}$$

where $a.c.\{G(\mathbf{k}, \omega)\}$ is given by (11.58). The function $a.c.\{g(\mathbf{k}, \omega)\}$ as defined by (11.62) has a branch cut along the line $\text{Re}\{\omega\} = \mu$. Furthermore, a peak in $A(\mathbf{k}, \omega)$ of the type shown in (11.55) appears as a peak in $\text{Im}\{\tilde{g}^<(\mathbf{k}, \omega)\}$ when $\varepsilon_{\mathbf{k}} < \mu$ or as a peak in $-\text{Im}\{\tilde{g}^>(\mathbf{k}, \omega)\}$ when $\varepsilon_{\mathbf{k}} > \mu$. Since $\tilde{g}^<$ ($\tilde{g}^>$) describes the propagation of a hole (particle), it follows that when $\varepsilon_{\mathbf{k}} < \mu$, the pole in $a.c.\{g(\mathbf{k}, \omega)\}$, which lies in the upper half-plane describes a quasihole; when $\varepsilon_{\mathbf{k}} > \mu$, the pole in $a.c.\{g(\mathbf{k}, \omega)\}$ which lies in the lower ω -half-plane, describes a quasiparticle. This situation is summarized in Fig. 11.3. When k is very small, the elementary excitation is expected to be a quasihole; this means that for very small k the pole $z_{\mathbf{k}}$ lies in region II of Fig. 11.3. On the other hand, for very large k the pole lies in region IV. Assuming that the trajectory defined by $z_{\mathbf{k}}$ as k increases from zero is a continuous one, it follows that this trajectory must cross the real ω -axis at the point $\omega = \mu$. Thus, a characteristic

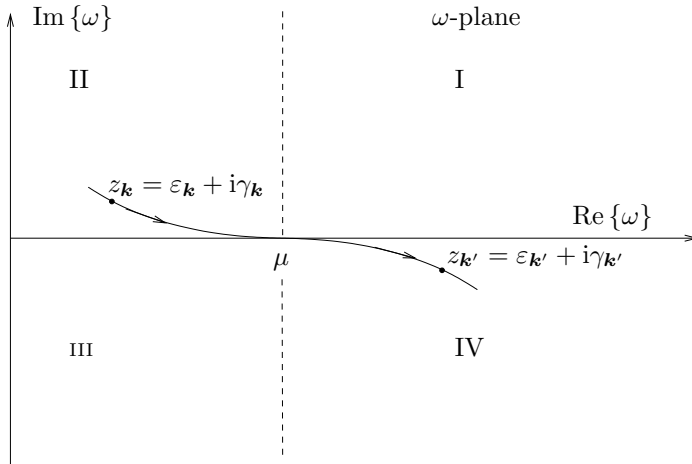


Fig. 11.3. Analytic structure in complex ω -plane of analytic continuation of $g(\mathbf{k}, \omega)$, $a.c.\{g(\mathbf{k}, \omega)\}$, as given by (11.62) for fermions at $T = 0$. A pole or any other singularity will appear either in region II (corresponding to a quasihole) or in region IV (corresponding to a quasiparticle). As k increases the pole moves along a trajectory, an example of which is shown. The function $a.c.\{g(\mathbf{k}, \omega)\}$ has a branch cut along the line $\text{Re}\{\omega\} = \mu$

surface in k -space, which is called the Fermi surface, can be defined by the relation

$$\varepsilon_{k_F} = \mu . \tag{11.63}$$

For a rotationally invariant system the Fermi surface is a sphere of radius k_F ; k_F is called the Fermi momentum. The Fermi surface as defined above has (under certain conditions) one property of the Fermi surface of a system of noninteracting particles, i.e., the quantity $\langle n(\mathbf{k}) \rangle$ is discontinuous at $k = k_F$. To show this, use (11.25) and (11.55) and assume that the slope of the pole trajectory is continuous at μ and of magnitude $s = \lim (|\gamma_k| / |\varepsilon_k - \mu|)$ as $k \rightarrow k_F$. Then we obtain

$$\langle n(\mathbf{k}_F^-) \rangle - \langle n(\mathbf{k}_F^+) \rangle = \frac{2w_{k_F}}{\pi} \tan^{-1} \left(\frac{1}{s} \right) . \tag{11.64}$$

Thus, if the slope is zero (as in Fig. 11.3), the discontinuity equals w_{k_F} . If the slope is infinite or if the trajectory is discontinuous at k_F , the difference $\langle n(\mathbf{k}_F^-) \rangle - \langle n(\mathbf{k}_F^+) \rangle$ is zero and the Fermi surface loses its usual physical meaning. In Fig. 11.4 we plot $n(\mathbf{k})$ vs. k for the case where $s = 0$. Systems for which the trajectory of the pole is continuous with a zero slope at μ are called *normal*.

We show now that for normal systems the quasiparticles (or quasiholes) near the Fermi surface can be used to analyze not only the thermodynamic behavior of the system but the dynamic behavior as well. For this purpose we try to calculate $g(\mathbf{k}, t)$, which, for $t > 0$, describes the propagation of an extra

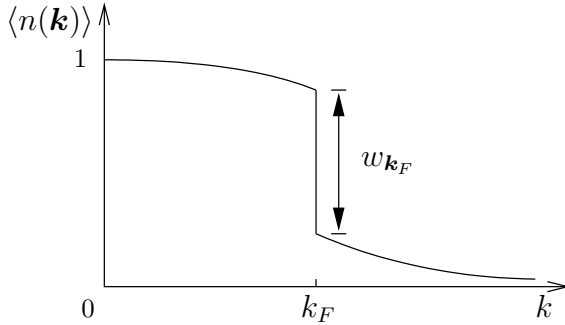


Fig. 11.4. Average particle number per unit volume in \mathbf{k} -space for a normal interacting Fermi system at $T = 0$; k_F is the Fermi momentum

particle added to the system at $t = 0$. As was mentioned before, for fermions at $T = 0$

$$g(\mathbf{k}, t) = \int_C \frac{d\omega}{2\pi} e^{-i\omega t} G(\mathbf{k}, \omega) = \int_C \frac{d\omega}{2\pi} e^{-i\omega t} a.c. \{g(\mathbf{k}, \omega)\}, \quad (11.65)$$

where the path C is shown in Fig. 11.1 a and (11.62) was used. For $t > 0$ the path can be closed by a semicircle in the lower ω -half-plane. The resulting contour can be deformed as shown in Fig. 11.5. We have assumed that there is a pole at $z_{\mathbf{k}}$, and any remaining singularities in region IV of the $a.c. \{g(\mathbf{k}, \omega)\}$ are below the line $\text{Im} \{\omega\} = -\Gamma$. The contribution from this line contains a factor $e^{-\Gamma t}$, and, consequently, it is negligible for $t \gg 1/\Gamma$. The contribution from the pole is

$$-i w_{\mathbf{k}} \exp(-i\varepsilon_{\mathbf{k}} t - |\gamma_{\mathbf{k}}| t), \quad (11.66)$$

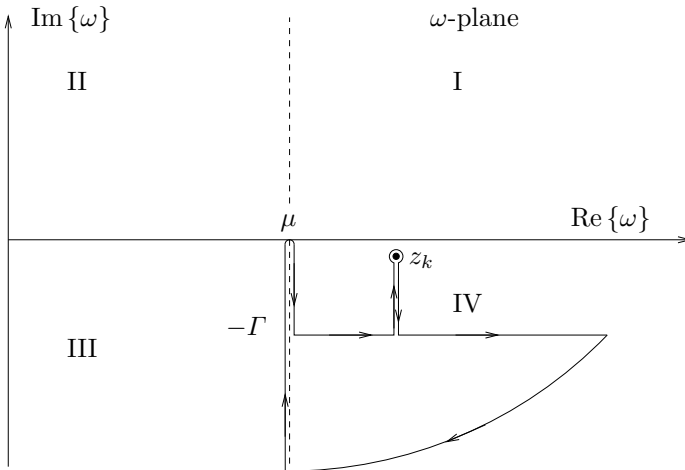


Fig. 11.5. Contour in ω -plane for evaluating $g(\mathbf{k}, t)$ for $t > 0$

and the contribution from the contour around the branch cut is, according to (11.62) and (11.58),

$$\begin{aligned} & \int_{\mu}^{\mu-i\infty} \frac{d\omega}{2\pi} e^{-i\omega t} [a.c. \{G(\mathbf{k}, \omega)\} - G(\mathbf{k}, \omega)] \\ & \approx \int_{\mu}^{\mu-i\infty} \frac{d\omega}{2\pi} e^{-i\omega t} \frac{-2\gamma_{\mathbf{k}} w_{\mathbf{k}} i}{(\omega - z_{\mathbf{k}})(\omega - z_{\mathbf{k}}^*)}. \end{aligned} \quad (11.67)$$

In obtaining the last expression we have omitted the quantity $-i.a.c.\{A_b(\mathbf{k}, \omega)\}$ in (11.58) because it is small in comparison with the last term in (11.58) when the pole $z_{\mathbf{k}}$ is close to the point $\omega = \mu$. The contribution of (11.67) is comparable to the contribution of (11.66) when $t \leq 1/(\varepsilon_{\mathbf{k}} - \mu)$. For $t \gg 1/(\varepsilon_{\mathbf{k}} - \mu)$ the contribution of (11.67) becomes about equal to

$$\frac{\gamma_{\mathbf{k}} w_{\mathbf{k}} e^{-i\mu t}}{\pi t (\varepsilon_{\mathbf{k}} - \mu)^2} = \frac{w_{\mathbf{k}} e^{-i\mu t}}{\pi t (\varepsilon_{\mathbf{k}} - \mu)} \frac{\gamma_{\mathbf{k}}}{\varepsilon_{\mathbf{k}} - \mu}. \quad (11.68)$$

Since $t(\varepsilon_{\mathbf{k}} - \mu) \gg 1$ and $\gamma_{\mathbf{k}}/(\varepsilon_{\mathbf{k}} - \mu) \rightarrow 0$ as $k \rightarrow k_F$, it follows that the contribution of (11.68) is negligible. We can thus conclude that for

$$\max \left\{ \frac{1}{\Gamma}, \frac{1}{|\varepsilon_{\mathbf{k}} - \mu|} \right\} \ll t \ll \frac{1}{|\gamma_{\mathbf{k}}|}, \quad (11.69)$$

the propagator $g(\mathbf{k}, t)$ is given by

$$g(\mathbf{k}, t) \simeq -i w_{\mathbf{k}} \exp(-i\varepsilon_{\mathbf{k}} t - |\gamma_{\mathbf{k}}| t), \quad (11.70)$$

which is the propagator of an entity of weight $w_{\mathbf{k}}$, of energy $\varepsilon_{\mathbf{k}}$, and of lifetime $1/|\gamma_{\mathbf{k}}|$, i.e., of the quasiparticle we have already introduced. We can interpret the results (11.69) and (11.70) physically as follows: following the addition of a new bare particle in our system, a time of order $1/|\varepsilon_{\mathbf{k}} - \mu|$ is required for its dressing, i.e., for the appearance of the quasiparticle. After the quasiparticle is formed, it behaves as an independent entity for a period of the order $1/|\gamma_{\mathbf{k}}|$. For a normal system $1/|\varepsilon_{\mathbf{k}} - \mu| \ll 1/|\gamma_{\mathbf{k}}| \rightarrow \infty$ as $k \rightarrow k_F$. Hence, for a normal system there is a considerable time span when the quasiparticles (and quasiholes) lying close to the Fermi surface are well-defined independent elementary excitations of the system. Further considerations supporting this last statement can be found in [423].

Physically we can understand the existence of long-lived quasiparticles because the available phase space for decaying processes is proportional to $(k - k_F)^2$ as $k \rightarrow k_F$ [113] [while $(\varepsilon_{\mathbf{k}} - \mu) \sim (k - k_F)$ as $k \rightarrow k_F$]. This $(k - k_F)^2$ result for the available phase space is based upon the conservation of energy and momentum and upon the assumption that the quasiparticles are fermions with a well-defined Fermi surface. Because of this last assumption the argument above only shows that the normal state is a consistent state of an interacting Fermi system and not necessarily the actual one. However, if this consistent state is the actual one for very small α (as in the case where

the perturbation expansion in powers of αV_i converges), then by a continuity argument, one expects that it may remain such for the real value $\alpha = 1$.

Examples of normal systems are a dense system of electrons repelling each other via Coulomb forces and moving in a positive background to ensure overall electrical neutrality and a system of fermions interacting through short-range repulsive forces. On the other hand, a system of fermions attracting each other is not a normal one. We have seen in Chap. 6 that no matter how weak the attraction, the system rearranges itself to a new state, the superconducting state, consisting of bound pairs.

Another system that is not a normal one is the so-called *Luttinger model* or Luttinger liquid, which is a 1-d exactly solvable model, such that any nonzero value of the interaction constant totally destroys the Fermi distribution and eliminates the concept of the Fermi momentum as a point of discontinuity of n_k [114, 135].

Although under the condition $\gamma_{\mathbf{k}} \ll |\varepsilon_{\mathbf{k}} - \mu|$ the poles of $a.c.\{G(\mathbf{k}, \omega)\}$ lying near the real ω -axis give the quasiparticles (or quasiholes), which are independent elementary excitations of the system, not all the elementary excitations appear as poles of $a.c.\{G(\mathbf{k}, \omega)\}$. Excitations made of pairs of particles must appear as poles of $a.c.\{g_2\}$, which describes the propagation of two particles. Also, even in normal systems there are excitations, such as plasmons or zero sound, that are elementary density waves. Such collective excitations must appear as poles of $a.c.\{D(\mathbf{k}, \omega)\}$, where $D(x, x') \equiv -i \langle T[n(x), n(x')] \rangle$ [$n(x) = \psi^\dagger(x)\psi(x)$ is the density operator]. Thus, in a typical normal system the role of the interactions is twofold: first, the bare particles are dressed and appear as independent quasiparticles characterized by a new dispersion relation $\varepsilon = f(\mathbf{k})$; second, new collective density wave-type excitations are created. In a system that is not normal the interactions play a more drastic role, creating a new ground state that, in general, is fundamentally different from the ground state of the noninteracting system.

11.4 Summary

11.4.1 Properties

The Green's functions defined in Chap. 10 for a many-body system have analytical properties that are similar but not identical to the Green's functions defined in Chap. 2 corresponding to a second-order (in time) differential equation. For a translationally invariant system the Fourier transforms of the g_s and \tilde{g}_s can be expressed in terms of a single real quantity $A(\mathbf{k}, \omega)$ that can be interpreted as 2π times a generalized density of states in \mathbf{k} - ω -space. We have for real ω

$$\tilde{g}(\mathbf{k}, \omega) = -iA(\mathbf{k}, \omega), \quad (11.5)$$

$$g^R(\mathbf{k}, \omega) = \lim_{s \rightarrow 0^+} G(\mathbf{k}, \omega + is), \quad (11.14)$$

$$g^A(\mathbf{k}, \omega) = \lim_{s \rightarrow 0^+} G(\mathbf{k}, \omega - is), \tag{11.15}$$

$$\tilde{g}^>(\mathbf{k}, \omega) = -iA(\mathbf{k}, \omega) [1 \pm f_{\mp}(\omega)], \tag{11.6}$$

$$\tilde{g}^<(\mathbf{k}, \omega) = \mp iA(\mathbf{k}, \omega) f_{\mp}(\omega), \tag{11.7}$$

$$g(\mathbf{k}, \omega) = g^R(\mathbf{k}, \omega) + \tilde{g}^<(\mathbf{k}, \omega), \tag{11.18,19}$$

where, for complex ω , $G(\mathbf{k}, \omega)$ is defined as

$$G(\mathbf{k}, \omega) = \int_{-\infty}^{\infty} \frac{d\omega'}{2\pi} \frac{A(\mathbf{k}, \omega')}{\omega - \omega'} \tag{11.10}$$

and

$$f_{\mp}(\omega) = \frac{1}{e^{\beta(\omega - \mu)} \mp 1}. \tag{11.8}$$

$A(\mathbf{k}, \omega)$ can be expressed in terms of G as follows:

$$A(\mathbf{k}, \omega) = i \lim_{s \rightarrow 0^+} [G(\mathbf{k}, \omega + is) - G(\mathbf{k}, \omega - is)]; \quad \omega \text{ real.} \tag{11.11}$$

Equations (11.5), (11.14), (11.15), (11.10), and (11.11) are the analogs of (1.22), (2.34), (2.35), (1.30), and (1.21), respectively. Equations (11.18) and (11.19) reduce to (2.33) only for fermions at $T = 0$ and with $\omega = \mu$ instead of $\omega = 0$; similarly for (11.6) and (11.7). The analogy can also be seen by comparing Fig. 11.1 with Fig. 2.2.

11.4.2 Use

1. Having the generalized density of states $A(\mathbf{k}, \omega)/2\pi$, one can obtain several quantities of physical interest, such as the density of particles in \mathbf{k} -space $\langle n(\mathbf{k}) \rangle$, the total kinetic energy $\langle T \rangle$, the total potential energy $\langle V_i \rangle$, the total Hamiltonian $\langle \mathcal{H} \rangle$, and the grand partition function Z_G . We have explicitly

$$\langle n(\mathbf{k}) \rangle = \int_{-\infty}^{\infty} \frac{d\omega}{2\pi} A(\mathbf{k}, \omega) f_{\mp}(\omega), \tag{11.25}$$

$$\langle T \rangle = \sum_{\mathbf{k}} \int_{-\infty}^{\infty} \frac{d\omega}{2\pi} \frac{k^2}{2m} A(\mathbf{k}, \omega) f_{\mp}(\omega), \tag{11.23}$$

$$\langle V_i \rangle = \sum_{\mathbf{k}} \int_{-\infty}^{\infty} \frac{d\omega}{2\pi} \left(\frac{\omega - k^2/2m}{2} \right) A(\mathbf{k}, \omega) f_{\mp}(\omega), \tag{11.29}$$

$$\langle \mathcal{H} \rangle = \sum_{\mathbf{k}} \int_{-\infty}^{\infty} \frac{d\omega}{2\pi} \frac{\omega + (k^2/2m)}{2} A(\mathbf{k}, \omega) f_{\mp}(\omega), \tag{11.30}$$

$$\begin{aligned} \ln(Z_G) &= \beta P \Omega = \beta P_0 \Omega - \beta \int_0^1 \frac{d\alpha}{\alpha} \sum_{\mathbf{k}} \int_{-\infty}^{\infty} \frac{d\omega}{2\pi} \\ &\quad \times \frac{1}{2} \left(\omega - \frac{k^2}{2m} \right) A_{\alpha}(\mathbf{k}, \omega) f_{\mp}(\omega), \end{aligned} \tag{11.37}$$

where $A_\alpha(\mathbf{k}, \omega)$ corresponds to an interaction part in the Hamiltonian equal to αV_i and $Z_{G_0} = \exp(\beta P_0 \Omega)$ is the grand partition function for $\alpha = 0$.

2. The poles of the analytic continuation of $G(\mathbf{k}, \omega)$, *a.c.* $\{G(\mathbf{k}, \omega)\}$, in the complex ω -plane can be interpreted as representing quasiparticles or dressed particles, i.e., weakly interacting entities determining the low-lying excitation spectrum of the many-body system. The real part, $\varepsilon_{\mathbf{k}}$, of the pole gives the energy of the quasiparticle, the inverse of the imaginary part, $\gamma_{\mathbf{k}}$, gives its lifetime, and the residue gives the percentage of the dressed particle consisting of a bare (actual) particle. Normal systems are those for which $\gamma_{\mathbf{k}}/|\varepsilon_{\mathbf{k}} - \mu| \rightarrow 0$ as $\varepsilon_{\mathbf{k}} \rightarrow \mu$. Not all systems are normal; superconductors and Luttinger liquids are two examples of nonnormal systems.
3. Green's functions also give the linear response of a system to an external perturbation. For example, the dielectric function $\varepsilon(\mathbf{k}, \omega)$ is given by

$$\frac{1}{\varepsilon(\mathbf{k}, \omega)} - 1 = \frac{4\pi e^2}{k^2} D^R(\mathbf{k}, \omega), \quad (11.45)$$

where D^R is a retarded Green's function with the field operator replaced by the total density operator $\psi^+(x)\psi(x) - n_0$.

Further Reading

The material of this chapter is presented in detail in the standard books on many-body theory such as the books by Fetter and Walecka [20], Mahan [114], Kadanoff and Baym [420], Abrikosov et al. [113], etc. For an introductory level the book by Mattuck [421] may be found very satisfactory. The subject of quasiparticles is treated in a thorough way in the book by Nozieres [423]; in the same book the reader will find an extensive examination of the dielectric function.

Problems

- 11.1. Prove (11.4).
- 11.2. Prove (11.19).
- 11.3. Prove (11.25).
- 11.4s. Prove (11.37) and recast it in terms of $G(\mathbf{k}, z_\nu)$.
- 11.5. Show how (11.46), (11.45), (11.42) can be recast in the form of (8.47).

Calculational Methods for g

There are two basic approaches to the approximate calculation of Green's functions. One is based upon the differential equation obeyed by g . In the other, a perturbation expansion is employed where g is expressed as a series whose terms involve the unperturbed g_0 and the interaction potential $v(\mathbf{r}-\mathbf{r}')$.

12.1 Equation of Motion Method

As was mentioned in Chap. 10, the Green's functions for an interacting many-body system obey a hierarchy of equations, the first of which has the form

$$\left(i \frac{\partial}{\partial t} + \frac{\nabla_r^2}{2m} \right) g(x, x') = \delta(x - x') \pm i \int d^3 r_1 v(\mathbf{r} - \mathbf{r}_1) g_2(x, x_1; x', x_1^+)_{t_1=t} \quad (12.1)$$

and connects the one-particle causal Green's function with the two-particle causal Green's function; the next equation in the hierarchy connects g_2 with g_3 ; and so on. A similar hierarchy of equations is obeyed by the retarded and advanced Green's functions [424]. The infinite number of coupled differential equations shows clearly the essential complication introduced by interparticle interactions. It is obvious that to obtain a solution, one has to terminate the hierarchy at some point by employing an approximate relation connecting g_n with g_{n-1} , g_{n-2} , etc. The simplest such approximation attempts to express g_2 in terms of g and then substitute in (12.1). Thus a nonlinear integrodifferential equation for g will result.

We consider first the simplest approximate relation expressing g_2 in terms of g , which is equivalent to the so-called Hartree approximation,

$$g_2(x_1, x_2; x'_1, x'_2) \simeq g(x_1, x'_1) g(x_2, x'_2) . \quad (12.2)$$

Remembering the physical interpretation of g_2 as describing the propagation of two additional particles from x_1, x_2 to x'_1, x'_2 , we can see that (12.2) means

that the two particles propagate independently, one from x_1 to x'_1 and the other from x_2 to x'_2 . Note that (12.2) does not satisfy the basic symmetry property demanding that g_2^2 be invariant under the exchange $x_1 \rightleftharpoons x_2$ or under the exchange $x'_1 \rightleftharpoons x'_2$. Thus (12.2) is a quite drastic approximation indeed.

Substituting (12.2) into (12.1) we obtain

$$\begin{aligned} & \left(i \frac{\partial}{\partial t} + \frac{\nabla_r^2}{2m} \right) g(x, x') \\ &= \delta(x - x') \pm ig(x, x') \int d^3r_1 v(\mathbf{r} - \mathbf{r}_1) g(x, x_1^+) \\ &= \delta(x - x') + g(x, x') \int d^3r_1 v(\mathbf{r} - \mathbf{r}_1) \langle n(\mathbf{r}_1) \rangle, \end{aligned} \quad (12.3)$$

where (11.24) was used. Introducing the effective one-body potential

$$V(\mathbf{r}) \equiv \int d^3r_1 v(\mathbf{r} - \mathbf{r}_1) \langle n(\mathbf{r}_1) \rangle, \quad (12.4)$$

we can rewrite (12.3) as

$$\left[i \frac{\partial}{\partial t} + \frac{\nabla_r^2}{2m} - V(\mathbf{r}) \right] g(x, x') = \delta(x - x'), \quad (12.5)$$

which shows that the added particle (or hole) moves (independently) in the average potential $V(\mathbf{r})$ created by the particles of the system. For a translationally invariant system, the density $\langle n(\mathbf{r}_1) \rangle$ is a constant n_0 ; as a result $V(\mathbf{r})$ is a constant $n_0 v_0$, where $v_0 = \int d^3r v(\mathbf{r})$. Then (12.5) becomes a simple differential equation that by a Fourier transformation can be written as

$$\left(\omega - \frac{k^2}{2m} - n_0 v_0 \right) g(\mathbf{k}, \omega) = 1. \quad (12.6)$$

The general solution of (12.6) is the sum of a particular solution plus the general solution of the corresponding homogeneous equation, which is proportional to $\delta(\omega - k^2/2m - n_0 v_0)$. In Chap. 1, to get rid of this indeterminacy, we have allowed ω to become complex, in which case the homogeneous equation has no solution, and then we have taken the limit of the solution as ω approaches the real axis. This method works here for *fermions* at $T = 0$ where $g(\mathbf{k}, \omega)$ is the limit of an analytic function, as can be seen from (11.19'). Thus for fermions at $T = 0$ we have, by combining (12.6) with (11.19'), that

$$g(\mathbf{k}, \omega) = \lim_{s \rightarrow 0^+} \frac{1}{\omega - k^2/2m - n_0 v_0 + is\bar{\epsilon}(\omega - \mu)}. \quad (12.7)$$

For $T \neq 0$, $g(\mathbf{k}, \omega)$ is not the limit of an analytic function, and consequently one cannot continue (12.6) in the complex ω -plane without further analysis. This point shows why the equation of motion method works well for g^R

(or g^A), since each one is the limit of an analytic function for all temperatures [see (11.14) and (11.15)]. There is also a trick that allows us to use the equation of motion method for the “imaginary time” causal Green’s functions. Consider the quantity

$$g(\mathbf{r}_1, -i\sigma_1, \mathbf{r}_2, -i\sigma_2) = \begin{cases} \tilde{g}^>(\mathbf{r}_1, -i\sigma_1, \mathbf{r}_2, -i\sigma_2) , & \sigma_1 > \sigma_2 , \\ \tilde{g}^<(\mathbf{r}_1, -i\sigma_1, \mathbf{r}_2, -i\sigma_2) , & \sigma_2 > \sigma_1 , \end{cases} \quad (12.8a)$$

which results from replacing in the causal Green’s function, $g(\mathbf{r}_1, t_1, \mathbf{r}_2, t_2)$, the time t_1 by $-i\sigma_1$, the time t_2 by $-i\sigma_2$, and the time ordering by σ -ordering; the quantities σ_1 and σ_2 are confined in the interval $[0, \beta]$, where β is the inverse temperature. For the systems we consider, $g(\mathbf{r}_1, -i\sigma_1, \mathbf{r}_2, -i\sigma_2)$ is a function of $\mathbf{r} = \mathbf{r}_1 - \mathbf{r}_2$ and $\sigma = \sigma_1 - \sigma_2$. Using the relation

$$\begin{aligned} & \tilde{g}^<(\mathbf{r}_1, t_1, \mathbf{r}_2, t_2) \\ &= \int_{-\infty}^{\infty} \frac{d\omega}{2\pi} \int \frac{d^3k}{(2\pi)^3} \exp[-i\omega(t_1 - t_2) + i\mathbf{k} \cdot (\mathbf{r}_1 - \mathbf{r}_2)] \tilde{g}^<(\mathbf{k}, \omega) , \end{aligned}$$

together with (12.8) and (11.7), we obtain

$$\begin{aligned} & \tilde{g}^<(\mathbf{r}_1, -i\sigma_1, \mathbf{r}_2, -i\sigma_2) \\ &= \mp i \int_{-\infty}^{\infty} \frac{d\omega}{2\pi} \int \frac{d^3k}{(2\pi)^3} \exp[-\omega\sigma + i\mathbf{k} \cdot (\mathbf{r}_1 - \mathbf{r}_2)] A(\mathbf{k}, \omega) f_{\mp}(\omega) , \end{aligned} \quad (12.9)$$

where $\sigma_1 - \sigma_2 \equiv \sigma < 0$. From the general equation (11.53) we have that

$$g(\mathbf{r}_1, -i\sigma_1, \mathbf{r}_2, -i\sigma_2) = \mp i \int \frac{d^3k}{(2\pi)^3} e^{i\mathbf{k} \cdot (\mathbf{r}_1 - \mathbf{r}_2)} \frac{\mp 1}{\beta} \sum_{\nu} e^{-z_{\nu}\sigma} G(\mathbf{k}, z_{\nu}) ,$$

which shows that the Fourier transform of $g(\mathbf{r}_1, -i\sigma_1, \mathbf{r}_2, -i\sigma_2)$ with respect to $\mathbf{r}_1 - \mathbf{r}_2$, $g(\mathbf{k}, -i\sigma)$, obeys the relation

$$g(\mathbf{k}, -i\sigma) = \frac{i}{\beta} \sum_{\nu} \exp(-z_{\nu}\sigma) G(\mathbf{k}, z_{\nu}) , \quad (12.10)$$

where z_{ν} is given by (11.49). In a similar way one obtains that (12.10) is valid also for $\sigma > 0$. Equation (12.10) shows that the imaginary time Green’s function, $g(\mathbf{k}, -i\sigma)$, can be expanded in a Fourier series whose coefficients are the values of the analytic function $G(\mathbf{k}, \omega)$ at points z_{ν} . Inverting (12.10) we have

$$G(\mathbf{k}, z_{\nu}) = -\frac{i}{2} \int_{-\beta}^{\beta} g(\mathbf{k}, -i\sigma) \exp(z_{\nu}\sigma) d\sigma . \quad (12.11)$$

From (12.10) it follows immediately that

$$g(\mathbf{k}, -i\sigma) = \pm e^{\beta\mu} g(\mathbf{k}, -i(\sigma + \beta)) , \quad \sigma < 0 . \quad (12.12)$$

From definition (12.8) it follows that $g(\mathbf{r}_1, -i\sigma_1, \mathbf{r}_2, -i\sigma_2)$ obeys the basic equation (12.1) with each t replaced by $-i\sigma$ and $\delta(t_1 - t_2)$ replaced by $i\delta(\sigma_1 - \sigma_2)$. Using (12.2) for the imaginary time Green's function, substituting in (12.1), and employing (12.10), we obtain

$$\left(z_\nu - \frac{k^2}{2m} - n_0 v_0\right) G(\mathbf{k}, z_\nu) = 1. \quad (12.13)$$

Because of the analyticity of $G(\mathbf{k}, \omega)$ in the complex ω -plane, it follows immediately from (12.13) that

$$G(\mathbf{k}, z_\nu) = \frac{1}{z_\nu - k^2/2m - n_0 v_0}, \quad (12.14)$$

which by analytic continuation gives

$$G(\mathbf{k}, \omega) = \frac{1}{\omega - k^2/2m - n_0 v_0}. \quad (12.15)$$

From $G(\mathbf{k}, \omega)$ one can obtain all the real time Green's functions by employing the general relations of Sect. 11.1. The above analysis shows that the imaginary time causal Green's functions are very convenient tools because, on the one hand, they obey the hierarchy of equations of motion and, on the other hand, their Fourier coefficients are the values of the analytic function $G(\mathbf{k}, \omega)$ at the points $\omega = z_\nu$.

To summarize the calculational procedure for $T \neq 0$:

1. The imaginary time causal Green's functions (resulting from substituting $t_1 = -i\sigma_1$, etc., into g, g_2, \dots) obey a hierarchy of equations, the first of which is (12.1) with $t = -i\sigma, \dots$ and $\delta(t - t') = i\delta(\sigma - \sigma')$.
2. The hierarchy is approximately terminated usually by expressing g_2 in terms of g . There is a systematic procedure for obtaining increasingly more accurate expressions of g_2 in terms of g [420].
3. Combining (12.1) and the approximate relation $g_2 \simeq f(g)$ one obtains an equation for g , which in view of (12.10) becomes an equation for $G(\mathbf{k}, z_\nu)$. The solution of this equation determines the analytic function $G(\mathbf{k}, \omega)$ at the points $\omega = z_\nu$. As we have seen in Sect. 11.2, the values of $G(\mathbf{k}, z_\nu)$ is all we need in order to calculate the thermodynamic quantities.
4. If the real time Green's functions are needed, one has to obtain $G(\mathbf{k}, \omega)$ by analytically continuing $G(\mathbf{k}, z_\nu)$ and by taking into account that $G(\mathbf{k}, \omega) \rightarrow 1/\omega$ as $\omega \rightarrow \infty$ [20]. This asymptotic behavior is a consequence of (11.9) and (11.10). Determining $G(\mathbf{k}, \omega)$ from its values at the points $\omega = z_\nu$ may be a difficult problem; however, in most practical cases it involves no more than substituting z_ν by ω . Having $G(\mathbf{k}, \omega)$, one can obtain all Green's functions by employing the equations of Sect. 11.1.

The above procedure was illustrated in the simple case of the Hartree approximation (12.2). As can be seen from (12.15), within the framework of this

approximation, a quasiparticle of momentum \mathbf{k} has energy $\varepsilon_{\mathbf{k}} = k^2/2m + n_0v_0$, infinite lifetime, and weight equal to 1, i.e., it is a free particle with the added energy n_0v_0 . The average energy is obtained by combining (11.30), (11.11), and (12.15); so

$$\langle \mathcal{H} \rangle = \sum_{\mathbf{k}} \varepsilon_{\mathbf{k}} f_{\mp}(\varepsilon_{\mathbf{k}}) - \frac{1}{2} \Omega n_0^2 v_0, \quad (12.16)$$

where the last term corrects for the double counting of the interaction n_0v_0 . The equation of state in the low-density limit is [420]

$$P - \frac{1}{2} n_0^2 v_0 = n_0 k_B T, \quad (12.17)$$

which is of the van der Waals type without the volume-exclusion effect [420].

An improvement over the Hartree approximation can be obtained by taking into account the symmetry (or antisymmetry) or g_2 under the exchange $x_1 \rightleftharpoons x_2$ or under the exchange $x'_1 \rightleftharpoons x'_2$, while still considering the added particles as moving independently of each other. Under these conditions we have the so-called Hartree–Fock approximation

$$g_2(x_1, x_2; x'_1, x'_2) \simeq g(x_1, x'_1) g(x_2, x'_2) \pm g(x_1, x'_2) g(x_2, x'_1). \quad (12.18)$$

Following the procedure outlined above one obtains within the framework of the Hartree–Fock approximation

$$G(\mathbf{k}, \omega) = \frac{1}{\omega - \varepsilon_{\mathbf{k}}}, \quad (12.19)$$

where

$$\varepsilon_{\mathbf{k}} = \frac{k^2}{2m} + n_0v_0 \pm \int \frac{d^3k'}{(2\pi)^3} v(\mathbf{k} - \mathbf{k}') \langle n(\mathbf{k}') \rangle \quad (12.20)$$

and $v(\mathbf{k}) = \int d^3r e^{-i\mathbf{k} \cdot \mathbf{r}} v(\mathbf{r})$ is the Fourier transform of the potential $v(\mathbf{r})$. Note that the quasiparticle energy $\varepsilon_{\mathbf{k}}$ depends implicitly on the temperature T through the density $\langle n(\mathbf{k}') \rangle$. In [420] more complicated $g_2 \simeq f(g)$ are examined.

12.2 Diagrammatic Method for Fermions at $T = 0$

This method is applicable to the important case where the total Hamiltonian can be decomposed as

$$\mathcal{H} = \mathcal{H}_0 + \mathcal{H}_1, \quad (12.21)$$

where \mathcal{H}_0 , the unperturbed part, is such that the Green's functions corresponding to \mathcal{H}_0 can be easily calculated. The method here is analogous to that presented in Chap. 4 where the eigenvalues and eigenfunctions of the one-body \mathcal{H} were determined from $G = (E - \mathcal{H})^{-1}$ and G was expressed as a perturbation series in terms of \mathcal{H}_1 and $G_0 = (E - \mathcal{H}_0)^{-1}$. In the present many-body case, working with g is much more advantageous than in the one-body case. The reason is that the causal Green's function g not only has

a simpler perturbation expansion than any other quantity, but it also provides a host of important physical information without unimportant details of the many-body system. For comparison we mentioned that while the perturbation expansion for the ground-state energy is more complicated than the expansion for g , the information we obtain is clearly less.

To obtain the perturbation expansion for g , we need to work within the interaction picture according to which the time development of the operators is determined by the unperturbed part, \mathcal{H}_0 , while the time development of the states is determined by the perturbation \mathcal{H}_1 . More explicitly, we have for any operator A [see (8.38b) and (8.38c)]

$$A_I(t) = \exp(i\mathcal{H}_0 t) A_S \exp(-i\mathcal{H}_0 t) , \quad (12.22)$$

which is equivalent to

$$i \frac{dA_I(t)}{dt} = [A_I(t), \mathcal{H}_0] . \quad (12.23)$$

We also have

$$|\Psi_I(t)\rangle = \exp(i\mathcal{H}_0 t) |\Psi_S(t)\rangle , \quad (12.24)$$

which leads immediately to

$$i \frac{d}{dt} |\Psi_I(t)\rangle = \mathcal{H}_{1I}(t) |\Psi_I(t)\rangle . \quad (12.25)$$

The subscript “ I ” denotes the interaction picture; the subscript “ S ” denotes the Schrödinger picture according to which

$$\frac{dA_S}{dt} = 0 \quad (12.26)$$

and

$$i \frac{d}{dt} |\Psi_S(t)\rangle = \mathcal{H}_S |\Psi_S(t)\rangle , \quad \mathcal{H}_S \equiv \mathcal{H} , \quad (12.27)$$

or, equivalently,

$$|\Psi_S(t)\rangle = e^{-i\mathcal{H}t} |\Psi_S(0)\rangle . \quad (12.28)$$

We consider also the Heisenberg picture where

$$A_H(t) = e^{i\mathcal{H}t} A_S e^{-i\mathcal{H}t} \quad (12.29)$$

or, equivalently,

$$i \frac{dA_H(t)}{dt} = [A_H(t), \mathcal{H}_H] \quad (12.29')$$

and

$$|\Psi_H(t)\rangle = |\Psi_S(0)\rangle . \quad (12.30)$$

From the above relations it is easy to see that the observable matrix elements are the same in all pictures:

$$\langle \Phi_S(t) | A_S(t) | \Psi_S(t) \rangle = \langle \Phi_H | A_H(t) | \Psi_H \rangle = \langle \Phi_I(t) | A_I(t) | \Psi_I(t) \rangle . \quad (12.31)$$

By integrating (12.25) or by employing (4.39), (4.42), and (12.24) we obtain

$$|\Psi_I(t)\rangle = S(t, t_0) |\Psi_I(t_0)\rangle, \quad (12.32)$$

where $S(t, t_0)$ is given by (4.55) with all the integration limits being t_0 and t ; as can be seen from (4.51) and (12.22), we have $\mathcal{H}_1^I(t) \equiv \mathcal{H}_{1I}(t)$. In what follows we assume that \mathcal{H}_1 contains a factor $e^{-s|t|}$ and that after the calculations are done, we will take the limit $s \rightarrow 0^+$. This means that the interaction is turned on adiabatically at $t = -\infty$ and is turned off adiabatically as $t = \infty$. We can now prove that

$$\langle \Psi_H | A_H(t) | \Psi_H \rangle = \frac{\langle \Phi | S(\infty, t) A_I(t) S(t, -\infty) | \Phi \rangle}{\langle \Phi | S | \Phi \rangle}, \quad (12.33)$$

where $|\Psi_H\rangle$ is the normalized ground state of the total Hamiltonian \mathcal{H} , $|\Phi\rangle$ is the ground state of the unperturbed Hamiltonian \mathcal{H}_0 , and $S \equiv S(\infty, -\infty)$. The proof is as follows:

$$\begin{aligned} \langle \Psi_H | A_H(t) | \Psi_H \rangle &= \langle \Psi_I(t) | A_I(t) | \Psi_I(t) \rangle \\ &= \langle \Psi_I(t_0) | S(t_0, t) A_I(t) S(t, t_0) | \Psi_I(t_0) \rangle \\ &= \langle \Phi | S(-\infty, \infty) S(\infty, t) A_I(t) S(t, -\infty) | \Phi \rangle. \end{aligned} \quad (12.34)$$

The second step follows from (12.32) and the third step from (12.24) and the fact that $|\Psi_I(t_0)\rangle = \exp(-i\mathcal{H}_0 t_0) |\Phi\rangle$ as $t_0 \rightarrow -\infty$, since $\mathcal{H}_1 \rightarrow 0$ as $t \rightarrow -\infty$: we have also used the basic property $S(t_1, t_2) = S(t_1, t_3) S(t_3, t_2)$ with $t_1 = -\infty$, $t_3 = \infty$, $t_2 = t$. Assuming that the ground state $|\Phi\rangle$ is nondegenerate, and taking the limit $s \rightarrow 0^+$, we can see from (4.46) that $S|\Phi\rangle$ is proportional to $|\Phi\rangle$, i.e.,

$$S|\Phi\rangle = e^{i\phi} |\Phi\rangle. \quad (12.35)$$

Equation (12.35) means that an interaction switched on and off adiabatically does not produce a transition from a nondegenerate state. From (12.35) we have

$$\langle \Phi | S(-\infty, \infty) = e^{-i\phi} \langle \Phi | \quad (12.36)$$

and

$$e^{-i\phi} = \frac{1}{\langle \Phi | S | \Phi \rangle}. \quad (12.37)$$

Combining (12.37) and (12.36) with (12.34), we obtain (12.33). With the help of (4.55) we can rewrite (12.33) in a more explicit way as follows:

$$\begin{aligned} \langle \Psi_H | A_H(t) | \Psi_H \rangle &= \frac{1}{\langle \Phi | S | \Phi \rangle} \\ &\times \left\langle \Phi \left| \sum_{n=0}^{\infty} \frac{(-i)^n}{n!} \int_{-\infty}^{\infty} dt_1 \cdots \int_{-\infty}^{\infty} dt_n T[\mathcal{H}_{1I}(t_1) \cdots \mathcal{H}_{1I}(t_n) A_I(t)] \right| \Phi \right\rangle. \end{aligned} \quad (12.38)$$

In a similar way we can prove that

$$\begin{aligned} \langle \Psi_H | T [A_{1H}(t)A_{2H}(t') \cdots] | \Psi_H \rangle &= \frac{1}{\langle \Phi | S | \Phi \rangle} \\ &\times \left\langle \Phi \left| \sum_{n=0}^{\infty} \frac{(-i)^n}{n!} \int_{-\infty}^{\infty} dt_1 \cdots \int_{-\infty}^{\infty} dt_n \right. \right. \\ &\quad \left. \left. \times T [\mathcal{H}_{1I}(t_1) \cdots \mathcal{H}_{1I}(t_n) A_{1H}(t)A_{2I}(t') \cdots] \right| \Phi \right\rangle . \end{aligned} \quad (12.39)$$

Equation (12.39) is the basis for the perturbative-diagrammatic expansion of the causal Green's function. We consider the case where the interaction part \mathcal{H}_1 is given by

$$\mathcal{H}_1 = \frac{1}{2} \int d^3r d^3r' \psi^\dagger(\mathbf{r}) \psi^\dagger(\mathbf{r}') v(\mathbf{r} - \mathbf{r}') \psi(\mathbf{r}') \psi(\mathbf{r}) , \quad (12.40)$$

which can be rewritten as

$$\int_{-\infty}^{\infty} \mathcal{H}_{1I}(t) dt = \frac{1}{2} \int dx dx' \psi_I^\dagger(x) \psi_I^\dagger(x') v(x - x') \psi_I(x') \psi_I(x) , \quad (12.41)$$

with

$$v(x - x') = v(\mathbf{r} - \mathbf{r}') \delta(t - t') \quad (12.42)$$

and

$$\psi_I(x) = \exp(i\mathcal{H}_0 t) \psi(\mathbf{r}) \exp(-i\mathcal{H}_0 t) . \quad (12.43)$$

Using the definition of $g(x, x')$, (12.39), and (12.41), we obtain the following expansion:

$$g(x, x') = \frac{N}{D} , \quad (12.44)$$

$$\begin{aligned} N &= -i \sum_{n=0}^{\infty} \left(\frac{1}{2}\right)^n \frac{(-i)^n}{n!} \int dx_1 dx'_1 \cdots \int dx_n dx'_n \\ &\quad \times \left\langle \Phi \left| T \left[\psi_I^\dagger(x_1) \psi_I^\dagger(x'_1) \psi_I(x'_1) \psi_I(x_1) \cdots \right. \right. \right. \\ &\quad \left. \left. \left. \times \psi_I^\dagger(x_n) \psi_I^\dagger(x'_n) \psi_I(x'_n) \psi_I(x_n) \psi_I(x) \psi_I^\dagger(x') \right] \right| \Phi \right\rangle \\ &\quad \times v(x_1 - x'_1) \cdots v(x_n - x'_n) , \end{aligned} \quad (12.45)$$

$$\begin{aligned} D &= \sum_{n=0}^{\infty} \left(\frac{1}{2}\right)^n \frac{(-i)^n}{n!} \int dx_1 dx'_1 \cdots \int dx_n dx'_n \\ &\quad \times \left\langle \Phi \left| T \left[\psi_I^\dagger(x_1) \psi_I^\dagger(x'_1) \cdots \psi_I(x'_n) \psi_I(x_n) \right] \right| \Phi \right\rangle \\ &\quad \times v(x_1 - x'_1) \cdots v(x_n - x'_n) . \end{aligned} \quad (12.46)$$

Taking into account (10.46) we can write (12.45) and (12.46) as follows:

$$\begin{aligned}
 N = \sum_{n=0}^{\infty} \left(\frac{1}{2}\right)^n \frac{i^n}{n!} \int dx_1 dx'_1 \cdots \int dx_n dx'_n \\
 \times g_{2n+1,0}(x, x_1, x'_1, \dots; x', x_1, x'_1, \dots) \\
 \times v(x_1 - x'_1) \cdots v(x_n - x'_n), \quad (12.47)
 \end{aligned}$$

$$\begin{aligned}
 D = \sum_{n=0}^{\infty} \left(\frac{1}{2}\right)^n \frac{i^n}{n!} \int dx_1 dx'_1 \cdots \int dx_n dx'_n \\
 \times g_{2n,0}(x_1, x'_1, \dots; x_1, x'_1, \dots) \\
 \times v(x_1 - x'_1) \cdots v(x_n - x'_n); \quad (12.48)
 \end{aligned}$$

the subscript “0” denotes that the Green’s functions g_{2n+1} and g_{2n} correspond to the unperturbed Hamiltonian \mathcal{H}_0 (since all ψ_{IS} , $\psi_I^{\dagger}S$ and $|\Phi\rangle$ refer to \mathcal{H}_0). Remembering the physical interpretation of g_m as describing the propagation of m additional particles, and taking into account that the unperturbed part \mathcal{H}_0 does not include any interparticle interactions, we can conclude that the m added particles propagate independently of each other, and hence $g_{m,0}$ can be written as a product of one-particle propagators. This product must be symmetrized (or antisymmetrized) in order to take into account the invariance of physical quantities under particle exchange. Thus, we have

$$\begin{aligned}
 g_{2n+1,0}(x, x_1, x'_1, \dots; x', x_1, x'_1, \dots) \\
 = \sum (-1)^P g_0(x, \tilde{x}') \cdots g_0(x'_n, \tilde{x}'_n), \quad (12.49)
 \end{aligned}$$

where $\{\tilde{x}', \tilde{x}_1, \tilde{x}'_1, \dots, \tilde{x}_n, \tilde{x}'_n\}$ is an arbitrary permutation of the set $\{x', x_1, x'_1, \dots, x_n, x'_n\}$, the summation is over all permutations, and P is even (odd) when the permutation is even (odd). Equal time g_0 must be interpreted as $\tilde{g}_0^<$; this can be seen from the starting equations (12.45) and (12.46), where the creation operator precedes the equal time annihilation operator.

Equation (12.49) can be proved formally [20]; it is known as *Wick’s theorem*. Combining (12.49) with (12.47), (12.48), and (12.44), we immediately see that we have succeeded in expressing g in powers of g_0 and $v(x - x')$; this expansion is substantially more complicated than the analogous expansion in the single-particle case.

It is obvious that the zero-order contributions to N and D are $N^{(0)} = g_0(x, x')$ and $D^{(0)} = 1$, so that, to zero order, $g(x, x') = g_0(x, x')$ as expected. The first-order contribution to N , $N^{(1)}$ contains $3! = 6$ terms; $N^{(2)}$ contains $5! = 120$ terms, and so on. At this point we introduce a set of diagrams, each of which is in one-to-one correspondence with each term in $N^{(n)}$ via certain well-defined rules to be presented below. We introduce also diagrams for each term contributing to $D^{(n)}$. The introduction of these diagrams, called *Feynman diagrams*, was done for the following reasons:

1. They facilitate the task of keeping track of the enormous number of terms contributing to N or D . We will also see that the diagrams have some additional very important advantages.
2. Certain cancellations are revealed by the introduction of diagrams.
3. One can ascribe a physical meaning to each diagram as representing a particular process associated with the propagation of the added particle in our system.

To be specific, consider the terms contributing to $N^{(1)}$; there are six terms in the summation (12.49) for $n = 1$. These six terms are in one-to-one correspondence with the six ways one can connect by directed lines the four points x, x', x_1 , and x'_1 shown in Fig. 12.1a. These six ways give the six diagrams shown in Fig. 12.1b. The rules for finding the contribution to $N^{(1)}$ from the corresponding diagrams can be obtained by simple inspection of (12.49) and (12.47). Thus each directed line starting at x_λ and ending at x_μ corresponds to $g_0(x_\mu, x_\lambda)$; the wavy line connecting x_1 with x'_1 corresponds to $v(x_1 - x'_1)$. We multiply these factors by $(i/2)(-1)^P$ and integrate them over the internal variables x_1 and x'_1 . Note that $(-1)^P$ equals $(-1)^m$, where m is the number of closed loops. The same rules allow us to calculate $D^{(1)}$ from the two diagrams shown in Fig. 12.2.

As one can see from Fig. 12.1b, the diagrams can be classified as connected (such as the third to sixth) and disconnected (such as the first and second). The contribution of a disconnected diagram consisting of two or more connected subdiagrams can be written as a product of terms each one corresponding to each subdiagram. The reason is that the subdiagrams have no common integration variables, and consequently the integral of the corresponding products is the product of the corresponding integrals. Thus, the contribution to N up to first order can be written as in Fig. 12.1c. Taking into account that $D^{(0)} = 1$ and that $D^{(1)}$ is given by the diagrams in Fig. 12.2, we see that the quantity in the second parenthesis in Fig. 12.1c equals the contribution to D up to first order. It follows that the contributions to g up to first order are given by the *connected* diagrams up to first order contributing to N and shown in the first parenthesis in Fig. 12.1c. It turns out [20] that this feature is correct to all orders, so that $g(x, x')$ is given by the sum of *connected* diagrams contributing to N .

Because we are left with connected diagrams only, we can make some further simplifications. We observe that n th-order diagrams resulting from each other by permutation of the pairs $(x_1, x'_1), (x_2, x'_2), \dots, (x_n, x'_n)$ are equal since this permutation is equivalent to renaming the integration variables. There are $n!$ such diagrams. Thus we can keep only one of them and drop the factor $1/n!$ in (12.47). Similarly, interchanging x_λ with x'_λ leaves the contribution of the diagram unchanged. Thus we can consider only one set of all diagrams resulting from interchanges of the type $x_\lambda \rightleftharpoons x'_\lambda$ and drop the factor $(1/2)^n$ in (12.47). We are now in a position to give the final rules for calculating the n th-order contribution to $g(x, x')$:

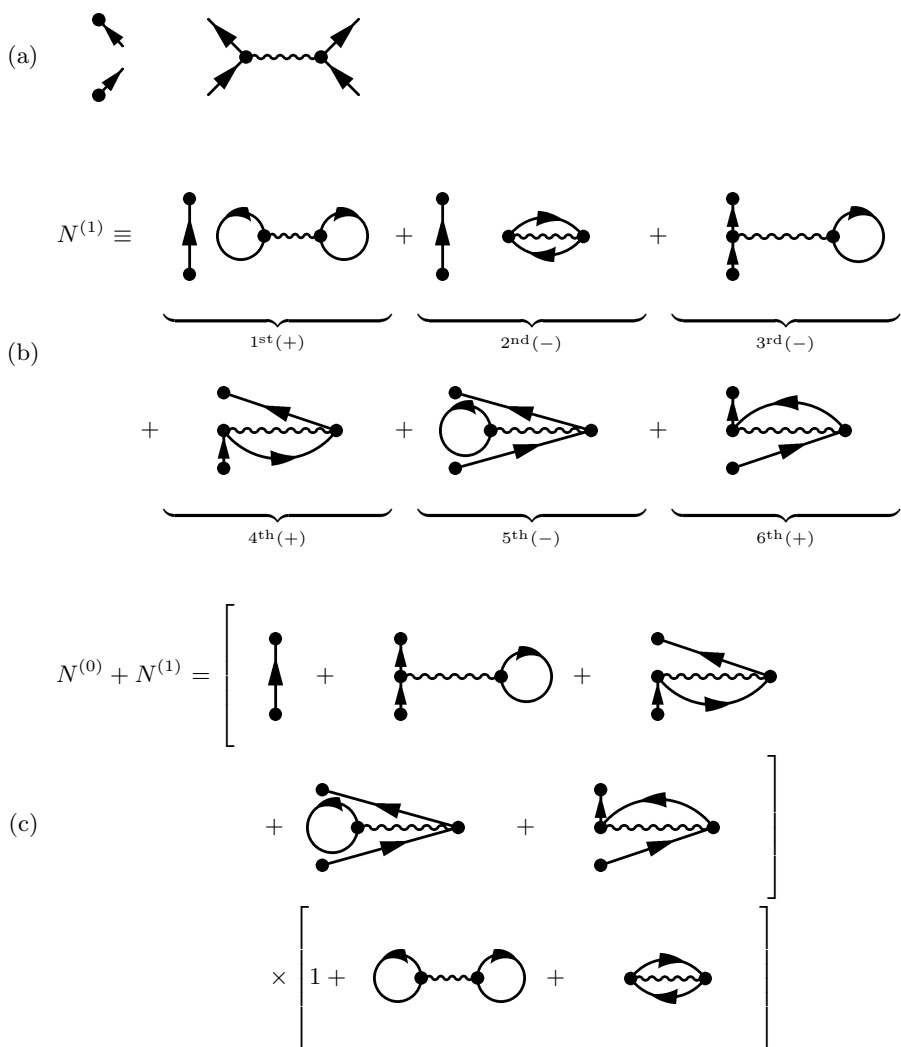


Fig. 12.1. The six terms contributing to $N^{(1)}$ (see text) are in one-to-one correspondence with the six diagrams (b) resulting from all possible ways of connecting the two external points x and x' and the two internal points x_1 and x'_1 (a) according to the following rules: a directed line must start from x' ; a directed line must end at x ; one directed line must start from and one must end at each internal point; and no directed line must start from or end at any other point except x , x' , x_1 , and x'_1 . The plus or minus sign in parentheses is the sign of $(-1)^P$ [see (12.49)] for the corresponding term. The terms $N^{(0)} + N^{(1)}$ can be written as in c, where up to first-order terms must be kept

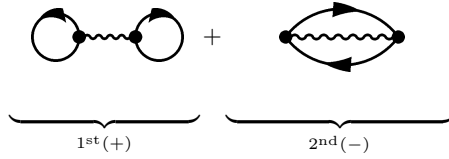


Fig. 12.2. The two diagrams contributing to $D^{(1)}$ (see text)

1. Draw all topologically distinct connected diagrams with n interaction (wavy) lines, two external points, and $2n + 1$ directed g_0 lines.
2. Label each vertex with a 4-d point $x_i \equiv \mathbf{r}_i, t_i$.
3. For each directed line starting from x_ν and ending at x_μ write a factor $g_0(x_\mu, x_\nu)$.
4. For each interaction (wavy) line between x_i and x'_i write a factor $iv(x_i - x'_i)$.
5. Integrate over all internal variables x_i, x'_i .
6. Multiply the expression by $(-1)^m$, where m is the number of closed fermion loops.
7. Interpret $g_0(\mathbf{r}_i, t_i, \mathbf{r}'_i, t_i)$ as being equal to $\tilde{g}_0^<(\mathbf{r}_i, t_i, \mathbf{r}'_i, t_i)$.

In Fig. 12.3 we plot all the diagrams for g up to second order. The contribution of the two first-order diagrams is, according to the rules above,

$$\begin{aligned}
 & -i \int g_0(x, x_1) g_0(x_1, x') g_0(x'_1, x'_1) v(x_1 - x'_1) dx_1 dx'_1 \\
 & +i \int g_0(x, x'_1) g_0(x'_1, x_1) g_0(x_1, x') v(x_1 - x'_1) dx_1 dx'_1 .
 \end{aligned}$$

For translationally invariant systems the calculations are facilitated by working in momentum-frequency space. This is achieved by expressing all $g(x_\nu - x_\mu)$ and $v(x_i - x'_i)$ in terms of their Fourier transforms with respect to the variables $x_\nu - x_\mu$ and $x_i - x'_i$, respectively. Then the integration over the internal variables x_i can be performed explicitly giving δ -functions expressing energy-momentum conservation at each vertex. Thus, in momentum space, we have rules resulting from the previous ones by the following replacement: $2 \rightarrow 2'$, $3 \rightarrow 3'$, $4 \rightarrow 4'$, $5 \rightarrow 5'$, and $7 \rightarrow 7'$, where

2'. Label each line with a four-momentum $q \equiv \mathbf{k}, \omega$; conserve energy-momentum at each vertex.

3'. For each directed line labeled with a four-momentum \mathbf{k}, ω write a factor

$$g_0(\mathbf{k}, \omega) = \lim_{s \rightarrow 0^+} \frac{1}{\omega - \varepsilon_k^0 + is\varepsilon(\omega - \mu)} .$$

4'. For each interaction (wavy) line labeled by \mathbf{k}, ω write a factor

$$iv(\mathbf{k}) = i \int d^3r v(\mathbf{r}) e^{-i\mathbf{k} \cdot \mathbf{r}} .$$

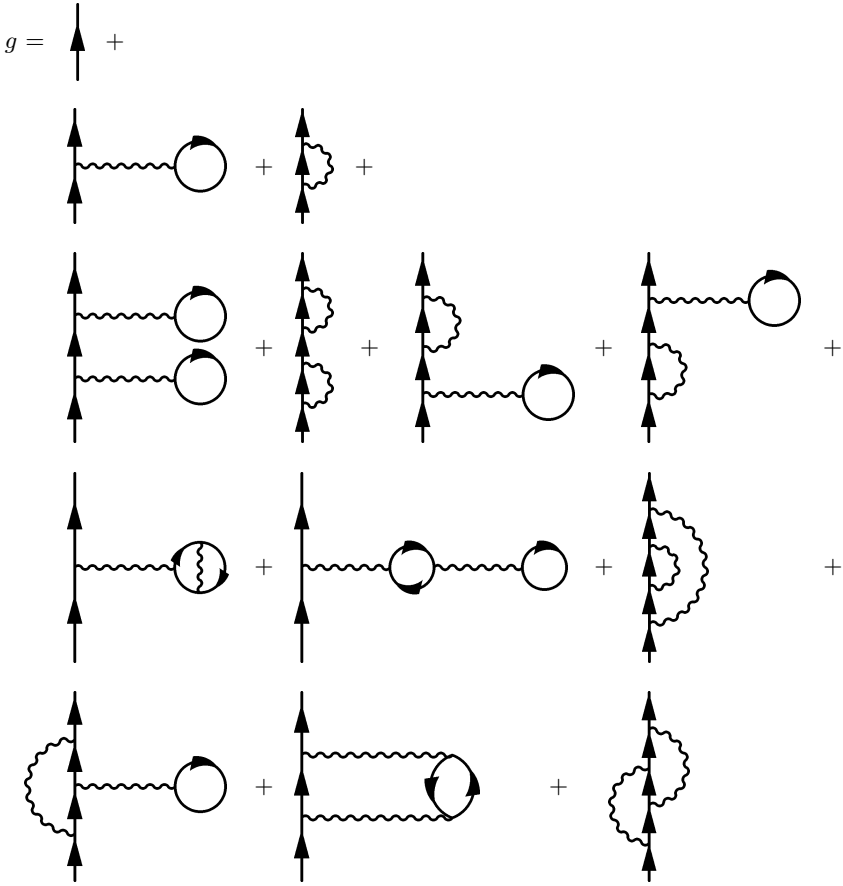


Fig. 12.3. Feynman diagrams for g of zero order (*first line*), first order (*second line*), and second order (*third, fourth, and fifth lines*)

5'. Integrate over all internal independent four-momenta (with a factor $1/2\pi$ for each single integration).

7'. Interpret each $g_0(\mathbf{k}, \omega)$ corresponding to a line starting from and ending at the same point (or linked by the same interaction line) as being $\tilde{g}_0^<(\mathbf{k}, \omega) = 2\pi i \delta(\omega - \varepsilon_k^0) \theta(k_F - k)$.

According to the above rules, the contribution to $g(q)$ from the first-order diagrams shown in Fig. 12.4 is

$$\begin{aligned}
 & -i \int \frac{d^4 q'}{(2\pi)^4} \tilde{g}_0^<(q') v(0) g_0(q) g_0(q) + i \int \frac{d^4 q'}{(2\pi)^4} g_0(q) g_0(q) \tilde{g}_0^<(q') v(\mathbf{k} - \mathbf{k}') \\
 & = g_0^2(q) \left[v(0) \int \frac{d^3 k'}{(2\pi)^3} \theta(k_F - k') - \int \frac{d^3 k'}{(2\pi)^3} v(\mathbf{k} - \mathbf{k}') \theta(k_F - k') \right].
 \end{aligned}$$



Fig. 12.4. First-order Feynman diagrams for g in the four-momentum space

It should be noted that the above rules for obtaining g are appropriate for an interaction term \mathcal{H}_1 of the form given by (12.40). Similar but not identical rules would apply for the case where $\mathcal{H}_0 = \mathcal{H}_{0e} + \mathcal{H}_{0p}$ and $\mathcal{H}_1 = \gamma \int d^3r \psi^\dagger(\mathbf{r}) \psi(\mathbf{r}) \phi(\mathbf{r})$, where \mathcal{H}_{0e} describes noninteracting electrons, \mathcal{H}_{0p} describes noninteracting phonons, and \mathcal{H}_1 is the electron–phonon interaction. In this case we have a causal Green’s function g for the electron field and another causal Green’s function D for the phonon field, for each of which we can write perturbative expansions involving both the unperturbed Green’s functions g_0 and D_0 and the interaction γ . For details the reader is referred to [20] or [113].

12.3 Diagrammatic Method for $T \neq 0$

In the last section we succeeded in expanding the $T = 0$ fermion g in terms of g_0 and v . This expansion was based upon: (1) (12.39), expressing the average (at $T = 0$) of a chronological product of Heisenberg operators as N/D , where N is the unperturbed average (at $T = 0$) of the chronological product of $S(\infty, -\infty)$ and the same operators in the interaction picture and D is the unperturbed average (at $T = 0$) of $S(\infty, -\infty)$; (2) Wick’s theorem (12.49), expressing $g_{m,0}$ in terms of products of g_0 s. For finite temperatures an equation analogous to (12.39) does not exist. Hence, the real time g for $T \neq 0$ cannot be expanded in terms of g_0 and v . However, it turns out that such an expansion for $T \neq 0$ is possible for the imaginary time Green’s functions introduced in Sect. 12.1. The basis for such an expansion is the following equation:

$$\begin{aligned} & \langle T [A_{1H}(-i\sigma) A_{2H}(-i\sigma') \cdots] \rangle \\ &= \frac{\langle T [S(-i\beta, 0) A_{1I}(-i\sigma) A_{2I}(-i\sigma') \cdots] \rangle_0}{\langle S(-i\beta, 0) \rangle_0}, \end{aligned} \quad (12.50)$$

where

$$\langle A \rangle \equiv \frac{\text{Tr} \{ A \exp[-\beta(\mathcal{H} - \mu N)] \}}{\text{Tr} \{ \exp[-\beta(\mathcal{H} - \mu N)] \}};$$

in $\langle A \rangle_0$, \mathcal{H} has been replaced by \mathcal{H}_0 . Equation (12.50) is the analog of (12.39). To prove (12.50) we use the relation

$$|\Psi_I(0)\rangle = |\Psi_S(0)\rangle = |\Psi_H\rangle, \quad (12.51)$$

which follows from (12.24) and (12.30). From (12.51), (12.32), and (12.31) it follows that

$$A_H(t) = S(0, t)A_I(t)S(t, 0). \quad (12.52)$$

We have also that

$$e^{-i\mathcal{H}t} = e^{-i\mathcal{H}_0 t}S(t, 0). \quad (12.53)$$

Equation (12.53) follows from (12.28), (12.24), (12.32), and (12.51). Replacing t by $-i\beta$ in (12.53) and multiplying by $e^{\beta\mu N}$, we obtain

$$e^{-\beta(\mathcal{H}-\mu N)} = e^{-\beta(\mathcal{H}_0-\mu N)}S(-i\beta, 0). \quad (12.54)$$

To arrive at (12.54) we need to assume that N commutes with \mathcal{H} and \mathcal{H}_0 . If this is not the case, then $\mu = 0$; consequently, (12.54) is always valid. Combining (12.54) with (12.52) and the property $S(t_1, t_2) = S(t_1, t_3)S(t_3, t_2)$, we obtain (12.50).

Taking into account (12.50), (12.49) (which holds for imaginary times as well [20]) and the definition of $g(\mathbf{r}_1, -i\sigma_1, \mathbf{r}_2, -i\sigma_2)$, we have a diagrammatic expansion of the latter in terms of $g_0(\mathbf{r}_i, -i\sigma_i, \mathbf{r}'_i, -i\sigma'_i)$ and $v(\mathbf{r}_i - \mathbf{r}'_i)$ based on rules resulting from the previous ones by the following substitutions: 2 by II, 4 by IV, 5 by V, and 7 by VII, where

II. Label each vertex with a 4-d point $x_i \equiv \mathbf{r}_i, -i\sigma_i$.

IV. For each interaction (wavy) line between x_i and x'_i write a factor

$$v(\mathbf{r}_i - \mathbf{r}'_i) \delta(\sigma_i - \sigma'_i).$$

V. Integrate over all internal variables \mathbf{r}_i and σ_i : $\int d^3r_i \int_0^\beta d\sigma_i$.

VII. Interpret $g_0(\mathbf{r}_i, -i\sigma_i, \mathbf{r}'_i, -i\sigma'_i)$ as being equal to $\tilde{g}_0^<(\mathbf{r}_i, -i\sigma_i, \mathbf{r}'_i, -i\sigma'_i)$.

The calculational effort is greatly simplified if we work in the \mathbf{k}, z_ν -space, i.e., if we try to calculate $G(\mathbf{k}, z_\nu)$ given by (12.11). The final rules for obtaining the n th-order contribution to $G(\mathbf{k}, z)$ are the following:

I'. Draw all topologically distinct connected diagrams with n interaction lines, two external points, and $2n + 1$ directed lines.

II'. Label each line with a four-momentum \mathbf{k}', z'_ν ; conserve momentum and $\text{Im}\{z'_\nu\}$ at each vertex.

III'. For each directed line labeled with a four-momentum \mathbf{k}, z_ν write a factor

$$G_0(\mathbf{k}, z_\nu) = \frac{1}{z_\nu - \varepsilon_k^0}.$$

IV'. For each interaction (wavy) line labeled \mathbf{k}, z_ν write a factor $-v(\mathbf{k})$.

V'. Integrate over all internal independent momenta $\mathbf{k} [(2\pi)^{-3} \int d^3k]$ and sum over all internal independent discrete frequencies $(\beta^{-1} \sum_\nu)$.

VI'. Multiply by $(-1)^m$, where m is the number of closed fermion loops.

VII'. Whenever a directed line either closes on itself or is joined by the same interaction line, insert a convergence factor $\exp(-z_\nu\sigma)$ with $\sigma \rightarrow 0^-$.

As an example we calculate the contributions of the first-order diagrams shown in Fig. 12.5. We have

$$G_0^2(\mathbf{k}, z_\nu) \left[\mp v(0) \int \frac{d^3k'}{(2\pi)^3} \frac{1}{\beta} \sum_{\nu'} \exp(-z'_\nu \sigma) G_0(\mathbf{k}', z'_\nu) - \int \frac{d^3k'}{(2\pi)^3} v(\mathbf{k} - \mathbf{k}') \frac{1}{\beta} \sum_{\nu'} \exp(-z'_\nu \sigma) G_0(\mathbf{k}', z'_\nu) \right],$$

which, with the help of (11.53) and $A_0(\mathbf{k}, \omega) = 2\pi\delta(\omega - \varepsilon_k^0)$, becomes

$$G_0^2(\mathbf{k}, z_\nu) \left[v(0) \int \frac{d^3k'}{(2\pi)^3} f_\mp(\varepsilon_{k'}^0) \pm \int \frac{d^3k'}{(2\pi)^3} v(\mathbf{k} - \mathbf{k}') f_\mp(\varepsilon_{k'}^0) \right]$$

(upper sign for bosons; lower sign for fermions).

It should be noted that the above rules for finite temperatures are appropriate for an interaction of the form (12.40). For other interactions, such as the electron–phonon interactions, the rules must be modified [20, 113].

Before concluding this section we remind the reader that the calculational schemes we have presented do not cover the case of bosons at low temperatures. The reason is that the unperturbed system for $T < T_c$ undergoes the phenomenon of Bose condensation according to which a finite fraction of the particles occupy a single quantum state, the $\mathbf{k} = 0$ state. This effect requires a special treatment, which is presented in [20] and [113]. Special treatment is also required for fermion systems, which are not normal (superfluid or superconducting systems). These questions will not be covered in the present work (with the exception of superconductivity).



Fig. 12.5. First-order Feynman diagrams for $G(\mathbf{k}, z_\nu)$

12.4 Partial Summations. Dyson’s Equation

It is very rare that a small number of lowest-order diagrams would be a good approximation for g . For this reason, in practical calculations we either try to obtain certain general results without employing approximations or, whenever specific results are sought, we try to find a class of diagrams such that the

contribution of the whole class is both calculable and dominant. Of course, it is not so often that such a happy situation occurs. Anyway, our calculational task is facilitated by reorganizing our expansion through certain partial summations. These partial summations can be performed in a graphical way. An example of such a summation is shown in Fig. 12.6. Square 1 denotes a part of the diagram connected to the rest by two directed lines; square 2 denotes a different part connected to the rest by two directed lines. The sum of the two diagrams can be found by calculating first the contributions of parts 1 and 2 according to the rules, summing these two contributions, and using this result for the part 1 + 2. This idea can be developed further so that starting from a few simple diagrams (called skeletons) and performing all possible summations in the lines and vertices (putting flesh to the skeletons [421]) we obtain g . Such a procedure requires care to ensure that all diagrams have been included and no diagram was counted more than once. To examine this question, we need to introduce some definitions and present some relations.

We call *self-energy* Σ the sum of the contributions from all parts that are connected to the rest by two directed lines (one in and one out). From the structure of the diagrams for g it follows that

$$G(\mathbf{k}, z_\nu) = G_0(\mathbf{k}, z_\nu) + G_0(\mathbf{k}, z_\nu)\Sigma(\mathbf{k}, z_\nu)G_0(\mathbf{k}, z_\nu). \quad (12.55)$$

Equation (12.55) can be written in a graphical way (Fig. 12.7), which shows that in x -space it would acquire an integral form. Note the similarity of (12.55) and (4.17). We define next the *proper self-energy*, Σ^* , which involves only those self-energy parts that cannot be divided into two pieces by cutting

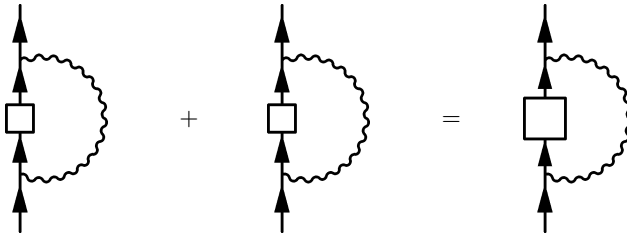


Fig. 12.6. An example of graphical summation

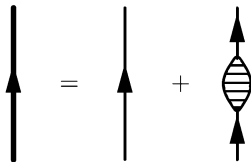


Fig. 12.7. Relation between Green's function G (thick line), unperturbed Green's function G_0 (thin line), and self-energy Σ

a single particle line. It is not difficult to see that

$$\begin{aligned} \Sigma &= \Sigma^* + \Sigma^* G_0 \Sigma^* + \Sigma^* G_0 \Sigma^* G_0 \Sigma^* + \dots \\ &= \Sigma^* + \Sigma^* G_0 \Sigma \\ &= \Sigma^* + \Sigma G_0 \Sigma^* . \end{aligned} \tag{12.56}$$

Note the analogy of (12.56) and (4.13), (4.15), and (4.16). Combining (12.55) and (12.56) we obtain

$$G = G_0 + G_0 \Sigma^* G = G_0 + G \Sigma^* G_0 , \tag{12.57}$$

which is the analog of (4.6) and (4.7). In \mathbf{k}, ω -space (12.57) can be rewritten as

$$G(\mathbf{k}, \omega) = \frac{G_0(\mathbf{k}, \omega)}{1 - G_0(\mathbf{k}, \omega) \Sigma^*(\mathbf{k}, \omega)} = \frac{1}{\omega - \varepsilon_k^0 - \Sigma^*(\mathbf{k}, \omega)} , \tag{12.58}$$

where we have taken into account that $G_0(\mathbf{k}, \omega) = (\omega - \varepsilon_k^0)^{-1}$. In Fig. 12.8 we show (12.57) in a diagrammatic way. It is clear that (12.58) has not solved the problem since Σ^* involves the summation of infinite diagrams. One could try to connect Σ^* with G by employing the idea of partial summations in the diagrams for Σ^* ; these partial summations would replace the G_0 -lines by G -lines. It turns out that one cannot express Σ^* with a few diagrams involving G -lines and interaction lines. This is to be expected since, as we have seen in the equation of motion method, one cannot obtain a system with a finite number of equations for a finite number of unknown functions that are related to the many-body g . However, one can express Σ^* in terms of G with the help of a new quantity Γ , which is called the *vertex part* and is defined as the sum of the contributions from all parts that are connected with four (two in and two out) directed lines (G_0 -lines) to the rest and that cannot be decomposed into disconnected parts. Γ is related to the two-particle Green's function g_2 , as shown in Fig. 12.9, i.e.,

$$\begin{aligned} g_2(x_1, x_2, x'_1, x'_2) &= g(x_1, x'_1) g(x_2, x'_2) \pm g(x_1, x'_2) g(x_2, x'_1) \\ &+ \int d\tilde{x}_1 d\tilde{x}_2 d\tilde{x}'_1 d\tilde{x}'_2 \Gamma(\tilde{x}_1, \tilde{x}_2; \tilde{x}'_1, \tilde{x}'_2) g(x_1, \tilde{x}_1) g(x_2, \tilde{x}_2) \\ &\times g(\tilde{x}'_1, x'_1) g(\tilde{x}'_2, x'_2) . \end{aligned} \tag{12.59}$$

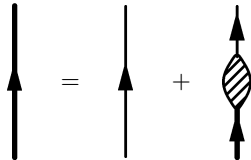


Fig. 12.8. Relation between G (thick line), G_0 (thin line) and proper self-energy Σ^*



Fig. 12.9. Relation between g_2 , g , and vertex part Γ

One can show [113] that Σ^* is given in terms of G and Γ as shown in Fig. 12.10a. One can easily prove that the relation shown in Fig. 12.10a is equivalent to the equation of motion (12.1). The proof makes use of (12.59) and (12.57). Figure 12.10 shows that Σ^* can be calculated by “putting flesh” to the four skeleton diagrams shown in Fig. 12.10b, i.e., by replacing the G_0 -lines by G -lines and one of the two interaction lines in the last two diagrams by the vertex part. (If both interaction lines in the same diagram are replaced by vertex parts, one would double count diagrams.) As expected, one cannot express Γ in a closed form involving G and Γ , i.e., the skeleton diagrams for Γ (to be fleshed by the substitution $G_0 \rightarrow G$ and $v \rightarrow \Gamma$) are infinite in number. Usually we stop this infinite hierarchy of relations by approximately expressing Γ in a closed form in terms of G and Γ . The simplest such approximation is to put $\Gamma = 0$ in the relation shown in Fig. 12.10a. This is the Hartree–Fock approximation. We obtain then for $\Sigma^*(\mathbf{k}, z_\nu)$ the expression

$$\begin{aligned} \Sigma^*(\mathbf{k}, z_\nu) = & \mp v(0) \int \frac{d^3 k'}{(2\pi)^3} \frac{1}{\beta} \sum_{\nu'} \exp(-z'_\nu \sigma) G(\mathbf{k}', z'_\nu) \\ & - \int \frac{d^3 k'}{(2\pi)^3} v(\mathbf{k} - \mathbf{k}') \frac{1}{\beta} \sum_{\nu'} \exp(-z'_\nu \sigma) G(\mathbf{k}', z'_\nu) \end{aligned} \quad (12.60)$$

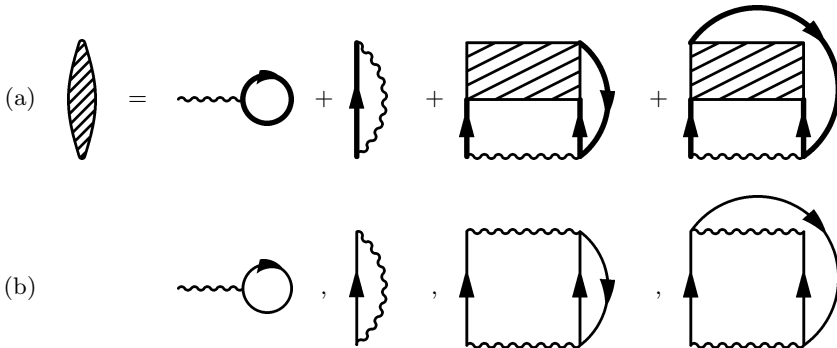


Fig. 12.10. The proper self-energy, Σ^* , can be calculated from the four diagrams (a) resulting by “fleshing” the skeleton diagrams (b)

$$\begin{aligned}
 &= v(0) \int \frac{d^4 q'}{(2\pi)^4} A(\mathbf{k}', \omega') f_{\mp}(\omega') \\
 &\quad \pm \int \frac{d^4 q'}{(2\pi)^4} v(\mathbf{k} - \mathbf{k}') A(\mathbf{k}', \omega') f_{\mp}(\omega') \\
 &= \Sigma^*(\mathbf{k}) .
 \end{aligned} \tag{12.61}$$

Combining (12.61) with (12.58) we obtain (12.19) and (12.20). The Hartree–Fock approximation is shown diagrammatically in Fig. 12.11. The basic equation (12.58) combined with the equation connecting Σ^* with G and I (Fig. 12.10a) is called *Dyson’s equation*.

We introduce also the concept of an *effective interparticle interaction* v_e as the sum of v plus the contributions (apart from a factor i or -1 for the $T = 0$ or $T \neq 0$ case, respectively) from all parts that have two external interaction lines. The effective interaction, v_e , can be expressed as shown in Fig. 12.12a in terms of the *polarization* Π ; the latter is defined as the sum of the contributions (apart from the above factors) of all parts that are connected to the rest by two interaction lines. Following an analysis similar to the one given for the self-energy, we can easily express the polarization, Π , in terms of the *proper polarization*, Π^* , as shown in Fig. 12.12b. The proper polarization Π^* is the sum of the contributions (apart from a factor $-i$ or -1 for the $T = 0$ or $T \neq 0$ case, respectively) of all parts that are connected to the rest by two interaction lines and that cannot be divided into two pieces by cutting a single interaction line. For a translationally invariant system and in the q -representation, the relations of Fig. 12.12 become

$$v_e(q) = v(q) + v^2(q)\Pi(q) , \tag{12.62}$$

$$\Pi(q) = \Pi^*(q) + \Pi^*(q)v(q)\Pi^*(q) + \dots = \Pi^*(q) + \Pi^*(q)v(q)\Pi(q) , \tag{12.63}$$

which leads to

$$\Pi(q) = \frac{\Pi^*(q)}{1 - v(q)\Pi^*(q)} \tag{12.63'}$$

and

$$v_e(q) = v(q) + v(q)\Pi^*(q)v_e(q) , \tag{12.64}$$

which can be solved for $v_e(q)$ to yield

$$v_e(q) = \frac{v(q)}{1 - v(q)\Pi^*(q)} . \tag{12.64'}$$

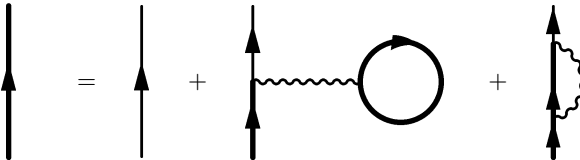


Fig. 12.11. Hartree–Fock approximation

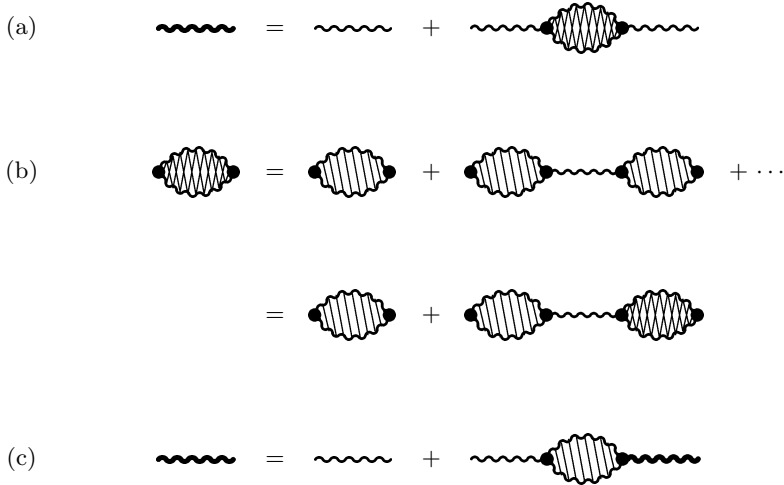


Fig. 12.12. Relation between: **a** v_e , v , and Π ; **b** v , Π , and Π^* ; **c** v_e , v , and Π^* for fermions at $T = 0$. For the $T \neq 0$ imaginary time case in \mathbf{k}, z_ν -space iv_e , iv , $-i\Pi$, and $-i\Pi^*$ must be replaced by $-v_e$, $-v$, $-\Pi$, and $-\Pi^*$, respectively

If we define a *dielectric function* $\varepsilon^C(\mathbf{k}, \omega)$ from the relation

$$v_e(q) = \frac{v(q)}{\varepsilon^C(q)}, \quad (12.65)$$

we obtain, by taking into account (12.62) and (12.64'),

$$\frac{1}{\varepsilon^C(q)} = 1 + v(q)\Pi(q) = \frac{1}{1 - v(q)\Pi^*(q)}. \quad (12.66)$$

To find the relation between the usual (*retarded*) *dielectric function* defined in Chap. 11 and $\varepsilon^C(\mathbf{k}, \omega)$, we observe first that the inverse Fourier transform of the polarization $\Pi(q)$ equals $D(x, x')$, where

$$D(x, x') \equiv -i \langle T [\tilde{n}_H(x) \tilde{n}_H(x')] \rangle \quad (12.67)$$

and

$$\tilde{n}_H(x) = n_H(x) - \langle n_H(x) \rangle = \psi_H^\dagger(x) \psi_H(x) - \langle \psi^\dagger(x) \psi(x) \rangle. \quad (12.68)$$

The proof of the relation $D = \Pi$ follows from a diagrammatic expansion of (12.67). The causal Green's function, $D(x, x')$, is connected with the retarded Green's function, $D^R(x, x')$, which was introduced in Chap. 11 in the usual way. Thus for fermions at $T = 0$

$$\begin{aligned} \text{Re} \{ D^R(q) \} &= \text{Re} \{ D(q) \} = \text{Re} \{ \Pi(q) \}, \\ \text{Im} \{ D^R(q) \} &= \bar{\varepsilon}(\omega) \text{Im} \{ D(q) \} = \bar{\varepsilon}(\omega) \text{Im} \{ \Pi(q) \}, \end{aligned} \quad (12.69)$$

where

$$\bar{\varepsilon}(\omega) = \begin{cases} +1 & \text{for } \omega > 0, \\ -1 & \text{for } \omega < 0. \end{cases}$$

Taking into account (12.66), (11.45), and (12.69) and the fact that $v(q) = 4\pi e^2/q^2$ (for a Coulomb interaction), we obtain that

$$\operatorname{Re} \{\varepsilon(\mathbf{k}, \omega)\} = \operatorname{Re} \{\varepsilon^C(\mathbf{k}, \omega)\}, \quad (12.70)$$

$$\operatorname{Im} \{\varepsilon(\mathbf{k}, \omega)\} = \bar{\varepsilon}(\omega) \operatorname{Im} \{\varepsilon^C(\mathbf{k}, \omega)\}. \quad (12.71)$$

In the $T \neq 0$ imaginary time formalism, the sum of all polarization diagrams gives $-\Pi(\mathbf{k}, z_\nu)$, from which, by analytic continuation, one obtains $\Pi(\mathbf{k}, z)$. The dielectric function $\varepsilon(\mathbf{k}, \omega)$ is then given by

$$\frac{1}{\varepsilon(\mathbf{k}, \omega)} = 1 + v(\mathbf{k}) \lim \Pi(\mathbf{k}, z), \quad (12.72)$$

as z approaches ω from above the real ω -axis. The conclusion is that from the polarization diagrams one can obtain the dielectric function for either $T = 0$ or $T \neq 0$.

Of course, the polarization Π or the proper polarization Π^* involves an infinite number of diagrams, which cannot be summed exactly. Thus the calculation of Π or Π^* must be done approximately. The approximation is usually implemented either by keeping a few diagrams for Π^* or by expressing Π in terms of g and Γ and then approximating Γ . An example will be examined in the next chapter.

12.5 Other Methods of Calculation

Several other methods of treating many-body systems have been developed. Besides the standard technique of *canonical transformations* various bosonization approaches are employed, such as the introduction of the so-called *slave boson operators* [135], or the reexpression of electron Hamiltonian in the Luttinger liquid model in terms of the *bosonic density operators* [114, 135]. The interested reader is referred to the books by Mahan [114] and Doniach and Sondheimer [135].

12.6 Summary

In all practical cases the total Hamiltonian \mathcal{H} can be decomposed into an unperturbed part \mathcal{H}_0 , such that the corresponding Green's functions can be easily calculated, and a perturbation \mathcal{H}_1 .

In the equation of motion method one writes a differential equation for one of the g s; this equation also contains a term involving \mathcal{H}_1 and a higher-order Green's function. The calculation is done by approximately expressing the higher-order Green's function in terms of g . This method is applicable to g^R , g^A (for $T = 0$ or $T \neq 0$), and g (for $T = 0$ only). It can be applied to the $T \neq 0$ causal g if complex times are considered.

In the perturbative diagrammatic method, g is expressed as a complicated series each term of which involves products of g_0 and \mathcal{H}_1 . Keeping track of the terms in the series is facilitated by associating diagrams with each term. The diagrams help in intermediate algebraic manipulations and permit also a physical interpretation of each term (this last feature can be used to develop meaningful approximations). The diagrammatic method is applicable to the causal Green's function g at $T = 0$; it is applicable to the imaginary time causal g for $T \neq 0$.

The calculational effort is facilitated by defining the summation of certain types of diagram parts. Thus, the self-energy, Σ , and the proper self-energy, Σ^* , are defined; their relation to the causal Green's function is shown in Fig. 12.7 and 12.8. We defined also the vertex part, Γ , which is related to g_2 , as shown in Fig. 12.9. The proper self-energy, Σ^* , can be expressed in terms of Γ and G . The system of equations can be closed by approximating Γ in terms of Γ and G . Finally, the polarization part, Π , and the proper polarization part, Π^* , are defined and related with the effective interaction, as shown in Fig. 12.12. The quantity Π (or Π^*) is directly related to the dielectric function.

Further Reading

For the equation of motion method the interested reader may consult the book by Kadanoff and Baym [420].

The diagrammatic approach for g , G , Σ , Σ^* , Γ , Π , and Π^* is presented in a clear way in the book by Fetter and Walecka [20]. The other classic books, such as the one by Abrikosov et al. [113] or the one by Mahan [114], provide extensive treatments of the diagrammatic approach and the partial summations leading to the concepts of the proper self-energy and the proper polarization.

Problems

12.1. Calculate the energy and the thermodynamic potential, $-P\Omega$, within the Hartree–Fock approximation.

Hint: Use (11.30) and (11.37) as a starting point and assume that v_0 in (12.20) is zero. For $T = 0$ obtain explicit results. See [20], pp. 121–127 and 261–267.

12.2. Express the energy, $\varepsilon_{\mathbf{k}}$, and the inverse lifetime, $\gamma_{\mathbf{k}}$, of a quasiparticle in terms of expansion of the proper self-energy around the pole of the Green's function.

Hint: See next chapter.

12.3. How is $w_{\mathbf{k}}$ related to the derivative of $\Sigma^*(\mathbf{k}, \omega)$?

Hint: See next chapter.

12.4s. Obtain (12.19) and (12.20) from Fig. 12.11 by employing the finite temperature diagrammatic approach.

12.5. Calculate the sum

$$\sum_{\nu} G_0 \left(\frac{z}{2} + z_{\nu}, \varepsilon_{\mathbf{k}} \right) G_0 \left(\frac{z}{2} - z_{\nu}, \varepsilon'_{\mathbf{k}} \right) .$$

Hint: Reexpress the product of $G_0 G_0$ as a difference of G_0 s, and use (11.47) and (11.53).

Applications

Summary. Some applications of the many-body Green's functions are briefly presented. They include the study of a high-density electronic system moving in a positive background; this model describes approximately electrons in metals. A low-density Fermi system with short-range interactions is also examined. The employment of the Green's function formalism to justify the widely used independent-particle approximation is emphasized. Superconductivity and the Hubbard model are also examined.

13.1 Normal Fermi Systems. Landau Theory

In Chap. 11 we defined a normal Fermi system as one for which the *a.c.* $\{g(\mathbf{k}, \omega)\}$ has a single pole with a trajectory (as k varies) that crosses the real ω -axis at $\omega = \mu$ (for $k = k_F$) with zero slope. Taking into account that

$$g(\mathbf{k}, \omega) = [\omega - \varepsilon_k^0 - \Sigma^*(\mathbf{k}, \omega)]^{-1}, \quad (13.1)$$

it follows that for a normal Fermi system $\Sigma_I^* = \text{Im} \{\Sigma^*(\mathbf{k}, \omega)\}$ must behave as

$$\Sigma_I^*(\mathbf{k}, \omega) = \bar{\varepsilon}(\mu - \omega)C_k |\omega - \mu|^n, \quad C_k \geq 0, \text{ real}, \quad (13.2)$$

for $\omega \approx \mu$ with $n > 1$. Luttinger [425] has proved that $n = 2$ is a consistent solution of the equations for g and Σ^* . The outline of the proof is the following. We substitute (13.2) into (13.1), and the resulting expression is used in the equation shown in Fig. 12.10a. The first two terms give $\Sigma_I^* = 0$. In the next two terms, Γ is replaced by an infinite series of diagrams involving the bare interaction v and the dressed propagator g . One can then show [425] that each of the resulting diagrams gives an imaginary part that behaves as

$$(\omega - \mu)^{2m}, \quad m = 1, 2, 3, \dots,$$

in the limit $\omega \rightarrow \mu^\pm$. Hence,

$$\lim_{\omega \rightarrow \mu} \Sigma_I^*(\mathbf{k}, \omega) \propto (\omega - \mu)^2, \quad (13.3)$$

as was assumed at the beginning. Thus, expression (13.1), subject to condition (13.3), is a solution of the equations for g , which means that the normal state of a strongly interacting Fermi system is a possible one. The pole $z_{\mathbf{k}} = \varepsilon_{\mathbf{k}} + i\gamma_{\mathbf{k}}$ is a solution of

$$z_{\mathbf{k}} - \varepsilon_{\mathbf{k}}^0 - \Sigma^*(\mathbf{k}, z_{\mathbf{k}}) = 0, \quad (13.4)$$

which for $k \approx k_F$ gives

$$\varepsilon_{\mathbf{k}} = \mu + \left| \frac{\partial \varepsilon_{\mathbf{k}}^0}{\partial \mathbf{k}} + \frac{\partial \Sigma_R^*}{\partial \mathbf{k}} \right| w_{\mathbf{k}} \cdot (\mathbf{k} - \mathbf{k}_F), \quad (13.5)$$

$$w_{\mathbf{k}} = \left[1 - \frac{\partial \Sigma_R^*}{\partial \omega} \right]^{-1}, \quad (13.6)$$

$$\gamma_{\mathbf{k}} = \bar{\varepsilon} (\mu - \varepsilon_{\mathbf{k}}) w_{\mathbf{k}} C_{\mathbf{k}} (\varepsilon_{\mathbf{k}} - \mu)^2, \quad (13.7)$$

where the derivatives are calculated for $\mathbf{k} = \mathbf{k}_F$ and $\omega = \mu$.

The Green's function g can be written as

$$g(\mathbf{k}, \omega) = \frac{w_{\mathbf{k}}}{\omega - \varepsilon_{\mathbf{k}} - i\gamma_{\mathbf{k}}} + g_b(\mathbf{k}, \omega), \quad (13.8)$$

where the smooth background contribution, $g_b(\mathbf{k}, \omega)$, can be omitted for $\omega \approx \varepsilon_{\mathbf{k}}$. We see that the normal solution, (13.8), not only is a possible solution of the interacting Fermi system but also goes continuously to the unperturbed $g_0(\mathbf{k}, \omega)$, since, as the coupling constant goes to zero, $C_{\mathbf{k}} \rightarrow 0$, $w_{\mathbf{k}} \rightarrow 1$, $\varepsilon_{\mathbf{k}} \rightarrow \varepsilon_{\mathbf{k}}^0$, and $g_b(\mathbf{k}, \omega) \rightarrow 0$. Thus, if we assume that the actual state of the interacting system develops in a unique and *continuous* way from the unperturbed state as the interactions are turned on, we can conclude that the normal solution, (13.5)–(13.8), is the actual one and that our system is a normal one. Obviously, if the perturbation expansion converges, the above assumptions are correct and the system is a normal one. However, it should be stressed that the continuity assumption may be valid while the expansion in powers of the coupling constant may diverge, which means that a system may be normal even if the perturbation expansion diverges. On the other hand, there are physical systems (e.g., a superconducting material) where the perturbed state does not develop from the unperturbed in a continuous way as the interactions are turned on; such systems are not normal, and the actual Green's function does not have the form (13.5)–(13.8).

Equation (13.5) shows that the dispersion relation $\varepsilon_{\mathbf{k}}$ for $k \approx k_F$ is characterized by a single quantity $v_F = |\partial \varepsilon_{\mathbf{k}}^0 / \partial \mathbf{k} + \partial \Sigma_R^* / \partial \mathbf{k}| w_{\mathbf{k}}$; the expansion coefficient v_F is the velocity of the quasiparticles at the Fermi level, and it is usually expressed as

$$v_F = \frac{k_F}{m^*}. \quad (13.9)$$

Equation (13.9) can be considered as the definition of the effective mass m^* . For a noninteracting system $m^* = m$.

For a normal system characterized by (13.5)–(13.8) with short-range forces, one can prove (see, e.g., [425]), by analyzing the diagrams for the vertex part $\Gamma(p_1, p_2; k)$, that

$$\Gamma(p_1, p_2; k) \simeq \Gamma^\omega(p_1, p_2) + \frac{w_{k_F}^2 k_F^2}{(2\pi)^3 v_F} \int \Gamma^\omega(p_1, q) \Gamma(q, p_2; k) \frac{\mathbf{v} \cdot \mathbf{k}}{\omega - \mathbf{v} \cdot \mathbf{k}} d\mathcal{O}. \quad (13.10)$$

In (13.10) $p_1 = \mathbf{p}_1, \omega_1$ and $p_2 = \mathbf{p}_2, \omega_2$ are the four momenta at the two “in” points of the vertex part Γ ; $p_1 + k, p_2 - k$ are the four momenta at the two “out” points of the vertex part Γ ; $k = \mathbf{k}, \omega$ is the four-momentum transfer; $\Gamma^\omega \equiv \lim_{\omega \rightarrow 0} \lim_{\mathbf{k} \rightarrow 0} \Gamma(k)$ (note the order of the limits); \mathbf{v} is a vector directed along \mathbf{q} with $|\mathbf{v}| = v_F$; the four-momentum q equals \mathbf{q}, μ with $|\mathbf{q}| = k_F$; $\int d\mathcal{O}$ denotes an integration over the direction of \mathbf{q} . Equation (13.10) is valid for small ω and $|\mathbf{k}|$.

Using (13.10) together with some relations connecting the derivatives $\partial g^{-1}/\partial\omega$, $\partial g^{-1}/\partial\mathbf{k}$, $\mathbf{k} \cdot \partial g^{-1}/\partial\mathbf{k}$, and $\partial g^{-1}/\partial\mu$ with the vertex part Γ (see [425]), one can prove the following two important relations first derived by Landau [426, 427].

The Fermi momentum k_F , which was defined by the equation $\varepsilon_{k_F} = \mu$, satisfies the relation

$$\frac{4\pi}{3} \frac{k_F^3}{(2\pi)^3} = \frac{N}{\Omega}, \quad (13.11)$$

where N is the total number of particles for each spin direction and Ω is the volume. We see that k_F for a normal interacting Fermi system satisfies the same basic equation as for the noninteracting system. Thus, for a normal system, turning on the interactions not only retains the concept of a Fermi surface; it leaves the Fermi surface unchanged.

The other relation connects the bare mass m with the effective mass m^* and the vertex part Γ^ω

$$\frac{1}{m^*} = \frac{1}{m} - \frac{k_F w_{k_F}^2}{2(2\pi)^3} \int \Gamma^\omega(p_1, p_2) \cos\theta d\mathcal{O}, \quad (13.12)$$

where $p_1 \equiv \mathbf{p}_1, \mu$; $p_2 \equiv \mathbf{p}_2, \mu$; $|\mathbf{p}_1| = |\mathbf{p}_2| = k_F$; θ is the angle between \mathbf{p}_1 and \mathbf{p}_2 ; and the integration is over all directions of \mathbf{p}_1 or \mathbf{p}_2 (the interaction is isotropic). For an alternative derivation of (13.11) and (13.12) the reader is referred to [423].

From (13.10) one can prove [113] that $\Gamma(p_1, p_2; k)$ develops a pole as a function of ω . Since $\Gamma(p_1, p_2; k)$ is directly related to the polarization part $\Pi(k)$, it follows that the pole of $\Gamma(p_1, p_2; k)$ appears as a pole in $\Pi(k) \equiv \Pi(\mathbf{k}, \omega)$. As was mentioned in Chap. 11, the pole of $\Pi(\mathbf{k}, \omega) [\equiv D(\mathbf{k}, \omega)]$ corresponds to a collective Bose excitation, which is an elementary density wave. Thus, a normal system possesses collective Bose excitations. For short-range interactions at $T = 0$, these excitations are given as the poles of the solution

of (13.10). It turns out [20, 113] that the eigenfrequency $\omega_{\mathbf{k}}$ of this collective excitation is of the form

$$\omega_{\mathbf{k}} = c_0 |\mathbf{k}| , \quad (13.13)$$

i.e., it resembles sound waves. For this reason it is called *zero sound*. Zero sound is clearly distinguished from ordinary sound because the former, in contrast to the latter, does not correspond to a local equilibrium condition (i.e., the variation in the distribution, $\delta f(\mathbf{r}, \mathbf{k})$, is not spherical in \mathbf{k} -space). This question was discussed by Abrikosov et al. [113] and Fetter and Walecka [20].

We close this section by mentioning that the leading term in the difference $\Phi(T) - \Phi(0)$ as $T \rightarrow 0^+$, where Φ is any thermodynamic quantity (such as specific heat, entropy, or energy), is given by replacing the bare mass m^* in the corresponding free-particle expression by the effective mass m^* [113]. In other words, for a normal Fermi system and for the purpose of calculating the temperature dependence of thermodynamic quantities in the limit $T \rightarrow 0$, one can replace the strongly interacting particles by noninteracting quasiparticles of an effective mass m^* .

In this section we have outlined how the many-body Green's function formalism can be used to justify and quantify the fundamental idea that an interacting system of particles can be replaced by a weakly interacting system of quasiparticles. For many purposes the interactions among quasiparticles can be omitted, and consequently the so-called one-body approximation is justified. For normal systems there is one-to-one correspondence between particles and quasiparticles, and each quasiparticle reduces to a real particle as the interactions are turned off. Note, though, that the interactions produce a Bose-type excitation (a density wave) that is absent in a noninteracting system.

We reiterate that there are systems (such as the superconducting materials or superfluid He^3) where the interactions play a fundamental role in reorganizing the low-lying states to a new configuration that cannot result from the unperturbed states in a continuous way. For such a system the Green's function formalism requires some modifications. The reader is referred to Sect. 13.4 or to the book by Mattuck, [421] for an introduction. More detailed treatment is given in [20], [111], and [113]. The modified Green's function formalism finds one of the most important applications in the study of these nonnormal fermion systems.

13.2 High-Density Electron Gas

In this section we consider a particular but important fermion system, the so-called *jellium model*, a high-density electronic system moving in the background of positive charge to ensure overall electrical neutrality. The jellium model is an idealization of a real metal; this idealization omits the discrete character of the positive background, its dynamics (phonons), and the interaction of the ion motion with the electrons. The high-density jellium model,

although a normal Fermi system, has certain peculiarities associated with the long-range character of the electron–electron interaction. The $1/r^2$ nature of the Coulomb force gives that the average potential energy per particle is proportional to $n^{1/3}$; on the other hand, the average kinetic energy per particle, as a result of the Pauli principle, is proportional to $k_F^2/2m$, i.e., proportional to $n^{2/3}$, where $n = N/\Omega$ is the number density. Thus, in contrast to ordinary gases, in the high-density limit, the kinetic energy of the electron system dominates the potential energy, and therefore the system behaves as a gas; on the other hand, in the low-density limit, the potential energy is the dominant one, and the system becomes a (Wigner) solid; for intermediate densities we have a liquid. We can express formally this feature by introducing the dimensionless interparticle spacing r_s , where

$$r_s = \frac{r_0}{a_B} ; \quad (13.14)$$

r_0 is defined by $4\pi r_0^3/3 = \Omega/N$ and $a_B = \hbar^2/me^2$ is the Bohr radius. By introducing the dimensionless quantities Ω' , \mathbf{k}' , \mathbf{p}' , and \mathbf{q}' , where

$$\Omega' = \Omega/r_0^3, \quad \mathbf{k}' = r_0\mathbf{k}, \quad \mathbf{p}' = r_0\mathbf{p}, \quad \mathbf{q}' = r_0\mathbf{q}, \quad (13.15)$$

we can rewrite the Hamiltonian of the jellium model (Appendix I) as

$$\mathcal{H} = \frac{e^2}{a_B r_s^2} \left(\frac{1}{2} \sum_{\mathbf{k}'} \mathbf{k}'^2 a_{\mathbf{k}'}^\dagger a_{\mathbf{k}'} + \frac{r_s}{2\Omega'} \sum_{\mathbf{k}'\mathbf{p}'\mathbf{q}'}' \frac{4\pi}{q'^2} a_{\mathbf{k}'+\mathbf{q}'}^\dagger a_{\mathbf{p}'-\mathbf{q}'}^\dagger a_{\mathbf{p}'} a_{\mathbf{k}'} \right), \quad (13.16)$$

which shows that in the high-density limit ($r_s \rightarrow 0$) the potential energy becomes negligible. Note that the prime in the summation means that the $q' = 0$ term must be excluded.

By inspection of (13.16) one may suspect that terms of higher than second order in the potential energy would give contributions that approach zero as $r_s \rightarrow 0$. Hence, it is reasonable to try to terminate the diagrammatic expansion in the second order. Because of the $q' = 0$ exclusion, the diagrams involving a $q' = 0$ interaction line give no contribution and can be omitted. Thus the only diagrams that contribute to the proper self-energy up to second order are those of Fig. 13.1. The Σ_1^* , Σ_{2a}^* , and Σ_{2b}^* diagrams can be calculated according to the rules and give no problems. Explicit results can be found in [20]. The Σ_{2r}^* diagram is troublesome and requires detailed consideration; we have

$$\Sigma_{2r}^*(\mathbf{k}, \omega) = i \int \frac{d^3q}{(2\pi)^3} \frac{d\omega_1}{2\pi} g_0(\mathbf{k} - \mathbf{q}, \omega - \omega_1) v^2(q) \Pi_0^*(\mathbf{q}, \omega_1), \quad (13.17)$$

where $-i\Pi_0^*$ is the contribution of the bubble, i.e., the contribution of the lowest order to the proper polarization

$$\Pi_0^*(\mathbf{q}, \omega_1) = -i \int \frac{d^3p_1}{(2\pi)^3} \frac{d\omega_2}{2\pi} g_0(\mathbf{p}_1, \omega_2) g_0(\mathbf{p}_1 + \mathbf{q}, \omega_1 + \omega_2). \quad (13.18)$$

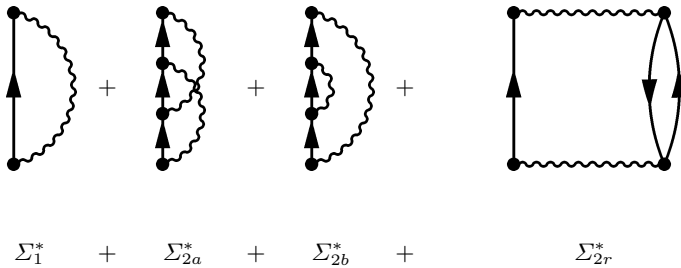


Fig. 13.1. All the contributions of up to second order to the proper self-energy of an electron gas

This quantity $\Pi_0^*(\mathbf{q}, \omega_1)$ is calculated explicitly in [20]. It turns out that

$$\lim_{\mathbf{q} \rightarrow 0} \Pi_0^*(\mathbf{q}, |\mathbf{q}|x) = F(x), \tag{13.19}$$

where $F(x)$ is an integrable function of $x \equiv \omega_1/|\mathbf{q}|$. Substituting (13.19) into (13.17), and taking into account that $v(\mathbf{q}) = 4\pi e^2/q^2$, we obtain that the integral over q behaves for small q as

$$\Sigma_{2r}^*(\mathbf{k}, \omega) \sim \int_0 \frac{d^3q}{q^4} q \sim \int_0 \frac{dq}{q}, \tag{13.20}$$

i.e., it diverges logarithmically. This logarithmic divergence simply indicates that the perturbation expansion in powers of the Coulomb potential $4\pi e^2/q^2$ does not converge. One way to avoid this difficulty is to replace the Coulomb potential by $e^2 e^{-\lambda r}/r$, which has a Fourier transform equal to

$$v_\lambda(\mathbf{q}) = \frac{4\pi e^2}{q^2 + \lambda^2}, \tag{13.21}$$

with λ being a small quantity. One can then try to sum the perturbation series in powers of v_λ and take the limit $\lambda \rightarrow 0$ in the final result. In summing the power series expansion, one must keep in mind that there are now two independent small quantities, namely, r_s and λ , and hence one cannot terminate the series at the second order because some of the higher-order terms (which tend to zero as $r_s \rightarrow 0$) may approach infinity as $\lambda \rightarrow 0$. To handle this problem correctly one must find for each order of perturbation series (i.e., for each power of r_s) the leading term(s) in λ . In second order the leading term λ is Σ_{2r}^* , which behaves as $\ln \lambda$ in the limit $\lambda \rightarrow 0$. This behavior stems from the fact that the two interaction lines in Σ_{2r}^* have the same \mathbf{q} . It is easy to see that the leading term in λ of n th order will come from the diagram that has the same \mathbf{q} in all interaction lines (Fig. 13.2). Such a diagram would give a contribution Σ_{nr}^* that is proportional to

$$\Sigma_{nr}^* \sim r_s^{n-2} \int_0 \frac{d^3q}{(q^2 + \lambda^2)^n} q \sim r_s^{n-2} \lambda^{2-n}, \quad n = 3, 4, \dots, \tag{13.22}$$

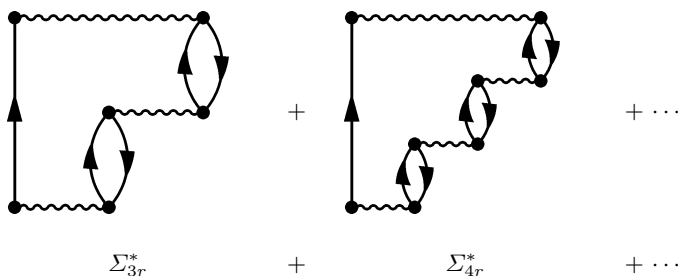


Fig. 13.2. Leading diagrams of third, fourth, etc. order for proper self-energy of an electron gas

while all the other diagrams of n th order give a contribution of the order $r_s^{n-2}\lambda^{3-n}$ or less. Thus, in the limit $\lambda \rightarrow 0$, the n th-order contribution to Σ^* and Σ_n^* equals Σ_{nr}^* . We can conclude that in the limit of small r_s and small λ the proper self-energy is given by

$$\Sigma^* \simeq \Sigma_1^* + \Sigma_{2a}^* + \Sigma_{2b}^* + \sum_{n=2}^{\infty} \Sigma_{nr}^* . \quad (13.23)$$

The quantity $\Sigma_1^* + \Sigma_{2r}^* + \Sigma_{3r}^* + \dots$ can be written as in Fig. 13.3, where

$$v_{e,\text{RPA}} = v\lambda + v\lambda^2\Pi_0^* + v\lambda^3\Pi_0^{*2} + \dots = \frac{v}{1 - v\Pi_0^*} . \quad (13.24)$$

Thus we have for $\Sigma_r^* = \sum_{n=2}^{\infty} \Sigma_{nr}^*$

$$\begin{aligned} \Sigma_r^* &= i \int \frac{d^3q}{(2\pi)^3} \frac{d\omega_1}{2\pi} g_0(\mathbf{k} - \mathbf{q}, \omega - \omega_1) [v_{e,\text{RPA}}(\mathbf{q}, \omega) - v(\mathbf{q})] \\ &= i \int \frac{d^3q}{(2\pi)^3} \frac{d\omega_1}{2\pi} g_0(\mathbf{k} - \mathbf{q}, \omega - \omega_1) \frac{v^2(\mathbf{q})\Pi_0^*(\mathbf{q}_1, \omega_1)}{1 - v(\mathbf{q})\Pi_0^*(\mathbf{q}_1, \omega_1)} . \end{aligned} \quad (13.25)$$

Note that $v_{e,\text{RPA}}$ results from the general expression (12.64') by replacing the proper polarization Π^* by its lowest approximation Π_0^* . The approximation

$$\Pi^*(\mathbf{q}, \omega_1) \simeq \Pi_0^*(\mathbf{q}, \omega_1) \quad (13.26)$$



Fig. 13.3. The sum $\Sigma_1^* + \Sigma_{2r}^* + \Sigma_{3r}^* + \dots$; $v_{e,\text{RPA}}$ is the effective interaction corresponding to the approximation $\Pi^* = \Pi_0^*$

is known, for historical reasons, as the *random phase approximation (RPA)*. It is also known as the summation of the ring diagrams. It must be stressed that on the rhs of (13.24) or (13.25) we can take the limit $\lambda \rightarrow 0$ without any divergence.

The approximation (13.26) coupled with the general equation (12.66) for the dielectric function gives

$$\varepsilon_{\text{RPA}}^c(\mathbf{q}, \omega) = 1 - v(\mathbf{q}) \Pi_0^*(\mathbf{q}, \omega) . \quad (13.27)$$

Having obtained Σ^* and ε^C we can calculate several quantities of physical interest:

- (a) *Quasiparticles* ε_k and γ_k . The reader is referred to [421] and references therein.
- (b) *Ground-state energy*. Taking into account the general thermodynamic relation

$$\left\langle \frac{\partial \mathcal{H}}{\partial a} \right\rangle = \frac{\partial E}{\partial a} \Big|_{N, \Omega} , \quad (13.28)$$

(11.29), (11.7), Fig. 11.1, and (12.58), we can express the ground-state energy E as follows:

$$E = E_0 - \frac{i}{2} \int \frac{da}{a} \sum_{\mathbf{k}} \int_C \frac{d\omega}{2\pi} \Sigma^*(\mathbf{k}, \omega) g(\mathbf{k}, \omega) , \quad (13.29)$$

where E_0 is the unperturbed ground-state energy, contour C consists of the path shown in Fig. 11.1 a and a semicircle in the upper half-plane, and Σ^* and g correspond to an interaction potential equal to $\alpha v(\mathbf{q})$. Equation (13.29) is more convenient for calculations than (11.30). Substituting (13.23) into (13.29) and expanding g in powers of the small quantity Σ^* , we obtain that

$$g\Sigma^* \simeq (\Sigma_1^* + \Sigma_{2a}^* + \Sigma_{2b}^* + \Sigma_r^*)g_0 + (\Sigma_1^*g_0)^2 , \quad (13.30)$$

where the omitted terms in (13.30) would give a contribution to E that would approach zero as $r_s \rightarrow 0$. Combining (13.29) with (13.30) and performing the integrations, we obtain for the ground-state energy

$$E = \frac{e^2 N}{2a_B} \left[\frac{2.21}{r_s^2} - \frac{0.916}{r_s} + 0.0622 \ln(r_s) - 0.094 + \dots \right] , \quad (13.30')$$

where the first term in parentheses is the unperturbed ground-state energy, the second corresponds to the first-order $g_0 \Sigma_1^*$ in (13.30), the third comes from $g_0 \Sigma_r^*$, and the fourth from the sum $g_0 (\Sigma_{2a}^* + \Sigma_{2b}^*) + (\Sigma_1^* g_0)^2$. The remaining terms approach zero as $r_s \rightarrow 0$. Equation (13.30') shows that we cannot obtain a series expansion of E in powers of r_s .

(c) *Effective interaction* $v_{e,RPA}$. Using (13.27) we have

$$v_{e,RPA} = \frac{v(\mathbf{q})}{\varepsilon_{RPA}^c(\mathbf{q})} = \frac{v(\mathbf{q})}{1 - v(\mathbf{q})\Pi_0^*(q)}, \quad (13.31)$$

which for the static case, $\omega = 0$, becomes [20]

$$v_{e,RPA} = \frac{4\pi e^2}{\mathbf{q}^2 + q_{TF}^2 f(q/k_F)}, \quad (13.32)$$

where the *Thomas–Fermi screening length*, q_{TF}^{-1} , is given by

$$q_{TF}^2 = \frac{4r_s}{\pi} \left(\frac{4}{9\pi} \right)^{1/3} k_F^2, \quad (13.33)$$

and the function $f(x)$ equals

$$f(x) = \frac{1}{2} - \frac{1}{2x} \left(1 - \frac{1}{4}x^2 \right) \ln \left| \frac{2-x}{2+x} \right|. \quad (13.34)$$

In the limit $q \rightarrow 0$, (13.32) becomes

$$v_{e,RPA}(\mathbf{q}, 0) \simeq \frac{4\pi e^2}{\mathbf{q}^2 + q_{TF}^2} \quad \text{as } q \rightarrow 0, \quad (13.35)$$

which shows clearly the effects of screening produced by the summation of the ring diagrams.

(d) *Response to an external static point charge*. From $\varepsilon^c(q)$ we can immediately obtain, with the use of (12.70) and (12.71), the retarded dielectric function $\varepsilon(q)$, which gives the following expression for the electronic charge density $\delta\rho(\mathbf{r})$ induced by a static point charge $Z|e|$ at the origin:

$$\delta\rho_r(\mathbf{r}) = -Z|e| \int \frac{d^3q}{(2\pi)^3} e^{i\mathbf{q}\cdot\mathbf{r}} \frac{q_{TF}^2 f(q/k_F)}{q^2 + q_{TF}^2 f(q/k_F)}; \quad (13.36)$$

the subscript r indicates that the ring approximation was used. Some interesting consequences of (13.36) are discussed in [20]. Here we mention that, as $r \rightarrow \infty$,

$$\delta\rho_r(\mathbf{r}) \rightarrow \frac{Z|e|}{\pi} \frac{2\xi}{(4+\xi)^2} \frac{\cos(2k_F r)}{r^3}; \quad \xi \equiv \frac{q_{TF}^2}{2k_F^2}, \quad (13.37)$$

i.e., the induced charge does not decay exponentially, as one would conclude from the approximate expression (13.35), but in an oscillating power law way. These *Friedel oscillations* [428, 429] arise from the sharp Fermi surface, which produces the singularity at $q = 2k_F$ of the function $f(q/k_F)$.

(e) *Collective (plasma) oscillations.* As was mentioned in Chap. 11, collective density oscillation modes appear as poles in the analytic continuation of $\Pi(\mathbf{k}, \omega)$ or, in view of (12.72), as zeros in the analytic continuation of $\varepsilon^c(\mathbf{k}, \omega)$ or $\varepsilon(\mathbf{k}, \omega)$. Within the RPA, $\varepsilon^c(\mathbf{k}, \omega)$ is given by (13.27), so the collective mode of the electron gas has a complex eigenfrequency $z_q = \omega_q - i\bar{\varepsilon}(\omega_q)\gamma_q$ that satisfies the equation

$$1 = v(\mathbf{q})a.c.\{\Pi_0^*(\mathbf{q}, z_q)\}. \quad (13.38)$$

Using the properties of $\Pi_0^*(\mathbf{q}, \omega)$ as $q \rightarrow 0$ and the fact that $v(\mathbf{q}) \sim q^{-2}$ as $q \rightarrow 0$, we can prove [20] that

$$z_q = \omega_q \simeq \omega_p \left[1 + \frac{9}{10} \left(\frac{q}{q_{TF}} \right)^2 \right] \quad \text{as } q \rightarrow 0, \quad (13.39)$$

where ω_p , the plasma frequency, is given by

$$\omega_p^2 = \frac{4\pi e^2 n}{m}. \quad (13.40)$$

Equation (13.39) shows that the plasma has a dispersion relation that starts from a finite value ω_p at $q = 0$ and grows quadratically with q .

Within the RPA, the lifetime $1/\gamma_q$ is exactly infinite for small q . If the RPA is relaxed, γ_q becomes different from zero for all $q \neq 0$. Note that if $v(\mathbf{q})$ were approaching a constant v as $q \rightarrow 0$, i.e., if $v(\mathbf{r})$ were of short range, then the solution of (13.38) would have a dispersion relation of the form

$$\omega_q = c_0 q \quad \text{as } q \rightarrow 0, \quad (13.41)$$

where the velocity c_0 would satisfy the equation [20]

$$1 = \frac{v_0 m k_F}{\pi^2} \left[\frac{1}{2} \frac{c_0}{v_F^0} \ln \left| \frac{c_0/v_F^0 + 1}{c_0/v_F^0 - 1} \right| - 1 - \frac{i\pi}{2} \frac{c_0}{v_F^0} \theta \left(1 - \left| \frac{c_0}{v_F^0} \right| \right) \right], \quad (13.42)$$

where $v_F^0 = k_F/m$. Equation (13.42) shows that $c_0/v_F^0 > 1$; otherwise there is no real solution. In the weak coupling limit, $v_0 m k_F \ll 1$, the solution of (13.42) is

$$c_0 \simeq v_F^0 \left[1 + 2 \exp \left(-\frac{2\pi^2}{m k_F v_0} - 2 \right) \right], \quad (13.43)$$

while in the strong coupling limit, $v_0 m k_F \gg 1$, we have

$$c_0 \simeq \sqrt{\frac{n v_0}{m}}. \quad (13.44)$$

As was mentioned in Sect. 13.1, the collective mode with the linear dispersion relation is called zero sound. For the Coulomb interaction case the collective mode is called plasmon and its dispersion is given by (13.39), i.e., it approaches a nonzero value ω_p as $q \rightarrow 0$. This nonzero ω_p implies a nonzero restoring

force as $q \rightarrow 0$, which is a result of the long-range character of the Coulomb interaction. Note that the zero sound or the plasmon dispersion is given in general as a solution of the same equation, $1 = v(\mathbf{q})a.c.\{\Pi^*(\mathbf{q}, z)\}$, which in the RPA reduces to (13.38).

13.3 Dilute Fermi Gas

In this section we examine the case of a low-density Fermi system with repulsive short-range interactions. This is a particular example of the general theory outlined in Sect. 13.1. Its interest lies in the fact that explicit results can be obtained that are of relevance to the studies of nuclear matter and He^3 .

The small parameter in this case is $k_F a$, where a is the scattering length defined by the relation

$$f(\mathbf{k}_f, \mathbf{k}) \rightarrow -a \quad \text{as} \quad k_f = k \rightarrow 0, \quad (13.45)$$

where $f(\mathbf{k}_f, \mathbf{k})$ is the scattering amplitude (Chap. 4) corresponding to the potential $v(\mathbf{r})$. Thus the theory outlined here is appropriate for either a dilute system ($k_F a \rightarrow 0$) or short-range interactions $a \rightarrow 0$. For nuclear matter $k_F a \simeq 1/3$.

Because $k_F a \rightarrow 0$, one could guess that the most important diagrams are those describing the interactions of pairs of particles to all orders. Quantitatively, this means that the vertex part Γ could be approximated by the so-called ladder diagrams shown in Fig. 13.4a. One can prove [20, 421] that the diagrams for Γ omitted in Fig. 13.4a give contributions to Σ^* of higher order in $k_F a$. This statement can be demonstrated by comparing the two diagrams for Σ^* in Fig. 13.5. Diagram a is proportional to $k_F a$, while diagram b

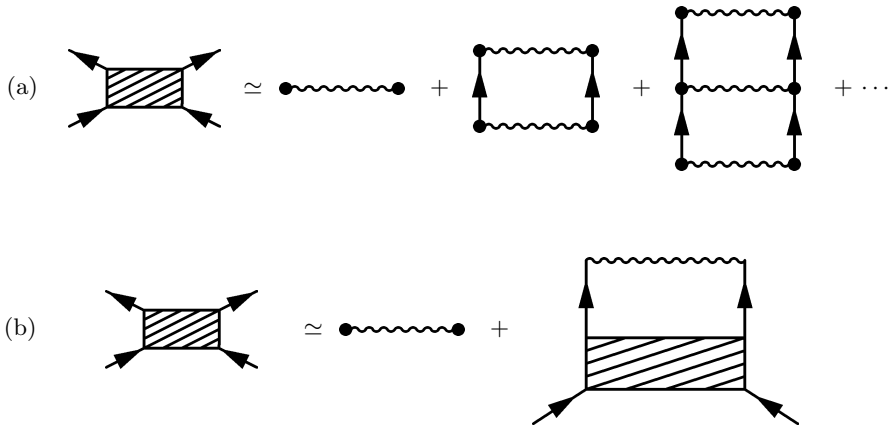


Fig. 13.4. **a** Vertex part Γ in ladder approximation. **b** Integral equation obeyed by Γ in ladder approximation

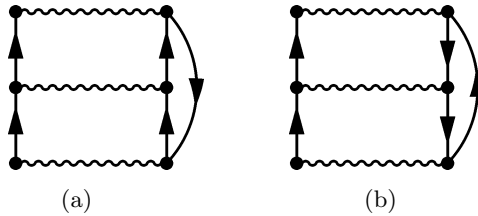


Fig. 13.5. Diagram **a** was retained in the ladder approximation, while diagram **b** was omitted

is proportional to $(k_F a)^2$; in general the power of $k_F a$ is determined by the number of reverse running g_0 -lines. It follows that the lowest order in $k_F a$ is obtained by keeping diagrams in Γ involving only parallel running g_0 -lines, i.e., by keeping the ladder diagrams. The summation of the ladder diagrams is equivalent to an integral equation for Γ , as shown in Fig. 13.4b. This integral equation is known as the ladder approximation to the *Bethe-Salpeter equation*; its kernel involves the product $v g_0 g_0$. For present purposes it is much more convenient to express the integral equation for Γ in terms of the scattering amplitude $f(\mathbf{k}_f, \mathbf{k})$, which is related to the potential $v(\mathbf{q})$ through (4.62). After some lengthy algebraic manipulations one obtains

$$\Gamma(\mathbf{p}, \mathbf{p}'; P) = \Gamma_0(\mathbf{p}, \mathbf{p}'; P) + m \int \frac{d^3 k}{(2\pi)^3} \Gamma_0(\mathbf{p}, \mathbf{k}; P) \\ \times \left[\frac{N(\mathbf{P}, \mathbf{k})}{mE - \mathbf{k}^2 + is} N(\mathbf{P}, \mathbf{k}) - \frac{1}{mE - \mathbf{k}^2 + is} \right] \Gamma(\mathbf{k}, \mathbf{p}', P), \quad (13.46)$$

with

$$\Gamma_0(\mathbf{p}, \mathbf{p}'; P) = -\frac{4\pi}{m} f(\mathbf{p}, \mathbf{p}') + \frac{(4\pi)^2}{m} \int \frac{d^3 k}{(2\pi)^3} \\ \times f(\mathbf{p}, \mathbf{k}) \left(\frac{1}{mE - \mathbf{k}^2 + is} + \frac{1}{\mathbf{k}^2 - \mathbf{p}'^2 - is} \right) f^*(\mathbf{p}', \mathbf{k}); \quad (13.47)$$

in the above equations $s \rightarrow 0^+$; the four-momentum P stands for $p_1 + p_2$; the four-momentum p stands for $(p_1 - p_2)/2 + k$ and $p' = (p_1 - p_2)/2$; $E = E_0 - \mathbf{P}^2/4m$ is the total energy of the pair in the center-of-mass frame; $E_0 = (p_1^2 + p_2^2)/2m$; $N(\mathbf{P}, \mathbf{k}) = 1(-1)$ if both $\mathbf{P}/2 \pm \mathbf{k}$ are outside (inside) the Fermi sea; $N(\mathbf{P}, \mathbf{k}) = 0$ otherwise. The quantity Γ_0 is the vertex part for two particles in the vacuum: $\Gamma \rightarrow \Gamma_0$ as $k_F \rightarrow 0$. The usefulness of (13.46) and (13.47) is that the quantity Γ is related to the observable scattering amplitude, which remains finite even for infinite potentials such as the hard-sphere potential. Equations (13.46) and (13.47) were obtained first by Galitskii [430] and Beliaev [431].

The integration over \mathbf{k} in (13.46) is essentially restricted within the Fermi sea because the integrand vanishes when both $\mathbf{P}/2 \pm \mathbf{k}$ are outside the Fermi sea. Since we are interested in energies of the order ε_F , the last term in (13.46) is of the order $m\Gamma_0 k_F \Gamma$, so that $(\Gamma - \Gamma_0)/\Gamma \sim m\Gamma_0 k_F \sim f k_F \sim k_F a$. Thus (13.46) can be solved by iteration in the present case where $k_F a \ll 1$. In the same limit only small values of \mathbf{p} , \mathbf{p}' , and \mathbf{k} are important in (13.47) for which the scattering amplitude $f(\mathbf{k}, \mathbf{k}')$ behaves as

$$f(\mathbf{k}, \mathbf{k}') = -a + ika^2 + O(k^2 a^3) ; \quad |\mathbf{k}| = |\mathbf{k}'| \rightarrow 0 . \quad (13.48)$$

Substituting (13.48) into (13.47), replacing Γ by Γ_0 in the last term of (13.46), and keeping terms of order a^2 , we obtain Γ to order a^2 . Replacing the result for Γ in the equation shown in Fig. 12.10a (with the g -lines approximated by g_0 -lines) we have the self-energy to order $(k_F a)^2$. For details the reader is referred to [20]. The final results for physical quantities are the following [20]:

$$\gamma_k = \frac{k_F^2}{2m} \frac{2}{\pi} (k_F a)^2 \left(\frac{k_F - k}{k_F} \right)^2 \bar{\varepsilon}(k_F - k) + \dots , \quad (13.49)$$

$$\mu \equiv \varepsilon_{k_F} = \frac{k_F^2}{2m} \left[1 + \frac{4}{3\pi} k_F a + \frac{4}{15\pi^2} (11 - 2 \ln 2) (k_F a)^2 + \dots \right] , \quad (13.50)$$

$$\frac{m^*}{m} = 1 + \frac{8}{15\pi^2} (7 \ln 2 - 1) (k_F a)^2 + \dots , \quad (13.51)$$

$$\langle \mathcal{H} \rangle = \frac{Nk_F^2}{2m} \left[\frac{3}{5} + \frac{2}{3\pi} k_F a + \frac{4}{35\pi^2} (11 - 2 \ln 2) (k_F a)^2 + \dots \right] . \quad (13.52)$$

The theory outlined above can be improved if in the equation shown in Fig. 13.4b the g_0 -lines are replaced by g -lines. The resulting integral equation together with the equation of Fig. 12.10a (which in view of the integral equation for Γ can be simplified as in Fig. 13.6) and the equation $g^{-1} = \omega - \varepsilon_k^0 - \Sigma^*$ form a complete set of equations. For a discussion of this improvement the reader is referred to [20].

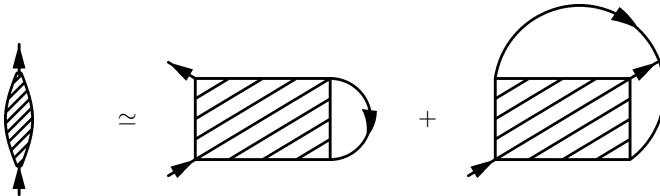


Fig. 13.6. In the self-consistent (i.e., with the g_0 -lines replaced by the g -lines) ladder approximation, Σ^* is related to Γ as shown

13.4 Superconductivity

13.4.1 Diagrammatic Approach

The ladder approximation of the previous section is a reasonable one for examining the phenomenon of superconductivity because it includes the characteristic physical process responsible for this phenomenon, i.e., the multiple scattering of two particles leading to the bound Cooper pair. Since the many-body Green's function incorporates the indistinguishability of the electrons, both the direct and the indirect processes, discussed in Chap. 6, are expected to show up automatically in the present formalism. We demonstrate here that this is indeed the case.

From Fig. 13.4 we see that the structure of the ladder approximation to the vertex part is of the form

$$T = -v - vGGT. \quad (13.53)$$

We have used the symbol T instead of Γ in order to stress the analogy with the t -matrix in one-body Green's function formalism. Referring to Fig. 13.4b, we denote by p the sum $p_1 + p_2$ and by s the difference $(p_1 - p_2)/2$, so that $p_1 = s + (p/2)$ and $p_2 = -s + (p/2)$, where $p \equiv (z, \mathbf{p})$, $s = (i\omega_n, \mathbf{s})$, $z = 2\mu + 2\text{Im}\{z\}$, and $i\omega_n = i\pi(2n - 1)/\beta$. Similarly, $p_1 + k$ is denoted by $s' + (p/2)$, $p_2 - k$ by $-s' + (p/2)$, $p_1 + k - q$ by $\bar{s} + (p/2)$, and $p_2 - k + q$ by $-\bar{s} + (p/2)$. Notice that, when p_1, p_2 corresponds to the same spin direction (e.g., both up), then within the ladder approximation both diagrams of Fig. 13.6 contribute to the proper self-energy. In contrast, when p_1 and p_2 are associated with opposite spins, only the first diagram of the rhs in Fig. 13.6 contributes to Σ^* . Furthermore, if the interaction v is proportional to a δ -function in real space [and, consequently, a constant in \mathbf{k} -space, for $|\varepsilon(k) - \mu| < \omega_D$], then for parallel spins the two diagrams in Fig. 13.6 exactly cancel each other (within the ladder approximation). This is physically obvious, since two electrons with parallel spins cannot be at the same point in space and thus they give no chance to the δ -function interaction to act. Two more remarks: for the purpose of calculating Σ^* in the framework of the diagrams in Fig. 13.4 and the first diagram in Fig. 13.6, we must put $p_2 - k = p_2$, or $s' = s$; then the presence of a δ -function interaction makes T depend only on p .

Taking into account the points above and the rules III' to VI' in Sect. 12.3 we can write (13.53) more explicitly as follows:

$$T(p) \left[1 + v \int \frac{d^3\bar{s}}{(2\pi)^3} \frac{1}{\beta} \sum_{\bar{n}} G\left(\bar{s} + \frac{p}{2}\right) G\left(-\bar{s} + \frac{p}{2}\right) \right] = -v. \quad (13.54)$$

To proceed further we shall replace the dressed propagators by the bare ones in the summation over \bar{n} :

$$\begin{aligned} & \frac{1}{\beta} \sum_{\bar{n}} G_0 \left(\bar{s} + \frac{p}{2} \right) G_0 \left(-\bar{s} + \frac{p}{2} \right) \\ &= \frac{1}{\beta} \sum_n \frac{1}{i\omega_n + (z/2) - \varepsilon_1} \frac{1}{-i\omega_n + (z/2) - \varepsilon_2}, \end{aligned} \quad (13.55)$$

where we have replaced the dummy index \bar{n} by n , and we set

$$\varepsilon_1 = \varepsilon_0 \left(\left| \bar{s} + \frac{p}{2} \right| \right) \quad \text{and} \quad \varepsilon_2 = \varepsilon_0 \left(\left| -\bar{s} + \frac{p}{2} \right| \right).$$

To perform the summation over n in (13.55) we write

$$\begin{aligned} & \frac{1}{i\omega_n + (z/2) - \varepsilon_1} \times \frac{1}{-i\omega_n + (z/2) - \varepsilon_2} \\ &= -\frac{1}{z - \varepsilon_1 - \varepsilon_2} \left[\frac{1}{i\omega_n - (z/2) + \varepsilon_2} - \frac{1}{i\omega_n + (z/2) - \varepsilon_1} \right]; \end{aligned} \quad (13.56)$$

then, according to (11.53), we have

$$\frac{1}{\beta} \sum_n \frac{1}{i\omega_n - (z/2) + \varepsilon_2} = \frac{1}{\exp[\beta(\mu - \varepsilon_2)] + 1}, \quad (13.57a)$$

$$\frac{1}{\beta} \sum_n \frac{1}{i\omega_n + (z/2) - \varepsilon_1} = \frac{1}{\exp[\beta(\varepsilon_1 - \mu)] + 1}. \quad (13.57b)$$

In (13.57a) and (13.57b) we have taken the limit $\text{Im}\{z\} = 0$ so that $z/2 = \mu$. As was discussed in Chap. 6 and can be verified by performing the integral in (13.54) numerically, the most favorable condition for the blowing up of $T(p)$ occurs when $p = 0$; in this case, $\varepsilon_1 = \varepsilon_2 = \varepsilon$, and (13.55) in view of (13.57a) and (13.57b) becomes

$$\frac{1}{\beta} \sum_{\bar{n}} G_0 \left(\bar{s} + \frac{p}{2} \right) G_0 \left(-\bar{s} + \frac{p}{2} \right) = -\frac{1 - 2f(\varepsilon)}{z - 2\varepsilon}, \quad (13.58)$$

where $f(\varepsilon) = [e^{\beta(\varepsilon - \mu)} + 1]^{-1}$ is the Fermi distribution.

The integration over $d^3\bar{s}$ can be transformed to an integration over $d\varepsilon$ times the DOS at E_F , ϱ_F , which can be taken out of the integral. Thus, the denominator of $T(p)$ becomes

$$1 - v\varrho_F \int_{\mu - \omega_D}^{\mu + \omega_D} d\varepsilon \frac{1 - 2f(\varepsilon)}{z - 2\varepsilon}. \quad (13.59)$$

By setting $z = E$ and $\varepsilon = E'/2$, the integral in (13.59) becomes identical to the one in (6.65), which was calculated for $E = 2\mu \simeq 2E_F$ in (6.67) and turned out to be negative. Thus the quantity T blows up only for negative v (i.e., for attractive interaction), signaling the creation of a bound state, i.e., the creation of a Cooper pair. The critical temperature is given by (6.68), where $\lambda = \varrho_F |v|$ ($|v|$ has dimensions of energy times volume).

13.4.2 Equation of Motion Approach

This approach is based on imaginary time Green's functions and on a factorization of g_2 in the spirit of the Hartree–Fock approximation, but with a crucial addition:

$$g_2(x_1, x_2; x'_1, x'_2) \simeq g(x_1, x'_1)g(x_2, x'_2) - g(x_1, x'_2)g(x_2, x'_1) + \langle T(\psi(x_1)\psi(x_2)) \rangle \langle T(\psi^\dagger(x'_1)\psi^\dagger(x'_2)) \rangle, \quad (13.60)$$

where $x_1, x_2, x'_1,$ and x'_2 are condensed notations for $(\mathbf{r}_1, -i\sigma_1, s_1), (\mathbf{r}_2, -i\sigma_2, s_2), (\mathbf{r}'_1, -i\sigma'_1, s'_1),$ and $(\mathbf{r}'_2, -i\sigma'_2, s'_2),$ respectively, and $s_1, s_2, s'_1,$ and s'_2 are spin indices taking values up or down. The last term in (13.60) describes the propagation of two holes and two particles. It was added for physical reasons in order to incorporate in the formalism the possibility of Cooper pairs and in the hope that the resulting theory will provide a self-consistent way for the formation of Cooper pairs as well as their properties.

One may argue that the last term in (13.60) is automatically zero; this is certainly true for a particle-conserving Hamiltonian. However, the factorization of the interaction part, $V_i,$ of the Hamiltonian,

$$V_i = \frac{1}{2} \int d^3r d^3r' v(\mathbf{r} - \mathbf{r}') \psi_s^\dagger(\mathbf{r}) \psi_{s'}^\dagger(\mathbf{r}') \psi_{s'}(\mathbf{r}') \psi_s(\mathbf{r}), \quad (13.61)$$

consistent with (13.60), will render V_i in a particle-nonconserving form:

$$V_i \simeq V_{iHF} + \int d^3r d^3r' v(\mathbf{r} - \mathbf{r}') \left[\langle \psi_\downarrow^\dagger(\mathbf{r}) \psi_\uparrow^\dagger(\mathbf{r}') \rangle \psi_\uparrow(\mathbf{r}') \psi_\downarrow(\mathbf{r}) + \langle \psi_\uparrow(\mathbf{r}') \psi_\downarrow(\mathbf{r}) \rangle \psi_\downarrow^\dagger(\mathbf{r}) \psi_\uparrow^\dagger(\mathbf{r}') \right], \quad (13.62)$$

which allows the possibility of nonzero $\langle T(\psi(x_1)\psi(x_2)) \rangle$ and $\langle T(\psi^\dagger(x'_1)\psi^\dagger(x'_2)) \rangle.$ The choice of spin indices in (13.62) reflects the fact that electrons in the Cooper pairs have opposite spins. The same choice of spin indices must be made in (13.60), where the imaginary time evolution of the operators is determined by the Hamiltonian $\mathcal{H} = \mathcal{H}_0 + V_i,$ where \mathcal{H}_0 is the kinetic energy and V_i is replaced by the rhs of (13.62). Actually, for simplicity we shall omit V_{iHF} and in explicit calculations we shall choose

$$v(\mathbf{r} - \mathbf{r}') = -|v| \delta(\mathbf{r} - \mathbf{r}'). \quad (13.63)$$

Note that the average value

$$\langle A(\sigma) \rangle = \frac{\text{Tr} \{ e^{-\beta(\mathcal{H} - \mu N)} e^{\sigma \mathcal{H}} A e^{-\sigma \mathcal{H}} \}}{\text{Tr} \{ e^{-\beta(\mathcal{H} - \mu N)} \}}$$

of any Heisenberg time-dependent operator remains invariant if $\sigma \mathcal{H}$ is replaced by $\sigma(\mathcal{H} - \mu N).$ This follows from the invariance of the trace in cyclic permutations (when \mathcal{H} and N commute), and by the fact that $\mu = 0,$ when \mathcal{H} and N do not commute. Thus, in calculating thermal averages, we can use for the time evolution either \mathcal{H} or $\mathcal{H} - \mu N.$ However, it is imperative to use $\mathcal{H} - \mu N$

instead of \mathcal{H} , in the case where \mathcal{H} and N commute, but \mathcal{H} has been replaced by a particle-nonconserving approximation, as in (13.62). The advantage of $\mathcal{H} - \mu N$, besides letting us attribute the nonconservation to particle exchange with a bath of chemical potential μ , is that it allows us to have a nonzero μ , defined by $\mu = (\partial F / \partial \bar{N})_{T,V}$ (where \bar{N} is the average number of particles within the grand canonical ensemble) despite the approximate nonconservation of particles. Henceforth we shall use $\mathcal{H} - \mu N$ for the time development of Heisenberg operators. As a result of this change, all single-particle energies, $\varepsilon_k \rightarrow \xi_k = \varepsilon_k - \mu$ and $z_n \rightarrow i\omega_n = z_n - \mu$ and $\omega_n = \pi(2n - 1)/\beta$.

The factorization (13.60) forces us to introduce two new closely related Green's functions

$$f(x, x') \equiv - \left\langle T \left[\psi_{\uparrow}(x) \psi_{\downarrow}(x') \right] \right\rangle, \quad (13.64a)$$

$$f^{\dagger}(x, x') \equiv - \left\langle T \left[\psi_{\downarrow}^{\dagger}(x) \psi_{\uparrow}^{\dagger}(x') \right] \right\rangle. \quad (13.64b)$$

Combining (12.1) (with $t \rightarrow -i\sigma$, etc.), (13.60), (13.62), and (13.63) with the approximation $V_{iHF} = 0$, we find the following equation for the time evolution of g :

$$\left(-\frac{\partial}{\partial \sigma} + \frac{1}{2m} \nabla^2 + \mu \right) g(x, x') = i\delta(\mathbf{r} - \mathbf{r}') \delta(\sigma - \sigma') \\ + i|v| \langle \psi_{\uparrow}(\mathbf{r}) \psi_{\downarrow}(\mathbf{r}) \rangle f^{\dagger}(x, x'). \quad (13.65)$$

It is clear from (13.65) that we need to find an equation for the time evolution of the new Green's function $f^{\dagger}(x, x')$. This can be achieved by employing the general time evolution equations, $\partial\psi/\partial\sigma = [\mathcal{H} - \mu N, \psi]$ and $\partial\psi^{\dagger}/\partial\sigma = [\mathcal{H} - \mu N, \psi^{\dagger}]$, and the approximate form of \mathcal{H} together with the definitions (13.64a) and (13.64b). We find

$$\left(-\frac{\partial}{\partial \sigma} + \frac{1}{2m} \nabla^2 + \mu \right) f(x, x') = -i\Delta(\mathbf{r}) g(x', x), \quad (13.66a)$$

$$\left(\frac{\partial}{\partial \sigma} + \frac{1}{2m} \nabla^2 + \mu \right) f^{\dagger}(x, x') = -i\Delta^*(\mathbf{r}) g(x, x'), \quad (13.66b)$$

where the so-called gap, $\Delta(\mathbf{r})$, is by definition

$$\Delta(\mathbf{r}) \equiv |v| \langle \psi_{\downarrow}(\mathbf{r}) \psi_{\uparrow}(\mathbf{r}) \rangle = -|v| \langle \psi_{\uparrow}(\mathbf{r}) \psi_{\downarrow}(\mathbf{r}) \rangle \equiv |v| f(x^+, x). \quad (13.67)$$

For a time and space translationally invariant system, it is convenient to use Fourier transforms with respect to the difference $x - x'$. Then, taking into account (12.9)–(12.11) and

$$f^{\dagger}(x, x') = \int \frac{d^3k}{(2\pi)^3} e^{i\mathbf{k} \cdot (\mathbf{r} - \mathbf{r}')} \frac{1}{\beta} \sum_n e^{-i\omega_n(\sigma - \sigma')} F^{\dagger}(\mathbf{k}, z_n), \quad (13.68)$$

$$\Delta^* = |v| f^{\dagger}(x^+ - x) \\ = \frac{|v|}{\beta} \sum_n e^{-i\omega_n s} F^{\dagger}(\mathbf{r} - \mathbf{r}' = 0, i\omega_n) \text{ as } s \rightarrow 0^+, \quad (13.69)$$

we obtain from (13.65) and (13.66b) the following pair of equations:

$$(i\omega_n - \xi_k) G(\mathbf{k}, i\omega_n) + \Delta F^\dagger(\mathbf{k}, i\omega_n) = 1, \quad (13.70a)$$

$$(-i\omega_n - \xi_k) F^\dagger(\mathbf{k}, i\omega_n) - \Delta^* G(\mathbf{k}, i\omega_n) = 0, \quad (13.70b)$$

where $\xi_k = (k^2/2m) - \mu$ and $\omega_n = \pi(2n - 1)/\beta$. The solution of (13.70a) and (13.70b) is

$$G(\mathbf{k}, i\omega_n) = \frac{u_k^2}{i\omega_n - E_k} + \frac{v_k^2}{i\omega_n + E_k}, \quad (13.71a)$$

$$F(\mathbf{k}, i\omega_n) = F^\dagger(\mathbf{k}, i\omega_n) = -u_k v_k \left(\frac{1}{i\omega_n - E_k} - \frac{1}{i\omega_n + E_k} \right), \quad (13.71b)$$

where

$$E_k = \sqrt{\Delta^2 + \xi_k^2}, \quad (13.72)$$

$$u_k v_k = \frac{\Delta}{2E_k}, \quad (13.73)$$

$$v_k^2 = 1 - u_k^2 = \frac{1}{2} \left(1 - \frac{\xi_k}{E_k} \right). \quad (13.74)$$

We have assumed, without loss of generality, that Δ is real.

It remains to use the definitions of Δ , (13.67), and (13.69) and the solution (13.71b) to find an equation that determines the gap Δ :

$$\Delta = \frac{|v|}{\beta} \sum_n \int \frac{d^3k}{(2\pi)^3} \frac{\Delta}{\omega_n^2 + E_k^2}$$

or

$$1 = \frac{|v|}{\beta} \sum_n \int \frac{d^3k}{(2\pi)^3} \frac{1}{\omega_n^2 + E_k^2}. \quad (13.75)$$

The series has been summed already [see (13.55) and (13.58) and set $z = 0$] and gives

$$\sum_n \frac{1}{\beta} \frac{1}{(\omega_n^2 + E_k^2)} = \frac{1}{2E_k} \tanh \left(\frac{\beta E_k}{2} \right),$$

while the integration over d^3k can be transformed to an integration over $d\xi$ times the DOS per unit volume at the Fermi level. Thus

$$1 = |v| \varrho_F \int_0^{\omega_D} \frac{d\xi}{\sqrt{\xi^2 + \Delta^2}} \tanh \left(\frac{\sqrt{\xi^2 + \Delta^2}}{2k_B T} \right). \quad (13.76)$$

Equation (13.76) allows us to determine the gap as a function of temperature. It turns out that $\Delta \neq 0$ for $T < T_c$ and $\Delta = 0$ for $T \geq T_c$. In particular, for $T = 0$ we find that

$$\Delta(0) = 2\omega_D e^{-1/\lambda}, \quad \lambda = |v| \varrho_F. \quad (13.77)$$

The critical temperature, T_c , is determined by letting $\Delta \rightarrow 0^+$ in (13.76). We find as before

$$k_B T_c = \frac{2e^\gamma}{\pi} \omega_D e^{-1/\lambda}. \quad (13.78)$$

Many other quantities of physical interest may be obtained by employing (13.71), (13.72)–(13.74), and (13.76). For details see, e.g., the book by Fetter and Walecka [20].

13.5 The Hubbard Model

The Hubbard model, within the LCAO framework, is as important as the interacting electrons [see (13.16)] within the jellium framework. Actually, it is richer, since it incorporates the discrete nature of the solid-state structure and is amenable to several generalizations so as to incorporate essential features characterizing various groups of materials.

In its simplest form, the Hubbard model is described by the following Hamiltonian:

$$\mathcal{H} = \sum_{i\sigma} V_{ij} a_{i\sigma}^\dagger a_{j\sigma} + U \sum_i n_{i\uparrow} n_{i\downarrow}. \quad (13.79)$$

The first term on the rhs of (13.79) is the usual TBH with one state per site; $a_{i\sigma}^\dagger$ creates a particle at state $|i\rangle$ with spin σ ($\sigma = \uparrow$ or \downarrow); $a_{j\sigma}$ destroys a particle with spin σ at the state $|j\rangle$. The last term in the rhs of (13.79) describes the on-site interaction of strength U , when two particles of opposite spin are on the same state $|i\rangle$. Usually, we assume for simplicity that $V_{ij} = V_{ji} = V$ when i, j nearest neighbors, and zero otherwise; furthermore, we shall take $U > 0$, i.e., repulsive interaction.

The most important parameter in the Hamiltonian (13.79) is the ratio $U/|V|$, which determines the relative weight of the two competing aspects incorporated in this model: U , the strength of the repulsive potential energy, which tells the particles to avoid each other as much as possible; and $|V|$, the strength of the kinetic energy, which favors the spreading of the particles over all sites of the system. Important factors in determining the outcome of this competition of conflicting tendencies are the number of particles per state, ζ , and the dimensionality, d , of the system. Depending on the values of $U/|V|$, ζ , and the dimensionality d , the system may exhibit magnetic ordering and/or undergo a metal-insulator transition. Thus, a phase diagram in the ζ - $U/|V|$ plane has to be constructed [392, 432–440].

Several generalizations of the simple Hubbard model can be achieved by adding more terms in the Hamiltonian (13.79) or by having more than one orbital per site. These generalizations seem to be necessary for allowing the appearance of important physical phenomena such as ferromagnetism. For example, we can add to (13.79) additional interactions, \mathcal{H}_1 , of the form

$$\begin{aligned}
\mathcal{H}_1 &= \frac{1}{2} \sum_{i \neq j} U_{j-i} n_i n_j + \frac{1}{2} \sum_{i \neq j} \sum_{\sigma \sigma'} J_{j-i} a_{i\sigma}^\dagger a_{j\sigma'}^\dagger a_{i\sigma'} a_{j\sigma} \\
&= \frac{1}{2} \sum_{i \neq j} \left(U_{j-i} - \frac{1}{2} J_{j-i} \right) n_i n_j - \sum_{i \neq j} J_{j-i} \mathbf{s}_i \cdot \mathbf{s}_j, \quad (13.80)
\end{aligned}$$

where $n_i = a_{i\uparrow}^\dagger a_{i\uparrow} + a_{i\downarrow}^\dagger a_{i\downarrow}$ and $2\mathbf{s}_i \mathbf{s}_j = 2s_{iz}s_{jz} + s_{i+}s_{j-} + s_{i-}s_{j+}$. The last term in (13.80), known as the *Heisenberg model*, favors ferromagnetic ordering for $J_{j-i} > 0$ and antiferromagnetic ordering for J_{j-i} negative between nearest neighbors and zero otherwise.

Returning now to the simple Hubbard model, (13.79), one can show that for $\zeta = 1$ and in the limit $U/|V| \rightarrow \infty$, it is equivalent to

$$\mathcal{H}' = \frac{2V^2}{U} \left(\sum'_{i \neq j} \mathbf{s}_i \cdot \mathbf{s}_j - \frac{N_s Z}{4} \right), \quad (13.81)$$

where the prime in the summation denotes restriction to the Z nearest neighbors only and N_s is the total number of sites. Equation (13.81) shows clearly that the simple Hubbard model is capable (at least in this limit) of creating magnetic ordering.

Within the Hartree approximation, the Green's function for the simple Hubbard model can be obtained by replacing the last term in (13.79) by $\sum_{i\sigma} \varepsilon_{i\sigma} n_{i\sigma}$, where self-consistency requires that

$$\varepsilon_{i\sigma} = U \langle n_{i\sigma'} \rangle, \quad (13.82)$$

where σ' is opposite to σ . Three of the possible choices for $\langle n_{i\sigma} \rangle$ are shown schematically in Fig. 13.7 and given below:

Case (a)

$$\langle n_{i\sigma} \rangle = \frac{1}{2} \zeta, \quad (13.83)$$

Case (b)

$$\langle n_{i\sigma} \rangle = \begin{cases} \frac{1}{2}(\zeta + \mu), & \sigma = \uparrow \\ \frac{1}{2}(\zeta - \mu), & \sigma = \downarrow \end{cases}, \quad (13.84)$$

Case (c)

$$\langle n_{i\sigma} \rangle = \begin{cases} \frac{1}{2}(\zeta + \mu), & \sigma = \uparrow, \text{ sublattice A or } \sigma = \downarrow, \text{ sublattice B,} \\ \frac{1}{2}(\zeta - \mu), & \sigma = \downarrow, \text{ sublattice A or } \sigma = \uparrow, \text{ sublattice B.} \end{cases} \quad (13.85)$$

Using the techniques of Chap. 5, we determine the diagonal matrix elements of the one-particle Green's functions for each of the three phases:

$$G_{i\sigma}^\dagger(E) = \lim_{s \rightarrow 0^+} \left\langle i \left| \frac{1}{E + is - \mathcal{H}_\sigma} \right| i \right\rangle, \quad (13.86)$$

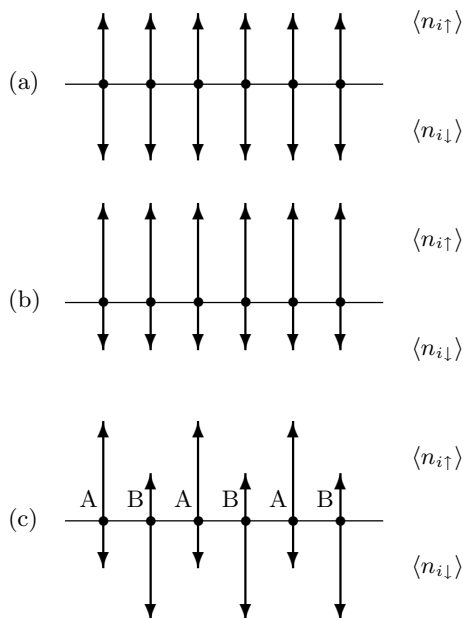


Fig. 13.7. Schematic representation of three possible choices for $\langle n_{i\uparrow} \rangle$ and $\langle n_{i\downarrow} \rangle$ within the Hartree approximation to the Hubbard model: **a** nonmagnetic fully symmetric phase, **b** ferromagnetic phase, **c** antiferromagnetic phase

where

$$\mathcal{H}_\sigma = \sum_i \varepsilon_{i\sigma} n_{i\sigma} + V \sum_{i \neq j}' a_{i\sigma}^\dagger a_{j\sigma} = \sum_i |i\sigma\rangle \varepsilon_{i\sigma} \langle i\sigma| + V \sum_{i \neq j}' |i\sigma\rangle \langle j\sigma|, \quad (13.87)$$

as well as the DOS per site

$$\varrho_{i\sigma}(E) = -\frac{1}{\pi} \text{Im} \{G_{i\sigma}(E)\}. \quad (13.88)$$

The number of electrons per site is given by

$$\zeta = \int^{E_F} dE \varrho_{i\uparrow}(E) + \int^{E_F} dE \varrho_{i\downarrow}(E), \quad (13.89)$$

and the local magnetic moment, μ , [for cases (b) and (c)]

$$\mu = |\langle n_{i\uparrow} \rangle - \langle n_{i\downarrow} \rangle| = \left| \int^{E_F} dE \varrho_{i\uparrow}(E) - \int^{E_F} dE \varrho_{i\downarrow}(E) \right|. \quad (13.90)$$

Equations (13.89) and (13.90) determine self-consistently the two unknowns, E_F and μ [in case (a) μ is identically zero]. Equation (11.30) [with $k^2/2m$

replaced by $\varepsilon_\sigma(\mathbf{k})$, the eigenvalues of \mathcal{H}_σ] yields for the average energy in the present case

$$\frac{\langle \mathcal{H} \rangle}{N_s} = \sum_\sigma \int_\sigma^{E_F} dE \varrho_{i\sigma}(E) E - \frac{U}{4} (\zeta^2 - \mu^2), \quad (13.91)$$

where the last term on the rhs of (13.91) corrects for the double counting of the interaction term present in both \mathcal{H}_\uparrow and \mathcal{H}_\downarrow .

For a given value of $U/|V|$ and ζ , the phase with the lowest value of $\langle \mathcal{H} \rangle$ is the preferable one among the three, but not necessarily the ground state. This is because a better approximation than the Hartree may change the ordering (e.g., it may make $\langle \mathcal{H} \rangle_{\text{ferromagnetic}}$ always larger than the minimum between the other two); furthermore, other, more complicated, configurations may have lower energy than those shown in Fig. 13.7 at least in some regions of the ζ - $U/|V|$ plane [432, 433, 441].

The model allows us to calculate the value of the magnetic couplings J_{j-i} (in the magnetic phases) by reversing one or two local moments and computing the resulting change in energy [439]. For example, if J_{j-i} is different from zero for nearest neighbors only, J is given by

$$|J| = \left| \frac{\delta \langle \mathcal{H} \rangle}{Z} \right|, \quad (13.92)$$

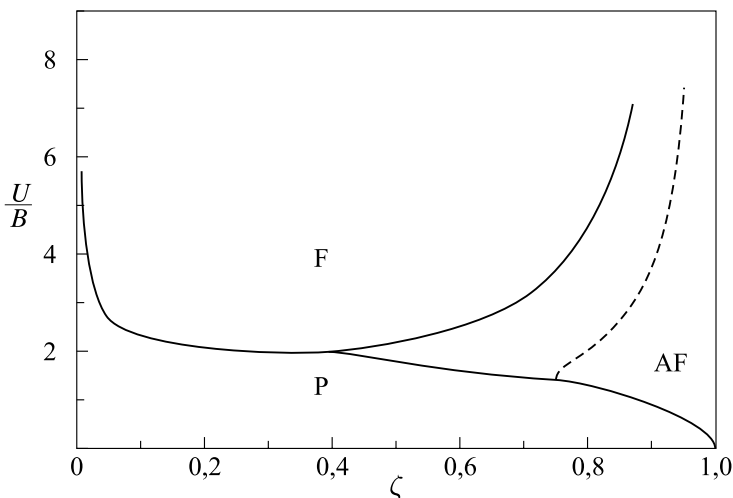


Fig. 13.8. Phase diagram for the 3-d simple Hubbard model in the Hartree approximation showing the regions where the nonmagnetic (**P**), the antiferromagnetic, (**AF**) and the ferromagnetic (**F**) phases have the lowest energy. In the F phase, $\mu = \zeta$; the exact solution is expected to shrink the F region probably until it disappears completely. B is half the bandwidth in the P phase. The results are the same for ζ and $2 - \zeta$

where $\delta \langle \mathcal{H} \rangle = \langle \mathcal{H}_r \rangle - \langle \mathcal{H} \rangle$, $\mathcal{H}_r = \mathcal{H}_{\uparrow r} + \mathcal{H}_{\downarrow r}$, and the subscript r indicates the sign reversal of a single moment, which creates a single impurity of strength $|\varepsilon| = U |\langle n_{i\uparrow} \rangle - \langle n_{i\downarrow} \rangle|$ in both $\mathcal{H}_{\uparrow r}$ and $\mathcal{H}_{\downarrow r}$. $\langle \mathcal{H}_r \rangle$ can be calculated using the formalism of Chap. 6.

The reader may verify the results [434, 440] of the Hartree approximation shown in Figs. 13.8–13.10 by following the procedures outlined in this section.

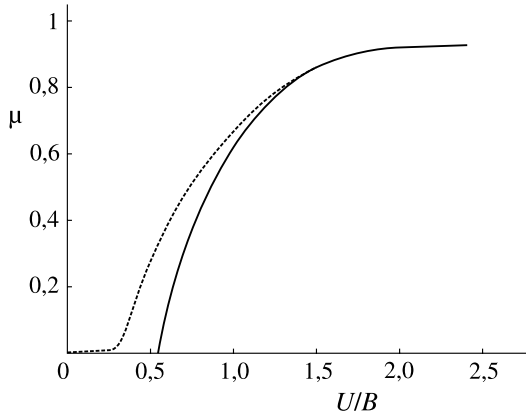


Fig. 13.9. The magnetic moment per site (in units of μ_B) vs. U/B ($B = Z|V|$) for the AF phase of the Hubbard model and for $\zeta = 1$ within the framework of the Hartree approximation. *Solid line:* simple cubic lattice; *dotted line:* Bethe lattice Green's function

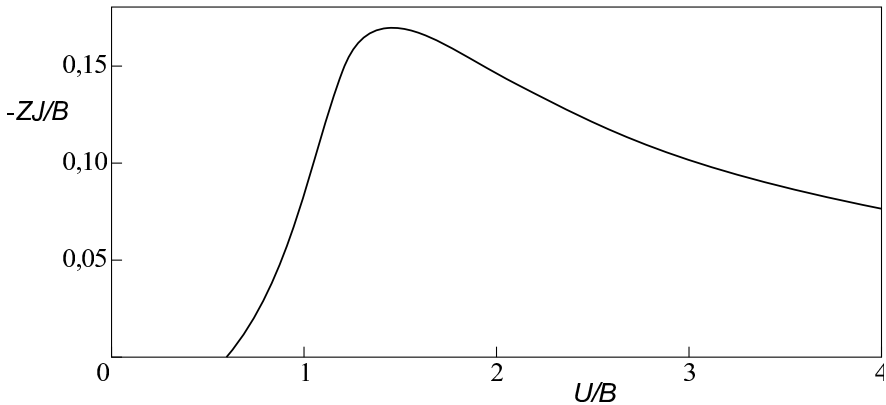


Fig. 13.10. Value of J (as defined in $-J \sum' s_i \cdot s_j$) vs. U/B ($B = Z|V|$) for AF phase of Hubbard model and for $\zeta = 1$ (for Hartree approximation). For large values of U/B , $J \rightarrow -2V^2/U$, in accordance with (13.81)

13.6 Summary

We first outlined the proof that the normal state of a Fermi system is a consistent solution of the equations, and it goes continuously to the free-particle state as the interactions are turned off. Thus, if the actual state of the interacting system develops in a continuous way as the interactions are turned on, the system is normal, i.e., it has a well-defined Fermi surface determined from the equation

$$\varepsilon_{k_F} = \mu ,$$

where ε_k is the quasiparticle energy. Moreover, the quasiparticle lifetime approaches infinity as $(k - k_F)^{-2}$ in the limit $k \rightarrow k_F$; and each quasiparticle is in one-to-one correspondence with the real particles.

We then indicated how the Green's function formalism can be used to justify Landau's theory. The most important results are: (1) The Fermi momentum k_F (as defined above) satisfies the simple equation (taking into account the two directions of spin)

$$2 \frac{4\pi}{3} \frac{k_F^3}{(2\pi)^3} = \frac{N}{\Omega} . \quad (13.11)$$

(2) The effective mass m^* defined by the equation

$$m^* = \frac{k_F}{|\partial\varepsilon_k/\partial k|_{k=k_F}} \quad (13.9)$$

is related to the bare mass m as follows:

$$\frac{1}{m^*} = \frac{1}{m} - \frac{k_F w_{k_F}^2}{2(2\pi)^3} \int \Gamma^\omega(p_1, p_2) \cos\theta d\mathcal{O} , \quad (13.12)$$

where Γ^ω is a limiting value of the vertex part. (3) There are also collective excitations (such as zero sound) in an interacting Fermi system with an acousticlike dispersion relation that is given by the poles of the vertex part Γ or the poles of the polarization part Π . The above results are quite important because they provide (for normal Fermi systems) a justification for the one-body approximation, which is widely used in solid-state and nuclear physics. Moreover, they give corrections and refinements; they also clarify the conditions under which the one-body approximation is valid.

We also examined four important specific examples for which explicit results were obtained:

- 1) The high-density electron gas moving in a uniform positive background. This is a normal Fermi system that approximates electrons in a metal. It exhibits some peculiarities associated with the long-range character of the Coulomb interaction; the most important consequence of this feature is that the collective excitation, which is called plasmon, has a dispersion relation of the form

$$\omega_q^2 = \omega_p^2 + Aq^2 \text{ as } q \rightarrow 0 . \quad (13.39)$$

- 2) A low-density Fermi system with short-range repulsive interactions. Explicit results for quasiparticles and ground-state energy were obtained; these results are applicable to nuclear matter and with appropriate refinements to liquid He³.
- 3) We revisited the problem of superconductivity within the framework of the diagrammatic approach and the equation of motion approach to the many-body Green's functions. The first approach confirms the results of §6.3.2 without the hand-waving physical arguments employed there. The second approach provides a full solution to the Green's function – and, hence, to the calculation of thermodynamic quantities of the superconducting state – through the gap function $\Delta(T)$ given by

$$1 = |v| \varrho_F \int_0^{\omega_D} \frac{d\xi}{\sqrt{\xi^2 + \Delta^2}} \tanh\left(\frac{\sqrt{\xi^2 + \Delta^2}}{2k_B T}\right). \quad (13.76)$$

- 4) The Hubbard model, which in its simpler form has the following Hamiltonian:

$$\mathcal{H} = \sum_{i\sigma} V_{ij} a_{i\sigma}^\dagger a_{j\sigma} + U \sum_i n_{i\uparrow} n_{i\downarrow}, \quad (13.79)$$

where usually $V_{ij} = V$ for nearest neighbors and zero otherwise. This model incorporates the essential competition between the spreading of the electrons throughout the system on the one hand and the requirement of avoiding double occupation of the same state $|i\rangle$ on the other. As a result of this, the model is capable of describing many-body-driven metal-insulator transitions as well as magnetic phases. For one electron per site and $U/|V| \rightarrow \infty$, the Hamiltonian (13.79) reduces to a Heisenberg type Hamiltonian

$$\mathcal{H} = - \sum_{i \neq j} J_{ij} \mathbf{s}_i \cdot \mathbf{s}_j + \text{const.} \quad (13.93)$$

with J given by

$$J = -\frac{2V^2}{U} \quad (13.94)$$

for nearest neighbors and zero otherwise.

We mention finally that the Green's function formalism is very useful in describing effects due to interactions among other elementary excitations in solids such as phonons and magnons as well as interactions of these excitations with electrons.

Further Reading

The material of Sects. 13.1, 13.2, 13.3, and 13.4.2 is presented in detail in the classic books on many-body theory such as those by Fetter and Walecka [20],

Mahan [114], and Abrikosov et al. [113]. The ladder approximation to the vertex part is treated also in the last chapter of the Kadanoff and Baym book [420]. Some relevant material can be found in solid-state books [30, 133].

The Hubbard model and the related subjects of magnetism and metal-insulator transitions are presented in several books, e.g., the books by Mott [442], Enz [134], Auerbach [443], Montorsi [444], Mattis [441], etc.

Problems

13.1. Consider the process $\mathbf{k}_1, \mathbf{k}_2 \rightarrow \mathbf{k}_3, \mathbf{k}_4$, where $k_1 > k_F, k_2 < k_F, k_3 > k_F, k_4 > k_F$. We have that $|k_i - k_F|/k_F \ll 1$, ($i = 1, \dots, 4$). Show that the available phase space for this process is proportional to $(k_1 - k_F)^2$. Conclude from this that $\text{Im}\{\Sigma^*(\mathbf{k}, \omega)\} \sim (\omega - \mu)^2$.

Hint: See [113], p. 17.

13.2. Calculate the quantity Π_0^* given by (13.18).

Hint: See [20], pp. 281–282.

13.3. Show that the specific heat for an *electron gas* within the Hartree–Fock approximation behaves like $-T/\ln T$ as $T \rightarrow 0$ while experimentally is proportional to T in this limit.

Hint: Consider the thermodynamic potential $-P\Omega = -k_B T \ln Z_G$ as given by (11.37); take into account that

$$d(P\Omega) = SdT + PdV + Nd\mu.$$

(See also [20], pp. 261–267; do not forget that we are dealing with a jellium model with long-range forces between the electrons and no screening.)

13.4. Prove that the finite temperature dielectric function, $\varepsilon_{\text{RPA}}(\mathbf{q}, \omega)$, can be brought to the form

$$\varepsilon_{\text{RPA}}(\mathbf{q}, \omega) = 1 - \frac{8\pi e^2}{q^2} \int \frac{d^3k}{(2\pi)^3} \frac{f(\varepsilon_{\mathbf{k}}) - f(\varepsilon_{\mathbf{k}+\mathbf{q}})}{\omega + i\delta - \varepsilon_{\mathbf{k}+\mathbf{q}} + \varepsilon_{\mathbf{k}}}.$$

13.5s. Prove (13.37).

13.6. Starting from the following expression for the thermodynamic potential $-P\Omega$

$$-P\Omega = 2k_B T \sum_{\mathbf{k}} \ln[1 - f(E_{\mathbf{k}})] + \sum_{\mathbf{k}} [\xi_{\mathbf{k}} - E_{\mathbf{k}}] v_{\mathbf{k}}^2 - \Delta^2 \sum_{\mathbf{k}} \frac{1}{E_{\mathbf{k}}},$$

show that the specific heat, C_V , of the superconducting state is given by

$$C_V = -\frac{2\varrho_F}{T} \int_{-\infty}^{\infty} d\varepsilon \left(E^2 + \frac{1}{2k_B T} \frac{\partial \Delta^2}{\partial \beta} \right) \frac{\partial f}{\partial E}, \quad E = \sqrt{\varepsilon^2 + \Delta^2}.$$

Hint: Take into account that

$$\frac{\partial(P\Omega)}{\partial E_{\mathbf{k}}} = \frac{\partial(P\Omega)}{\partial u_{\mathbf{k}}} = 0,$$

since the potential, $-P\Omega$, must be minimum at equilibrium.

13.7. Following (13.82)–(13.91), verify the results shown in Figs. 13.8–13.10. Use Bethe lattice Green's functions in the limit $K \rightarrow \infty$ with $2|V'| \sqrt{K} = B = Z|V|$. How are the results modified for the 1-d case?

A

Dirac's delta Function

The 1-d delta function, $\delta(x)$, is defined through a limiting procedure so that

$$\delta(x) = 0 \quad \text{for } x \neq 0 \quad (\text{A.1a})$$

and $\delta(0) = \infty$. The meaning of this last relation, taking into account (A.1a), is that

$$\int_a^b dx f(x) \delta(x) = f(0) \quad (\text{A.1b})$$

for any well-behaved function $f(x)$ and for any pair a, b such that $a < 0 < b$.

Some functions producing in the limit the delta function, as defined by (A.1a, A.1b), are given below:

$$\delta(x) = \begin{cases} \lim_{\varepsilon \rightarrow 0^+} \frac{1}{\pi} \frac{\varepsilon}{x^2 + \varepsilon^2}, & \text{Lorentzian,} & (\text{A.2a}) \\ \lim_{\sigma \rightarrow 0^+} \frac{1}{\sigma\sqrt{2\pi}} \exp\left(-\frac{x^2}{2\sigma^2}\right), & \text{Gaussian,} & (\text{A.2b}) \\ \lim_{\varepsilon \rightarrow 0^+} \frac{\sin(x/\varepsilon)}{\pi x}, & \text{Dirichlet,} & (\text{A.2c}) \\ \lim_{L \rightarrow \infty} \frac{1}{2\pi} \int_{-|L|}^{|L|} e^{ikx} dk, & \text{Fourier.} & (\text{A.2d}) \end{cases}$$

From the definition of the delta function it follows that

$$\delta(g(x)) = \sum_n \frac{\delta(x - x_n)}{|g'(x_n)|}, \quad (\text{A.3})$$

where $g(x)$ is a well-behaved function of x , the sum runs over the real roots, $\{x_n\}$, of $g(x) = 0$, and $g'(x_n) \equiv (dg/dx)_{x=x_n} \neq 0$ for all x_n .

The derivative of the delta function is properly defined as

$$\delta'(x) = 0, \quad x \neq 0 \quad (\text{A.4a})$$

and

$$\int_a^b dx f(x) \delta'(x) = -f'(0) \quad (\text{A.4b})$$

for any well-behaved function $f(x)$ and for any pair a, b such that $a < 0 < b$.

The integral of the delta function is the so-called theta function

$$\delta(x) = \frac{d\theta(x)}{dx}, \quad (\text{A.5a})$$

where

$$\theta(x) \equiv \begin{cases} 1, & \text{for } x > 0, \\ 0, & \text{for } x < 0. \end{cases} \quad (\text{A.5b})$$

The definition of the delta function is generalized to more than one independent cartesian variable:

$$\delta(\mathbf{r}) = \delta(x_1) \delta(x_2) \dots \delta(x_n) \quad (\text{A.6})$$

in an n -dimensional space. More explicitly we have

$$\delta(\mathbf{r} - \mathbf{r}') = \delta(x - x') \delta(y - y') = \frac{1}{r} \delta(r - r') \delta(\phi - \phi'), \quad \text{2-d,} \quad (\text{A.7})$$

$$\begin{aligned} \delta(\mathbf{r} - \mathbf{r}') &= \delta(x - x') \delta(y - y') \delta(z - z') \\ &= \frac{1}{r^2} \delta(r - r') \delta(\cos \theta - \cos \theta') \delta(\phi - \phi') \\ &= \frac{1}{r^2 \sin \theta} \delta(r - r') \delta(\theta - \theta') \delta(\phi - \phi'), \quad \text{3-d.} \end{aligned} \quad (\text{A.8})$$

The completeness relation (1.4) of Chap. 1 allows us to obtain many series or integral representations of the delta function. For example, the Fourier representation of the d -dimensional delta function is, according to (1.4) and the footnote on p. 3,

$$\begin{aligned} \delta(\mathbf{r} - \mathbf{r}') &= \sum_{\mathbf{k}} \phi_{\mathbf{k}}(\mathbf{r}) \phi_{\mathbf{k}}^*(\mathbf{r}') = \frac{1}{\Omega} \sum_{\mathbf{k}} e^{i\mathbf{k} \cdot (\mathbf{r} - \mathbf{r}')} \xrightarrow{\Omega \rightarrow \infty} \\ &= \frac{1}{\Omega} \frac{\Omega}{(2\pi)^d} \int d\mathbf{k} e^{i\mathbf{k} \cdot (\mathbf{r} - \mathbf{r}')} = \frac{1}{(2\pi)^d} \int d\mathbf{k} e^{i\mathbf{k} \cdot (\mathbf{r} - \mathbf{r}')} . \end{aligned} \quad (\text{A.9})$$

Equation (A.9) generalizes in d -dimensions (A.2d).

Similarly, the delta function over the spherical angles θ and ϕ can be expressed as a sum over spherical harmonics, $Y_{\ell m}(\theta, \phi)$, according to (1.4):

$$\begin{aligned} \delta(\cos \theta - \cos \theta') \delta(\phi - \phi') &= \frac{1}{\sin \theta} \delta(\theta - \theta') \delta(\phi - \phi') \\ &= \sum_{\ell=0}^{\infty} \sum_{m=-\ell}^{\ell} Y_{\ell m}(\theta, \phi) Y_{\ell m}^*(\theta', \phi'), \end{aligned} \quad (\text{A.10})$$

where the spherical harmonics are given in terms of the associated Legendre polynomials, $P_\ell^{|m|}$, by the following expression:

$$Y_{\ell m}(\theta, \phi) = i^\ell (-1)^{(|m|+m)/2} \sqrt{\frac{(2\ell+1)(\ell-|m|)!}{4\pi(\ell+|m|)!}} P_\ell^{|m|}(\cos\theta) e^{im\phi} . \quad (\text{A.11})$$

Equation (A.10) is valid because the set $Y_{\ell m}(\theta, \phi)$ is orthonormal

$$\int_0^\pi \sin\theta d\theta \int_0^{2\pi} d\phi Y_{\ell m}^*(\theta, \phi) Y_{\ell' m'}(\theta, \phi) = \delta_{\ell\ell'} \delta_{mm'} .$$

B

Dirac's bra and ket Notation

In quantum mechanics, the states of a particle are described by eigenfunctions, $\phi_n(\mathbf{r})$, of any hermitian operator, \mathcal{L} , corresponding to a physical quantity such as its momentum, its Hamiltonian, etc. The same physical states can equally well be described by the Fourier transforms, $\tilde{\phi}_n(\mathbf{k})$, of $\phi_n(\mathbf{r})$ or by any other representation of $\phi_n(\mathbf{r})$ such as the set $\{a_{n,\ell}\}$ of the expansion

$$\phi_n(\mathbf{r}) = \sum_{\ell} a_{n,\ell} \psi_{\ell}(\mathbf{r}) \quad (\text{B.1})$$

in terms of a complete orthonormal set of functions $\{\psi_{\ell}\}$.

It is very convenient to introduce for a physical state a single symbol that will be independent of any particular representation and such that the various representations, $\phi_n(\mathbf{r})$, $\tilde{\phi}_n(\mathbf{k})$, and $\{a_{n,\ell}\}$, can be reproduced easily whenever they are needed. This symbol is denoted by $|n\rangle$ or by $|\phi_n\rangle$ and is called a *ket*. Thus

State of a particle characterized by quantum number(s) $n \iff |\phi_n\rangle$ or $|n\rangle$

To each ket $|\phi_n\rangle$ corresponds one and only one conjugate entity denoted by $\langle\phi_n|$ and called a *bra*. We define also the inner product of two kets, $|\phi\rangle$ and $|\psi\rangle$, (in that order) as a complex quantity denoted by $\langle\phi|\psi\rangle$ and such that

$$\langle\phi|\psi\rangle^* = \langle\psi|\phi\rangle. \quad (\text{B.2})$$

In particular, for an orthonormal set we have

$$\langle\phi_n|\phi_m\rangle = \delta_{nm}. \quad (\text{B.3})$$

Physically, the inner product $\langle\phi|\psi\rangle$ gives the probability amplitude for a particle being in state $|\psi\rangle$ to be observed in state $|\phi\rangle$.

A complete set of kets, $\{|\phi_n\rangle\}$, defines an abstract Hilbert space. Some usual complete sets of kets for a spinless particle are the following:

- (a) The position kets $\{|\mathbf{r}\rangle\}$, where \mathbf{r} runs over all positions in the domain Ω ; $|\mathbf{r}\rangle$ corresponds to the state where the particle is completely localized at the point \mathbf{r} .

- (b) The momentum kets $\{|\mathbf{k}\rangle\}$; $|\mathbf{k}\rangle$ corresponds to the state where the particle has momentum $\hbar\mathbf{k}$.
- (c) The Bloch kets $\{|\mathbf{k}, n\rangle\}$; $|\mathbf{k}, n\rangle$ corresponds to the state where the particle has crystal momentum $\hbar\mathbf{k}$ and belongs to the n th band.
- (d) The kets $\{|\phi_\ell\rangle\}$; $|\phi_\ell\rangle$ is an eigenstate of the Hamiltonian. The indexes fully characterize this eigenstate.

According to the above, the inner product $\langle \mathbf{r} | \psi \rangle$ gives the probability amplitude for a particle being in the state $|\psi\rangle$ to be observed at the point \mathbf{r} ; but this probability amplitude is nothing other than $\psi(\mathbf{r})$. Hence

$$\psi(\mathbf{r}) = \langle \mathbf{r} | \psi \rangle . \quad (\text{B.4})$$

Similarly,

$$\tilde{\psi}(\mathbf{k}) = \langle \mathbf{k} | \psi \rangle . \quad (\text{B.5})$$

If in (B.4) we choose $|\psi\rangle = |\mathbf{k}\rangle$, then we obtain

$$\langle \mathbf{r} | \mathbf{k} \rangle = \frac{1}{\sqrt{\Omega}} e^{i\mathbf{k} \cdot \mathbf{r}} . \quad (\text{B.6})$$

The rhs is the \mathbf{r} -representation of a normalized plane wave; if in (B.4) we choose $|\psi\rangle = |\mathbf{r}'\rangle$, then we have

$$\langle \mathbf{r} | \mathbf{r}' \rangle = \delta(\mathbf{r} - \mathbf{r}') . \quad (\text{B.7})$$

Equation (B.7) follows from the orthonormality of the set $\{|\mathbf{r}'\rangle\}$.

From (B.4) and (B.7) we obtain

$$\begin{aligned} \psi(\mathbf{r}) &= \langle \mathbf{r} | \psi \rangle = \int d\mathbf{r}' \delta(\mathbf{r} - \mathbf{r}') \langle \mathbf{r}' | \psi \rangle = \int d\mathbf{r}' \langle \mathbf{r} | \mathbf{r}' \rangle \langle \mathbf{r}' | \psi \rangle \\ &= \langle \mathbf{r} | \int d\mathbf{r}' |\mathbf{r}'\rangle \langle \mathbf{r}' | \psi \rangle . \end{aligned} \quad (\text{B.8})$$

Since (B.8) is valid for every $\langle \mathbf{r} |$ and every $|\psi\rangle$, we end up with the completeness relation for the set $\{|\mathbf{r}'\rangle\}$:

$$\int d\mathbf{r}' |\mathbf{r}'\rangle \langle \mathbf{r}' | = 1 . \quad (\text{B.9})$$

Similarly, we obtain the relation

$$1 = \sum_{\mathbf{k}} |\mathbf{k}\rangle \langle \mathbf{k} | \xrightarrow{\Omega \rightarrow \infty} \frac{\Omega}{(2\pi)^d} \int d\mathbf{k} |\mathbf{k}\rangle \langle \mathbf{k} | . \quad (\text{B.10})$$

Using (B.9) and (B.10) we can easily transform from $\psi(\mathbf{r})$ to $\tilde{\psi}(\mathbf{k})$ and vice versa

$$\begin{aligned} \tilde{\psi}(\mathbf{k}) &= \langle \mathbf{k} | \psi \rangle = \int d\mathbf{r} \langle \mathbf{k} | \mathbf{r} \rangle \langle \mathbf{r} | \psi \rangle = \int d\mathbf{r} \frac{1}{\sqrt{\Omega}} e^{-i\mathbf{k} \cdot \mathbf{r}} \psi(\mathbf{r}) \\ &= \frac{1}{\sqrt{\Omega}} \int d\mathbf{r} e^{-i\mathbf{k} \cdot \mathbf{r}} \psi(\mathbf{r}) , \end{aligned} \quad (\text{B.11})$$

$$\begin{aligned}\psi(\mathbf{r}) = \langle \mathbf{r} | \psi \rangle &= \sum_{\mathbf{k}} \langle \mathbf{r} | \mathbf{k} \rangle \langle \mathbf{k} | \psi \rangle = \frac{1}{\sqrt{\Omega}} \sum_{\mathbf{k}} e^{i\mathbf{k} \cdot \mathbf{r}} \tilde{\psi}(\mathbf{k}) \\ &= \frac{\sqrt{\Omega}}{(2\pi)^d} \int d\mathbf{k} e^{i\mathbf{k} \cdot \mathbf{r}} \tilde{\psi}(\mathbf{k}) .\end{aligned}\quad (\text{B.12})$$

Notice that the definition of the inner product coincides with the usual definition in the \mathbf{r} -representation:

$$\langle \phi | \psi \rangle = \int d\mathbf{r} \langle \phi | \mathbf{r} \rangle \langle \mathbf{r} | \psi \rangle = \int d\mathbf{r} \phi^*(\mathbf{r}) \psi(\mathbf{r}) . \quad (\text{B.13})$$

The form of any operator in the Dirac notation follows by calculating its matrix elements. For example, taking into account that the position operator, $\hat{\mathbf{r}}$, satisfies by definition the relation $\langle \mathbf{r} | \hat{\mathbf{r}} = \langle \mathbf{r} | \mathbf{r}$ and that the momentum operator, $\hat{\mathbf{p}}$, satisfies the relation $\langle \mathbf{k} | \hat{\mathbf{p}} = \langle \mathbf{k} | \hbar \mathbf{k}$, we have

$$\langle \mathbf{r} | \hat{\mathbf{r}} | \psi \rangle = \mathbf{r} \langle \mathbf{r} | \psi \rangle = \mathbf{r} \psi(\mathbf{r}) , \quad (\text{B.14})$$

$$\langle \mathbf{k} | \hat{\mathbf{p}} | \psi \rangle = \hbar \mathbf{k} \langle \mathbf{k} | \psi \rangle = \hbar \mathbf{k} \tilde{\psi}(\mathbf{k}) . \quad (\text{B.15})$$

Using (B.10) and (B.15) we obtain the matrix element $\langle \mathbf{r} | \hat{\mathbf{p}} | \psi \rangle$:

$$\begin{aligned}\langle \mathbf{r} | \hat{\mathbf{p}} | \psi \rangle &= \sum_{\mathbf{k}} \langle \mathbf{r} | \mathbf{k} \rangle \langle \mathbf{k} | \hat{\mathbf{p}} | \psi \rangle = \sum_{\mathbf{k}} \frac{1}{\sqrt{\Omega}} e^{i\mathbf{k} \cdot \mathbf{r}} \hbar \mathbf{k} \tilde{\psi}(\mathbf{k}) \\ &= \sum_{\mathbf{k}} -i\hbar \frac{\partial}{\partial \mathbf{r}} e^{i\mathbf{k} \cdot \mathbf{r}} \frac{1}{\sqrt{\Omega}} \tilde{\psi}(\mathbf{k}) = -i\hbar \frac{\partial}{\partial \mathbf{r}} \sum_{\mathbf{k}} \frac{1}{\sqrt{\Omega}} e^{i\mathbf{k} \cdot \mathbf{r}} \tilde{\psi}(\mathbf{k}) \\ &= -i\hbar \frac{\partial}{\partial \mathbf{r}} \psi(\mathbf{r}) .\end{aligned}\quad (\text{B.16})$$

The last relation follows from (B.12). In a similar way one can show that

$$\langle \mathbf{k} | \hat{\mathbf{r}} | \psi \rangle = i \frac{\partial}{\partial \mathbf{k}} \tilde{\psi}(\mathbf{k}) . \quad (\text{B.17})$$

The relations (B.14)–(B.17) can be generalized for operators that are functions of $\hat{\mathbf{r}}$ or $\hat{\mathbf{p}}$. Since by definition the function $f(\hat{\mathcal{A}})$ of any operator $\hat{\mathcal{A}}$ is an operator with the same eigenstates as $\hat{\mathcal{A}}$ and eigenvalues $f(A_i)$, where A_i are the eigenvalues of $\hat{\mathcal{A}}$, we have

$$\langle \mathbf{r} | f(\hat{\mathbf{r}}) | \psi \rangle = f^*(\mathbf{r}) \psi(\mathbf{r}) , \quad (\text{B.18})$$

$$\langle \mathbf{k} | g(\hat{\mathbf{p}}) | \psi \rangle = g^*(\hbar \mathbf{k}) \tilde{\psi}(\mathbf{k}) , \quad (\text{B.19})$$

$$\langle \mathbf{r} | g(\hat{\mathbf{p}}) | \psi \rangle = g^* \left(-i\hbar \frac{\partial}{\partial \mathbf{r}} \right) \psi(\mathbf{r}) , \quad (\text{B.20})$$

$$\langle \mathbf{k} | f(\hat{\mathbf{r}}) | \psi \rangle = f^* \left(i \frac{\partial}{\partial \mathbf{k}} \right) \tilde{\psi}(\mathbf{k}) . \quad (\text{B.21})$$

For hermitian operators $f^*(\mathbf{r}) = f(\mathbf{r})$ and $g^*(\hbar\mathbf{k}) = g(\hbar\mathbf{k})$. As an application of (B.18) and (B.20) we have

$$\left\langle \mathbf{r} \left| \frac{\hat{\mathbf{p}}^2}{2m} + V(\hat{\mathbf{r}}) \right| \psi \right\rangle = \left[-\frac{\hbar^2}{2m} \nabla_r^2 + V(\mathbf{r}) \right] \psi(\mathbf{r}) . \quad (\text{B.22})$$

For particles with spin $1/2$ we have to specify whether the spin is up (\uparrow) or down (\downarrow). Thus a complete set is $\{|\mathbf{r}, \uparrow\rangle, |\mathbf{r}, \downarrow\rangle\}$ or $\{|\mathbf{k}, \uparrow\rangle, |\mathbf{k}, \downarrow\rangle\}$. Assuming that the spin quantization axis is the z -axis, we have for the spin operator $\mathbf{s} = \mathbf{x}_0 s_x + \mathbf{y}_0 s_y + \mathbf{z}_0 s_z$:

$$s_z |\mathbf{r}, \sigma\rangle = \frac{1}{2} \sigma |\mathbf{r}, \sigma\rangle , \quad \begin{array}{l} \sigma = +1 \quad \text{for spin up ,} \\ \sigma = -1 \quad \text{for spin down ,} \end{array} \quad (\text{B.23})$$

$$\left| \begin{array}{l} \langle \mathbf{r}, \uparrow | \mathbf{s} | \psi \rangle \\ \langle \mathbf{r}, \downarrow | \mathbf{s} | \psi \rangle \end{array} \right| = \frac{1}{2} \boldsymbol{\sigma} \left| \begin{array}{l} \langle \mathbf{r}, \uparrow | \psi \rangle \\ \langle \mathbf{r}, \downarrow | \psi \rangle \end{array} \right| , \quad (\text{B.24})$$

where $\boldsymbol{\sigma}$ is the vector defined by the three Pauli matrices

$$\boldsymbol{\sigma} = \begin{pmatrix} 0 & 1 \\ 1 & 0 \end{pmatrix} \mathbf{x}_0 + \begin{pmatrix} 0 & -i \\ i & 0 \end{pmatrix} \mathbf{y}_0 + \begin{pmatrix} 1 & 0 \\ 0 & -1 \end{pmatrix} \mathbf{z}_0 . \quad (\text{B.25})$$

C

Solutions of Laplace and Helmholtz Equations in Various Coordinate Systems¹

C.1 Helmholtz Equation $(\nabla^2 + k^2) \psi(\mathbf{r}) = 0$

C.1.1 Cartesian Coordinates x, y, z

$$\begin{aligned} \psi(\mathbf{r}) = \sum_{\ell m} \left\{ A_{\ell m} [\sin(\ell x_1) + b_\ell \cos(\ell x_1)] \right. \\ \times \left[\sinh(\sqrt{\ell^2 + m^2} x_2) + c_{\ell m} \cosh(\sqrt{\ell^2 + m^2} x_2) \right] \\ \left. \times \left[\sin(\sqrt{m^2 + k^2} x_3) + d_m \cos(\sqrt{m^2 + k^2} x_3) \right] \right\}. \quad (\text{C.1}) \end{aligned}$$

The set $\{x_1, x_2, x_3\}$ represents any permutation of the set $\{x, y, z\}$. Boundary conditions (BCs) and normalization may fully determine the various eigensolutions and eigenvalues. Instead of $\sin(\ell x_1) + b_\ell \cos(\ell x_1)$, one can use $\exp(i\ell x_1) + b'_\ell \exp(-i\ell x_1)$; similar replacements can be employed in the other factors of (C.1).

The solution of the *Laplace equation* $\nabla^2 \phi = 0$ is obtained immediately by setting $k = 0$ in (C.1).

C.1.2 Cylindrical Coordinates z, ϕ, ρ

$$\begin{aligned} \psi(\mathbf{r}) = \sum_{m,n} A_{mn} [\sinh(mz) + b_m \cosh(mz)] [\sin(n\phi) + c_n \cos(n\phi)] \\ \times \left[J_n(\sqrt{m^2 + k^2} \rho) + d_{nm} Y_n(\sqrt{m^2 + k^2} \rho) \right]. \quad (\text{C.2}) \end{aligned}$$

In the first factor of the rhs of (C.2) one can use instead of $\sinh(mz) + b_m \cosh(mz)$ the sum $e^{mz} + b'_m e^{-mz}$. Similarly, in the second factor one can use $e^{in\phi} + c'_n e^{-in\phi}$. Finally, in the last factor one may use

$$H_n^{(1)}(w) = J_n(w) + iY_n(w)$$

¹ For the definition and properties of the most common special functions see [1].

and/or

$$H_n^{(2)}(w) = J_n(w) - iY_n(w)$$

instead of J_n and Y_n , where $w = \sqrt{m^2 + k^2}\varrho$. Recall that

$$J_n(w) \rightarrow \frac{(w/2)^n}{\Gamma(n+1)}, \quad w \rightarrow 0, \quad n \neq -1, -2, \dots, \quad (\text{C.3a})$$

$$Y_n(w) \rightarrow -\frac{1}{\pi}\Gamma(n)(w/2)^{-n}, \quad w \rightarrow 0, \quad \text{Re}\{n\} > 0, \quad (\text{C.3b})$$

$$Y_0(w) \rightarrow \frac{2}{\pi} \ln w + \text{const.}, \quad w \rightarrow 0, \quad (\text{C.3c})$$

$$H_n^{(1)}(w) \rightarrow \sqrt{\frac{2}{\pi w}} e^{i(w-n\pi/2-\pi/4)}, \quad w \rightarrow \infty, \quad (\text{C.3d})$$

$$H_n^{(2)}(w) \rightarrow \sqrt{\frac{2}{\pi w}} e^{-i(w-n\pi/2-\pi/4)}, \quad w \rightarrow \infty. \quad (\text{C.3e})$$

Thus, $Y_n(w)$ blows up for $w \rightarrow 0$; $H_n^{(1)}(w)$ and $H_n^{(2)}(w)$ represent for $w \rightarrow \infty$ outgoing and ingoing waves, respectively, while for $\text{Im}\{w\} > 0$, $H_n^{(1)}(w)$ and $H_n^{(2)}(w)$ blow up as $w \rightarrow 0$.

The solution of the *Laplace equation*, $\nabla^2\phi = 0$, is obtained by setting $k = 0$ in (C.2). The solutions of the *Helmholtz equation* in 2-d polar coordinates, ϕ and ϱ , are produced by setting $m = 0$ in (C.2). Finally, for the solution of the *Laplace equation* in 2-d polar coordinates, we must take $m = 0$ and $k \rightarrow 0$ so that

$$\begin{aligned} \phi(\mathbf{r}) = & \sum_{n \neq 0} A_n [\sin(n\phi) + c_n \cos(n\phi)] (\varrho^n + d_n \varrho^{-n}) \\ & + A_0 (1 + d_0 \ln \varrho). \end{aligned} \quad (\text{C.4})$$

C.1.3 Spherical coordinates r, θ, ϕ

$$\begin{aligned} \psi(\mathbf{r}) = & \sum_{\ell m} A_{\ell m} (e^{im\phi} + b_m e^{-im\phi}) [P_\ell^m(\cos \theta) + c_{\ell m} Q_\ell^m(\cos \theta)] \\ & \times [j_\ell(kr) + d_\ell y_\ell(kr)]. \end{aligned} \quad (\text{C.5})$$

$Q_\ell^m(\cos \theta)$ is singular for $\theta = 0$ and $\theta = \pi$; similarly, $P_\ell^m(\cos \theta)$ is singular for $\theta = 0$ and $\theta = \pi$ unless ℓ is a nonnegative integer. Thus, $c_{\ell m}$ must be zero and ℓ must a nonnegative integer if $\theta = 0$ or π is included in the problem.

The spherical Bessel functions, $j_\ell(w)$ and $y_\ell(w)$, are defined by the relations

$$\begin{aligned} j_\ell(w) = & \sqrt{\frac{\pi}{2w}} J_{\ell+\frac{1}{2}}(w) \\ \rightarrow & \frac{w^\ell}{1 \times 3 \times \dots \times (2\ell + 1)} \quad \text{as } w \rightarrow 0, \end{aligned} \quad (\text{C.6a})$$

$$\begin{aligned}
 y_\ell(w) &= \sqrt{\frac{\pi}{2w}} Y_{\ell+\frac{1}{2}}(w) \\
 &\rightarrow -\frac{1 \times 3 \times \dots \times (2\ell-1)}{w^{\ell+1}} \quad \text{as } w \rightarrow 0. \quad (\text{C.7a})
 \end{aligned}$$

In a similar way we define the spherical Hankel functions $h_\ell^{(1)}(w) = j_\ell(w) + iy_\ell(w)$ and $h_\ell^{(2)}(w) = j_\ell(w) - iy_\ell(w)$, which represent outgoing and ingoing spherical waves, respectively.

For problems covering the full range of values of ϕ ($0 \leq \phi \leq 2\pi$) and θ ($0 \leq \theta \leq \pi$), $c_{\ell m}$ must be set equal to zero, ℓ must be a nonnegative integer for the reasons explained above, m must be an integer running from $-\ell$ to $+\ell$, and the first two factors in brackets on the rhs of (C.5) are then represented by the spherical harmonic $Y_{\ell m}(\theta, \phi)$ [not to be confused with the Bessel function $Y_n(w)$] given by (A.11) in Appendix A. The set $\{Y_{\ell m}(\theta, \phi)\}$ is an orthonormal complete set of functions over the whole surface of the 3-d unit sphere.

The solution of the *Laplace equation*, $\nabla^2\phi = 0$, is obtained by taking the limit $k \rightarrow 0$ in (C.5) and using (C.6a) and (C.7a):

$$\begin{aligned}
 \phi(\mathbf{r}) &= \sum_{\ell m} A_{\ell m} [e^{im\phi} + b_m e^{-im\phi}] \\
 &\quad \times [P_\ell^m(\cos\theta) + c_{\ell m} Q_\ell^m(\cos\theta)] (r^\ell + d'_\ell/r^{\ell+1}). \quad (\text{C.8})
 \end{aligned}$$

If ϕ and θ cover the full range of their values, then the first two factors in brackets on the rhs of (C.8) must be replaced by $Y_{\ell m}(\theta, \phi)$, as given by (A.11).

C.2 Vector Derivatives

We shall conclude this Appendix by giving the formulae for some vector derivatives in spherical and cylindrical coordinates.

C.2.1 Spherical Coordinates r, θ, ϕ

$$\text{grad}\psi(\mathbf{r}) \equiv \nabla\psi(\mathbf{r}) = \frac{\partial\psi}{\partial r} \mathbf{i}_r + \frac{1}{r} \frac{\partial\psi}{\partial\theta} \mathbf{i}_\theta + \frac{1}{r \sin\theta} \frac{\partial\psi}{\partial\phi} \mathbf{i}_\phi. \quad (\text{C.9})$$

$$\begin{aligned}
 \text{div}\mathbf{A}(\mathbf{r}) &\equiv \nabla \cdot \mathbf{A}(\mathbf{r}) \\
 &= \frac{1}{r^2} \frac{\partial}{\partial r} (r^2 A_r) + \frac{1}{r \sin\theta} \frac{\partial}{\partial\theta} (\sin\theta A_\theta) + \frac{1}{r \sin\theta} \frac{\partial A_\phi}{\partial\phi}. \quad (\text{C.10})
 \end{aligned}$$

$$\nabla^2\psi(\mathbf{r}) = \frac{1}{r^2} \frac{\partial}{\partial r} \left(r^2 \frac{\partial\psi}{\partial r} \right) + \frac{1}{r^2 \sin\theta} \frac{\partial}{\partial\theta} \left(\sin\theta \frac{\partial\psi}{\partial\theta} \right) + \frac{1}{r^2 \sin^2\theta} \frac{\partial^2\psi}{\partial\phi^2}. \quad (\text{C.11})$$

C.2.2 Cylindrical Coordinates z, ϱ, ϕ

$$\text{grad}\psi(\mathbf{r}) \equiv \nabla\psi(\mathbf{r}) = \frac{\partial\psi}{\partial z}\mathbf{i}_z + \frac{\partial\psi}{\partial\varrho}\mathbf{i}_\varrho + \frac{1}{\varrho}\frac{\partial\psi}{\partial\phi}\mathbf{i}_\phi. \quad (\text{C.12})$$

$$\text{div}\mathbf{A}(\mathbf{r}) \equiv \nabla \cdot \mathbf{A}(\mathbf{r}) = \frac{\partial A_z}{\partial z} + \frac{1}{\varrho}\frac{\partial}{\partial\varrho}(\varrho A_\varrho) + \frac{1}{\varrho}\frac{\partial A_\phi}{\partial\phi}. \quad (\text{C.13})$$

$$\nabla^2\psi(\mathbf{r}) = \frac{\partial^2\psi}{\partial z^2} + \frac{1}{\varrho}\frac{\partial}{\partial\varrho}\left(\varrho\frac{\partial\psi}{\partial\varrho}\right) + \frac{1}{\varrho^2}\frac{\partial^2\psi}{\partial\phi^2}. \quad (\text{C.14})$$

C.3 Schrödinger Equation in Centrally Symmetric 3- and 2-Dimensional Potential V

$$-\frac{\hbar^2}{2m}\nabla^2\psi + V\psi = E\psi. \quad (\text{C.15})$$

For the 3-d case we write

$$\psi(\mathbf{r}) = \frac{u(r)}{r}Y_{\ell m}(\theta, \phi), \quad (\text{C.16})$$

and we obtain

$$-\frac{\hbar^2}{2m}\frac{d^2u}{dr^2} + \left[V(r) + \frac{\hbar^2\ell(\ell+1)}{2mr^2}\right]u = Eu, \quad (\text{C.17a})$$

$$\begin{aligned} (\mathbf{r} \times \mathbf{p})^2 &= -\hbar^2(\mathbf{r} \times \nabla)^2 \\ &= -\hbar^2\left[\frac{1}{\sin^2\theta}\frac{\partial^2}{\partial\phi^2} + \frac{1}{\sin\theta}\frac{\partial}{\partial\theta}\left(\sin\theta\frac{\partial}{\partial\theta}\right)\right], \end{aligned} \quad (\text{C.17b})$$

$$(\mathbf{r} \times \mathbf{p})^2 Y_{\ell m}(\theta, \phi) = \hbar^2\ell(\ell+1)Y_{\ell m}(\theta, \phi), \quad (\text{C.17c})$$

where $Y_{\ell m}(\theta, \phi)$ is given by (A.11); in particular,

$$Y_{\ell 0}(\theta, \phi) = i^\ell \sqrt{\frac{2\ell+1}{4\pi}}P_\ell(\cos\theta). \quad (\text{C.17d})$$

Equation (C.17a) is a 1-d Schrödinger equation with an effective potential consisting of the actual potential $V(r)$ plus the centrifugal part; the latter equals the eigenvalue, $\hbar^2\ell(\ell+1)$, of the square of the angular momentum, $\mathbf{r} \times \mathbf{p}$, over twice the “moment of inertia” mr^2 .

For the 2-d polar coordinates we write

$$\psi(\mathbf{r}) = R(\varrho)\Phi(\phi), \quad (\text{C.18})$$

and we obtain

$$\Phi(\phi) = e^{in\phi} + b_n e^{-in\phi} \quad (\text{C.19a})$$

and

$$\varrho^2 \frac{d^2 R}{d\varrho^2} + \varrho \frac{dR}{d\varrho} + R \left[\left(\frac{2mE}{\hbar^2} - \frac{2mV(\varrho)}{\hbar^2} \right) \varrho^2 - n^2 \right] = 0. \quad (\text{C.19b})$$

If $V(\varrho)$ is a constant such that $E - V > 0$, we define $k^2 = 2m(E - V)/\hbar^2$ and (C.19b) becomes the ordinary Bessel equation with solutions $J_n(k\varrho)$ and $Y_n(k\varrho)$ [see (C.2) for $m = 0$].

If $V(\varrho)$ is a constant such that $E - V < 0$, then we define $-k^2 = 2m(E - V)/\hbar^2$, and (C.19b) becomes the modified Bessel equation with solutions $I_n(k\varrho)$ and $K_n(k\varrho)$ satisfying the following relations:

$$I_n(w) = \begin{cases} e^{-in\pi/2} J_n(iw), & -\pi < \arg w \leq \pi/2, \\ e^{3in\pi/2} J_n(iw), & \pi/2 < \arg w \leq \pi; \end{cases} \quad (\text{C.20})$$

$$K_n(w) = \begin{cases} \frac{i\pi}{2} e^{in\pi/2} H_n^{(1)}(iw), & -\pi < \arg w \leq \pi/2, \\ -\frac{i\pi}{2} e^{-in\pi/2} H_n^{(2)}(-iw), & \pi/2 < \arg w \leq \pi. \end{cases} \quad (\text{C.21})$$

Other useful properties of $I_n(w)$ and $K_n(w)$ are given in [1].

D

Analytic Behavior of $G(z)$ Near a Band Edge

The Green's function $G(z)$ can be expressed in terms of the discontinuity $\tilde{G}(E) \equiv G^+(E) - G^-(E)$ as follows:

$$G(z) = \frac{i}{2\pi} \int_{-\infty}^{\infty} dE \frac{\tilde{G}(E)}{z - E}. \quad (\text{D.1})$$

The derivative of $G(z)$ is obtained by differentiation under the integral. Integrating by parts we obtain

$$G'(z) = \frac{i}{2\pi} \int_{-\infty}^{\infty} dE \frac{\tilde{G}'(E)}{z - E}, \quad (\text{D.2})$$

where the prime denotes differentiation with respect to the argument. In obtaining (D.2) we have assumed that $\tilde{G}'(E)$ exists and is integrable and that $\tilde{G}(E)/E \rightarrow 0$ as $|E| \rightarrow \infty$. By taking the limits $\text{Im}\{z\} \rightarrow 0^\pm$ and using (1.20) we obtain

$$G^\pm(E) = \frac{i}{2\pi} \text{P} \int_{-\infty}^{\infty} dE' \frac{\tilde{G}(E')}{E - E'} \pm \frac{1}{2} \tilde{G}(E), \quad (\text{D.3})$$

$$\frac{d}{dE} G^\pm(E) = \frac{i}{2\pi} \text{P} \int_{-\infty}^{\infty} dE' \frac{\tilde{G}'(E')}{E - E'} \pm \frac{1}{2} \tilde{G}'(E), \quad (\text{D.4})$$

where one can show under the above assumptions that

$$G'(z) \xrightarrow{\text{Im}\{z\} \rightarrow 0^\pm} \frac{d}{dE} G^\pm(E).$$

We would like to connect the behavior of $G(z)$ and $G'(z)$ as $z \rightarrow E_0$ with the behavior of $\tilde{G}(E)$ around E_0 . One can prove the following theorems [15] about $F(z)$ given by

$$F(z) = \frac{i}{2\pi} \int_{-\infty}^{\infty} dx \frac{f(x)}{z - x} = \frac{1}{2\pi i} \int_{-\infty}^{\infty} \frac{f(x)}{x - z} dx. \quad (\text{D.5})$$

Theorem 1. *If $f(x)$ satisfies the condition*

$$|f(x_1) - f(x_2)| \leq A|x_1 - x_2|^\mu \tag{D.6}$$

for all x_1 and x_2 in the neighborhood of x_0 , where A and μ are positive constants, then

$$|F(z_1) - F(z_2)| \leq A'|z_1 - z_2|^\mu \quad \text{when } \mu < 1, \tag{D.7}$$

and

$$|F(z_1) - F(z_2)| \leq A'|z_1 - z_2|^{1-\varepsilon} \quad \text{when } \mu = 1, \tag{D.8}$$

for all z_1 and z_2 in the neighborhood of x_0 and $Im\{z_1\}Im\{z_2\} > 0$; A' is a positive constant and ε is an arbitrary positive number.

Inequalities (D.7) and (D.8) are valid as one or both of z_1 and z_2 reach the real axis either from above or from below. Thus, e.g.,

$$|F^+(x_1) - F^+(x_2)| \leq A'|x_1 - x_2|^\mu \quad \text{when } \mu < 1, \tag{D.9}$$

with a similar relation for $F^-(x_1) - F^-(x_2)$.

Theorem 2. *If $f(x)$ is discontinuous at $x = x_0$, i.e.,*

$$f(x_0^+) - f(x_0^-) = D \neq 0, \tag{D.10}$$

but otherwise $f(x)$ satisfies condition (D.6) for both x_1 and x_2 being either to the left or to the right of x_0 , then

$$F(z) = \frac{D}{2\pi i} \ln\left(\frac{1}{x_0 - z}\right) + F_0(z), \tag{D.11}$$

where $F_0(z)$ satisfies (D.7) or (D.8).

Theorem 3. *If $f(x)$ behaves around x_0 as*

$$f(x) = f_0(x) + f_1(x)\theta(\pm x \mp x_0) [\pm x \mp x_0]^{-\gamma}, \tag{D.12}$$

where $f_0(x)$ and $f_1(x)$ satisfy condition (D.6) and $0 < \gamma < 1$, then

$$F(z) = \pm \frac{e^{\pm\gamma\pi i}}{2i \sin(\gamma\pi)} \frac{f_1(x_0)}{(\pm z \mp x_0)^\gamma} + F_0(z), \tag{D.13}$$

where $(\pm z \mp x_0)^{-\gamma}$ is the branch that coincides with the branch $(\pm x \mp x_0)^{-\gamma}$ in (D.12) as z approaches x from the upper half-plane and

$$|F_0(z)| < \frac{C}{|z - x_0|^{\gamma_0}}, \tag{D.14}$$

where C and γ_0 are positive constants such that $\gamma_0 < \gamma$.

The above theorems allow us to obtain the analytic behavior of $G(z)$ near a band edge. Thus:

- (a) When $G(E)$ goes to zero as $(E - E_B)^\mu$ ($\mu > 0$) near the band edge E_B , then, according to Theorem 1 above, $G(z)$ and $G^\pm(E)$ are bounded in the neighborhood of E_B . The derivatives $G'(z)$ and $G^{\pm'}(E)$ can be obtained using (D.2). Since $\tilde{G}'(E)$ behaves as $(E - E_B)^{\mu-1}$ inside the band and near the band edge, then, according to Theorem 3 above, the quantities $G'(z)$ and $G^{\pm'}(E)$ behave as $(z - E_B)^{\mu-1}$ and $(E - E_B)^{\mu-1}$ as z and E approach E_B . For a free particle in 3-d, $\mu = 1/2$.
- (b) When $\tilde{G}(E)$ goes to zero in a discontinuous way at the band edge (as in the 2-d free-particle case), one can apply Theorem 2 above. Consequently, $G(z)$ and $G^\pm(E)$ exhibit a logarithmic singularity as shown in (D.11).
- (c) When $\tilde{G}(E)$ behaves as $|E - E_B|^{-\gamma}$ with $0 < \gamma < 1$ in the interior of the band and near the band edge E_B , then, according to Theorem 3 above, $G(z)$ and $G^\pm(E)$ behave as $(z - E_B)^{-\gamma}$ and $(E - E_B)^{-\gamma}$, respectively. For a free particle in 1-d, $\gamma = 1/2$.

E

Wannier Functions

For many purposes it is useful to introduce the Wannier functions. The Wannier function associated with the band index n and the lattice site $\boldsymbol{\ell}$ is defined as [27, 28, 30]

$$w_n(\boldsymbol{r} - \boldsymbol{\ell}) = \frac{1}{\sqrt{N}} \sum_{\boldsymbol{k}} e^{-i\boldsymbol{k} \cdot \boldsymbol{\ell}} \psi_{n\boldsymbol{k}}(\boldsymbol{r}) , \quad (\text{E.1})$$

where $\psi_{n\boldsymbol{k}}(\boldsymbol{r})$ are the Bloch eigenfunctions given by (5.2). The Wannier functions $w_n(\boldsymbol{r} - \boldsymbol{\ell})$ are localized around the lattice site $\boldsymbol{\ell}$.

The functions $w_n(\boldsymbol{r} - \boldsymbol{\ell})$ for all n and $\boldsymbol{\ell}$ form a complete orthonormal set; thus any operator, e.g., the Hamiltonian, can be expressed in a Wannier representation. It may happen that the eigenenergies associated with a particular band index n_0 are well separated from all the other eigenenergies. In this case the matrix elements of the Hamiltonian \mathcal{H} between $w_{n_0}(\boldsymbol{r} - \boldsymbol{\ell})$ and $w_n(\boldsymbol{r} - \boldsymbol{m})$, where $n \neq n_0$, may be much smaller than $|\varepsilon_n - \varepsilon_{n_0}|$. Then these small matrix elements to a first approximation can be omitted, and the subspace spanned by the states $w_{n_0}(\boldsymbol{r} - \boldsymbol{\ell})$, where $\boldsymbol{\ell}$ runs over all lattice vectors, becomes decoupled from the rest. Let us assume that the band n_0 is associated with a single atomic orbital $\phi(\boldsymbol{r} - \boldsymbol{\ell})$ per atom; then, the set $\{w_{n_0}(\boldsymbol{r} - \boldsymbol{\ell})\}$ is nothing other than an orthonormalized version of the set $\{\phi(\boldsymbol{r} - \boldsymbol{\ell})\}$. If the latter is assumed to be orthonormal, then the Wannier functions $w_{n_0}(\boldsymbol{r} - \boldsymbol{\ell})$ and the atomic orbitals $\phi(\boldsymbol{r} - \boldsymbol{\ell})$ coincide. However, in general, the Wannier functions are hybridized atomiclike orbitals that possess two important features: completeness and orthonormality.

F

Renormalized Perturbation Expansion (RPE)

Consider the tight-binding Hamiltonian $\mathcal{H} = \mathcal{H}_0 + \mathcal{H}_1$, where

$$\mathcal{H}_0 = \sum_{\ell} |\ell\rangle \varepsilon_{\ell} \langle \ell|, \quad (\text{F.1})$$

$$\mathcal{H}_1 = V \sum'_{\ell m} |\ell\rangle \langle m|, \quad (\text{F.2})$$

and the summation in (F.2) extends over nearest-neighbor sites only. If we consider \mathcal{H}_0 as the unperturbed Hamiltonian and \mathcal{H}_1 as a perturbation, we can apply the formalism developed in Chap. 4. Thus we have for $G(z) \equiv (z - \mathcal{H})^{-1}$

$$G = G_0 + G_0 \mathcal{H}_1 G_0 + G_0 \mathcal{H}_1 G_0 \mathcal{H}_1 G_0 + \dots$$

or

$$\begin{aligned} G(\ell, \mathbf{m}) &= G_0(\ell, \mathbf{m}) + \sum_{\mathbf{n}_1 \mathbf{n}_2} G_0(\ell, \mathbf{n}_1) \langle \mathbf{n}_1 | \mathcal{H}_1 | \mathbf{n}_2 \rangle G_0(\mathbf{n}_2, \mathbf{m}) \\ &+ \sum_{\mathbf{n}_1 \dots \mathbf{n}_4} G_0(\ell, \mathbf{n}_1) \langle \mathbf{n}_1 | \mathcal{H}_1 | \mathbf{n}_2 \rangle G_0(\mathbf{n}_2, \mathbf{n}_3) \\ &\quad \times \langle \mathbf{n}_3 | \mathcal{H}_1 | \mathbf{n}_4 \rangle G_0(\mathbf{n}_4, \mathbf{m}) \\ &+ \dots \end{aligned} \quad (\text{F.3})$$

It is clear from (F.1) that $G_0(\mathbf{n}_1, \mathbf{n}_2) = \delta_{\mathbf{n}_1 \mathbf{n}_2} G_0(\mathbf{n}_1)$, where $G_0(\mathbf{n})$ is

$$G_0(\mathbf{n}) = \frac{1}{z - \varepsilon_{\mathbf{n}}}. \quad (\text{F.4})$$

Similarly, $\langle \mathbf{n}_1 | \mathcal{H}_1 | \mathbf{n}_2 \rangle$ is different from zero only when \mathbf{n}_1 and \mathbf{n}_2 are nearest neighbors. Hence (F.3) can be simplified as follows:

$$\begin{aligned} G(\ell, \mathbf{m}) &= \delta_{\ell, \mathbf{m}} G_0(\ell) + G_0(\ell) V G_0(\mathbf{m}) \delta_{\ell, \mathbf{m}+1} \\ &+ \sum_{\mathbf{n}_1} G_0(\ell) V G_0(\mathbf{n}_1) V G_0(\mathbf{m}) + \dots \end{aligned} \quad (\text{F.5})$$

One way of keeping track of the various terms in the expansion (F.5) is to consider all possible paths in the lattice starting from site ℓ and ending at site m with steps connecting one lattice site with a nearest-neighbor site. There is a one-to-one correspondence between the terms in (F.5) and the set of all such paths. Each term in (F.5) can be obtained from the corresponding path by calculating a product according to the following rules. (1) For each lattice site n (including the initial ℓ and the final m) visited by the path, include a factor $G_0(n)$. (2) For each step from one site to a nearest-neighbor site, include a factor V . Thus, the contribution to $G(\ell, m)$ corresponding to the path shown in Fig. F.1 is

$$G_0(\ell) V G_0(n_1) V G_0(n_2) V G_0(n_1) V G_0(n_2) V G_0(m) .$$

The most general path starting from ℓ and ending at m can be constructed by “decorating” a “skeleton” path. The latter is a self-avoiding (no site is visited more than once) path starting from ℓ and ending at m ; the “decorations” consist of closed paths starting from and ending at sites visited by the self-avoiding path. The skeleton path in Fig. F.1 is the self-avoiding path $\ell \rightarrow n_1 \rightarrow n_2 \rightarrow m$. There is one decoration $n_1 \rightarrow n_2 \rightarrow n_1$ at site n_1 giving an extra factor $G(n_1) V^2 G(n_2)$; the same decoration can be considered as associated with site n_2 [being $n_2 \rightarrow n_1 \rightarrow n_2$ and giving an extra factor $G(n_1) V^2 G(n_2)$]. Because of this ambiguity one must be careful not to count the same decoration twice. The above remarks allow us to perform a partial summation. Consider the subset of all paths whose only difference is the decorations starting and ending at site ℓ . The contribution of all these paths is

$$V G_0(n_1) \cdots V G_0(m) \sum_{\ell} ,$$

where \sum_{ℓ} is the sum of *all* the decorations of site ℓ , i.e., the sum of the contributions of all paths starting from and ending at ℓ , which equals the Green’s function $G(\ell, \ell)$. Thus, one can omit all decorations of site ℓ if at the same time one replaces $G_0(\ell)$ by $G(\ell, \ell)$. The same is true for the next

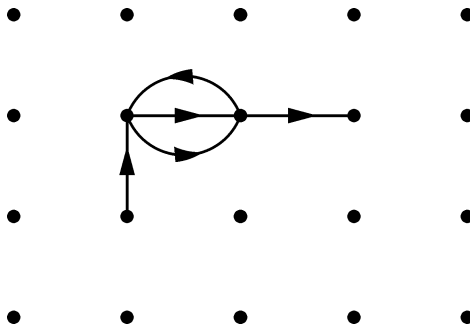


Fig. F.1. A path starting from site ℓ and ending at site m involving five steps

site \mathbf{n}_1 , but with one difference: decorations of site \mathbf{n}_1 that visit site ℓ must be omitted because these decorations have been included already as decorations associated with site ℓ . The decorations at site \mathbf{n}_1 can be omitted if $G_0(\mathbf{n}_1)$ is replaced by $G(\mathbf{n}_1, \mathbf{n}_1[\ell])$, where the symbol $[\ell]$ denotes that in evaluating $G(\mathbf{n}_1, \mathbf{n}_1[\ell])$ the paths visiting site ℓ must be excluded. This exclusion is obtained automatically if one assumes that $\varepsilon_\ell = \infty$ [because then $G_0(\ell) = 0$]. Hence, $G(\mathbf{n}_1, \mathbf{n}_1[\ell])$ is the $\mathbf{n}_1, \mathbf{n}_1$ matrix element of \mathcal{H} with $\varepsilon_\ell = \infty$. Similarly, all the decorations at site \mathbf{n}_2 can be omitted if at the same time one replaces $G_0(\mathbf{n}_2)$ by $G(\mathbf{n}_2, \mathbf{n}_2[\ell, \mathbf{n}_1])$, where the symbol $[\ell, \mathbf{n}_1]$ denotes that both ε_ℓ and $\varepsilon_{\mathbf{n}_1}$ are infinite. This way one avoids double counting decorations passing through \mathbf{n}_2 that have been already counted as decorations associated with site ℓ or site \mathbf{n}_1 . As a result of these partial summations one can write for $G(\ell, \mathbf{m})$

$$G(\ell, \mathbf{m}) = \sum G(\ell, \ell) V G(\mathbf{n}_1, \mathbf{n}_1[\ell]) V \times G(\mathbf{n}_2, \mathbf{n}_2[\ell, \mathbf{n}_1]) V \cdots V G(\mathbf{m}, \mathbf{m}[\ell, \mathbf{n}_1, \mathbf{n}_2, \dots]) , \quad (\text{F.6})$$

where the summation is over all self-avoiding paths starting from ℓ and ending at \mathbf{m} , $\ell \rightarrow \mathbf{n}_1 \rightarrow \mathbf{n}_2 \rightarrow \cdots \rightarrow \mathbf{m}$. In particular, for the diagonal matrix elements $G(\ell, \ell)$ we have

$$G(\ell, \ell) = G_0(\ell) + \sum G(\ell, \ell) V G(\mathbf{n}_1, \mathbf{n}_1[\ell]) V \cdots G_0(\ell) , \quad (\text{F.7})$$

where again the summation extends over all closed self-avoiding paths starting from and ending at ℓ . The last factor is $G_0(\ell)$ because all decorations of the final site ℓ have already been counted as decorations of the initial site ℓ . Equation (F.7) can be rewritten as

$$G(\ell, \ell) = G_0(\ell) + G(\ell, \ell) \Delta(\ell) G_0(\ell) , \quad (\text{F.8})$$

where $\Delta(\ell)$ is called the self-energy¹ and is given by

$$\Delta(\ell) = \sum V G(\mathbf{n}_1, \mathbf{n}_1[\ell]) V \cdots V . \quad (\text{F.9})$$

Equation (F.8) can be solved for $G(\ell, \ell)$ to give

$$G(\ell, \ell; z) = \frac{G_0(\ell)}{1 - G_0(\ell) \Delta(\ell; z)} = \frac{1}{z - \varepsilon_\ell - \Delta(\ell; z)} . \quad (\text{F.10})$$

The last step follows from (F.4). Equation (F.10) justifies the name self-energy for $\Delta(\ell)$. The expansions (F.6), (F.7), and (F.9) for $G(\ell, \mathbf{m})$, $G(\ell, \ell)$, and $\Delta(\ell)$, respectively, are called the renormalized perturbation expansions (RPEs), [388, 445, 446]. Their characteristic property is that they involve summation over terms that are in one-to-one correspondence with the *self-avoiding*

¹ The name self-energy is used in the literature for different quantities depending on the forms of \mathcal{H}_0 and \mathcal{H}_1 .

paths in the lattice. The price for the simplification of having self-avoiding paths is that the factors associated with lattice sites are complicated Green's functions of the type $G(\mathbf{n}, \mathbf{n}[\ell, \mathbf{n}_1, \dots])$. These Green's functions can be evaluated by using again the RPE. One can iterate this procedure. Note that for a system involving only a *finite* number of sites, the summations associated with the RPE involve only a *finite* number of terms. The iteration procedure *terminates* also, since with every new step in the iteration at least one additional site is excluded. Thus, the RPE iterated as indicated above gives a *closed* expression for the Green's functions of a system involving a finite number of sites. For a system having an infinite number of sites the terms in each summation and the steps in the iteration procedure are infinite; thus for an infinite system the question of the convergence of the RPE arises.

The RPE can be used very successfully to calculate Green's functions for Bethe lattices. For the double periodic case shown in Fig. 5.11, we have for the self-energy $\Delta(\ell)$

$$\Delta(\ell) = (K + 1)V^2G(\ell + 1, \ell + 1[\ell]), \tag{F.11}$$

since there are only $K + 1$ self-avoiding paths starting from and ending at site ℓ (each one visiting a nearest neighbor). The quantity $G(\ell + 1, \ell + 1[\ell])$ can be written according to (F.10) as

$$G(\ell + 1, \ell + 1[\ell]) = \frac{1}{z - \varepsilon_{\ell+1} - \Delta(\ell + 1[\ell])}. \tag{F.12}$$

Using the RPE, the self-energy $\Delta(\ell + 1[\ell])$ can be written as

$$\Delta(\ell + 1[\ell]) = KV^2G(\ell + 2, \ell + 2[\ell + 1]). \tag{F.13}$$

We use K and not $(K + 1)$ since the self-avoiding path involving site ℓ is excluded. By combining (F.12) and (F.13), we have

$$G(\ell + 1, \ell + 1[\ell]) = \frac{1}{z - \varepsilon_{\ell+1} - KV^2G(\ell + 2, \ell + 2[\ell + 1])}. \tag{F.14}$$

Similarly,

$$G(\ell + 2, \ell + 2[\ell + 1]) = \frac{1}{z - \varepsilon_{\ell+2} - KV^2G(\ell + 3, \ell + 3[\ell + 2])}. \tag{F.15}$$

Because of the periodicity shown in Fig. 5.11, $G(\ell + 3, \ell + 3[\ell + 2]) = G(\ell + 1, \ell + 1[\ell])$. Thus (F.14) and (F.15) become a set of two equations for the two unknown quantities $G(\ell + 1, \ell + 1[\ell])$ and $G(\ell + 2, \ell + 2[\ell + 1]) = G(\ell, \ell[\ell + 1])$. By solving this system we obtain

$$\begin{aligned} &G(\ell + 1, \ell + 1[\ell]) \\ &= \frac{(z - \varepsilon_1)(z - \varepsilon_2) - \sqrt{(z - \varepsilon_1)(z - \varepsilon_2)[(z - \varepsilon_1)(z - \varepsilon_2) - 4KV^2]}}{2K(z - \varepsilon_{\ell+1})V^2}, \end{aligned} \tag{F.16}$$

$$\begin{aligned} &G(\ell, \ell[\ell + 1]) \\ &= \frac{(z - \varepsilon_1)(z - \varepsilon_2) - \sqrt{(z - \varepsilon_1)(z - \varepsilon_2)[(z - \varepsilon_1)(z - \varepsilon_2) - 4KV^2]}}{2K(z - \varepsilon_\ell)V^2}. \end{aligned} \tag{F.17}$$

Substituting in (F.11) and (F.10) we obtain for $G(\ell, \ell)$ the expression given in (5.57) and (5.58).

For the calculation of the off-diagonal matrix element, $G(\ell, m)$, one can apply (F.6). For a Bethe lattice there is just one self-avoiding diagram connecting site ℓ with site m ; $G(\ell + 1, \ell + 1[\ell])$ has already been calculated, and $G(\ell + 2, \ell + 2[\ell, \ell + 1])$ equals $G(\ell + 2, \ell + 2[\ell + 1])$, which has been evaluated. These two quantities alternate as we proceed along the sites of the unique path connecting ℓ with m . Thus one obtains the expressions (5.59a), (5.59b), and (5.60) for $G(\ell, m)$.

We mention without proof two theorems concerning products of the form

$$P = G(\boldsymbol{\ell}, \boldsymbol{\ell}, z)G(\mathbf{n}_1, \mathbf{n}_1[\boldsymbol{\ell}]; z) \\ \times G(\mathbf{n}_2, \mathbf{n}_2[\boldsymbol{\ell}, \mathbf{n}_1]; z) \cdots G(\mathbf{m}, \mathbf{m}[\boldsymbol{\ell}, \mathbf{n}_1, \mathbf{n}_2 \dots]; z) .$$

The first states that

$$P = \frac{\prod_i (z - E_i^a)}{\prod_j (z - E_j)} , \tag{F.18}$$

where $\{E_i^a\}$ is the eigenenergies of \mathcal{H} with sites $\boldsymbol{\ell}, \mathbf{n}_1, \mathbf{n}_2, \dots, \mathbf{m}$ removed, i.e., $\varepsilon_{\boldsymbol{\ell}} = \varepsilon_{\mathbf{n}_1} = \varepsilon_{\mathbf{n}_2} = \dots = \varepsilon_{\mathbf{m}} = \infty$, and $\{E_j\}$ is the eigenenergies of \mathcal{H} . The second theorem states that

$$P = \det\{G\} , \tag{F.19}$$

where G is a matrix with matrix elements $G(\mathbf{s}, \mathbf{r}, z)$, where both \mathbf{s} and \mathbf{r} belong to the set $\{\boldsymbol{\ell}, \mathbf{n}_1, \mathbf{n}_2, \dots, \mathbf{m}\}$.

G

Boltzmann's Equation

The function to be determined by employing Boltzmann's equation (BE) is the density, $f(\mathbf{r}, \mathbf{k}; t)$, of particles in phase space, defined by the relation

$$dN \equiv (2s + 1) \frac{d^d r d^d k}{(2\pi)^d} f(\mathbf{r}, \mathbf{k}; t) ,$$

where dN is the number of particles in the phase space volume element $d^d r d^d k$ around the point \mathbf{r}, \mathbf{k} at time t . In what follows, we shall assume that the spin $s = 1/2$. Since we specify both the position, \mathbf{r} , and the (crystal) momentum, $\hbar\mathbf{k}$, it is clear that we work within the framework of the semiclassical approximation.

If there were no interactions among the particles or collisions with defects and other departures from periodicity, the total time derivative, df/dt , would be equal to zero according to Liouville's theorem

$$\frac{df}{dt} \equiv \frac{\partial f}{\partial t} + \frac{\partial f}{\partial \mathbf{r}} \cdot \frac{d\mathbf{r}}{dt} + \frac{\partial f}{\partial \mathbf{k}} \cdot \frac{d\mathbf{k}}{dt} = 0 . \quad (\text{G.1})$$

However, because of collisions with defects and particle interactions, the rhs of (G.1) is not zero but equal to $(\partial f/\partial t)_c$, where the subscript c indicates any kind of collision or interaction.

The simplest expression of $(\partial f/\partial t)_c$ is through the introduction of a phenomenological relaxation time τ :

$$\left(\frac{\partial f}{\partial t} \right)_c \simeq -\frac{f - f_0}{\tau} \equiv -\frac{f_1}{\tau} , \quad (\text{G.2})$$

where f_0 is the form of f in a state of thermodynamic equilibrium,

$$f_0(\varepsilon_k) = \frac{1}{\exp[\beta(\varepsilon_k - \mu)] + 1} , \quad (\text{G.3})$$

the chemical potential μ is determined by the condition

$$2 \int d\mathbf{r} d\mathbf{k} \frac{f_0(\varepsilon_{\mathbf{k}})}{(2\pi)^d} = N ,$$

and $f_1 \equiv f - f_0$. More realistic choices for $(\partial f / \partial t)_c$ do exist. For example, if the particles are fermions and if the only collisions are elastic scatterings by static short-range defect potentials, then we have

$$\left(\frac{\partial f(\mathbf{r}, \mathbf{k}; t)}{\partial t} \right)_c = \Omega \int \frac{d\mathbf{k}'}{(2\pi)^d} \times \{f(\mathbf{r}, \mathbf{k}'; t) [1 - f(\mathbf{r}, \mathbf{k}; t)] - f(\mathbf{r}, \mathbf{k}; t) [1 - f(\mathbf{r}, \mathbf{k}'; t)]\} Q(\mathbf{k}, \mathbf{k}') , \quad (\text{G.4})$$

where $Q(\mathbf{k}, \mathbf{k}')$ is the probability per unit time that a particle of initial wavevector \mathbf{k} will find itself with a wavevector \mathbf{k}' after a collision. We assume that $Q(\mathbf{k}, \mathbf{k}') = Q(\mathbf{k}', \mathbf{k})$ as a result of time reversal. According to (4.48)

$$Q(\mathbf{k}, \mathbf{k}') = N_{\text{imp}} W_{\mathbf{k}, \mathbf{k}'} = \Omega n_{\text{imp}} (2\pi/\hbar) |\langle \mathbf{k} | T | \mathbf{k}' \rangle|^2 \delta(\varepsilon_{\mathbf{k}} - \varepsilon'_{\mathbf{k}}) ,$$

where $n_{\text{imp}} \equiv N_{\text{imp}}/\Omega$ is the concentration of the scattering centers and T is the t -matrix for each of those centers. The rate for the process $\mathbf{k}' \rightarrow \mathbf{k}$ is also proportional to the occupation, f' , of the state \mathbf{k}' and to the availability, $1 - f$, of the state \mathbf{k} ; the same is true for the rate of the inverse process, $\mathbf{k} \rightarrow \mathbf{k}'$, which enters with a minus sign since it reduces the magnitude of $f(\mathbf{r}, \mathbf{k}; t)$.

In (G.1), $d\mathbf{r}/dt = \mathbf{v}$ and $d\mathbf{k}/dt = \hbar^{-1}q(\mathbf{E} + \mathbf{v} \times \mathbf{B}/c)$, where \mathbf{E} and \mathbf{B} are the imposed electric and magnetic fields, respectively, and q is the charge of the carrier ($-e$ for electrons). Hence

$$\begin{aligned} \frac{\partial f}{\partial \mathbf{k}} \cdot \frac{d\mathbf{k}}{dt} &= \left(\frac{\partial f_0}{\partial \mathbf{k}} + \frac{\partial f_1}{\partial \mathbf{k}} \right) \cdot \left(\mathbf{E} + \frac{\mathbf{v}}{c} \times \mathbf{B} \right) \hbar^{-1}q \\ &= \left(\frac{\partial f_0}{\partial \varepsilon_{\mathbf{k}}} \frac{\partial \varepsilon_{\mathbf{k}}}{\partial \mathbf{k}} + \frac{\partial f_1}{\partial \mathbf{k}} \right) \cdot \left(\mathbf{E} + \frac{\mathbf{v}}{c} \times \mathbf{B} \right) \hbar^{-1}q \\ &= q \frac{\partial f_0}{\partial \varepsilon_{\mathbf{k}}} \mathbf{v}_{\mathbf{k}} \cdot \mathbf{E} + \frac{q}{c\hbar} \frac{\partial f_1}{\partial \mathbf{k}} \cdot (\mathbf{v} \times \mathbf{B}) . \end{aligned} \quad (\text{G.5})$$

In the last relation we have used the fact that $(\partial \varepsilon_{\mathbf{k}} / \partial \mathbf{k}) \cdot (\mathbf{v} \times \mathbf{B}) = 0$, since $\partial \varepsilon_{\mathbf{k}} / \partial \mathbf{k} = \hbar \mathbf{v}$, and we have omitted the term $(\partial f_1 / \partial \mathbf{k}) \cdot \mathbf{E} \hbar^{-1}q$, since it is of second order in \mathbf{E} (taking into account that f_1 is of first order in \mathbf{E}). In calculating quantities as the conductivity that represent linear response to \mathbf{E} , there is no need to keep terms of higher order than the first in \mathbf{E} .

If we take into account that $\varepsilon_{\mathbf{k}} = \varepsilon'_{\mathbf{k}}$ (since the collisions are elastic) and, consequently, $f_0(\varepsilon_{\mathbf{k}}) = f_0(\varepsilon_{\mathbf{k}'})$, (G.4) becomes

$$\left(\frac{\partial f(\mathbf{r}, \mathbf{k}; t)}{\partial t} \right)_c = \Omega \int \frac{d\mathbf{k}'}{(2\pi)^d} [f_1(\mathbf{r}, \mathbf{k}'; t) - f_1(\mathbf{r}, \mathbf{k}; t)] Q(\mathbf{k}, \mathbf{k}') . \quad (\text{G.6})$$

If the fields \mathbf{E} and \mathbf{B} are taken as constant, the density $f(\mathbf{r}, \mathbf{k}; t)$ does not depend on \mathbf{r} and t and the linearized BE takes the form

$$\frac{q}{c\hbar} \frac{\partial f_1}{\partial \mathbf{k}} \cdot (\mathbf{v}_{\mathbf{k}} \times \mathbf{B}) + \frac{f_1}{\tau} = -q \frac{\partial f_0}{\partial \varepsilon_{\mathbf{k}}} \mathbf{v}_{\mathbf{k}} \cdot \mathbf{E} \quad (\text{G.7})$$

[if we make the simplest assumption (G.2) for the collision term], and the form

$$\begin{aligned} & \frac{q}{c\hbar} \frac{\partial f_1}{\partial \mathbf{k}} \cdot (\mathbf{v} \times \mathbf{B}) + \Omega \int \frac{d\mathbf{k}'}{(2\pi)^d} [f_1(\mathbf{k}) - f_1(\mathbf{k}')] Q(\mathbf{k}, \mathbf{k}') \\ & = -q \frac{\partial f_0}{\partial \varepsilon_{\mathbf{k}}} \mathbf{v}_{\mathbf{k}} \cdot \mathbf{E} \end{aligned} \quad (\text{G.8})$$

if we use the more realistic expression (G.6).

We examine first the case of no magnetic field, $\mathbf{B} = 0$. Equation (G.7) gives immediately the solution

$$f_1(\mathbf{k}) = -q\tau \frac{\partial f_0}{\partial \varepsilon_{\mathbf{k}}} \mathbf{v}_{\mathbf{k}} \cdot \mathbf{E}, \quad (\text{G.9})$$

while the more realistic case (G.8) may again admit a solution of the form (G.9) [in view of the rhs of (G.8)] with an energy-dependent τ , $\tau(\varepsilon_{\mathbf{k}})$, which can be obtained in terms of $Q(\mathbf{k}, \mathbf{k}')$. Indeed, taking into account the form of $f_1(\mathbf{k})$ and that the direction of \mathbf{E} is arbitrary, we find

$$\tau(\varepsilon_{\mathbf{k}}) \Omega \left\{ \mathbf{v}_{\mathbf{k}} \int \frac{d\mathbf{k}'}{(2\pi)^d} Q(\mathbf{k}, \mathbf{k}') - \int \frac{d\mathbf{k}'}{(2\pi)^d} Q(\mathbf{k}, \mathbf{k}') \mathbf{v}_{\mathbf{k}'} \right\} = \mathbf{v}_{\mathbf{k}}. \quad (\text{G.10})$$

Since two of the three terms in (G.10) are proportional to $\mathbf{v}_{\mathbf{k}}$, the third term, $\int (d\mathbf{k}'/(2\pi)^d) Q(\mathbf{k}, \mathbf{k}') \mathbf{v}_{\mathbf{k}'}$, must be proportional to $\mathbf{v}_{\mathbf{k}}$. Hence, by analyzing $\mathbf{v}_{\mathbf{k}'}$ to $\mathbf{v}_{\mathbf{k}'\parallel} = (\mathbf{v}_{\mathbf{k}}/v_{\mathbf{k}}) v_{\mathbf{k}'} \cos \theta$ and to $\mathbf{v}_{\mathbf{k}'\perp}$, we see that only $\mathbf{v}_{\mathbf{k}'\parallel}$ makes a contribution to the third term; the angle θ is between \mathbf{k} and \mathbf{k}' . Furthermore, if $\varepsilon_{\mathbf{k}}$ is isotropic, then $v_{\mathbf{k}} = v_{\mathbf{k}'}$ and

$$\tau(\varepsilon_{\mathbf{k}}) \Omega \int \frac{d\mathbf{k}'}{(2\pi)^d} Q(\mathbf{k}, \mathbf{k}') (1 - \cos \theta) = 1. \quad (\text{G.11})$$

Taking into account the expression for $Q(\mathbf{k}, \mathbf{k}')$ and the fact that

$$\frac{d\mathbf{k}'}{(2\pi)^3} = \frac{d\varepsilon_{\mathbf{k}} \varrho(\varepsilon'_{\mathbf{k}}) d\mathcal{O}}{4\pi},$$

we find

$$\frac{1}{\tau(\varepsilon_{\mathbf{k}})} = \frac{2\pi}{\hbar} \varrho(\varepsilon_{\mathbf{k}}) \frac{n_{\text{imp}} \Omega^2}{4\pi} \int d\mathcal{O} |\langle \mathbf{k} | T(\varepsilon_{\mathbf{k}}) | \mathbf{k}' \rangle|^2 (1 - \cos \theta), \quad (\text{G.12})$$

which coincides with (8.22) by setting $\varepsilon_{\mathbf{k}} = E_F$ and $T' = \Omega T$.

Assuming that $\varepsilon(k) = \hbar^2 k^2 / 2m^*$, we have that

$$\rho(\varepsilon_k) = \frac{m^{*2} v}{2\pi^2 \hbar^3}$$

and

$$|\langle \mathbf{k} | T'(\varepsilon_k) | \mathbf{k}' \rangle|^2 = \frac{4\pi^2 \hbar^4}{m^{*2}} \frac{d\sigma}{d\mathcal{O}}.$$

Substituting these expressions into (G.12) we can recast it as follows:

$$\frac{1}{\tau_{\text{tr}}} = v n_{\text{imp}} \sigma_{\text{tr}}$$

or

$$\frac{1}{\ell_{\text{tr}}} = n_{\text{imp}} \sigma_{\text{tr}}, \tag{G.12'}$$

where $v = \partial\varepsilon(k)/\hbar\partial k$ and $\ell_{\text{tr}} = v\tau_{\text{tr}}$.

We return now to the case where there is a nonzero magnetic field, \mathbf{B} , whose direction is taken as the z -axis. We assume further that the collision term is given by (G.2) and (G.12). Instead of the triad k_x, k_y, k_z , we shall use the triad ϕ, ε_k, k_z , where the phase $\phi = \phi(t) + \phi_0$ is given by the formula

$$\phi = \phi(t) + \phi_0 = \omega_c t + \phi_0,$$

and ω_c is the cyclotron frequency, $\omega_c = |q| B / m^* c$ (in SI $\omega_c = |q| B / m^*$).

In the new variables only ϕ changes with \mathbf{B} :

$$\frac{\partial f}{\partial \mathbf{k}} \cdot \left(\frac{d\mathbf{k}}{dt} \right)_{\mathbf{B}} = \frac{\partial f_1}{\partial \phi} \left(\frac{\partial \phi}{\partial t} \right)_{\mathbf{B}} = \omega_c \frac{\partial f_1}{\partial \phi}. \tag{G.13}$$

Substituting (G.13) into (G.7) we have

$$\omega_c \frac{\partial f_1}{\partial \phi} + \frac{f_1}{\tau_{\text{tr}}} = -q \frac{\partial f_0}{\partial \varepsilon_{\mathbf{k}}} \mathbf{v} \cdot \mathbf{E}. \tag{G.14}$$

This equation can be solved by employing Green's function techniques (Problem 8.8). The solution is

$$f_1(\phi, \varepsilon_k, k_z) = \frac{q}{\omega_c} \left(-\frac{\partial f_0}{\partial \varepsilon_{\mathbf{k}}} \right) \int_{-\infty}^{\phi} d\phi' \exp\left(\frac{\phi' - \phi}{\omega_c \tau_{\text{tr}}} \right) \mathbf{v}(\phi', \varepsilon_k, k_z) \cdot \mathbf{E}. \tag{G.15}$$

Assuming that $\varepsilon_{\mathbf{k}} = \hbar^2 k^2 / 2m^*$, we have that

$$d^3 k = \left(\frac{m^*}{\hbar^2} \right) d\phi d\varepsilon_k dk_z.$$

Substituting this last relation into the expression for the current density,

$$\mathbf{j} = 2q \int \frac{d^3 k}{(2\pi)^3} \mathbf{v}_k f_1(\mathbf{k}),$$

and taking into account (G.15), we find for the conductivity tensor in the presence of magnetic field the following expression:

$$\begin{aligned} \sigma_{ij} = & \frac{q^2}{4\pi^3\hbar^2} \int d\varepsilon_k \left(-\frac{\partial f_0}{\partial \varepsilon_k} \right) \int dk_z \frac{m^*}{\omega_c} \\ & \times \int_0^{2\pi} d\phi \int_{-\infty}^0 d\phi' v_i(\phi) v_j(\phi') \exp\left(\frac{\phi' - \phi}{\omega_c \tau}\right). \end{aligned} \quad (\text{G.16})$$

Notice that both $v_i(\phi)$ and $v_j(\phi')$ depend also on ε_k and k_z . For metals, where $-\partial f_0/\partial \varepsilon_k = \delta(\varepsilon_k - E_F)$, (G.16) becomes

$$\sigma_{ij} = \frac{q^2}{4\pi^3\hbar^2} \int dk_z \frac{m^*}{\omega_c} \int_0^{2\pi} d\phi \int_{-\infty}^0 d\phi' v_i(\phi) v_j(\phi + \phi') \exp(\phi'/\omega_c \tau), \quad (\text{G.17})$$

where $q = -e$ for electrons.

Equations (G.16) and (G.17) are known as *Shockley's tube-integral formulae* and constitute the basis for calculating the magnetoresistance tensor.

H

Transfer Matrix, S -Matrix, etc.

We shall consider first a 1-d model described by the hermitian Hamiltonian $\mathcal{H} = \mathcal{H}_0 + \mathcal{H}_1$, where

$$\mathcal{H}_0 = -\frac{\hbar^2}{2m} \frac{d^2}{dx^2} \quad (\text{H.1a})$$

and

$$\mathcal{H}_1 = \begin{cases} 0, & x < 0, \\ V(x), & 0 < x < L, \\ V_0, & L < x, \end{cases} \quad (\text{H.1b})$$

with V_0 being constant and $V(x)$ an arbitrary real function of x .

The eigenfunction(s) corresponding to the eigenenergy E (where $E > 0$ and $E > V_0$) is (are) of the form

$$\psi(x) = \begin{cases} A_1 \exp(ik_1x) + B_1 \exp(-ik_1x), & x < 0, \\ A_2 \exp(ik_2x) + B_2 \exp(-ik_2x), & L < x, \end{cases} \quad (\text{H.2a})$$

$$(\text{H.2b})$$

where $k_1 > 0$, $k_2 > 0$, $E = \hbar^2 k_1^2 / 2m$, and $E = V_0 + \hbar^2 k_2^2 / 2m$.

If we know the solution in the region $x < 0$, we can obtain, in principle, the solution everywhere (since ψ obeys Schrödinger equation). Hence, both A_2 and B_2 are linear functions of A_1 and B_1 :

$$A_2 = \alpha A_1 + \beta B_1, \quad (\text{H.3})$$

where the coefficients α and β are functions of E , V_0 , and L and functionals of $V(x)$.

Since the Hamiltonian is hermitian, there is *time-reversal symmetry*, which means that $\psi^*(x)$ is also an eigensolution with the same eigenenergy as that of $\psi(x)$:

$$\psi^*(x) = \begin{cases} A_1^* \exp(-ik_1x) + B_1^* \exp(ik_1x), & x < 0, \\ A_2^* \exp(-ik_2x) + B_2^* \exp(ik_2x), & L < x. \end{cases} \quad (\text{H.4a})$$

$$(\text{H.4b})$$

Comparing (H.4) with (H.2) we see that the former results from the latter by the substitutions $A_1 \rightarrow B_1^*$, $B_1 \rightarrow A_1^*$, $A_2 \rightarrow B_2^*$, and $B_2 \rightarrow A_2^*$. Hence, (H.3) with these substitutions is transformed into

$$B_2^* = \alpha B_1^* + \beta A_1^* \quad (\text{H.5})$$

or

$$B_2 = \alpha^* B_1 + \beta^* A_1. \quad (\text{H.5}')$$

Combining (H.3) and (H.5') we can write in matrix form

$$\begin{pmatrix} A_2 \\ B_2 \end{pmatrix} = M \begin{pmatrix} A_1 \\ B_1 \end{pmatrix}, \quad (\text{H.6})$$

where

$$M = \begin{pmatrix} \alpha & \beta \\ \beta^* & \alpha^* \end{pmatrix}; \quad (\text{H.7})$$

M is the so-called *transfer matrix*. The advantage of this matrix is that it allows us to transfer our knowledge of the solution from the region $x < 0$ to the region $x > L$.

Furthermore, in the case of more complicated Hamiltonians consisting of alternating regions of constant and varying potentials, we can propagate the solution by repeated applications of relation (H.6), which is equivalent to the multiplication of consecutive transfer matrices.

The coefficients α and β of the transfer matrix are related to the transmission and reflection amplitudes. Indeed, if $B_2 = 0$, then we have an incoming wave coming from the left; then the transmission amplitude, $t_{21} \equiv t_{2 \leftarrow 1}$, equals the ratio A_2/A_1 and the reflection amplitude, $r_{11} = B_1/A_1$. From (H.5') we have that

$$r_{11} = \left(\frac{B_1}{A_1} \right)_{B_2=0} = -\frac{\beta^*}{\alpha^*}, \quad (\text{H.8})$$

since $B_2 = 0$. Using (H.8) and (H.3) we find that

$$t_{21} = \left(\frac{A_2}{A_1} \right)_{B_2=0} = \frac{|\alpha|^2 - |\beta|^2}{\alpha^*}. \quad (\text{H.9})$$

Similarly, if the wave is coming from the right, we have that $A_1 = 0$, and then the reflection amplitude is $r_{22} = A_2/B_2$, while the transmission amplitude $t_{12} \equiv t_{1 \leftarrow 2} = B_1/B_2$.

From (H.5') we have

$$t_{12} = \left(\frac{B_1}{B_2} \right)_{A_1=0} = \frac{1}{\alpha^*}. \quad (\text{H.10})$$

Combining (H.10) and (H.3) we find

$$r_{22} = \left(\frac{A_2}{B_2} \right)_{A_1=0} = \frac{\beta}{\alpha^*}. \quad (\text{H.11})$$

We can express α and β in terms of the transmission and reflection amplitudes by employing (H.8), (H.9), (H.10), and (H.11):

$$\alpha = \frac{1}{t_{12}^*} = \frac{t_{21}}{1 - |r_{11}|^2}, \quad (\text{H.12})$$

$$\beta = \frac{r_{22}}{t_{12}} = -\frac{t_{21}r_{11}^*}{1 - |r_{11}|^2}. \quad (\text{H.13})$$

Conservation of probability, i.e., conservation of the number of particles, provides another relation between α and β , since the flux in the left, $k_1 (|A_1|^2 - |B_1|^2)$, must be the same as the flux in the right, $k_2 (|A_2|^2 - |B_2|^2)$. By setting B_2 or A_1 equal to zero we have, respectively,

$$k_1 (1 - |r_{11}|^2) = k_2 |t_{21}|^2, \quad (\text{H.14})$$

$$k_2 (1 - |r_{22}|^2) = k_1 |t_{12}|^2. \quad (\text{H.15})$$

We have

$$\begin{aligned} |r_{11}|^2 &= R_{11}, \\ |r_{22}|^2 &= R_{22}, \\ \left(\frac{k_2}{k_1}\right) |t_{21}|^2 &= T_{21}, \end{aligned}$$

and

$$\left(\frac{k_1}{k_2}\right) |t_{12}|^2 = T_{12},$$

where R_{11} and R_{22} are the reflection coefficients from the left and the right, respectively, and T_{21} and T_{12} are the transmission coefficients from the left and the right, respectively. Thus (H.14) is equivalent to $R_{11} + T_{21} = 1$ and (H.15) to $R_{22} + T_{12} = 1$. Comparing (H.8) with (H.11) we find that $|r_{22}| = |r_{11}|$. Hence

$$R_{11} = R_{22} \quad \text{and} \quad T_{21} = T_{12}. \quad (\text{H.16})$$

Dividing (H.14) by (H.15) we find that

$$\frac{|t_{21}|^2}{|t_{12}|^2} = \frac{k_1^2}{k_2^2},$$

which, in view of (H.9) and (H.10), leads to

$$|\alpha|^2 - |\beta|^2 = \frac{k_1}{k_2}. \quad (\text{H.17})$$

To simplify the notation, we introduce *current* amplitudes \hat{A}_i, \hat{B}_i , ($i = 1, 2$), related to the corresponding wavefunction amplitudes A_i and B_i by the relations

$$\hat{A}_i = \sqrt{v_i} A_i \quad \text{and} \quad \hat{B}_i = \sqrt{v_i} B_i, \quad (i = 1, 2),$$

where v_i , ($i = 1, 2$) is the velocity $\hbar k_i/m$ in segment i . Then, the *current* reflection and transmission amplitudes are defined by ratios of \hat{B} s and \hat{A} s, analogous to (H.8), (H.9), (H.10), and (H.11). As a result, $\hat{r}_{ii} = r_{ii}$, but

$$\hat{t}_{ij} = \sqrt{\frac{v_i}{v_j}} t_{ij} \quad \text{and} \quad t_{ij} = \sqrt{\frac{v_j}{v_i}} \hat{t}_{ij}. \quad (\text{H.18})$$

In terms of the \hat{t}_{ij} , the transmission coefficient T_{ij} is given by

$$T_{ij} = |\hat{t}_{ij}|^2. \quad (\text{H.19})$$

Similarly, (H.14) and (H.15) simplify to

$$1 - |\hat{r}_{ii}|^2 = |\hat{t}_{ji}|^2. \quad (\text{H.14}')$$

Furthermore, (H.6) becomes

$$\begin{pmatrix} \hat{A}_2 \\ \hat{B}_2 \end{pmatrix} = \hat{M} \begin{pmatrix} \hat{A}_1 \\ \hat{B}_1 \end{pmatrix}, \quad (\text{H.6}')$$

where

$$\hat{M} = \begin{pmatrix} \hat{\alpha} & \hat{\beta} \\ \hat{\beta}^* & \hat{\alpha}^* \end{pmatrix} = \sqrt{\frac{v_2}{v_1}} \begin{pmatrix} \alpha & \beta \\ \beta^* & \alpha^* \end{pmatrix}, \quad (\text{H.20})$$

i.e.,

$$\hat{\alpha} = \sqrt{\frac{v_2}{v_1}} \alpha, \quad \hat{\beta} = \sqrt{\frac{v_2}{v_1}} \beta. \quad (\text{H.20}')$$

Then, in terms of the hatted quantities, (H.8)–(H.11) remain valid. Finally, matrix \hat{M} is unitary, $\hat{M}\hat{M}^\dagger = 1$, which implies that

$$|\hat{\alpha}|^2 - |\hat{\beta}|^2 = 1. \quad (\text{H.17}')$$

We shall define another matrix, called the *S-matrix*, which relates the outgoing waves to the incoming waves. As we shall see, the *S-matrix* is the 1-d analog of the *S-matrix* we defined in Chap. 4:

$$\begin{pmatrix} \hat{B}_1 \\ \hat{A}_2 \end{pmatrix} \equiv \hat{S} \begin{pmatrix} \hat{A}_1 \\ \hat{B}_2 \end{pmatrix}. \quad (\text{H.21})$$

It follows immediately (by setting either \hat{B}_2 or \hat{A}_1 equal to zero) that

$$\hat{S} = \begin{pmatrix} \hat{r}_{11} & \hat{t}_{12} \\ \hat{t}_{21} & \hat{r}_{22} \end{pmatrix} \quad (\text{H.22a})$$

$$= \frac{1}{\hat{\alpha}^*} \begin{pmatrix} -\hat{\beta}^* & 1 \\ (|\hat{\alpha}|^2 - |\hat{\beta}|^2) & \hat{\beta} \end{pmatrix}. \quad (\text{H.22b})$$

Of special interest is the case where $V_0 = 0$; then the ratios of current amplitudes and wavefunction amplitudes are identical. Since the perturbation \mathcal{H}_1 is confined within the finite region $(0, L)$, the reflection and transmission amplitudes can be found by employing (4.31)

$$\begin{aligned} \langle x | \psi \rangle &= \langle x | k \rangle + \langle x | G_0^+ T^+ | k \rangle \\ &= \frac{1}{\sqrt{L}} e^{ikx} + \sum_{k'} \langle x | G_0^+ | k' \rangle \langle k' | T^+ | k \rangle, \quad k > 0, \end{aligned} \quad (\text{H.23})$$

where, taking into account (3.32), we have

$$\begin{aligned} \langle x | G_0^+ | k' \rangle &= \int dx' \langle x | G_0^+ | x' \rangle \langle x' | k' \rangle = \frac{1}{\sqrt{L}} \int dx' G_0^+(x, x') \exp(ik'x') \\ &= \frac{1}{\sqrt{L}} \frac{-im}{\hbar^2 k} \int dx' \exp(ik|x - x'|) \exp(ik'x'). \end{aligned} \quad (\text{H.24})$$

For the transmission amplitude, we must choose $x > L$, which implies $x > x'$. Then, substituting (H.24) into (H.23), multiplying by \sqrt{L} , and performing the integration over x' [which gives $2\pi\delta(k - k')$], we find

$$\sqrt{L}\psi(x) = e^{ikx} \left(1 + \frac{-im}{\hbar^2 k} \langle k | T'^+ | k \rangle \right), \quad T' = LT. \quad (\text{H.25})$$

Hence

$$t_{21} = 1 + G_0^+(x, x) \langle k | T'^+ | k \rangle, \quad (\text{H.26})$$

where $G_0^+(x, x) = -im/\hbar^2 k = -i/\hbar v_k$ (v_k is the velocity) and

$$\langle k | T'^+ | k \rangle = \int dx' dx'' \exp[ik(x' - x'')] \langle x'' | T^+ | x' \rangle. \quad (\text{H.27})$$

Choosing $x < 0$, which implies $|x - x'| = x' - x$, we find for the reflection amplitude, r_{11} , the following expression:

$$r_{11} = G_0^+(x, x) \langle -k | T'^+ | k \rangle, \quad (\text{H.28})$$

where

$$\langle -k | T'^+ | k \rangle = \int dx' dx'' \exp[ik(x' + x'')] \langle x'' | T^+ | x' \rangle. \quad (\text{H.29})$$

Similarly, we find

$$t_{12} = 1 + G_0^+(x, x) \langle -k | T'^+ | -k \rangle, \quad k > 0, \quad (\text{H.30})$$

$$r_{22} = G_0^+(x, x) \langle k | T'^+ | -k \rangle, \quad k > 0. \quad (\text{H.31})$$

Equations (H.26), (H.28), (H.30), and (H.31) are the 1-d analog of (4.46).

Quite similar expressions to those in (H.26)–(H.31) for t_{21} , r_{11} , t_{12} , r_{22} , and S are valid for a 1-d TBM with

$$\langle \ell | \mathcal{H}_0 | m \rangle = \varepsilon_0 \delta_{\ell m} + V(1 - \delta_{\ell m})$$

and

$$\mathcal{H}_1 = \sum_{\ell=1}^{\ell_0} |\ell\rangle \varepsilon_\ell \langle \ell|$$

($\ell_0 a$ being equal to the length L). Combining (5.31) and (5.17), and taking into account that $v_k = \partial E_k / \hbar \partial k$, instead of

$$G_0^+(x, x) = -\frac{im}{\hbar^2 k} = -\frac{i}{\hbar v_k},$$

we must set

$$G_0^+(\ell, \ell) = -\frac{i}{B |\sin(ka)|} = -\frac{i}{\hbar v_k}.$$

In the limit $k \rightarrow 0$, $v_k \rightarrow \hbar k / m^*$, where $m^* = \hbar^2 / B a^2$, $B = 2|V|$. Furthermore, we have

$$\langle k | T'^+ | k \rangle = \sum_{\ell, m} e^{ika(\ell-m)} \langle m | T^+ | \ell \rangle, \quad k > 0, \quad (\text{H.32})$$

$$\langle -k | T'^+ | k \rangle = \sum_{\ell, m} e^{ika(\ell+m)} \langle m | T^+ | \ell \rangle, \quad k > 0, \quad (\text{H.33})$$

$$\langle -k | T'^+ | -k \rangle = \sum_{\ell, m} e^{-ika(\ell-m)} \langle m | T^+ | \ell \rangle, \quad k > 0, \quad (\text{H.34})$$

$$\langle k | T'^+ | -k \rangle = \sum_{\ell, m} e^{-ika(\ell+m)} \langle m | T^+ | \ell \rangle, \quad k > 0. \quad (\text{H.35})$$

The transfer matrix for $V_0 = 0$,

$$\hat{M} = M = M(0) = \begin{pmatrix} \alpha & \beta \\ \beta^* & \alpha^* \end{pmatrix},$$

was associated with the potential $V(x)$ placed between 0 and L . If the same potential is rigidly transposed by a length L_0 so as to be located between L_0 and $L_0 + L$, then the transfer matrix would be $M(L_0)$. To find the relation between $M(L_0)$ and $M(0)$, it is sufficient to introduce a new coordinate $x' =$

$x - L_0$; then $A_1 e^{ikx}$ would become $A_1 \exp(ikL_0) \exp(ikx')$, $B_1 e^{-ikx}$ would become $B_1 \exp(-ikL_0) \exp(-ikx')$, and so on.

The potential between L_0 and $L_0 + L$ expressed in terms of x' is exactly equivalent to the potential between 0 and L expressed in terms of x . Hence, the quantities $A_2 \exp(ikL_0)$, $B_2 \exp(-ikL_0)$ and $A_1 \exp(ikL_0)$, $B_1 \exp(-ikL_0)$ are connected through $M(0)$:

$$\begin{pmatrix} A_2 \exp(ikL_0) \\ B_2 \exp(-ikL_0) \end{pmatrix} = M(0) \begin{pmatrix} A_1 \exp(ikL_0) \\ B_1 \exp(-ikL_0) \end{pmatrix}. \tag{H.36}$$

By introducing the $V = 0$ transfer matrix for length L_0 :

$$M_0(L_0) = \begin{pmatrix} \exp(ikL_0) & 0 \\ 0 & \exp(-ikL_0) \end{pmatrix}, \tag{H.37}$$

(H.36) becomes

$$\begin{pmatrix} A_2 \\ B_2 \end{pmatrix} = M(L_0) \begin{pmatrix} A_1 \\ B_1 \end{pmatrix},$$

with

$$M(L_0) = M_0^*(L_0) M(0) M_0(L_0). \tag{H.38}$$

Equation (H.38) allows us to propagate easily the solution along a linear chain consisting of alternating segments of $V = 0$ and $V(x) \neq 0$ as shown in Fig. H.1. Indeed, we have the recursive relation that, by repeated application, connects A_{n+1} , B_{n+1} to A_1 , B_1 :

$$\begin{aligned} \begin{pmatrix} A_{n+1} \\ B_{n+1} \end{pmatrix} &= M_0^*(L_n) M_n(0) M_0(L_n) \begin{pmatrix} A_n \\ B_n \end{pmatrix} \equiv M_n(L_n) \begin{pmatrix} A_n \\ B_n \end{pmatrix} \\ &= M_n(L_n) M_{n-1}(L_{n-1}) \cdots M_1(0) \begin{pmatrix} A_1 \\ B_1 \end{pmatrix} \end{aligned}$$

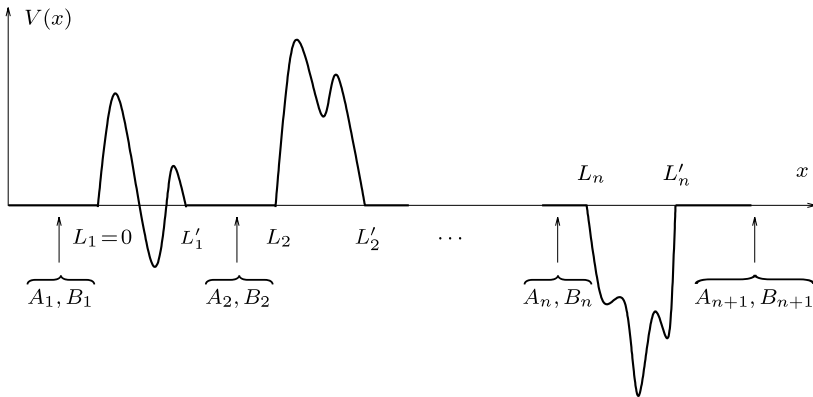


Fig. H.1. A 1-d potential of alternating segments where $V(x) \neq 0$ and $V(x) = 0$

$$\begin{aligned}
 &= M_0^*(L_n) M_n(0) M_0(L_n) M_0^*(L_{n-1}) M_{n-1}(0) M_0(L_{n-1}) \cdots \\
 &\quad \cdots M_0^*(L_2) M_2(0) M_0(L_2) M_1(0) \begin{pmatrix} A_1 \\ B_1 \end{pmatrix} \\
 &= M_0^*(L_n) M_n(0) M_0(L_n - L_{n-1}) M_{n-1}(0) M_0(L_{n-1} - L_{n-2}) \cdots \\
 &\quad \cdots M_0(L_3 - L_2) M_2(0) M_0(L_2 - L_1) M_1(0) \begin{pmatrix} A_1 \\ B_1 \end{pmatrix}. \tag{H.39}
 \end{aligned}$$

If the system is periodic with period a , the result is

$$\begin{pmatrix} A_{n+1} \\ B_{n+1} \end{pmatrix} = M_0^*((n-1)a) [\tilde{M}]^{n-1} M(0) \begin{pmatrix} A_1 \\ B_1 \end{pmatrix}, \tag{H.40}$$

where

$$\tilde{M} = \begin{pmatrix} e^{ika} & 0 \\ 0 & e^{-ika} \end{pmatrix} M(0) = \begin{pmatrix} e^{ika} \alpha & e^{ika} \beta \\ e^{-ika} \beta^* & e^{-ika} \alpha^* \end{pmatrix}. \tag{H.41}$$

For piecewise constant potentials it is more convenient to define and employ an alternative transfer matrix connecting $\psi(x)$ and $\psi'(x)$ at the arbitrary point x to $\psi(0)$ and $\psi'(0)$. Indeed, if between x_n and x_{n+1} ($n = 1, 2, \dots$) the potential is constant, equal to V_n , we have

$$\begin{aligned}
 &\begin{pmatrix} \psi(x) \\ \psi'(x) \end{pmatrix} \\
 &= \begin{pmatrix} \cos[k_n(x-x_n)] & \sin[k_n(x-x_n)]/k_n \\ -k_n \sin[k_n(x-x_n)] & \cos[k_n(x-x_n)] \end{pmatrix} \begin{pmatrix} \psi(x_n) \\ \psi'(x_n) \end{pmatrix}, \tag{H.42}
 \end{aligned}$$

where $x_n \leq x \leq x_{n+1}$ and $\hbar^2 k_n^2 / 2m = E - V_n$.

The continuity of $\psi(x)$ and $\psi'(x)$ and application of (H.42) give

$$\begin{aligned}
 \begin{pmatrix} \psi(x) \\ \psi'(x) \end{pmatrix} &= N_n(x-x_n) N_{n-1}(x_n-x_{n-1}) \times \cdots \\
 &\quad \cdots \times N_1(x_2-x_1) \begin{pmatrix} \psi(x_1) \\ \psi'(x_1) \end{pmatrix}, \tag{H.43}
 \end{aligned}$$

where

$$\begin{aligned}
 &N_\ell(x_{\ell+1}-x_\ell) \\
 &= \begin{pmatrix} \cos[k_\ell(x_{\ell+1}-x_\ell)] & \sin[k_\ell(x_{\ell+1}-x_\ell)]/k_\ell \\ -k_\ell \sin[k_\ell(x_{\ell+1}-x_\ell)] & \cos[k_\ell(x_{\ell+1}-x_\ell)] \end{pmatrix}, \\
 &\ell = 1, \dots, n-1, \tag{H.44}
 \end{aligned}$$

and $x_n \leq x \leq x_{n+1}$.

We can easily connect matrix $N(L)$ with matrix M defined in (H.6), assuming that $V(x)$ is a constant, $V(x) = V$. Indeed, since

$$\begin{aligned}
 A_2 \exp(ik_2L) + B_2 \exp(-ik_2L) &= \psi(L), \\
 ik_2 A_2 \exp(ik_2L) - ik_2 B_2 \exp(-ik_2L) &= \psi'(L) \\
 A_1 + B_1 &= \psi(0),
 \end{aligned}$$

and

$$ik_1 A_1 - ik_1 B_1 = \psi'(0),$$

we have

$$\begin{aligned} & \begin{pmatrix} A_2 \exp(ik_2 L) + B_2 \exp(-ik_2 L) \\ ik_2 A_2 \exp(ik_2 L) - ik_2 B_2 \exp(-ik_2 L) \end{pmatrix} \\ &= \begin{pmatrix} \exp(ik_2 L) & \exp(-ik_2 L) \\ ik_2 \exp(ik_2 L) & -ik_2 \exp(-ik_2 L) \end{pmatrix} \begin{pmatrix} A_2 \\ B_2 \end{pmatrix} \\ &= \begin{pmatrix} \cos(qL) & \sin(qL)/q \\ -q \sin(qL) & \cos(qL) \end{pmatrix} \begin{pmatrix} 1 & 1 \\ ik_1 & -ik_1 \end{pmatrix} \begin{pmatrix} A_1 \\ B_1 \end{pmatrix}, \end{aligned}$$

where

$$E = \frac{\hbar^2 k_1^2}{2m} = \frac{\hbar^2 k_2^2}{2m} + V_0 = \frac{\hbar^2 q^2}{2m} + V.$$

Hence

$$M = \frac{i}{2k_2} \begin{pmatrix} -ik_2 \exp(-ik_2 L) - \exp(-ik_2 L) \\ -ik_2 \exp(ik_2 L) \exp(ik_2 L) \end{pmatrix} N(L) \begin{pmatrix} 1 & 1 \\ ik_1 & -ik_1 \end{pmatrix}. \quad (\text{H.45})$$

In *electromagnetism*, a transfer matrix analogous to that in (H.42) is quite widespread (see, e.g., the book by Born and Wolf [447], pp. 5–70). For a wave propagating in the x -direction normal to consecutive films each of constant permittivity ε and permeability μ , the role of $\psi(x)$ is played by $E_y(x)$ (assuming that the EM wave is linearly polarized with the y -axis chosen in the direction of the electric field) and the role of $\psi'(x)$ by $H_z(x)$, since

$$\frac{\partial E_y}{\partial x} = \frac{i\mu\omega}{c} H_z$$

and

$$\frac{\partial H_z}{\partial x} = \frac{i\omega\varepsilon}{c} E_y.$$

Then, the electromagnetic analog of (H.42) is

$$\begin{pmatrix} E_y(x) \\ H_z(x) \end{pmatrix} = N(x - x_n) \begin{pmatrix} E_y(x_n) \\ H_z(x_n) \end{pmatrix}, \quad (\text{H.46})$$

where

$$N(x - x_n) = \begin{pmatrix} \cos[k_n(x - x_n)] & iz_n \sin[k_n(x - x_n)] \\ \frac{i}{z_n} \sin[k_n(x - x_n)] & \cos[k_n(x - x_n)] \end{pmatrix}. \quad (\text{H.47})$$

In (H.46) and (H.47) $x_n \leq x \leq x_{n+1}$, $z_n = \sqrt{\mu_n/\varepsilon_n}$ is the surface impedance of a film of constant permittivity and permeability bounded by the planes $x = x_n$ and $x = x_{n+1}$, and $k_n = \omega\sqrt{\varepsilon_n\mu_n}/c$.

Equation (H.47) can be easily generalized to the case where the angle of incidence is θ and not zero as in (H.47). Then for a TE wave (i.e., one with $E_z = E_x = 0$), (H.47) is still valid if k_n is replaced by $q_n = k_n \cos \theta$ and z_n by $t_n = z_n / \cos \theta$; for a TM wave (i.e., one with $H_z = H_x = 0$), the relation between $H_y(x)$, $-E_z(x)$ and $H_y(x_n)$, $-E_z(x_n)$ is still given by (H.47) with the replacements $k_n \rightarrow q_n = k_n \cos \theta$ and $z_n \rightarrow s_n = 1/z_n \cos \theta$ (see the book by Born and Wolf [447], pp. 51–70).

Further Reading

Because of its wide applicability, the subject of transfer matrix is treated in several books, starting from an elementary level and extending to various generalizations. For an introduction similar to the one presented here see the books by Landau and Lifshitz [12], Merzbacher [13], and Born and Wolf [447].

For a more advanced level see the review paper by Kramer and MacKinnon [376] and the recent book edited by Brandes and Kettermann [381], especially pp. 21–30.

I

Second Quantization

There are several ways to introduce the formalism of second quantization. Here we shall follow a field-theoretical approach that unifies both the Schrödinger and the classical wave case. For the latter case, second quantization is of critical importance, since it introduces the particle aspect of the wave/particle duality; for both cases this formalism is very convenient for treating systems of many interacting or noninteracting wave-particles, because it incorporates naturally, among other advantages, the generalized Pauli principle.

We consider first the Schrödinger equation describing the motion of a single particle in an external potential,

$$\left(i\hbar \frac{\partial}{\partial t} + \frac{\hbar^2}{2m} \nabla^2 - V \right) \psi(\mathbf{r}, t) = 0, \quad (\text{I.1})$$

and the wave equation

$$\left(\nabla^2 - \frac{1}{c^2} \frac{\partial^2}{\partial t^2} \right) u(\mathbf{r}, t) = 0, \quad (\text{I.2})$$

where $u(\mathbf{r}, t)$ is a real field.

Equations (I.1) and (I.2) can be derived, respectively, from the Lagrangian densities [19, 29]

$$\ell = i\hbar\psi^*\dot{\psi} - \frac{\hbar^2}{2m}\nabla\psi^* \cdot \nabla\psi - V\psi^*\psi, \quad (\text{I.3})$$

$$\ell = \frac{1}{2c^2}\dot{u}^2 - \frac{1}{2}(\nabla u)^2, \quad (\text{I.4})$$

by applying the principle of least action, which leads to the basic equation

$$\frac{\partial \ell}{\partial \phi} - \frac{\partial}{\partial t} \frac{\partial \ell}{\partial \dot{\phi}} - \sum_{\nu=1}^3 \frac{\partial}{\partial x_\nu} \frac{\partial \ell}{\partial (\partial \phi / \partial x_\nu)} = 0, \quad (\text{I.5})$$

where the dot denotes differentiation with respect to t and ϕ stands for ψ , ψ^* or for u ; x_1 , x_2 , and x_3 are the three cartesian coordinates of \mathbf{r} .

Substituting (I.3) and (I.4) into (I.5) we obtain (I.1) (or its complex conjugate) and (I.2), respectively.

The field momentum conjugate to the field variable ϕ ($\phi = \psi$, ψ^* or u) is obtained from the general relation

$$\pi = \frac{\partial \ell}{\partial \dot{\phi}} . \quad (\text{I.6})$$

We obtain for the field momenta conjugate to ψ and u , respectively,

$$\pi = i\hbar\psi^* , \quad (\text{I.7})$$

$$\pi = \frac{\dot{u}}{c^2} . \quad (\text{I.8})$$

The Hamiltonian densities are obtained from the general relation

$$h = \sum \pi \dot{\phi} - \ell ; \quad (\text{I.9})$$

the summation in (I.9) is over all independent fields ϕ [ψ , ψ^* in case (I.3), or u in case (I.4)]. We obtain by substituting in (I.9) from (I.7), (I.8) and (I.3), (I.4), respectively,

$$h = -\frac{i\hbar}{2m} (\nabla\pi) \cdot (\nabla\psi) - \frac{i}{\hbar} V\pi\psi , \quad (\text{I.10})$$

$$h = \frac{1}{2}c^2\pi^2 + \frac{1}{2}(\nabla u)^2 . \quad (\text{I.11})$$

The most general solution of (I.1) and (I.2) can be written as a linear superposition of the corresponding eigensolutions. Thus we have

$$\psi(\mathbf{r}, t) = \sum_n a_n \psi_n(\mathbf{r}) \exp(-iE_n t/\hbar) , \quad (\text{I.12})$$

$$u(\mathbf{r}, t) = \frac{1}{\sqrt{\Omega}} \sum_{\mathbf{k}} \{ P_{\mathbf{k}} \exp[i(\omega_k t - \mathbf{k} \cdot \mathbf{r})] + N_{\mathbf{k}} \exp[-i(\omega_k t - \mathbf{k} \cdot \mathbf{r})] \} , \quad (\text{I.13})$$

where

$$\left(-\frac{\hbar^2}{2m} \nabla^2 + V \right) \psi_n = E_n \psi_n$$

and $\omega_k = ck$. For $V = 0$, $\psi = e^{i\mathbf{k} \cdot \mathbf{r}}/\sqrt{\Omega}$ and $E_n = \hbar^2 k^2/2m$. Note that in (I.13), in contrast to (I.12), there are two terms for each \mathbf{k} , one associated with the positive frequency ω_k and the other with the negative frequency $-\omega_k$. This feature is a consequence of the second-order (in time) nature of the wave equation. Note also that as a consequence of u being real, we have the relation

$$P_{\mathbf{k}} = N_{\mathbf{k}}^* . \quad (\text{I.14})$$

Substituting (I.12) and (I.13) into (I.10) and (I.11), taking into account (I.7) and (I.8), and integrating over the whole volume Ω , we obtain the total energy of the system in terms of the coefficients a_n or $P_{\mathbf{k}}$, and $N_{\mathbf{k}}$, respectively. We have explicitly

$$\mathcal{H} = \sum_n a_n^* a_n E_n , \quad (\text{I.15})$$

$$\mathcal{H} = \sum_{\mathbf{k}} \frac{\omega_{\mathbf{k}}^2}{c^2} (N_{\mathbf{k}}^* N_{\mathbf{k}} + N_{\mathbf{k}} N_{\mathbf{k}}^*) . \quad (\text{I.16})$$

We can rewrite (I.16) by introducing the quantities

$$b_{\mathbf{k}} = \sqrt{\frac{2\omega_{\mathbf{k}}}{\hbar c^2}} N_{\mathbf{k}} \quad (\text{I.17})$$

as follows:

$$\mathcal{H} = \frac{1}{2} \sum_{\mathbf{k}} \hbar \omega_{\mathbf{k}} (b_{\mathbf{k}}^* b_{\mathbf{k}} + b_{\mathbf{k}} b_{\mathbf{k}}^*) . \quad (\text{I.18})$$

A general way to quantize a field ϕ is to replace $\phi(r, t)$ by an operator $\hat{\phi}(r, t)$ that satisfies the commutation relation

$$\hat{\phi}(\mathbf{r}, t) \pi(\mathbf{r}', t) \mp \pi(\mathbf{r}', t) \hat{\phi}(\mathbf{r}, t) = i\hbar \delta(\mathbf{r} - \mathbf{r}') , \quad (\text{I.19})$$

where the upper sign corresponds to the case where ϕ describes bosons (i.e., particles with integer spin) and the lower sign corresponds to the case where ϕ describes fermions (i.e., particles with integer plus $1/2$ spin).

The field u , being a classical field, corresponds to integer spin and as such is associated with the upper sign in (I.19). The field ψ may describe either fermions (e.g., electrons) or bosons (e.g., He^4 atoms). The operator $\hat{\phi}(\mathbf{r}, t)$ commutes (anticommutes) with $\hat{\phi}(\mathbf{r}', t)$; similarly, $\pi(\mathbf{r}, t)$ commutes (anticommutes) with $\pi(\mathbf{r}', t)$. Combining this last statement with (I.19) and expressing everything in terms of ψ or u , we have the equal time commutation (anticommutation) relation

$$\begin{aligned} \psi(\mathbf{r}, t) \psi^\dagger(\mathbf{r}', t) \mp \psi^\dagger(\mathbf{r}', t) \psi(\mathbf{r}, t) &= \delta(\mathbf{r} - \mathbf{r}') , \\ \psi(\mathbf{r}, t) \psi(\mathbf{r}', t) \mp \psi(\mathbf{r}', t) \psi(\mathbf{r}, t) &= 0 , \\ \psi^\dagger(\mathbf{r}, t) \psi^\dagger(\mathbf{r}', t) \mp \psi^\dagger(\mathbf{r}', t) \psi^\dagger(\mathbf{r}, t) &= 0 , \end{aligned} \quad (\text{I.20})$$

$$\begin{aligned} u(\mathbf{r}, t) \dot{u}(\mathbf{r}', t) - \dot{u}(\mathbf{r}', t) u(\mathbf{r}, t) &= i\hbar c^2 \delta(\mathbf{r} - \mathbf{r}') , \\ u(\mathbf{r}, t) u(\mathbf{r}', t) - u(\mathbf{r}', t) u(\mathbf{r}, t) &= 0 , \\ \dot{u}(\mathbf{r}, t) \dot{u}(\mathbf{r}', t) - \dot{u}(\mathbf{r}', t) \dot{u}(\mathbf{r}, t) &= 0 , \end{aligned} \quad (\text{I.21})$$

where the quantity ψ^* , which is the complex conjugate of ψ , has been replaced by the operator ψ^\dagger , which is the adjoint of the operator ψ . Since ψ

and u became operators, the coefficients a_n and b_k are operators obeying certain commutation (or anticommutation) relations. To find these relations we substitute (I.12), (I.13), and (I.17) into (I.20) and (I.21). After some straightforward algebra we obtain

$$\begin{aligned} a_n a_{n'}^\dagger \mp a_{n'}^\dagger a_n &= \delta_{nn'} , \\ a_n a_{n'} \mp a_{n'} a_n &= 0 , \\ a_n^\dagger a_{n'}^\dagger \mp a_{n'}^\dagger a_n^\dagger &= 0 , \end{aligned} \quad (\text{I.22})$$

$$\begin{aligned} b_k b_q^\dagger - b_q^\dagger b_k &= \delta_{kq} , \\ b_k b_q - b_q b_k &= 0 , \\ b_k^\dagger b_q^\dagger - b_q^\dagger b_k^\dagger &= 0 . \end{aligned} \quad (\text{I.23})$$

By right-multiplying the first of equations (I.22) by a_n , setting $n' = n$, and taking into account that the operators $a_n^\dagger a_n$ are nonnegative, we find that $a_n^\dagger a_n$ has the eigenvalues $0, 1, 2, \dots$ if the upper sign is taken and the eigenvalues $0, 1, 2, \dots$ if the lower sign is taken. Similarly, the operator $b_k^\dagger b_k$ takes the eigenvalues $0, 1, 2, \dots$. For this reason the operator $a_n^\dagger a_n$ or $b_k^\dagger b_k$ is called the number operator and is symbolized by n_n or n_k ; its eigenvalues show how many particles we have in the state $\psi_n(\mathbf{r})$ or how many quanta have been excited in the mode \mathbf{k} . The previous proof implies that the operator a_n or b_k annihilates a particle or quantum from the state $|\psi_n\rangle$ or $|\mathbf{k}\rangle$; similarly, we can show that a_n^\dagger or b_k^\dagger creates a particle in this state. These operators can be used to create a complete set of states starting from the vacuum state $|0\rangle$, i.e., from the state that has no particle or quanta. Obviously,

$$a_n |0\rangle = 0 , \quad (\text{I.24})$$

$$b_k |0\rangle = 0 . \quad (\text{I.25})$$

All the one-particle states can be obtained by applying the operator a_n^\dagger (or b_k^\dagger) to $|0\rangle$, i.e., $a_n^\dagger |0\rangle$ (or $b_k^\dagger |0\rangle$), where the index n (or \mathbf{k}) takes all possible values. By applying two creation operators we can construct the two-particle states, and so on. Note that the correct symmetry or antisymmetry of the state is automatically included in this formalism.

We can define different sets of operators $\{a_n\}$ and $\{a_n^\dagger\}$ depending on which complete set of one-particle states $\{\psi_n\}$ we choose. Let us have another complete orthonormal set $\{\psi_m\}$ to which a different set of operators $\{a_m\}$ and $\{a_m^\dagger\}$ corresponds. Taking into account that

$$|m\rangle = \sum_n \langle n | m \rangle |n\rangle ,$$

and that $|m\rangle = a_m^\dagger |0\rangle$ and $|n\rangle = a_n^\dagger |0\rangle$, we obtain

$$a_m^\dagger = \sum_n \langle n | m \rangle a_n^\dagger , \quad (\text{I.26})$$

from which it follows that

$$a_m = \sum_n \langle m | n \rangle a_n . \quad (\text{I.27})$$

Usually, the set $\{\psi_n\}$ is: (1) The position eigenstates $|\mathbf{r}\rangle$; (2) The momentum eigenstates $|\mathbf{k}\rangle$; (3) The eigenstates of the Hamiltonian $-\hbar^2\nabla^2/2m + V$. Of course, when $V = 0$, set (2) is identical to (3). Let us apply (I.27) when the set $\{|m\rangle\}$ is the set $\{|\mathbf{r}\rangle\}$ and the set $\{|n\rangle\}$ is set (3) above. We obtain

$$a_{\mathbf{r}} = \sum_n \langle \mathbf{r} | n \rangle a_n = \sum_n \psi_n(\mathbf{r}) a_n ;$$

comparing with (I.12), we see that $a_{\mathbf{r}} = \psi(\mathbf{r}, 0)$, i.e., $\psi(\mathbf{r}, 0) [\psi^\dagger(\mathbf{r}, 0)]$ is an annihilation (creation) operator annihilating (creating) a particle at point \mathbf{r} . Similarly, $\psi^\dagger(\mathbf{r}, 0)\psi(\mathbf{r}, 0)$ is the number operator at point \mathbf{r} , i.e., the number density operator (or concentration) $\varrho(\mathbf{r})$

$$\varrho(\mathbf{r}) = \psi^\dagger(\mathbf{r}, 0)\psi(\mathbf{r}, 0) . \quad (\text{I.28})$$

The relation between the operators $\psi(\mathbf{r})$, $\psi^\dagger(\mathbf{r})$ and $a_{\mathbf{k}}$, $a_{\mathbf{k}}^\dagger$ is, according to (I.26) and (I.27),

$$\psi(\mathbf{r}) = \sum_{\mathbf{k}} \langle \mathbf{r} | \mathbf{k} \rangle a_{\mathbf{k}} = \frac{1}{\sqrt{\Omega}} \sum_{\mathbf{k}} e^{i\mathbf{k}\cdot\mathbf{r}} a_{\mathbf{k}} , \quad (\text{I.29})$$

$$a_{\mathbf{k}} = \int d^3r \langle \mathbf{k} | \mathbf{r} \rangle \psi(\mathbf{r}) = \frac{1}{\sqrt{\Omega}} \int d^3r e^{-i\mathbf{k}\cdot\mathbf{r}} \psi(\mathbf{r}) . \quad (\text{I.30})$$

All the operators can be expressed in terms of creation and annihilation operators. We have already seen that

$$\varrho(\mathbf{r}) = \psi^\dagger(\mathbf{r})\psi(\mathbf{r}) .$$

Hence, the total number operator is

$$N = \int d^3r \psi^\dagger(\mathbf{r})\psi(\mathbf{r}) = \sum_{\mathbf{k}} a_{\mathbf{k}}^\dagger a_{\mathbf{k}} . \quad (\text{I.31})$$

The last relation follows with the help of (I.29). The kinetic energy operator is obtained by setting $V = 0$ in (I.10) and integrating over \mathbf{r} :

$$T = \frac{\hbar^2}{2m} \int \nabla\psi^\dagger\nabla\psi d^3r = -\frac{\hbar^2}{2m} \int d^3r \psi^\dagger\nabla^2\psi = \sum_{\mathbf{k}} \frac{\hbar^2 k^2}{2m} a_{\mathbf{k}}^\dagger a_{\mathbf{k}} . \quad (\text{I.32})$$

The second step follows by integrating by parts the first expression; the last expression is obtained with the help of (I.29).

The potential energy in the presence of an external potential $V(\mathbf{r})$ is obtained by integrating over \mathbf{r} the second term on the rhs of (I.10). We have

$$V_e = \int V(\mathbf{r}) \psi^\dagger(\mathbf{r})\psi(\mathbf{r}) d^3r = \int V(\mathbf{r}) \varrho(\mathbf{r}) d^3r , \quad (\text{I.33})$$

as was expected. The operators ρ , N , T , and V_e involve the product of one creation and one annihilation operator. This is a general feature for operators that correspond to additive quantities. On the other hand, operators involving summation over pairs of particles (such as the Coulomb interaction energy of a system of particles) contain a product of two creation and two annihilation operators. For example, we consider the interaction energy

$$V_i = \frac{1}{2} \sum_{ij} v(\mathbf{r}_i, \mathbf{r}_j) .$$

This expression can be written in terms of the density ρ as follows:

$$V_i = \frac{1}{2} \int \rho(\mathbf{r}) v(\mathbf{r}, \mathbf{r}') \rho(\mathbf{r}') d^3r d^3r' ; \quad (\text{I.34})$$

using (I.28) we obtain

$$V_i = \frac{1}{2} \int d^3r d^3r' \psi^\dagger(\mathbf{r}) \psi^\dagger(\mathbf{r}') v(\mathbf{r}, \mathbf{r}') \psi(\mathbf{r}') \psi(\mathbf{r}) . \quad (\text{I.35})$$

Note that in our derivation of (I.35) there is an uncertainty in the ordering of the four creation and annihilation operators. One can verify that the ordering in (I.35) is the correct one by evaluating the matrix elements of V_i among states with a fixed total number of particles [20, 448].

The total Hamiltonian of a system of particles interacting with each other via the pairwise potential $v(\mathbf{r}, \mathbf{r}')$ and placed in an external potential $V(\mathbf{r})$ is given by

$$\mathcal{H} = T + V_e + V_i , \quad (\text{I.36})$$

where the quantities T , V_e , and V_i are given by (I.32), (I.33), and (I.35), respectively.

Note that the Hamiltonian (I.36) cannot be brought to the form (I.15) because of the presence of the interaction term V_i . Furthermore, the field operator $\psi(\mathbf{r}, t)$ does not satisfy the simple equation (I.1). There are two ways to find the equation obeyed by ψ : (1) by applying the general equation (I.5) with ℓ containing an extra term $-V_i$ or (2) using the general equation

$$i\hbar \frac{\partial \psi}{\partial t} = [\psi, \mathcal{H}] ,$$

which leads to

$$\begin{aligned} & \left[i\hbar \frac{\partial}{\partial t} + \frac{\hbar^2 \nabla^2}{2m} - V(\mathbf{r}) \right] \psi(\mathbf{r}, t) \\ &= \int d^3r' v(\mathbf{r}, \mathbf{r}') \psi^\dagger(\mathbf{r}', t) \psi(\mathbf{r}', t) \psi(\mathbf{r}, t) , \end{aligned} \quad (\text{I.37})$$

with a similar equation for $\psi^\dagger(\mathbf{r}, t)$. For the particular but important case of a system of electrons moving in a positive background (to ensure overall

electrical neutrality) and repelling each other through $v(r, r') = e^2/|r - r'|$, the total Hamiltonian \mathcal{H} can be expressed in terms of $a_{\mathbf{k}}^\dagger$, $a_{\mathbf{k}}$ as follows:

$$\mathcal{H} = \sum_{\mathbf{k}} \frac{\hbar^2 k^2}{2m} a_{\mathbf{k}}^\dagger a_{\mathbf{k}} + \frac{e^2}{2\Omega} \sum_{\mathbf{k}, \mathbf{p}, \mathbf{q} \neq 0} \frac{4\pi}{q^2} a_{\mathbf{k}+\mathbf{q}}^\dagger a_{\mathbf{p}-\mathbf{q}}^\dagger a_{\mathbf{p}} a_{\mathbf{k}}. \quad (\text{I.38})$$

We can also express various operators associated with the field $u(\mathbf{r}, t)$ in terms of the field operator $u(\mathbf{r}, t)$ or in terms of the operators $b_{\mathbf{k}}$ and $b_{\mathbf{k}}^\dagger$. To be more specific, we consider the particular case of the longitudinal vibrations of an isotropic continuous solid. In this case, each operator $b_{\mathbf{k}}^\dagger$ creates a quantum of a plane wave longitudinal oscillation that carries a momentum equal to $\hbar\mathbf{k}$ and an energy equal to $\hbar\omega_{\mathbf{k}}$. This quantum is called a *longitudinal acoustic (LA) phonon*.

The theory we have presented for the field $u(\mathbf{r}, t)$ requires some modifications to be applicable to the longitudinal vibrations of a continuum; the reason is that the latter are described by a *vector* field, namely, the displacement, $\mathbf{d}(\mathbf{r}, t)$, from the equilibrium position; since we are dealing with longitudinal vibrations, it follows that $\nabla \times \mathbf{d} = 0$. The various quantities of physical interest can be expressed in terms of LA phonon creation and annihilation operators as follows (for detailed derivations see [20]). The displacement operator, $\mathbf{d}(\mathbf{r}, t)$, is

$$\mathbf{d}(\mathbf{r}, t) = -i \sum_{\mathbf{k}} \sqrt{\frac{\hbar}{2\omega_{\mathbf{k}}\varrho\Omega}} \frac{\mathbf{k}}{k} \left[b_{\mathbf{k}} e^{-i(\omega_{\mathbf{k}}t - \mathbf{k} \cdot \mathbf{r})} - b_{\mathbf{k}}^\dagger e^{i(\omega_{\mathbf{k}}t - \mathbf{k} \cdot \mathbf{r})} \right], \quad (\text{I.39})$$

where ϱ is the constant equilibrium mass density. The conjugate momentum, $\boldsymbol{\pi}(\mathbf{r}, t)$, is

$$\begin{aligned} \boldsymbol{\pi}(\mathbf{r}, t) &= \varrho \frac{\partial \mathbf{d}}{\partial t} = - \sum_{\mathbf{k}} \sqrt{\frac{\hbar\omega_{\mathbf{k}}\varrho}{2\Omega}} \frac{\mathbf{k}}{k} \\ &\times \left(b_{\mathbf{k}} \exp[-i(\omega_{\mathbf{k}}t - \mathbf{k} \cdot \mathbf{r})] + b_{\mathbf{k}}^\dagger \exp[i(\omega_{\mathbf{k}}t - \mathbf{k} \cdot \mathbf{r})] \right). \end{aligned} \quad (\text{I.40})$$

The Lagrangian and Hamiltonian densities are

$$\ell = \frac{1}{2}\varrho \dot{\mathbf{d}}^2 - \frac{1}{2}B(\nabla \cdot \mathbf{d})^2, \quad (\text{I.41})$$

$$h = \frac{1}{2\varrho}\boldsymbol{\pi}^2 + \frac{1}{2}B(\nabla \cdot \mathbf{d})^2, \quad (\text{I.42})$$

where

$$B = \varrho c^2 \quad (\text{I.43})$$

is the adiabatic bulk modulus, $B = -\Omega(\partial P/\partial \Omega)_S$, and c is the speed of sound in the medium. The Hamiltonian expressed in terms of $b_{\mathbf{k}}^\dagger$, $b_{\mathbf{k}}$ has exactly the form (I.18), which can be rewritten as

$$\mathcal{H} = \sum_{\mathbf{k}} \hbar\omega_{\mathbf{k}} \left(b_{\mathbf{k}}^\dagger b_{\mathbf{k}} + \frac{1}{2} \right) \quad (\text{I.44})$$

by taking into account (I.23). Equation (I.44) means that the phonons are non-interacting. If the harmonic approximation is relaxed, the Lagrangian (I.41) will contain extra terms involving powers of $\nabla \cdot \mathbf{d}$ higher than the second. Since \mathbf{d} is a linear combination of $b_{\mathbf{k}}^\dagger$ and $b_{\mathbf{k}}$, these third- and higher-order terms will add to the Hamiltonian (I.44) an \mathcal{H}_i that will involve terms of the form $b_{\mathbf{k}} b_{\mathbf{q}} b_{\mathbf{p}}$, $b_{\mathbf{k}}^\dagger b_{\mathbf{q}} b_{\mathbf{p}}$, $b_{\mathbf{k}}^\dagger b_{\mathbf{q}}^\dagger b_{\mathbf{p}}$, and $b_{\mathbf{k}}^\dagger b_{\mathbf{q}}^\dagger b_{\mathbf{p}}^\dagger$ and terms involving four, five, etc. creation and annihilation operators. Thus the term \mathcal{H}_i represents complicated interactions among the phonons, and as a result the equation of motion (I.2) is modified; the new equation can be found from (I.5) with ℓ containing whatever anharmonic terms are present.

In a solid there are interactions between the electrons [which are described by the field $\psi(\mathbf{r}, t)$] and the longitudinal phonons [which are described by the field $\mathbf{d}(\mathbf{r}, t)$]. It is customary and convenient to describe the longitudinal phonons through the scalar field $\phi(\mathbf{r}, t)$, which is defined as

$$\phi(\mathbf{r}, t) = c\sqrt{\varrho} \nabla \cdot \mathbf{d}. \quad (\text{I.45})$$

Substituting in (I.45) from (I.39), we obtain for the phonon field $\phi(\mathbf{r}, 0)$ the following expression:

$$\phi(\mathbf{r}, 0) = \sum_{\mathbf{k}} \sqrt{\frac{\hbar\omega_{\mathbf{k}}}{2\Omega}} \left(b_{\mathbf{k}}^\dagger e^{-i\mathbf{k} \cdot \mathbf{r}} + b_{\mathbf{k}} e^{i\mathbf{k} \cdot \mathbf{r}} \right); \quad (\text{I.46})$$

the summation over \mathbf{k} is restricted by the condition $k \leq k_D$, where k_D is the *Debye wave number*: $k_D = (6\pi^2 N_a / \Omega)^{1/3}$, where N_a is the total number of atoms. This restriction ensures that the degrees of freedom in our isotropic continuum are equal to the vibrational degrees of freedom of a real solid. In terms of the fields $\psi(\mathbf{r})$ and $\phi(\mathbf{r})$ the electron-phonon interaction Hamiltonian is [20]

$$\mathcal{H}_{e-p} = \gamma \int d^3r \psi^\dagger(\mathbf{r}) \psi(\mathbf{r}) \phi(\mathbf{r}), \quad (\text{I.47})$$

where

$$\gamma = \frac{\pi^2 \hbar^2 z \varrho}{m k_F M \sqrt{B}}; \quad (\text{I.48})$$

z is the valence and M is the mass of each ion, m is the mass of the electron, and k_F is the Fermi momentum of the electron gas. If the various interactions discussed up to now are included, the total Hamiltonian \mathcal{H}_t of an electron-phonon system can be written as follows:

$$\mathcal{H}_t = \mathcal{H}_e + \mathcal{H}_p + \mathcal{H}_{e-e} + \mathcal{H}_{p-p} + \mathcal{H}_{e-p}, \quad (\text{I.49})$$

where \mathcal{H}_e , \mathcal{H}_p , \mathcal{H}_{e-e} , and \mathcal{H}_{e-p} are given by (I.15), (I.44), (I.35), and (I.47), respectively; \mathcal{H}_{p-p} contains terms involving the product of at least three phonon creation and annihilation operators, as was discussed above; \mathcal{H}_e can be written also as the sum of (I.32) and (I.33). The time dependence of the operators $\psi(\mathbf{r}, t)$ and $\phi(\mathbf{r}, t)$ can be obtained from the general relation

$$i\hbar \frac{\partial \psi(\mathbf{r}, t)}{\partial t} = [\psi(\mathbf{r}, t), \mathcal{H}_t] , \quad (\text{I.50})$$

$$i\hbar \frac{\partial \phi(\mathbf{r}, t)}{\partial t} = [\phi(\mathbf{r}, t), \mathcal{H}_t] . \quad (\text{I.51})$$

If the interaction terms were absent, (I.50) would give (I.12) and (I.51) would give

$$\begin{aligned} \phi(\mathbf{r}, t) = \sum_{\mathbf{k}} \sqrt{\frac{\hbar\omega_{\mathbf{k}}}{2\Omega}} \left(b_{\mathbf{k}}^{\dagger} \exp[i(\omega_{\mathbf{k}}t - \mathbf{k} \cdot \mathbf{r})] \right. \\ \left. + b_{\mathbf{k}} \exp[-i(\omega_{\mathbf{k}}t - \mathbf{k} \cdot \mathbf{r})] \right) . \end{aligned} \quad (\text{I.52})$$

We shall conclude by expressing some common electronic and phononic operators in second quantization language.

Electronic Hamiltonian Including the Spin Variable σ ($\sigma = \pm 1$)

$$\begin{aligned} \mathcal{H}_e + \mathcal{H}_{e-e} = \sum_{\sigma} \int d\mathbf{r} \psi_{\sigma}^{\dagger}(\mathbf{r}) \left[-\frac{\hbar^2}{2m} \nabla^2 + V(\mathbf{r}) \right] \psi_{\sigma}(\mathbf{r}) \\ + \frac{1}{2} \sum_{\sigma\sigma'} \int d\mathbf{r} \int d\mathbf{r}' \psi_{\sigma}^{\dagger}(\mathbf{r}) \psi_{\sigma'}^{\dagger}(\mathbf{r}') v(\mathbf{r}, \mathbf{r}') \psi_{\sigma'}(\mathbf{r}') \psi_{\sigma}(\mathbf{r}) . \end{aligned} \quad (\text{I.53})$$

Total Electronic Momentum

$$\mathbf{P} = \sum_{\sigma} \int d\mathbf{r} \psi_{\sigma}(\mathbf{r}) (-i\hbar\nabla) \psi_{\sigma}^{\dagger}(\mathbf{r}) = \sum_{\sigma\mathbf{k}} \hbar\mathbf{k} a_{\mathbf{k}\sigma}^{\dagger} a_{\mathbf{k}\sigma} . \quad (\text{I.54})$$

Electronic Current Density

$$\mathbf{j}(\mathbf{r}) = \frac{\hbar}{2mi} \sum_{\sigma} [\psi_{\sigma}^{\dagger}(\mathbf{r}) \nabla \psi_{\sigma}(\mathbf{r}) - (\nabla \psi_{\sigma}^{\dagger}(\mathbf{r})) \psi_{\sigma}(\mathbf{r})] \quad (\text{I.55a})$$

$$= \frac{\hbar}{\Omega m} \sum_{\mathbf{k}, \mathbf{q}, \sigma} e^{i\mathbf{q} \cdot \mathbf{r}} \left(\mathbf{k} + \frac{\mathbf{q}}{2} \right) a_{\mathbf{k}, \sigma}^{\dagger} a_{\mathbf{k}+\mathbf{q}, \sigma} . \quad (\text{I.55b})$$

Total Electronic Spin Density

$$\mathbf{S}(\mathbf{r}) = \frac{1}{2} \sum_{\sigma\sigma'} \psi_{\sigma}^{\dagger}(\mathbf{r}) (\boldsymbol{\sigma})_{\sigma\sigma'} \psi_{\sigma'}(\mathbf{r}) \quad (\text{I.56a})$$

$$= \frac{1}{2\Omega} \sum_{\mathbf{k}, \mathbf{q}, \sigma, \sigma'} e^{i\mathbf{q} \cdot \mathbf{r}} a_{\mathbf{k}\sigma}^{\dagger} (\boldsymbol{\sigma})_{\sigma\sigma'} a_{\mathbf{k}+\mathbf{q}, \sigma'} , \quad (\text{I.56b})$$

where $\boldsymbol{\sigma}$ is the vector whose cartesian components are the three Pauli matrices.

In a discrete periodic lattice, the atomic (or ionic) displacement vector, $\mathbf{d}_{\mathbf{R},\nu}(t)$, is characterized by the index \mathbf{R} (which determines the primitive cell in which the atom is located) and the index ν (which specifies the atom within the primitive cell \mathbf{R}). The eigenmodes are characterized by the crystal momentum \mathbf{q} and the branch index s ($s = 1, 2, 3, \dots, 3p$), where p is the number of atoms in each primitive cell. By introducing the abbreviations $Q \equiv \mathbf{q}, s$ and $x \equiv \mathbf{R}, \nu, i$ (where $i = 1, 2, 3$ denote the three cartesian coordinates of $\mathbf{d}_{\mathbf{R},\nu}(t)$), we have

$$d(x, t) = \frac{1}{\sqrt{N}} \sum_Q \sqrt{\frac{\hbar}{2M\omega_Q}} \left[w_Q(x) e^{-i\omega_Q t} b_Q + w_Q^*(x) e^{i\omega_Q t} b_Q^\dagger \right], \quad (\text{I.57})$$

$$p(x, t) = \frac{-i}{\sqrt{N}} \sum_Q \sqrt{\frac{\hbar M_\nu^2 \omega_Q}{2M}} \left[w_Q(x) e^{-i\omega_Q t} b_Q - w_Q^*(x) e^{i\omega_Q t} b_Q^\dagger \right], \quad (\text{I.58})$$

$$b_Q = \frac{1}{\sqrt{N}} \sum_x \left[\sqrt{\frac{M_\nu^2 \omega_Q}{2\hbar M}} d(x, 0) + i \sqrt{\frac{1}{2\hbar M \omega_Q}} p(x, 0) \right] w_Q^*(x), \quad (\text{I.59})$$

$$b_Q^\dagger = \frac{1}{\sqrt{N}} \sum_x \left[\sqrt{\frac{M_\nu^2 \omega_Q}{2\hbar M}} d(x, 0) - i \sqrt{\frac{1}{2\hbar M \omega_Q}} p(x, 0) \right] w_Q(x); \quad (\text{I.60})$$

$$\mathcal{H}_p = \sum_Q \hbar \omega_Q \left(b_Q^\dagger b_Q + \frac{1}{2} \right),$$

where M_ν is the mass of the ν th atom, N is the total number of atoms in the solid, $\bar{M} = \sum_{\nu=1}^p M_\nu/p$, $w_Q(x) = \varepsilon_{\nu i, Q} e^{i\mathbf{q} \cdot \mathbf{R}}$ satisfies the equation

$$M_\nu \omega_{\mathbf{q}, s}^2 w_{\mathbf{q}, s}(\mathbf{R}, \nu, i) = \sum_{\nu' i'} D_{\nu i, \nu' i'}(\mathbf{q}) w_{\mathbf{q}, s}(\mathbf{R}, \nu', i'), \quad (\text{I.61})$$

and $p(x, t) = M_\nu \dot{d}(x, t)$ is the i th cartesian component of the momentum of the atom ν located at the \mathbf{R} primitive cell. The harmonic potential energy, U , in terms of the displacement $d_{\mathbf{R},\nu,i}$, is given by

$$U = U_0 + \frac{1}{2} \sum_{\mathbf{R}, \mathbf{R}'} \sum_{\nu, \nu'} \sum_{ii'} d_{\mathbf{R},\nu,i} D_{\nu i, \nu' i'}(\mathbf{R} - \mathbf{R}') d_{\mathbf{R}',\nu',i'} \quad (\text{I.62})$$

and

$$D_{\nu i, \nu' i'}(\mathbf{q}) = \sum_{\mathbf{R}} D_{\nu i, \nu' i'}(\mathbf{R}) e^{-i\mathbf{q} \cdot \mathbf{R}}. \quad (\text{I.63})$$

The eigenmodes $w_Q(x)$ are orthonormal in the following sense:

$$\sum_x M_\nu w_Q^*(x) w_{Q'}(x) = M_0 \delta_{QQ'}, \quad (\text{I.64})$$

where $M_0 = N\bar{M}$ is the total mass of the solid; they satisfy also the completeness relation

$$\frac{M_\nu}{M_0} \sum_Q w_Q(x)w_Q(x') = \delta_{xx'} . \quad (\text{I.65})$$

If there is only one atom per primitive cell, equation (I.57) simplifies to

$$\begin{aligned} \mathbf{d}(\mathbf{R}, t) = \frac{1}{\sqrt{N}} \sum_{\mathbf{q}s} \sqrt{\frac{\hbar}{2M\omega_{\mathbf{q}s}}} & [\varepsilon_{\mathbf{q}s} \exp[i(\mathbf{q} \cdot \mathbf{R} - \omega_{\mathbf{q}s}t)]b_{\mathbf{q}s} \\ & + \varepsilon_{\mathbf{q}s}^* \exp[-i(\mathbf{q} \cdot \mathbf{R} - \omega_{\mathbf{q}s}t)]b_{\mathbf{q}s}^\dagger] , \quad (\text{I.66}) \end{aligned}$$

which reduces to (I.39) by setting $\mathbf{q} = \mathbf{k}$, $s = \text{longitudinal only}$, $\varepsilon_{\mathbf{q}} = -i\mathbf{k}/|\mathbf{k}|$, and $NM = \rho\Omega$.

Solutions of Selected Problems

Chapter 1

1.1s. We start with the relations

$$\mathcal{L}\phi_n = \lambda_n\phi_n, \quad (1)$$

$$\mathcal{L}\phi_m = \lambda_m\phi_m, \quad (2)$$

where $\lambda_n \neq \lambda_m$. We multiply (1) by ϕ_m^* and (2) by ϕ_n^* , and we integrate

$$\int_{\Omega} \phi_m^* \mathcal{L}\phi_n \, d\mathbf{r} = \lambda_n \int_{\Omega} \phi_m^* \phi_n \, d\mathbf{r}, \quad (3)$$

$$\int_{\Omega} \phi_n^* \mathcal{L}\phi_m \, d\mathbf{r} = \lambda_m \int_{\Omega} \phi_n^* \phi_m \, d\mathbf{r}. \quad (4)$$

By taking the complex conjugate of (4) and employing the hermitian nature of \mathcal{L} we find

$$\left[\int_{\Omega} \phi_n^* \mathcal{L}\phi_m \, d\mathbf{r} \right]^* = \int_{\Omega} \phi_m^* \mathcal{L}\phi_n \, d\mathbf{r} = \lambda_m \int_{\Omega} \phi_m^* \phi_n \, d\mathbf{r}. \quad (5)$$

In (5) we have used the fact that the eigenvalues of a hermitian operator are real [for a proof set $n = m$ in (3) and then take its complex conjugate].

Subtracting (5) from (3) we have

$$(\lambda_n - \lambda_m) \int_{\Omega} \phi_m^* \phi_n \, d\mathbf{r} = 0. \quad (6)$$

Thus, if $\lambda_n \neq \lambda_m$, then ϕ_m and ϕ_n are orthogonal. By incorporating an appropriate constant multiplying factor in the definition of ϕ_n , ϕ_m , we can always have that

$$\int_{\Omega} \phi_n^* \phi_n \, d\mathbf{r} = 1 \quad (7)$$

for every n .

Now, if $\lambda_n = \lambda_m$, while $\phi_n \neq \phi_m$ with $\int_{\Omega} \phi_n^* \phi_m \, d\mathbf{r} \neq 0$, we can always choose a new eigenfunction $\phi'_m = \alpha_1 \phi_n + \alpha_2 \phi_m$ associated with the same eigenvalue $\lambda_m = \lambda_n$, such that

$$\int_{\Omega} \phi_n^* \phi'_m \, d\mathbf{r} = \alpha_1 + \alpha_2 \int_{\Omega} \phi_n^* \phi_m \, d\mathbf{r} = 0, \tag{8}$$

and

$$\int_{\Omega} \phi'^*_m \phi'_m \, d\mathbf{r} = |\alpha_1|^2 + |\alpha_2|^2 + \alpha_1^* \alpha_2 \int_{\Omega} \phi_n^* \phi_m \, d\mathbf{r} + \alpha_2^* \alpha_1 \int_{\Omega} \phi_m^* \phi_n \, d\mathbf{r} = 1. \tag{9}$$

Thus, by appropriate selection of α_1 and α_2 , we can impose orthonormality even in the case of degenerate eigenvalues. \square

1.2s. By definition, a set of functions $\{\phi_n\}$ is complete if any well-behaved function ψ defined on Ω and satisfying proper boundary conditions can be written as a linear combination of ϕ_n s:

$$\psi(\mathbf{r}) = \sum_n c_n \phi_n(\mathbf{r}). \tag{1}$$

By multiplying by ϕ_m^* , integrating over \mathbf{r} , and taking into account the orthonormality of the set $\{\phi_n\}$, we determine the coefficients $\{c_m\}$:

$$\int_{\Omega} \phi_m^* \psi \, d\mathbf{r}' = \sum_n c_n \int_{\Omega} \phi_m^* \phi_n \, d\mathbf{r}' = c_m. \tag{2}$$

Substituting (2) into (1) we have

$$\psi(\mathbf{r}) = \int_{\Omega} \left\{ \sum_m \phi_m^*(\mathbf{r}') \phi_m(\mathbf{r}) \right\} \psi(\mathbf{r}') \, d\mathbf{r}'. \tag{3}$$

For (3) to be true for any function ψ , the kernel

$$\sum_m \phi_m^*(\mathbf{r}') \phi_m(\mathbf{r})$$

must be equal to $\delta(\mathbf{r} - \mathbf{r}')$. \square

1.3s. The true meaning of (1.20) is the following:

$$\begin{aligned} & \lim_{y \rightarrow 0^+} \int_A^B \frac{f(x)}{x \pm iy} \, dx \\ &= \lim_{\alpha \rightarrow 0^+} \left[\int_A^{-\alpha} \frac{f(x)}{x} \, dx + \int_{\alpha}^B \frac{f(x)}{x} \, dx \right] \mp i\pi \int dx f(x) \delta(x), \end{aligned} \tag{1}$$

where $A < 0 < B$, and $f(x)$ is any function well behaved in the interval $[A, B]$. The limit of the expression in brackets on the rhs of (1) is denoted by

$$P \int_A^B \frac{f(x)}{x} dx \text{ or by } \oint_A^B \frac{f(x)}{x} dx$$

and is called the *principal value* of the integral.

The lhs of (1), before taking the limit $y \rightarrow 0^+$, can be written as follows by multiplying the numerator and the denominator of the integrand by $x \mp iy$:

$$\int_A^B \frac{f(x)}{x \pm iy} dx = \int_A^B \frac{xf(x)}{x^2 + y^2} dx \mp i \int_A^B \frac{yf(x)}{x^2 + y^2} dx . \tag{2}$$

According to (A.2a) of Appendix A, the limit of $y/(x^2 + y^2)$ as $y \rightarrow 0^+$ equals $\pi\delta(x)$. Hence the imaginary part of the lhs of (1) equals the imaginary part of the rhs of (1). Let us examine now the real part of the lhs of (1). We have

$$\int_A^B dx I(x, y) = \int_A^{-\alpha} dx I(x, y) + \int_{-\alpha}^{\alpha} dx I(x, y) + \int_{\alpha}^B dx I(x, y) , \tag{3}$$

where $I(x, y) = xf(x)/(x^2 + y^2)$. In the first and third integral of the rhs of (3) we can take the limit $y \rightarrow 0^+$ and thus recover the expression in brackets on the rhs of (1). In the second integral of the rhs of (3) and in the limit $\alpha \rightarrow 0^+$, $I(x, y)$ can be replaced by $xf(0)/(x^2 + y^2)$ since $f(x)$ is well behaved in the whole interval (A, B) . Hence, we have

$$\lim_{\alpha \rightarrow 0^+} \int_{-\alpha}^{\alpha} dx I(x, y) = f(0) \lim_{\alpha \rightarrow 0^+} \int_{-\alpha}^{\alpha} dx \frac{x}{x^2 + y^2} = 0 . \tag{4}$$

Thus the real parts of the two sides of (1) are equal to each other as well. \square

1.5s. The state of a classical point particle moving in a d-dimensional real space is fully determined by fixing the d-component position vector \mathbf{r} and the d-component momentum vector \mathbf{p} , i.e., by giving the corresponding point in phase space (the latter is the combined \mathbf{r}, \mathbf{p} space). Thus, the number of states associated with a region of phase space, although classically infinite, is proportional to the volume of that region (the dimension of this volume is action to the d th power). Quantum mechanics, because of Heisenberg’s uncertainty relation, $\delta x \delta p_x \geq \hbar/2$, sets an absolute minimum, $(c\hbar)^d$, to the volume of phase space (c is a numerical constant). Hence, to the elementary volume $(c\hbar)^d$ corresponds just one state and to the volume $d\mathbf{r}d\mathbf{p}$ correspond

$$\frac{d\mathbf{r}d\mathbf{p}}{(c\hbar)^d} \tag{1}$$

states. To determine the numerical constant c , it is enough to consider a free particle in a 1-d real space of total length L as $L \rightarrow \infty$. Without loss of generality we can impose periodic boundary conditions:

$$\psi(0) = \psi(L) , \tag{2}$$

where ψ is the eigenfunction,

$$\psi(x) = \frac{1}{\sqrt{L}} e^{ikx}, \quad (3)$$

of momentum $p = \hbar k$. Because of (2) we have

$$e^{ikL} = 1 \Rightarrow kL = 2\pi\ell, \quad \ell = \text{integer}. \quad (4)$$

Thus, the allowed values of k are

$$k_\ell = \frac{2\pi}{L} \ell,$$

with a spacing between consecutive eigenvalues equal to $2\pi/L$. As a result, the number of states in an interval δk equals

$$\frac{\delta k}{2\pi/L} = \frac{L}{2\pi} \delta k = \frac{L\delta p}{2\pi\hbar}. \quad (5)$$

Hence the constant c in (1) equals 2π , and the final formula for the number of states in the phase space volume element $d\mathbf{r}d\mathbf{p} = \hbar^d d\mathbf{r}d\mathbf{k}$ is the following:

$$\frac{d\mathbf{r}d\mathbf{p}}{h^d} = \frac{d\mathbf{r}d\mathbf{k}}{(2\pi)^d}. \quad (6)$$

For a uniform $|\psi(\mathbf{r})|^2$, integration over $d\mathbf{r}$ gives

$$\frac{\Omega d\mathbf{k}}{(2\pi)^d} \quad (7)$$

for the number of states associated with the \mathbf{k} -space volume element $d\mathbf{k}$ and the whole real space volume, Ω .

Notice that (6) and (7) are valid not only for plane waves but for Bloch waves as well, i.e., for wavefunctions $\psi(x)$ of the form

$$\psi(x) = u(x)e^{ikx}, \quad (8)$$

where $u(x)$ is a periodic function with the same period as the potential acting on the particle. For these wavefunctions, (4) is valid, which implies (5), (6), and (7). \square

1.6s. The normalized eigenfunctions of the operator, $-d^2/dx^2$, in the domain $(0, 1)$ with BC $\phi_n(0) = \phi_n(1) = 0$ are obviously

$$\phi_n(x) = \sqrt{2} \sin(n\pi x), \quad n = 1, 2, 3, \dots \quad (1)$$

Hence, according to (1.13), the Green's function $G(x, x'; z)$ is given by the following sum:

$$G(x, x'; z) = 2 \sum_{n=1}^{\infty} \frac{\sin(n\pi x) \sin(n\pi x')}{z - n^2\pi^2}. \quad (2)$$

The second method of calculation gives G as the sum G^∞ , the Green's function satisfying the same inhomogeneous equation in the infinite domain

$(-\infty, +\infty)$, plus the general solution, ϕ , of the corresponding homogeneous equation

$$\left(z + \frac{d^2}{dx^2}\right)\phi(x) = 0. \quad (3)$$

Equation (3) gives for $\phi(x)$

$$\phi(x) = Ae^{i\sqrt{z}x} + Be^{-i\sqrt{z}x}. \quad (4)$$

Taking into account (1.55) and the BC for $G(x, x'; z) = G^\infty(x, x'; z) + \phi(x)$, we obtain two linear algebraic equations for A and B :

$$G(0, x'; z) = 0 \Rightarrow \frac{e^{i\sqrt{z}x'}}{2i\sqrt{z}} + A + B = 0, \quad (5)$$

$$G(1, x'; z) = 0 \Rightarrow \frac{e^{i\sqrt{z}(1-x')}}{2i\sqrt{z}} + Ae^{i\sqrt{z}} + Be^{-i\sqrt{z}} = 0. \quad (6)$$

Solving the set of (5) and (6) we find

$$A = i \frac{\sin[\sqrt{z}(1-x')]}{2\sqrt{z}\sin\sqrt{z}}, \quad B = ie^{i\sqrt{z}} \frac{\sin(\sqrt{z}x')}{2\sqrt{z}\sin\sqrt{z}}. \quad (7)$$

Substituting A and B from (7) into (4) and adding $\phi(x)$ to G^∞ we obtain after some algebra

$$G(x, x'; z) = \begin{cases} -\frac{\sin[\sqrt{z}(1-x')]\sin(\sqrt{z}x)}{\sqrt{z}\sin\sqrt{z}} \xrightarrow{z \rightarrow 0} -(1-x')x, & x < x', \quad (8a) \\ -\frac{\sin[\sqrt{z}(1-x)]\sin(\sqrt{z}x')}{\sqrt{z}\sin\sqrt{z}} \xrightarrow{z \rightarrow 0} -(1-x)x', & x' < x. \quad (8b) \end{cases}$$

The reader can easily prove that expression (8) satisfies (3) for $0 \leq x < x'$ and for $x' < x \leq 1$, exhibits a discontinuity equal to 1 in the derivative (dG/dx) at $x = x'$ [which is equivalent to $d^2G/dx^2 = \delta(x-x')$], and satisfies the BC at $x, x' = 0$, and $x, x' = 1$. Thus (8) gives indeed the requested Green's function in closed form.

According to the third method of calculation, we find the Green's function separately in the regions $0 \leq x < x'$ and $x' < x \leq 1$ together with the corresponding BC. In these regions the Green's function satisfies (3), which together with the BC gives

$$G(x, x'; z) = \begin{cases} C(x') \sin(\sqrt{z}x), & x < x', \quad (9a) \\ D(x') \sin[\sqrt{z}(1-x)], & x' < x. \quad (9b) \end{cases}$$

The unknown quantities $C(x')$ and $D(x')$ are determined by the continuity of G at $x = x'$, which implies

$$C(x') \sin(\sqrt{z}x') = D(x') \sin[\sqrt{z}(1-x')] \quad (10)$$

and the relation

$$\left(\frac{dG}{dx}\right)_{x=x'+} - \left(\frac{dG}{dx}\right)_{x=x'-} = 1. \tag{11}$$

Equation (11) is obtained by integrating (1.1) over x ,

$$\left(z + \frac{d}{dx^2}\right) G(x, x'; z) = \delta(x - x'), \tag{12}$$

once from $x' - \alpha$ to $x' + \alpha$ as $\alpha \rightarrow 0^+$; one more integration of (11) leads to (10). Taking into account that $G(x, x'; z)$ remains invariant under interchanging x and x' , we conclude that (10) implies that

$$C(x') = A \sin [\sqrt{z}(1 - x')] \tag{13a}$$

and

$$D(x') = A \sin (\sqrt{z}x'). \tag{13b}$$

Substituting (13a) and (13b) into (11) we determine the constant A :

$$A = -\frac{1}{\sqrt{z} \sin \sqrt{z}}. \tag{14}$$

Combining (14), (13a, 13b), and (9), we end up again with (8) for $G(x, x'; z)$.

To find the sum $\sum_{n=1}^{\infty} (\alpha^2 + n^2)^{-1}$, we equate the two expressions for $G(x, x'; z)$ [(2) and (8)], set $x = x'$, and then integrate over x from 0 to 1. We then find

$$\frac{1}{2\sqrt{z}} \cot \sqrt{z} - \frac{1}{2z} = \sum_{n=1}^{\infty} \frac{1}{z - n^2\pi^2}. \tag{15}$$

Setting $z = -\pi^2\alpha^2$ in (15) we have

$$\sum_{n=1}^{\infty} \frac{1}{\alpha^2 + n^2} = \frac{1}{2\alpha^2} [-1 + \alpha\pi \coth(\alpha\pi)] \xrightarrow{\alpha \rightarrow 0} \frac{\pi^2}{6}. \tag{16}$$

If we choose $x = x' = 1/2$ in both (2) and (8), we obtain

$$-\frac{\sin^2(\sqrt{z}/2)}{\sqrt{z} \sin \sqrt{z}} = 2 \sum'_{n=1}^{\infty} \frac{1}{z - n^2\pi^2}, \tag{17}$$

where the prime in the sum indicates that only odd values of n are involved. Taking the limit $z \rightarrow 0$ in (17) we have

$$\sum'_{n=1}^{\infty} \frac{1}{n^2} = \frac{\pi^2}{8}. \tag{18}$$

□

1.7s. The solutions of the 2-dimensional Helmholtz equation, $(z + \nabla^2)\phi = 0$, in polar coordinates are given by setting $m = 0$ in (C.2) of Appendix C:

$$\psi(\boldsymbol{\varrho}) = A_n e^{in\phi} J_{|n|}(\sqrt{z}\varrho) , \tag{1}$$

where n is an integer, since ϕ covers the whole range $[0, 2\pi]$. The BC of $\psi(\boldsymbol{\varrho})$, being finite at the origin, excludes the presence of the other Bessel function, Y_n . The BC at $\varrho = a$, $\psi(a, \phi) = 0$ implies that

$$J_{|n|}(\sqrt{z}a) = 0 . \tag{2}$$

Let us call the roots of $J_{|n|}(x) = 0$, λ_{nm} , $m = 1, 2, 3, \dots$. It then follows from (2) that

$$z = \frac{\lambda_{nm}^2}{a^2} .$$

Hence the eigenfunctions we are looking for are of the form

$$\psi_{nm}(\boldsymbol{\varrho}) = A_{nm} e^{in\phi} J_{|n|}(\lambda_{nm}\varrho/a) , \tag{3}$$

where the constant A_{nm} is determined from the normalization condition,

$$\int \psi_{nm}^*(\boldsymbol{\varrho}) \psi_{nm}(\boldsymbol{\varrho}) \varrho d\varrho d\phi = 1 ,$$

which, in connection with the relation¹

$$\int_0^1 dx x J_{|n|}(\alpha x) J_{|n|}(\beta x) = \frac{1}{2} \delta_{\alpha\beta} [J_{|n|+1}(\alpha)]^2 , \text{ if } J_{|n|}(\alpha) = J_{|n|}(\beta) = 0 , \tag{4}$$

gives

$$A_{nm} = \sqrt{\frac{1}{\pi a} \frac{1}{J_{n+1}(\lambda_{nm})}} . \tag{5}$$

Taking into account (3) and (5) and combining the $\pm |n|$ terms, we have [according to the basic formula (1.13)]:

$$\begin{aligned} G(\boldsymbol{\varrho}, \boldsymbol{\varrho}'; z) &= \frac{2}{\pi a^2} \sum_{n=1}^{\infty} \sum_{m=1}^{\infty} \frac{J_n(\lambda_{nm}\varrho/a) J_n(\lambda_{nm}\varrho'/a) \cos[n(\phi - \phi')]}{J_{n+1}^2(\lambda_{nm}) [z - (\lambda_{nm}/a)^2]} \\ &+ \frac{1}{\pi a^2} \sum_{m=1}^{\infty} \frac{J_0(\lambda_{0m}\varrho/a) J_0(\lambda_{0m}\varrho'/a)}{J_1^2(\lambda_{0m}) [z - (\lambda_{0m}/a)^2]} \end{aligned} \tag{6}$$

¹ See the GR table of integrals on p. 672 of [11].

Combination of the Fourth and Third methods

In 2-dimensional polar coordinates the delta function $\delta(\varrho - \varrho')$ can be written as

$$\delta(\varrho - \varrho') = \frac{1}{\varrho} \delta(\varrho - \varrho') \delta(\phi - \phi') = \frac{1}{2\pi} \sum_{m=-\infty}^{\infty} \frac{1}{\varrho} \delta(\varrho - \varrho') e^{im(\phi - \phi')} . \quad (7)$$

We shall express the Green's function we are trying to determine as

$$G(\varrho, \varrho'; z) = \frac{1}{2\pi} \sum_{m=-\infty}^{\infty} g_m(\varrho, \varrho'; z) e^{im(\phi - \phi')} . \quad (8)$$

In the regions $0 \leq \varrho \leq \varrho'$ and $\varrho' < \varrho \leq a$, G satisfies the homogeneous equation $(z + \nabla^2)G = 0$, and consequently g_m is given by Bessel functions:

$$g_m(\varrho, \varrho'; z) = \begin{cases} A_m(\varrho', z) J_m(\sqrt{z}\varrho) , & 0 \leq \varrho < \varrho' \\ B_m(\varrho', z) L_m(\sqrt{z}\varrho) , & \varrho' < \varrho \leq a \end{cases} \quad (9a)$$

$$(9b)$$

where

$$L_m(\sqrt{z}\varrho) = J_m(\sqrt{z}\varrho) - c_m Y_m(\sqrt{z}\varrho) , \quad (9c)$$

such that $L_m(\sqrt{z}a) = 0$, which implies

$$c_m = J_m(\sqrt{z}a) / Y_m(\sqrt{z}a) . \quad (9d)$$

In (9a) we have excluded $Y_m(\sqrt{z}\varrho)$ because it blows up for $\varrho = 0$. The invariance under interchanging ϱ and ϱ' and the continuity of $G(\varrho, \varrho'; z)$ at $\varrho = \varrho'$ lead to the relations

$$A_m(\varrho', z) = D_m L_m(\sqrt{z}\varrho') , \quad (10a)$$

$$B_m(\varrho', z) = D_m J_m(\sqrt{z}\varrho') , \quad (10b)$$

where D_m is a constant depending only on m . By integrating the singularity $\delta(\varrho - \varrho')/\varrho$ from $\varrho' - \alpha$ to $\varrho' + \alpha$ in the limit $\alpha \rightarrow 0^+$, we transform it to a discontinuity $1/\varrho$ at the point $\varrho = \varrho'$. Thus

$$\left(\frac{dg_m}{d\varrho} \right)_{\varrho=\varrho'+} - \left(\frac{dg_m}{d\varrho} \right)_{\varrho=\varrho'-} = \frac{1}{\varrho} . \quad (11)$$

Substituting (9a), (9b), (9c), (9d), (10a), and (10b) into (11), we determine D_m :

$$\begin{aligned} D_m &= \frac{1}{\varrho [(dL_m/d\varrho) J_m - (dJ_m/d\varrho) L_m]_{\varrho=\varrho'}} \\ &= \frac{1}{c_m \varrho \sqrt{z} [J'_m Y_m - J_m Y'_m]_{\varrho=\varrho'}} = \frac{1}{c_m \varrho \sqrt{z} \left(\frac{-2}{\pi \varrho \sqrt{z}} \right)} \\ &= -\frac{\pi}{2c_m} , \end{aligned} \quad (12)$$

where

$$J'_m = \left[\frac{dJ_m}{d(\sqrt{z}\varrho)} \right]_{\varrho=\varrho'} , \quad Y'_m = \left[\frac{dY_m}{d(\sqrt{z}\varrho)} \right]_{\varrho=\varrho'} ;$$

use was made of the fact that the Wronskian

$$W \{ J_m(\sqrt{z}\varrho), Y_m(\sqrt{z}\varrho) \} \equiv J_m Y'_m - J'_m Y_m = \frac{2}{\pi\sqrt{z}\varrho} .$$

Thus

$$g_m(\varrho, \varrho'; z) = \begin{cases} J_m(\sqrt{z}\varrho) K_m(\sqrt{z}\varrho') , & \varrho < \varrho' , \\ J_m(\sqrt{z}\varrho') K_m(\sqrt{z}\varrho) , & \varrho' < \varrho , \end{cases} \quad (13a)$$

$$(13b)$$

where

$$K_m(x) = \frac{\pi}{2} \left[Y_m(x) - \frac{Y_m(\sqrt{z}a)}{J_m(\sqrt{z}a)} J_m(x) \right] . \quad (13c)$$

The case $a = \infty$ (meaning that the BC at infinity is such that the Green's function describes an outgoing wave) is obtained by replacing $K_m(x)$ by $-(i\pi/2)H_m^{(1)}(x)$. Notice that the case $a = \infty$ cannot be obtained from (13c) by taking the limit $a \rightarrow \infty$ since the BC $G(\varrho, \varrho'; z) = 0$ implies the existence of a reflected ingoing wave in addition to the outgoing. Formally the $K_m(x)$ can be transformed to $-(i\pi/2)H_m^{(1)}(x)$ by replacing $Y_m(\sqrt{z}a)/J_m(\sqrt{z}a)$ by i . The case $a = \infty$ has already been obtained in closed form in (1.48). Comparing the two expressions (1.48) and (8) combined with (13a) and $K_m \rightarrow -(i\pi/2)H_m^{(1)}$ we have

$$-\frac{i}{4}H_0^{(1)}(\sqrt{z}|\varrho - \varrho'|) = -\frac{i}{4} \sum_{m=-\infty}^{\infty} e^{im(\phi-\phi')} \times \begin{cases} J_m(\sqrt{z}\varrho) H_m^{(1)}(\sqrt{z}\varrho') , & \varrho < \varrho' \\ J_m(\sqrt{z}\varrho') H_m^{(1)}(\sqrt{z}\varrho) , & \varrho' < \varrho \end{cases} . \quad (14)$$

Knowing (14) allows us to use the *second method* for the calculation of G , i.e., $G = G^\infty + \psi$, where ψ is the general solution of the homogeneous equation $(z + \nabla^2)\psi = 0$; ψ according to (1) has the following general form:

$$\psi = \frac{i}{4} \sum_{m=-\infty}^{\infty} A_m e^{im(\phi-\phi')} J_m(\sqrt{z}\varrho) . \quad (15)$$

Hence the Green's function G is given by [taking into account (14)]

$$G = \frac{i}{4} \sum_m e^{im(\phi-\phi')} \times \begin{cases} A_m J_m(\sqrt{z}\varrho) - J_m(\sqrt{z}\varrho) H_m^{(1)}(\sqrt{z}\varrho') , & \varrho < \varrho' , \\ A_m J_m(\sqrt{z}\varrho) - J_m(\sqrt{z}\varrho') H_m^{(1)}(\sqrt{z}\varrho) , & \varrho' < \varrho . \end{cases} \quad (16)$$

To satisfy the BC $G = 0$ for $\varrho = a$, we must have

$$A_m = J_m(\sqrt{z}\varrho') \frac{H_m^{(1)}(\sqrt{z}a)}{J_m(\sqrt{z}a)}. \quad (17)$$

We substitute (17) into (16) and find, taking into account that $H_m^{(1)} = J_m + iY_m$,

$$\begin{aligned} A_m J_m(\sqrt{z}\varrho) - J_m(\sqrt{z}\varrho) H^{(1)}(\sqrt{z}\varrho') &= -i \left[Y_m(\sqrt{z}\varrho') - \frac{Y_m(\sqrt{z}a)}{J_m(\sqrt{z}a)} J_m(\sqrt{z}\varrho') \right] J_m(\sqrt{z}\varrho) \\ &= -\frac{2i}{\pi} K_m(\sqrt{z}\varrho') J_m(\sqrt{z}\varrho), \quad \varrho < \varrho'; \end{aligned} \quad (18)$$

$$\begin{aligned} A_m J_m(\sqrt{z}\varrho) - J_m(\sqrt{z}\varrho') H_m^{(1)}(\sqrt{z}\varrho) &= -\frac{2i}{\pi} K_m(\sqrt{z}\varrho) J_m(\sqrt{z}\varrho'), \quad \varrho' < \varrho. \end{aligned} \quad (19)$$

Substituting (18) and (19) into (16) we find the same expression as the one obtained by combining (8) with (13a).

The reader may verify, by taking the limit $z \rightarrow 0$ in (13a, 13b, 13c) and using (C.3a-C.3c) of Appendix C, that the Green's function satisfying the relation $\nabla^2 G = \delta(\varrho - \varrho')$ and the BC $G = 0$ for $\varrho = a$ is given by

$$G = \frac{1}{2\pi} \begin{cases} \ln\left(\frac{\varrho'}{a}\right) + \sum_{m=1}^{\infty} \frac{\cos[m(\phi - \phi')]}{m} \left[\left(\frac{\varrho\varrho'}{a^2}\right)^m - \left(\frac{\varrho}{\varrho'}\right)^m \right], & \varrho < \varrho', \\ \ln\left(\frac{\varrho}{a}\right) + \sum_{m=1}^{\infty} \frac{\cos[m(\phi - \phi')]}{m} \left[\left(\frac{\varrho\varrho'}{a^2}\right)^m - \left(\frac{\varrho'}{\varrho}\right)^m \right], & \varrho' < \varrho. \end{cases}$$

The above function, multiplied by -4π , gives the electrostatic potential, ψ , of a line unit charge located at the point (ϱ', ϕ') inside a hollow grounded metallic circular cylindrical shell of radius a . \square

1.8s.

First method by employing the eigenfunctions of $-\nabla^2$

The eigenfunctions of $-\nabla^2$ satisfying the BC at $r = 0$ and $r = a$ are of the form

$$f_{n\ell m} = A_{n\ell m} Y_{\ell m}(\theta, \phi) j_{\ell}(\sqrt{z'}r), \quad (1)$$

where $\sqrt{z'}a = \lambda_{\ell n}$ and $j_{\ell}(\lambda_{\ell n}) = 0$, i.e., $z' = \lambda_{\ell n}^2/a^2$.

The coefficients $A_{n\ell m}$ are determined from the normalization condition

$$\int f_{n\ell m}^* f_{n\ell m} d\mathbf{r} = 1, \quad (2a)$$

or

$$\begin{aligned}
 & A_{n\ell m}^2 \int_0^a dr r^2 \left[j_\ell(\sqrt{z}r) \right]^2 \\
 &= A_{n\ell m}^2 a^3 \int_0^1 dx x^2 [j_\ell(\lambda_{\ell n}x)]^2 = A_{n\ell m}^2 \frac{a^3}{2} [j_{\ell+1}(\lambda_{\ell n})]^2 = 1. \quad (2b)
 \end{aligned}$$

Hence, according to (1.13), the Green's function is given by

$$\begin{aligned}
 & G(\mathbf{r}, \mathbf{r}'; z) \\
 &= \frac{2}{a^3} \sum_{n=1}^{\infty} \sum_{\ell=0}^{\infty} \sum_{m=-\ell}^{\ell} \frac{Y_{\ell m}(\theta, \phi) Y_{\ell m}^*(\theta', \phi') j_\ell(\lambda_{\ell n}r/a) j_\ell(\lambda_{\ell n}r'/a)}{[j_{\ell+1}(\lambda_{\ell n})]^2 [z - (\lambda_{\ell n}^2/a^2)]}. \quad (3)
 \end{aligned}$$

Combining the Third and Fourth methods

Following the corresponding approach in 1.7s and taking into account that

$$\delta(\mathbf{r} - \mathbf{r}') = \frac{\delta(r - r')}{r^2} \sum_{\ell m} Y_{\ell m}(\theta, \phi) Y_{\ell m}^*(\theta', \phi'), \quad (4)$$

we expect $G(\mathbf{r}, \mathbf{r}'; z)$ to be of the form

$$G(\mathbf{r}, \mathbf{r}'; z) = \sum_{\ell m} Y_{\ell m}(\theta, \phi) Y_{\ell m}^*(\theta', \phi') \begin{cases} j_\ell(\sqrt{z}r) k_\ell(\sqrt{z}r'), & r < r', \quad (5a) \\ j_\ell(\sqrt{z}r') k_\ell(\sqrt{z}r), & r' < r, \quad (5b) \end{cases}$$

where

$$k_\ell(x) = d_\ell [j_\ell(x) - c_\ell y_\ell(x)] \quad (6a)$$

and

$$k_\ell(\sqrt{z}a) = 0. \quad (6b)$$

Equation (6b) implies that

$$c_\ell = \frac{j_\ell(\sqrt{z}a)}{y_\ell(\sqrt{z}a)}. \quad (7)$$

Using (C.11) with G in the place of ψ in connection with (C.17b) and (C.17c) we find

$$(z + \nabla^2) G = \frac{1}{r^2} \frac{\partial}{\partial r} \left(r^2 \frac{\partial G}{\partial r} \right) + [zr^2 - \ell(\ell + 1)] \frac{1}{r^2} G = \delta(\mathbf{r} - \mathbf{r}'). \quad (8a)$$

Substituting in (8a) from (4) and (5) and integrating over r from $r' - s$ to $r' + s$ as $s \rightarrow 0^+$ we find

$$\sqrt{z} [j_\ell(x) k'_\ell(x) - j'_\ell(x) k_\ell(x)] = \frac{1}{r^2}, \quad x = \sqrt{z}r. \quad (8b)$$

The Wronskian in brackets equals

$$-d_\ell c_\ell W(j_\ell, y_\ell) = -\frac{d_\ell c_\ell}{x^2} = -\frac{d_\ell c_\ell}{zr^2}.$$

Thus

$$d_\ell = -\frac{\sqrt{z}}{c_\ell}, \tag{9}$$

and

$$k_\ell(x) = \sqrt{z} \left[y_\ell(x) - \frac{1}{c_\ell} j_\ell(x) \right]. \tag{10}$$

The case $a = \infty$ with no ingoing reflected wave is obtained by replacing $1/c_\ell$ by i so that

$$k_\ell(x) \rightarrow -i\sqrt{z}h_\ell^{(1)}(x). \tag{11}$$

Equating (5), in conjunction with (11), with expression (1.39) for $G(\mathbf{r}, \mathbf{r}'; z)$, we have the following relation:

$$\begin{aligned} & \frac{e^{i\sqrt{z}|\mathbf{r}-\mathbf{r}'|}}{4\pi|\mathbf{r}-\mathbf{r}'|} \\ &= -i\sqrt{z} \sum_{\ell m} Y_{\ell m}(\theta, \phi) Y_{\ell m}^*(\theta', \phi') \begin{cases} j_\ell(\sqrt{z}r) h_\ell^{(1)}(\sqrt{z}r'), & r < r' \\ j_\ell(\sqrt{z}r') h_\ell^{(1)}(\sqrt{z}r), & r' < r \end{cases} \\ &= -i\sqrt{z} \sum_{\ell=0}^{\infty} \sum_{m=0}^{\ell} (2 - \delta_{m0}) \frac{2\ell + 1}{4\pi} \frac{(\ell - m)!}{(\ell + m)!} P_\ell^m(\cos \theta) P_\ell^m(\cos \theta') \\ & \quad \times \cos[m(\phi - \phi')] \begin{cases} j_\ell(\sqrt{z}r) h_\ell^{(1)}(\sqrt{z}r'), & r < r' \\ j_\ell(\sqrt{z}r') h_\ell^{(1)}(\sqrt{z}r), & r' < r \end{cases}. \tag{12} \end{aligned}$$

If we choose the z -axis to coincide with the direction θ', ϕ' and we call γ the angle between θ, ϕ , and the new z -axis, then the above expression simplifies because it is symmetric around the new z -axis and consequently $m = 0$; furthermore, $P_\ell(\cos 0) = P_\ell(1) = 1$. Thus comparing the two expressions for $G(\mathbf{r}, \mathbf{r}'; z)$ in the old and the new z -axis we obtain

$$\begin{aligned} P_\ell(\cos \gamma) &= P_\ell(\mathbf{n} \cdot \mathbf{n}') \\ &= \sum_{m=0}^{\ell} (2 - \delta_{m0}) \frac{(\ell - m)!}{(\ell + m)!} P_\ell^m(\cos \theta) P_\ell^m(\cos \theta') \cos[m(\phi - \phi')] \tag{13a} \end{aligned}$$

$$= \frac{4\pi}{2\ell + 1} \sum_{m=-\ell}^{\ell} Y_{\ell m}(\mathbf{n}) Y_{\ell m}^*(\mathbf{n}'), \tag{13b}$$

where \mathbf{n}, \mathbf{n}' are the unit vectors along the directions (θ, ϕ) and (θ', ϕ') , respectively. To obtain (12) and (13a), we used (A.11) in Appendix A.

Taking the limit $z \rightarrow 0$ in (12) we have

$$\frac{1}{|\mathbf{r} - \mathbf{r}'|} = \sum_{\ell m} \frac{4\pi}{2\ell + 1} Y_{\ell m}(\theta, \phi) Y_{\ell m}^*(\theta', \phi') \begin{cases} r^\ell / r'^{\ell+1}, & r < r' \\ r'^\ell / r^{\ell+1}, & r' < r \end{cases} \quad (14a)$$

$$= \sum_{\ell=0}^{\infty} P_\ell(\mathbf{n} \cdot \mathbf{n}') \begin{cases} r^\ell / r'^{\ell+1}, & r < r' \\ r'^\ell / r^{\ell+1}, & r' < r \end{cases} \quad (14b)$$

$$= \sum_{\ell=0}^{\infty} \sum_{m=0}^{\ell} (2 - \delta_{m0}) \frac{(\ell - m)!}{(\ell + m)!} P_\ell^m(\cos \theta) P_\ell^m(\cos \theta') \times \cos[m(\phi - \phi')] \begin{cases} r^\ell / r'^{\ell+1}, & r < r' \\ r'^\ell / r^{\ell+1}, & r' < r \end{cases} \quad (14c)$$

Equations (14a), (14b), and (14c) are the basis for the multipole expansions in electrostatics.

We quote here for completeness the expansion of a plane wave in spherical harmonics:

$$e^{i\mathbf{k} \cdot \mathbf{r}} = 4\pi \sum_{\ell=0}^{\infty} \sum_{m=-\ell}^{\ell} i^\ell Y_{\ell m}^*(\mathbf{k}_0) Y_{\ell m}(\mathbf{r}_0) j_\ell(kr) \quad (15a)$$

$$= \sum_{\ell=0}^{\infty} i^\ell (2\ell + 1) P_\ell(\mathbf{k}_0 \cdot \mathbf{r}_0) j_\ell(kr), \quad (15b)$$

where \mathbf{k}_0 and \mathbf{r}_0 are the unit vectors along the directions of \mathbf{k} and \mathbf{r} , respectively. \square

1.9s. We wish to calculate the integral

$$G(z) = \frac{1}{\pi} \int_{-B}^B \frac{dE}{(z - E)\sqrt{(B^2 - E^2)}}, \quad B = 2|V|. \quad (1)$$

We change variables by introducing ϕ through

$$E = B \cos \phi \quad (2)$$

so that

$$G(z) = \frac{1}{\pi} \int_{-\pi}^0 \frac{-B \sin \phi d\phi}{(z - B \cos \phi)B \sin \phi} = -\frac{1}{\pi} \int_{-\pi}^0 \frac{d\phi}{z - B \cos \phi}. \quad (3)$$

We put $w = e^{i\phi}$ so that $dw = iwd\phi$ and $\cos \phi = (w + w^{-1})/2 = (w^2 + 1)/2w$. Hence

$$G(z) = \frac{i}{\pi} \int_{-1}^1 \frac{dw}{zw - \frac{B}{2}(w^2 + 1)} = -\frac{i}{\pi} \frac{2}{B} \int_{-1}^1 \frac{dw}{w^2 - (2z/B)w + 1} \quad (4)$$

$$= -\frac{2i}{\pi B} \int_{-1}^1 \frac{dw}{(w - w_1)(w - w_2)} = -\frac{i}{\pi B} \oint \frac{dw}{(w - w_1)(w - w_2)},$$

where w_1, w_2 are the roots of the polynomial $w^2 - (2z/B)w + 1$. Obviously, $w_1w_2 = 1, w_1 + w_2 = 2z/B$, and $w_2 - w_1 = 2\sqrt{(z/B)^2 - 1}$. The last integral is over the unit circle; it was obtained by adding to (3) the integral

$$-\frac{1}{\pi} \int_0^\pi \frac{d\phi}{z - B \cos \phi} = G(z)$$

and dividing by 2.

Case 1: $|w_1| \neq |w_2|$; then one of the two roots, e.g., $|w_1|$, is less than one (since $w_1w_2 = 1$). By the residue theorem we then have

$$G(z) = \frac{2}{B(w_2 - w_1)} = \frac{1}{\sqrt{z^2 - B^2}}, \tag{5}$$

where the square root is the one that has the same sign of the imaginary part as the sign of $\text{Im}\{z\}$. Thus $\text{Im}\{z\} \times \text{Im}\{G(z)\} < 0$, unless $\text{Im}\{z\} = 0$; in this case $G(z)$ is negative for $z < -B$ and positive for $B < z$.

Case 2: $|w_1| = |w_2|$; this occurs only when $z = \cos \phi$, i.e., only when z is real and in the interval $(-B, B)$. To prove that, take into account that, since $|w_1| = |w_2| = 1$ and $w_1w_2 = 1, w_1 = e^{i\phi}$ and $w_2 = e^{-i\phi}$; hence $w_1 + w_2 = 2z/B = 2 \cos \phi$. Thus in this case we must follow a limiting procedure by setting $z = B \cos \phi + i\varepsilon$ and take the limit $\varepsilon \rightarrow 0^\pm$. Using (5) and the relation $\varepsilon \text{Im}\{G(\cos \phi + i\varepsilon)\} < 0$, we obtain, remembering that $E = B \cos \phi$,

$$G^\pm(B \cos \phi) = \lim_{\varepsilon \rightarrow 0^\pm} G(E + i\varepsilon) = \frac{\mp i}{\sqrt{B^2 - E^2}} = \frac{\mp i}{B |\sin \phi|}. \tag{6}$$

The density of states (DOS) is

$$\varrho(E) = -\frac{1}{\pi} \text{Im}\{G^+(E)\} = \frac{1}{\pi \sqrt{B^2 - E^2}}, \tag{7}$$

which coincides, as it should, with the original DOS. \square

1.11s. We have that

$$\begin{aligned} \psi(\boldsymbol{\varrho}) &= \int_\Omega u(\mathbf{r}) G(\mathbf{r}, \boldsymbol{\varrho}) d\mathbf{r} + \int_\Omega \psi(\mathbf{r}) \mathcal{L}_r G(\mathbf{r}, \boldsymbol{\varrho}) d\mathbf{r} \\ &\quad - \int_\Omega G(\mathbf{r}, \boldsymbol{\varrho}) \mathcal{L}_r \psi(\mathbf{r}) d\mathbf{r}. \end{aligned} \tag{1}$$

Equation (1) is valid because the third term cancels the first since $\mathcal{L}_r \psi(\mathbf{r}) = u(\mathbf{r})$ and the second term is equal to $\psi(\mathbf{r})$ in view of the fact that $\mathcal{L}_r G(\mathbf{r}, \boldsymbol{\varrho}) = \delta(\mathbf{r} - \boldsymbol{\varrho})$. The last two terms in (1) can be transformed as follows, taking into account that $\mathcal{L}_r = \nabla_r (f(\mathbf{r}) \nabla_r) + g(\mathbf{r})$:

$$\begin{aligned}
& \int_{\Omega} [\psi(\mathbf{r}) \mathcal{L}_r G(\mathbf{r}, \boldsymbol{\rho}) - G(\mathbf{r}, \boldsymbol{\rho}) \mathcal{L}_r \psi(\mathbf{r})] d\mathbf{r} \\
&= \int_{\Omega} \psi(\mathbf{r}) \nabla_r [f(\mathbf{r}) \nabla_r G(\mathbf{r}, \boldsymbol{\rho})] d\mathbf{r} + \int_{\Omega} \psi(\mathbf{r}) g(\mathbf{r}) G(\mathbf{r}, \boldsymbol{\rho}) d\mathbf{r} \\
&\quad - \int_{\Omega} G(\mathbf{r}, \boldsymbol{\rho}) \nabla_r [f(\mathbf{r}) \nabla_r \psi(\mathbf{r})] d\mathbf{r} - \int_{\Omega} G(\mathbf{r}, \boldsymbol{\rho}) g(\mathbf{r}) \psi(\mathbf{r}) d\mathbf{r}; \quad (2)
\end{aligned}$$

the second and fourth terms on the rhs of (2) cancel each other; the remaining two terms can be written as follows:

$$\begin{aligned}
& \int_{\Omega} \{\psi(\mathbf{r}) \nabla_r [f(\mathbf{r}) \nabla_r G(\mathbf{r}, \boldsymbol{\rho})] - G(\mathbf{r}, \boldsymbol{\rho}) \nabla_r [f(\mathbf{r}) \nabla_r \psi(\mathbf{r})]\} d\mathbf{r} \\
&= \int_{\Omega} \nabla_r [\psi(\mathbf{r}) f(\mathbf{r}) \nabla_r G(\mathbf{r}, \boldsymbol{\rho}) - G(\mathbf{r}, \boldsymbol{\rho}) f(\mathbf{r}) \nabla_r \psi(\mathbf{r})] d\mathbf{r} \\
&= \int_S [\psi(\mathbf{r}) f(\mathbf{r}) \nabla_r G(\mathbf{r}, \boldsymbol{\rho}) - G(\mathbf{r}, \boldsymbol{\rho}) f(\mathbf{r}) \nabla_r \psi(\mathbf{r})] \cdot d\mathbf{S}. \quad (3)
\end{aligned}$$

Substituting (3) into (1) we have

$$\begin{aligned}
\psi(\boldsymbol{\rho}) &= \int_{\Omega} G(\mathbf{r}, \boldsymbol{\rho}) u(\mathbf{r}) d\mathbf{r} \\
&\quad + \int_S [\psi(\mathbf{r}) f(\mathbf{r}) \nabla_r G(\mathbf{r}, \boldsymbol{\rho}) - G(\mathbf{r}, \boldsymbol{\rho}) f(\mathbf{r}) \nabla_r \psi(\mathbf{r})] \cdot d\mathbf{S}. \quad (4)
\end{aligned}$$

Thus, if we know that $\psi(\mathbf{r})$ satisfies the BC $\psi(\mathbf{r}) = u_1(\mathbf{r})$ for \mathbf{r} on the bounding surface S , we can choose the BC for $G(\mathbf{r}, \boldsymbol{\rho}) = 0$ on S . Then

$$\psi(\boldsymbol{\rho}) = \int_{\Omega} G(\mathbf{r}, \boldsymbol{\rho}) u(\mathbf{r}) d\mathbf{r} + \int_S u_1(\mathbf{r}) f(\mathbf{r}) \nabla_r G(\mathbf{r}, \boldsymbol{\rho}) \cdot d\mathbf{S}. \quad (4a)$$

If, on the other hand, $\nabla_r \psi(\mathbf{r})$ is given for \mathbf{r} on S [$\nabla_r \psi = \mathbf{u}_2(\mathbf{r})$], we can choose $\nabla_r G(\mathbf{r}, \boldsymbol{\rho}) = 0$ on S ; then we have

$$\psi(\boldsymbol{\rho}) = \int_{\Omega} G(\mathbf{r}, \boldsymbol{\rho}) u(\mathbf{r}) d\mathbf{r} - \int_S G(\mathbf{r}, \boldsymbol{\rho}) f(\mathbf{r}) \mathbf{u}_2(\mathbf{r}) \cdot d\mathbf{S}. \quad (4b)$$

Equations (4a) and (4b) show that the unknown function ψ can be expressed in terms of a volume and a surface integral involving the Green's functions and known functions. If $u_1 \nabla_r G$ or $G \mathbf{u}_2$ in (4a) and (4b), respectively, is zero on the surface S , then only the volume integral survives.

In the special case $f(\mathbf{r}) = 1$ and $g(\mathbf{r}) = z$, we have

$$\psi(\boldsymbol{\rho}) = \int_{\Omega} G(\mathbf{r}, \boldsymbol{\rho}) u(\mathbf{r}) d\mathbf{r} + \int_S u_1(\mathbf{r}) \nabla_r G(\mathbf{r}, \boldsymbol{\rho}) \cdot d\mathbf{S} \quad (4a')$$

or

$$\psi(\boldsymbol{\rho}) = \int_{\Omega} G(\mathbf{r}, \boldsymbol{\rho}) u(\mathbf{r}) d\mathbf{r} - \int_S G(\mathbf{r}, \boldsymbol{\rho}) \mathbf{u}_2(\mathbf{r}) \cdot d\mathbf{S}. \quad (4b')$$

Notice that, in this case, $G(\mathbf{r}, \boldsymbol{\rho}) = G(\boldsymbol{\rho}, \mathbf{r})$. \square

Chapter 2

2.2s. Taking into account that

$$\frac{d^d k}{(2\pi)^d} = \frac{dk_1}{2\pi} \times \cdots \times \frac{dk_d}{2\pi} \quad (1)$$

and

$$\begin{aligned} \exp(\mathbf{i}\mathbf{k} \cdot \boldsymbol{\varrho} - ic\mathbf{k}^2\tau) &= \exp \left[i \sum_{\nu=1}^d (k_\nu \varrho_\nu - ck_\nu^2\tau) \right] \\ &= \exp [i(k_1\varrho_1 - ck_1^2\tau)] \times \cdots \times \exp [i(k_d\varrho_d - ck_d^2\tau)] , \end{aligned}$$

we obtain that

$$\begin{aligned} g(\mathbf{r}, \mathbf{r}'; \tau) &= -ic \int_{-\infty}^{\infty} \frac{dk_1}{2\pi} \exp [i(k_1\varrho_1 - ck_1^2\tau)] \\ &\quad \times \cdots \times \int_{-\infty}^{\infty} \frac{dk_d}{2\pi} \exp [i(k_d\varrho_d - ck_d^2\tau)] . \end{aligned} \quad (2)$$

Each of the quantities

$$k_\nu \varrho_\nu - ck_\nu^2\tau = -c\tau \left(k_\nu^2 - \frac{\varrho_\nu}{c\tau} k_\nu \right)$$

can be transformed to a perfect square by adding and subtracting $\varrho_\nu^2/4c\tau$. Indeed

$$-c\tau \left(k_\nu^2 - \frac{\varrho_\nu}{c\tau} k_\nu \right) = - \left[\left(k_\nu - \frac{\varrho_\nu}{2c\tau} \right)^2 - \frac{\varrho_\nu^2}{4c^2\tau^2} \right] c\tau . \quad (3)$$

In each of the integrands in (2) we take into account (3), and we change variables by the substitution $x_\nu = k_\nu - (\varrho_\nu/2c\tau)$. Then each integral becomes

$$\begin{aligned} &\int_{-\infty}^{\infty} \frac{dx_\nu}{2\pi} \exp \left[-ic\tau x_\nu^2 + i\frac{\varrho_\nu^2}{4c\tau} \right] \\ &= \frac{1}{2\pi} \exp \left(i\frac{\varrho_\nu^2}{4c\tau} \right) \int_{-\infty}^{\infty} dx_\nu \exp (-ic\tau x_\nu^2) = \sqrt{\frac{1}{4\pi ic\tau}} \exp \left(i\frac{\varrho_\nu^2}{4c\tau} \right) . \end{aligned} \quad (4)$$

Substituting (4) into (2) and taking into account that

$$\begin{aligned} \exp \left(i\frac{\varrho_1^2}{4c\tau} \right) \times \cdots \times \exp \left(i\frac{\varrho_d^2}{4c\tau} \right) &= \exp \left[\frac{i}{4c\tau} (\varrho_1^2 + \cdots + \varrho_d^2) \right] \\ &= \exp \left(\frac{i\boldsymbol{\varrho}^2}{4c\tau} \right) , \end{aligned}$$

we obtain (2.24). \square

Chapter 3

3.1s. Consider a point \mathbf{r} far from the boundaries of the cube of volume L^d within which the particle is confined. Eventually we shall let $L \rightarrow \infty$. The local DOS is according to (1.25)

$$\varrho(\mathbf{r}, E) = \sum_n \delta(E - E_n) \psi_n^*(\mathbf{r} - \mathbf{r}_n) \psi_n(\mathbf{r} - \mathbf{r}_n) . \quad (1)$$

We can separate the eigenstates $\psi_n(\mathbf{r} - \mathbf{r}_n)$ (located around \mathbf{r}_n) into two groups: the first contains those centered away from the boundary by at least a length of the order L_c ; the second contains those centered close to the boundary within a distance of the order L_c . The number, N_1 , of eigenstates in the first group is proportional to $(L - \alpha L_c)^d \rightarrow L^d$ as $L \rightarrow \infty$, while the number, N_2 , in the second group is proportional to $L_c L^{d-1}$. Thus, in the limit $L \rightarrow \infty$, $N_2/N_1 \sim L_c/L \rightarrow 0$. Since each of the eigenstates of the first group is essentially confined within a volume L_c^d around \mathbf{r}_n , it is not in contact with the boundary; thus the quantities $\psi_n^* \psi_n$ and E_n converge as $L \rightarrow \infty$ to nonzero finite values. The average separation between two consecutive levels, $\bar{\delta E}$, is of the order L^{-d} , while the coefficients $\psi_n^* \psi_n$ in front of the δ functions remain finite (for the first group), although most of them are quite small. Let us integrate (1) from $E = -\infty$ to $E = E$:

$$R(\mathbf{r}, E) = \sum_n \theta(E - E_n) \psi_n^*(\mathbf{r} - \mathbf{r}_n) \psi_n(\mathbf{r} - \mathbf{r}_n) . \quad (2)$$

The function $R(\mathbf{r}, E)$ has almost everywhere steps (since their average separation $L^{-d} \rightarrow 0$ as $L \rightarrow \infty$) of finite size. Obviously, neither $R(\mathbf{r}, E)$ nor $\varrho(\mathbf{r}, E)$ converges to a well-defined function at any point E as $L \rightarrow \infty$. Neither of the side limits

$$\lim_{s \rightarrow 0^\pm} \lim_{L \rightarrow \infty} \sum_n \frac{s/\pi}{(E - E_n)^2 + s^2} \psi_n^*(\mathbf{r} - \mathbf{r}_n) \psi_n(\mathbf{r} - \mathbf{r}_n) \quad (3)$$

exists.

On the other hand, if the eigenstates were extended over the whole volume L^d , the quantity $\psi_n \psi_n$ would be on the average equal to L^{-d} , while the average separation of two consecutive levels would be of the order of L^{-d} . Thus, (2) would look as in Fig. 1, where both b and $b' \rightarrow 0$ as $L \rightarrow \infty$ with b'/b finite. It is clear that taking the limits as in (3), a smooth, differentiable (except at some isolated singular points) function will be produced. \square

3.2s. From (3.13') and (3.20) we have, for $d = 1$,

$$\begin{aligned} \psi(x, t) &= i\hbar \int_{-\infty}^{\infty} \tilde{g}(x, x'; t) \psi(x', 0) dx \\ &= \sqrt{\frac{m}{2\pi i\hbar t}} \frac{1}{\sqrt{\delta x} (2\pi)^{1/4}} \\ &\quad \times \int_{-\infty}^{\infty} dx' \exp \left[i \frac{m(x-x')^2}{2\hbar t} + i \frac{p_0 x'}{\hbar} - \frac{x'^2}{4\delta x^2} \right] . \end{aligned} \quad (1)$$

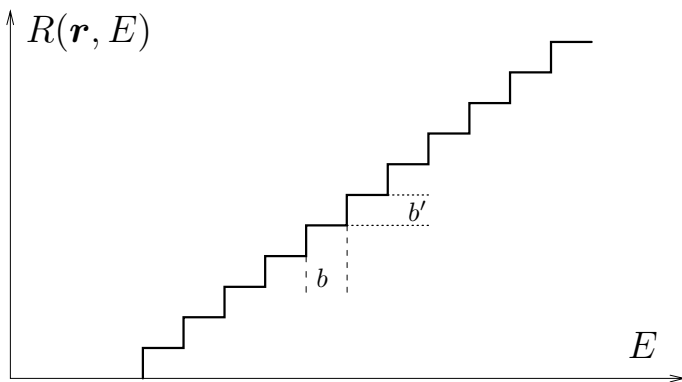


Fig. 1. The number of states per unit volume for a finite system

The integral in (1) can be written as

$$\exp\left(i\frac{mx^2}{2\hbar t}\right) \int_{-\infty}^{\infty} dx' \exp(-a x'^2 + bx') , \tag{2}$$

where

$$a = \frac{1}{4\delta x^2} - \frac{im}{2\hbar t} \tag{3a}$$

and

$$b = -\frac{im}{\hbar t} (x - v_0 t) , \quad v_0 = \frac{p_0}{m} . \tag{3b}$$

The quantity $-a x'^2 + bx'$ can be written as

$$-a \left(x' - \frac{b}{2a}\right)^2 + \frac{b^2}{4a}$$

and hence the integral in (2) is given by

$$\int_{-\infty}^{\infty} dx' \exp(-ax'^2 + bx') = \sqrt{\frac{\pi}{a}} \exp\left(\frac{b^2}{4a}\right) , \quad \text{Re}\{a\} > 0 . \tag{4}$$

Substituting (4) into (2) and taking into account (3a) and (3b) we find

$$\begin{aligned} & \sqrt{\frac{\pi}{a}} \exp\left(i\frac{mx^2}{2\hbar t}\right) \exp\left[-\frac{m^2}{\hbar^2 t^2} (x - v_0 t)^2 \frac{1}{4\left(-\frac{im}{2\hbar t}\right) \left[1 + i\frac{\hbar t}{2m\delta x^2}\right]}\right] \\ &= \sqrt{\frac{\pi}{a}} \exp\left[\frac{imx^2}{2\hbar t} - \frac{im(x - v_0 t)^2}{2\hbar t \left(1 + i\frac{\hbar t}{2m\delta x^2}\right)}\right] \end{aligned}$$

$$\begin{aligned}
&= \sqrt{\frac{\pi}{a}} \exp \left[\frac{im}{2\hbar t} \left(x^2 - \frac{(x - v_0 t)^2}{1 + i \frac{\hbar t}{2m\delta x^2}} \right) \right] \\
&= \sqrt{\frac{\pi}{a}} \exp \left[\frac{-\frac{x^2}{4\delta x^2} + i \frac{mv_0}{\hbar} x - i \frac{mv_0^2 t}{2\hbar}}{1 + i \frac{\hbar t}{2m\delta x^2}} \right].
\end{aligned}$$

Substituting the last expression for the integral into (1) we obtain finally

$$\begin{aligned}
\psi(x, t) &= (2\pi\delta x^2)^{-1/4} \left[1 + \frac{i\hbar t}{2m\delta x^2} \right]^{-1/2} \\
&\times \exp \left(\frac{-\frac{x^2}{4\delta x^2} + i \frac{mv_0}{\hbar} x - i \frac{mv_0^2 t}{2\hbar}}{1 + i \frac{\hbar t}{2m\delta x^2}} \right). \quad (5)
\end{aligned}$$

The absolute value of the square of $\psi(x, t)$ is

$$|\psi(x, t)|^2 = \frac{1}{\delta x(t)\sqrt{2\pi}} \exp \left[-\frac{(x - v_0 t)^2}{2[\delta x(t)]^2} \right], \quad (6)$$

where

$$[\delta x(t)]^2 = \delta x^2 + \frac{\hbar^2 t^2}{4m^2\delta x^2} \quad (7)$$

is the variance of x that increases with time as shown in (7).

Thus, the free particle with an initial average velocity $v_0 = p_0/m$ and an initial Gaussian probability distribution propagates with the same average velocity v_0 and preserves its Gaussian probability distribution, but centered now at $x(t) = v_0 t$ and with monotonically increasing width $\delta x(t)$. It is worthwhile to point out that the coefficient of t^2 in (7) is inversely proportional to δx^2 . Can you provide a physical explanation of this inverse dependence on δx^2 ?

We define $\tilde{\psi}(p, t)$ as the Fourier transform of $\psi(x, t)$:

$$\tilde{\psi}(p, t) \equiv \int_{-\infty}^{\infty} dx e^{-ipx/\hbar} \psi(x, t). \quad (8)$$

It suffices to calculate $\tilde{\psi}(p, t)$ for $t = 0$, since $\mathcal{H}|p\rangle = \varepsilon_p|p\rangle$, where $\varepsilon_p = p^2/2m$, and consequently

$$\begin{aligned}
\tilde{\psi}(p, t) &= \langle p | \psi(t) \rangle = \langle p | e^{i\mathcal{H}t/\hbar} | \psi(0) \rangle = \exp \left(-i \frac{\varepsilon_p t}{\hbar} \right) \langle p | \psi(0) \rangle \\
&= \exp \left(-i \frac{\varepsilon_p t}{\hbar} \right) \tilde{\psi}(p, 0). \quad (9)
\end{aligned}$$

To obtain $\tilde{\psi}(p, 0)$, we use (4) and find

$$\tilde{\psi}(p, 0) = \sqrt{2\delta x} (2\pi)^{1/4} \exp \left[-\frac{(p - p_0)^2 \delta x^2}{\hbar^2} \right], \quad (10a)$$

$$\tilde{\psi}(p, t) = \sqrt{2\delta x} (2\pi)^{1/4} \exp \left[-\frac{\delta x^2}{\hbar^2} (p - p_0)^2 - i \frac{\varepsilon_p t}{\hbar} \right], \quad (10b)$$

$$\left| \tilde{\psi}(p, t) \right|^2 = 2\delta x \sqrt{2\pi} \exp \left[-\frac{2\delta x^2}{\hbar^2} (p - p_0)^2 \right]. \quad (11)$$

From the last relation, (11), we see that the variance $\delta p^2(t)$ is given by²

$$\delta p^2(t) = \frac{\hbar^2}{4\delta x^2}, \quad (12)$$

i.e., it does not change with time.

Notice that at $t = 0$

$$\delta x \delta p = \frac{\hbar}{2}, \quad (13)$$

which means that the initial state, $\psi(x, 0)$, is a minimum uncertainty wave packet no matter what the value of δx is. However, because of (7), this property is not preserved for $t \neq 0$ since

$$\delta x(t) \delta p(t) = \frac{\hbar}{2} \sqrt{1 + \frac{\hbar^2 t^2}{4m^2 \delta x^4}}. \quad (14)$$

It is worthwhile to compare the increase with time of $[\delta x(t)]^2$ for the diffusion case (see the solution of Problem 2.3) and the Schrödinger case (7). Can you provide a physical explanation for the differences? \square

3.4s.

a. For $E < \Delta$,

$$\frac{R(E)}{\Omega_r} = \frac{1}{(2\pi)^3} \frac{4\pi}{3} k^3 = \frac{1}{6\pi^2} \frac{E^3}{\hbar^3 c^3}.$$

b. For $E = \Delta + \delta E$ ($\delta E \ll \Delta$),

$$\frac{R(E)}{\Omega_r} = \frac{1}{6\pi^2} \frac{E^3}{\hbar^3 c^3} + \frac{1}{(2\pi)^3} \frac{4\pi}{3} (k_+^3 - k_-^3),$$

² Keep in mind that the normalization condition for $\left| \tilde{\psi}(p, t) \right|^2$ is

$$\int_{-\infty}^{\infty} \frac{dp}{2\pi\hbar} \left| \tilde{\psi}(p, t) \right|^2 = 1.$$

where

$$(k_{\pm} - k_0)^2 = \frac{2m_0\delta E}{\hbar^2}$$

or

$$k_{\pm} = k_0 \pm \sqrt{\frac{2m_0\delta E}{\hbar^2}}$$

and

$$k_{\pm}^3 \approx k_0^3 \pm 3k_0^2 \sqrt{\frac{2m_0\delta E}{\hbar^2}}.$$

Thus,

$$k_+^3 - k_-^3 = 6k_0^2 \sqrt{\frac{2m_0\delta E}{\hbar^2}}$$

and

$$\begin{aligned} \frac{R(E)}{\Omega_r} &= \frac{1}{6\pi^2} \frac{E^3}{\hbar^3 c^3} + \frac{6}{6\pi^2} k_0^2 \sqrt{\frac{2m_0}{\hbar^2} (E - \Delta)} \\ &= \frac{1}{6\pi^2} \frac{E^3}{\hbar^3 c^3} + \frac{k_0^2}{\pi^2} \sqrt{\frac{2m_0}{\hbar^2} (E - \Delta)}. \end{aligned}$$

c. For $E = \Delta' - \delta E'$ ($0 < \delta E' \ll \Delta'$)

$$\begin{aligned} \frac{R(E)}{\Omega_r} &= \frac{1}{6\pi^2} k^3 - \frac{1}{6\pi^2} (k_+^3 - k_-^3) \\ &= \frac{1}{6\pi^2} \left(\frac{2mE}{\hbar^2} \right)^{3/2} - \frac{1}{6\pi^2} (k_+^3 - k_-^3), \\ \Delta' - \frac{\hbar^2}{2m'_0} (k'_{\pm} - k_1)^2 &= \Delta' - \delta E' \Rightarrow k'_{\pm} = k_1 \pm \sqrt{\frac{2m'_0}{\hbar^2} \delta E'}, \\ k'^3_{\pm} &= k_1^3 \pm 3k_1^2 \sqrt{\frac{2m'_0 \delta E'}{\hbar^2}} \Rightarrow k'^3_+ - k'^3_- \\ &= 6k_1^2 \sqrt{\frac{2m'_0 \delta E'}{\hbar^2}}. \end{aligned}$$

Hence,

$$\frac{R(E)}{\Omega_r} = \frac{1}{6\pi^2} \left(\frac{2mE}{\hbar^2} \right)^{3/2} - \frac{k_1^2}{\pi^2} \sqrt{\frac{2m'_0}{\hbar^2} (\Delta' - E)}.$$

d. For $E > \Delta'$

$$\frac{R(E)}{\Omega_r} = \frac{1}{6\pi^2} \left(\frac{2mE}{\hbar^2} \right)^{3/2}.$$

Thus, the number of states per volume and the DOS per volume are as shown schematically in Fig. 2a,b respectively. \square

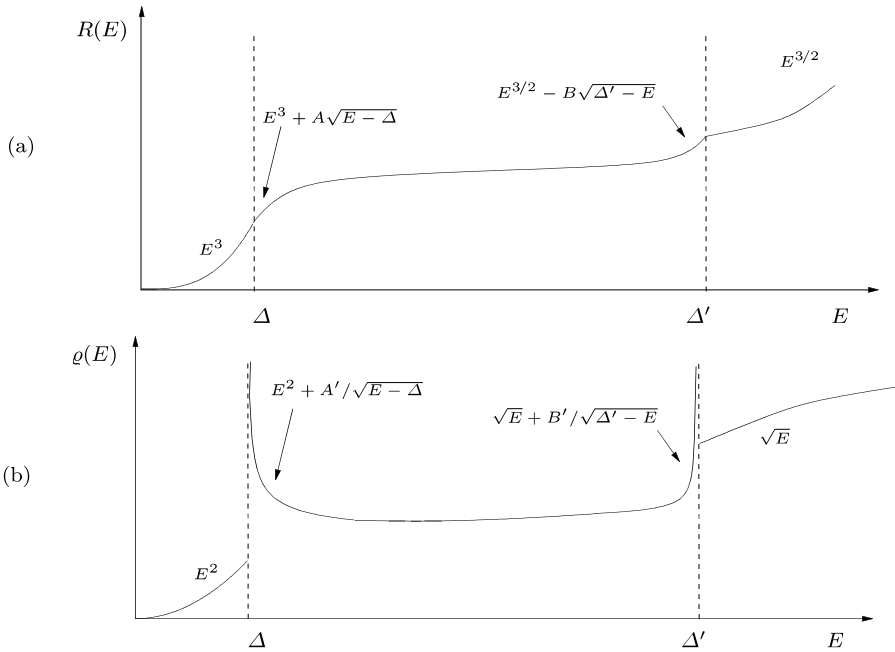


Fig. 2. **a** The number of states per unit volume, $R(E)$, and **b** the DOS per unit volume for $E(k)$ as in Fig. 3.3

Chapter 4

4.3s. According to (4.46) we have

$$\langle n | S^\dagger | m \rangle = \delta_{nm} + 2\pi i \delta(E_n - E_m) \langle \phi_n | T^-(E_n) | \phi_m \rangle \quad (1)$$

and

$$\langle m | S | \ell \rangle = \delta_{m\ell} - 2\pi i \delta(E_\ell - E_m) \langle \phi_m | T^+(E_\ell) | \phi_\ell \rangle . \quad (2)$$

Multiplying (1) by (2) and summing over m (summation over repeated indices is implied) we have to show that

$$\begin{aligned} \langle n | S^\dagger | m \rangle \langle m | S | \ell \rangle &= \langle n | S^\dagger S | \ell \rangle = \delta_{n\ell} \\ &= \delta_{nm} \delta_{m\ell} + 2\pi i [\delta_{m\ell} \delta(E_n - E_m) \langle \phi_n | T^-(E_n) | \phi_m \rangle \\ &\quad - \delta_{nm} \delta(E_\ell - E_m) \langle \phi_m | T^+(E_\ell) | \phi_\ell \rangle] \\ &\quad - (2\pi i)^2 \delta(E_n - E_m) \delta(E_\ell - E_m) \\ &\quad \times \langle \phi_n | T^-(E_n) | \phi_m \rangle \langle \phi_m | T^+(E_\ell) | \phi_\ell \rangle . \quad (3) \end{aligned}$$

Now, $\sum_m \delta_{nm} \delta_{m\ell} = \delta_{n\ell}$, which cancels the $\delta_{n\ell}$ on the lhs of (3). Because of the term $\delta_{m\ell}$ we have $E_m = E_\ell$; because of δ_{nm} we have that $E_m = E_n$; furthermore, in the last term

$$\delta(E_n - E_m) \delta(E_\ell - E_m) = \delta(E_\ell - E_n) \delta(E_m - E_n) .$$

Hence (3) gives

$$\begin{aligned} & \langle \phi_n | T^+ (E_n) | \phi_\ell \rangle - \langle \phi_n | T^- (E_n) | \phi_\ell \rangle \\ &= -2\pi i \sum_m \delta(E_m - E_n) \langle \phi_n | T^- (E_n) | \phi_m \rangle \langle \phi_m | T^+ (E_n) | \phi_\ell \rangle, \end{aligned} \quad (4)$$

which is (4.50).

If we start from the relation $T = \mathcal{H}_1 + \mathcal{H}_1 G \mathcal{H}_1$, we have

$$T^+ - T^- = -2\pi i \mathcal{H}_1 \delta(E - \mathcal{H}) \mathcal{H}_1. \quad (5)$$

Choosing $E = E_n$ and taking the $\langle \phi_n |, | \phi_\ell \rangle$ matrix element of (5) we have

$$\begin{aligned} & \langle \phi_n | T^+ (E_n) | \phi_\ell \rangle - \langle \phi_n | T^- (E_n) | \phi_\ell \rangle \\ &= -2\pi i \langle \phi_n | \mathcal{H}_1 \delta(E_n - \mathcal{H}) \mathcal{H}_1 | \phi_\ell \rangle. \end{aligned} \quad (6)$$

Introducing the unit operator $\sum_m |\psi_m^- \rangle \langle \psi_m^-|$, we have for the rhs of (6)

$$\begin{aligned} & -2\pi i \sum_m \langle \phi_n | \mathcal{H}_1 \delta(E_n - \mathcal{H}) | \psi_m^- \rangle \langle \psi_m^- | \mathcal{H}_1 | \phi_\ell \rangle \\ &= -2\pi i \sum_m \delta(E_n - E_m) \langle \phi_n | \mathcal{H}_1 | \psi_m^- \rangle \langle \psi_m^- | \mathcal{H}_1 | \phi_\ell \rangle \\ &= -2\pi i \sum_m \delta(E_n - E_m) \langle \phi_n | T^- (E_n) | \phi_m \rangle \langle \phi_m | T^+ (E_n) | \phi_\ell \rangle. \end{aligned} \quad (7)$$

Substituting in (6) we obtain (4.50). The last relation follows from (4.34). \square

4.6s. Consider a particle of mass m acted upon by a d -dimensional potential well of depth $-V_0$, and radius a ($d = 1, 2, 3$). Assume that the ground state is a smooth function of total linear extent L . Then, the kinetic energy, E_k , of the particle is

$$E_k = c_1 \frac{\hbar^2}{2mL^2}, \quad (1)$$

where c_1 is a numerical constant. The potential energy, E_p , is

$$E_p = -c_2 V_0 \left(\frac{a}{L} \right)^d, \quad a < L, \quad (2)$$

assuming that $a < L$. Hence the total energy, E_t , is

$$E_t = c_1 \frac{\hbar^2}{2mL^2} - c_2 V_0 \frac{a^d}{L^d}, \quad a < L. \quad (3)$$

By introducing the natural unit of kinetic energy, $K_0 = \hbar^2/2ma^2$, we have

$$\frac{E_t}{K_0} = c_1 \frac{a^2}{L^2} - c_2 \frac{V_0}{K_0} \frac{a^d}{L^d}. \quad (4)$$

Assuming that $V_0 \ll K_0$, we plot in Fig. 3 E_t/K_0 vs. L/a for $d < 2$ and $d > 2$. We see from the plot that for $d < 2$ there is always a minimum at a finite $L/a \gg 1$ no matter how small the ratio V_0/K_0 is. On the other hand, for $d > 2$ and for a very shallow potential well ($V_0 \ll K_0$) there is no minimum for L/a and hence no bound state unless $c_2 V_0/c_1 K_0$ becomes comparable to unity. Actually, the critical value of V_0/K_0 is $\pi^2/4$. (See Problem 4.7s; in that problem, the critical dimension, $d = 2$, is also examined). \square

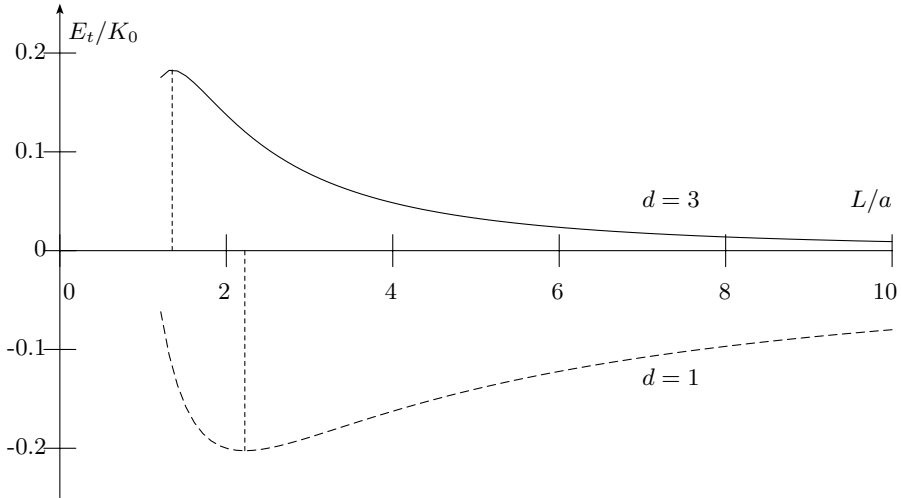


Fig. 3. Plot of dimensionless energy, E_t/K_0 , vs. linear extent, L/a , of wavefunction for d -dimensional system ($d = 1, 3$)

4.7s.

1-dimensional case In Fig. 4 we plot the potential $V(x)$ vs. x : The ground state is an even function of x without nodes. Thus it is enough to consider only positive values of x . For $0 \leq x \leq a$, the solution is of the form

$$\psi(x) = A \cos(\lambda x), \quad 0 \leq x \leq a, \tag{1a}$$

while for $a \leq x$

$$\psi(x) = B e^{-kx}, \quad a \leq x. \tag{1b}$$

Substituting in the Schrödinger equation we find that

$$\lambda^2 = \frac{2mV_0}{\hbar^2} - \frac{2mE_d}{\hbar^2}, \quad d = 1, \tag{2a}$$

$$k^2 = \frac{2mE_d}{\hbar^2}, \quad d = 1. \tag{2b}$$

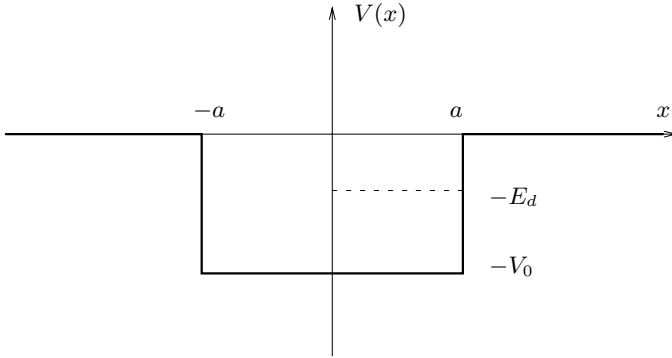


Fig. 4. A 1-d potential well

The continuity of $\psi'(x)/\psi(x)$ at $x = a$ gives

$$a\lambda \tan(a\lambda) = ak, \tag{3a}$$

or

$$\sqrt{b-z} \tan(\sqrt{b-z}) = \sqrt{z}, \tag{3b}$$

where b and z are the dimensionless quantities

$$z \equiv \frac{E_d}{\hbar^2/2ma^2}, \quad d = 1, \tag{4a}$$

$$b \equiv \frac{V_0}{\hbar^2/2ma^2}. \tag{4b}$$

From (3b) it follows that

$$z \rightarrow b^2 \quad \text{or} \quad E_1 \rightarrow \frac{V_0^2}{\hbar^2/2ma^2} \quad \text{as} \quad V_0 \rightarrow 0, \tag{5a}$$

$$z \rightarrow b - \frac{\pi^2}{4} \quad \text{or} \quad E_1 \rightarrow V_0 - \frac{\pi^2 \hbar^2}{8ma^2} \quad \text{as} \quad V_0 \rightarrow \infty. \tag{5b}$$

The decay length, $1/k$, divided by the radius a is directly related to z :

$$\frac{1}{ka} = \frac{1}{\sqrt{z}} \rightarrow \begin{cases} \frac{1}{b} = \frac{\hbar^2/2ma^2}{V_0} & \text{as } V_0 \rightarrow 0, \\ \frac{1}{\sqrt{b}} = \sqrt{\frac{\hbar^2/2ma^2}{V_0}} & \text{as } V_0 \rightarrow \infty. \end{cases} \tag{6a}$$

$$\tag{6b}$$

2-dimensional case The general solution of the Schrödinger equation for $\varrho < a$ has the form [see (C.18–C.19b)]

$$A_n [J_n(\lambda\varrho) + b_n Y_n(\lambda\varrho)] (e^{in\phi} + c_n e^{-in\phi}), \quad \varrho < a, \tag{7a}$$

where λ is given by (2a). For $\varrho > a$, the general solution, according to (C.18–C.21), is of the form

$$B_n [K_n(k\varrho) + b'_n I_n(k\varrho)] (e^{in\phi} + c_n e^{-in\phi}) , \quad \varrho > a , \quad (7b)$$

where k is given by (2b).

Since $\psi(\varrho)$ is finite at the origin, we must exclude $Y_n(\lambda\varrho)$ by setting $b_n = 0$. Similarly, $b'_n = 0$ since $I_n(k\varrho)$ blows up at infinity. Furthermore, since we are looking for the ground state, we must take $n = 0$ (an $n \neq 0$ adds to the Hamiltonian a positive term proportional to $\hbar^2 n^2 / 2m\varrho^2$).

The continuity of the solution and its derivative at $\varrho = a$ gives

$$\frac{\lambda J'_0(\lambda a)}{J_0(\lambda a)} = \frac{k K'_0(ka)}{K_0(ka)} , \quad (8)$$

where the prime denotes differentiation with respect to λa or ka , respectively. In the limit $b \equiv V_0 / (\hbar^2 / 2ma^2) \rightarrow 0$, we have that both λa and $ka \rightarrow 0$, and consequently

$$J_0(\lambda a) \rightarrow 1 - \frac{1}{4}(\lambda a)^2 + O(\lambda^4 a^4) , \quad (9a)$$

$$J'_0(\lambda a) \rightarrow -\frac{1}{2}\lambda a + O(\lambda^3 a^3) , \quad (9b)$$

$$K_0(ka) \rightarrow -\left[\ln\left(\frac{ka}{2}\right) + \gamma \right] \left[1 + \frac{(ka)^2}{4} \right] + \frac{(ka)^2}{4} + O\left(\ln\left(\frac{ka}{2}\right) k^4 a^4\right) \quad (9c)$$

$$K'_0(ka) \rightarrow -\frac{1}{ka} + O(ka \ln(ka)) . \quad (9d)$$

Thus (8) in the limit $b \rightarrow 0$ becomes

$$-\frac{\lambda^2 a}{2} = -\frac{1/a}{-\ln\left(\frac{e^\gamma}{2} ka\right)} \text{ as } b \rightarrow 0 \quad (10)$$

or

$$\ln\left(\frac{e^\gamma}{2} ka\right) = -\frac{2}{\lambda^2 a^2} \simeq -\frac{2}{b}$$

or

$$ka = \frac{2}{e^\gamma} e^{-2/b} . \quad (11)$$

Taking into account (2b) we find

$$\frac{E_2}{\hbar^2 / 2ma^2} = \frac{4}{e^{2\gamma}} \exp\left[-\frac{4\hbar^2}{2ma^2 V_0}\right] = \frac{4}{e^{2\gamma}} \exp\left[-\frac{2\hbar^2}{ma^2 V_0}\right] ,$$

or, by introducing the area, $\Omega_0 = \pi a^2$, of the potential well,

$$E_2 = \frac{2\pi}{e^{2\gamma}} \frac{\hbar^2}{m\Omega_0} \exp\left[-\frac{2\pi\hbar^2}{V_0 m\Omega_0}\right], \quad b \rightarrow 0. \quad (12)$$

The dimensionless decay length, $1/ka$, is given by inverting (11):

$$\frac{1}{ka} = \frac{e^\gamma}{2} e^{2/b} = \frac{e^\gamma}{2} \exp\left[\frac{\pi\hbar^2}{V_0 m\Omega_0}\right], \quad b \rightarrow 0. \quad (13)$$

Notice the nonanalytic behavior of E_2 and $(ka)^{-1}$ as $b = V_0/(\hbar^2/2ma^2) \rightarrow 0$.

3-dimensional case Taking into account that the ground state corresponds to $\ell = 0$, we have from (C.17a)

$$\frac{du^2}{dr^2} - \frac{2m}{\hbar^2}(V - E)u = 0 \quad (14)$$

with BC $u = 0$ for $r = 0$ [because $u(r)/r$ must be finite at $r = 0$] and $u \rightarrow 0$ as $r \rightarrow \infty$.

By introducing λ^2 and k^2 from (2a) and (2b), respectively, we obtain for $u(r)$

$$u(r) = \begin{cases} A \sin(\lambda r), & r < a, \\ B e^{-kr}, & r > a. \end{cases} \quad (15a)$$

$$(15b)$$

The continuity of $u(r)$ and du/dr at $r = a$ gives

$$\frac{a\lambda \cos(a\lambda)}{\sin(a\lambda)} = -ka \quad (16)$$

or

$$\sqrt{b-z} \cot \sqrt{b-z} = -\sqrt{z}. \quad (16')$$

For (16') to have any solution, the quantity $\cot \sqrt{b-z}$ must be negative, which means that $\sqrt{b-z}$ must exceed $\pi/2$. Thus $b = \pi^2/4$ is the critical value for the first bound state to appear; then $\sqrt{b-z} \rightarrow (\pi/2)^+$ as $\sqrt{z} \rightarrow 0^+$. Hence, in order to have a bound state, the following must hold:

$$b > b_c = \frac{\pi^2}{4} \quad (17)$$

or

$$V_0 > V_{0c} = \frac{\pi^2}{8} \frac{\hbar^2}{ma^2}. \quad (17')$$

We write $b = b_c + \delta b$. As $\delta b \rightarrow 0$ we have

$$\sqrt{b-z} \rightarrow \sqrt{b_c + \delta b - z} \rightarrow \sqrt{b_c + \delta b} \rightarrow \sqrt{b_c} + \frac{\delta b}{2\sqrt{b_c}}, \quad (18)$$

$$\cot \sqrt{b-z} \rightarrow -\frac{\delta b}{2\sqrt{b_c}}. \quad (19)$$

In (18) we took into account that $z \sim \delta b^2$ as $\delta b \rightarrow 0$. In view of (18) and (19), (16') becomes in the limit $\delta b \rightarrow 0$

$$\sqrt{z} = \frac{\delta b}{2}, \quad \delta b \rightarrow 0^+ \tag{20a}$$

or

$$z = \frac{1}{4} (b - b_c)^2 = \frac{1}{4} \left(b - \frac{\pi^2}{4} \right)^2, \quad b \rightarrow \left(\frac{\pi^2}{4} \right)^+ \tag{20b}$$

or

$$E_3 = \frac{1}{4\hbar^2/2ma^2} (V_0 - V_{0c})^2, \quad V_0 \rightarrow V_{0c}^+. \tag{20c}$$

The dimensionless decay length, $(ka)^{-1}$, is obtained by inverting (20a):

$$\frac{1}{ka} = \frac{2}{b - (\pi^2/4)} = \frac{\hbar^2/ma^2}{V_0 - V_{0c}}. \tag{21}$$

In the opposite limit of $V_0 \rightarrow \infty$ we obtain

$$E_3 = V_0 - \frac{\pi^2 \hbar^2}{2ma^2} = V_0 - 4V_{0c}, \quad V_0 \rightarrow \infty, \tag{22}$$

and $(ka)^{-1} \rightarrow 0$ as $V_0 \rightarrow \infty$.

In Fig. 5 we plot z as a function of b^2 , according to (16'), (8), and (3b) for 3-d, 2-d, and 1-d, respectively ($\lambda a = \sqrt{b - z}$ and $ka = \sqrt{z}$). \square

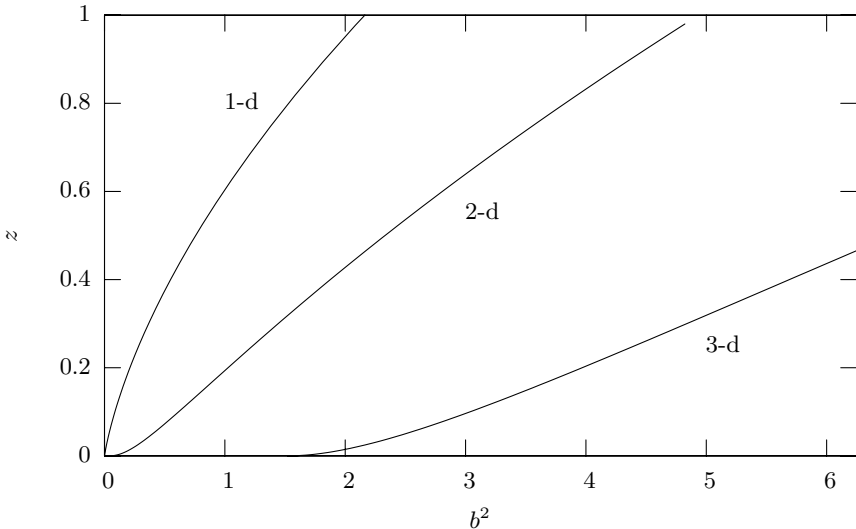


Fig. 5. Plot of dimensionless binding energy $z \equiv E_d/K_0$, where $K_0 = \hbar^2/2ma^2$, vs. b^2 , where $b \equiv V_0/K_0$ and $d = 1, 2, 3$

Chapter 5

5.1s. Since $\varrho_1\varrho_2 = 1$ we can write $\varrho_1 = r_1e^{i\theta}$ and $\varrho_2 = r_2e^{-i\theta}$ with $r_1r_2 = 1$, where $r_1 = |\varrho_1|$ and $r_2 = |\varrho_2|$. The equality $|\varrho_1| = |\varrho_2|$ implies that $\varrho_1 + \varrho_2 = 2\cos\theta$. But $\varrho_1 + \varrho_2 = -2x$. Hence $|\varrho_1| = |\varrho_2|$ is equivalent to $-x = \cos\theta$, or $-1 \leq x \leq 1$. Given the definition of $\sqrt{x^2 - 1}$, we have that the sign of $\text{Im}\{\varrho_2\} = -r_2\sin\theta$ is the same as the sign of $-\text{Im}\{x\}$; but the sign of $-\text{Im}\{x\}$ is the same as the sign of $\text{Im}\{\varrho_1\} + \text{Im}\{\varrho_2\} = r_1\sin\theta - r_2\sin\theta = (r_1 - r_2)\sin\theta$, since $\varrho_1 + \varrho_2 = -2x$. Hence, the sign of $(r_1 - r_2)\sin\theta$ is the same as the sign of $-r_2\sin\theta$. For $\sin\theta \neq 0$ this implies that $r_2 > r_1$. \square

5.2s. We know that

$$E(\mathbf{k}) = \varepsilon_0 + 2V(\cos\phi_1 + \cos\phi_2) = \varepsilon_0 - 2|V|(\cos\phi_1 + \cos\phi_2), \quad (1)$$

where $\phi_1 = k_x a$, $\phi_2 = k_y a$.

$$\lim G(\mathbf{R}; z) = G^+(\mathbf{R}; E) = \lim \frac{a^2}{(2\pi)^2} \int_{1\text{BZ}} d^2k \frac{e^{i\mathbf{k} \cdot \mathbf{R}}}{z - E(\mathbf{k})}, \quad (2)$$

as $\text{Im}\{z\} \rightarrow 0^+$, where $\mathbf{R} = \mathbf{m}a = m_1 a \mathbf{i} + m_2 a \mathbf{j}$.

Equation (2) can be rewritten as follows:

$$G^+(\mathbf{R}; E) = \frac{-ia^2}{(2\pi)^2} \int_0^\infty dt \int d^2k \exp\{i[\mathbf{k} \cdot \mathbf{R} + (E - E(\mathbf{k}))t]\}. \quad (3)$$

We shall follow the method of stationary phase for the evaluation of integral (3) for $R \gg a$. For this purpose we expand the exponent in (3) up to the second order around the points \mathbf{k}_0 and t_0 to be determined shortly:

$$\mathbf{k} = \mathbf{k}_0 + \mathbf{q}, \quad t = t_0 + \tau; \quad (4)$$

we have then

$$\begin{aligned} A &\equiv \mathbf{k} \cdot \mathbf{R} + (E - E(\mathbf{k}))t \\ &= \mathbf{k}_0 \cdot \mathbf{R} + \mathbf{q} \cdot \mathbf{R} + (E - E_0)t_0 + (E - E_0)\tau \\ &\quad - \left. \frac{\partial E}{\partial \mathbf{k}} \right|_0 \cdot \mathbf{q}t_0 - \left. \frac{\partial E}{\partial \mathbf{k}} \right|_0 \cdot \mathbf{q}\tau - \frac{1}{2} \sum_{ij} \left. \frac{\partial^2 E}{\partial k_i \partial k_j} \right|_0 q_i q_j t_0. \end{aligned} \quad (5)$$

To get rid of the first-order terms (so as to make the phase stationary), we choose

$$\left. \frac{\partial E}{\partial \mathbf{k}} \right|_0 t_0 = \mathbf{R}, \quad (6a)$$

$$E_0 \equiv E(\mathbf{k}_0) = E. \quad (6b)$$

Then

$$A = \mathbf{k}_0 \cdot \mathbf{R} - \left. \frac{\partial E}{\partial \mathbf{k}} \right|_0 \cdot \mathbf{q}\tau - \frac{1}{2} \sum_{ij} \left. \frac{\partial^2 E}{\partial k_i \partial k_j} \right|_0 q_i q_j t_0. \quad (7)$$

Using (1) we have

$$\left. \frac{\partial E}{\partial k_x} \right|_0 \equiv \beta_1 = 2|V|a \sin(k_{0x}a), \tag{8a}$$

$$\left. \frac{\partial E}{\partial k_y} \right|_0 \equiv \beta_2 = 2|V|a \sin(k_{0y}a), \tag{8b}$$

$$\left. \frac{\partial^2 E}{\partial k_x^2} \right|_0 \equiv \alpha_1 = 2|V|a^2 \cos(k_{0x}a), \tag{8c}$$

$$\left. \frac{\partial^2 E}{\partial k_y^2} \right|_0 \equiv \alpha_2 = 2|V|a^2 \cos(k_{0y}a). \tag{8d}$$

Then

$$A = \mathbf{k}_0 \cdot \mathbf{R} - \sum_{i=1}^2 \beta_i q_i \tau - \frac{1}{2} \sum_{i=1}^2 \alpha_i q_i^2 t_0. \tag{9}$$

We substitute (9) into (3) and perform the integrations first over q_i ($i = 1, 2$) and then over τ , keeping in mind that only small values of q_i and τ contribute, since for larger values the strong phase oscillations (due to the very large value of R) would render the integral zero. Thus we can extend the limits of integrations to $\mp\infty$ without appreciable error:

$$\begin{aligned} I_i &\equiv \int_{-\infty}^{\infty} dq_i \exp \left[-i \left(\sum_i \beta_i q_i \tau + \frac{1}{2} \sum_i \alpha_i q_i^2 t_0 \right) \right] \\ &= \sqrt{\frac{\pi}{|\alpha_i| t_0}} (1 \pm i) \exp \left[i \frac{\beta_i^2 \tau^2}{2t_0 \alpha_i} \right]; \end{aligned} \tag{10}$$

the upper sign is for negative α_i and the lower for positive α_i . We define

$$\lambda \equiv \frac{\beta_1^2}{2t_0 \alpha_1} + \frac{\beta_2^2}{2t_0 \alpha_2} = \frac{\beta_1^2 \alpha_2 + \beta_2^2 \alpha_1}{2t_0 \alpha_1 \alpha_2}. \tag{11}$$

Substituting (10) and (11) into (3) we find

$$\begin{aligned} G^+(\mathbf{R}; E) &= \frac{-ia^2}{(2\pi)^2} \int_{-\infty}^{\infty} d\tau \frac{\pi}{\sqrt{|\alpha_1 \alpha_2|} t_0} (1 \pm i)(1 \pm i) e^{i\lambda t^2} e^{i\mathbf{k}_0 \cdot \mathbf{R}} \\ &= \frac{-ia^2}{4\pi} \frac{(1 \pm i)(1 \pm i)}{\sqrt{|\alpha_1 \alpha_2|} t_0} \int_{-\infty}^{\infty} d\tau e^{i\lambda \tau^2} e^{i\mathbf{k} \cdot \mathbf{R}} \\ &= \frac{-i(1 \pm i)(1 \pm i)(1 \pm i)a^2 \sqrt{\pi}}{4\pi \sqrt{2|\lambda|} \sqrt{|\alpha_1 \alpha_2|} t_0} e^{i\mathbf{k} \cdot \mathbf{R}}; \end{aligned} \tag{12}$$

in the last $(1 \pm i)$ factor the upper sign is for positive λ and the lower for negative λ . Substituting (6a) and (11) into (12) we have

$$G^+(\mathbf{R}; E) = \frac{-i(1 \pm i)(1 \pm i)(1 \pm i)a^2}{4\sqrt{\pi}} \frac{(\beta_1^2 + \beta_2^2)^{1/4}}{\sqrt{|\beta_1^2 \alpha_2 + \beta_2^2 \alpha_1|}} \frac{e^{i\mathbf{k}_0 \cdot \mathbf{R}}}{\sqrt{R}}. \tag{13}$$

For $\alpha_1 > 0$ and $\alpha_2 > 0$ the first fraction is equal to $-(1+i)a^2/2\sqrt{\pi}$, while for $a_1 < 0$ and $a_2 < 0$ the first fraction is equal to $(1-i)a^2/2\sqrt{\pi}$. Finally, for $\alpha_1\alpha_2 < 0$ the first fraction is equal to $(\pm 1-i)a^2/2\sqrt{\pi}$ with the upper sign for $\lambda > 0$ and the lower for $\lambda < 0$. The second fraction becomes [by employing (8a-8d)]:

$$\begin{aligned} & \frac{\sqrt{2|V|} a (\sin^2 \phi_{01} + \sin^2 \phi_{02})^{1/4}}{\sqrt{2|V|} 2|V| a^2 \sqrt{|\sin^2 \phi_{01} \cos \phi_{02} + \sin^2 \phi_{02} \cos \phi_{01}|}} \\ &= \frac{\sqrt{a} (\sin^2 \phi_{01} + \sin^2 \phi_{02})^{1/4}}{2|V| a^2 \sqrt{[(\cos \phi_{01} + \cos \phi_{02})(1 - \cos \phi_{01} \cos \phi_{02})]}} \\ &= \frac{\sqrt{a} (\sin^2 \phi_{01} + \sin^2 \phi_{02})^{1/4}}{2|V| a^2 \left| \frac{\varepsilon_0 - E}{2|V|} (1 - \cos \phi_{01} \cos \phi_{02}) \right|^{1/2}}. \end{aligned} \quad (14)$$

Substituting in (13) we have finally

$$G^+(\mathbf{R}; E) = \frac{(\pm 1 - i)}{2\sqrt{\pi}} \frac{\sqrt{a} (\sin^2 \phi_{01} + \sin^2 \phi_{02})^{1/4}}{2|V| \left| \frac{\varepsilon_0 - E}{2|V|} (1 - \cos \phi_{01} \cos \phi_{02}) \right|^{1/2}} \frac{e^{i\mathbf{k}_0 \cdot \mathbf{R}}}{\sqrt{R}}. \quad (15)$$

Equation (15) must be reduced to the free electron Green's function, as $R \rightarrow \infty$, times a^2 by taking the limits $\varepsilon_0 = 4|V|$, $|E|/|V| \rightarrow 0$, $\phi_{01}, \phi_{02} \rightarrow 0$, and $|V| = \hbar^2/2ma^2$. We have then (taking into account that, in these limits, \mathbf{k}_0 is parallel to \mathbf{R})

$$\begin{aligned} G^+(\mathbf{R}; E) &= \frac{-(1+i)}{2\sqrt{\pi}} \frac{\sqrt{a} (k_0^2 a^2)^{1/4}}{(\hbar^2/ma^2) \sqrt{2} \sqrt{k_0^2 a^2/2}} \frac{e^{ik_0 R}}{\sqrt{R}} \\ &= \frac{-(1+i)}{2\sqrt{\pi}} \frac{ma^2}{\hbar^2} \frac{e^{ik_0 R}}{\sqrt{k_0 R}}. \end{aligned} \quad (16)$$

Now the free electron $G^+(R; E)$ in the limit $R \rightarrow \infty$ is

$$\begin{aligned} G^+(R; E) &= \lim_{R \rightarrow \infty} \frac{-im}{2\hbar^2} H_0^{(1)}(k_0 R), \quad E > 0, \\ &= \frac{-im}{2\hbar^2} \sqrt{\frac{2}{k_0 R \pi}} e^{ik_0 R} e^{-i\pi/4} \\ &= \frac{-im(1-i)}{\sqrt{22}\hbar^2} \sqrt{\frac{2}{\pi k_0 R}} e^{ik_0 R} = \frac{-(1+i)}{2\sqrt{\pi}} \frac{m}{\hbar^2} \frac{e^{ik_0 R}}{\sqrt{k_0 R}}. \end{aligned} \quad (17)$$

□

5.5s. The position vectors of the nearest-neighbor sites in a bcc lattice are:

$$\begin{aligned}
 \boldsymbol{\ell}_1 &= \frac{a}{2} (\mathbf{i} + \mathbf{j} + \mathbf{k}) = -\boldsymbol{\ell}'_1, \\
 \boldsymbol{\ell}_2 &= \frac{a}{2} (-\mathbf{i} + \mathbf{j} + \mathbf{k}) = -\boldsymbol{\ell}'_2, \\
 \boldsymbol{\ell}_3 &= \frac{a}{2} (\mathbf{i} - \mathbf{j} + \mathbf{k}) = -\boldsymbol{\ell}'_3, \\
 \boldsymbol{\ell}_4 &= \frac{a}{2} (\mathbf{i} + \mathbf{j} - \mathbf{k}) = -\boldsymbol{\ell}'_4,
 \end{aligned}
 \tag{1}$$

where a is the linear size of the cubic unit cell (which for bcc has a volume twice as big as the primitive cell). Substituting (1) into (5.15) we find

$$\begin{aligned}
 E(\mathbf{k}) &= \varepsilon_0 + 2V [\cos(\phi_1 + \phi_2 + \phi_3) + \cos(-\phi_1 + \phi_2 + \phi_3) \\
 &\quad + \cos(\phi_1 - \phi_2 + \phi_3) + \cos(\phi_1 + \phi_2 - \phi_3)] \\
 &= \varepsilon_0 + 8V \cos \phi_1 \cos \phi_2 \cos \phi_3, \quad \phi_i = \frac{k_i a}{2}, \quad i = x, y, z,
 \end{aligned}
 \tag{2}$$

$$\frac{\partial E}{\partial \phi_i} = -8V \sin \phi_i \cos \phi_j \cos \phi_k.
 \tag{3}$$

In the spirit of Fig. 5.3, we plot $E(\mathbf{k})$ as \mathbf{k} moves along straight segments of the 1BZ shown in the insert of Fig. 6.

Thus, the minimum, E_m , of $E(\mathbf{k})$ is at the point $\phi_1 = \phi_2 = \phi_3 = 0$ and is equal to $\varepsilon_0 - 8|V|$. The maximum, $E_m = \varepsilon_0 + 8|V|$, is at point H , $\phi_1 = 0$,

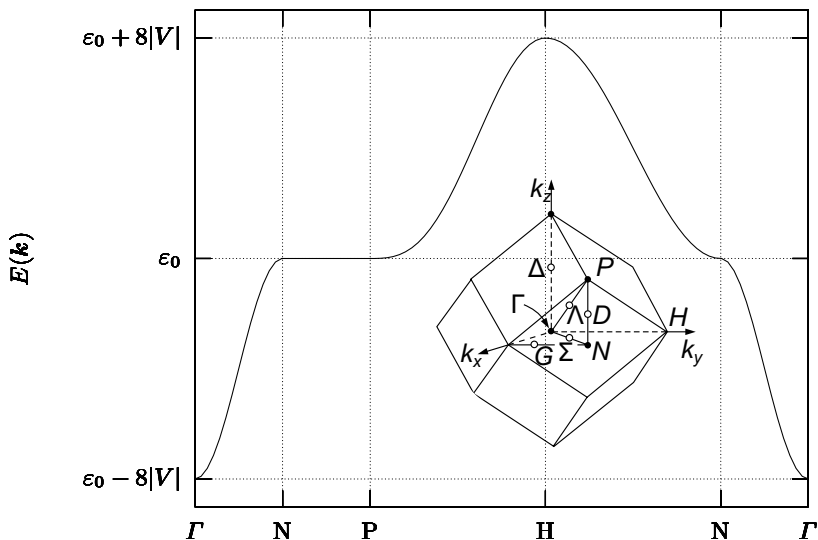


Fig. 6. E vs. \mathbf{k} for the 3-d bcc tight-binding case with nearest-neighbor coupling $V (< 0)$, as \mathbf{k} varies along the straight-line segments of the first Brillouin zone (1BZ) for bcc

$\phi_2 = \pi, \phi_3 = 0$ (plus two others resulting from cyclic permutations). Along the line segment PNP' ($\phi_1 = \pi/2, \phi_2 = \pi/2, -\pi/2 \leq \phi_3 \leq \pi/2$) (plus 11 more resulting from cyclic permutations and changing the signs to $\pm\pi/2$) $E(\mathbf{k}) = \varepsilon_0$ and $\partial E/\partial\phi_i = 0$ for all $i = x, y, z$. Hence the DOS must exhibit a logarithmic singularity at $E = \varepsilon_0$ and be of the form depicted in Fig. 7.

The position vectors for nearest neighbors in an fcc lattice are:

$$\begin{aligned}\ell_{1\pm} &= \frac{a}{2}(\mathbf{i} \pm \mathbf{j}) = -\ell'_{1\pm}, \\ \ell_{2\pm} &= \frac{a}{2}(\mathbf{j} \pm \mathbf{k}) = -\ell'_{2\pm}, \\ \ell_{3\pm} &= \frac{a}{2}(\mathbf{k} \pm \mathbf{i}) = -\ell'_{3\pm}.\end{aligned}$$

Substituting (4) into (5.15) we find after some algebra

$$E = \varepsilon_0 - 4|V|(\cos\phi_1 \cos\phi_2 + \cos\phi_2 \cos\phi_3 + \cos\phi_3 \cos\phi_1), \quad (4)$$

where $\phi_i = k_i a/2$ and a is the linear size of the cubic unit cell (which for fcc has a volume four times the volume of the primitive cell).

In Fig. 8 we plot E vs. \mathbf{k} in the spirit of Fig. 5.3.

Thus the minimum value, $E_m = \varepsilon_0 - 12|V|$, of $E(\mathbf{k})$ is obtained at the point Γ ($\phi_1 = \phi_2 = \phi_3 = 0$) and the maximum, E_M , along line segment XW ($-\pi/2 \leq \phi_1 \leq \pi/2, \phi_2 = \pi, \phi_3 = 0$) and five more resulting from symmetry considerations. The derivatives

$$\frac{\partial E}{\partial\phi_i} = 4|V|\sin\phi_i(\cos\phi_j + \cos\phi_k), \quad i \neq j \neq k \neq i, \text{ for all } i$$

indeed vanish along XW (and symmetric lines) as well as on the isolated point L (and points symmetric to it). Point L is a saddle point with two positive As

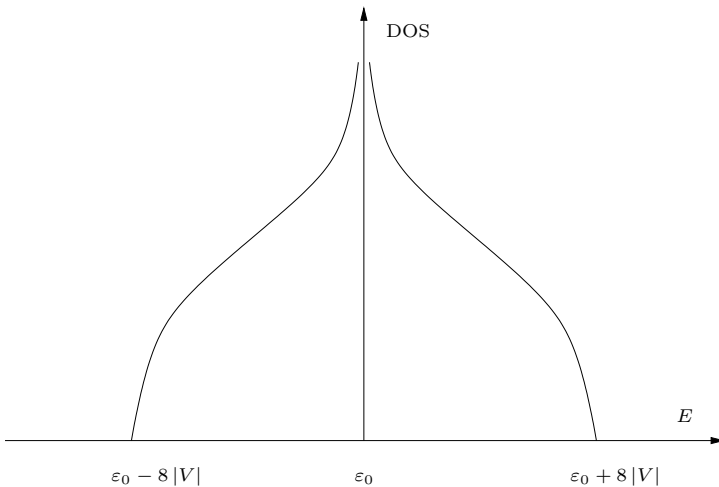


Fig. 7. Schematic plot of DOS for bcc TBM (see text)

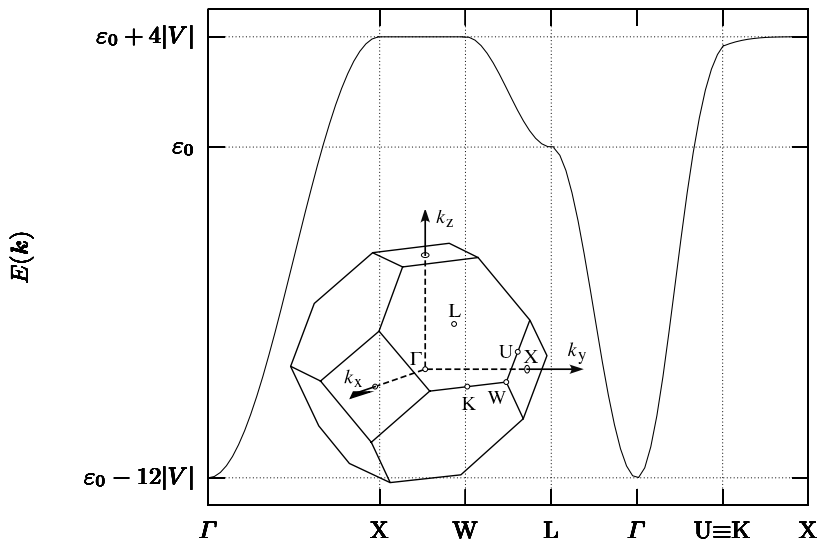


Fig. 8. E vs. \mathbf{k} for 3-d fcc tight-binding case with nearest-neighbor coupling $V (< 0)$, as \mathbf{k} varies along straight-line segments of first Brillouin zone (1BZ) for fcc

along directions perpendicular to $(1, 1, 1)$ and one negative along the direction $(1, 1, 1)$. Thus the DOS for the fcc resembles that in the sketch in Fig. 9. \square

5.7s. Let us call G_1 , \bar{G}_1 , and \bar{G}_2 the quantities $G(1, 1)$, $G(1, 1[2])$, and $G(2, 2[1])$, respectively. Combining (F.10) and (F.11) we have

$$\frac{1}{G_1} = z - \varepsilon_1 - \Delta = z - \varepsilon_1 - (K + 1)V^2\bar{G}_2. \tag{1}$$

From (F.12) and (F.13) we find

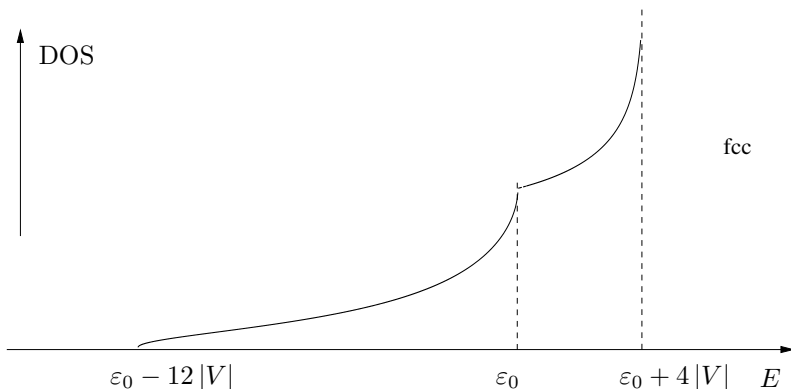


Fig. 9. Schematic plot of DOS for fcc TBM (see text)

$$\frac{1}{\bar{G}_1} = z - \varepsilon_1 - KV^2\bar{G}_2. \quad (2)$$

We multiply (1) by K and (2) by $K + 1$, and we subtract

$$\frac{K+1}{\bar{G}_1} - \frac{K}{G_1} = (K+1)(z - \varepsilon_1) - K(z - \varepsilon_1) = z - \varepsilon_1,$$

or

$$\bar{G}_1 = \frac{K+1}{z - \varepsilon_1 + KG_1^{-1}}. \quad (3)$$

□

Chapter 6

6.3s.

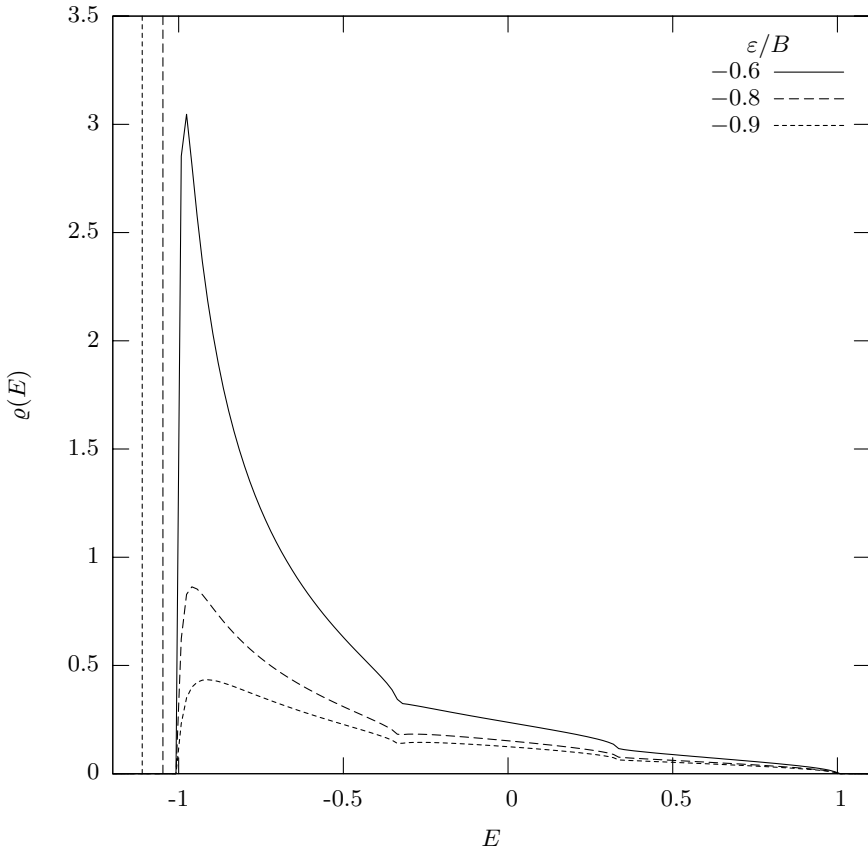


Fig. 10. Plot of DOS for simple cubic TBM at site of impurity

□

6.4s. We start from (6.25). The quantity $\langle n | G_0^+ | \ell \rangle$, according to (5.28), is given by

$$\langle n | G_0^+ | \ell \rangle = G_0^+(\ell, \ell) \varrho_1^{|\ell|}, \quad (1)$$

where

$$\begin{aligned} \varrho_1 &= -\frac{z - \varepsilon_0}{B} + i\sqrt{1 - \left(\frac{z - \varepsilon_0}{B}\right)^2} \\ &= \cos(ka) + i\sqrt{1 - \cos^2(ka)} \\ &= \cos(ka) + i\sin(ka) = e^{ik} \end{aligned} \quad (2)$$

since

$$z = E(k) = \varepsilon_0 - B \cos(ka). \quad (3)$$

We then have, by substituting (2) into (6.25),

$$\langle n | \psi_E \rangle = \langle n | k \rangle + \frac{\varepsilon G_0^+(\ell, \ell; E) e^{ik|\ell-n|} e^{ik\ell}}{\sqrt{N} [1 - \varepsilon G_0^+(\ell, \ell; E)]}. \quad (4)$$

- For $n > \ell$, i.e., for transmission, we have

$$\begin{aligned} \sqrt{N} \langle n | \psi_E \rangle &= e^{ikn} + \frac{\varepsilon G_0^+(\ell, \ell; E)}{1 - \varepsilon G_0^+(\ell, \ell; E)} e^{ikn} \\ &= \frac{1}{1 - \varepsilon G_0^+(\ell, \ell; E)} e^{ikn}, \quad n > \ell. \end{aligned} \quad (5)$$

- For $n < \ell$, i.e., for reflection, we have

$$\begin{aligned} \sqrt{N} \langle n | \psi_E \rangle &= e^{ikn} + \frac{\varepsilon G_0^+(\ell, \ell; E) e^{2ik\ell} e^{-ikn}}{1 - \varepsilon G_0^+(\ell, \ell; E)} \\ &= e^{ikn} + e^{-ikn} e^{2ik\ell} \frac{\varepsilon G_0^+(\ell, \ell; E)}{1 - \varepsilon G_0^+(\ell, \ell; E)} \end{aligned} \quad (6)$$

$$\begin{aligned} &= \frac{1}{e^{-ik\ell}} \\ &\quad \times \left[e^{ik(n-\ell)} + e^{-ik(n-\ell)} \frac{\varepsilon G_0^+(\ell, \ell; E)}{1 - \varepsilon G_0^+(\ell, \ell; E)} \right], \quad n < \ell. \end{aligned} \quad (7)$$

Thus

$$t = \frac{1}{1 - \varepsilon G_0^+(\ell, \ell; E)} \quad (8)$$

and

$$r = \frac{\varepsilon G_0^+(\ell, \ell; E)}{1 - \varepsilon G_0^+(\ell, \ell; E)}. \quad (9)$$

□

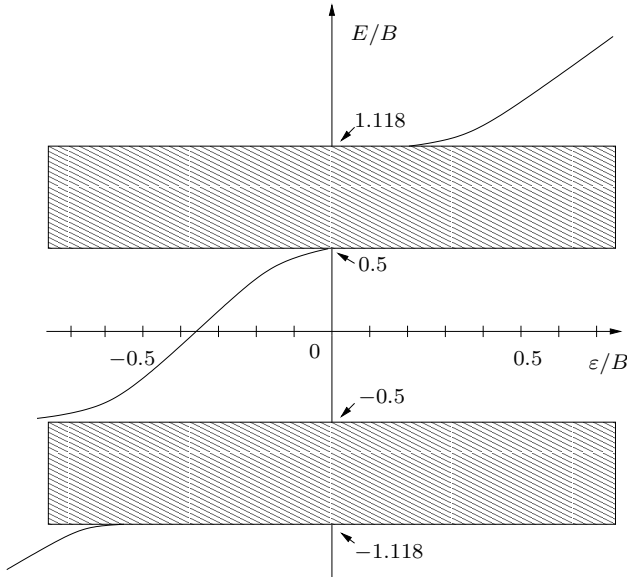


Fig. 11. Plot of the bound states eigenenergy(ies) vs. the local perturbation for a two-band (shaded areas) model shown in Fig. 5.12

6.5s. Schematic plot of the bound-state eigenenergies, E_p , vs. the local perturbation $|1\rangle \varepsilon \langle 1|$ for the double spacing periodic Cayley tree with $K = 3$, $\varepsilon_1 = -\varepsilon_2 = B/2$. The upper and lower edges of the two subbands are also shown. Notice that for $\varepsilon < -0.539B$ there are two bound eigenenergies (one in the gap and the other below the lower band); for $0 < \varepsilon < 0.206B$ there is no bound state; finally, for $0.206B < \varepsilon$ there is only one bound state above the upper band. \square

6.6s. We introduce the center of mass, \mathbf{K} , and the relative, \mathbf{k} , by the relations $\mathbf{K} = \mathbf{k}_1 + \mathbf{k}_2$ and $\mathbf{k} = (\mathbf{k}_1 - \mathbf{k}_2)/2$ so that

$$\mathbf{k}_1 = \frac{1}{2}\mathbf{K} + \mathbf{k} , \tag{1a}$$

$$\mathbf{k}_2 = \frac{1}{2}\mathbf{K} - \mathbf{k} . \tag{1b}$$

We have the inequalities

$$k_1^2 = \frac{K^2}{4} + k^2 + \mathbf{K} \cdot \mathbf{k} > k_F^2 , \tag{2a}$$

$$k_2^2 = \frac{K^2}{4} + k^2 - \mathbf{K} \cdot \mathbf{k} > k_F^2 . \tag{2b}$$

Furthermore,

$$E = \frac{\hbar^2}{2m} (k_1^2 + k_2^2) = \frac{\hbar^2}{m} \left(\frac{K^2}{4} + k^2 \right) \tag{3}$$

or

$$k = \sqrt{\frac{mE}{\hbar^2} - \frac{K^2}{4}}. \quad (4)$$

From (2a) and (2b) in combination with (3) we have

$$-\left(\frac{mE}{\hbar^2} - k_F^2\right) < \mathbf{K} \cdot \mathbf{k} < \frac{mE}{\hbar^2} - k_F^2, \quad (5)$$

which, in view of (4), becomes

$$|\cos \theta| < \frac{\frac{mE}{\hbar^2} - k_F^2}{K \sqrt{\frac{mE}{\hbar^2} - \frac{K^2}{4}}}. \quad (6)$$

The DOS per unit volume, $\varrho(E; K)$, equals $(2\pi)^{-3} d\Omega_k/dE$, where $d\Omega_k$ is the elementary available volume in phase space between E and $E + dE$. Thus

$$\varrho(E; K) = \frac{1}{(2\pi)^3} \int d\phi d\theta \sin \theta k^2 dk \frac{\delta\left(k - \sqrt{\frac{mE}{\hbar^2} - \frac{K^2}{4}}\right)}{dE} \times \theta(E - 2E_F), \quad (7)$$

where, according to (3), $dE/dk = 2\hbar^2 k/m$. If we denote by A the maximum value of $|\cos \theta|$ [taking into account (6)] and perform the integrations in (7), we find

$$\varrho_0(E; K) = \frac{A}{4\pi^2} \frac{m}{\hbar^2} \sqrt{\frac{mE}{\hbar^2} - \frac{K^2}{4}} \theta(E - 2E_F), \quad (8)$$

where

$$A = \min \left[1, \frac{\frac{mE}{\hbar^2} - k_F^2}{K \sqrt{\frac{mE}{\hbar^2} - \frac{K^2}{4}}} \right]. \quad (8')$$

For $K = 0$ we obtain

$$\begin{aligned} \varrho_0(E; 0) &= \frac{1}{4\pi^2} \left(\frac{m}{\hbar^2}\right)^{3/2} \sqrt{E} \theta(E - 2E_F) \\ &= \frac{1}{2\sqrt{2}\pi^2} \left(\frac{m}{\hbar^2}\right)^{3/2} \sqrt{\frac{E}{2}} \theta(E - 2E_F) \\ &= \frac{1}{2} \varrho\left(\frac{E}{2}\right) \theta(E - 2E_F), \end{aligned} \quad (9)$$

where $\varrho(E)$ is the DOS for a single free particle of mass m . For $K \neq 0$, $E \rightarrow 2E_F$, and taking into account (3), we have for the quantity A

$$A \rightarrow \frac{E - 2E_F}{\hbar^2 K k/m},$$

and consequently

$$\varrho_0(E; K) \rightarrow \frac{1}{4\pi^2} \left(\frac{m}{\hbar^2}\right)^2 \frac{E - 2E_F}{K} \theta(E - 2E_F), \quad K \neq 0, \quad E \rightarrow 2E_F. \quad (10)$$

□

6.7s. The DOS is given by

$$\varrho_0(E) = \varrho_F \frac{1}{2} \left[1 - 2f \left(\frac{E}{2} \right) \right] = \frac{\varrho_F}{2} \frac{e^{\beta(E/2 - E_F)} - 1}{e^{\beta(E/2 - E_F)} + 1} = \frac{\varrho_F}{2} \tanh x, \quad (1)$$

where $x \equiv \frac{\beta}{2} (E/2 - E_F)$ and $dE = \frac{4}{\beta} dx$ and the integration limits are $x = -\beta\hbar\omega_D/2$ and $\beta\hbar\omega_D/2$. Thus we have for $G_0(E)$

$$G_0(z) = \int_{-\beta\hbar\omega_D/2}^{\beta\hbar\omega_D/2} dx \frac{\varrho_F}{2} \frac{4}{\beta} \frac{\tanh x}{z - (4x/\beta) - 2E_F}, \quad (2)$$

and the value of $G_0(z)$ for $z = 2E_F$ is

$$G_0(2E_F) = -\frac{\varrho_F}{2} \int_{-\beta\hbar\omega_D/2}^{\beta\hbar\omega_D/2} \frac{dx \tanh x}{x} = -\varrho_F \int_0^{\beta\hbar\omega_D/2} \frac{dx \tanh x}{x}. \quad (3)$$

Integrating by parts we have

$$\begin{aligned} G_0(2E_F) &= -\varrho_F \left(\ln x \tanh x \Big|_0^{\beta\hbar\omega_D/2} - \int_0^{\beta\hbar\omega_D/2} dx \frac{\ln x}{\cosh^2 x} \right) \\ &= -\varrho_F \left(\ln \frac{\beta\hbar\omega_D}{2} \tanh \frac{\beta\hbar\omega_D}{2} - \int_0^{\beta\hbar\omega_D/2} \frac{dx \ln x}{\cosh^2 x} \right). \end{aligned} \quad (4)$$

In the limit $\beta\hbar\omega_D \gg 2$ or $k_B T \ll \hbar\omega_D/2$ we have approximately

$$G_0(2E_F) = -\varrho_F \left(\ln \frac{\beta\hbar\omega_D}{2} - \int_0^\infty dx \frac{\ln x}{\cosh^2 x} \right). \quad (5)$$

The integral in (5) equals $\ln \pi - \ln 4 - \gamma$, where $\gamma = 0.577215 \dots$ is the so-called Euler's constant. We can write (5) as follows:

$$G_0(2E_F) = -\varrho_F \ln \frac{2e^\gamma \hbar\omega_D}{\pi k_B T}, \quad k_B T \ll \hbar\omega_D. \quad (6)$$

□

Chapter 7

7.1s. Following a procedure similar to that of Problem 6.4s (and taking into account that $\varrho_1 = e^{ik_a} = e^{i\phi}$) we obtain the following expressions for the transmission, t , and the reflection, r , amplitudes:

$$t = 1 + G_0 T_f, \quad (1a)$$

$$r = G_0 T_b, \quad (1b)$$

where G_0 is the diagonal matrix element of the unperturbed Green's function $G_0 = G_0(\ell, \ell)$, and T_f and T_b are the forward and backward matrix elements of T , respectively, given by

$$T_f = T_{\ell\ell} + T_{mm} + T_{\ell m}e^{ika} + T_{m\ell}e^{-ika} , \tag{2a}$$

$$T_b = e^{2ika\ell}T_{\ell\ell} + e^{2ikam}T_{mm} + e^{ika(\ell+m)}T_{\ell m} + e^{ika(\ell+m)}T_{m\ell} . \tag{2b}$$

More generally, if we have impurities at the sites ℓ_1, \dots, ℓ_p (which are not necessarily consecutive), the expressions for T_f and T_b are

$$T_f = \sum_{\ell_i \ell_j} \exp [ika(\ell_i - \ell_j)] \langle \ell_j | T | \ell_i \rangle , \tag{3a}$$

$$T_b = \sum_{\ell_i \ell_j} \exp [ika(\ell_i + \ell_j)] \langle \ell_j | T | \ell_i \rangle . \tag{3b}$$

The matrix elements $T_{\ell\ell}, T_{mm}, T_{\ell m}, T_{m\ell}$ in (2a) and (2b) are given by employing (7.12) and (7.13). The result is the following:

$$T_f = f_{m\ell} [t_\ell + t_m + 2t_\ell t_m G_0(\ell, m) \cos(ka)] \tag{4a}$$

$$= f_{m\ell} [t_\ell + t_m + 2t_\ell t_m G_0 e^{ika} \cos(ka)] , \tag{4b}$$

where $G_0 \equiv G_0(\ell, \ell)$ and

$$f_{m\ell} = [1 - t_\ell t_m G_0^2 e^{2ika}]^{-1} . \tag{5}$$

The reader may calculate numerically and plot $|t|^2 = |1 + G_0 T_f|^2$ vs. $x \equiv E/B = -\cos(ka)$ for various values of ε and ε' (especially for those close to the boundaries in Fig. 7.3a). \square

7.2s. In matrix notation the unperturbed Hamiltonian, \mathcal{H}_0 , satisfies the relations

$$\langle \ell | H_0 | \ell \rangle = \begin{vmatrix} \varepsilon_s & 0 \\ 0 & \varepsilon_p \end{vmatrix} , \tag{1}$$

$$\langle \ell | H_0 | \ell \pm 1 \rangle = \begin{vmatrix} V_{ss} & \pm V_{sp} \\ \mp V_{sp} & V_{pp} \end{vmatrix} = \begin{vmatrix} V_2 & \pm V_2'' \\ \mp V_2'' & V_2' \end{vmatrix} . \tag{2}$$

We define the matrix state $|k\rangle = [|ks\rangle, |kp\rangle]$ by

$$|k\rangle = \frac{1}{\sqrt{N}} \sum_{\ell} e^{ik\ell a} |\ell\rangle . \tag{3}$$

The $|k\rangle$ states are orthonormal in the sense that

$$\langle k | k' \rangle = \delta_{kk'} \mathbf{1} , \tag{4}$$

where $\mathbf{1}$ is the 2×2 unit matrix.

Let us calculate the matrix elements of \mathcal{H}_0 in the $|k\rangle$ basis

$$\begin{aligned} \langle k | \mathcal{H}_0 | k' \rangle &= \frac{1}{N} \sum_{\ell m} e^{ik'ma - ik\ell a} \langle \ell | \mathcal{H}_0 | m \rangle = \\ &= \frac{1}{N} \sum_m \left[e^{i(k'-k)ma} \begin{vmatrix} \varepsilon_s & 0 \\ 0 & \varepsilon_p \end{vmatrix} + e^{i(k'-k)ma} e^{-ika} \begin{vmatrix} V_2 & -V_2'' \\ V_2'' & V_2' \end{vmatrix} \right. \\ &\quad \left. + e^{i(k'-k)ma} e^{ika} \begin{vmatrix} V_2 & V_2'' \\ -V_2'' & V_2' \end{vmatrix} \right], \end{aligned}$$

or (taking into account that $\sum_m e^{i(k'-k)ma} = N\delta_{kk'}$)

$$\langle k | \mathcal{H}_0 | k' \rangle = \delta_{kk'} \begin{vmatrix} \varepsilon_s + 2V_2 \cos(ka) & 2iV_2'' \sin(ka) \\ -2iV_2'' \sin(ka) & \varepsilon_p + 2V_2' \cos(ka) \end{vmatrix}. \quad (5)$$

Now the matrix elements of the Green's function G_0 in the initial $\{|\ell\rangle\}$ basis is

$$\begin{aligned} \langle \ell | (z - \mathcal{H}_0)^{-1} | m \rangle &= \sum_{kk'} \langle \ell | k \rangle \langle k | (z - \mathcal{H}_0)^{-1} | k' \rangle \langle k' | m \rangle \\ &= \frac{1}{N} \sum_k e^{ik(\ell-m)a} [z\mathbf{1} - E_2(k)]^{-1}, \end{aligned} \quad (6)$$

where $E_2(k)$ is the matrix in (5) and $\mathbf{1}$ is the unit 2×2 matrix. Thus we have to find the inverse of the matrix

$$z\mathbf{1} - E_2(k) = \begin{vmatrix} z - \varepsilon_s - 2V_2 \cos(ka) & -2iV_2'' \sin(ka) \\ 2iV_2'' \sin(ka) & z - \varepsilon_p - 2V_2' \cos(ka) \end{vmatrix}. \quad (7)$$

We have

$$[z\mathbf{1} - E_2(k)]^{-1} = \frac{1}{D(k)} \begin{vmatrix} z - \varepsilon_p - 2V_2' \cos \phi & 2iV_2'' \sin \phi \\ -2iV_2'' \sin \phi & z - \varepsilon_s - 2V_2 \cos \phi \end{vmatrix}, \quad (8)$$

where $\phi = ka$ and

$$D(k) = (z - \varepsilon_s - 2V_2 \cos \phi)(z - \varepsilon_p - 2V_2' \cos \phi) - 4V_2''^2 \sin^2 \phi.$$

The summation over k from $-\pi/a$ to π/a and the division by N would be transformed to an integration over ϕ from $-\pi$ to π (over 2π). The off-diagonal matrix elements in (8) are odd functions of k or ϕ , and consequently the $\ell = m$ matrix element would be diagonal:

$$\langle \ell | (z - \mathcal{H}_0)^{-1} | \ell \rangle = \begin{vmatrix} G_{0ss}(z) & 0 \\ 0 & G_{0pp}(z) \end{vmatrix}, \quad (9)$$

where

$$G_{0ss}(z) = \int_{-\pi}^{\pi} \frac{d\phi}{2\pi} \frac{z - \varepsilon_p - 2V_2' \cos \phi}{D(\phi)}, \quad (9a)$$

$$G_{0pp}(z) = \int_{-\pi}^{\pi} \frac{d\phi}{2\pi} \frac{z - \varepsilon_s - 2V_2 \cos \phi}{D(\phi)}. \quad (9b)$$

The perturbing Hamiltonian corresponding to the impurity at the n -site, $|n\rangle \varepsilon' \langle n|$, where ε' is a 2×2 diagonal matrix with ε'_s and ε'_p , shall modify the Green's function as in (6.8) and (6.10):

$$\begin{aligned} G(\ell, m) - G_0(\ell, m) &= G_0(\ell, n) \varepsilon' [1 - G_0(n, n) \varepsilon']^{-1} G_0(n, m) \\ &= G_0(\ell, n) [1 - \varepsilon' G_0(n, n)]^{-1} \varepsilon' G_0(n, m), \end{aligned} \quad (10)$$

where $G_0(n, n)$ is a 2×2 matrix given by (9), (9a), and (9b). Since in general both ε' and $G_0(\ell, m)$ are matrices, the ordering is important [not in the present case since the matrices ε' and $G_0(n, n)$ are both diagonal]. We have for them

$$\begin{aligned} [1 - \varepsilon' G_0(n, n)]^{-1} &= [1 - G_0(n, n) \varepsilon']^{-1} \\ &= \begin{vmatrix} [1 - \varepsilon'_s G_{0ss}]^{-1} & 0 \\ 0 & [1 - \varepsilon'_p G_{0pp}]^{-1} \end{vmatrix}. \end{aligned} \quad (11)$$

Thus, the bound states would appear as solutions to the equations

$$\frac{1}{\varepsilon'_s} = G_{0ss}(E), \quad (12a)$$

$$\frac{1}{\varepsilon'_p} = G_{0pp}(E). \quad (12b)$$

In particular, for a vacancy (for which $\varepsilon'_s = \varepsilon'_p = \infty$) we have

$$G_{0ss}(E) = 0, \quad (13a)$$

$$G_{0pp}(E) = 0. \quad (13b)$$

The reader may calculate $G_{0ss}(E)$ and $G_{0pp}(E)$ numerically for $\varepsilon_s, \varepsilon_p, V_2, V'_2$, and V''_2 appropriate for Si as given in Problem 5.6. He can compare his result with those of a more realistic model for Si in [52]. \square

7.5s. We introduce the dimensionless quantities $z = E/B, \sigma = \Sigma^+/B, a = \varepsilon/B$, and $g = BG^+ = BG^+_0 (E - \Sigma^+)$. Then (7.59a) becomes

$$\sigma = \frac{1}{2} \left[\frac{a}{1 - (a - \sigma)g} - \frac{a}{1 + (a + \sigma)g} \right], \quad (1)$$

where for the Hubbard Green's function we have

$$g = 2 \left(z - \sigma - \sqrt{(z - \sigma)^2 - 1} \right). \quad (2)$$

Keep in mind that $\text{Im}\{z\} \rightarrow 0^+, \text{Im}\{\sigma\} \leq 0, \text{Im}\{g\} \leq 0$.

Iterate (1) for each value of a and z until you obtain convergence, which is facilitated by starting with a nonnegligible value of $\text{Im}\{z\}$ and large values of $\text{Re}\{z\}$ ($\text{Re}\{z\} = 1 + a$). Sometimes, convergence is accelerated if, in each step n , you employ as a starting value of σ half the sum of the input plus the output value of σ .

The results are shown in Fig. 12. Note that as ε is increasing, a deep develops at the center of the band that becomes deeper and deeper, and eventually the band splits into two subbands separated by a gap. \square

7.6s. The CPA obtains Σ from (7.59a), which can be recast as

$$\Sigma(E) = \int d\varepsilon p(\varepsilon) \frac{\varepsilon}{1 - (\varepsilon - \Sigma)G}, \quad G = \langle n | G_0 (E - \Sigma) | n \rangle. \quad (1)$$

We shall examine the case of weak disorder, i.e., $(w/|V|) \leq 1$, and we shall distinguish two subcases (a) $|\varepsilon| \leq w$, (b) $|\varepsilon| \gg w$, where w is the standard deviation of the Gaussian probability function, $p(\varepsilon)$.

In subcase (a) we can expand the denominator in (1) in powers of $(\varepsilon - \Sigma)G$ and keep terms up to third order. We find

$$\Sigma \simeq w^2 G - (2w^4 - \mu_4) G^3 + O(w^6), \quad (2)$$

where $\mu_4 \equiv \langle \varepsilon^4 \rangle = 3w^4$.

In subcase (b), the main contribution to the integral in (1) comes from the pole of the denominator. Thus

$$\Sigma \simeq -i \frac{\pi}{G_0^2(E)} p(G_0^{-1}), \quad (3)$$

since $|\Sigma| \ll |\varepsilon|$ in this case. Hence, in subcase (b) the DOS per unit volume is

$$\varrho(E) = \frac{1}{a^d} \frac{G'_0(E)}{G_0^2(E)} p(G_0^{-1}(E)). \quad (4)$$

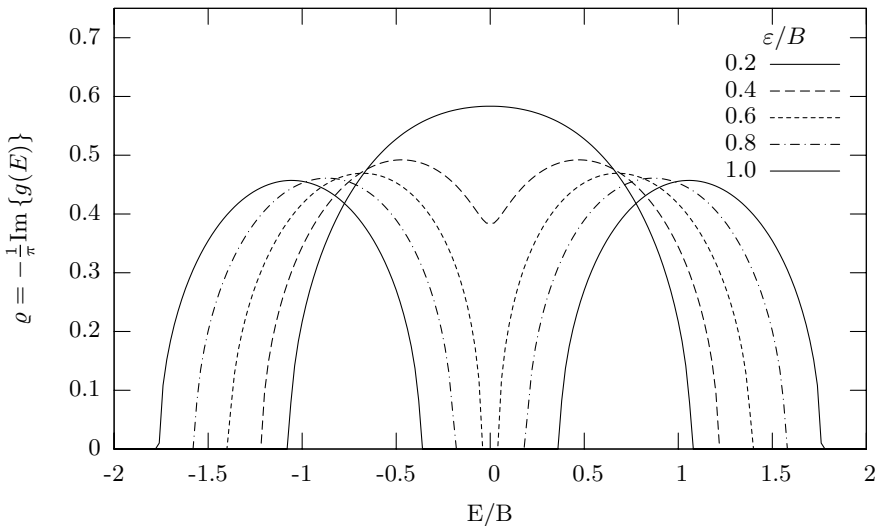


Fig. 12. Density of states for a random binary alloy $A_x B_{1-x}$ ($x = 0.5$) with $\varepsilon_A + \varepsilon_B = 0$ and $\varepsilon_A - \varepsilon_B = 2\varepsilon$. The unperturbed bandwidth is $2B$; B has been taken as the unit of energy

The reader may verify, by using Table 5.2, that for a simple cubic lattice

$$G_0^{-2}(E) \simeq 18.6V^2 - 15.76|V|E, \quad 3V \leq E \leq 0.1V, \quad (5)$$

where $E = 0$ coincides with the unperturbed lower band edge, and $V < 0$.

Substituting (5) into (4) we obtain the DOS at the tail, which over the range shown in (5) is exponential in E

$$\rho_{\text{tail}} \sim \exp\left(-\frac{|E|}{E_0}\right), \quad E_0 = \frac{w^2}{7.88|V|}. \quad (6)$$

This exponential tailing in the DOS leads to exponential subgap optical absorption in crystalline and amorphous semiconductors (Urbach tails) with an E_0 of the form $E_0 = E_{0s} + E_{0T}$, where E_{0s} is due to static disorder and $E_{0T} \sim k_B T$ is due to thermal disorder.

Returning now to subcase (a) and taking into account that $G_0(E) = G_0(0) + \alpha\sqrt{-E}$ as $E \rightarrow 0^-$ with $\alpha = 1/4\pi|V|^{3/2}$ and $G_0(0) = -0.2527/|V|$, we have from (2)

$$\Sigma = w^2 G_0(0) + \alpha w^2 \sqrt{\Sigma - E} + w^4 G_0^3(0). \quad (7)$$

This is a quadratic equation for Σ . The CPA band ‘‘edge,’’ E_{CPA} , is determined when $\text{Im}\{\Sigma\} = 0$, where Σ is the solution of (7). This condition leads to

$$\begin{aligned} E_{CPA} &= G_0(0)w^2 + \left[\frac{\alpha^2}{4} + G_0^3(0)\right]w^4 \\ &= -\frac{0.2527w^2}{|V|} + \left[\frac{1}{64\pi^2} - (0.2527)^3\right]\frac{w^4}{|V|^3}. \end{aligned} \quad (8)$$

The quantity $w^2 G_0(0) + w^4 G_0^3(0)$ in (7) can be replaced by $E_{CPA} - (\alpha^2 w^4/4)$, in view of (8), so that (7) becomes

$$\Sigma - E = \alpha w^2 \sqrt{\Sigma - E} - (E - E_{CPA}) - \frac{\alpha^2 w^4}{4}. \quad (9)$$

By introducing the unit of energy

$$\varepsilon_0 = \frac{\alpha^2 w^4}{4} = \frac{w^4}{4(4\pi)^2 |V|^3},$$

(9) is reduced to a dimensionless universal form

$$\bar{\Sigma} - \bar{E} = 2\sqrt{\bar{\Sigma} - \bar{E}} - x - 1, \quad (10)$$

where $\bar{\Sigma} = \Sigma/\varepsilon_0$, $\bar{E} = E/\varepsilon_0$, and $x = (E - E_{CPA})/\varepsilon_0$. The solution of (10) is $\bar{\Sigma} - \bar{E} = 1 - x + 2\sqrt{-x}$. \square

7.9s. We introduce the notation

$$\begin{aligned} q_0 &= \omega/c_0, \quad c_0 = \sqrt{B_0/\varrho_0}, \quad c = \sqrt{B/\varrho}, \\ q &= \omega/c, \quad \Delta = \varrho_0/\varrho, \quad M = c_0/c. \end{aligned}$$

The incident wave, ϕ_i , is

$$\phi_i = \exp(iq_0 z) = \sum_{\ell=0}^{\infty} i^\ell (2\ell + 1) j_\ell(q_0 r) P_\ell(\cos \theta). \quad (1)$$

The scattered wave, ϕ_s , and the wave inside the sphere, ϕ_{ins} , are of the form

$$\phi_s = - \sum_{\ell=0}^{\infty} i^\ell (2\ell + 1) r_\ell h_\ell(q_0 r) P_\ell(\cos \theta), \quad h_\ell \equiv h_\ell^{(1)}, \quad (2a)$$

$$\phi_{\text{ins}} = \sum_{\ell=0}^{\infty} i^\ell (2\ell + 1) I_\ell j_\ell(qr) P_\ell(\cos \theta). \quad (2b)$$

The coefficients r_ℓ and I_ℓ are determined from the BC

$$j_{\ell 0} - r_{\ell 0} h_{\ell 0} = \frac{1}{\Delta} I_\ell j_\ell, \quad (3a)$$

$$q_0 j'_{\ell 0} - r_{\ell 0} q_0 h'_{\ell 0} = I_\ell q j'_\ell, \quad (3b)$$

where the argument of $j_{\ell 0}$ and $h_{\ell 0}$ is $q_0 a$, while that of j_ℓ is qa ; prime denotes differentiation with respect to $q_0 r$ or qr .

The result for r_ℓ is

$$r_\ell = \frac{j'_{\ell 0} j_\ell - x j_{\ell 0} j'_\ell}{h'_{\ell 0} j_\ell - x h_{\ell 0} j'_\ell}, \quad x = \frac{q\varrho_0}{q_0\varrho}. \quad (4)$$

The equation for the energy flux can be written

$$\mathbf{j} = - \frac{2\varrho_0}{B_0 + B_0^*} \text{Re} \left\{ B_0^* \dot{\phi} \nabla \phi^* \right\}. \quad (5)$$

Substituting $\phi = \phi_i + \phi_s$ into (5) we find that

$$\mathbf{j} = \mathbf{j}_i + \mathbf{j}_s + \mathbf{j}_{is}, \quad (6)$$

where

$$\mathbf{j}_{is} = - \frac{2\varrho_0}{B_0 + B_0^*} \text{Re} \left\{ B^* \dot{\phi}_i \nabla \phi_s^* + B^* \dot{\phi}_s \nabla \phi_i^* \right\}. \quad (7)$$

From energy conservation,

$$\int_{r \leq a} d^3 r \nabla \cdot \mathbf{j} + Q = 0,$$

where Q is the energy dissipation within the sphere; taking into account (6), we have

$$-\int \mathbf{j}_{is} \cdot d\mathbf{S} = \int \mathbf{j}_i \cdot d\mathbf{S} + \int \mathbf{j}_s \cdot d\mathbf{S} + Q. \quad (8)$$

The first integral on the rhs of (8) is zero, the second one gives the scattering cross section (times $|\mathbf{j}_i|$), while Q gives the absorption cross section (due to dissipation inside the sphere) times $|\mathbf{j}_i|$. Thus, the total cross section (TCS), which is also called the extinction cross section, is given by minus the integral of \mathbf{j}_{is} over the surface of the sphere divided by $|\mathbf{j}_i|$.

Performing the integral of \mathbf{j}_{is} over the surface of the sphere we find, after a lengthy but straightforward calculation, that

$$TCS = 4\pi \frac{\text{Im}\{C\}}{\text{Re}\{B_0 q_0\}}, \quad (9)$$

where

$$C = B_0 q_0 a^2 \sum_{\ell=0}^{\infty} (2\ell + 1) (j_{\ell 0}^* h'_{\ell 0} r_{\ell} + j'_{\ell 0} h_{\ell 0}^* r_{\ell}^*), \quad (10)$$

and the subscript zero indicates that the argument of the Bessel and the Hankel functions is $q_0 a$.

It is left to the reader to show that in the absence of losses in the host material (i.e., when $\text{Im}\{B_0\} = 0$), (9) and (10) reduce to the usual formulae for the total scattering section

$$TCS = \frac{4\pi}{q_0} \text{Im}\{f(0)\} = \frac{4\pi}{q_0^2} \sum_{\ell=0}^{\infty} (2\ell + 1) \text{Re}\{r_{\ell}\}. \quad (11)$$

□

8.1s. In the presence of an electric potential ϕ , the chemical potential, μ , becomes

$$\mu = \mu_0 + q\phi, \quad (1)$$

where μ_0 is its expression in the absence of ϕ and q is the charge of each particle. Equilibrium demands that μ must be a constant throughout the system. If this is not the case, a particle current is set up proportional to $-\nabla\mu$ (for not-so-large values of $|\nabla\mu|$):

$$\mathbf{j}_p = -c\nabla\mu = -c \frac{\delta\mu_0}{\delta n} \nabla n - cq\nabla\phi. \quad (2)$$

By definition, the diffusion coefficient is the coefficient of $-\nabla n$:

$$D = c \frac{\delta\mu_0}{\delta n}; \quad (3)$$

the coefficient of $-\nabla\phi = E$ is by definition the conductivity divided by q :

$$\sigma = cq^2. \quad (4)$$

Substituting the linear coefficient c from (3) into (4) we have

$$\sigma = q^2 D \frac{\delta n}{\delta \mu_0} . \quad (5)$$

By making explicit the spatial nonlocal dependencies of σ , D , and $\delta n/\delta \mu_0$ we obtain (8.10).

For $k_B T \gg E_F$ the relation

$$n = \int d\varepsilon \varrho(\varepsilon) \frac{1}{e^{\beta(\varepsilon-\mu)} + 1}$$

reduces to

$$n = \int d\varepsilon \varrho(\varepsilon) e^{-\beta(\varepsilon-\mu)} .$$

Hence

$$\frac{\partial n}{\partial \mu} = \beta n ,$$

from which (8.11b) follows. \square

9.1s. The conductance, \mathcal{G} , of a wire of cross section A and length L is given by

$$\mathcal{G} = \sigma \frac{A}{L} , \quad (1)$$

where σ is the conductivity of the material in the limits $L \rightarrow \infty$ and $A = L^2 \rightarrow \infty$.

Generalizing (9.42) and (9.43) to a wire we have

$$\mathcal{G} = \frac{e^2}{2\pi\hbar} \frac{c\lambda_A}{L} - \frac{e^2}{2\pi\hbar} , \quad (2)$$

where in the place of ξ (the localization length of a 1-d system) we have substituted $c\lambda_A$; λ_A is the localization length of the wire given by $\lambda_A = A/4.82\xi'$ and c is a numerical factor which, by the method of §9.6.1, turns out to be about 2. Combining (1) and (2) and the expression for λ_A we obtain

$$\sigma = \frac{c}{4.82 \times 2\pi} \frac{e^2}{\hbar} \frac{1}{\xi'} \quad \text{for } L \rightarrow \infty . \quad (3)$$

When $L^{-1} > 0$ we have to add to (3) a term proportional to L^{-1} , which, according to (9.2c), is equal to

$$\frac{1}{2\sqrt{2}\pi^2} \frac{e^2}{\hbar} \frac{1}{L_M} = \frac{\sqrt{c_1}}{2\sqrt{2}\pi^2} \frac{e^2}{\hbar} \frac{1}{L} . \quad (4)$$

In (4) we took into account (9.5) and assumed that $L_\phi^{-1} = L_\omega^{-1} = L_\beta^{-1} = 0$. Combining (3) and (4) we obtain

$$\sigma = \frac{e^2}{\hbar} \left(\frac{0.066}{\xi'} + \frac{0.036\sqrt{c_1}}{L} \right) . \quad (5)$$

According to the potential well analogy, ξ' blows up at a critical value $(S\ell_{tr}^2)_c$ [see (9.30)] with a critical exponent $s = 1$ (keep in mind that the correct critical exponent is larger, $s \simeq 1.54$). Thus

$$\xi' = \frac{C}{S\ell_{tr}^2 - (S\ell_{tr}^2)_c} ;$$

from (9.2c), the critical value turns out to be $12c'_1$, where $c'_1 = \ell_{tr}/L_m$. The quantity C is determined by going to the weak scattering case, where $S\ell_{tr}^2 \gg (S\ell_{tr}^2)_c$ and $\sigma = (e^2/12\pi^3\hbar)S\ell_{tr}$. Equating this value of σ with the value $0.066e^2/\hbar\xi'$, where $\xi' = C/S\ell_{tr}^2$, we find

$$C = 12\pi^3 \times 0.066 \simeq 24.56 .$$

□

9.5s. We shall employ (9.106a) and (9.106b) [for a discrete system $\sqrt{v_p v_q}$ must be divided by the lattice spacing a as in (9.111)]. The Green's function will be calculated by the same trick as in Problem 9.9 below, i.e., we shall introduce a 2×2 Hamiltonian of the form

$$\mathcal{H} \equiv \begin{pmatrix} \mathcal{H}_0 & \mathcal{H}_{01} \\ \mathcal{H}_{01} & \mathcal{H}_1 \end{pmatrix} , \tag{1}$$

where \mathcal{H}_0 describes an infinite periodic 1-d TBM, \mathcal{H}_1 a semi-infinite periodic TBM terminated at point 1_d (i.e., the perpendicular leg of T) and $\mathcal{H}_{01} = V'(|0\rangle\langle 1_d| + |1_d\rangle\langle 0|)$. Corresponding to \mathcal{H} is a 2×2 Green's function that satisfies the matrix equation

$$\begin{pmatrix} E - \mathcal{H}_0 & -\mathcal{H}_{01} \\ -\mathcal{H}_{01} & E - \mathcal{H}_1 \end{pmatrix} \begin{pmatrix} \mathcal{G}_0 & \mathcal{G}_{01} \\ \mathcal{G}_{10} & \mathcal{G}_1 \end{pmatrix} = \begin{pmatrix} 1 & 0 \\ 0 & 1 \end{pmatrix} . \tag{2}$$

More explicitly, (2) is equivalent to the following four equations:

$$(E - \mathcal{H}_0)\mathcal{G}_0 - \mathcal{H}_{01}\mathcal{G}_{10} = 1 , \tag{2a}$$

$$-\mathcal{H}_{01}\mathcal{G}_0 + (E - \mathcal{H}_1)\mathcal{G}_{10} = 0 , \tag{2b}$$

$$-\mathcal{H}_{01}\mathcal{G}_1 + (E - \mathcal{H}_0)\mathcal{G}_{01} = 0 , \tag{2c}$$

$$(E - \mathcal{H}_1)\mathcal{G}_1 - \mathcal{H}_{01}\mathcal{G}_{01} = 1 . \tag{2d}$$

Combining (2a) and (2b) we obtain

$$\mathcal{G}_0 = G_0 + G_0\mathcal{H}_{01}G_1\mathcal{H}_{01}G_0 , \tag{3}$$

where

$$G_0 = (E - \mathcal{H}_0)^{-1} \quad \text{and} \quad G_1 = (E - \mathcal{H}_1)^{-1} . \tag{4}$$

Similarly, from (2c) and (2d) we have

$$\mathcal{G}_1 = G_1 + G_1\mathcal{H}_{01}G_0\mathcal{H}_{01}G_1 . \tag{5}$$

Let us calculate first $\langle 0 | \mathcal{G}_0 | m \rangle = \mathcal{G}_0(0, m)$ from (3):

$$\mathcal{G}_0(0, m) = G_0(0, m) + G_0(0, 0)V'G_1(1_d, 1_d)V'\mathcal{G}_0(0, m), \quad (6)$$

or

$$\mathcal{G}_0(0, m) = \frac{G_0(0, m)}{1 - V'^2 G_0(0, 0)G_1(1_d, 1_d)}. \quad (6')$$

We remind the reader that

$$G_0(n, m) = \frac{-i}{2|V|\sin\phi} e^{i|n-m|\phi}, \quad \phi = ka. \quad (7)$$

From (3), (6'), and (7) we can easily show that

$$\mathcal{G}_0(n, m) = G_0(n, m) + G_0(n, 0)G_1(1_d, 1_d)V'^2\mathcal{G}_0(0, m). \quad (8)$$

To find the current transmission amplitude from left to right we have from (9.106a)

$$\hat{t}_{r\ell} = i\hbar v e^{-i\phi(|n|+|m|)} \frac{\mathcal{G}_0(n, m)}{a}. \quad (9)$$

Taking into account that $\hbar v = -2Va \sin\phi$, and substituting in (9) from (8), (7), and (6') we obtain

$$\hat{t}_{r\ell} = \left[1 + i \frac{V'^2}{2|V|\sin\phi} G_1(1_d, 1_d) \right]^{-1}. \quad (10)$$

It remains to calculate $G_1(1_d, 1_d)$; this corresponds to a Hamiltonian where site 0 is a vacancy. Hence

$$G_1 = G_0 - G_0 \frac{|0\rangle\langle 0|}{G_0(1_d, 1_d)} G_0$$

or

$$G_1(1_d, 1_d) = G_0(1_d, 1_d) - G_0(1_d, 1_d) e^{2i\phi} = \frac{-i}{2|V|\sin\phi} (1 - e^{2i\phi}). \quad (11)$$

Substituting in (10) we have

$$\hat{t}_{r\ell} = \left(1 + \frac{V'^2}{V^2} \frac{1 - e^{2i\phi}}{4\sin^2\phi} \right)^{-1} = \frac{1 - e^{-2i\phi}}{1 + x^2 - e^{-2i\phi}}, \quad x^2 = \frac{V'^2}{V^2}. \quad (12)$$

The reader may obtain the remaining matrix elements of \hat{s} by the same approach. \square

9.6s. Because of the one-parameter scaling assumption we have that

$$Q = f(L/\xi'), \quad (1)$$

where ξ' is a function of Q such that $\xi' = c(Q - Q_c)^{-s}$, as $Q \rightarrow Q_c^+$. Differentiating this last relation we have

$$\frac{d}{dQ} \left(\frac{1}{\xi'} \right) = \frac{s}{c} (Q - Q_c)^{s-1}. \quad (2)$$

By definition of β we obtain from (1)

$$\beta = \frac{L}{Q} \frac{dQ}{dL} = \frac{L}{Q} \dot{f} \frac{1}{\xi'}, \quad (3)$$

where the dot over f denotes differentiation with respect to the argument L/ξ' . Now, using the relation

$$\frac{d}{dQ} \left(\frac{L}{\xi'} \right) = \left[\frac{dQ}{d(L/\xi')} \right]^{-1} = \frac{1}{\dot{f}}, \quad (4)$$

and keeping L constant, we have that

$$\frac{d}{dQ} \left(\frac{1}{\xi'} \right) = \frac{1}{L} \frac{1}{\dot{f}} = \frac{1}{L} \frac{L}{Q} \frac{1}{\xi'} \frac{1}{\beta} = \frac{1}{Q\xi'\beta}. \quad (5)$$

In (5) we have replaced \dot{f} from (3). Substituting in (5) ξ' by $c(Q - Q_c)^{-s}$, $d(1/\xi')/dQ$ from (2), and setting $\beta = (d\beta/dQ)_c (Q - Q_c)$ as $Q \rightarrow Q_c$ [since by definition $\beta(Q_c) = 0$], we find that

$$s = \frac{1}{Q_c (d\beta/dQ)_c}. \quad (6)$$

□

9.7s. We have from (9.72)

$$\begin{aligned} \xi^{-1} &= \frac{1}{2} \int_{-\infty}^{\infty} d\varepsilon p(\varepsilon) \int_{-\infty}^{\infty} dx f_0(x) \ln \left| 1 + \frac{\varepsilon}{x} \right| \\ &= \frac{1}{4} \int_{-\infty}^{\infty} d\varepsilon p(\varepsilon) \int_{-\infty}^{\infty} dx f_0(x) \ln \left| 1 - \frac{\varepsilon^2}{x^2} \right| \\ &= \frac{1}{2} \int_{-\infty}^{\infty} d\varepsilon p(\varepsilon) \int_0^{\infty} dx f_0(x) \ln \left| 1 - \frac{\varepsilon^2}{x^2} \right|. \end{aligned} \quad (1)$$

Taking into account that $f_0(x) = C/\sqrt{1+x^4}$, we have for the integral

$$\begin{aligned} I &\equiv \int_0^{\infty} dx \frac{1}{\sqrt{1+x^4}} \ln \left| 1 - \frac{\varepsilon^2}{x^2} \right| \\ &= \int_0^{\infty} dx \left(\frac{1}{\sqrt{1+x^4}} - 1 \right) \ln \left| 1 - \frac{\varepsilon^2}{x^2} \right|, \end{aligned} \quad (2)$$

since

$$\int_0^{\mu} dx \ln \left| 1 - \frac{\varepsilon^2}{x^2} \right| \xrightarrow{\mu \rightarrow \infty} \frac{\varepsilon^2}{\mu} \rightarrow 0. \quad (3)$$

We split integral (2) from 0 to ε and from ε to ∞ . In the first integral we write

$$\frac{1}{\sqrt{1+x^4}} \approx 1 - \frac{1}{2}x^4$$

since $\varepsilon \rightarrow 0$, while in the second we expand the logarithm

$$\ln \left| 1 - \frac{\varepsilon^2}{x^2} \right| = - \sum_{n=1}^{\infty} \frac{1}{n} \left(\frac{\varepsilon}{x} \right)^{2n}. \quad (4)$$

Thus

$$I = I_1 + I_2,$$

where

$$I_1 = \int_0^\varepsilon dx \left(-\frac{x^4}{2} \right) \ln \left| 1 - \frac{\varepsilon^2}{x^2} \right| \rightarrow O(\varepsilon^5) \quad \text{for } \varepsilon \rightarrow 0, \quad (5)$$

$$I_2 = \sum_{n=1}^{\infty} \frac{\varepsilon^{2n}}{n} \int_\varepsilon^\infty dx \left(1 - \frac{1}{\sqrt{1+x^4}} \right) \frac{1}{x^{2n}}. \quad (6)$$

Each term in the series (6) is of order higher than ε^2 , except for the $n = 1$, for which we have

$$I_2^{(1)} = \varepsilon^2 \int_\varepsilon^\infty \left(1 - \frac{1}{\sqrt{1+x^4}} \right) \frac{1}{x^2}. \quad (7)$$

This integral can be expressed in terms of elliptic functions (see [11], p. 261):

$$I_2^{(1)} = -\frac{\varepsilon^2}{2} [\mathcal{F}(\alpha, r) - 2\mathcal{E}(\alpha, r)] + O(\varepsilon^3), \quad (8)$$

where

$$\alpha = \arccos \left(\frac{\varepsilon^2 - 1}{\varepsilon^2 + 1} \right) \rightarrow \pi \quad \text{as } \varepsilon \rightarrow 0,$$

$$r = \frac{1}{\sqrt{2}}.$$

But

$$\mathcal{F}(\pi, r) = 2\mathcal{K}(r) \quad \text{and} \quad \mathcal{E}(\pi, r) \equiv 2\mathcal{E}(r). \quad (9)$$

Thus finally

$$I = I_2^{(1)} + O(\varepsilon^3) = -\varepsilon^2 [\mathcal{K}(r) - 2\mathcal{E}(r)] + O(\varepsilon^3). \quad (10)$$

Hence the inverse localization length to order σ^2 is given by

$$\xi^{-1} = \frac{C}{2} \int_{-\infty}^{\infty} d\varepsilon p(\varepsilon) I_2^{(1)}, \quad \text{where } C = \frac{1}{2\mathcal{K}(r)} \quad (11)$$

according to (9.77). Thus finally

$$\xi^{-1} = \frac{2\mathcal{E}(r) - \mathcal{K}(r)}{4\mathcal{K}(r)} \sigma^2,$$

where σ is the standard deviation of $p(\varepsilon)$. \square

9.10s. From (8.75) we have

$$s \langle G(0, 0; E + is) G(0, 0; E - is) \rangle = \frac{s}{N} \sum_{\mathbf{q}} \frac{A(\mathbf{q})}{1 - uA(\mathbf{q})}, \quad (1)$$

where, according to (8.82),

$$u(z, z') A(\mathbf{q}; z, z') \rightarrow 1 + a_1(z - z') - a_2 q^2 \quad (2)$$

as $z \rightarrow z'$ and $q \rightarrow 0$; $a_1 = i/2 |\Sigma_2|$ and $a_2 = \hbar D^{(0)}/2 |\Sigma_2|$ according to (8.83) and (8.85), respectively. In the present case, $z - z' = 2is$.

Substituting in (1) we have

$$\begin{aligned} s \langle G^+ G^- \rangle &= c \frac{s}{N} \frac{\Omega}{(2\pi)^d} \int d\mathbf{q} \frac{(1/u) |\Sigma_2|}{s + (\hbar D^{(0)}/2) q^2} \\ &= \frac{c}{(2\pi)^d} \frac{\Omega}{N} s \int d\mathbf{q} \frac{\pi \rho'}{s + (\hbar D^{(0)}/2) q^2}, \end{aligned} \quad (3)$$

where we have taken into account that $u = |\Sigma_2|/\pi \rho'$ and we have introduced a numerical factor c to correct for the fact that expansion (2) is valid for small values of q .

For $d = 3$ the q^2 term in the denominator (in the limit $s \rightarrow 0^+$) is cancelled by a q^2 phase space factor in the numerator (coming from $d\mathbf{q} \sim q^2 dq$), and hence (3) approaches zero linearly in s , indicating thus the validity of the perturbation expansion. In contrast, for $d = 2$ or $d = 1$ the phase space factor is q or 1, respectively, and the integral blows up. Although the integral blows up as $s \rightarrow 0$, the quantity $s \langle G^+ G^- \rangle$ still approaches zero: as $\sqrt{s/\hbar D^{(0)}}$ in one dimension and as $(s/\hbar D^{(0)}) \ln |s/\hbar D^{(0)}|$ in two dimensions. If this result is accepted, one must conclude that the eigenstates are neither extended nor normalizable; instead, they decay very slowly to zero. However, we know that, at least in one dimension, the states are exponentially localized. Hence, we must conclude that the singularities of the vertex part obtained through the CPA or the post-CPA, although indicative of localization effects, are not capable of fully describing the situation at all length scales. It is assumed that at short length scales, when one does not sample the extreme tails of the eigenfunctions, the CPA and the post-CPA vertex corrections are satisfactory.

One way of improving the present method is to replace in (3) $D^{(0)}$ by D , the corrected diffusion coefficient, which in general is ω and q dependent. Since $D(\omega)$ is proportional to $i\omega$, then $s \langle G^+ G^- \rangle$ goes to a nonzero limit as $\omega \rightarrow 0$ first and then $s \rightarrow 0^+$, and thus regular localization is recovered. \square

10.6s. Since the particles do not interact, their Hamiltonian has the form

$$\mathcal{H} = \sum_i \varepsilon_i a_i^\dagger a_i. \quad (1)$$

The quantity $\langle a_i^\dagger a_i \rangle$ to be calculated is by definition

$$\langle a_i^\dagger a_i \rangle = \frac{\text{Tr} \left\{ a_i^\dagger a_i e^{-\beta(\mathcal{H}-\mu N)} \right\}}{\text{Tr} \left\{ e^{-\beta(\mathcal{H}-\mu N)} \right\}}. \quad (2)$$

We have that

$$a_i \exp \left(-x a_i^\dagger a_i \right) = e^{-x} \exp \left(-x a_i^\dagger a_i \right) a_i. \quad (3)$$

Equation (3) can be proved by acting on any eigenfunction of $a_i^\dagger a_i$ ($a_i^\dagger a_i |\phi\rangle = n_i |\phi\rangle$) and taking into account that $f(a_i^\dagger a_i) a_i |\phi\rangle = f(n_i - 1) a_i |\phi\rangle$. Then we write

$$\mathcal{H} - \mu N = (\varepsilon_i - \mu) a_i^\dagger a_i + \sum_{j \neq i} (\varepsilon_j - \mu) a_j^\dagger a_j,$$

and we have

$$\begin{aligned} & \text{Tr} \left\{ a_i^\dagger a_i e^{-\beta(\mathcal{H}-\mu N)} \right\} \\ &= \text{Tr} \left\{ a_i^\dagger a_i \exp \left[-\beta (\varepsilon_i - \mu) a_i^\dagger a_i \right] \exp \left[-\beta \sum_{j \neq i} (\varepsilon_j - \mu) a_j^\dagger a_j \right] \right\} \\ &= \text{Tr} \left\{ a_i^\dagger \exp \left[-\beta (\varepsilon_i - \mu) \right] \exp \left[-\beta \sum_j (\varepsilon_j - \mu) a_j^\dagger a_j \right] a_i \right\} \\ &= \exp \left[-\beta (\varepsilon_i - \mu) \right] \text{Tr} \left\{ a_i a_i^\dagger \exp \left[-\beta \sum_j (\varepsilon_j - \mu) a_j^\dagger a_j \right] \right\} \\ &= \exp \left[-\beta (\varepsilon_i - \mu) \right] \left\{ \text{Tr} \left[e^{-\beta(\mathcal{H}-\mu N)} \right] \pm \text{Tr} \left[a_i^\dagger a_i e^{-\beta(\mathcal{H}-\mu N)} \right] \right\}. \quad (4) \end{aligned}$$

From (4) and definition (2) we obtain the desired result

$$\langle a_i^\dagger a_i \rangle = \frac{1}{\exp \left[\beta (\varepsilon_i - \mu) \right] \mp 1}. \quad (5)$$

□

11.4s. From (11.36) we have

$$\frac{\partial}{\partial a} (\ln Z_{G_a}) = -\beta \langle V_i \rangle = -\beta \frac{1}{a} \langle V_{ia} \rangle. \quad (1)$$

We integrate (1) from $a = 0$ to $a = 1$:

$$\ln Z_G = \ln Z_{G_0} - \beta \int_0^1 \frac{da}{a} \langle V_{ia} \rangle. \quad (2)$$

The quantity $\langle V_{ia} \rangle$ is given by (11.29):

$$\langle V_{ia} \rangle = \sum_{\mathbf{k}} \int \frac{d\omega}{2\pi} \frac{1}{2} \left(\omega - \frac{k^2}{2m} \right) A_a(\mathbf{k}, \omega) f_{\mp}(\omega) . \quad (3)$$

Substituting (3) into (2) we obtain (11.37). The integration over ω can be transformed to a sum over z_ν according to (11.47) and (11.53). We have

$$\beta P \Omega = \beta P_0 \Omega \pm \int_0^1 \frac{da}{a} \sum_{\mathbf{k}} \sum_{\nu} \frac{1}{2} \left(z_\nu - \frac{k^2}{2m} \right) G_a(\mathbf{k}, z_\nu) . \quad (4)$$

□

12.4s. From Figs. 12.11) and (12.8, and rules I' to VII' on p. 299, we have for the proper self-energy Σ^*

$$\begin{aligned} \Sigma^*(\mathbf{k}, z_\nu) &= \mp \frac{1}{\beta} \sum_{\nu'} \int \frac{d^3 k'}{(2\pi)^3} v(0) G(\mathbf{k}', z'_\nu) \exp(-z'_\nu \sigma) \\ &\quad - \frac{1}{\beta} \sum_{\nu'} \int \frac{d^3 k'}{(2\pi)^3} v(\mathbf{k} - \mathbf{k}') G(\mathbf{k}', z'_\nu) \exp(-z'_\nu \sigma) , \end{aligned} \quad (1)$$

where the first term on the rhs corresponds to the loop diagram in Fig. 12.11 and the last term in the last diagram.

Now, by employing (11.47) and (11.53) we can rewrite (1) as follows:

$$\begin{aligned} \Sigma^*(\mathbf{k}) &= \int \frac{d\omega'}{2\pi} \int \frac{d^3 k'}{(2\pi)^3} v(0) A(\mathbf{k}', \omega') f_{\mp}(\omega') \\ &\quad \pm \int \frac{d\omega'}{2\pi} \int \frac{d^3 k'}{(2\pi)^3} v(\mathbf{k} - \mathbf{k}') A(\mathbf{k}', \omega') f_{\mp}(\omega') \\ &= v(0)n_0 \pm \int \frac{d^3 k'}{(2\pi)^3} v(\mathbf{k} - \mathbf{k}') \langle n(\mathbf{k}') \rangle . \end{aligned} \quad (2)$$

The bottom line in (2) was obtained from (11.24) and (11.25) by taking into account that the particle density, $\langle n(\mathbf{k}') \rangle$, is independent of \mathbf{r} and equal to n_0 .

Since

$$G(\mathbf{k}, \omega) = [\omega - \varepsilon_k^0 - \Sigma^*(k, \omega)]^{-1} ,$$

we have that the quantity ε_k in (12.19) equals

$$\varepsilon_k = \varepsilon_k^0 + v(0)n_0 \pm \int \frac{d^3 k'}{(2\pi)^3} v(\mathbf{k} - \mathbf{k}') \langle n(\mathbf{k}') \rangle , \quad (3)$$

which coincides with (12.20) since $\varepsilon_k^0 = k^2/2m$. □

13.5s. We shall outline here the proof:

(a) We first do the integral over the angles, and we have

$$\delta_{\varrho}(\mathbf{r}) = -\frac{Z|e|}{2\pi^2 r} \int_0^{\infty} dq q \sin(qr) F(q), \quad (1)$$

where

$$F(q) = \frac{q_{TF}^2 f(q/k_F)}{q^2 + q_{TF}^2 f(q/k_F)}. \quad (2)$$

We integrate (1) twice by parts

$$\begin{aligned} \delta_{\varrho}(\mathbf{r}) &= \frac{Z|e|}{2\pi^2 r^3} \int_0^{\infty} dq \sin(qr) \frac{d^2}{dq^2} [qF(q)] \\ &= \frac{Z|e|}{(2\pi)^2 i r^3} \int_{-\infty}^{\infty} dq e^{iqr} \frac{d^2}{dq^2} [qF(q)]. \end{aligned} \quad (3)$$

The function $qF(q)$ has a singularity at $q = \pm 2k_F$ of the form $(q \mp 2k_F) \ln(|q \mp 2k_F|)$. Thus, the second derivative of $qF(q)$ would produce two poles, $(q \mp 2k_F)^{-1}$, which would dominate the integral as $r \rightarrow \infty$. \square

References

Chapter 1

- [1] M. Abramowitz and I. A. Stegun, editors. *Handbook of Mathematical Functions*. Dover, London, 1974.
- [2] J. Mathews and R. L. Walker. *Mathematical Method of Physics*. Addison-Wesley, Reading, MA, second edition, 1970.
- [3] F. W. Byron and R. W. Fuller. *Mathematics of Classical and Quantum Physics*. Dover, reprint edition, 1992. Two volumes in one.
- [4] D. G. Duffy. *Green's Functions with Applications*. Chapman and Hall/CRC, Boca Raton, FL, 2001.
- [5] G. Barton. *Elements of Green's Functions and Propagation: Potentials, Diffusion and Waves*. Clarendon, Oxford, 1989.
- [6] G. F. Roach. *Green's Functions*. Cambridge University Press, Cambridge, second edition, 1982.
- [7] I. Stakgold. *Green's Functions and Boundary Value Problems*. Wiley, New York, second edition, 1998.
- [8] P. M. Morse and H. Feshbach. *Methods of Theoretical Physics*, volume I&II. McGraw-Hill, New York, 1953.
- [9] W. R. Smythe. *Static and Dynamic Electricity*. McGraw-Hill, New York, 1968.
- [10] J. D. Jackson. *Classical Electrodynamics*. Wiley, New York, third edition, 1998.
- [11] I. S. Gradshteyn and I. M. Ryzhik. *Table of Integrals, Series, and Products*. Academic, New York, sixth edition, 2000.

Chapter 2

- [12] L. D. Landau and E. M. Lifshitz. *Quantum Mechanics*. Pergamon, Oxford, third edition, 1977.
- [13] E. Merzbacher. *Quantum Mechanics*. Wiley, New York, third edition, 1998.
- [14] N. N. Bogoliubov and D. V. Shirkov. *Introduction to the Theory of Quantized Fields*. Wiley-Interscience, New York, 1959.

Chapter 3

- [15] N. I. Muskhelishvili. *Singular Integral Equations: Boundary Problems of Function Theory and Their Applications to Mathematical Physics*. Dover, second edition, 1992. Corrected reprint of the Noordhoff translation (1953) of the Russian original of 1946.
- [16] J. J. Sakurai. *Modern Quantum Mechanics*. Addison-Wesley, Reading, MA, 1994.
- [17] H. A. Bethe. *Intermediate Quantum Mechanics*. Benjamin, New York, 1964.
- [18] S. Flügge. *Practical Quantum Mechanics*. Springer, Heidelberg, 1974.
- [19] L. I. Schiff. *Quantum Mechanics*. McGraw-Hill, New York, second edition, 1955.

Chapter 4

- [20] A. L. Fetter and J. D. Walecka. *Quantum Theory of Many-Particle Systems*. McGraw-Hill, New York, 1971.
- [21] P. Sheng. *Introduction to Wave Scattering, Localization and Mesoscopic Phenomena*. Academic, San Diego, 1995.

Chapter 5

- [22] C. Kittel. *Introduction to Solid State Physics*. Wiley, New York, seventh edition, 1996.
- [23] H. Ibach and H. Lüth. *Solid State Physics: An Introduction to Theory and Experiment*. Springer, Berlin, 1991.
- [24] G. Burns. *Solid State Physics*. Academic, London, 1985.
- [25] W. A. Harrison. *Electronic Structure and the Properties of Solids*. W. H. Freeman, San Francisco, 1980. Reprinted by Dover, New York, 1989.
- [26] W. A. Harrison. *Elementary Electronic Structure*. World Scientific, Singapore, 1999.
- [27] J. M. Ziman. *Principles of the Theory of Solids*. Cambridge University Press, London, 1964.
- [28] N. W. Ashcroft and N. D. Mermin. *Solid State Physics*. Holt, Rinehart & Winston, London, 1976.
- [29] C. Kittel. *Quantum Theory of Solids*. Wiley, New York, 1973.
- [30] M. P. Marder. *Condensed Matter Physics*. Wiley-Interscience, New York, 2000.
- [31] W. A. Harrison. *Pseudopotentials in the Theory of Metals*. Benjamin, New York, 1966.
- [32] V. Heine and D. Weaire. In H. Ehrenreich, F. Seitz, and D. Turnbull, editors, *Solid State Physics*, volume 24, page 249. Academic, New York, 1970.
- [33] J. C. Phillips and L. Kleinman. *Phys. Rev.*, 116:287, 1959.
- [34] M. L. Cohen and V. Heine. *Phys. Rev.*, 122(6):1821–1826, 1961.
- [35] M. L. Cohen and V. Heine. In H. Ehrenreich, F. Seitz, and D. Turnbull, editors, *Solid State Physics*, volume 24, page 37. Academic, New York, 1970.
- [36] J. Hafner and H. Nowotny. *Phys. Status Solidi B*, 51:107, 1972.
- [37] J. R. Chelikowsky and M. L. Cohen. *Phys. Rev. Lett.*, 36:229, 1976. See also [38].

- [38] J. R. Chelikowsky and M. L. Cohen. *Phys. Rev. B*, 14:556, 1976.
- [39] D. J. Chadi and M. L. Cohen. *Phys. Status Solidi B*, 68:405, 1975.
- [40] J. C. Phillips. *Rev. Mod. Phys.*, 42:317, 1970.
- [41] S. T. Pantelides and W. A. Harrison. *Phys. Rev. B*, 11(8):3006–3021, 1975.
- [42] W. A. Harrison. *Phys. Rev. B*, 8(10):4487–4498, 1973.
- [43] S. Froyen and W. A. Harrison. *Phys. Rev. B*, 20(6):2420–2422, 1979.
- [44] W. A. Harrison. *Phys. Rev. B*, 24(10):5835–5843, 1981.
- [45] J. C. Slater and G. F. Koster. *Phys. Rev.*, 94(6):1498–1524, 1954.
- [46] E. O. Kane and A. B. Kane. *Phys. Rev. B*, 17(6):2691–2704, 1978.
- [47] J. D. Joannopoulos, M. Schluter, and M. L. Cohen. The Density of States of Amorphous and Trigonal Se and Te. In M. Pilkuhn, editor, *in Proceedings of the 12th International Conference on Semiconductors*, page 1304, Stuttgart, 1974. Teubner.
- [48] R. M. Martin, G. Lucovsky, and K. Helliwel. *Phys. Rev. B*, 4(13):1383–1395, 1976.
- [49] D. J. Chadi. *Phys. Rev. B*, 16(2):790–796, 1977.
- [50] D. J. Chadi. *Phys. Rev. B*, 16(8):3572–3578, 1977.
- [51] K. C. Pandey and J. C. Phillips. *Phys. Rev. B*, 13(2):750–760, 1976.
- [52] D. A. Papaconstantopoulos and E. N. Economou. *Phys. Rev. B*, 22(6):2903–2907, 1980.
- [53] S. T. Pantelides. *Phys. Rev. B*, 11(12):5082–5093, 1975.
- [54] J. R. Smith and J. G. Gay. *Phys. Rev. B*, 12(10):4238, 1975.
- [55] L. Hodges and H. Ehrenreich. *Phys. Lett.*, 16:203, 1965.
- [56] F. M. Mueller. *Phys. Rev.*, 153(3):659–669, 1967.
- [57] J. Rath and J. Callaway. *Phys. Rev. B*, 8:5398–5403, 1973.
- [58] L. F. Mattheiss. *Phys. Rev. B*, 5(2):290–306, 1972. See also [59].
- [59] L. F. Mattheiss. *Phys. Rev. B*, 5(2):306–315, 1972.
- [60] L. F. Mattheiss. *Phys. Rev. B*, 6(12):4718–4740, 1972.
- [61] L. F. Mattheiss. *Phys. Rev. B*, 13(6):2433–2450, 1972.
- [62] L. F. Mattheiss. *Phys. Rev. B*, 12(6):2161–2180, 1975.
- [63] B. M. Klein, L. L. Boyer, D. A. Papaconstantopoulos, and L. F. Mattheiss. *Phys. Rev. B*, 18(12):6411–6438, 1978.
- [64] W. A. Harrison. *Phys. Rev. B*, 38:270, 1988.
- [65] T. Morita. *J. Math. Phys.*, 12:1744, 1971.
- [66] L. van Hove. *Phys. Rev.*, 89(6):1189, 1953.
- [67] H. B. Rosenstock. *Phys. Rev.*, 97(2):290–303, 1955.
- [68] J. Callaway. *J. Math. Phys.*, 5:783, 1964.
- [69] S. Katsura and S. Inawashiro. *J. Math. Phys.*, 12(1622), 1971.
- [70] T. Horiguchi. *J. Math. Phys.*, 13:1411, 1972.
- [71] T. Horiguchi and C. C. Chen. *J. Math. Phys.*, 15:659, 1974.
- [72] T. Morita and T. Horiguchi. *J. Math. Phys.*, 12:981, 1971.
- [73] T. Horiguchi. *J. Phys. Soc. Jpn.*, 30:1261, 1971.
- [74] G. S. Joyce. *Philos. Trans. R. Soc. Lond. Ser. A*, 273:583, 1973.
- [75] T. Morita. *J. Phys. A*, 8:478–489, 1975.
- [76] T. Horiguchi and T. Morita. *J. Phys. C*, 8(11):L232–L235, 1975.
- [77] D. J. Austen and P. D. Loly. *J. Comput. Phys.*, 11:315, 1973.
- [78] F. T. Hioe. *J. Math. Phys.*, 19:1065, 1978.
- [79] M. A. Rashid. *J. Math. Phys.*, 21:2549, 1980.
- [80] S. Inawashiro, S. Katsura, and Y. Abe. *J. Math. Phys.*, 14:560, 1973.

- [81] S. Katsura, S. Inawashiro, and Y. Abe. *J. Math. Phys.*, 12:895, 1971.
- [82] G. S. Joyce. *J. Phys. A*, 5:L65, 1972.
- [83] S. Katsura, T. Morita, S. Inawashiro, T. Horiguchi, and Y. Abe. *J. Math. Phys.*, 12:892, 1971.
- [84] T. Morita and T. Horiguchi. *J. Math. Phys.*, 12:986, 1971.
- [85] K. Mano. *J. Math. Phys.*, 15(12):2175–2176, 1974.
- [86] K. Mano. *J. Math. Phys.*, 16:1726, 1975.
- [87] G. S. Joyce. *J. Math. Phys.*, 12:1390, 1971.
- [88] M. Inoue. *J. Math. Phys.*, 15:704, 1974.
- [89] J. D. Joannopoulos and F. Yndurain. *Phys. Rev. B*, 10:5164, 1974. See also [90].
- [90] F. Yndurain and J. D. Joannopoulos. *Phys. Rev. B*, 11:2957, 1975.
- [91] D. C. Allan and J. D. Joannopoulos. *Phys. Rev. Lett.*, 44:43, 1980. See also [92].
- [92] J. D. Joannopoulos. *J. Non-Cryst. Solids*, 35–36:781, 1980.
- [93] M. F. Thorpe. In M. F. Thorpe, editor, *Excitations in Disordered Systems*, volume B78 of *NATO Advanced Study Institute Series*, pages 85–107. Plenum, New York, 1981.

Chapter 6

- [94] G. F. Koster and J. C. Slater. *Phys. Rev.*, 95:1167, 1954.
- [95] G. F. Koster and J. C. Slater. *Phys. Rev.*, 96:1208, 1954.
- [96] J. Callaway. *Phys. Rev.*, 154:515, 1967.
- [97] J. Callaway and A. Hughes. *Phys. Rev.*, 156:860, 1967.
- [98] J. Callaway and A. Hughes. *Phys. Rev.*, 164:1043, 1967.
- [99] J. Bernholc and S. T. Pantelides. *Phys. Rev. B*, 18:1780, 1978.
- [100] J. Bernholc, N. O. Lipari, and S. T. Pantelides. *Phys. Rev. B*, 21:3545, 1980.
- [101] M. Lannoo and J. Bourgoin. *Point Defects in Semiconductors I*, volume 22 of *Solid-State Sci.* Springer, Berlin Heidelberg New York, 1981.
- [102] G. A. Baraff and M. Schlüter. *Phys. Rev. B*, 19:4965, 1979.
- [103] G. A. Baraff, E. O. Kane, and M. Schlüter. *Phys. Rev. Lett.*, 43:956, 1979.
- [104] N. O. Lipari, J. Bernholc, and S. T. Pantelides. *Phys. Rev. Lett.*, 43:1354, 1979.
- [105] L. N. Cooper. *Phys. Rev.*, 104:1189, 1956.
- [106] L. D. Landau and E. M. Lifshitz. *Statistical Physics*, pages 202–206. Pergamon, London, first edition, 1958.
- [107] E. M. Lifshitz and L. P. Pitaevskii. *Statistical Physics*, volume 2, pages 88–93. Pergamon, London, 1980.
- [108] J. Bardeen, L. N. Cooper, and J. R. Schrieffer. *Phys. Rev.*, 106:162, 1957.
- [109] J. Bardeen, L. N. Cooper, and J. R. Schrieffer. *Phys. Rev.*, 108:1175, 1957.
- [110] J. R. Schrieffer. *Theory of Superconductivity*. Benjamin, Reading, MA, 1964.
- [111] G. Rickayzen. *Theory of Superconductivity*. Wiley, New York, 1964.
- [112] R. D. Parks, editor. *Superconductivity*. Dekker, New York, 1969.
- [113] A. A. Abrikosov, L. P. Gorkov, and I. E. Dzyaloshinski. *Methods of Quantum Field Theory in Statistical Physics*. Prentice-Hall, Englewood Cliffs, NJ, 1963.
- [114] G. D. Mahan. *Many-Particle Physics*. Plenum, New York, second edition, 1990.
- [115] E. N. Economou. In G. Bambakidis, editor, *Metal Hydrides*, pages 1–19. Plenum, New York, 1981.
- [116] G. Grimvall. *Phys. Scripta*, 14:63, 1976.

- [117] W. L. McMillan. *Phys. Rev.*, 167:331, 1968.
- [118] P. B. Allen and R. C. Dynes. *Phys. Rev. B*, 12:905, 1975.
- [119] J. Kondo. *Progr. Theor. Phys.*, 37:32, 1964.
- [120] A. A. Abrikosov. *Physics*, 2:5, 1965.
- [121] H. Suhl. *Phys. Rev. A*, 138:515, 1965.
- [122] Y. Nagaoka. *Phys. Rev. A*, 138:1112, 1965.
- [123] Y. Nagaoka. *Progr. Theor. Phys.*, 37:13, 1967.
- [124] J. Kondo. In H. Ehrenreich, F. Seitz, and D. Turnbull, editors, *Solid State Physics*, volume 23, page 183. Academic, New York, 1969.
- [125] P. W. Anderson and G. Yuval. *Phys. Rev. B*, 1:1522, 1970.
- [126] P. W. Anderson and G. Yuval. *J. Phys. C*, 4:607, 1971.
- [127] M. Fowler and A. Zawadowski. *Solid State Commun.*, 9:471, 1971.
- [128] G. T. Rado and H. Suhl, editors. *Magnetism*, volume 5. Academic, New York, 1973.
- [129] K. G. Wilson. *Rev. Mod. Phys.*, 67:773, 1975.
- [130] Philippe Nozieres. In M. Krusius and M. Vuorio, editors, *Proc. 14th Int. Conf. Low Temperature Physics*, page 339, Amsterdam, 1975. North-Holland.
- [131] N. Andrei. *Phys. Rev. Lett.*, 45:379, 1980.
- [132] P. B. Wiegmann. *Pis'ma Zh. Eksp. Teor. Fiz.*, 31:392, 1980. [*JETP Lett.* 31, 364 (1980)].
- [133] P. L. Taylor and O. Heinonen. *Condensed Matter Physics*. Cambridge University Press, Cambridge, 2002.
- [134] C. P. Enz. *A Course on Many-Body Theory Applied to Solid State Physics*. World Scientific, Singapore, 1992.
- [135] S. Doniach and E. H. Sondheimer. *Green's Functions for Solid State Physicists*. Imperial College Press, London, 1998. Reedition.

Chapter 7

- [136] P. Lloyd. *J. Phys. C*, 2:1717, 1969.
- [137] J. M. Ziman. *Models of Disorder*. Cambridge University Press, London, 1979.
- [138] R. J. Elliott, J. A. Krumhansl, and P. L. Leath. *Rev. Mod. Phys.*, 46:465, 1974.
- [139] H. Ehrenreich and L. M. Schwartz. In H. Ehrenreich, F. Seitz, and D. Turnbull, editors, *Solid State Physics*, volume 31, page 150. Academic, New York, 1976.
- [140] L. M. Schwartz. In M. F. Thorpe, editor, *Excitations in Disordered Systems*, volume B78 of *NATO Advanced Study Institute Series*, pages 177–224. Plenum, New York, 1981.
- [141] A. Bansil. In M. F. Thorpe, editor, *Excitations in Disordered Systems*, volume B78 of *NATO Advanced Study Institute Series*, pages 225–240. Plenum, New York, 1981.
- [142] A. Bansil, L. Schwartz, and H. Ehrenreich. *Phys. Rev. B*, 12:2893, 1975.
- [143] P. E. Mijnaerends and A. Bansil. *Phys. Rev. B*, 13:2381, 1976.
- [144] P. E. Mijnaerends and A. Bansil. *Phys. Rev. B*, 19:2912, 1979.
- [145] A. Bansil, R. S. Rao, P. E. Mijnaerends, and L. Schwartz. *Phys. Rev. B*, 23:3608, 1981.
- [146] A. Bansil. *Phys. Rev. B*, 20:4025, 1979.
- [147] A. Bansil. *Phys. Rev. B*, 20:4035, 1979.

- [148] P. N. Sen. In M. F. Thorpe, editor, *Excitations in Disordered Systems*, volume B78 of *NATO Advanced Study Institute Series*, pages 647–659. Plenum, New York, 1981.
- [149] S. C. Maxwell. *A treatise on Electricity and Magnetism (1873)*. Dover, New York, 1945.
- [150] J. Hubbard. *Proc. R. Soc. A*, 281:401, 1964.
- [151] D. W. Taylor. *Phys. Rev.*, 156:1017, 1967.
- [152] P. Soven. *Phys. Rev.*, 156:809, 1967.
- [153] P. L. Leath. *Phys. Rev.*, 171:725, 1968.
- [154] P. L. Leath. *Phys. Rev. B*, 5:1643, 1972.
- [155] R. N. Aiyer, R. J. Elliott, J. A. Krumhansl, and P. L. Leath. *Phys. Rev.*, 181:1006, 1969.
- [156] B. G. Nickel and J. A. Krumhansl. *Phys. Rev. B*, 4:4354, 1971.
- [157] S. F. Edwards. *Philos. Mag.*, 3:1020, 1958.
- [158] J. S. Langer. *Phys. Rev.*, 120:714, 1960.
- [159] R. Klaunder. *Ann. Phys.*, 14:43, 1961.
- [160] T. Matsubara and Y. Toyozawa. *Progr. Theor. Phys.*, 26:739, 1961.
- [161] P. L. Leath and B. Goodman. *Phys. Rev.*, 148:968, 1966.
- [162] P. L. Leath and B. Goodman. *Phys. Rev.*, 175:963, 1968.
- [163] F. Yonezawa and T. Matsubara. *Progr. Theor. Phys.*, 35:357, 1966.
- [164] F. Yonezawa and T. Matsubara. *Progr. Theor. Phys.*, 35:759, 1966.
- [165] F. Yonezawa and T. Matsubara. *Progr. Theor. Phys.*, 37:1346, 1967.
- [166] P. L. Leath. *Phys. Rev. B*, 2:3078, 1970.
- [167] T. Matsubara and T. Kaneyoshi. *Progr. Theor. Phys.*, 36:695, 1966.
- [168] B. Velicky, S. Kirkpatrick, and H. Ehrenreich. *Phys. Rev.*, 175:747, 1968.
- [169] B. Velicky, S. Kirkpatrick, and H. Ehrenreich. *Phys. Rev. B*, 1:3250, 1970.
- [170] Y. Onodera and Y. Toyozawa. *J. Phys. Soc. Jpn.*, 24:341, 1968.
- [171] F. Yonezawa. *Progr. Theor. Phys.*, 39:1076, 1968.
- [172] F. Yonezawa. *Progr. Theor. Phys.*, 40:734, 1968.
- [173] W. H. Butler. *Phys. Lett. A*, 39:203, 1972.
- [174] F. Brouers, M. Cyrot, and F. Cyrot-Lackmann. *Phys. Rev. B*, 7:4370, 1973.
- [175] F. Yonezawa and K. Morigaki. *Progr. Theor. Phys. Suppl.*, 53:1, 1973.
- [176] J. A. Stratton. *Electromagnetic Theory*. McGraw-Hill, New York, 1941.
- [177] Craig F. Bohren and Donald R. Huffman. *Absorption and Scattering of Light by Small Particles*. Wiley Science Paperback. Wiley-Interscience, New York, 1998.
- [178] M. Kafesaki and E. N. Economou. *Phys. Rev. B*, 52:13317–13331, 1995.
- [179] M. Kafesaki and E. N. Economou. *Phys. Rev. B*, 60:11993, 1999.
- [180] R. S. Penciu, H. Kriegs, G. Petekidis, G. Fytas, and E. N. Economou. *J. Chem. Phys.*, 118(11):5224–5240, 2003.
- [181] E. N. Economou and C. M. Soukoulis. *Phys. Rev. B*, 40:7977–7980, 1989.
- [182] C. M. Soukoulis, S. Datta, and E. N. Economou. *Phys. Rev. B*, 49(6):3800–3810, 1994.
- [183] K. Busch, C. M. Soukoulis, and E. N. Economou. *Phys. Rev. B*, 50(1):93–98, 1994.
- [184] K. Busch, C. M. Soukoulis, and E. N. Economou. *Phys. Rev. B*, 52(15):10834–10840, 1995.
- [185] X. Jing, P. Sheng, and M. Zhou. *Phys. Rev. Lett.*, 66(9):1240–1243, 1991.
- [186] X. J., P. Sheng, and M. Zhou. *Phys. Rev. A*, 46(10):6531–6534, 1992.

- [187] P. Sheng, X. Jing, and M. Zhou. *Physica A*, 207(1–3):37–45, 1994.
- [188] M. Kafesaki and E. N. Economou. *Ann. Physik (Leipzig)*, 7:383, 1998.
- [189] F. Yonezawa and T. Odagaki. *Solid State Commun.*, 27:1199 and 1203, 1978.
- [190] F. Yonezawa and T. Odagaki. *J. Phys. Soc. Jpn.*, 47:388, 1979.
- [191] J. S. Faulkner. *Phys. Rev. B*, 13:2391, 1976.
- [192] J. S. Faulkner and G. M. Stocks. *Phys. Rev. B*, 23:5628, 1981.
- [193] J. S. Faulkner and G. M. Stocks. *Phys. Rev. B*, 21:3222, 1980.
- [194] D. A. Papaconstantopoulos, B. M. Klein, J. S. Faulkner, and L. L. Boyer. *Phys. Rev. B*, 18:2784, 1978.
- [195] D. A. Papaconstantopoulos and E. N. Economou. *Phys. Rev. B*, 24:7233, 1981.
- [196] B. L. Gyorffy and G. M. Stocks. In P. Phariseau, B. L. Gyorffy, and L. Scheire, editors, *Electrons in Disordered Metals and at Metallic Surfaces*. Plenum, New York, 1979.
- [197] J. S. Faulkner. *Progr. Mat. Sci.*, 27:1, 1982.
- [198] G. M. Stocks, W. M. Temmerman, and B. L. Gyorffy. *Phys. Rev. Lett.*, 41:339, 1978.
- [199] J. Koringa and R. L. Mills. *Phys. Rev. B*, 5:1654, 1972.
- [200] L. Roth. *Phys. Rev. B*, 9:2476, 1974.
- [201] E. Balanovski. *Phys. Rev. B*, 20:5094, 1979.
- [202] L. Schwartz, H. Krakauer, and H. Fukuyama. *Phys. Rev. Lett.*, 30:746, 1973.
- [203] T. Kaplan and M. Mostoller. *Phys. Rev. B*, 9:1983, 1974.
- [204] A. B. Harris, P. L. Leath, B. G. Nickel, and R. J. Elliott. *J. Phys. C*, 7:1693, 1974.
- [205] R. A. Tahir-Kheli. *Phys. Rev. B*, 6:2808, 1972.
- [206] R. A. Tahir-Kheli. *Phys. Rev. B*, 6:2826, 1972.
- [207] R. A. Tahir-Kheli, T. Fujiwara, and R. J. Elliott. *J. Phys. C*, 11:497, 1978.
- [208] R. J. Elliott. In M. F. Thorpe, editor, *Excitations in Disordered Systems*, volume B78 of *NATO Advanced Study Institute Series*, pages 3–25. Plenum, New York, 1981.
- [209] H. Shiba. *Progr. Theor. Phys.*, 46:77, 1971.
- [210] E-Ni Foo, A. Amar, and M. Austloos. *Phys. Rev. B*, 4:3350, 1971.
- [211] J. A. Blackman, D. M. Esterling, and N. F. Berk. *Phys. Rev. B*, 4:2412, 1971.
- [212] D. J. Whitelaw. *J. Phys. C*, 14:2871, 1981.
- [213] P. L. Leath. In M. F. Thorpe, editor, *Excitations in Disordered Systems*, volume B78 of *NATO Advanced Study Institute Series*, pages 109–127. Plenum, New York, 1981.
- [214] E. Müller-Hartmann. *Solid State Commun.*, 12:1269, 1973.
- [215] F. Ducastelle. *J. Phys. C*, 4:L75, 1971.
- [216] F. Ducastelle. *J. Phys. C*, 7:1795, 1974.
- [217] W. H. Butler and B. G. Nickel. *Phys. Rev. Lett.*, 30:373, 1973.
- [218] V. Čapek. *Phys. Status Solidi B*, 43:61, 1971.
- [219] P. L. Leath. *J. Phys. C*, 6:1559, 1973.
- [220] A. Gonis and J. W. Garland. *Phys. Rev. B*, 16:1495, 1977.
- [221] A. Gonis and J. W. Garland. *Phys. Rev. B*, 16:2424, 1977.
- [222] L. M. Falicov and F. Yndurain. *Phys. Rev. B*, 12:5664, 1975.
- [223] R. Haydock. In M. F. Thorpe, editor, *Excitations in Disordered Systems*, volume B78 of *NATO Advanced Study Institute Series*, pages 29–57. Plenum, New York, 1981.

- [224] F. Cyrot-Lackmann and S. N. Khanna. In M. F. Thorpe, editor, *Excitations in Disordered Systems*, volume B78 of *NATO Advanced Study Institute Series*, pages 59–83. Plenum, New York, 1981.
- [225] K. F. Freed and M. H. Cohen. *Phys. Rev. B*, 3:3400, 1971.
- [226] C. T. White and E. N. Economou. *Phys. Rev. B*, 15:3742, 1977.
- [227] K. Aoi. *Solid State Commun.*, 14:929, 1974.
- [228] T. Miwa. *Progr. Theor. Phys.*, 52:1, 1974.
- [229] F. Brouers and F. Ducastelle. *J. Phys. F*, 5:45, 1975.
- [230] A. R. Bishop and A. Mookerjee. *J. Phys. C*, 7:2165, 1974.
- [231] P. R. Best and P. Lloyd. *J. Phys. C*, 8:2219, 1975.
- [232] I. Takahashi and M. Shimizu. *Progr. Theor. Phys.*, 51:1678, 1973.
- [233] S. Wu and M. Chao. *Phys. Status Solidi B*, 68:349, 1975.
- [234] A. R. McGurn and R. A. Tahir-Kheli. *J. Phys. C*, 10:4385, 1977.
- [235] H. Schmidt. *Phys. Rev.*, 105:425, 1957.
- [236] R. Mills and P. Ratanavararaksa. *Phys. Rev. B*, 18:5291, 1978.
- [237] A. Mookerjee. *J. Phys. C*, 6:L205, 1973.
- [238] A. Mookerjee. *J. Phys. C*, 6:1340, 1973.
- [239] T. Kaplan, P. L. Leath, L. J. Gray, and H. W. Diehl. *Phys. Rev. B*, 21:4230, 1980.
- [240] L. J. Gray and T. Kaplan. *Phys. Rev. B*, 24:1872, 1981.
- [241] T. Kaplan and L. J. Gray. In M. F. Thorpe, editor, *Excitations in Disordered Systems*, volume B78 of *NATO Advanced Study Institute Series*, pages 129–143. Plenum, New York, 1981.
- [242] Antonios Gonis. *Green Functions for Ordered and Disordered Systems*, volume 4 of *Studies in Mathematical Physics*. North-Holland, Amsterdam, 1992.
- [243] P. Sheng. *Scattering and Localization of Classical Waves in Random Media*, volume 8 of *World Scientific Series on Directions in Condensed Matter Physics*. World Scientific, Singapore, 1990.
- [244] E. M. Lifshitz, S. A. Grestscul, and L. A. Pastur. *Introduction to the Theory of Disordered Systems*. Wiley, New York, 1988.

Chapter 8

- [245] M. H. Cohen, E. N. Economou, and C. M. Soukoulis. *Phys. Rev. B*, 30:4493, 1984.
- [246] J. M. Ziman. *Electrons and Phonons*. Oxford University Press, London, 1960.
- [247] B. R. Nag. *Electron Transport in Compound Semiconductors*, volume 11 of *Solid State Sci*. Springer, Berlin Heidelberg New York, 1980.
- [248] N. F. Mott and E. A. Davis. *Electronic Processes in Non-Crystalline Materials*. Clarendon, Oxford, second edition, 1979.
- [249] J. Callaway. *Quantum Theory of the Solid State*. Academic, New York, second edition, 1991.
- [250] Y. Imry. *Introduction to mesoscopic physics*. Oxford University Press, Oxford, second edition, 2002.
- [251] D. J. Thouless. In R. Balian, R. Maynard, and G. Toulouse, editors, *III-Condensed Matter*, pages 1–62. North-Holland, Amsterdam, 1979.
- [252] R. Kubo. *Can. J. Phys.*, 34:1274, 1956.
- [253] R. Kubo. *J. Phys. Soc. Jpn.*, 12:570, 1957.
- [254] A. D. Greenwood. *Proc. Phys. Soc.*, 71:585, 1958.

- [255] E. N. Economou and C. M. Soukoulis. *Phys. Rev. Lett.*, 46:618, 1981.
- [256] B. S. Andereck and E. Abrahams. *J. Phys. C*, 13:L383, 1980.
- [257] P. W. Anderson, D. J. Thouless, E. Abrahams, and D. S. Fisher. *Phys. Rev. B*, 22:3519, 1980.
- [258] A. A. Abrikosov. *Solid State Commun.*, 37:997, 1981.
- [259] S. F. Edwards. *Philos. Mag.*, 4:1171, 1959.
- [260] B. Velicky. *Phys. Rev.*, 184:614, 1969.
- [261] M. Janssen. *Fluctuations and Localization in Mesoscopic Electron Systems*. World Scientific, Singapore, 2001.

Chapter 9

- [262] M. Kaveh. *Can. J. Phys.*, 60:746, 1982.
- [263] D. C. Licciardello and E. N. Economou. *Phys. Rev. B*, 11:3697, 1975.
- [264] A. Kawabata. *J. Phys. Soc. Jpn.*, 53:3540, 1984.
- [265] S. Hikami, A. I. Larkin, and Y. Nagaoka. *Progr. Theor. Phys.*, 63:707, 1980.
- [266] B. L. Altshuler, A. G. Aronov, B. Z. Spivak, D. Yu. Sharvin, and Yu. V. Sharvin. *JEPT Lett.*, 35:588, 1982.
- [267] G. Bergman. *Phys. Rep.*, 107:1, 1984.
- [268] P. A. Lee and T. V. Ramakrishnan. *Rev. Mod. Phys.*, 57:287, 1985.
- [269] A. G. Aronov and Yu. V. Sharvin. *Rev. Mod. Phys.*, 59:755, 1987.
- [270] S. Hikami. *Phys. Rev. B*, 29:3726–3729, 1984.
- [271] D. Vollhardt and P. Wölfle. *Phys. Rev. B*, 22:4666, 1980.
- [272] W. Götze. *Solid State Commun.*, 27:1392, 1978.
- [273] W. Götze. *J. Phys. C*, 12:1279, 1979.
- [274] A. Kawabata. *Solid State Commun.*, 38:823, 1981.
- [275] A. Kawabata. *J. Phys. Soc. Jpn.*, 49:628, 1980.
- [276] E. N. Economou and C. M. Soukoulis. *Phys. Rev. B*, 28:1093, 1983.
- [277] E. N. Economou, C. M. Soukoulis, and A. D. Zdetsis. *Phys. Rev. B*, 30:1686, 1984.
- [278] E. N. Economou. *Phys. Rev. B*, 31:7710, 1985.
- [279] A. D. Zdetsis, C. M. Soukoulis, and E. N. Economou. *Phys. Rev. B*, 33:4936, 1986.
- [280] S. N. Evangelou and E. N. Economou. *Phys. Lett. A*, 345:151, 1990.
- [281] Elihu Abrahams, Sergey V. Kravchenko, and Myriam P. Sarachik. *Rev. Mod. Phys.*, 73(2):251–266, 2001.
- [282] R. Landauer and J. C. Helland. *J. Chem. Phys.*, 22:1655, 1954.
- [283] N. F. Mott and W. D. Twose. *Adv. Phys.*, 10:107, 1961.
- [284] R. E. Borland. *Proc. Phys. Soc.*, 77:705, 1961.
- [285] R. E. Borland. *Proc. Phys. Soc.*, 78:926, 1961.
- [286] R. E. Borland. *Proc. R. Soc. A*, 274:529, 1963.
- [287] R. E. Borland. *Proc. Phys. Soc.*, 83:1027, 1964.
- [288] F. J. Wegner. *Z. Phys. B*, 22:273, 1975.
- [289] B. I. Halperin. *Adv. Chem. Phys.*, 13:123, 1967.
- [290] J. Hori. *Spectral Properties of Disordered Chains and Lattices*. Pergamon, London, 1968.
- [291] E. H. Lieb and D. C. Mattis. *Mathematical Physics in One Dimension*. Academic, New York, 1966.
- [292] K. Ishii. *Progr. Theor. Phys. Suppl.*, 53:77, 1973.
- [293] H. Furstenberg. *Trans. Amer. Math. Soc.*, 108:377–428, 1963.

- [294] J. Sak and B. Kramer. *Phys. Rev. B*, 24:1761, 1981.
- [295] C. M. Soukoulis and E. N. Economou. *Phys. Rev. B*, 24:5698, 1981.
- [296] A. Douglas Stone and J. D. Joannopoulos. *Phys. Rev. B*, 24:3592, 1981.
- [297] A. Douglas Stone and J. D. Joannopoulos. *Phys. Rev. B*, 25:1431, 1982.
- [298] P. W. Anderson. *Phys. Rev. B*, 23:4828, 1981.
- [299] V. L. Berezinskii. *Zh. Eksp. Teor. Fiz.*, 65:1251, 1973. [*Sov. Phys. JETP* 38, 630 (1974)].
- [300] A. A. Gogolin. *Sov. Phys. JETP*, 50:827, 1979.
- [301] A. A. Abrikosov and I. A. Ryzhkin. *Adv. Phys.*, 27:147, 1978.
- [302] P. Erdős and R. C. Herndon. *Adv. Phys.*, 31:65, 1982.
- [303] G. Theodorou and M. H. Cohen. *Phys. Rev. B*, 13:4597, 1976.
- [304] L. Fleishman and D. Licciardello. *J. Phys. C*, 10:L125, 1977.
- [305] B. Y. Tong. *Phys. Rev. A*, 1:52, 1970.
- [306] R. Landauer. *Philos. Mag.*, 21:863, 1970.
- [307] S. Datta. *Electronic Transport in Mesoscopic Systems*. Cambridge University Press, Cambridge, 1995.
- [308] D. S. Fisher and P. A. Lee. *Phys. Rev. B*, 23:6851, 1981.
- [309] E. N. Economou and C. M. Soukoulis. *Phys. Rev. Lett.*, 47:973, 1981.
- [310] R. Landauer. *Phys. Lett. A*, 85:91, 1981.
- [311] D. J. Thouless. *Phys. Rev. Lett.*, 47:972, 1981.
- [312] D. J. Thouless and S. Kirkpatrick. *J. Phys. C*, 14:235, 1981.
- [313] V. I. Mel'nikov. *Fiz. Tverd. Tela*, 22:2404, 1980. [*Sov. Phys. Sol. St.* 22, 1398 (1980)].
- [314] M. Ya. Azbel. *Phys. Rev. B*, 22:4045, 1980.
- [315] D. Lenstra and W. van Haeringen. *J. Phys. C*, 14:L819, 1981.
- [316] Y. Imry, G. Grinstein, and G. Mazenko. *Directions in Condensed Matter Physics*. World Scientific, Singapore, 1986.
- [317] M. Büttiker, Y. Imry, R. Landauer, and S. Pinhas. *Phys. Rev. B*, 31:6207, 1985.
- [318] M. Büttiker. *IBM I. Res. Dev.*, 32:317, 1988.
- [319] E. Abrahams, P. W. Anderson, D. C. Licciardello, and T. V. Ramakrishnan. *Phys. Rev. Lett.*, 42:673, 1979.
- [320] D. C. Licciardello and D. J. Thouless. *J. Phys. C*, 11:925, 1978.
- [321] S. Sarker and E. Domany. *Phys. Rev. B*, 23:6018, 1981.
- [322] N. F. Mott. *Philos. Mag. B.*, 44(2):265, 1981.
- [323] F. J. Wegner. *Z. Phys. B*, 25:327, 1976.
- [324] F. J. Wegner. *J. Phys. B*, 35:207, 1979.
- [325] L. Schäfer and F. J. Wegner. *J. Phys. B.*, 38:113, 1980.
- [326] A. Houghton, A. Jevicki, R. D. Kenway, and A. M. M. Pruisken. *Phys. Rev. Lett.*, 45:394, 1980.
- [327] K. B. Efetov, A. I. Larkin, and D. E. Kheml'nitskii. *Zh. Eksp. Teor. Fiz.*, 79:1120, 1980. [*Sov. Phys. JETP* 52(3), 568 (1981)].
- [328] G. A. Thomas, Y. Ootuka, S. Katsumoto, S. Kobayashi, and W. Sasaki. *Phys. Rev. B*, 25:4288, 1982.
- [329] G. A. Thomas, Y. Ootuka, S. Kobayashi, and W. Sasaki. *Phys. Rev. B*, 24:4886, 1981.
- [330] Y. Imry. *Phys. Rev. Lett.*, 44:469, 1980.
- [331] W. L. McMillan. *Phys. Rev. B*, 24:2739, 1981.
- [332] S. Hikami. *Phys. Rev. B*, 24:2671, 1981.

- [333] T. F. Rosenbaum, K. Andres, G. A. Thomas, and R. N. Bhatt. *Phys. Rev. Lett.*, 45:1723, 1980.
- [334] T. F. Rosenbaum, K. Andres, G. A. Thomas, and P. Lee. *Phys. Rev. Lett.*, 46:568, 1981.
- [335] R. A. Römer and M. Schreiber. In T. Brandes and S. Kettermann, editors, *Anderson Localization and its Ramifications*. Springer, Heidelberg, 2003.
- [336] T. Ohtsuki and K. Slevin. In T. Brandes and S. Kettermann, editors, *Anderson Localization and its Ramifications*. Springer, Heidelberg, 2003.
- [337] A. Kawabata. In T. Brandes and S. Kettermann, editors, *Anderson Localization and its Ramifications*. Springer, Heidelberg, 2003.
- [338] M. J. Vren, R. A. Davis, M. Kaveh, and M. Pepper. *J. Phys. C*, 14:5737, 1981.
- [339] G. J. Dolan and D. D. Osheroff. *Phys. Rev. Lett.*, 43:721, 1979.
- [340] L. Van den Dries, C. Van Haesendonck, Y. Bruynseraede, and G. Deutscher. *Phys. Rev. Lett.*, 46:565, 1981.
- [341] L. Van den Dries, C. Van Haesendonck, Y. Bruynseraede, and G. Deutscher. *Physica B+C*, 107:7, 1981.
- [342] D. J. Bishop, D. C. Tsui, and R. C. Dynes. *Phys. Rev. Lett.*, 44:1153, 1980.
- [343] D. J. Bishop, D. C. Tsui, and R. C. Dynes. *Phys. Rev. Lett.*, 46:360, 1981.
- [344] Y. Kawaguchi and S. Kawaji. *J. Phys. Soc. Jpn.*, 48:699, 1980.
- [345] G. Bergmann. *Phys. Rev. Lett.*, 49:162, 1982.
- [346] G. Bergmann. *Phys. Rev. B*, 25:2937, 1982.
- [347] G. Bergmann. *Solid State Commun.*, 42:815, 1982.
- [348] N. Giordano, W. Gilson, and D. E. Prober. *Phys. Rev. Lett.*, 43:725, 1979.
- [349] N. Giordano. *Phys. Rev. B*, 22:5635, 1980.
- [350] J. T. Masden and N. Giordano. *Physica B+C*, 107:3, 1981.
- [351] P. Chaudhari and H. V. Hebermeier. *Solid State Commun.*, 34:687, 1980.
- [352] P. Chaudhari, A. N. Broers, C. C. Chi, R. Laibowitz, E. Spiller, and J. Viggiano. *Phys. Rev. Lett.*, 45:930, 1980.
- [353] A. E. White, M. Tinkham, W. J. Skocpol, and D. C. Flanders. *Phys. Rev. Lett.*, 48:1752, 1982.
- [354] T. F. Rosenbaum, R. F. Milligan, G. A. Thomas, P. A. Lee, T. V. Ramakrishnan, R. N. Bhatt, K. DeConde, H. Hess, and T. Perry. *Phys. Rev. Lett.*, 47:1758, 1981.
- [355] S. Maekawa and H. Fukuyama. *J. Phys. Soc. Jpn.*, 50:2516, 1981.
- [356] S. Yoshino and M. Okazaki. *J. Phys. Soc. Jpn.*, 43:415, 1977.
- [357] F. Yonezawa. *J. Noncrystall. Solids*, 35 and 36:29, 1980.
- [358] J. Stein and U. Krey. *Solid State Commun.*, 27:797, 1978.
- [359] J. Stein and U. Krey. *Solid State Commun.*, 27:1405, 1978.
- [360] D. Weaire and V. Srivastava. *J. Phys. C*, 10:4309, 1977.
- [361] P. Prelovšek. *Phys. Rev. B*, 18:3657, 1978.
- [362] P. Prelovšek. *Solid State Commun.*, 31:179, 1979.
- [363] P. Lee. *Phys. Rev. Lett.*, 42:1492, 1978.
- [364] P. Lee. *J. Noncrystall. Solids*, 35 and 36:21, 1980.
- [365] P. B. Allen. *J. Phys. C*, 13:L667, 1980.
- [366] M. Kaveh and N. F. Mott. *J. Phys. C*, 14:L177, 1981.
- [367] N. F. Mott and M. Kaveh. *J. Phys. C*, 14:L659, 1981.
- [368] H. G. Schuster. *Z. Phys. B.*, 31:99, 1978.
- [369] J. L. Pichard and G. Sarma. *J. Phys. C*, 14:L127, 1981.
- [370] J. L. Pichard and G. Sarma. *J. Phys. C*, 14:L617, 1981.

- [371] A. MacKinnon and B. Kramer. *Phys. Rev. Lett.*, 47:1546, 1981.
- [372] C. M. Soukoulis, I. Webman, G. S. Crest, and E. N. Economou. *Phys. Rev. B*, 26:1838, 1982.
- [373] R. Haydock. In M. F. Thorpe, editor, *Excitations in Disordered Systems*, volume B78 of *NATO Advanced Study Institute Series*, pages 553–563. Plenum, New York, 1981.
- [374] R. Haydock. *J. Phys. C*, 14:229, 1981.
- [375] R. Haydock. *Philos. Mag. B.*, 43:203, 1981.
- [376] B. Kramer and A. MacKinnon. *Reports on Progress in Physics*, 56:1469, 1993.
- [377] E. N. Economou, C. M. Soukoulis, M. H. Cohen, and A. D. Zdetsis. *Phys. Rev. B*, 31:6172, 1985.
- [378] E. N. Economou, C. M. Soukoulis, and A. D. Zdetsis. *Phys. Rev. B*, 31:6483, 1985.
- [379] I. Zambetaki, Q. Li, E. N. Economou, and C. M. Soukoulis. *Phys. Rev. Lett.*, 76:3614, 1996.
- [380] Q. Li, S. Katsoprinakis, E. N. Economou, and C. M. Soukoulis. *Phys. Rev. B*, 56(8):R4297–R4300, 1997.
- [381] T. Brandes and S. Kettermann, editors. Springer, Heidelberg, 2003.
- [382] D. J. Thouless. *J. Phys. C*, 5:77, 1972.
- [383] M. Kappus and F. Wegner. *Z. Phys. B.*, 45:15, 1981.
- [384] S. Sarker. *Phys. Rev. B*, 25:4304, 1982.
- [385] E. N. Economou and C. T. Papatriantafillou. *Phys. Rev. Lett.*, 32:1130, 1974.
- [386] C. Papatriantafillou, E. N. Economou, and T. P. Eggarter. *Phys. Rev. B*, 13:910, 1976.
- [387] C. Papatriantafillou and E. N. Economou. *Phys. Rev. B*, 13:920, 1976.
- [388] P. W. Anderson. *Phys. Rev.*, 109:1492, 1958.
- [389] J. M. Ziman. *J. Phys. C*, 2:1230, 1969.
- [390] M. Kikuchi. *J. Phys. Soc. Jpn.*, 29:296, 1970.
- [391] D. C. Herbert and R. Jones. *J. Phys. C*, 4:1145, 1971.
- [392] D. J. Thouless. *J. Phys. C*, 3:1559, 1970.
- [393] E. N. Economou and M. H. Cohen. *Phys. Rev. Lett.*, 25:1445, 1970.
- [394] E. N. Economou and M. H. Cohen. *Phys. Rev. B*, 5:2931, 1972.
- [395] R. Abou-Chacra, P. W. Anderson, and D. J. Thouless. *J. Phys. C*, 6:1734, 1973.
- [396] C. M. Soukoulis and E. N. Economou. *Phys. Rev. Lett.*, 45:1590, 1980.
- [397] J. Bernasconi and T. Schneider, editors. *Physics in One Dimension*, volume 23 of *Springer Ser. Solid-State Sci.* Springer, Berlin Heidelberg New York, 1981.
- [398] Gert R. Strobl. *The Physics of Polymers: Concepts for Understanding Their Structures and Behavior*. Springer, second edition, 1997.
- [399] F. Yonezawa, editor. *Fundamental Physics of Amorphous Semiconductors*, volume 25 of *Springer Ser. Solid-State Sci.* Springer, Berlin Heidelberg New York, 1980.
- [400] N. E. Cusack. *The Physics of Structurally Disordered Matter: An Introduction*. Graduate Student Series in Physics. Institute of Physics Publishing, Bristol, 1987.
- [401] W. A. Phillips, editor. *Amorphous Solids*, volume 24 of *Topics in Current Physics*. Springer, Berlin Heidelberg New York, 1980.
- [402] C. M. Soukoulis, editor. *Photonic Crystals and Light Localization in the 21st Century*. Kluwer, Dordrecht, 2001.

- [403] J. D. Joannopoulos, R. D. Meade, and J. N. Winn. *Photonic Crystals*. Princeton University Press, Princeton, 1995.
- [404] D. S. Wiersma, P. Bartolini, A. Lagendijk, and R. Righini. *Nature*, 390:671–673, 1997.
- [405] A. Lagendijk. In C. M. Soukoulis, editor, *Photonic Crystals and Light Localization in the 21st Century*, page 447. Kluwer, Dordrecht, 2001.
- [406] S. John. *Nature*, 390:661, 1997.
- [407] M. S. Kushwaha. *Recent Res. Dev. Applied Phys.*, 2:743, 1999.
- [408] M. Kafesaki, R. S. Penciu, and E. N. Economou. Air Bubbles in Water: a Strongly Multiple Scattering Medium for Acoustic Waves. *Phys. Rev. Lett.*, 84:6050, 2000.
- [409] F. Scheffold, R. Lenke, R. Tweert, and G. Maret. *Nature*, 398(6724):206, 1999.
- [410] R. Martel, T. Schmidt, H. R. Shea, T. Hertel, and Ph. Avouris. Single - and multi - wall carbon nanotube field-effect transistors. *Appl. Phys. Lett.*, 73:2447, 1998.
- [411] H. R. Shea, R. Martel, and Ph. Avouris. Electrical transport in rings of single-wall nanotubes. *Phys. Rev. Lett.*, 84:4441, 2000.
- [412] S. Heinze, J. Tersoff, R. Martel, V. Derycke, J. Appenzeller, and Ph. Avouris. Carbon nanotubes as schottky barrier transistors. *Phys. Rev. Lett.*, 89:106801, 2002.
- [413] Y. M. Lin, J. Appenzeller, and Ph. Avouris. Ambipolar-to-unipolar conversion of carbon nanotube transistors by gate structure engineering. *Nanoletters*, 4:947, 2004.
- [414] A. N. Andriotis and M. Menon. Green’s function embedding approach to quantum conductivity of single wall carbon nanotubes. *J. Chem. Phys.*, 115:2737, 2001.
- [415] A. N. Andriotis, M. Menon, D. Srivastava, and L. Chernozatonskii. Transport properties of single wall carbon nanotube y-junctions. *Phys. Rev. B*, 65:165416, 2002.
- [416] A. N. Andriotis, M. Menon, and D. Srivastava. Transfer matrix approach to quantum conductivity calculations in single wall carbon nanotubes. *J. Chem. Phys.*, 117:2836, 2002.
- [417] D. K. Ferry and St. M. Goodnick. *Transport in Nanostructures*. Cambridge University Press, Cambridge, 1997.

Chapter 10

- [418] G. Rickayzen. *Green’s Functions and Condensed Matter*. Academic, London, 1980.
- [419] N. N. Bogoliubov and S. V. Tyablikov. Retarded and advanced green’s functions in statistical physics. *Dokl. Akad. Nauk SSSR*, 126:53, 1959.
- [420] L. P. Kadanoff and G. Baym. *Quantum Statistical Mechanics*. Benjamin, New York, 1962.

Chapter 11

- [421] R. D. Mattuck. *A Guide to Feynman Diagrams in the Many-Body Problem*. McGraw-Hill, New York, second edition, 1976.
- [422] L. D. Landau and E. M. Lifshitz. *Statistical Physics*, pages 39,70. Pergamon, London, first edition, 1959.

- [423] Philippe Nozieres. *Theory of Interacting Fermi Systems*. Benjamin, New York, 1964.

Chapter 12

- [424] D. N. Zubarev. Double Time Green's Functions in Statistical Physics. *Uspekhi Fiz. Nauk*, 21:71, 1960. English translation, *Sov. Phys. Uspekhi* 3, 320 (1960).

Chapter 13

- [425] J. M. Luttinger. *Phys. Rev.*, 121:942, 1961.
 [426] L. D. Landau. *Sov. Phys. JETP*, 3:920, 1956.
 [427] L. D. Landau. *Sov. Phys. JETP*, 5:101, 1957.
 [428] J. Friedel. *Philos. Mag.*, 43:153, 1952.
 [429] J. Friedel. *Nuovo Cimento*, 7:287, 1958.
 [430] V. M. Galitskii. *Sov. Phys. JETP*, 7:104, 1958.
 [431] S. T. Beliaev. *Sov. Phys. JETP*, 7:299, 1958.
 [432] M. Marder, N. Papanicolaou, and G. C. Psaltakis. *Phys. Rev. B*, 41:6920–6932, 1990.
 [433] V. J. Emery, S. A. Kivelson, and H. Q. Lin. *Phys. Rev. Lett.*, 64(4):475–478, 1990.
 [434] E. N. Economou, C. T. White, and R. R. DeMarco. *Phys. Rev. B*, 18:3946–3958, 1978.
 [435] A. N. Andriotis, E. N. Economou, Q. Li, and C. M. Soukoulis. *Phys. Rev. B*, 47:9208, 1993.
 [436] M. Cyrot and C. Lyon-Caen. *Le Journal de Physique*, 36:253, 1975.
 [437] R. Strack and D. Vollhardt. *Phys. Rev. Lett.*, 70:2637, 1993.
 [438] Shun-Qing Shen, Zhao-Ming Qiu, and Guang-Shan Tian. *Phys. Rev. Lett.*, 72(8):1280–1282, 1994.
 [439] E. N. Economou and P. Mihas. *J. Phys. C*, 10:5017, 1977.
 [440] R. R. DeMarco, E. N. Economou, and C. T. White. *Phys. Rev. B*, 18:3968–3975, 1978.
 [441] D. C. Mattis. *The Theory of Magnetism*, volume I and II. Springer, 1988.
 [442] N. Mott. *Metal-insulator Transitions*. Taylor and Francis, London, 1974.
 [443] A. Auerbach. *Interacting Electrons and Quantum Magnetism*. Springer, Berlin, 1994.
 [444] A. Montorsi. *The Hubbard Model*. World Scientific, Singapore, 1992. A Reprint Volume.

Appendix F

- [445] E. Feenberg. *Phys. Rev.*, 74:206, 1948.
 [446] K. M. Watson. *Phys. Rev.*, 105:1388, 1957.

Appendix H

- [447] M. Born and E. Wolf. *Principles of Optics*. Cambridge University Press, Cambridge, sixth edition, 1997.

Appendix I

- [448] G. Baym. *Lectures on Quantum Mechanics*. Benjamin, New York, 1969.

Index

- S -matrix, **61**, 73, 74, 235, 244, **372**
- σ -model
 - nonlinear, 224
- δ -function singularity, 114
- k -representation, 5, 65
- r -representation, **4**, 43, 64
- t -matrix, **57**, 63, 65, **72**, 75, 115, 134, 139, 142, 144, 149, 152, 159, 161, 168, 171, 177, 178, 186, 322, 364
 - average, 153
- 1BZ (first Brillouin zone), 85–87
- A15 compound, 80
- absorption, 162, 171, 239
 - cross section, 162, 171
 - optical, 100, 210
- acceleration, 120
- Aharonov–Bohm effect, **207**, **208**, **241**
- amplitude, 83, 115
 - current, 372
 - exponential decay, 230
 - fluctuation, 240
 - reflection, 217, 237, 370, 373, 429
 - current, 372
 - scattering, 46, **65**, 67, 73, **159**, 161, 171, 319, 320
 - forward, 66
 - transmission, 217, 237, 370, 373, 429
 - current, 372
 - transmission current, 217, 218
- analytic
 - behavior, 353
 - continuation, 9, 117, 276–278, 283
- Anderson
 - localization, 240, 243
 - model, **201**
 - transition, 212, **212**
- annihilation operator, **250**, 252, 255, **383**
 - phonon, 258
- anti-ferromagnetic
 - ordering, 328
- anticommutation relation, 252, 381
- anticommutator, 35, 36
- antiferromagnetic
 - coupling, 134
 - phase, 329, 330
- approximation
 - Born, 65, 75, 131
 - Hartree, 285, 288, 328–331
 - Hartree–Fock, 289, 303, 307, 334
 - independent-particle, 183
 - ladder, 319, 321, 322
- ATA (average t -matrix approximation), **152**, 153, 154, 163, 164, 168
- atomic orbital, 79
 - hybrid, 79, 104
- attraction
 - phonon mediated, 131, 132
- average, 150
 - t -matrix, 153
 - energy, 289, 330
 - thermal, 324
- average t -matrix approximation (ATA), **152**
- ballistic motion, 205
- band, **78**, 80, 91, 94, 96, 101, 104, 145

- conduction, **126**, 210
 - tail, 210
- edge, **46**, 69, **78**, 84, 89, 91, 96, 97, 99, 104, 119, 121, 122, 124, 136, 137, 170, 210, 353
- index, **78**, 104
- tail, 157
- valence, **126**, 210
 - tail, 210
- bandwidth, 84, 85, 89, 96, 101
- BC (boundary condition), 345
- bcc (body-centered cubic), 103
- BCS, 130, 139
- BE (Boltzmann's equation), **363**
- Bessel
 - equation, **349**
 - function, 12, 45
 - modified, 45, **349**
 - spherical, **346**
- Bessel function, 118
- Bethe lattice, 98–102, 145, 147, 360, 361
 - double spacing periodic case, 98
- Bethe–Salpeter equation, 320
- binary
 - alloy, 150, 164, 170
 - case, 157
 - distribution, 165–167, 201
- binding energy, 128, 129, 135, 139
- Bloch
 - eigenfunction, 355
 - function, **78**, 138
 - ket, **342**
 - wave, **115**, 394
- Bloch's
 - theorem, **70**
- body-centered cubic (bcc) lattice, 103
- Bohr radius, 313
- Boltzmann's equation, 177, 196, 197, **363**
 - linearized, **365**
- bond, 164
- Born approximation, 65, 75, 131
- Bose
 - condensation, 258, 265, 300
 - function, **257**
 - thermal equilibrium distribution, 263
- Bose–Einstein distribution, 262
- boson, 252, 254, **381**
- bosonic density operator, 306
- bound, 137
- bound pair, 128, 130
- bound state, 74, 75
- boundary
 - natural, **6**, 15, 233
- boundary condition, **3**, 11, 15, 41, 345
- branch cut, **6**, 9, 15, 22, 42, 44, 57, 72, 117, 232
- Brillouin zone
 - first, **78**, 84–87, 90, 94, **102**, 105
- bulk modulus, 85, 158, 159, 171, 385
- canonical transformation, 276, 306
- capacitance, 239
- cartesian coordinate, 25, 173
- Cauchy's theorem, 114
- causality, 174
- Cayley tree, 98, 99, 126, 140
 - double spacing periodic case, 98
- center of mass, 127
- cermet topology, **158**
- channel, 217, 218
- characteristic length, 225
- charge density, 8
- chemical potential, 175, 219, 242, **364**, 436
- chronological product, 298
- classical wave, 238
- cluster, 157, 165, 168
 - scattering, 165
- cluster–Bethe–lattice, 101
- coefficient
 - diffusion, **25**, 193, 197, 204, 208, 220, 240
 - Lamé, 158
 - reflection, 125, 170, 215, 371
 - transmission, 125, 170, 215–217, 371, 372
- coherent potential approximation (CPA), 141, 153, 169
- collective (plasma) oscillation, 318
- commutation relation, 252, 381
- commutator, 35, 36
 - current–current, 273
- completeness, 355
 - of a set, **4**
 - relation, 338, **342**, 389
- complex propagation constant, 155
- concentration, 37, 175, 177

- condensate, 128
- conductance, 216, 218, 220, 221, 239, 242, 437
 - Hall, 239
 - of nanotube, 240
- conduction
 - band, **126**, 210
 - tail, 210
- conductivity, 126, **173**, 189, 193, 204, 210, 212, 213, 216, 222, 240, 241, 244, 273, 364
 - AC, 175
 - DC, 175, 209
 - electrical, 173, 195, 197
 - local, 179
 - metallic, 199
 - post-CPA correction, 192
 - tensor, 174, 367
 - thermal, **25**
- conductor
 - perfect, 180, 197, 239
 - quasi 1-d, 218
 - quasi-1-d, 243
- configuration, 150
- conjugate momentum, 385
- connected diagram, 294
- connection of the notation, 269
- conservation of probability, **371**
- constant
 - complex propagation, 155
 - diffusion, 37
 - Euler's, **69**, **130**
 - propagation, 161, 162
- contact, 217, 218
 - resistance, 217
- continuation
 - analytic, 9, 117, 276–278, 283
- continued fraction method, 166
- continuum, 145, 169
- contribution
 - diamagnetic, 179, 197
 - paramagnetic, 179
- convergence, 234
- Cooper pair, 111, 322–324
- coordinate
 - cartesian, 25, 173
 - relative, 127
- Copper oxide, 131
- correction
 - post-CPA, 194, 199, 201
- Coulomb
 - blockade, **240**
 - force, 313
 - interaction
 - energy, 384
 - screened, 176
 - potential
 - attractive, 66, 67
 - repulsion, 132
 - screened, 132
- coupled pendula, 81, 83, 101, 200
- equations of motion, 81
- coupling
 - magnetic, 330
- coupling limit
 - strong, 318
 - weak, 318
- covalent solid, 79
- CPA, 141, 153, 154, 156–158, 160, 162–168, 170, 186, 189, 195, 210, 245
 - for classical wave, 158
 - homomorphic, **164**
 - muffin-tin, 164
- creation operator, **250**, 252, 255, **383**
 - phonon, 258
- critical
 - dimensionality, 201, 213, 242
 - energy, 235
 - exponent, 50, 223
 - temperature, 130, 327
 - value, 138, 223
 - voltage, 239
- cross section, 115, 163, 177
 - absorption, 162, 171
 - differential, **65**, **66**, 75
 - inelastic, 176
 - extinction, 162
 - scattering, 115, 118, 125, 159, 162, 171
 - total, 66, 73, 75, 161, 162, 171, 436
- crossover, 134
- crystal cell
 - primitive, 79
- crystal wavevector, 104
- CsI, 100
- current, 219
 - amplitude, 372

- density, 173
- current reflection amplitude, 236
- current transmission amplitude, 236, 242
- current–current commutator, 273
- cutoff
 - energy, 130, 134, 139
 - length
 - upper, 199, 205, 240
- cyclotron radius, **200**, 240

- Debye frequency, 131
- Debye wave number, 386
- decay length, 75
- defect, 126
- degeneracy, 42, 112
- delta function, **337**
 - derivative, **337**
 - in cartesian variables, 338
- density, 158, 161, 171, 270, 271
 - electronic, 273
 - fluctuation, 128
 - high, 312
 - low, 313, 319
 - matrix, **180**
 - of particles, 282
 - wave, 281, 312
 - elementary, 311
- density of states, **7**, 16, 42, 46, 51, 72, 78, 91, 104, 157, 166, 167, 211, 268, 433
 - generalized, 275, 281
- derivative
 - logarithmic, 220
- device
 - double-barrier, 239
- devil's staircase, **52**
- diagram, 142, 144, 307
 - connected, 294
 - Feynman, 293, 297, 298, 300
 - ladder, 319
 - maximally crossed, 191, 192
 - phase, 327, 330
 - ring, 316, 317
 - skeleton, 301, 303
- diagrammatic representation, 169
- dielectric function, 283, 305, 334
 - retarded, 305
- differential
 - cross section, **65**, **66**, 75
 - equation, 18, 285
 - homogeneous, second-order, 26
 - inhomogeneous, 3
 - inhomogeneous, second-order, 26
 - second-order, 27, 34
 - diffuse, 220
 - diffusion, 25, 239
 - classical, 224
 - coefficient, **25**, 193, 197, 204, 208, 220, 240
 - constant, 37
 - equation, **25**, 37
 - function, 174
 - length, 200, 240
 - inelastic, 222
 - digamma function, **207**
 - dilute limit, 156
 - dimensionality
 - critical, 75, 201, 213, 242
- Dirac notation
 - inner product, **343**
- Dirac's notation
 - bra, 4, 5, 19, 42, **341**
 - inner product, **341**
 - ket, 4, 5, 19, 42, **341**
- Dirichlet function, 337
- discontinuity, 278
- disorder, 156, 173, 200, 235
 - diagonal, 164, 168
 - binary, 244
 - environmental, 151, 165, 168
 - limit
 - weak, 229
 - off-diagonal, 151, 164, 165, 168
 - strong, 221
 - topological, 151
- displacement
 - operator, 385
 - vector, 388
- dissipation
 - of energy, 273
- distribution
 - binary, 165–167, 201
 - Bose thermal equilibrium, 263
 - Bose–Einstein, 262
 - Fermi, 127, 129, 139, 178, 183
 - Fermi thermal equilibrium, 263
 - Fermi–Dirac, 262

- Gaussian, 170
- Lorentzian, 201
- rectangular, 150, 201
- divergence, 209, 234
- logarithmic, 69, 314
- DOS, 44–46, 48, 49, 51, 52, 58, 91, 94, 96, 97, 99, 103, 104, 106, 113, 114, 118, 120–125, 127–129, 132, 139–141, 150, 156, 157, 168, 170, 173, 175, 177, 193, 210, 245, 323, 329, 428
- average, 154, 228
- direct process, 135
- direct-process, 134
- for bcc, 423
- generalized, 263, 264
- indirect process, 135
- indirect-process, 134
- tail, 210, 434
- total, 220
- DOS (density of states), **7**
- drift velocity, 176
- dynamic behavior, 278
- Dyson's equation, 300, 304
- effect
 - Aharonov–Bohm, **207, 208, 241**
 - interference, 203, 204
 - Kondo, 111, 129, 135, 139
 - weak localization, 213
- effective
 - interaction, 307, 317
 - interparticle, 304
 - mass, 120, 310–312, 332
 - medium, 158
- eigenenergy, 64, 70, 81, 83, 104, 224, 227
 - discrete, 42, 66, 67
 - resonance, 115, 120, 140
- eigenfrequency, 83, 130, 131, 176, 177
 - discrete, 136
- eigenfunction, **4, 9, 16, 55, 57–59, 70, 71, 81, 83, 102, 156, 224**
 - Bloch, 355
 - bound, 114
 - causal, 60
 - discrete, 59, 113, 118
 - localized, 113
 - nondegenerate, 9
 - orthogonal, 17
 - scattering, 118
- eigenmode, 83
- eigensolution
 - linear superposition of, 380
- eigenstate, **6, 42, 114, 138, 157**
 - bound, 115
 - extended, 6, 42, 116, 139, 196, **200, 201, 226, 231, 232**
 - localized, 6, 42, 116, 157, 196, **200, 201, 221, 226, 231, 232, 233**
 - nondegenerate, 42
 - normalized, 6
 - propagating, 6, 42, 116, 139
 - resonance, 115–118, 136
 - scattering, 138
 - extended, 169
- eigenvalue, **3, 5, 10, 11, 15, 16, 19, 41, 55, 71, 102**
 - discrete, 5, 9, 15, 16, 57–59, 118
 - nondegenerate, 19
- eigenvector, **4, 19**
- Einstein's relation, 174, 175
- electric
 - field, 8, 173, 364
 - susceptibility, 175, 182, 209
- electrical
 - conductivity, 173, 195, 197
 - resistivity, 131, 133
- electrochemical potential, 217, 218
- electromagnetic
 - equation, 48
 - theory, 31
 - wave, 238
- electromagnetism, 14, 377
- electron
 - dressed, **132**
 - gas
 - high-density, 332
 - pair, 132
 - quasi, **132**
- electron–electron interaction, 201, 239
- electron–phonon interaction, 131, 132
- electronic
 - current density, **387**
 - density, 273
 - Hamiltonian, **387**
 - momentum, **387**
 - polarizability, 100

- potential energy, 176
- spectrum, 137
- spin density, **387**
- structure, 164
- trajectory, 86
- electrostatics, 11
- elementary excitation, 281
- Eliashberg gap equation, 133
- elliptic integral, 94, 97
 - complete, 90, 91
- energy
 - average, 289, 330
 - binding, 128, 129, 135, 139
 - conservation of, 128
 - critical, 235
 - cutoff, 130, 134, 139
 - flux, 171
 - ground-state, 316
 - interaction, 270
 - kinetic, 270, 282, 313, 383
 - mismatch, 219
 - potential, 282, 313, 383
 - electronic, 176
 - resonance, 116, 120
 - total, 126, 271, 381
- ensemble, 150, 199
 - canonical, 182
 - grand canonical, 254
- equation
 - Bessel, **349**
 - Bethe–Salpeter, 320
 - Boltzmann's, 177, 196, 197, **363**
 - linearized, **365**
 - diffusion, **25**, 37
 - diffusion type, 33
 - Dyson's, 300, 304
 - electromagnetic, 48
 - Helmholtz, **345**, 397
 - in cartesian coordinates, **345**
 - in cylindrical coordinates, **345**
 - in polar coordinates, **346**
 - in spherical coordinates, **346**
 - homogeneous, 9, 14–16, 22, 24, 28, 29, 35
 - inhomogeneous, 9, 16, 17, 24, 27, 30, 35, 59
 - integral, 320
 - Klein–Gordon, 31, **47**, 48, 51
 - Laplace, **11**, 12, **345–347**
 - Lippman–Schwinger, **59**
 - Newton's, **176**
 - of motion, 135
 - of state, 289
 - Poisson's, **11**, 13, 126, 273
 - relativistic, 33
 - Schrödinger, 41, 43, 44, 46, 52, 58, 69, 75, 158, 159, 251, 348
 - time-dependent, **60**
 - Schrödinger type, 33
 - time-evolution, 325
 - weak localization, 201
- equation of motion approach, **324**
- equation of motion method, 307
- equations
 - hierarchy of, 256
- Euler's constant, **69**, **130**
- excitation
 - elementary, 281
- expansion
 - asymptotic, 97, 103
 - power series, 314
- exponent, 212
 - critical, 50, 223
 - Lyapunov, **214**, 215
- external static point charge
 - response to, 317
- extinction
 - cross section, 162
- face-centered cubic (fcc) lattice, 103
- fcc (face-centered cubic), 103
- Fermi
 - distribution, 127, 129, 139, 178, 183
 - energy, 127
 - function, **257**
 - level, 219, 310
 - momentum, **278**, 281, 311, 332
 - sea, 127, 129
 - surface, 131, 210, 278, **278**, 280
 - system
 - low-density, 333
 - normal, 309, 332
 - thermal equilibrium distribution, 263
- Fermi's golden rule, **62**, 75, 178
- Fermi–Dirac distribution, 262
- fermion, 252, 254, 278, **381**
 - closed loop, 296, 299
- ferromagnetic

- ordering, 328
- phase, 329, 330
- ferromagnetism, 327
- Feynman diagram, 293, 297, 298, 300
- Feynman's path integral, 203
- field
 - elastic wave, 162
 - electric, 8, 173, 364
 - electromagnetic, 162
 - EM, 163, 171
 - magnetic, 86, 202, 239, 364, 366
 - external, 223
 - momentum, 380
 - operator, 35, 36, 250
 - for noninteracting quantum fields, 36
 - transverse, 162
 - vector classical, 162
- film, 196, 238
 - metallic, 212
- first Brillouin zone, **78**, 84–87, 90, 94, **102**, 105
- fluctuation–dissipation theorem, **182**, 273
- flux
 - average, **206**
 - magnetic, **206**, 208, 241
 - quantum, **206**
- force
 - Coulomb, 313
 - friction, 176
 - magnetic, 212
 - restoring harmonic, 177
 - short-range, 311
- formalism
 - second quantization, 249
- formula
 - Kubo–Greenwood, **180**, 195
- four probe, 218
- Fourier
 - function, 337
 - series, 287
 - transform, **5**, **21**, 25, 27, 33, 34, 57, 58, 174, 176, 255, 258
- frequency
 - Debye, 131
 - mismatch, 200
 - natural, 177
 - phonon, 131
 - plasma, **318**
- friction force, 176
- Friedel oscillation, **317**
- fullerene, 131
- function
 - analytic, 5, 9, 22
 - Bessel, 12, 45, 118
 - modified, 45, **349**
 - spherical, **346**
 - Bloch, **78**, 138
 - Bose, **257**
 - delta, **337**
 - derivative, **337**
 - in cartesian variables, 338
 - dielectric, 283, 305, 334
 - retarded, 305
 - diffusion, 174
 - digamma, **207**
 - Dirichlet, 337
 - Fermi, **257**
 - Fourier, 337
 - gamma, 67, 207
 - gap, 333
 - Gaussian, 337
 - grand partition, **271**, 282
 - Hankel, 12, 45
 - spherical, 163, **347**
 - Hubbard dielectric, 132
 - linear response, 263, 272
 - longitudinal dielectric, 273
 - Lorentzian, 337
 - orthogonal to, 9, 16
 - response, 273
 - step, **23**
 - theta, **338**
 - Wannier, 79, **355**
- Furstenberg's theorem, 215
- gamma function, 67, 207
- gap, **78**, 100, 104, 120, 126, **325**, 326
 - function, 333
 - level, 111
- Gauss' theorem, **11**
- Gaussian, 157
 - distribution, 170
 - function, 337
- generalized DOS-like, 265
- geometric
 - average, 150

- optics, 159
- grand partition function, **271**, 282
- Green's function, 250, 255, 265, 325
 - n -particle, **256**
 - 1-d, 227
 - advanced, **27**, 35
 - causal, **27**, 35
 - imaginary time, 287, 288
 - perturbative expansion, 292
 - diffusion, 37
 - for noninteracting particles, 257
 - for the LA phonon field, 258
 - Hubbard, **97**, 101, 120, 122, 170
 - retarded, **27**, 35, 272
 - two-particle, **256**
 - wave, 37
- ground state, 281
- ground-state
 - energy, 316
- group velocity, 85, 155
 - of sound, 85
- Hall
 - conductance, 239
 - effect
 - integral quantum, 213, **239**
 - voltage, **239**
- Hamiltonian, 384, 385
 - density, 380
 - electron-phonon, **386**
 - total, **386**
 - electronic, **387**
 - Heisenberg type, **333**
 - Kondo, 134
 - periodic, 47, 77, 78
 - eigenfunction of, 78
 - eigenvalue of, 78
 - tight-binding, **77**, **80**, 83, 87, **101**, 111
 - total, 282
- Hankel function, 12, 45
 - spherical, 163, **347**
- harmonic
 - approximation, 386
 - interaction, 135
 - oscillator, 78
 - potential energy, 388
- Hartree
 - approximation, 285, 288, 328–331
- Hartree–Fock
 - approximation, 289, 303, 307, 334
- heat
 - specific, 334
- Heisenberg
 - model, 328
 - picture, 250, **290**
- Helmholtz equation, **345**, 397
 - in cartesian coordinates, **345**
 - in cylindrical coordinates, **345**
 - in polar coordinates, **346**
 - in spherical coordinates, **346**
- hermitian operator, 3, 5, 14, 15, 17, 19, 33, 391
- hierarchy of equations, 256, 285
- high T_c superconductivity, 131
- Hilbert space, 80, **341**
- hole, 129
- Hubbard
 - dielectric function, 132
 - Green's function, **97**, 101, 120, 122, 170
 - model, 327–331, 333
- hyperbola, 107, 145
- imaginary time, 299
- imperfection, 77, 78
- impurity, 113, 115, 136, 137, 141, 144, 145, 169
 - band, 202
 - single-isotope, **136**
 - substitutional, 111
- independent-particle approximation, 183
- inequality, 352
- inertia, 176
- inner product, **341**, **343**
- instability
 - numerical, 91
- insulator, 126
- integral, 17
 - elliptic, 94, 97
 - complete, 90, 91
 - equation, 56, 57, 59, 227, 229, 320
 - inhomogeneous, 72
- integral quantum Hall effect (IQHE), 213, **239**
- interaction
 - effective, 307, 317

- electron–electron, 196, 201, 239
- electron–phonon, 131, 132
- energy, 270
- harmonic, 135
- on-site, 327
- picture, **290**
- repulsive, 333
- screened Coulomb, 176
- short-range
 - repulsive, 319
- spin-orbit, 223
- interface, 196, 212, 213, 238
- interference, 203, 204
 - constructive, 199
 - destructive, 199
 - quantum, 240
- ionic
 - crystal, 99
 - motion, 78, 82
 - solid, 79
- jellium model, **312**
 - high-density, 313
- kernel, 56
- KKR method, **70**
- Klein–Gordon
 - case, **47**, 50
 - equation, 31, **47**, 48, 51
- Kondo
 - effect, 111, 129, 135, 139
 - Hamiltonian, 134
 - problem, 133, 139
- Kramers–Krönig relation, 174
- Kubo–Greenwood
 - formalism, 217
 - formula, **180**, 195
- LA (longitudinal acoustic), **385**
- ladder
 - approximation, 319, 321, 322
 - diagram, 319
- Lagrangian, 203
 - density, 379
- Lamé coefficient, 158
- Landau’s theory, 332
- Laplace
 - equation, **11**, 12, **345–347**
 - transform, 25
- lattice, 77, 101
 - bcc, 422
 - Bethe, 98–102, 145, 147, 360, 361
 - body-centered, 97
 - body-centered cubic (bcc), 103
 - constant, 84, 90
 - diced, 94
 - face-centered, 97
 - face-centered cubic (fcc), 103
 - fcc, 423
 - honeycomb, 94
 - path in, 358
 - relaxation, **126**
 - simple cubic, **94**, 96, 97, 119–121, 147, 170
 - square, 84, 89, 92, 95, 124
 - triangular, 94
 - vector, 78
 - vibration, 100, 131, 136, 137, 164, 165
- LCAO, **79**, 102
- Legendre polynomial, 339
- length
 - localization, 212
 - screening, **317**
 - Thomas–Fermi, **317**
- level
 - bound, 119, 120, 122, 124–126, 129, 209
 - discrete, 66, 68, 69, 73, 74, 120, 122, 123, 138, 145–147
 - Fermi, 310
 - non-degenerate, 138
 - repulsion, 226
 - resonance, 122, 123, 139
 - spacing, 226
 - statistics, **225**
- LiF, 100
- lifetime, 118, 276, 277, 283, 318, 332
- line, 301
- line of singularity, **6**
- linear
 - chain, 375
 - density, 85
 - response, 283
 - function, 263, 272
 - theory, **180**
- linear combination of atomic orbitals (LCAO), **79**, 102
- Liouville’s theorem, 363

- Lippman–Schwinger equation, **59**
- liquid, 313
 Luttinger, 281, 283
- liquid He-4, 52
- local
 conductivity, 179
 moment, 133, 134, 139
 oscillation, **136**
- localization, 192, 197, 209, 219, 224, 230
 Anderson, 240, 243
 effect
 weak, 213
 function, **234**
 in disordered system, 209
 length, 209, 210, 213–215, 221, 225, 229, 240, 241
 inverse, 227
 problem, 201
 regime
 strong, 210
 weak, 216, 240
 theory, 238
 weak, 205
- locator, **144**
 expansion, 165
- logarithmic
 derivative, 220
 divergence, 69, 314
- longitudinal, 163
 dielectric function, 273
- Lorentzian, 150, 168, 170
 distribution, 201
 function, 337
 shape, 277
- Luttinger
 liquid, 281, 283
 model, 281
- Lyapunov exponent, **214**, 215
- magnetic
 coupling, 330
 excitation, 164, 165
 field, 86, 192, 202, 239, 364, 366
 external, 223
 flux, **206**, 208, 241
 quantum, **206**
 force, 212
 moment, 329, 331
 ordering, 327, 328
 phase, 333
 susceptibility, 134
- magnetoresistance
 negative, 202, 213, 241
 tensor, 367
- magnon, 333
- mass
 center of, 127
 effective, 120, **310**, 311, 312, 332
- material, 238
 superconducting, 312
- mathematical data, 17
- matrix, 148
 Pauli, **344**, 387
- matrix element, 61, 79, 80, 101, 150
 diagonal, 7–9, 42, 80, 81, 87, 89, 92, 95, 96, 111, 231
 of current operator, 179
 off-diagonal, 80, 81, 89, 99, 101, 103, 151, 155, 165
- maximally crossed diagram, 191, 192
- mean
 arithmetic, 184
 geometric, 184
- mean free path, 155, **155**, 156, 159, 210, 230, 240
 elastic, 194
 scattering, **178**, 229
 transport, 180, 204, 229
- medium
 effective, 166
 homogeneous, 49
 periodic, 49
 polarizable, 130
 random, 163
 strongly scattering, 158
 disordered, 158
 periodic, 158
- metal, 80, 312
 transition, 80
- metal–insulator transition, 173
- metallic
 conductivity, 199
 regime, 221
- method
 continued fraction, 166
 equation of motion, 307
 of residues, 88
 of stationary phase, 92

- pseudopotential, 79
- recursion, 166, 224
- mobility
 - averaged, 175
 - edge, 201, 210, 211, 235
 - microscopic, 175
- model
 - XY , 224
 - Anderson, **201**
 - Heisenberg, 328
 - Hubbard, 327–331, 333
 - Luttinger, 281
 - nearly-free electron, **78**
 - tight-binding, 79, **80**
- moment
 - local, 133, 134, 139
 - magnetic, 329, 331
 - of inertia, 348
- momentum, 18, 46, 388
 - angular, 348
 - conjugate, 385
 - conservation of, 128
 - eigenstate, 383
 - electronic, **387**
 - Fermi, **278**, 281, 311, 332
 - ket, **342**
 - operator, **343**
 - total, 127
- motion
 - ballistic, 205
 - equation of, 135
 - ionic, 78, 82
- multichannel case, 237
- NaCl, 100
- nanoelectronics, 240
- nanotube
 - carbon, **240**
- nearly-free electron model, **78**
- negative energy solution, 48
- network topology, **158**
- Newton's equation, **176**
- NFE, **78**, 79
- nonanalyticity, 165
- nonmagnetic
 - phase, 329, 330
- normal state, 280
- normalized eigenstate, 6
- number density operator, **383**
- number of states, **7**, 18, 49–52, 104, 394
- number operator, **382**
- numerical technique, 224
- occupation number, 175
- one-dimensional
 - quasi, 217
- operator, 18, 23, 61
 - adjoint, **19**, 381
 - annihilation, **250**, 252, 255, **383**
 - phonon, 258
 - bosonic density, 306
 - chronological, **251**
 - creation, **250**, 252, 255, **383**
 - phonon, 258
 - differential, 14
 - displacement, 385
 - field, 250
 - hermitian, 3, 5, 14, 15, 17, 19, 33, 391
 - linear, 3, 14, 33
 - momentum, **343**
 - number, **382**
 - number density, **383**
 - position, 4, **343**
 - positive definite, 8
 - slave boson, 306
 - spin, **344**
 - time-evolution, **23**, **43**
 - time-independent, 33
 - unit, 5
- optical
 - absorption, 100, 210
 - theorem, 63, **66**, 73, 161
- orbital, 77
 - d -like, 79
 - p -like, 79
 - s -like, 79
 - antibonding, 104
 - atomic, 79
 - hybrid, 79, 104
 - atomiclike, 101, 126
 - bonding, 104
 - local, 163
 - tube, 204
- order
 - short-range, 151, 168
- ordering
 - anti-ferromagnetic, 328
 - chronological, 63

- ferromagnetic, 328
- magnetic, 328
- orthonormal, 388
- orthonormality, 79, 355, 392
- oscillation
 - charge
 - longitudinal, 176
 - collective
 - transverse, 176
 - collective (plasma), 318
 - Friedel, **317**
 - local, **136**
 - small, **135**
- oscillator
 - harmonic, 78
- oxide superconductor, 80
- pair
 - bound, 281
 - electron, 132
 - of equations, 326
- partial differential equation
 - first-order, 33
 - homogeneous
 - first-order, 21
 - inhomogeneous
 - first-order, 21
- partial summation, 301
- particle
 - dressed, **276**, 283
 - number, 279
- particles
 - interacting, 253
- path, 142
 - integral, 203
 - self-avoiding, 358, 360
 - skeleton, **358**
- Pauli matrix, **344**, 387
- Pauli principle, 127, 129, 313, 379
- permeability, 158, 163, 377
- permittivity, 158, 175, 176, 195, 377
- perturbation, **55**, 64, 70, 142
 - expansion, 14, 285
 - series, 55
 - theory, **55**
 - second-order, 133
 - time-dependent, 61
- perturbative approach, 36
- phase, 42, 83
 - antiferromagnetic, 329, 330
 - diagram, 327, 330
 - ferromagnetic, 329, 330
 - incoherence, 214, 230
 - inelastic length, 204
 - inelastic time, 204, 205, 240
 - length, 204
 - time, 200
 - magnetic, 333
 - nonmagnetic, 329, 330
 - shift, 162
 - space, 18, 280, 363
 - velocity, 85, 156
 - of sound, 85
- phonon, **48**, 132, 333, 386
 - frequency, 131
 - longitudinal acoustic (LA), 255, **385**
- photoconductivity, 100
- photon, **48**
- plane wave
 - expansion of, 403
 - normalized, **342**
- plasma frequency, 131, **318**
- plasmon, 128, 281, 318, 332
- Poisson's equation, **11**, 13, 126, 273
- polarizability, 176
 - electronic, 100
- polarization, 162, **304**, 306
 - part, 307
 - proper, **304**, 306, 313
 - part, 307
- pole, 9, 10, 16, 22, 42, 57, 66–69, 72, 73, 117, 145, 277, 310, 332
 - simple, **5**, 15
- polynomial
 - Legendre, 339
- position
 - eigenstate, 383
 - ket, **341**
 - operator, **4**, **343**
- positive energy solution, 48
- post-CPA, 222
 - contribution to σ , 196
 - correction, 194
 - correction to conductivity, 192
 - vertex inclusion, 195
- potential
 - attractive, 145
 - centrifugal, 348

- chemical, 175, 219, 242, **364**, 436
- Coulomb
 - attractive, 66, 67
 - disordered, 51
 - electrochemical, 217, 218
 - thermodynamic, 307
 - vector, **206**
 - well, 69, 209
 - analogy, 210, 212, 244
 - circular, 69
 - shallow, 67, 68, 73
- power, 178
- power series expansion, 314
- pressure, 159, 171, 271
- primitive cell, 87
- primitive crystal cell, 79
- principal
 - axis, 106
 - value, **393**
- principle of least action, 379
- probability, 150
 - amplitude, 60, 61, 73, 117, 203, 231, **341**
 - conservation of, **371**
 - distribution, 150, 226
 - joint, 229
 - reflection, 216
 - transmission, 216, 218
- process
 - direct, 322
 - indirect, 129, 322
- propagation constant, 161, 162
- propagator, **23**, 133, **144**, 280
 - bare, 322
 - dressed, 322
- proper self-energy, **132**
- property
 - optical, 176
- pseudopotential method, 79
- PWA (potential well analogy), 216

- quantized sound wave, 128
- quantum
 - condensation, 128
 - dot, **239**
 - field theory, 35
 - interference, 240
- quantum-mechanical, 14
- quasihole, 278

- quasiparticle, 263, 276, 278, 280, 283, 312, 316, 332

- radius
 - Bohr, 313
 - cyclotron, **200**, 240
- random
 - 1-d system, 214
 - matrix, 214
 - medium, 163
 - variable, 156
 - Gaussian, 180
- random phase approximation (RPA), 316
- random walk problem, 224
- randomness
 - off-diagonal, 164
- ray approximation, 159
- Rayleigh scattering, **159**
- reciprocity relation, **9**
- rectangular
 - case, 157
 - distribution, 150, 201
- recurrence relation, 90, 91, 93, 103
- recursion method, 166, 224
- recursion relation, 93
- reflection
 - amplitude, 237, 370, 373, 429
 - current, 372
 - coefficient, 125, 170, 215, 371
- regime
 - critical, 239
 - extended, 239
 - strong localization, 210
 - weak localization, 216, 240
- relation
 - anticommutation, 252
 - commutation, 252
 - Einstein's, 174, 175
 - Kramers–Krönig, 174
- relaxation time, 156, **156**, 159, 196, **363**
 - transport, 176, 196
- renormalized perturbation expansion (RPE), 98, 230, 234, **359**
- representation, 341
 - diagrammatic, 169
- residue, 9, 16, 42, 72, 112, 277, 283
 - theorem, 10
- resistance, 213, 216

- contact, 217
 - total, 217
- resistivity, 134, 135, 139
 - electrical, 131, 133
 - tensor, 174
- resonance, **66**, 121, 122, 125, 146
 - eigenenergy, 120, 140
 - eigenstate, 117, 118, 136
 - energy, 116, 120
 - level, 139
 - state, 212
 - tunneling, 239
- response, 9, 24
 - function, 273
 - linear, 283
- ring, 208
- role, 173
- RPA
 - (random phase approximation), 316, 318, 319
- RPE (renormalized perturbation expansion), 98, 227
- rule, 295, 299
 - final, 294
- saddle point, 91, 106, 107
- scaling, 133
 - approach, **219**, 223, 224, 243
 - one-parameter, 223, 439
- scattered wave, 163
- scattering, 64, 144, 176
 - amplitude, 46, **65**, 67, 73, **159**, 161, 171, 319, 320
 - forward, 66
 - backward, 229
 - cross section, 115, 118, 125, 159, 162, 171
 - elastic, 173
 - forward, 229
 - inelastic, 173
 - length, **319**
 - limit
 - strong, **156**
 - mean free path, **178**, 229
 - multiple, 144, 157, 165, 169, 199, 217, 322
 - probability, 131
 - process, 239
 - Rayleigh, **159**
- regime
 - weak, 222
- spin flip, 133
- spin-orbit, 223
- theory, 57, 63
- weak, 134
- Schrödinger
 - case, 49
 - equation, 41, 43, 44, 46, 52, 58, 69, 75, 158, 159, 251, 348
 - time-dependent, **60**
 - picture, **290**
- second quantization, 379
 - formalism, 249
- self-consistency, 126
- self-energy, **153**, 154–156, 160, 166, 169, 185, 190, 240, 243, 301, **301**, 307, **359**, 360
 - proper, **132**, **301**, 302, 307, 314, 315
- semiconductor, 103, 126, 210
 - amorphous, 151
 - doped, **126**
 - heavily doped, 202
- set
 - complete, 355
 - orthonormal, 341, 355
- set of eigenfunctions
 - complete, 3, 15, 17, 33, 41
 - orthonormal, 3, 15, 17, 41
- Shockley's tube-integral formula, **367**
- Si, 103, 104, 127
- simple cubic, 84, 108
 - lattice, 119–121, 147, 170
- single-isotope impurity, **136**
- singlet state, **128**
- singular point, 93, 94
- singularity, 23, 26–28, 34, 42, 52, 57, 104, 133
 - δ -function, 114
 - logarithmic, 47, 50, 91, 94
 - square root, 89
 - Van Hove, 94, 96, 97
- skeleton
 - diagram, 301, 303
 - path, **358**
- slave boson operator, 306
- small oscillation, 83, **135**
- solid
 - covalent, 79

- crystalline, 77, 78
- ionic, 79
- periodic, 70
- tetrahedral, 79
- Wigner, 313
- solid-state physics, 46
- solution
 - normal, 310
 - outgoing, 115
- sound
 - propagation, 171
 - velocity, 159
 - wave, 48, 312
 - quantized, 128
- source, 9, 24
 - unit point, 9
- spacing
 - interparticle, 313
- specific heat, **25**, 334
- spectrum, **4**, 78, 136
 - band, 84
 - continuous, 8–10, 15, 42, 44, 57–59, 64, 72, 113, 120, 122, 200
 - discrete, 8, 200
 - electronic, 137
- speed of sound, 385
- spherical harmonic, **339**, 347
- spin, 127
 - flip, 134, 139
 - scattering, 133
 - operator, **344**
 - part, 128
- spring constant, 83, 164
- state
 - bound, 74, 75, 111, 114, 118, 120, 124, 128, 134, 135, 139, 170, 323, 427
 - extended, 210, 226, 233
 - ground, 128, 281
 - localized, 209–211, 226
 - normal, 332
 - propagating, 52
 - resonance, 111, 212
 - scattering, 111
 - singlet, **128**
 - superconducting, 334
 - triplet, 128
- step function, **23**
- strip case, 225
- strong coupling, 130, 132
 - limit, 318
- subband, 99
 - width, 100
- sublattice, 80, 81
- substitutional impurity, 111
- sum rule, 114, 265
- supercell, 166
- superconducting system, 129
- superconductivity, 124, 139, 322, 333
 - high T_c , 131
 - theory of, 69
- superconductor, 129, 283
- superfluid, 312
 - system, 129
- superlattice, 166
- surface impedance, 377
- susceptibility, 176
 - electric, 175, 182
 - magnetic, 134
- symmetry
 - of time reversal, 192
 - time reversal, 204
- system
 - disordered, 6, 15, 141, **150**, 167, 169, 209, 221, 240
 - Fermi
 - low-density, 333
 - normal, 332
 - many-body, 249
 - normal, **278**, 283, 311
 - quasi one-dimensional, 223
 - quasi-1-d, 215, 242
 - quasi-one-dimensional, 225
 - random, **150**, 151, 169
 - 1-d, 214
 - superconducting, 129
 - superfluid, 129
 - TB
 - 2-d, 238
 - three-dimensional, 223
 - two-dimensional, 223
- tail
 - in DOS, 210, 434
 - Urbach, **210**, 434
- TBH, 81, 101, 111, 137, 327
- TBM, **79**, 80, 83, 103, 136, 141, 151, 186, 201, 210, 220, 238, 374

- TCS (total cross section), 436
- technique
- transfer matrix, 214
- temperature
- critical, 130, 327
 - finite, 219
- tensor
- conductivity, 174, 367
 - magnetoresistance, 367
 - resistivity, 174
- tetrahedral solid, 79
- theorem
- Bloch's, **70**
 - Cauchy's, 114
 - fluctuation–dissipation, **182**, 273
 - Furstenberg's, 215
 - Gauss', **11**
 - Liouville's, 363
 - optical, 63, **66**, 73, 161
 - residue, 10
 - Wick's, **293**, 298
- theory
- electromagnetic, 31
 - Landau's, 332
 - linear response, **180**
 - of superconductivity, 69
 - perturbation, **55**, 133
 - scattering, 57, 63
- thermal
- average, 254, 324
 - conductivity, **25**
- thermodynamic
- potential, 307
 - property, 45
 - quantity, 263, 275
 - relation, 271
- theta function, **338**
- Thomas–Fermi screening length, **317**
- tight-binding, 84
- bcc, 422
 - for fcc, 424
 - Hamiltonian, **77**, 83, 87, **101**, 111
 - coupled pendulum analog of, **82**
 - coupled pendulum double spacing analog of, **82**
 - Hamiltonian (TBH), **80**
 - model (TBM), **79**, **80**
 - simple cubic, 85
- time
- imaginary, 299
- time-evolution
- equation, 325
 - operator, **23**, **43**
- time-reversal symmetry, 369
- topology
- cermet, **158**
 - network, **158**
- total
- cross section, 66, 73, 75, 161, 162, 171, 436
 - energy, 271, 381
- trajectory
- classical, 204
- transfer matrix, 214, **370**, 376, 377
- element, 81, 83, 220
 - technique, 214
- transformation
- canonical, 276, 306
- transition
- metal, 79, 80
 - metal compound, 80
 - metal–insulator, 173
 - metal-insulator, 327, 333
 - probability, 46, 75
 - rate of, **62**
- transmission, 239, 242
- amplitude, 237, 370, 373, 429
 - current, 372
 - coefficient, 125, 170, 215, 371, 372
 - in quasi-1-d system, **235**
- transport
- mean free path, 180, 204, 229
 - property, 173, 186, 226, 238
 - relaxation time, 176, 196
- transverse, 163
- triplet state, 128
- tunneling, 132
- two-band model, 427
- unitarity
- of S , 63
- unitary, 63, 372
- Urbach tail, **210**, 434
- vacancy, **170**
- vacuum state, **382**
- valence
- band, **126**, 210

- tail, 210
- value
 - critical, 138, 222, 223
- values
 - continuous, 4
 - discrete, 4
- van der Waals, 289
- Van Hove singularity, 94, 96, 97
- VCA, **151**, 152, 168
- vector
 - classical field, 162
 - derivative
 - in cylindrical coordinates, 347
 - in spherical coordinates, 347
 - displacement, 388
 - potential, **206**
 - space, **4**
- velocity, 158, 159, 161, 310, 318
 - longitudinal, 158
 - of light, 48
 - of sound, 48
 - sound, 159
 - transverse, 158
- vertex, 301
 - correction, 184, **186**, 188–193, **196**, 208, 222
 - inclusion
 - post-CPA, 195
 - part, 187, 188, **302**, 307, 311, 319, 320, 322, 332
- vibration
 - longitudinal, 385
- Virtual Crystal Approximation (VCA), **151**
- voltage, 219
 - critical, 239
 - probe, 218
- Wannier function, 79, **355**
- wave
 - acoustic, 161, 163
 - classical, 158, 159, 238
 - acoustic, 158
 - elastic, 158
 - electromagnetic, 158
 - elastic, 163
 - electromagnetic, 238
 - scattering of, 169
 - equation, 31, 33, 49, 51, 171
 - 2-d, 31
 - homogeneous, 36
 - inhomogeneous, **30**, 36
 - scalar, 37
 - function, 41
 - ingoing, 12, 65
 - outgoing, 12
 - packet
 - free quantum-mechanical, 25
 - minimum uncertainty, 25
 - plane, **4**
 - propagating, 83
 - reflected, 145
 - spherical, 65
 - TE, **378**
 - TM, **378**
 - transmitted, 145
- wavelength, **155**, 156, 158
- wavevector, 49, 52
 - crystal, 104
- weak coupling limit, 318
- weak localization equation, **201**
- weak scattering limit, 156, 221
- Wick's theorem, **293**, 298
- Wigner solid, 313
- wire, 196
 - case, 225
 - thin, 238
- zero sound, 281, 312, 318, 332
- zone
 - first Brillouin, **78**, 84–87, 90, 94, **102**, 105